Proceedings of the Third Lunar Science Conference
(Supplement 3, *Geochimica et Cosmochimica Acta*)
Vol. 2, pp. 1637–1644
The M.I.T. Press, 1972

^{237}Np, ^{236}U, and other actinides on the moon*

P. R. Fields, H. Diamond, D. N. Metta, D. J. Rokop, and C. M. Stevens
Chemistry Division, Argonne National Laboratory,
Argonne, Illinois 60439

Abstract—Widely varying amounts of ^{236}U (2.4×10^7 y half-life) have been observed in samples 12070,91, 12013,10,42, 12073,34, and 14305,80. In samples 10084,75 and 14163,135 the ratio $^{236}U : ^{238}U < 3 \times 10^{-9}$. The $^{236}U : ^{238}U$ ratio in the whole 12070 sample is much higher than it is in the coarsest component of that sample. Arguments are presented to show that lunar ^{236}U is produced mostly by solar flare protons irradiating the indigenous ^{238}U. The ^{237}Np (2.14×10^6 y half-life) also predicted by this mechanism was sought and found in sample 12070. Preliminary calculations imply that the solar flare proton flux more than two million years ago was greater than it has been more recently.

Measurements of $^{235}U : ^{238}U$ mol ratios, total thorium and uranium contents, $^{234}U : ^{238}U$ activity ratios, and limits to ^{239}Pu and ^{244}Pu contents were made on samples 14305 and 14163.

Introduction

The first observation of naturally occuring ^{236}U (2.4×10^7 y half-life) was in sample 12070 by Fields *et al.* (1971). Six more measurements of ^{236}U in lunar samples have been made, and in a separate paper by Rokop *et al.* (1972) ^{236}U in terrestrial uranium has been reported. We suggest that most of the lunar ^{236}U was made by the reaction of solar flare protons with the ^{238}U in lunar soil. Since the same reaction should also produce ^{237}Np, the neptunium fraction of the most ^{236}U-rich sample was investigated, and ^{237}Np was found.

Ultimately the ^{236}U and ^{237}Np contents of lunar samples may serve as long-lived solar proton flux monitors, but since the surface exposure and mixing history of the samples are not well defined and the pertinent cross sections are not known, only broad inferences are now possible. The very high ^{236}U content of 12070 and some crude cross-section assumptions imply that the ^{236}U was produced by a proton flux much more intense than that implied by the ^{26}Al content of many lunar samples (Reedy and Arnold, 1972). This high proton flux exposure must have occurred at such a time that the ^{26}Al would have had time to decay away, but not so long ago that ^{236}U would be lost, that is, 2–100 million years ago.

Further actinide data has been collected for samples 14163,135 and 14305,80. Uranium and thorium contents and limits to ^{239}Pu and ^{244}Pu and other actinides are given. The mass spectrometric $^{235}U : ^{238}U$ ratios and the $^{234}U : ^{238}U$ activity ratios are reported.

* Work was performed under NASA Contract No. T76536 and U.S. Atomic Energy Commission.

EXPERIMENTAL METHODS

The chemical procedures have been described earlier in Fields *et al.* (1970). Uranium, thorium, neptunium, and plutonium are all extracted into tricaporyl methyl ammonium chloride (Alequat 336) in xylene from HNO_3 solution and are resolved into their components with Dowex A–1 ion exchange columns with HCl and HI elutriants.

Isotopic dilution with ^{230}Th (8.0×10^4 y) and ^{233}U [$(1.585 \pm 0.018) \times 10^5$ y] (Ellis, 1971) added to the dissolving sample was used for thorium and uranium analyses. ^{239}Np, obtained from mass-separated ^{243}Am, was added to the already isolated neptunium fraction of 12070,91. This was then reduced with HI to ensure exchange and then purified with another anion exchange column. The chemical yield of neptunium at the point of adding tracer was estimated from the yields of two dummy runs employing ^{237}Np tracer. ^{236}Pu tracer was also added to separated plutonium fractions whose chemical yields were estimated. The uncertainties of estimation were included in the stated errors and were incorporated into the upper limits of ^{239}Pu and ^{244}Pu that are reported.

The uranium and thorium determinations and the ^{235}U : ^{238}U ratios employed a 30 cm radius, 60° sector, permanent magnet mass spectrometer with a multiple filament surface ionization source and electron multiplier detection.

The very high sensitivity of the 100-inch mass spectrometer (Moreland *et al.*, 1967) was required for the ^{239}Pu, ^{244}Pu limits and for finding ^{237}Np.

Because the ^{236}U : ^{238}U ratio can be very small, measurements were made with a 32.4 cm, 44° sector tandem magnetic mass spectrometer, specifically designed to measure widely disparate isotope ratios at adjacent mass peaks (Kaiser and Stevens, 1967; Moreland *et al.*, 1970). A high-pass energy filter exploited the 1.2 eV difference in the kinetic energy between $^{236}U^+$ and $^{235}UH^+$ to suppress the latter. Further discrimination was based upon the 5.7 MeV mass difference between $^{236}U^+$ and $^{235}UH^+$.

Interference at the ^{236}U mass position by $^{235}UH^+$ can be estimated from the works of Moreland *et al.* (1970) to be less than 2×10^{-13} of the ^{238}U. Known mass 236 ions from surface ionization such as $^{39}K_5\,^{41}K^+$, $^{204}Pb\,^{16}O_2^+$, $^{187}Re\,^{16}O_2\,^{17}O^+$, and $^{12}C_{18}H_{20}^+$, have sufficiently different masses from $^{236}U^+$ to be displaced: the tandem mass spectrometer can resolve full peaks at mass 1500. Other isometic hydrocarbons such as $^{12}C_{19}H_8^+$ have also been ruled out by ancillary studies of their normal abundance ratios to more easily discerned peaks (Rokop *et al.*, 1972).

The data on ^{236}U in terrestrial uranium reported elsewhere by Rokop *et al.* (1972) are included here to demonstrate the capability of the machine to achieve even greater sensitivity than was available with the much smaller amounts of uranium from lunar samples.

Each measurement reported in this paper was accompanied by one or more appropriate blanks. Except for one unreported result, the blanks were very small, and the corrections are incorporated into the results.

RESULTS AND DISCUSSION

^{236}U

^{236}U, with a half life of 2.4×10^7 y, is the longest-lived radioactive nuclide perceptible on the moon that could not have survived since the last known nucleogenetic event, 4.7×10^9 years ago. As such, its abundance reflects radionuclide generating conditions for a greater time span than do the abundances of other radioactive nuclei. In this section we will consider the possible sources of ^{236}U in lunar material and will argue against the alternatives to production of ^{236}U by solar flare proton reactions with the ^{238}U, which is present at about one part per million in lunar surface material.

The ratios of ^{236}U : ^{238}U in six lunar samples are shown in Table 1. In a separate investigation (Fields *et al.*, 1971) the finest particles in 12070 (1/7 by volume) were

Table 1. ^{236}U in lunar and terrestrial samples.

Sample	^{236}U/^{238}U ($\times 10^{-9}$)	^{26}Al (Literature) (c/m/Kg)
10084,75 (soil)	< 3	107–147
12070,91 (soil)	233 ± 15	146–171
12070,91 (coarsest fraction of < 1 mm soil)	31 ± 6	
12013–10,42*	9.4 ± 2	115
12073,34 (breccia)	47 ± 10	110 ± 10
14163,135 (soil)	< 3	78
14305,80 (breccia)	4 ± 2	85 ± 17
Uraninite (Shinkolobwe Katanga, Congo)†	0.23 ± 0.08	
Shroeckingerite (Lost Creek, Wyoming)†	< 0.2	
Thucolite (Parry Sound, Ontario)†	0.08 ± 0.15	
Pitchblend (Great Bear Lake, Port Hope Refinery, Ontario)†	0.62 ± 0.22	

* Supplied, already isolated and purified, by J. Rosholt.
† Rokop *et al.*, 1972.

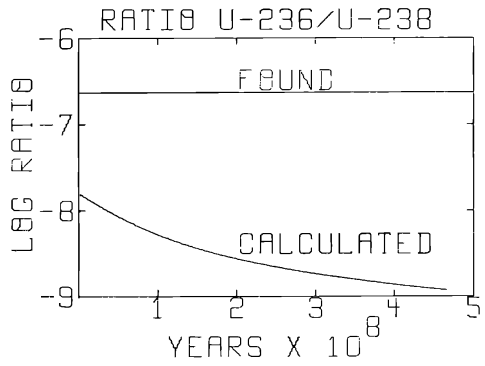

Fig. 1. ^{236}U : ^{238}U expectation from neutron capture by ^{235}U if the nvt were 2.1×10^{16} and the time of radiation were given by the abcissa. This is compared to the ratio found in 12070.

removed by collecting only those particles that settled faster than 0.17 cm/min. In this coarser portion of 12070 the ^{236}U : ^{238}U was nearly 8-fold lower than it was in the sample as a whole. This means that in the finest fraction of 12070 (less than 10 microns) the ^{236}U : ^{238}U ratio must have been greater than 2.33×10^{-7}. This places severe limits upon the possible modes of ^{236}U formation.

The isotopic composition of the gadolinium in 12070 (Burnett *et al.*, 1971) indicates that the total number of neutrons (< 0.2 eV) to which 12070 was exposed is 2.1×10^{16} n/cm^2. No information about the time distribution of this neutron exposure is available, but Fig. 1 shows the calculated ^{236}U : ^{238}U ratios one would expect if ^{236}U were made from the capture of neutrons by ^{235}U (σ = 106 barns) and if the time of the irradiation were given by the abcissa and continued until now.

There are two problems with the above reasoning: (1) There might be a much larger flux of slightly higher energy neutrons that would not be reflected by the gadolinium isotopic distribution but could affect the ^{235}U capture; (2) since 12070

is a mixture, the gadolinium might have acquired its irradiation history prior to its having been mixed with the uranium. The neutron flux estimated by Begemann *et al.* (1972) of 1 n/(cm^2 · sec) from ^{36}Cl and by Fields *et al.* (1971) of less than 80 n/(cm^2 · sec) in 12070 from a ^{239}Pu limit do not have the dependence upon low energy resonances of the gadolinium isotopes, and these also establish the inadequacy (at least recently) of the neutron flux for production of the required amount of ^{236}U. Although separation of rare earths and uranium is possible, Hubbard and Gast (1971) and others have shown a fairly close correlation between the uranium and gadolinium contents in many lunar fractions.

The very wide variation of ^{236}U content from sample to sample is more consistent with the source being solar flare protons, whose effective depth is only several centimeters, than it is with a neutron or galactic cosmic ray source, whose ranges would be meters. Just as is the case with neutrons, there are not enough galactic cosmic rays to produce the observed ^{236}U (Reedy and Arnold, 1972; Armstrong and Alsmiller, 1971).

The steep decline of activity with depth within a lunar rock shows that all but about 60 d/min/Kg of ^{26}Al activity is formed by solar flare protons (Finkel *et al.*, 1971). It can be seen in Table 1 that there is some correspondence between the high ^{236}U contents and the high ^{26}Al contents. Although the appropriate depth dependence measurements have not been made for ^{236}U, the absence of reasonable alternative modes of formation, the high variability of ^{236}U content, the crude correlation with ^{26}Al, and the presence of ^{237}Np in 12070 (discussed later) all point to the production of ^{236}U by solar protons acting upon ^{238}U. The pertinent reactions in order of importance would be (p, t), $(p, 3n)$, $(p, p2n)$, and $(p, 2pn)$. Only 49% of the ^{236}Np from ^{238}U $(p, 3n)$ reactions decays into ^{236}U.

There are very few measurements of proton spallation cross-sections for ^{238}U. These are shown in Fig. 2 along with an assumed curve for all proton reactions transforming ^{238}U to ^{236}U. It is hoped that this curve might be within a factor of 2 or 3 of being correct—more sophisticated calculations are in progress. This curve was applied to a proton spectrum whose rigidity is 100 MV (Finkel *et al.*, 1971), and the flux required to produce 2.33×10^{-7} ^{236}U : ^{238}U (in equilibrium) was calculated to be about 5000 protons/(sec · cm^2) above 10 MeV. This is about 2 orders of magnitude more protons than is invoked by Reedy and Arnold (1972) to explain the ^{26}Al on the moon. These results suggest that there was a far greater proton flux 2–100 million years ago than at present, and hence the sun might have been much more active then than now.

The possibility that ^{236}U was formed elsewhere and accreted upon the lunar surface cannot be excluded. However, such ^{236}U could not have arisen from some supernova explosion, for then we would expect much more ^{244}Pu, and we have reported a ^{244}Pu content for 12070 of $< 2 \times 10^{-4}$ lower than ^{236}U in that sample (Fields *et al.*, 1971).

^{237}Np

The protons reacting with ^{238}U can be expected to produce 2.2×10^6 y ^{237}Np. The neptunium fraction in the chemical separations of the various Apollo samples

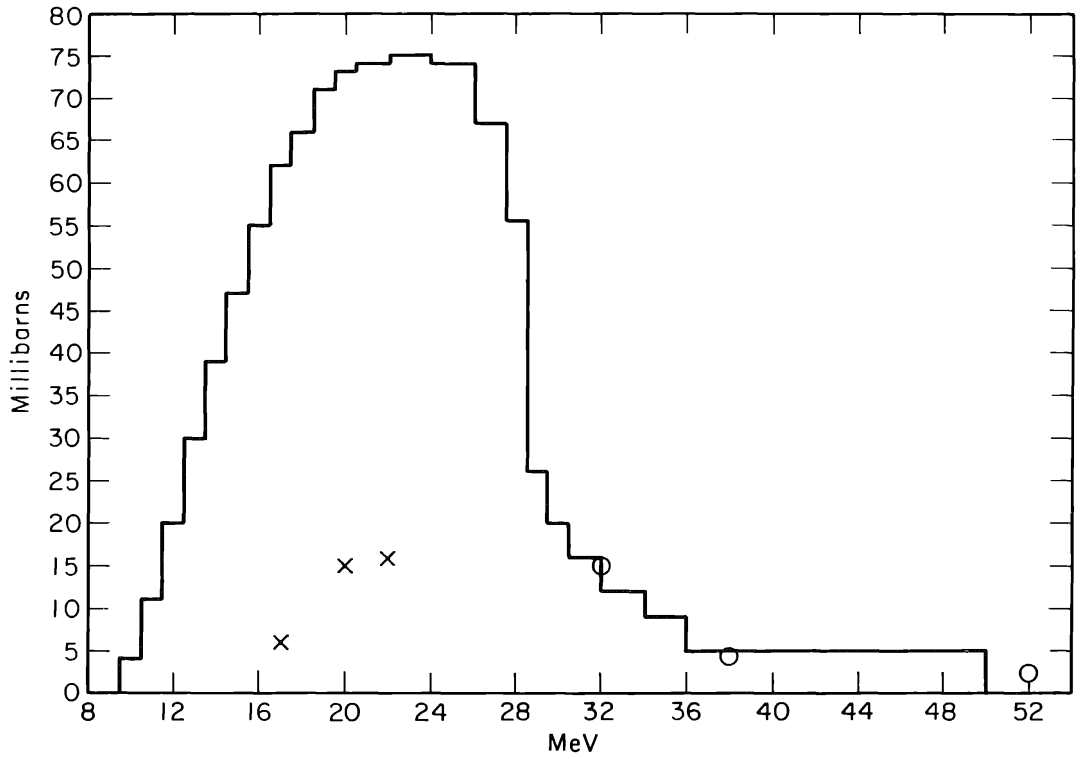

Fig. 2. Histogram of an assumed cross-section curve for all proton reactions transforming ^{238}U into ^{236}U. This was employed in calculations leading to the conclusion that the proton flux creating ^{236}U was more intense than the flux used to explain the production of ^{26}Al. The circles are from Lefort's (1961) ^{238}U (p, $3n$) cross sections. The crosses are from McCormick and Cohen's (1954) ^{238}U (p, $3n$). Forty-nine percent of these reactions result in ^{236}U. See also Wade *et al.* (1957).

had previously been isolated, and tracer experiments had measured the chemical yield of neptunium in these fractions. ^{239}Np tracer was added to a fraction of 12070, and after further purification the ^{237}Np/^{239}Np ratio was measured with the 100-inch mass spectrometer. There are $1.1 \pm 0.3 \times 10^{-13}$ g ^{237}Np per g of 12070,91. This is 0.28 as much as the ^{236}U content; if one assumes a steady equilibrium bombardment for the last 10^8 years, the cross section for formation of ^{237}Np would be 3.2 times the cross section for production of ^{236}U.

Here, as in ^{236}U, there appears to be no reasonable alternative to solar flare protons acting upon ^{238}U as a source for the observed ^{237}Np.

$^{235}U/^{238}U$

The isotopic ratios of ^{235}U : ^{238}U in five samples are shown in Table 2. Although deviation from terrestrial standards as much as 2.6 σ are reported, the lunar and terrestrial uraniums appear to have the same ratio.

Sample 14163,159 has been measured more precisely by Barnes *et al.* (1972) at 7257 and 7256 atoms of ^{235}U per 10^6 atoms ^{238}U.

Table 2. Isotopic ratios of $^{235}U/^{238}U(\times 10^6)$

Sample	Ratio
10084,75	7233 ± 15
12070,91	7153 ± 20
12073,34	7390 ± 200
14163,135	7230 ± 40
14305,80,41	7294 ± 15
Terrestrial uranium (assumed)	7257

^{244}Pu, ^{239}Pu, Uranium, and Thorium

The results of isotopic dilution analyses for two Apollo 14 samples are shown in Table 3. Two adjacent 1/3 g fragments of 14305,80,41 (taken from an outer portion of the breccia) exhibited varying amounts of thorium: the 17.2 ppm value in fragment b leads to the unusual thorium/uranium ratio of 4.16. The thorium/uranium ratio in 14163 is 3.88.

The uranium and thorium contents are in agreement with the less precise gamma-ray analyses from LSPET (1971).

The report by Hoffman *et al.* (1971) of 8.2×10^7 y ^{244}Pu in terrestrial bastnesite is supported by some unpublished evidence at Argonne National Laboratory for ^{244}Pu in terrestrial gadolinite (Metta *et al.*, 1971). In each case the observed ^{244}Pu appears to be too abundant to have survived from the amount estimated to have been present during the condensation of the solar system. Despite the absence of ^{244}Pu in five lunar samples, the lunar surface remains a promising collector of any ^{244}Pu that might come from accretion of extrasolar sources.

The limits to ^{239}Pu (24410 y) in Table 3 imply that recent thermal neutron fluxes were less than 33 n/(cm^2 · sec) and 370 n/(cm^2 · sec) for samples 14305,80 and 14163.

COMMENT

The broad survey of lunar actinides has proven productive in finding new monitors for solar flare protons. Since ^{236}U and ^{237}Np both arise from ^{238}U and protons, and since their half-lives differ by a factor of 11, one can reasonably expect to extract at least relative proton exposure histories by comparing $^{237}Np/^{236}U$ ratios in different samples.

Table 3. Thorium, uranium, ^{239}Pu, and ^{244}Pu content in two Apollo 14 samples.

	14163,135	14305,80,41
Thorium (ppm)	13.2 ± 0.4	15.6 ± 0.5[a] 17.2 ± 0.5[b]
Uranium (ppm)	3.4 ± 0.1	4.13 ± 0.12[b]
^{239}Pu (ppm)	$<4.5 \times 10^{-9}$	$<4 \times 10^{-10}$
^{244}Pu (ppm)	$4^{+1}_{-4} \times 10^{-9}$	$<2 \times 10^{-10}$
$^{238}U/^{234}U$ activity ratio	1.01 ± 0.01	1.01 ± 0.02

[a] Fragment a.
[b] Fragment b.

Although no ^{244}Pu or ^{239}Pu have been observed, one can now consider looking for them in larger samples whose radioactive contents indicate a long history of surface exposure.

Several schemes have been developed to isolate lunar superheavy elements (Z = 110–114), should they exist. However, no unambiguous scheme for identification of such elements now looks attractive enough to warrant the expenditure of large amounts of lunar samples. Here, too, samples whose radioactive contents indicate long exposure on the lunar surface would greatly enhance the probability of finding such elements.

References

Armstrong T. W. and Alsmiller R. G. Jr. (1971) Calculation of cosmogenic radionuclides in the moon and comparison with Apollo measurements. *Proc. Second Lunar Sci. Conf., Geochim. Cosmochim. Acta* Suppl. 2, Vol. 2, pp. 1729–1745. MIT Press.

Barnes I. L., Carpenter B. S., Garner E. L., Gramlich J. W., Keuhner E. C., Machlan L. A., Mainethal E. J., Moody J. R., Moore L. J., Murphy T. J., Paulsen P. J., Sappenfield K. M., and Shields W. R. (1972) Isotopic abundance ratio and assay analysis of selected elements in Apollo 14 samples (abstract). In *Lunar Science—III* (editor C. Watkins), pp. 41–43, Lunar Science Institute Contr. No. 88.

Begemann F., Born W., Palme H., Vilcsek E., and Wänke H. (1972) Cosmic ray produced radio isotopes in Apollo 12 and Apollo 14. *Third Lunar Science Conf.* (verbal presentation).

Burnett D. S., Huneke J. C., Podosek F. A., Russ G. P. III, and Wasserburg G. J. (1971) Irradiation history of lunar samples. *Proc. Second Lunar Sci. Conf., Geochim. Cosmochim. Acta* Suppl. 2, Vol. 2, pp. 1671–1679. MIT Press.

Ellis Y. A. (compiler) (1971) Nuclear Data Sheets **6,** 257.

Fields P. R., Diamond H., Metta D. N., Stevens C. M., Rokop D. J., and Moreland P. E. (1970) Isotopic abundances of actinide elements in lunar material. *Proc. Apollo 11 Lunar Sci. Conf., Geochim. Cosmochim. Acta* Suppl. 1, Vol. 2, pp. 1097–1102. Pergamon.

Fields P. R., Diamond H., Metta D. N., Stevens C. M., and Rokop D. J. (1971) Isotopic abundances of actinide elements in Apollo 12 samples. *Proc. Second Lunar Sci. Conf., Geochim. Cosmochim. Acta* Suppl. 2, Vol. 2, pp. 1571–1576. MIT Press.

Finkel R. C., Arnold J. R., Imamura M., Reedy R. C., Fruchter J. S., Loosli H. H., Evans J. C., Delany A. C., and Shedlovsky J. P. (1971) Depth variation of cosmogenic nuclides in a lunar surface rock and lunar soil. *Proc. Second Lunar Sci. Conf., Geochim. Cosmochim. Acta* Suppl. 2, Vol. 2, pp. 1773–1789. MIT Press.

Hoffman D. C., Lawrence F. O., Mewherter J. L., and Rourke F. M. (1971) Detection of Plutonium-244 in Nature, *Science* **234,** 132–134.

Hubbard N. J. and Gast P. W. (1971) Chemical composition and origin of nonmare basalts. *Proc. Second Lunar Sci. Conf., Geochim. Cosmochim. Acta* Suppl. 2, Vol. 2, pp. 999–1020. MIT Press.

Kaiser K. A. and Stevens C. M. (1967) Ion-retarding lens to improve the abundance sensitivity of tandem mass spectrometers. Argonne National Laboratory Report ANL-7393.

Leforte M. (1961) Fonction d'excitation de la réaction nucléaire ^{238}U (p, $3n$) ^{236}Np entre 30 et 150 MeV. *Compt. Rend.* **253,** 2221.

LSPET (Lunar Sample Preliminary Examination Team) (1971) Preliminary examination of lunar samples from Apollo 14. *Science* **173,** 681–693.

McCormick G. H. and Cohen B. L. (1954) Fission and total reaction cross sections for 22-MeV protons on ^{232}Th, ^{235}U and ^{238}U. *Phys. Rev.* **96,** 722.

Metta D. N., Rokop D. J., and Stevens C. M. (1971) (unpublished).

Moreland P. E. Jr., Stevens C. M., and Wahling D. B. (1967) Semiautomatic data-collection systems for the mass spectrometer. *Rev. Sci. Inst.* **38,** 760–764.

Moreland P. E. Jr., Rokop D. J., and Stevens C. M. (1970) Observations of uranium and plutonium hydrides formed by ion-molecule reactions. *Int. J. Mass Spectroscopy and Ion Physics* **5,** 127–136.

Reedy R. C. and Arnold J. R. (1972) Interaction of solar and galactic cosmic ray particles with the moon. *J. Geophys. Res.* (to be published).

Rokop D. J., Metta D. N., and Stevens C. M. (1972) $^{236}U/^{238}U$ measurements for three terrestrial minerals and one processed ore. *Int. J. of Mass. Spect. and Ion Physics* (to be published).

Wade W. H., Gazales-Vidal J., Glass R. A., and Seaborg G. T. (1957) Spallation-fission competition in the heaviest elements: triton production. *Phys. Rev.* **107,** 1311.

Proceedings of the Third Lunar Science Conference
(Supplement 3, *Geochimica et Cosmochimica Acta*)
Vol. 2, pp. 1645–1650
The M.I.T. Press, 1972

^{204}Pb in Apollo 14 samples and inferences regarding primordial Pb lunar geochemistry*

R. O. ALLEN, JR.,† S. JOVANOVIC, and G. W. REED, JR.

Argonne National Laboratory, Argonne, Illinois 60439

Abstract—^{204}Pb has been measured in Apollo 14 samples and its aqueous (pH 5–6) leachability determined. Soils contain 5–9 ppb of ^{204}Pb with 7–35% leachable; a fragmental rock contains 1.5 ppb ^{204}Pb with ~30% leachable. ^{208}Pb and Bi were also measured in some samples; both were more leachable on the average than ^{204}Pb. Primordial lead is present in two forms, as a volatile, soluble salt on surfaces and as a constituent of a metal or metal related phase.

INTRODUCTION

PRIMORDIAL Pb IN lunar samples can be studied only via its 204-isotope. The concentration and distribution of this element are of interest because of the volatility of its compounds, their presence as sublimates during terrestrial vulcanism, the tendency of Pb to be associated with terrestrial sulfides and with meteoritic sulfides and metal. Measurement of its distribution in lunar matter may help to determine, by analogy, its lunar geochemistry.

We have used fast neutron activation analysis to measure ^{204}Pb as a method which avoids to a great extent the uncertainties arising from blank corrections of the same order as the ppb ^{204}Pb concentrations found. The lability of ^{204}Pb was also studied by its leachability in aqueous (pH 5–6) solution. ^{208}Pb and Bi were measured in a few experiments along with ^{204}Pb.

EXPERIMENTAL

Neutron activation analysis using fast neutrons for ^{204}Pb and slow neutrons for ^{208}Pb and Bi was used in this work and has been adequately described by Turkevich *et al.* (1971). All previous irradiations were in reactors; in this work fast neutrons produced by (*d*, *n*) reactions at the ANL 60-in. cyclotron were used as well. The advantage in the latter irradiation technique is that the samples are considerably less radioactive; the disadvantage is that Bi levels are too low to be detected. The ^{206}Pb (n, α) ^{203}Hg reaction makes the measurement of ^{206}Pb feasible. Short reactor irradiations subsequent to the cyclotron run permit ^{208}Pb and Bi measurements.

Samples prepared in a N_2 dry-box were sealed in supersil fused silica ampoules for irradiation. After irradiation all samples were leached for 10–15 min in a hot dilute HNO_3 solution at pH 5–6. The leached Pb as well as that remaining in the sample were determined. After the aqueous leach the samples were rinsed with alcohol and ether; these washes were discarded. They might be expected to remove any contaminant organic lead (lead tetraethyl) adsorbed on surfaces.

Bulk and sieved fractions of soils 14163,152 and 14259,119, the soil breccia 14049,35 and fragmental rock 14321,185 were determined. In the case of the latter sample a 620 mg piece, freed of cut surfaces, was crushed and 470 mg run as a "representative" sample.

*Work sponsored by USAEC and NASA.

†Permanent address: Chemistry Dept., University of Virginia, Charlottesville, Va.

RESULTS

The ^{204}Pb concentrations in the leach and the sample are given in Table 1. ^{204}Pb

Table 1. Lead and bismuth in Apollo 14 samples.

Sample*	^{204}Pb (ppb)		^{208}Pb (ppm)		Bi (ppb)	
	Residue	Leach	Residue	Leach	Residue	Leach
14163,152	5.6 ± 1.7	3.0 ± 1.4	2.3 ± 0.3	1.0 ± 0.1	—	—
14163,152 > 150μ	2.3 ± 0.14	0.05 ± 0.08	—	—	—	—
< 150μ	10 ± 1	2.8 ± 0.5	—	—	—	—
Sum of fractions	8.2	2.1	—	—	—	—
14259,119	4.4 ± 0.5	0.5 ± 0.2	—	—	—	—
14259,119	5.1 ± 0.6	0.4 ± 0.2	1.8 ± 0.5	0.5 ± 0.2	1.7	< 0.4
14259 (119,112)						
> 150μ	7.0 ± 1.4	4.1 ± 1.0	—	—	—	—
< 150μ	5.8 ± 0.7	1.1 ± 0.2	—	—	—	—
Sum of fractions	6.0	1.6	—	—	—	—
14049,35	4.7 ± 0.8	1.3 ± 0.2	—	—	1.1	4.8
14321,185	1.1 ± 0.2	0.45 ± 0.23	—	—	0.9	0.6

* Sample weights were 0.3–1.0 g.

contents range from about 1.5 ppb in fragmental rock 14321,185 to 5–9 ppb in the soil samples and the friable soil breccia 14049,35. Within the experimental uncertainties, which are essentially counting statistics, replicate determinations are in good agreement. From 7–35% of the total ^{204}Pb in soils and 29% in rock 14321,185 are leached under the mild conditions used.

The ^{204}Pb concentrations in the > 150 μ and < 150 μ sieved fractions of soil 14163 are 2.4 and 12.8 ppb, respectively, with essentially no leachable ^{204}Pb in the coarser grained fraction and about 22% leachable in the finer grained fraction. In soil 14259 the > 150 μ sieve fraction contains 11.1 ppb ^{204}Pb and the < 150 μ fraction contains 6.9 ppb; in these respective size fractions 37% and 16% are leachable. The summations of ^{204}Pb in the sieve fractions fall statistically within the amounts in the bulk samples but are higher by ~1 ppb in both residual samples and in the leach of one. This may be due to sampling since both residual and labile Pb would not be expected to be effected by contamination. Nevertheless, the possibility of contamination should be examined.

A number of observations which argue against contamination and in support of the ^{204}Pb in these samples being indigenous are: (1) The almost constant ^{204}Pb in the replicates of soil 14259,119, including the sieved sample, run at different times, and in the soil breccia; (2) the lack of a consistent grain size dependence of the labile Pb, even the apparent absence of any labile Pb in the 14163,152 > 150 μ fraction; (3) the fact that the fragmental rock sample 14321,185, freshly broken out and crushed in our N_2-box, has a low total ^{204}Pb and an amount of leachable Pb similar to the 14259,119 soil sample.

^{208}Pb concentrations measured in 14163,152 and 14259,119 are given in Table 1; the residual and leachable fractions are 2.3 ± 0.3 and 1.0 ± 0.1, and 1.8 ± 0.5 and 0.5 ± 0.2 ppm, respectively.

Table 2. Literature data comparison.

Sample	Isotope or Element	This Work	Literature
14163	^{204}Pb (ppb)	8.6	9.40,[a] 10.3,[b] 7.05[c]
	^{208}Pb (ppm)	3.3	3.45,[a] 3.3,[b] 3.44[c]
14259	^{204}Pb (ppb)	5.2	4.08,[a] 4.3[d]
	^{208}Pb (ppm)	2.3	2.8,[a] 2.9,[a] 2.41[d]
	Bi (ppb)	2.1	1.8[e]
14321	^{204}Pb (ppb)	1.6	1.91[c]

[a] Tatsumoto *et al.*, 1972.
[b] Silver, 1972.
[c] Barnes *et al.*, 1972.
[d] Doe and Tatsumoto, 1972.
[e] Morgan *et al.*, 1972.

The Bi contents of three of the samples are given in Table 1 and range from 1.5 to 5.9 ppb. As in the case of Pb a significant fraction of the Bi is leachable, up to 81% in soil breccia 14049,35.

Results reported here and literature values are given in Table 2.

Discussion

Measurements of the labile and nonlabile Pb permit us to attempt some deductions concerning how primordial lead is contained in lunar material. The amounts of ^{204}Pb released from the samples under the mild leaching conditions are fairly uniform at 0.4 to 1.3 ppb with the exception of 14163,152 in which leachable Pb is higher but statistically within this range. Soil 14259,119 and fragmental rock 14321,185 have the least amounts of leachable ^{204}Pb. Other investigators have observed the lability of Pb in lunar samples under sometimes more drastic conditions than employed here, these include concentrated acid leaching (Silver, 1970) and volatilization (Silver, 1970, 1972; Huey *et al.*, 1971; Golpalan *et al.*, 1970; and Doe and Tatsumoto, 1972). In the strong acid treatment Silver (1970) reports 50% of the ^{204}Pb leached from soil 10084 and igneous rock 10017. Huey *et al.* (1971) find 50–80% ^{204}Pb volatilized from Apollo 11 and 12 soil at temperatures of 400–800°C, however, blank corrections were uncertain in these experiments. In other experiments Doe and Tatsumoto (1972) and Silver (1972) have found that on heating to the relatively low temperature of 600°C amounts of ^{204}Pb are volatile that are about the same as reported here in the aqueous leach. The results on the readily labile ^{204}Pb are summarized in Table 3. The two types

Table 3. Labile ^{204}Pb.

Sample	Conditions for Release	Fraction ^{204}Pb Released	Amount ^{204}Pb Released (ppb)	Investigator
14163	Leached, 15 min (pH 5–6)	35%	3.0	This work
14049	Leached, 15 min (pH 5–6)	19%	1.3	This work
14321	Leached, 15 min (pH 5–6)	29%	0.45	This work
14259	Leached, 15 min (pH 5–6)	7–21%	0.4–0.5	This work
14259	Heated, 600°C	20%	0.66	Doe and Tatsumoto (1972)
12033	Heated, 600°C	27%	0.33	Doe and Tatsumoto (1972)
12070	Heated, 600°C	26%	1.44	Doe and Tatsumoto (1972)
10084	Heated, 615°C	15%	1.47	Silver (1971)

of observations suggest that the labile ^{204}Pb is both soluble and volatile, possibly $PbCl_2$, a common terrestrial volcanic sublimate. If the correspondence between water-leachable and readily volatilized Pb holds for all samples then all sites appear to contain this labile ^{204}Pb component in comparable amounts.

A clue to the site of the nonleachable Pb may be gleaned from the metal contents of samples. The metal contents determined by Gose *et al.* (1972) and nonleachable ^{204}Pb in soil, breccia, and fragmental rock from this work along with estimates of nonlabile ^{204}Pb based on measurements by other investigators are given in Table 4. A correlation appears to exist. The Pb in 12070 measured by Doe and Tatsumoto (1972) consists of 4.56 ppb ^{204}Pb that is not volatilized at 600°C. The 1.5 ppb ^{204}Pb extracted from 10084 by concentrated HNO_3 (Silver, 1970) could for the most part be in the metal and is consistent with the trend. This 1.5 ppb ^{204}Pb may represent the indigenous (noncontamination) amount; the lowest reported ^{204}Pb concentrations in 10084 are 2.16, 1.95, and 2.16 ppb (Gopalan *et al.*, 1970; Tatsumoto, 1970; and Turkevich *et al.*, 1971; respectively). Even the ^{204}Pb in Apollo 12 igneous rocks 12021 and 12063 reflect the trend.

We conclude then that (1) some primordial lead is present in lunar material as a readily volatile, soluble sublimate, possibly $PbCl_2$, and that (2) some of it is present in solid solution in metal phases or incorporated in phases closely correlated with metal.

We have less extensive data on radiogenic lead but shall examine our results on ^{208}Pb as well as relevant ^{204}Pb data for implications concerning the evolution of lead that are consistent with or complementary to mass spectrometric isotope results.

^{208}Pb, which is primarily radiogenic, is relatively more leachable than it is volatile at low temperatures. Silver (1972b) reports 9% (~0.18 ppm) of the total Pb in 14163,184 is released at low (600°C) temperatures; from his isotopic data we estimate this to correspond to 0.06 ppm ^{208}Pb. Doe and Tatsumoto (1972) report 7% of the total Pb in 14259 volatilized at 600°C corresponding to 0.17 ppm ^{208}Pb. We observe 20–30% (1.0 ± 0.2 and 0.5 ± 0.2 ppm for 14163,152 and 14259,117, respectively) readily (pH 5–6) leachable ^{208}Pb. Thus, in contrast to primordial Pb only a fraction of the leachable radiogenic Pb (as ^{208}Pb) is volatile at 600°C. The enhanced solubility relative to volatility may be due to the fact that the radiogenic Pb is incorporated in phases which are soluble but relatively nonvolatile or it may be that the radiogenic Pb is not deposited as a relatively volatile volcanic sublimate.

A grain-size correlated, readily volatilized ^{207}Pb component has been reported

Table 4. Nonleachable ^{204}Pb-metal content comparison.

Sample	14163	14049	14321	12070	10084	14310	12063	12021
Nonleachable ^{204}Pb (ppb)	5.6[a]	4.7[a]	1.1[a]	4.56[b]	1.5[c]	< 1.0[d]	< 0.26[e]	< 0.184[e]
Metal[f] (wt. %)	0.58	0.59	0.19	0.31	0.4	0.1	0.06	0.04
$\frac{^{204}Pb\ (ppb)}{Metal\ (wt.\%)}$	10	8	5	15	4	< 10	< 4.3	< 4.5

[a] This work; [b] Doe and Tatsumoto, 1972; [c] Silver, 1970; [d] Tatsumoto *et al.*, 1972; [e] Tatsumoto *et al.*, 1971; [f] Gose *et al.*, 1972.

by Tatsumoto (1970), Tatsumoto *et al.* (1971), and Silver (1972b). We find that ^{204}Pb is not consistently grain-size correlated. As a possible explanation for this difference we can assume that the apparent relative amounts of ^{204}Pb on surfaces may be related to the mechanics of regolith formation. Lateral transport as discussed by Huey *et al.* (1971), for instance, can introduce material from diverse source regions each with a unique amount of surface related Pb. Soil samples then are mixtures and may or may not exhibit a labile-Pb grain-size correlation. The ^{207}Pb, on the other hand, may have been introduced during Tatsumoto *et al.* (1971) "third event" subsequent to regolith formation; in this case the deposited volatiles would be grain-size correlated.

Acknowledgments—We thank the crews of the ANL 60-in. cyclotron and the BNL High Flux Beam Reactor for irradiations. Milan C. Oselka of ANL modified the cyclotron target to make irradiations feasible. We are grateful to Dr. H. R. Heydegger, University of Chicago, who suggested several constructive changes in the manuscript. Association of G. W. Reed with and the use of facilities at the Enrico Fermi Institute, University of Chicago, are gratefully acknowledged.

References

Barnes I. L., Carpenter B. S., Garner E. L., Gramlich J. W., Kuehner E. C., Machlan L. A., Mainethal E. J., Moody J. R., Moore L. J., Murphy T. J., Paulsen P. J., Sappenfield K. M., Shields W. R. (1972) The isotopic abundance ratio and assay analysis of selected elements in Apollo 14 samples (abstract). In *Lunar Science—III* (editor C. Watkins), pp. 41–43. Lunar Science Institute Contr. No. 88.

Cliff R. A., Lee-Hu C., Wetherill G. W. (1971) Rb–Sr and U, Th–Pb measurements on Apollo 12 material. *Proc. Second Lunar Sci. Conf., Geochim. Cosmochim. Acta* Suppl. 2, Vol. 2, pp. 1493–1502. M.I.T. Press.

Doe B. R. and Tatsumoto M. (1972) Volatilized lead from Apollo 12 and 14 soils (abstract). In *Lunar Science—III* (editor C. Watkins), pp. 177–179, Lunar Science Institute Contr. No. 88.

Gopalan K., Kaushal S., Lee-Hu C., and Wetherill G. W. (1970) Rb–Sr and U, Th–Pb ages of lunar materials. *Proc. Apollo 11 Lunar Sci. Conf., Geochim. Cosmochim. Acta* Suppl. 1, Vol. 2, pp. 1195–1205. Pergamon.

Gose W. A., Pearce G. W., Strangeway D. W., Larson E. E. (1972) On the magnetic properties of lunar breccias (abstract). In *Lunar Science—III* (editor C. Watkins), pp. 332–334, Lunar Science Institute Contr. No. 88.

Huey J. M., Inochi H., Black L. P., Ostic R. G., and Kohman T. P. (1971) Lead isotopes and volatile transfer in the lunar soil. *Proc. Second Lunar Sci. Conf., Geochim. Cosmochim. Acta* Suppl. 2, Vol. 2, pp. 1547–1564. M.I.T. Press.

Morgan J. W., Laul J. C., Krähenbühl U., Ganapathy R., and Anders E. (1972) Major impacts on the moon: Chemical characterization of projectiles (abstract). In *Lunar Science—III* (editor C. Watkins), pp. 552–554, Lunar Science Institute Contr. No. 88.

Silver L. T. (1970) Uranium–thorium–lead isotopes in some Tranquility base samples and their implications for lunar history. *Proc. Apollo 11 Lunar Sci. Conf., Geochim. Cosmochim. Acta* Suppl. 1, Vol. 2, pp. 1533–1574. Pergamon.

Silver L. T. (1972a) U–Th–Pb abundances and isotopic characteristics in some Apollo 14 rocks and soils and an Apollo 15 soil (abstract). In *Lunar Science—III* (editor C. Watkins), pp. 704–706, Lunar Science Institute Contr. No. 88.

Silver L. T. (1972b) Lead volatilization and volatile transfer processes on the moon (abstract). In *Lunar Science—III* (editor C. Watkins), pp. 701–703, Lunar Science Intsitute Contr. No. 88.

Tatsumoto M. (1970) Age of the moon: An isotopic study of U–Th–Pb systematics of Apollo 11 lunar samples—II. *Proc. Apollo 11 Lunar Sci. Conf., Geochim. Cosmochim. Acta* Suppl. 2, Vol. 2, pp. 1595–1612. M.I.T. Press.

Tatsumoto M., Knight R. J., and Doe B. R. (1971) U–Th–Pb systematics of Apollo 12 lunar samples. *Proc. Second Lunar Sci. Conf., Geochim. Cosmochim. Acta* Suppl. 2, Vol. 2, pp. 1521–1546. M.I.T. Press.

Tatsumoto M., Hedge C. E., Doe B. R., and Unruh D. (1972) U–Th–Pb and Rb–Sr measurements on some Apollo 14 lunar samples (abstract). In *Lunar Science—III* (editor C. Watkins), pp. 741–743, Lunar Science Institute Contr. No. 88.

Turkevich A., Reed G. W. Jr., Heydegger H. R., Collister J. (1971) Activation analysis determination of uranium and ^{204}Pb in Apollo 11 lunar fines. *Proc. Second Lunar Sci. Conf., Geochim. Cosmochim. Acta* Suppl. 2, Vol. 2, pp. 1565–1570. M.I.T. Press.

Proceedings of the Third Lunar Science Conference
(Supplement 3, *Geochimica et Cosmochimica Acta*)
Vol. 2, pp. 1651–1658
The M.I.T. Press, 1972

Abundances of primordial and cosmogenic radionuclides in Apollo 14 rocks and fines

JAMES S. ELDRIDGE, G. DAVIS O'KELLEY, and K. J. NORTHCUTT
Oak Ridge National Laboratory, Oak Ridge, Tennessee 37830

Abstract—Potassium, thorium, uranium, ^{26}Al, and ^{22}Na concentrations were determined non-destructively by gamma-ray spectrometry in a group of breccias or clastic rocks and three samples of fines from Fra Mauro. Samples investigated were rocks 14169, 14170, 14265, 14271, 14272, 14273, 14321,38, and sawdust 14321,256. Fines samples 14148, 14156, and 14149,62 from the top, middle, and bottom, respectively, of the Soil Mechanics Experiment trench were measured in the same study. These samples were collected from the Comprehensive Sample and Station G from the smooth terrain, and from Station Cl in the blocky rim deposit of Cone Crater. There is a remarkable uniformity in the primordial radioelement content in all samples, and average concentrations exceed those of samples returned by Apollo 11 and 12 missions, with the exception of 12034 and 12013.

A simple two-component mixing model developed earlier for our K/U systematics yields KREEP contents of 60–85% for Apollo 14 soils and breccias.

Sawdust from extensive cutting of heterogeneous rocks is a valuable sample matrix for many analytical determinations, but dilution by saw-wire contamination must be accurately determined.

INTRODUCTION

APOLLO 14 SAMPLES from the Fra Mauro formation were expected to be representative of the terra or highlands region as opposed to the mare regions of Apollo 11 and 12 and Luna 16 samples. Ejecta blanket material from the Imbrium Basin, ray material from Copernicus Crater, and Fra Mauro base material excavated by the 340 m diameter Cone Crater were expected to be present at the landing site. Stratigraphic data had indicated that the Apollo 14 landing site was an area considered to be older than the Apollo 11 and 12 mare sites.

LSPET (1971) reported gamma-ray analyses on seven clastic rocks, two crystalline rocks, and five samples of fines. A striking feature of the primordial radioelement content of those samples reported by LSPET (1971) is the high average values for K, Th, and U, compared to the content of these elements in samples from the Apollo 11 and 12 sites. In addition, the fragmental rock to basaltic rock ratio (by number of rocks) was found to be approximately 9 to 1, in contrast to Apollo 11 rocks, where the ratio is 1 : 1, and Apollo 12, where the ratio is 1 : 9.

Our previous gamma-ray spectrometry studies on Apollo 11 and 12 materials have shown distinct differences in the mass ratio K/U for the earth and moon (O'Kelley *et al.*, 1970a, 1970b, 1971a). With the availability of samples from the 43 kg of returned lunar material from the Apollo 14 landing site, we continued our characterization of primordial and cosmogenic radionuclide concentrations in these highland materials.

EXPERIMENTAL METHODS

The gamma scintillation spectrometer used for these analyses contained two NaI(Tl) detectors, each 23 cm in diameter and 13 cm long, with 10 cm pure NaI light guides. The detectors were operated in a coincidence mode along with a large plastic scintillator in anticoincidence with the NaI(Tl) detectors. Further background reduction was achieved with a massive lead shield 20 cm thick. The data acquisition system included a coincidence-anticoincidence logic circuit interfaced with a 4096-channel analyzer containing dual 12-bit analog-to-digital converters. Coincident gamma-ray interactions were recorded in a 64 × 64 channel matrix configuration. Data analysis included the use of two IBM 360/91 programs; one to preprocess the matrix data and the second to perform the quantitative radionuclide determinations by the method of least squares (O'Kelley *et al.*, 1971a; Schonfeld, 1967).

Stainless steel cans of three different diameters and heights from 2.5 to 10 cm were used as sample containers for all rock and fine samples analyzed in this study. Sample weights ranged from 22 to 1100 grams. Calibrations of the system were performed for all the samples measured in this study by constructing exact replicas of them with a separate replica for each nuclide sought (typically eight), along with a blank replica. Electrolytically reduced iron powder was used as the dispersing medium for the nuclide standards in order to match the electronic density of the lunar materials. Bulk density adjustments were made by the addition of 3-mm polyurethane spheres.

Thus, all radionuclide determinations reported in this study were obtained from least-squares analysis of single—and coincident—gamma-ray spectra of all lunar samples using a library of calibration nuclides from exact replicas measured in the same stainless steel containers used for each lunar sample. This technique removes many of the uncertainties associated with the use of absorption corrections for geometrical inconsistencies associated with inexact replicas or with the use of corrections for the stainless-steel can attenuation of gamma rays. The least-squares method of quantitative radionuclide determination used in this study permits the choice of the matrix region used for the analysis. In general, the entire folded, processed matrix yields the highest statistical accuracy, but adjustment of the region of fit helps improve the quality of the data for some samples. Determinations of thorium, uranium, and potassium are based on the use of standards containing terrestrial isotopic abundances, and radioactive equilibrium is assumed for the thorium decay series through the ^{208}Tl daughter and for the uranium decay chain through the ^{214}Bi daughter. Errors reported in this study are conservative estimates of overall uncertainties, including counting statistics and calibration uncertainties.

RESULTS AND DISCUSSION

Primordial radioelement content of rocks and fines

Concentrations of K, Th, U, ^{26}Al, and ^{22}Na for seven clastic or brecciated rocks, three sieved samples of fines, and one composite sample of sawdust from extensive rock cutting of a fragmental rock are listed in Table 1. Two features of the tabular data are apparent from a cursory examination: (1) Levels of the primordial radionuclides are higher than those of the Apollo 11 and 12 samples by a factor of as much as 10; and (2) the spread in the concentrations of these radioelements is very narrow in all samples listed.

Figure 1 is a map of the Apollo 14 landing site and shows the location of samples measured in this study. Swann *et al.* (1971) described the local geologic setting and outlined three map units traversed during the EVA periods: a smooth terrain unit on which the LM landed, slopes of a cratered ridge of the Fra Mauro formation, and the blocky rim deposit of Cone Crater. The regolith in the Fra Mauro region is estimated to range from 10 to 29 m in thickness. All of the samples measured in this study, with the exception of 14321, came from the smooth terrain geologic unit,

Table 1. Gamma-ray analyses of rocks and fines from Apollo 14. (Concentration values have been corrected for decay to 1848 hours, GMT, 5 February 1971.)

Sample No.	Weight (g)	K* (ppm)	Th* (ppm)	U* (ppm)	^{26}Al (dpm/kg)	^{22}Na (dpm/kg)
			Clastic Rocks			
14169,0	78.66	5500 ± 300	14.2 ± 0.2	3.9 ± 0.1	82 ± 6	54 ± 7
14170,0	26.34	5850 ± 300	14.9 ± 0.5	4.1 ± 0.1	88 ± 6	39 ± 9
14265,0	65.79	4100 ± 200	10.9 ± 0.6	3.3 ± 0.2	102 ± 8	70 ± 7
14271,0	96.58	5250 ± 250	15.6 ± 0.2	4.5 ± 0.3	118 ± 6	61 ± 5
14272,0	46.20	4500 ± 200	11.3 ± 0.5	3.3 ± 0.2	94 ± 6	78 ± 9
14273,0	22.40	4560 ± 200	11.7 ± 0.5	3.1 ± 0.2	73 ± 7	66 ± 8
14321,38	1100.0	4050 ± 220	12.7 ± 0.5	3.9 ± 0.4	50 ± 20	35 ± 20
14321.256	200.2	3900 ± 200	10.8 ± 0.5	2.9 ± 0.4	70 ± 7	42 ± 5
			Fines of less than 1 mm			
14148,0	45.3	4150 ± 200	11.4 ± 0.5	3.3 ± 0.2	130 ± 10	74 ± 7
14149,62	50.0	4650 ± 200	11.4 ± 0.5	3.2 ± 0.2	105 ± 10	66 ± 6
14156,46	100.0	4410 ± 200	11.9 ± 0.5	3.3 ± 0.2	148 ± 12	68 ± 7

* Standardization for the assay of K, Th, and U made with reference standards of terrestrial isotopic abundances. Equilibrium of Th and U decay series is also assumed.

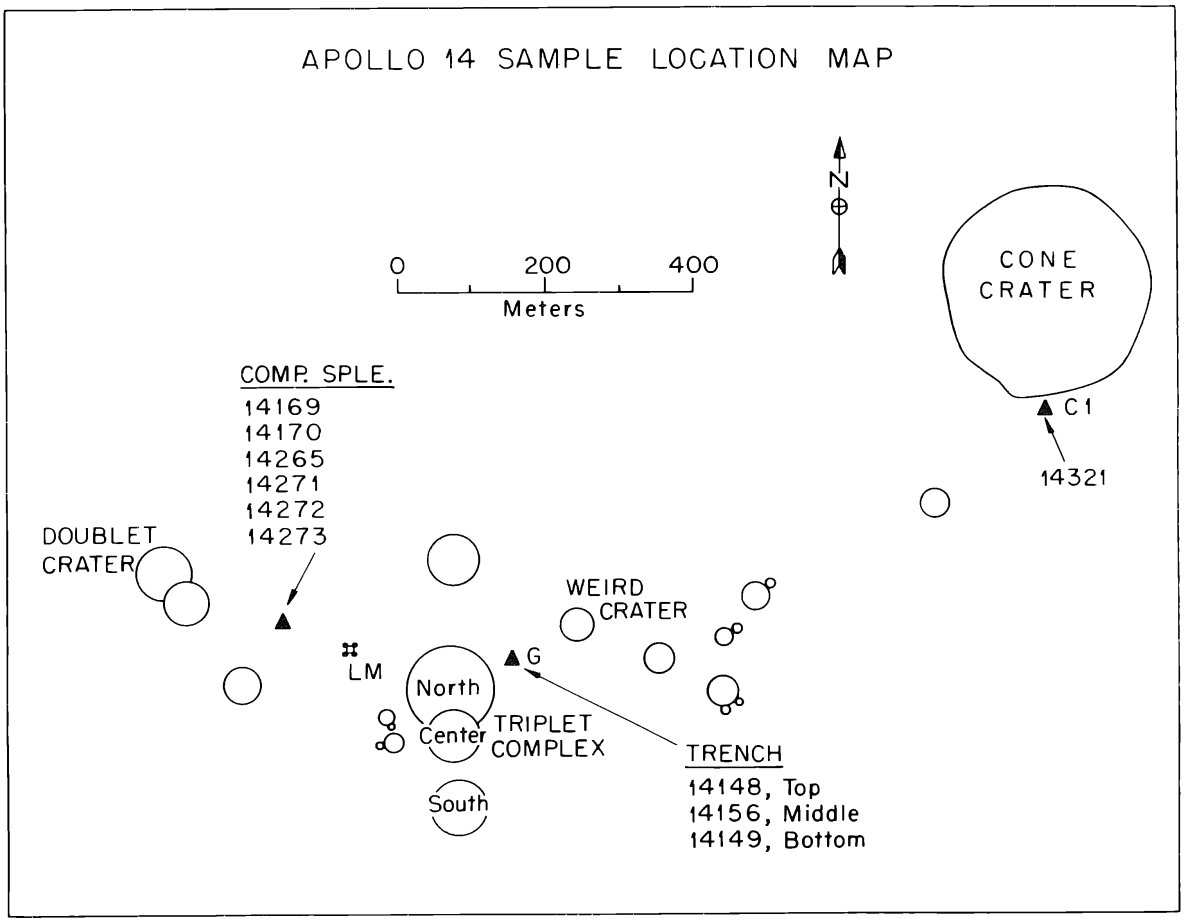

Fig. 1. Sample location map for rocks and fines described in this report. Open circles indicate craters, and sampling stations are shown as solid black triangles. The coordinates of the lunar module (LM) are 3.67°S 17.47°W.

which is densely populated with subdued crater forms several tens of meters to several hundred meters across and generally several meters to several tens of meters deep. Sample 14321 was collected at Station C1 on the second EVA and was collected from the hummocky ejecta blanket of Cone Crater. The rock was well rounded and partially buried (Swann *et al.* 1971).

Cosmic-ray exposure ages have been measured for samples 14053, 14063, 14066, 14167,8, 14305, and 14321 by LSPET (1971) and by Turner *et al.* (1971), yielding exposure ages in the range of 10 to 30 m.y. Turner *et al.* (1971) interpret the low exposure age and the sample location at the Cone Crater rim as evidence that samples 14053 and 14321 are Cone Crater ejecta; thus, the age of Cone Crater may be taken as <30 m.y. From the location on the rim, they conclude that sample 14321 was ejected from a depth >10 m.

LSPET (1971) calculated exposure ages of 10 to 20 m.y. for 14066 and 14305, whose locations were ~ 300 meters east and 100 meters west of the LM, respectively. Thus, if we make the assumption that rocks with exposure ages of 10–20 m.y. originated from the Cone Crater event, then it is obvious that the entire landing site is partially strewn with Cone Crater ejecta. From documentary photographs, Swann *et al.* (1971) predicted that 14305 landed in its position on the lunar surface as a result of a recent impact that produced a nearby crater and not as a result of the formation of any of the large older craters such as Cone. However, the exposure age is essentially the same as that of 14321, found partially buried on Cone Crater rim. Sample 14167,8,1, a 67 mg fragment from the comprehensive sample fines (smooth terrain unit) yielded an exposure age of 29 m.y. and was identified by Turner *et al.* (1971) as Cone Crater ejecta.

Exposure ages calculated for samples 14001, 14259, and 14310 fall in a range of 170 to 590 m.y. and are distinctively different from those of the Cone Crater age (LSPET 1971; Turner *et al.*, 1971). The primordial radionuclide content of at least two of these older exposure age samples (14310 and 14259) is high and is bracketed by the values shown in Table 1 (Keith *et al.*, 1972).

From the preceding discussion, it can be seen that the material returned from Fra Mauro Base sampled a wide area containing Cone Crater ejecta from depths >10 m, as well as surface materials with long exposure ages. From an analysis of our sample suite coupled with those of Keith *et al.* (1972) we can calculate an *average* thorium content of 12.9 ppm for 24 samples weighing 29 kg out of the total sample inventory of 43 kg. Thus, at least 68% by weight of the entire Fra Mauro sample collection contains ~ 13 ppm Th, and from the Th/U ratio of ~ 3.6 and the K/U ratio of ~ 1400, we calculate an *average* uranium content of ~ 3.6 ppm and an *average* potassium content of ~ 5000 ppm. To the extent that the Fra Mauro sample collection is considered a representative sample of the Fra Mauro formation and Imbrium Basin ejecta, we can speculate that these concentrations of K, Th, and U will be found in a wide area of the lunar surface in and around the Imbrium Basin.

Figure 2 shows a simple two-component mixing diagram fitting our K/U systematics, which were developed for Apollo 12 soils and breccias (O'Kelley *et al.*, 1971a). The solid lines are shown as previously described for the Apollo 12 samples with the additional data points added for Apollo 14 soils and breccias from this work and for

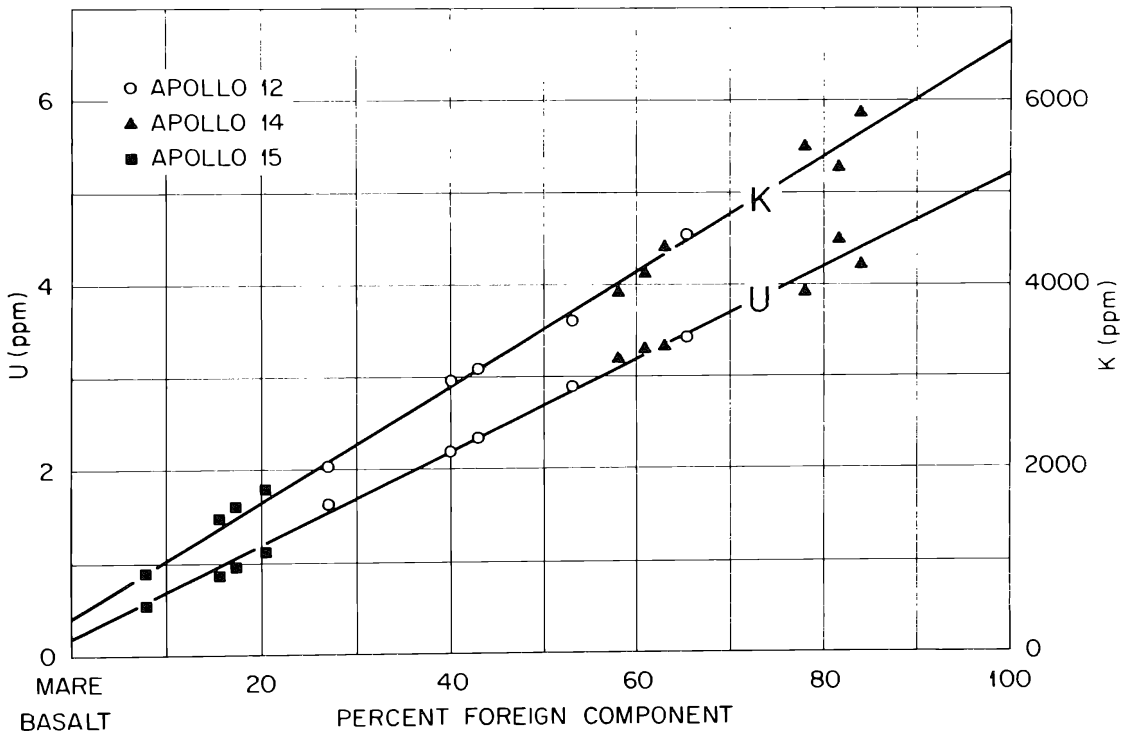

Fig. 2. Two-component mixing lines for K and U concentrations in lunar soils and breccias from Apollo 12, 14, and 15. KREEP has characteristics similar to the foreign component indicated here, with 6500 ppm K and 5.2 ppm U.

Apollo 15 samples as reported by O'Kelley *et al.* (1972a). This simple mixing diagram indicates ~60 to 85% content of foreign component (KREEP) in our collection of Apollo 14 soils and breccias. This finding is in excellent agreement with that of Schonfeld (1972), who used a 26-element linear mixing model and found a 60 to 95% KREEP content in Apollo 14 soils and breccias.

Rock 14321,38 and 14321,256 sawdust

Sample 14321,38 is an 1100 g piece sawed from the north side of the 8996 g 14321 collected near Station C1 during the second EVA. The lunar orientation was well documented by lunar surface photographs (Swann *et al.*, 1971). Cutting diagrams prepared by the NASA-MSC Curator's staff indicate that section 14321,38 has a top surface area of ~60 cm^2 from a total top surface area of ~420 cm^2. Sample 14321,256 is a 200 g aliquot of ~1 kg of sawdust obtained from multiple slab- and wire-saw cuttings of rock 14321. Wrigley (1972) measured Th, U, ^{26}Al, and ^{22}Na concentrations in 14321 sawdust and obtained excellent agreement with values shown in Table 1. Keith *et al.* (1972) measured radionuclide concentrations in 14321,38 and obtained good agreement with values shown in Table 1.

Showalter *et al.* (1972) measured 11 major and minor elements and 11 trace elements from two Apollo 12013 rock fragments and from a sample of 12013,17 sawdust. They found a dilution of the sawdust of 27% by contamination during the sawing process. They report that sawdust analyses should be quite valuable for overall

whole rock compositions for complex materials such as the Apollo 14 clastic rocks if suitable corrections are made for dilutions by the saw-wire debris. From a comparison of our 14321 sawdust and 14321,38 rock values in Table 1, we can calculate an average dilution of the sawdust of ~15%, based on the dilution of the thorium content from the rock.

Potassium and uranium dilutions yield different decrements, but the approximate 15% value is within the error range of the potassium and uranium dilutions. Rhodes (1972) found contamination of ~15% copper along with an unknown contamination of a fibrous material in the sawdust from the cutting of the breccia 14307. It is obvious that sawdust samples can be used for a variety of determinations to obtain whole rock or average concentrations for heterogeneous materials; however, the homogenized sawdust should be carefully analyzed in order to determine the type and quantity of diluents added by the cutting process.

Cosmogenic radionuclide concentrations

Galactic and solar cosmic rays produce many radionuclides in lunar samples by a variety of nuclear reactions. Many of these radionuclides may be determined by non-destructive gamma-ray spectrometry. In our suite of Apollo 11 and 12 samples, we determined nine radionuclides ranging in half-life from 5.7 d. (^{52}Mn) to 740,000 y. (^{26}Al) (O'Kelley *et al.*, 1970b, 1971b). The distribution schedule for Apollo 14 samples precluded any studies of short-lived radionuclides in our laboratory, since 115 days elapsed after the samples left the moon and 127 days after the intense solar flare of January 25, 1971, before we received our first sample (14321,38). In addition, the high concentrations of thorium and uranium masked the minor cosmogenic radionuclides. Concentrations of ^{26}Al and ^{22}Na were determined in all samples and are shown in Table 1. Cosmogenic radionuclide determinations reported here show little differences from those found in previous Apollo missions, with the exception of the three soil samples, which show unexpected results.

The Soil Mechanics Experiment trench was planned to be a 60 cm-deep trench about one crater diameter away from North Triplet Crater at Station G. The astronauts were instructed to dig the trench with one vertical sidewall to provide a means for sampling at depth. The trenching did not yield a vertical side wall; sloping occurred with walls of 60°–80°, and a maximum depth of 36 cm was achieved (Mitchell *et al.*, 1971). Samples 14148, 14149, and 14156, shown in Table 1, were taken from the top, bottom, and middle, respectively, of the trench and are all <1 mm sieved fractions. It was expected that there would be pronounced decreases in the concentrations of the cosmogenic species ^{26}Al and ^{22}Na with depth. Instead, all three samples show a surprising uniformity in concentrations of these nuclides. Calculations of ^{26}Al and ^{22}Na concentrations at depths of 36 cm show that sample 14149,62 should contain ~40 and ~35 dpm/kg for ^{26}Al and ^{22}Na, respectively (Armstrong and Alsmiller, 1971). Due to the uniform distribution of ^{26}Al and ^{22}Na and their high concentrations in the "bottom" sample, we must conclude that extensive mixing occurred and that sample 14149,62 is not representative of the soil at a 36 cm sampling depth. This also gives reason to question the uniformity of K, Th, and U concentrations in the different

soil layers. In addition, the separation of the <1 mm fraction from the trench bottom sample has further emphasized the sampling defect, because the bottom sample has a median grain size of 0.41 mm compared to 0.09 and 0.007 mm for the surface and middle trench samples (LSPET, 1971). Sample 14140, the 4–10 mm sieved fraction, is probably a more representative sample to characterize the trench bottom. The ^{26}Al contents of 14150, 14151 (1–2 mm sieved fraction), and 14152 (2–4 mm sieved fraction) could be used to predict the most characteristic trench bottom sample. All three of these samples are ~11 g fractions from the trench bottom sample (Warner and Duke, 1971).

Our studies with similar trench samples from Hadley Base showed the expected decrease in ^{26}Al and ^{22}Na content with increasing depth in the trench (O'Kelley *et al.*, 1972a, 1972b).

Summary

The Apollo 14 samples from Fra Mauro are unique in the uniformity of primordial radioelement content from all areas of the landing site and from samples ejected from depths ~10 m. These samples yielded average potassium, uranium, and thorium contents of 5000, 3.6, and 13 ppm, respectively. The K/U ratio of ~1400 compares favorably with that of Apollo 12 fines and breccias and to the value of 1250 predicted for KREEP (O'Kelley *et al.*, 1971a).

The K/U systematics developed for our Apollo 12 studies were used to estimate KREEP contents of Apollo 14 samples (O'Kelley *et al.*, 1971a). KREEP contents of 60–85% were determined for samples of this study.

Sawdust from cutting of lunar samples may be used for analytical purposes to obtain whole rock average concentrations of many elements if suitable corrections are made for dilution of the sawdust by saw-wire debris.

Care should be exercised in using sieved samples of fines or soils when there is a possibility that mixing of adjacent samples has occurred. This was found from trench samples collected at Station G. The bottom layer was known to be considerably more coarse-grained than the upper layers in the trench. Fine-grained material from the top layer contaminated the bottom of the trench; sieving of <1 mm fractions from the coarse grains of the bottom thus enhanced the contamination effect.

Acknowledgments—The authors gratefully acknowledge contributions to the work reported here by R. S. Clark, M. B. Duke, R. E. Laughon, V. A. McKay, and E. Schonfeld. This research was carried out under Union Carbide's contract with the U.S. Atomic Energy Commission through interagency agreements with the National Aeronautics and Space Administration.

References

Armstrong T. W. and Alsmiller R. G. Jr. (1971) Calculation of cosmogenic radionuclides in the moon and comparison with Apollo measurements. *Proc. Second Lunar Sci. Conf., Geochim. Cosmochim. Acta* Suppl. 2, Vol. 2, pp. 1729–1745. MIT Press.

Keith J. E., Clark R. S., and Richardson K. A. (1972) Gamma ray measurements of Apollo 12, 14, and 15 lunar samples (abstract). In *Lunar Science—III* (editor C. Watkins), pp. 445–448, Lunar Science Institute Contr. No. 88.

LSPET (Lunar Sample Preliminary Examination Team) (1971) Preliminary examination of lunar samples from Apollo 14. *Science* **173,** 681–693.

Mitchell J. K., Bromwell L. G., Carrier W. R. III, Costes N. C., and Scott R. F. (1971) Soil mechanics experiment. Sec. 4 of Apollo 14 Preliminary Science Report NASA SP-272, 1971.

O'Kelley G. D., Eldridge J. S., Schonfeld E., and Bell P. R. (1970a) Elemental compositions and ages of lunar samples by nondestructive gamma-ray spectrometry. *Science* **167,** 580–582.

O'Kelley G. D., Eldridge J. S., Schonfeld E., and Bell P. R. (1970b) Primordial radionuclide abundances, solar-proton and cosmic-ray effects and ages of Apollo 11 lunar samples by non-destructive gamma-ray spectrometry. *Proc. Apollo 11 Lunar Sci. Conf., Geochim. Cosmochim. Acta* Suppl. 1, Vol. 2, pp. 1407–1423. Pergamon.

O'Kelley G. D., Eldridge J. S., Schonfeld E., and Bell P. R. (1971a) Abundances of the primordial radionuclides K, Th, and U in Apollo 12 lunar samples by nondestructive gamma-ray spectrometry: Implications for origin of lunar soils. *Proc. Second Lunar Sci. Conf., Geochim. Cosmochim. Acta* Suppl. 2, Vol. 2, pp. 1159–1168. MIT Press.

O'Kelley G. D., Eldridge J. S., Schonfeld E., and Bell P. R. (1971b) Cosmogenic radionuclide concentrations and exposure ages of lunar samples from Apollo 12. *Proc. Second Lunar Sci. Conf., Geochim. Cosmochim. Acta* Suppl. 2, Vol. 2, pp. 1747–1755. MIT Press.

O'Kelley G. D., Eldridge J. S., Schonfeld E., and Northcutt K. J. (1972a) Concentrations of primordial radioelements and cosmogenic radionuclides in Apollo 15 samples by nondestructive gamma-ray spectrometry (abstract). In *Lunar Science—III* (editor C. Watkins), pp. 587–590, Lunar Science Institute Contr. No. 88.

O'Kelley G. D., Eldridge J. S., Schonfeld E., and Northcutt K. J. (1972b) Concentrations of primordial radioelements and cosmogenic radionuclides in Apollo 15 samples by nondestructive gamma-ray spectrometry. *Proc. Third Lunar Sci. Conf., Geochim. Cosmochim. Acta* Suppl. 3 (this volume).

Rhodes M. (1972) Private communication of unpublished results, NASA-MSC.

Schonfeld E. (1967) ALPHA M—an improved computer program for determining radioisotopes by least-squares resolution of the gamma-ray spectra. *Nucl. Instrum. Methods* **52,** 177–178.

Schonfeld E. (1972) Component abundance and ages in soils and breccia (abstract). In *Lunar Science—III* (editor C. Watkins), pp. 683–685, Lunar Science Institute Contr. No. 88.

Showalter D. L., Wakita H., Smith R. H., Schmitt R. A., Gillum D. E., and Ehmann W. D. (1972) Chemical composition of sawdust from lunar rock 12013 and comparison of a Java tektite with the rock. *Science* **175,** 170–172.

Swann G. A., Bailey N. G., Batson R. J., Eggleton R. E., Hait M. H., Holt, H. E., Larson K. B., McEwen M. C., Mitchell E. D., Schaber G. G., Schafer J. P., Shepard A. B., Sutton R. L., Trask N. J., Ulrich G. E., Wilshire H. G., and Wolfe E. W. (1971) Preliminary geologic investigations of the Apollo 14 landing site. Sec. 3 of Apollo 14 Preliminary Science Report, NASA SP-272, 1971.

Turner G., Huneke J. C., Podosek F. A., and Wasserburg G. J. (1971) ^{40}Ar–^{39}Ar ages and cosmic ray exposure ages of Apollo 14 samples. *Earth Planet. Sci. Lett.* **12,** 19–35.

Warner J. L. and Duke M. B. (1971) Apollo 14 lunar sample information catalog. NASA TM X-58062, 1971.

Wrigley R. C. (1972) Radionuclides at Fra Mauro (abstract). In *Lunar Science—III* (editor C. Watkins), pp. 814–815, Lunar Science Institute Contr. No. 88.

Proceedings of the Third Lunar Science Conference
(Supplement 3, *Geochimica et Cosmochimica Acta*)
Vol. 2, pp. 1659–1670
The M.I.T. Press, 1972

Primordial radioelements and cosmogenic radionuclides in lunar samples from Apollo 15

G. DAVIS O'KELLEY, JAMES S. ELDRIDGE, and K. J. NORTHCUTT

Oak Ridge National Laboratory,
Oak Ridge, Tennessee 37830

and

E. SCHONFELD

Manned Spacecraft Center,
Houston, Texas 77058

Abstract—Gamma-ray spectrometers with low background were used to determine nondestructively the concentrations of K, Th, U, and cosmogenic radionuclides in Hadley Base basalts 15016, 15475, and 15495; in breccias 15285 and 15455; and in soils 15031, 15041, 15101, and 15601. Bulk densities were determined for six of the samples. The basalts of Apollo 15 are somewhat lower in K, Th, and U (respectively, about 400, 0.54, and 0.14 ppm) than basalts of Apollo 12 or the low-K basalts of Apollo 11 (about 520, 0.97, and 0.25 ppm). KREEP is ubiquitous in the Apollo 15 soils and breccias and ranges from 8 to 21% in the samples studied. Samples of soil or soil breccia from the mature, relatively undisturbed mare regolith and from the Apennine Front are highest in KREEP, while a sample of soil from the edge of Hadley Rille was significantly lower.

Two rocks have concentrations of ^{26}Al less than their saturation values; 15475 and 15495 may have been ejected onto the lunar surface as recently as 0.7 m.y. and 2.0 m.y. ago, respectively. Trench samples from the LM-ALSEP site show variations in radionuclide concentrations with depth similar to those of the Apollo 12 cores. The galactic cosmic-ray production rate of ^{48}V was determined as 57 ± 11 dpm/kg Fe. The concentration of ^{56}Co in rock 15016 leads to the conclusion that the solar flare of 24 January 1971 was 1.91 ± 0.45 times more intense than the flare of 3 November 1969, in agreement with other radiochemical data and with preliminary satellite measurements.

INTRODUCTION

THE APOLLO 15 LANDING marked a notable scientific advance over previous Apollo missions. The increased astronaut mobility made possible the exploration of a large and diverse area of the Hadley-Apennine region. Well-documented rocks and rock fragments with a wide range of textures were returned, together with a variety of soil samples with significant geochemical differences from the igneous rocks and from each other. Thus, the samples from the selenological structures of the region offer unique opportunities to study the detailed geochemistry of the Apollo 15 landing site.

The techniques of nondestructive gamma-ray spectrometry have proved to be very useful for scanning a large number of samples to determine the concentrations of K, Th, and U. In addition to such chemical data, it is also possible to study in some detail the irradiation history of lunar samples by measuring the concentrations of radionuclides produced in the bombardment of lunar surface material by the solar and galactic cosmic rays. Our studies and related efforts by other investigators are included in papers on lunar samples from Apollo 11 (O'Kelley *et al.*, 1970a, 1970b),

Apollo 12 (O'Kelley *et al.*, 1971a, 1971b), and Apollo 14 (Eldridge *et al.*, 1972). A preliminary account of measurements on some of the Apollo 15 samples reported here was published by O'Kelley *et al.* (1972).

Samples from the Apollo 15 manned lunar landing have special significance to nuclear geochemistry because, unlike previous missions, sampling was not closely preceded by an intense solar flare. Thus, the Apollo 15 materials could be used to determine the galactic production rates of some short-lived radionuclides that previously were detected chiefly as products of solar-proton bombardment. Because no quarantine restrictions were imposed on samples from Apollo 15, it was possible to obtain samples for time-dependent studies in our laboratory rather soon after their arrival at the Lunar Receiving Laboratory (LRL).

DESCRIPTION OF SAMPLES

The suite of nine samples to be discussed here includes specimens from the principal geological structures at the Hadley-Apennine landing site. Locations of the samples are shown in Fig. 1, which is a simplified map of Hadley Base drawn from the preliminary report of the Apollo Lunar Geology Investigation Team (1972). Unlike that of previous missions, documentation is rather complete on Apollo 15 samples. For the benefit of later discussion, brief sample descriptions follow. Further details may be found in the Sample Information Catalog (LRL, 1971).

Three of the samples are mare basalts. Sample 15016 is a porphyritic, highly vesicular basalt. Our measured bulk density of 2.4 (Table 1) suggests void space of

Table 1. Concentrations of primordial radionuclides in Apollo 15 samples.*

Sample	Weight (g)	Density (g/cm^3)	K (ppm)	Th (ppm)	U (ppm)	K/U mass ratio	Th/U mass ratio
			Crystalline rocks				
15016,0	924	2.4	374 ± 20	0.52 ± 0.02	0.15 ± 0.01	2493 ± 213	3.47 ± 0.27
15475,0	288	2.9	354 ± 20	0.40 ± 0.02	0.12 ± 0.01	2950 ± 297	3.33 ± 0.32
15495,0	909	2.9	495 ± 25	0.60 ± 0.03	0.16 ± 0.01	3094 ± 248	3.75 ± 0.30
Average, crystalline rocks						2846	
			Breccias				
15285,0	251	2.4	1610 ± 80	3.4 ± 0.1	0.93 ± 0.05	1731 ± 127	3.66 ± 0.22
15455,0†	833		900 ± 150	2.0 ± 0.3	0.53 ± 0.08	1698 ± 382	3.77 ± 0.80
			Fines				
15031,86‡	100		1860 ± 95	4.3 ± 0.2	1.10 ± 0.05	1690 ± 116	3.91 ± 0.25
15041,100‡	100		1740 ± 90	4.0 ± 0.2	1.10 ± 0.05	1582 ± 109	3.64 ± 0.24
15101,1	116	~1.2	1484 ± 74	3.1 ± 0.3	0.86 ± 0.08	1725 ± 182	3.60 ± 0.48
15601,2	204	~1.7	900 ± 45	1.8 ± 0.2	0.51 ± 0.05	1765 ± 194	3.53 ± 0.52
Average, fines and breccias						1699	
Average, all samples							3.63 ± 0.15

* Calibration for assay of K, Th, and U assumed terrestrial isotopic abundances and equilibrium of Th and U decay series.

† "Black and white" breccia. Analysis given emphasizes the dark portion; determined with Ge(Li) detector.

‡ Trench samples near ALSEP (Station 8). Sample 15031 from bottom, 15041 from top.

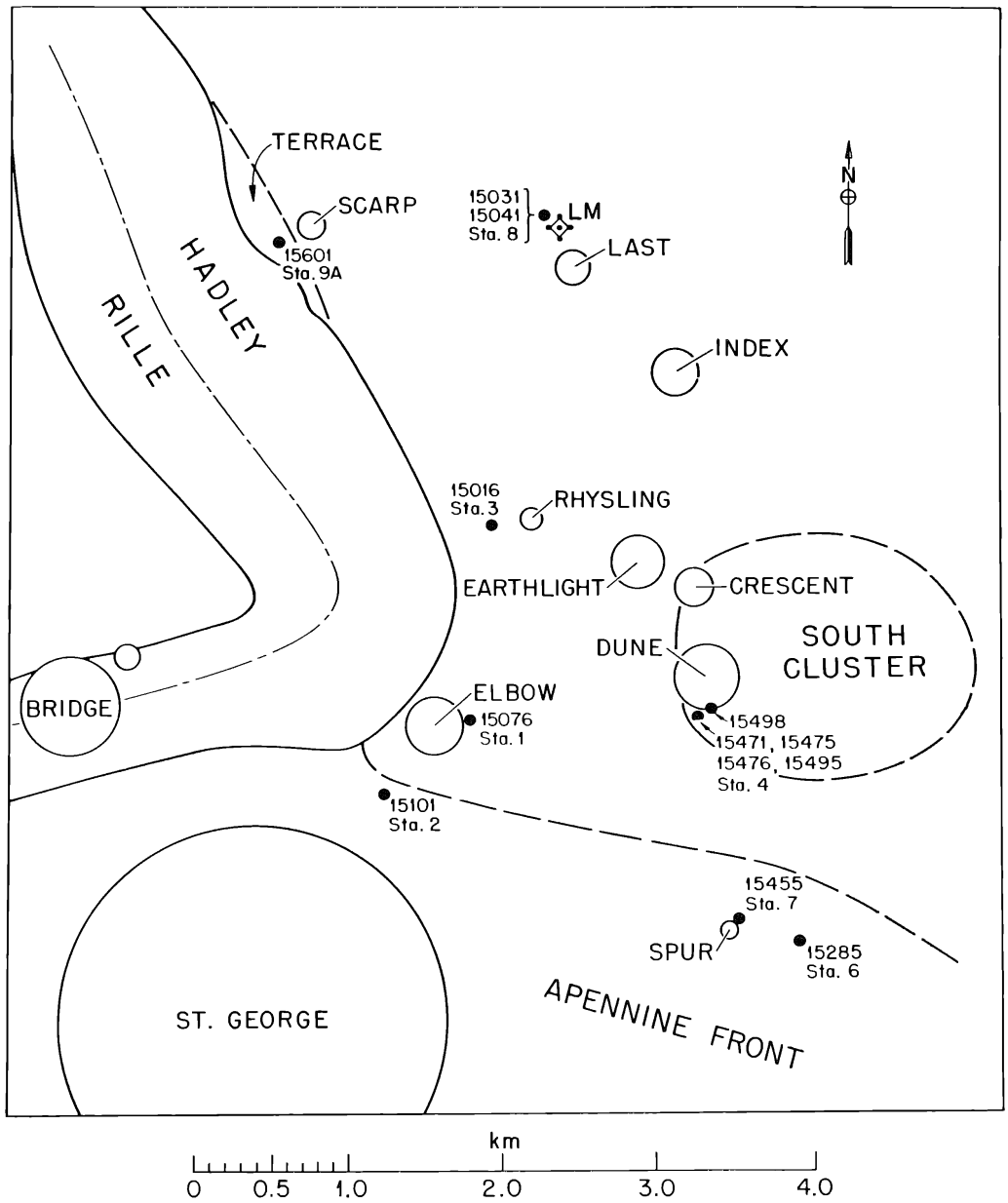

Fig. 1. Map showing original locations of samples measured in this study. Craters are shown as open circles, and sampling stations are shown as solid black circles. The coordinates of the lunar module (LM) are 26.43° N lat, 3.66° E long.

20%. Cavities are mostly vesicles, with about 2% void space as vugs. This sample can not be related clearly to the underlying bedrock. The ubiquitous porphyritic clinopyroxene basalts are typified by 15475 and 15495; sample 15475 represents the coarse basalts, while 15495, at the other extreme, may be classified as a gabbro by its grain size. Such variations suggest that these basalts may have been ejected from different depths of a thick, widespread unit that underlies the regolith at Hadley Base (LSPET, 1972).

Breccia sample 15285 from the Apennine Front is apparently very homogeneous in composition, with various amounts of glass coating on its surfaces. Its mineral

content suggests a largely nonmare origin. The "black and white rock," sample 15455, is a dark breccia with white, norite clasts. It has been described by LSPET (1972).

Four soil samples were provided, all with particle sizes less than 1 mm. Photographs of the Hadley landing site show a south-trending ray that passes through the LM-ALSEP area (Station 8). Sample 15041 is from the top of the Soil Mechanics Trench in the LM-ALSEP area and is of chemical interest because of the possible presence of ray material. Sample 15031 is from the bottom of the trench, about 36 cm below the surface, and provides an opportunity to study cosmogenic radionuclide concentrations at depth. Soil sample 15101 consists of low-density fines (~ 1.2 g/cm^3, Table 1) from an area off the ray, near St. George Crater. Sample 15601 from the "terrace" of Hadley Rille has the higher density (~ 1.7 g/cm^3) associated with mare soils from the Apollo 12 site but shows interesting chemical differences discussed later.

EXPERIMENTAL METHODS

The gamma-ray spectrometer of low background used for most of the analyses reported in this study is located at Oak Ridge National Laboratory (ORNL). It consists of two large scintillation detectors at 180° with the sample between them, completely surrounded by an anticoincidence mantle of plastic scintillator. Background is further reduced by enclosing detectors and anticoincidence mantle inside a large lead shield. The detector and shield system at ORNL is identical to that described by O'Kelley *et al.* (1970b) for the Houston LRL.

Spectra are recorded by a suitable data acquisition system either as noncoincident, or "singles," data if an event occurs in one detector only, or as a gamma-gamma coincidence event if a signal is produced in both detectors simultaneously. Data reduction procedures for the ORNL scintillation spectrometer system were described previously by O'Kelley *et al.* (1971a).

The analysis of rock 15455 used a high-efficiency, low-background Ge(Li) semiconductor radiation detector at the NASA Manned Spacecraft Center, Houston, Texas.

All samples were enclosed in stainless steel containers for measurement. Libraries of standard spectra for quantitative analysis with the least-squares computer program were acquired with the aid of replicas that contained accurate additions of radionuclide standards. With the exception of 15455, all calibrations were carried out with exact replicas placed inside stainless-steel containers identical to those used for the lunar samples.

The internal consistency of the experimental procedures was checked with the help of standard radionuclide test mixtures incorporated in lunar sample replicas. Amounts taken and found agreed in each case within counting statistics, usually 2 to 5%. In his evaluation of 28 analyses of Apollo 12 soil 12070, Morrison (1971) showed that our analyses of that sample (O'Kelley *et al.*, 1971a) for K, Th, and U fall within an average deviation from the mean of $\pm 2.6\%$, which is smaller than our reported errors. Thus, the experimental method appears well established. As before, error statements given here are conservative estimates of the overall uncertainties, including counting statistics and calibration errors.

RESULTS AND DISCUSSION

Radionuclide concentrations of the samples described above are listed in Tables 1 and 2. Additional samples are under study in connection with specific geological problems and will be reported later. Preliminary results on these new samples are consistent with the discussion here. Except for a few exceptions noted later, agreement with other work (Keith *et al.*, 1972; LSPET, 1972; Rancitelli *et al.*, 1972; Wänke *et al.*, 1972) was obtained within the experimental errors in cases where measurements on the same samples could be compared.

Table 2. Concentrations (dpm/kg) of spallogenic radionuclides in Apollo 15 samples* (decays corrected to 1711 hours GMT, 2 August 1971).

Sample	^{22}Na	^{26}Al	^{46}Sc	^{48}V	^{54}Mn	^{56}Co
			Crystalline rocks			
15016,0	29 ± 2	82 ± 4	3 ± 1	10 ± 2	31 ± 4	16 ± 3
15475,0	32 ± 3	40 ± 3	3 ± 2	—	23 ± 3	11 ± 5
15495,0	29 ± 3	69 ± 3	3 ± 1	trace	25 ± 2	11 ± 2
			Breccias and fines			
15285,0	50 ± 4	85 ± 4	3 ± 2		30 ± 5	
15031,86	33 ± 3	49 ± 3			40 ± 10	
15041,100	57 ± 4	99 ± 7	3 ± 2		33 ± 10	17 ± 5
15101,1	44 ± 5	120 ± 12	≤4	9 ± 6	28 ± 8	11 ± 6
15601,2	55 ± 6	112 ± 11	≤4		32 ± 8	28 ± 9

* Upper limits are 2σ evaluated from least-squares analysis.

Primordial radioelements K, Th, and U

The primordial radioelement concentrations are listed in Table 1. A large number of samples from Apollo 11, 12, 14, and 15 have been determined by gamma-ray spectrometry, both by our group and by others. Thus, it is now possible to make some detailed comparisons between the chemistry of Hadley Base and that of previous landing sites.

Patterns of primordial radioelement distributions in the Apollo 15 materials show subtle differences from distributions in lunar material from other sites. The new data add significantly to the K, Th, and U systematics developed by O'Kelley *et al.* (1971a). Concentrations of K, Th, and U in Apollo 15 samples show trends similar to those observed for the rocks and soils of Apollo 12 but quite distinct from the distributions observed for Apollo 14 samples. The basalts of Apollo 15 are somewhat lower in K, Th, and U (respectively, about 400, 0.54, and 0.14 ppm) than the basalts of Apollo 12 or the low-K basalts of Apollo 11 (about 520, 0.97, and 0.25 ppm). Like the soils and breccias of the Apollo 12 site, the soils and breccias of Hadley Base have concentrations of K, Th, and U much higher and more variable than for the crystalline rocks; however, the amount of foreign component (KREEP) in the Apollo 15 soils and breccias is less than that for comparable Apollo 12 materials.

As we have shown earlier (O'Kelley *et al.*, 1970b, 1971a), mass ratios K/U for the moon (1000–3000) lie significantly below the terrestrial values (8000–20,000). These differences are believed to be characteristic of each planet. The relatively narrow range of values for the ratio K/U implies that this parameter was determined by early chemical fractionation and was little altered by later igneous processes. The low values of K/U are another result of the depletion of volatile elements, such as potassium (Ganapathy *et al.*, 1970), accompanied by an anomalously high content of refractory elements, such as uranium or thorium (Hubbard and Gast, 1971). This correlation between potassium and uranium concentrations also implies a similar relationship between potassium and thorium, because concentration ratios Th/U are nearly constant in lunar material (typically, 3.6–3.8). Schmitt (1972) has shown that potassium correlates similarly with hafnium, another refractory element. The most convincing

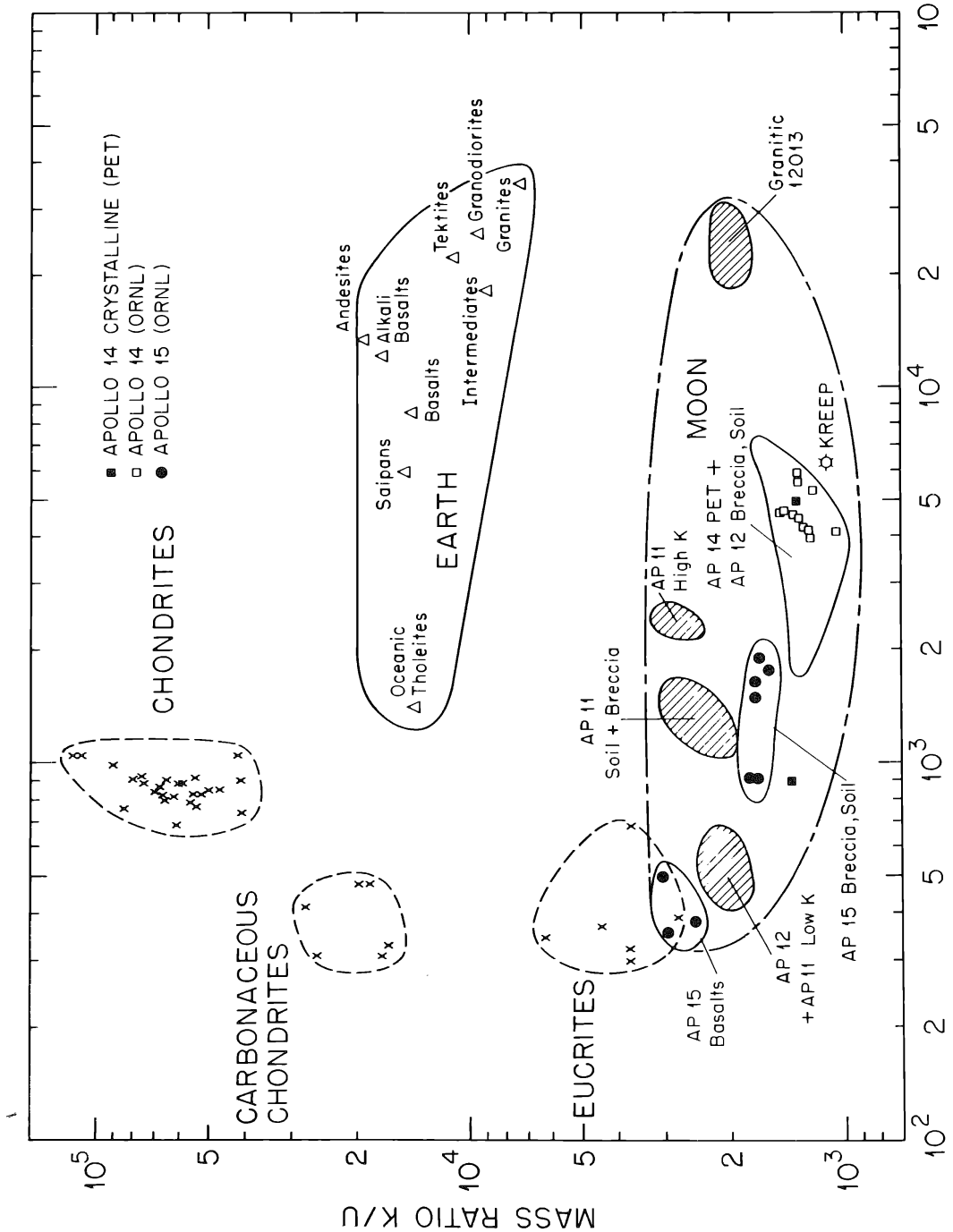

Fig. 2. Plot of concentration ratios K/U as a function of K concentration for terrestrial, meteoritic, and lunar materials. Data from this study are shown as solid circles.

interpretation of the situation is that the igneous liquids that formed the lunar samples were derived from an outer surface enriched in refractory elements and depleted in volatile elements (see Gast and McConnell, 1972).

Values of K/U from Hadley Base materials are displayed graphically in Fig. 2, which is redrawn from our systematics of Apollo 11 and Apollo 12 sample data (O'Kelley *et al.*, 1971a), with the addition of some recent results for Apollo 14 (LSPET, 1971; Eldridge *et al.*, 1972). Unlike our previous plots, the potassium concentrations of Fig. 2 were not normalized to 18% silicon.

A grouping according to sample type is apparent from Fig. 2. The points representing the data on Apollo 15 basaltic rocks overlap the eucrite zone and fall on a trend line for both meteorites and lunar materials. Data on 15085 and 15256 by Keith *et al.* (1972) and on 15556 by Rancitelli *et al.* (1972) are in good agreement with the boundaries of the Apollo 15 basalt zone. In their concentrations of potassium and uranium the Apollo 15 basalts show a remarkable similarity to the Nuevo Laredo eucrite. These gross similarities between the lunar mare basalts and the eucrites are further indications that both materials underwent similar genetic processes in the early history of the solar system (Silver and Duke, 1971).

The soils and breccias of Apollo 15 are much higher in primordial radioelements than the basalts from the same area. On a "trend line" connecting the Apollo 15 basalts and the lunar material KREEP (Meyer *et al.*, 1971) in Fig. 2, the Apollo 15 soils and breccias lie in a hitherto unfilled zone intermediate between the Apollo 12 basalts and the soils and breccias of Apollo 12 and 14. It is apparent that a simple, two-component mixing model that makes Apollo 15 soils and breccias from mare basalt as one end member requires as the other end member a material very similar to KREEP, because other materials shown in the figure would yield higher K/U ratios than those observed.

Two-component mixing diagrams that meet the requirements of our K/U systematics are shown in Fig. 3 for potassium and uranium in samples from Apollo 12 (O'Kelley *et al.*, 1971a), Apollo 14 (Eldridge *et al.*, 1972), and Apollo 15 (Table 1). Although such a two-component model is oversimplified in its neglect of anorthositic constituents, it yields the correct relative concentrations of KREEP, because anorthosites are very low in primordial radioelements and would simply act as diluents. It is seen that KREEP is ubiquitous at the Apollo 15 site but only varies from about 8 to 21%. The Apollo 12 samples show a range from 27 to 65%, but the Apollo 14 soils and breccias are very rich in KREEP, 58 to 84% for the samples shown.

Concentrations of KREEP in Hadley Base materials derived from the mixing lines of Fig. 3 compare favorably with the results of an extensive analysis by Schonfeld (1972a), who determined amounts of mare basalt, anorthosite, granitic material (light portion of 12013), ultramafic material, meteoritic components, and KREEP by use of a least-squares fit to a linear mixing model based on chemical concentrations of up to 26 elements. Schonfeld reports 18% KREEP for 15101 and 12% for 15601.

Although the breccias of the Apennine Front resemble the Fra Mauro breccias texturally, the Apennine Front breccias and soils we have measured are quite distinct chemically from their Fra Mauro counterparts. Table 1 and Fig. 3 show that the primordial radioelement and KREEP concentrations of soil 15101 and soil breccia

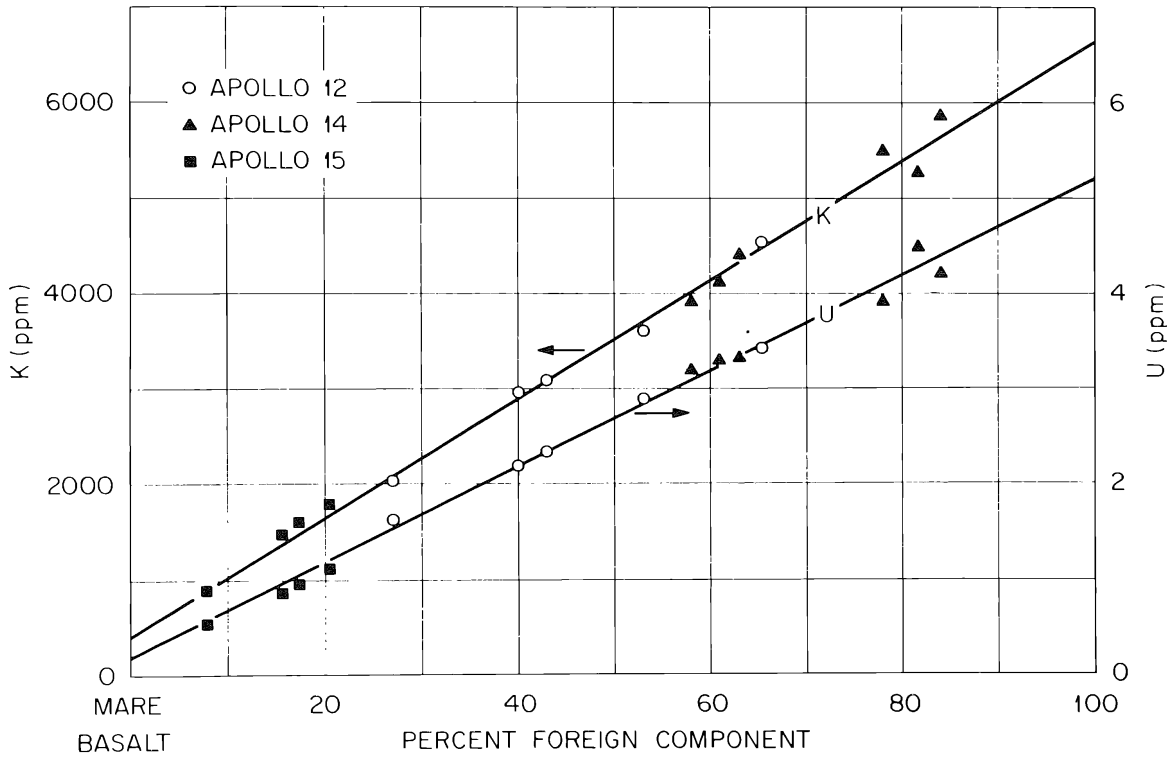

Fig. 3. Two-component mixing diagrams for K and U concentrations in lunar soils and breccias. Apollo 12 data from O'Kelley *et al.* (1971a), Apollo 14 data from Eldridge *et al.* (1972), Apollo 15 data from Table 1. Samples (and percent foreign component, or KREEP) are: 15601 and 15455 (8%), 15101 (16%), 15285 (17%), 15031 and 15041 (20%).

15285 lie well below the limits for Apollo 14 materials. This concentration of KREEP (~20%) is typical of soils and soil breccias along the Front. Further, Schonfeld (1972a) finds that these Front materials are lowest in basaltic component and highest in "anorthositic gabbro" of the materials from Hadley Base. Breccias 15455 (the "black and white" rock), 15426, and 15923 ("green clods") (Keith *et al.*, 1972; LSPET, 1972) all share a much lower concentration of primordial radioelements and, by inference, a lower concentration of KREEP. Two breccia samples (15205 and 15206) from the largest rock examined on the Front do approach the high primordial radioelement concentrations of the Apollo 14 samples (LSPET, 1972; Keith *et al.*, 1972; Rancitelli *et al.*, 1972). Such samples may prove to be Imbrium ejecta, like the Fra Mauro formation.

The mature, relatively undisturbed mare regolith appears to be high in KREEP. Soil sample 15041 from the surface at the LM-ALSEP site and 15031 from a depth of 36 cm have the highest concentrations of KREEP in our samples (~20%). The concentrations of potassium, thorium, and uranium do not show any significant variations with depth. It is not possible to associate the high concentration of KREEP at this location with ray material, although it may be significant that soil at the edge of Hadley Rille (15601, Table 1) is dramatically lower in radioelement concentrations and contains only about 8% KREEP.

The smaller amounts of potassium, thorium, and uranium in Rille soil 15601 may have originated *via* an erosion mechanism. Sample 15601 was collected only 20 m from the edge of the Hadley Rille. It is reasonable to assume that this area at the edge of the Rille was at one time covered by a layer of lunar material as rich in KREEP as the adjoining region (up to 20%) but that erosion by meteorite impacts at the margin of the Rille removed a large part of the layer. The effect of such impact erosion is much greater at an edge than on a horizontal plane, because the eroded material tends to fall away inside the Rille. It was reported that in the region under discussion, the regolith was almost absent 25 m from the edge of the Rille (Swann *et al.*, 1971). Thus, the soil of the terrace is believed to be thin, relatively young, and characteristic of the bedrock underlying this region.

Cosmogenic radionuclides

The general concentration patterns for spallogenic radionuclides shown in Table 2 resemble those observed on previous Apollo missions. Because chemical analysis data are lacking for many of the samples reported here, detailed interpretations cannot be made in some cases. However, it is possible to discern important trends in the data in many cases and to calculate quantitative results in others.

The three crystalline rocks yielded especially precise results on cosmogenic species, because spectra of such weak components suffer less interference from the thorium and uranium decay series than spectra of lunar soils and breccias. The concentrations of ^{56}Co, ^{54}Mn, and ^{22}Na for rocks 15016, 15475, and 15495 shown in Table 2 are close to the saturation values expected for basaltic rocks exposed to solar and galactic cosmic rays at the lunar surface. Photographic studies by Swann *et al.* (1971) noted the lack of extensive burial of these rocks. The ^{22}Na concentration only measures exposure on about a 10-year time scale, while ^{26}Al determines cosmic-ray exposure on a scale of a few million years. Rock 15016 appears to have a saturation value for ^{26}Al. For 15475, the concentration of ^{26}Al is only about one-half the saturation value; a detailed analysis indicates that this sample was ejected onto the lunar surface about 0.7×10^6 yr ago. The exposure of 15495 may also be low; if its chemical composition is the same as the other basalts in Table 2, its ^{26}Al concentration may be consistent with an exposure as short as 2×10^6 yr.

Soil samples 15101 and 15601 appear to have been taken from relatively thin surface layers. The high concentrations of ^{22}Na, ^{26}Al, and ^{56}Co are consistent with a mean sampling depth of about 3.5 cm for 15101 and a somewhat shallower depth of 2.3 cm for 15601, if it is assumed that their chemical compositions and radioactivity variations with depth are the same as found (Rancitelli *et al.*, 1971; Eldridge *et al.*, 1971) for Apollo 12 soils.

The trench samples from the LM-ALSEP area (Station 8) show the general trends expected for such samples. However, 15041 from the top of the trench seems to have been several cm thick; as in other Apollo surface samples, it seems difficult to obtain material representative of a thin surface layer. Our measurements of ^{22}Na and ^{26}Al in 15041 and those by Keith *et al.* (1972) and by Rancitelli *et al.* (1972) lead to mean depths of sampling of 2.9–2.1 cm. The spread in estimated sampling depth reflects a

small, systematic difference in ^{22}Na and ^{26}Al concentrations of 15031 and 15041 between our measurements and those of Keith *et al.* (1972) and Rancitelli *et al.* (1972). The aliquots of samples measured by us were different from the aliquots measured by the other groups. Small differences in assays for thorium and uranium, together with the differences just noted, suggest that the aliquots may have been taken from samples that originally were slightly nonuniform in composition.

The radionuclide concentrations to be expected at a depth of 36 cm are not well established, but the amounts of ^{22}Na and ^{26}Al determined for 15031 are in approximate agreement with expectations. It is not possible to detect any difference in ^{54}Mn content between 15041 and 15031. Calculations by Reedy and Arnold (1971) suggest a ^{54}Mn concentration for 15041 of about 34 dpm/kg from solar and galactic cosmic-ray production, decreasing to about 30 dpm/kg for 15031, for which only galactic cosmic-ray production is significant.

During the preliminary examinations of the Apollo 11 and Apollo 12 samples in the LRL, we were able to detect two relatively short-lived radionuclides (O'Kelley *et al.*, 1970b, 1971b); 5.7-day ^{52}Mn was determined in four rocks and 16-day ^{48}V was determined in six rocks. Our studies showed that the concentrations of ^{48}V were well correlated with the titanium concentrations of the rocks, as expected if most of the ^{48}V was produced by solar-flare protons *via* the ^{48}Ti (p, n) reaction. From the ^{48}V content of rock 12062, which appeared to have been buried, we inferred a yield from galactic proton bombardment of about 40 $\pm$ 20 dpm/kg Fe. Samples from Apollo 15 offered the best opportunity so far to determine the galactic production rate of ^{48}V almost free from solar flare effects.

As shown in Table 2, we were able to determine ^{48}V quantitatively in the first two samples received, 15016 and 15101. However, the results on 15016 were superior, because weak components of the gamma-ray spectra of mare basalts suffer less interference from the spectra of the thorium and uranium decay series than spectra of lunar soils and breccias. The concentration of ^{48}V in 15016 leads to a galactic production rate for ^{48}V of 57 $\pm$ 11 dpm/kg Fe, based on an FeO concentration of 22.6% (LSPET, 1972). This result agrees within the experimental errors with our earlier estimate, with the value of 90 $\pm$ 45 dpm/kg Fe determined by Honda and Arnold (1961) for the Aroos iron meteorite and with the value 75 $\pm$ 23 dpm/kg Fe obtained by Cressy (1970) for the St. Séverin amphoterite.

Solar flare of 25 January 1971

Unlike previous Apollo manned lunar landings, no intense solar flare directly preceded the Apollo 15 mission; however, 77.3-day ^{56}Co was detected in some of the samples. Because ^{56}Co is almost totally produced by solar flare protons *via* the ^{56}Fe (p, n) reaction, the ^{56}Co detected in our Apollo 15 samples was effectively produced by the intense solar flare of 24 January 1971, which preceded the collection of Apollo 14 samples. In our preliminary report on Apollo 15 samples (O'Kelley *et al.*, 1972) we compared the ^{56}Co yields for our Apollo 15 samples with concentrations of ^{56}Co in Apollo 12 samples and concluded that the flare of 24 January 1971 was at least 30% more intense than the well-characterized event of 3 November 1969. The

^{56}Co concentration of 16 ± 3 dpm/kg for rock 15016 was corrected for iron content and for decay from 24 January 1971 and was then applied to a more careful estimate of the relative intensity of the solar flare that produced the ^{56}Co of the Apollo 14 and 15 samples.

The threshold of the reaction ^{56}Fe (p, n) ^{56}Co is about 6 MeV, and the peak of the excitation function is about 13 MeV, so relative solar production rates for ^{56}Co relate rather well to solar proton fluxes of particles with energies above 10 MeV. Data on the concentration of ^{56}Co in rock 12002 (O'Kelley *et al.*, 1971b) were used to monitor the flare of 3 November 1969; a necessary correction for ^{56}Co already present from the flare of 12 April 1969 was estimated from our measurements on Apollo 11 rock 10017 (O'Kelley *et al.*, 1970a, 1970b). Differences in densities and geometries of the rocks were calculated. The new calculation concludes that the solar flare of 24 January 1971 was 1.91 ± 0.45 more intense than the flare of 3 November 1969. No absolute satellite measurements have been published; however, Bostrom (1972) obtained 2.0 for the above ratio from a preliminary analysis of satellite data. Also in excellent agreement are other radiochemical flux ratios of 1.6 ± 0.5 by Arnold *et al.* (1972), from a study of rock 14321; and 2.2 ± 0.3 by Schonfeld (1972b), from measurements on rock 14310.

Acknowledgments—The authors thank M. B. Duke and J. O. Annexstad for their rapid and efficient preparation of lunar material, the Lunar Sample Analysis Planning Team for their assistance and advice, and V. A. McKay and R. S. Clark for help with design and procurement of sample containers. Discussions with J. R. Arnold and P. W. Gast helped formulate our ideas. Research was carried out under Union Carbide's contract with the U.S. Atomic Energy Commission through interagency agreements with the National Aeronautics and Space Administration.

References

Apollo Lunar Geology Investigation Team (1972) Geologic setting of the Apollo 15 samples. *Science* **175,** 407–415.

Arnold J. R., Finkel R. C., and Wahlen M. (1972) Personal communication.

Bostrom C. O. (1972) Unpublished data.

Cressy P. J. Jr. (1970) Multiparameter analysis of gamma radiation from the Barwell, St. Séverin, and Tatlith meteorites. *Geochim. Cosmochim. Acta* **34,** 771–779.

Eldridge J. S., Northcutt K. J., and O'Kelley G. D. (1971) Unpublished data.

Eldridge J. S., O'Kelley G. D., and Northcutt K. J. (1972) Abundances of primordial and cosmogenic radionuclides in Apollo 14 rocks and fines (abstract). In *Lunar Science—III* (editor C. Watkins), pp. 221–223, Lunar Science Institute Contr. No. 88.

Ganapathy R., Keays R. R., Laul J. C., and Anders E. (1970) Trace elements in Apollo 11 lunar rocks: Implications for meteorite influx and origin of moon. *Proc. Apollo 11 Lunar Sci. Conf., Geochim. Cosmochim. Acta* Suppl. 1, Vol. 2, pp. 1117–1143. Pergamon.

Gast P. W. and McConnell R. K. Jr. (1972) Evidence for initial chemical layering of the moon (abstract). In *Lunar Science—III* (editor C. Watkins), pp. 289–290, Lunar Science Institute Contr. No. 88.

Honda M. and Arnold J. R. (1961) Radioactive species produced by cosmic rays in the Aroos iron meteorite. *Geochim. Cosmochim. Acta* **23,** 219–232.

Hubbard N. J. and Gast P. W. (1971) Chemical composition and origin of nonmare lunar basalts. *Proc. Second Lunar Sci. Conf., Geochim. Cosmochim. Acta* Suppl. 2, Vol. 2, pp. 999–1020. MIT Press.

Keith J. E., Clark R. S., and Richardson K. A. (1972) Gamma ray measurements of Apollo 12,

14, and 15 lunar samples (abstract). In *Lunar Science—III* (editor C. Watkins), pp. 446–448, Lunar Science Institute Contr. No. 88.

LSPET (Lunar Sample Preliminary Examination Team) (1971) Preliminary examination of lunar samples from Apollo 14. *Science* **173,** 681–693.

LSPET (Lunar Sample Preliminary Examination Team) (1972) The Apollo 15 lunar samples: A preliminary description. *Science* **175,** 363–375.

Lunar Receiving Laboratory (1971) *Lunar Sample Information Catalog—Apollo 15*. NASA Manned Spacecraft Center Report MSC 03209.

Meyer C. Jr., Brett R., Hubbard N. J., Morrison D. A., McKay D. S., Aitken F. K., Takeda H., and Schonfeld E. (1971) Mineralogy, chemistry, and origin of the KREEP component in soil samples from the Ocean of Storms. *Proc. Second Lunar Sci. Conf., Geochim. Cosmochim. Acta* Suppl. 2, Vol. 1, pp. 393–411. MIT Press.

Morrison G. H. (1971) Evaluation of lunar elemental analyses. *Anal. Chem.* **43,** No. 7, 22A–31A.

O'Kelley G. D., Eldridge J. S., Schonfeld E., and Bell P. R. (1970a) Elemental compositions and ages of lunar samples by nondestructive gamma-ray spectrometry. *Science* **167,** 580–582.

O'Kelley G. D., Eldridge J. S., Schonfeld E., and Bell P. R. (1970b) Primordial radionuclide abundances, solar proton and cosmic-ray effects, and ages of Apollo 11 lunar samples by nondestructive gamma-ray spectrometry. *Proc. Apollo 11 Lunar Sci. Conf., Geochim. Cosmochim. Acta* Suppl. 1, Vol. 2, pp. 1407–1423. Pergamon.

O'Kelley G. D., Eldridge J. S., Schonfeld E., and Bell P. R. (1971a) Abundances of the primordial radionuclides K, Th, and U in Apollo 12 lunar samples by nondestructive gamma-ray spectrometry: Implications for origin of lunar soils. *Proc. Second Lunar Sci. Conf., Geochim. Cosmochim. Acta* Suppl. 2, Vol. 2, pp. 1159–1168. MIT Press.

O'Kelley G. D., Eldridge J. S., Schonfeld E., and Bell P. R. (1971b) Cosmogenic radionuclide concentrations and exposure ages of lunar samples from Apollo 12. *Proc. Second Lunar Sci. Conf., Geochim. Cosmochim. Acta* Suppl. 2, Vol. 2, pp. 1747–1755. MIT Press.

O'Kelley G. D., Eldridge J. S., Schonfeld E., and Northcutt K. J. (1972) Primordial radioelements and cosmogenic radionuclides in lunar samples from Apollo 15. *Science* **175,** 440–443.

Rancitelli L. A., Perkins R. W., Felix W. D., and Wogman N. A. (1972) Cosmic ray flux and lunar surface processes characterized from radionuclide measurements in Apollo 14 and 15 lunar samples (abstract). In *Lunar Science—III* (editor C. Watkins), pp. 630–632, Lunar Science Institute Contr. No. 88.

Reedy R. C. and Arnold J. R. (1971) Interaction of solar and galactic cosmic-ray particles with the moon. *J. Geophys. Res.* (in press).

Schmitt R. A. (1972) Personal communication.

Schonfeld E. (1972a) Component abundance and ages in soils and breccia (abstract). In *Lunar Science—III* (editor C. Watkins), pp. 683–685, Lunar Science Institute Contr. No. 88.

Schonfeld E. (1972b) Unpublished data.

Silver L. T. and Duke M. B. (1971) U–Th–Pb isotope relations in some basaltic achondrites (abstract). *EOS-Trans. Am. Geophys. Union* **52,** 269.

Swann G. A., Hait M. H., Schaber G. G., Freeman V. L., Ulrich G. E., Wolfe E. W., Reed V. S., and Sutton R. L. (1971) Preliminary description of Apollo 15 sample environments. U.S. Geological Survey Interagency Report 36.

Wänke H., Baddenhausen H., Balacescu A., Teschke F., Spettel B., Dreibus G., Quijano M., Kruse H., Wlotzka F., and Begemann F. (1972) Multielement analyses of lunar samples (abstract). In *Lunar Science—III* (editor C. Watkins), pp. 779–781, Lunar Science Institute Contr. No. 88.

Proceedings of the Third Lunar Science Conference
(Supplement 3, *Geochimica et Cosmochimica Acta*)
Vol. 2, pp. 1671–1680
The M.I.T. Press, 1972

Gamma-ray measurements of Apollo 12, 14, and 15 lunar samples

J. E. KEITH, R. S. CLARK, and K. A. RICHARDSON*

National Aeronautics and Space Administration, Manned Spacecraft Center,
Houston, Texas 77058

Abstract—Two Apollo 12 samples, eighteen Apollo 14 samples, and twenty-four Apollo 15 samples were analyzed by gamma ray spectroscopic methods. The measurements were made on the low level NaI(Tl) spectrometer at the Lunar Receiving Laboratory. Potassium, U, and Th levels in the fragmental rocks from Apollo 14 are higher (the K ranging from 0.2% to 0.7%) than those returned from the other lunar landing missions. Fragmental rocks from Apollo 15 show a wide range (in K, 86 ppm to 0.49%) in these elements. An Apollo 15 crystalline rock (15415) and an Apollo 15 breccia (15418) exhibit the lowest levels of the natural radioactivities seen in lunar materials.

Levels of cosmic ray induced radionuclides reflect their chemical composition and their exposure history. Three Apollo 15 samples (15205, 15206, and 15085) are shown to be unsaturated in ^{26}Al, suggesting that they have only recently been exposed on the lunar surface. One Apollo 14 and two Apollo 15 (14045, 15426, and 15431) rocks show low ^{26}Al activity, probably as a result of a high erosion rate. Apollo 15 samples show a lower ^{56}Co activity than Apollo 12 or Apollo 14 samples, largely as a consequence of the absence of solar flares since January 1971.

INTRODUCTION

NONDESTRUCTIVE GAMMA-RAY SPECTROSCOPY has been shown to be an effective means of obtaining much information about the nature of lunar materials (O'Kelley *et al.*, 1970, 1971a, 1971b; Perkins *et al.*, 1970; Rancitelli *et al.*, 1971; Wrigley and Quaide, 1970; Wrigley, 1971). The method does not compromise the samples in any way and gives average concentrations of potassium, uranium, and thorium that may not be easily obtained in any other way in the case of inhomogeneous samples. The short range (about a centimeter) of solar particles and the meter to dekameter range of galactic cosmic rays combined with a suite of radionuclides whose half-lives range from a few days to a million years combine to preserve for us a record of the motions of the lunar regolith, the erosion rate of regolith materials, and the behavior of the sun during the last million years, both as a source of energetic particles and as a modulator of even more energetic particles in cislunar space.

In this paper we present the results of the measurement of the gamma-ray spectra of 44 lunar samples and some of the inferences that may be drawn from them.

PROCEDURE

Data acquisition

The gamma-ray spectrometer data acquisition system in the Radiation Counting Laboratory has been previously described in detail by its developers (O'Kelley *et al.*, 1970, 1971a, 1971b), and the location and facility has been described by McLane *et al.* (1967).

* Now with the Geological Survey of Canada, Ottawa, Canada.

All of the samples were counted in stainless steel containers, the most common of which has been described by O'Kelley *et al.* (1971). One large Apollo 14 sample (14321) was counted in a stainless steel container of 10.2 cm height and 20.4 cm diameter. An additional type, the O'Kelley container, was employed for the measurement of some Apollo 15 samples. These stainless steel containers are of 10.2 cm diameter and of 2.5 cm or 5.1 cm height.

Soil samples were placed in cylindrical aluminum containers of 7.6 cm diameter and 2.0 cm height or 9.1 cm diameter and 5.0 cm height, which were then sealed in one of the above stainless steel containers.

Apollo 15 samples were sealed in two 2-mil teflon bags before being sealed in the stainless steel containers. The stainless steel container was then sealed in another 2-mil teflon bag.

The procedures used here are essentially the same as those described by O'Kelley *et al.* (1970, 1971a, 1971b); however, calculations have been added to the data acquisition program to facilitate gain and balance control. The gain is controlled manually to within $\pm 0.2\%$ by monitoring the centroid of the ^{40}K peak. The balance refers to the relative number of events in the two crystals due to the sample, and in order for our data reduction schemes to work in the predetermined way, the number of events in the two crystals must be equal. By varying the spacing of the samples at a constant intercrystal distance, this equality is achieved to within $\pm 3\%$. The centroid of the ^{40}K peak, its standard deviation, the ratio of the net number of counts in the upper detector to the lower detector over our standard energy regions (that is, the ^{40}K peak and 0.10 to 2.0 MeV), and the ratio's standard deviation are all calculated by the data acquisition program.

Data reduction

The sets of standard spectra (now 32 sets of 8 or more spectra) comprising the library with which we reduce our data were obtained before the measurement of the spectra of our samples. Most of the standards whose spectra comprise this library have been described by O'Kelley *et al.* (1970, 1971a, 1971b) or are very similar to them. To choose the most appropriate set, we first limit ourselves to those standards counted at the same gain and intercrystal spacing and choose that standard in which the ratio of the Compton backscatter area to the photopeak area for the 0.583 MeV gamma ray of ^{208}Tl, measured in coincidence with its 2.62 MeV gamma ray, most closely approximates this ratio in the unknown spectrum. Since there is some uncertainty in this ratio, and since there may be some slight interference from other radionuclides in the unknown spectrum, several standards approximating this ratio are usually tried. The most appropriate is chosen by the examination of the residuals after data reduction.

The unknown spectrum is resolved into its components by sequentially comparing the unknown spectrum to a set of standard spectra. The bases of these comparisons are certain critical areas in the spectrum, one for each radionuclide, selected for minimum interference from other radionuclides. Those in the coincidence matrix are shown in Fig. 1. Those radionuclides emitting only one gamma ray are assigned the average of the areas of their photopeaks in the singles spectra of upper and lower detectors as their critical areas. The proportions of the standards resulting from these comparisons are subtracted from the unknown spectra and recorded, and the amount of the various radionuclides in the unknown are then calculated from the proportion subtracted, the counting times, the activity of the standard, and the sample weight. If the potassium content is greater than 0.2%, the order in which they are subtracted is Th, U, K, ^{26}Al, ^{22}Na, ^{56}Co, ^{46}Sc, and ^{54}Mn. If the potassium content is less than 2%, it is subtracted after the ^{22}Na.

This operation is currently being performed by a paper-tape-controlled floating point program STRIP, which can be called into the computer to operate in background while data acquisition continues in foreground. Since the program is controlled by paper-tape, it is possible to vary the order or the choice of critical regions easily (the standard areas are shown in Fig. 1) to meet changing conditions. STRIP stores the entire library, background, and unknown or its partial residual at any stage of the program on a 242 K word disc in floating point. A complete analysis currently takes about 22 minutes.

The appropriateness of the standard chosen is judged by the examination of the residuals. The quickest and most intuitively satisfying method is to look at the oscilloscope display of the residuals.

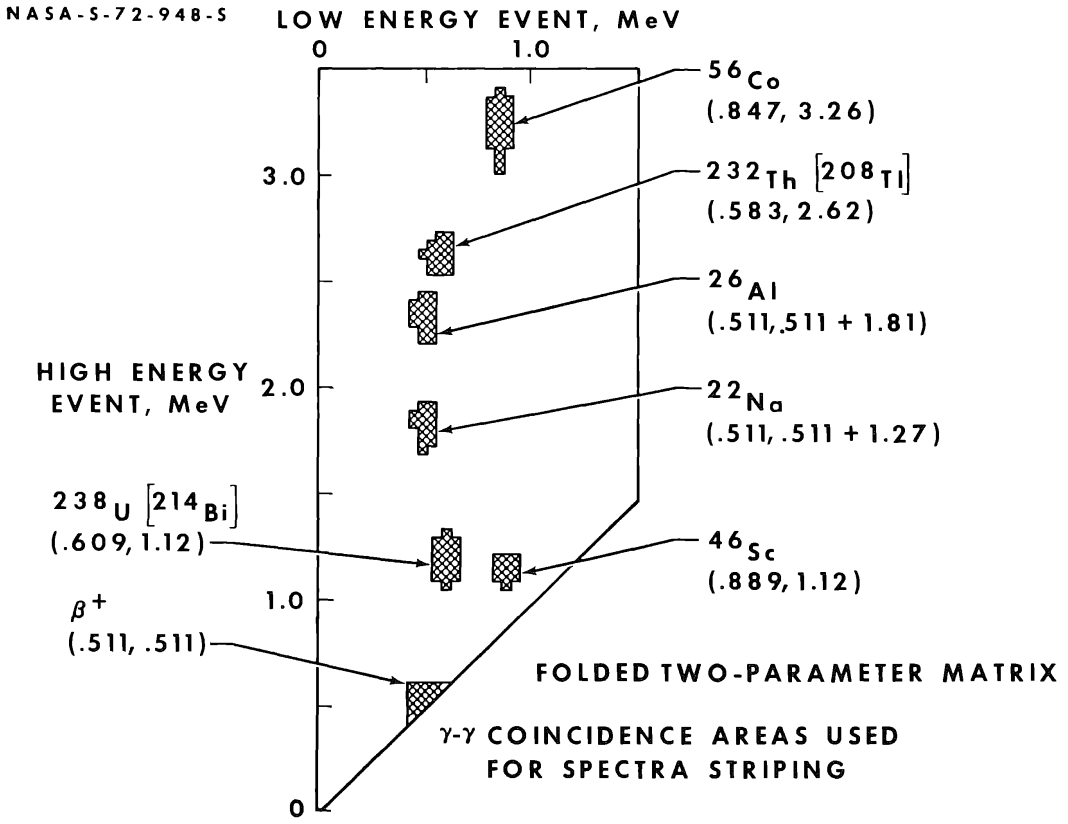

Fig. 1. Critical areas in the folded γ-γ coincidence matrix used in STRIP. Data is taken as a 127 by 127 channel matrix folded along its minor diagonal so that in every event, the position to be incremented is formed by assigning the greater energy in the Y direction, the lesser in the X direction. Only part of the matrix is shown. The entire matrix is an isosceles right triangle stretching from 0 to 5.12 MeV (that is, 40 keV per channel).

A random, uncorrelated distribution symmetric about zero is persuasive, since all 8900 data points are manipulated by STRIP and appear in the residuals, and the sum of the data points in all the critical areas is a small fraction of these. The 0.511 × 0.511 MeV region is not used as a critical area in STRIP, but its area is compared with that due to the position emitters after stripping as a check. The algebraic sum of the residuals for each singles spectrum and the sum-coincidence spectrum is also calculated and is less than 2% of the corresponding sums for the original unknown spectrum if the standard is appropriate.

Results

The results of these measurements and stripping of two Apollo 12 samples, eighteen Apollo 14 samples, and twenty-four Apollo 15 samples are presented in Tables 1 and 2. Those measurements made during preliminary examinations generally lasted about 2500 minutes; those made afterward generally lasted about 5000 minutes.

The sample spectra were resolved into their components by comparison with spectra obtained from various known distributed sources, as described previously. The errors listed in the tables are one standard deviation. They are derived from estimates of the errors due to counting statistics, errors in the standards, and the lack of fit due to inappropriateness of the standards. The errors due to counting

Table 1. Apollo 12 and 14 results.

Sample	Weight (grams)	Th (ppm)	U (ppm)	K (%)	^{26}Al (dpm/kg)	^{22}Na (dpm/kg)	^{54}Mn (dpm/kg)	^{56}Co (dpm/kg)	^{46}Sc (dpm/kg)
Clastic Rocks									
14066	497.5	15.3 ± 1.3	4.2 ± 0.2	0.72 ± 0.02	103 ± 6	43 ± 6	5 ± 12	31 ± 7	6 ± 3
14301	1370.0	13.2 ± 1.0	3.6 ± 0.5	0.604 ± 0.006	62 ± 18	27 ± 6	< 33	8 ± 2	0.4 ± 0.5
14305,18	380.6	13.9 ± 1.7	3.8 ± 0.2	0.533 ± 0.010	74 ± 13	46 ± 11	4 ± 13	3 ± 6	0.6 ± 1.6
14318	600.2	12.0 ± 2.5	3.27 ± 0.14	0.49 ± 0.03	117 ± 7	41 ± 3	10 ± 11	28 ± 10	4 ± 3
14321,38	1100.0	12.7 ± 0.8	3.6 ± 0.2	0.402 ± 0.015	72 ± 11	38 ± 7	16 ± 6	< 11	< 4
14045	64.2	13.8 ± 1.3	3.6 ± 0.4	0.39 ± 0.03	139 ± 19	84 ± 9	< 70	80 ± 20	5 ± 3
14315	115.0	8.8 ± 0.7	2.14 ± 0.08	0.328 ± 0.007	146 ± 16	58 ± 3	< 28	52 ± 10	4 ± 3
14082	63.0	4.2 ± 0.3	1.24 ± 0.11	0.206 ± 0.009	120 ± 13	53 ± 4	6 ± 11	34 ± 10	1.6 ± 1.6
Crystalline Rocks									
14310,42	455.0	10.5 ± 0.8	3.0 ± 0.2	0.414 ± 0.013	97 ± 6	33 ± 9	< 50	30 ± 30	1 ± 3
14053	251.3	2.29 ± 0.12	0.57 ± 0.05	0.0877 ± 0.0014	101 ± 4	57 ± 5	30 ± 2	44 ± 8	5 ± 1
Fines									
14259,8	496.4	14.4 ± 0.7	3.5 ± 0.3	0.416 ± 0.005	222 ± 9	91 ± 8	60 ± 20	60 ± 30	0.7 ± 1.5
14163	490.9	13.7 ± 0.7	3.9 ± 0.3	0.472 ± 0.011	79 ± 4	46 ± 5	4 ± 7	21 ± 6	0.7 ± 1.0
14160,11	100.0	14.2 ± 1.5	4.0 ± 0.5	0.52 ± 0.04	68 ± 10	44 ± 5	< 60	< 20	6 ± 3
14161,8	100.0	14.4 ± 1.2	3.9 ± 0.4	0.53 ± 0.08	73 ± 15	46 ± 5	< 70	14 ± 19	4 ± 4
14162,10	100.0	14.3 ± 1.5	3.9 ± 0.5	0.52 ± 0.04	76 ± 9	49 ± 5	9 ± 9	60 ± 50	11 ± 5
14148	69.8	13.4 ± 1.0	3.7 ± 0.3	0.43 ± 0.02	170 ± 18	71 ± 5	< 40	85 ± 16	1 ± 2
14156	136.0	13.9 ± 1.0	3.8 ± 0.3	0.40 ± 0.02	176 ± 17	66 ± 4	20 ± 20	64 ± 9	4.9 ± 1.7
14149	85.4	13.3 ± 1.0	3.5 ± 0.3	0.48 ± 0.02	132 ± 14	63 ± 4	< 40	44 ± 9	0.1 ± 0.4
Two Apollo 12 Rocks									
12010	288.7	2.5 ± 0.6	0.60 ± 0.10	0.104 ± 0.013	83 ± 19	54 ± 14	42 ± 6	< 70	5 ± 3
12031	185.0	0.94 ± 0.11	0.238 ± 0.013	0.0529 ± 0.0017	81 ± 5	54 ± 6	25 ± 8	20 ± 20	9 ± 3

Note: The errors listed include estimates of the errors due to counting statistics, the uncertainties of the standards, and the lack of fit in data reductions and are one standard deviation. Upper limits are three standard deviations above zero.

Table 2. Apollo 15 results.

Sample	Weight (gms)	Th (ppm)	U (ppm)	K (%)	^{26}Al (dpm/kg)	^{22}Na (dpm/kg)	^{54}Mn (dpm/kg)	^{56}Co (dpm/kg)	^{46}Sc (dpm/kg)
Clastic Rocks									
15206	85.5	12.0 ± 1.3	3.2 ± 0.4	0.487 ± 0.018	40 ± 5	49 ± 5	7 ± 8	< 30	< 8
15205	334.4	12.0 ± 0.4	2.9 ± 0.5	0.440 ± 0.008	48 ± 6	48 ± 4	50 ± 30	< 13	< 7
15465	364.9	5.9 ± 0.11	1.46 ± 0.13	0.234 ± 0.004	120 ± 30	56 ± 14	31 ± 18	< 19	< 5
15265	314.2	5.05 ± 0.12	1.27 ± 0.07	0.211 ± 0.08	72 ± 8	37 ± 3	12 ± 15	8 ± 6	< 15
15558	1333.3	3.42 ± 0.18	1.01 ± 0.04	0.170 ± 0.006	84 ± 5	36 ± 5	23 ± 5	9 ± 3	3.0 ± 0.7
15255	240.4	3.5 ± 0.3	0.92 ± 0.07	0.156 ± 0.019	111 ± 7	43 ± 4	26 ± 3	11 ± 8	4 ± 4
15466	117.8	3.5 ± 0.2	0.86 ± 0.08	0.156 ± 0.004	79 ± 8	36 ± 4	4 ± 5	5 ± 4	0.5 ± 1.3
15086	172.1	3.2 ± 0.2	0.76 ± 0.03	0.143 ± 0.003	39 ± 6	50 ± 6	22 ± 6	11 ± 3	2.5 ± 0.7
15459	92.0	2.9 ± 0.4	0.70 ± 0.04	0.137 ± 0.004	120 ± 40	39 ± 3	16 ± 13	8 ± 9	3.9 ± 1.7
15455	881.1	2.0 ± 0.3	0.53 ± 0.16	0.106 ± 0.004	70 ± 30	42 ± 4	10 ± 6	6 ± 2	5 ± 11
15445	270.8	2.40 ± 0.18	0.63 ± 0.08	0.106 ± 0.014	81 ± 16	45 ± 5	< 50	< 18	0.8 ± 1.5
15426	125.7	1.89 ± 0.09	0.41 ± 0.02	0.090 ± 0.008	61 ± 5	39 ± 3	20 ± 20	7 ± 3	3.1 ± 1.2
15418	1127.5	0.102 ± 0.016	0.043 ± 0.002	0.0086 ± 0.0007	120 ± 5	26.6 ± 1.5	7.7 ± 0.9	1.9 ± 0.8	0.8 ± 0.2
Crystalline Rocks									
15085	471.0	0.57 ± 0.05	0.138 ± 0.010	0.0404 ± 0.0009	84 ± 10	37 ± 3	23 ± 3	12 ± 2	3.9 ± 1.1
15256	201.0	0.42 ± 0.04	0.139 ± 0.009	0.030 ± 0.005	97 ± 6	37 ± 3	25 ± 5	6 ± 7	3.6 ± 1.8
15415	269.4	0.028 ± 0.014	0.003 ± 0.005	0.0124 ± 0.0005	116 ± 9	36 ± 5	0.4 ± 0.9	3 ± 4	< 8
Fines									
15021	132.3	5.0 ± 0.16	1.32 ± 0.04	0.161 ± 0.006	179 ± 9	51 ± 2	18 ± 6	15 ± 4	3.3 ± 1.5
15031	142.4	4.85 ± 0.12	1.25 ± 0.08	0.184 ± 0.006	55 ± 4	34 ± 3	10 ± 20	< 7	6.8 ± 1.9
15041	145.7	4.64 ± 0.14	1.20 ± 0.05	0.174 ± 0.008	127 ± 8	61 ± 4	15 ± 30	35 ± 13	5.4 ± 1.9
15211	104.2	3.75 ± 0.17	0.98 ± 0.06	0.149 ± 0.002	130 ± 13	59 ± 6	19 ± 8	16 ± 4	3.4 ± 1.0
15271	527.9	4.1 ± 0.4	1.21 ± 0.04	0.162 ± 0.008	130 ± 30	37 ± 4	9 ± 6	5 ± 11	3 ± 2
15301	557.2	3.38 ± 0.19	0.80 ± 0.19	0.122 ± 0.002	104 ± 6	45 ± 6	22 ± 7	< 12	3.6 ± 1.6
15401	86.3	3.4 ± 0.2	0.90 ± 0.11	0.143 ± 0.002	73 ± 13	58 ± 12	29 ± 17	12 ± 4	4.1 ± 1.3
15431	145.4	4.86 ± 0.15	1.12 ± 0.09	0.186 ± 0.005	66 ± 7	36 ± 4	< 12	12 ± 12	3 ± 4

Note: The errors listed include estimates of the errors due to counting statistics, the uncertainties of the standards, and the lack of fit in data reductions and are one standard deviation. Upper limits are three standard deviations above zero.

statistics are calculated in the standard manner. The errors in the activities of the potassium, uranium, and thorium standards are estimated to be 1%, and all other standards, 5%. The error due to inappropriateness of the standards is in many cases the largest and is the product of the estimates of the degree of inappropriateness and the change of the value as a function of the degree of inappropriateness, as estimated by several strips with different sets of standards. In 12 cases, the sample was measured more than once. In these cases, the weighted average of the results of measurements appears in the table. In these measurements, no case of inappropriate dependence of activity on time was found. When a peak cannot be distinguished, an upper limit of three standard deviations is reported.

As an examination of the tables will reveal, high thorium contents impair the measurement of less abundant radionuclides, especially ^{54}Mn. Since the details of the shape and thickness of the sample affect the composite thorium peak lying just above the ^{54}Mn peak, this peak is zeroed separately in the residuals to estimate the ^{54}Mn photopeak.

Discussion

Apollo 12 samples

Only three breccias that weighed over 50 g were returned in the Apollo 12 mission. Sample 12010 has a K content of 0.104% as compared to 0.46% and 0.3% for samples 12034 and 12073, respectively (O'Kelley *et al.*, 1971a). McKay *et al.* (1971) and Meyer *et al.* (1971) emphasize the heterogeneity of sample 12010 and the difficulty of getting a representative sample. Our value compares to 0.103% K for a piece of 12010 (Compston *et al.*, 1971), indicating that the value of McKay *et al.* (1971) of 9% KREEP (Hubbard *et al.*, 1971; Hubbard and Gast, 1971; Meyer *et al.*, 1971) based on the K mixing model is applicable to the entire rock. This is comparable to the $\leq$5% KREEP for total element mixing model used by Meyer *et al.* (1971), since the value for the Apollo 12 basalt component is 95 $\pm$ 5%.

Apollo 14 samples

The K, U, and Th contents of the Apollo 14 samples are high, as compared to samples from previous missions (with the exception of sample 12013). Only two large crystalline rocks were collected during this mission, and they differ by a factor of 5 in these naturally occurring radioactive elements.

The clastic rocks show a variation of K from 0.2% to 0.7%. Most of the samples have approximately the same (0.40 to 0.53%) potassium content as the Apollo 14 soils. This is consistent with the formation of the soil mainly by breakdown of the breccias.

Various workers have calculated erosion rates of lunar rocks. Finkel *et al.* (1971) calculate the erosion rate for sample 12002 to be 0.5 mm/10^6 yr. Rancitelli *et al.* (1971) calculate an erosion rate of 1 mm/10^6 yr and suggest that the erosion rate for 12002 could be as high as 4 or 5 mm per m.y. Hörz *et al.* (1971) calculate a lower limit of 0.2 to 0.4 mm/10^6 yr based on pit concentrations in the surface of lunar rock. Different erosion rates can have a significant effect on the ^{26}Al present near the surface

of lunar rocks due to the steep gradient of the ^{26}Al (Finkel *et al.*, 1971) produced by solar protons.

With one exception, sample 14045, all of the Apollo 14 samples that we measured seem to be saturated with respect to ^{26}Al. Sample 14045 is more friable than any Apollo 11 or Apollo 12 rock whose ^{26}Al concentration is known. This friability could cause the unsaturation by allowing the surface to be eroded fast enough to prevent saturation due to solar proton bombardment. Unfortunately, erosion rates of highly friable samples have not been investigated by physical methods, but considerable variation exists in the erosion rates of less friable samples (Crozaz *et al.*, 1971).

Sample 14310 has a high $^{26}Al/^{22}Na$ ratio. This can be explained by the high Al_2O_3/MgO (LSPET, 1972) ratio in this particular sample as compared to the Apollo 14 basalt and the Apollo 14 clastic rocks.

It is obvious from the low levels of ^{26}Al and ^{22}Na in sample 14301 that this sample was buried to a considerable extent in the lunar regolith. Photographic location of the sample (Swann *et al.*, 1971a) shows that only a very small portion of this sample was exposed on the lunar surface and that portion had a considerable amount of dust cover.

Samples 14148, 14156, and 14149 were the <1 mm fraction of the top, middle, and bottom of the trench. The high values for the ^{26}Al and ^{22}Na in the middle and bottom trench samples indicate that there was considerable amount of contamination in the sampling of the trench. Cobalt-56, which can only be produced to any extent at the lunar surface by solar protons (Heydegger and Turkevich, 1971), shows this contamination and also indicates that approximately 75% of the middle trench sample and 50% of the bottom trench sample are equivalent to the top of the trench in surface exposure.

In the soil samples, the ^{26}Al concentrations for the <1 mm fines ranges from 79 to 222 dpm/kg, with the lower limit of the range representing the bulk fines and the upper limit representing the comprehensive fines that were collected from the top centimeter of the lunar surface. All of the sieve fractions of the bulk sample were analyzed, and no significant differences in the ^{26}Al and ^{22}Na were seen. This indicates that the different size fractions were evenly distributed within the depth sampled in the lunar surface.

Apollo 15 samples

The Apollo 15 samples vary widely in their K, Th, and U concentrations. Two samples (15418 and 15415) contain the lowest concentrations of these elements yet found in a lunar sample. The clastic rocks seem to contain three distinct levels of naturally occurring radioactive elements, the majority of which resemble the fines, the low-K 15418, and two samples (15205 and 15206) of the same boulder, which have K, U, and Th contents more similar to Apollo 14 clastic rocks than the rest of the Apollo 15 samples.

In contrast to the trench sampling on Apollo 14, the Apollo 15 bottom trench sample (15031) was not appreciably contaminated with material from the surface. The Apollo 15 trench was about 35 to 40 cm deep (Swann *et al.*, 1971b), and no

significant difference could be seen in ^{26}Al and ^{22}Na levels at the bottom of the trench or in levels of these nuclides seen in other lunar samples known to be buried at least a few centimeters. However, the concentrations of K found in the top and bottom of the trench, as estimated by the weighted averages of the values reported in this work and those of Rancitelli *et al.* (1972) and O'Kelley *et al.* (1972), are significantly different at the 90% confidence level and suggest vertical variations. The U and Th levels found by all three investigators also are consistent with this explanation. Layering has been shown to exist in core tubes and drill stems samples from the lunar regolith (LSPET 1970, 1971, and 1972).

The ^{22}Na concentration in the top of the trench (15041) is significantly higher than that of the contingency sample (15021), while the ^{26}Al concentration in 15041 is significantly lower than that of 15021. Rancitelli *et al.* (1971) showed that the ^{26}Al gradient in the regolith is severely affected by gardening, and Swann *et al.* (1971b) has shown that an area within a meter of the contingency sampling area was disturbed by the LM landing. While no variation in depth of sampling can explain the discrepancy, it can be explained either by the removal of the top few millimeters of the regolith by the LM exhaust or by local differences in the gardening rate.

Sample 15401 is a sample of fines from the "saddle" of a large boulder sample at Station 6A. No chemical analysis for major elements is available to show if 15401 is derived by erosion from this boulder or not. Although the error limits are large, the sample appears to be grossly unsaturated in ^{26}Al. The most likely possibility is that within the last one million years a nearby cratering event has thrown dust into the "saddle" of the boulder.

Forty percent of the samples that we analyzed were from Station 7, and a wide variety of samples were collected in this area. Rock 15415 has the lowest abundance of U and Th yet observed in any lunar sample and the lowest ratio of U/K and Th/K observed in lunar samples. The absence of Fe and Mg in this rock accounts for low activities of ^{54}Mn, ^{56}Co, and ^{22}Na.

Sample 15418, a breccia with a very fine matrix, exhibits the lowest K content seen in any lunar sample. The ratios of U/K and Th/K are abnormally low compared to other lunar samples except 15415. The very low Fe and Mg contents of 15418 also account for the low levels of ^{54}Mn, ^{56}Co, and ^{22}Na.

Other than the two unique samples just mentioned, the range of K for the breccia samples from Station 7 ran from 0.234% for 15465 to 0.09% for 15426.

Two samples from this area are very friable. Sample 15431 is the <1 mm fraction of the debris from the pedestal rock. Sample 15415 was sitting on top of this rock and is thought to be a clast from this very friable breccia (Swann *et al.*, 1971b). Samples 15431 to 15433 were portions of this breccia that were broken up during sampling and sample return. Sample 15426 represents a portion of the "green rocks." Both samples 15426 and 15431 are very friable and appear to be unsaturated in ^{26}Al for the same reason as ascribed previously to sample 14045; that is, the erosion rate was high enough so that the ^{26}Al could not build up to saturation on the existing surfaces.

Samples 15085 and 15086 were sampled from 60 m east of Elbow Crater. Since there are small fresh craters very close to each of these samples that are considered

their own secondary craters (Swann *et al.*, 1971), it may be expected that these samples were thrown out by a common event. However, the induced radioactivity and other evidence do not support this hypothesis. The ^{26}Al in 15086 is very low and is definitely unsaturated. The sample was probably moved from depth in the regolith in the last 200,000 to 500,000 years. Sample 15085 is apparently saturated in ^{26}Al, so it would have to have been on the surface for at least the last few million years. Also, 15086 does not have a fillet, whereas 15085 does.

Rancitelli *et al.* (1972a, 1972b) have made an extensive study of the samples collected near the big boulder at Elbow Crater and have determined that the boulder was moved to this location about one million years ago. We also measured samples 15205 and 15206 and are in complete agreement with these data and conclusions. We also measured sample 15211 fines. This sample was thought to be derived from the boulder by erosion, but in the abundance of K, U, and Th it resembles the Apollo 15 fines and not the boulder.

SUMMARY

The lack of saturation of ^{26}Al shown in three samples from Apollo 15 is probably due to the recent movement of the samples to the surface from some depth in the lunar regolith. Variation in cosmic ray induced radionuclide concentrations have been observed and shown to be due to burial, erosion, and chemical composition. Estimations of the concentration of the naturally occurring radioactive elements and cosmic ray induced radionuclides have made possible the recognition of genetic relationships among the samples. Most of these measurements were made with counting times of a few days, and survey by gamma-ray spectroscopy has been shown to be a valuable, rapid, noncompromising way to recognize interesting lunar samples.

Acknowledgments—Technical support in the operation and maintenance of the equipment in our laboratory was provided by Warren R. Portenier and Marshall K. Robbins of Brown and Root-Northrop. Miss Linda Bennett assisted us in the data reduction. Software for our computer systems was developed by C. Wendell Richardson and Ric C. Davies of Idaho Nuclear Corporation. Standards were prepared by Joe C. Northcutt and James S. Eldridge of Oak Ridge National Laboratory. Containers and tools used for our lunar samples were developed by Vern A. McKay of ORNL.

We wish to thank Louis A. Rancitelli, Richard W. Perkins of Battelle, Pacific Northwest Laboratories, G. Davis O'Kelley, and James S. Eldridge of Oak Ridge National Laboratory, and Donald A. Morrison of MSC for many helpful suggestions and discussions.

REFERENCES

Compston W., Berry H., Vernon M. J., Chappell B. W., and Kaye M. J. (1971) Rubidium–strontium chronology and chemistry of lunar material from the Ocean of Storms. *Proc. Second Lunar Sci. Conf., Geochim. Cosmochim. Acta* Suppl. 2, Vol. 2, pp. 1471–1485. M.I.T. Press.

Crozaz G., Walker R., and Woolum D. (1971) Nuclear track studies of dynamic surface processes on the moon and the constancy of solar activity. *Proc. Second Lunar Sci. Conf., Geochim. Cosmochim. Acta* Suppl. 2, Vol. 3, pp. 2543–2558. MIT Press.

Finkel R. C., Arnold J. R., Imamura M., Reedy R. C., Fruchter J. S., Loosli H. H., Evans J. C., and Delany A. C. (1971). Depth variation of cosmogenic nuclides in a lunar surface rock and lunar soil. *Proc. Second Lunar Sci. Conf., Geochim. Cosmochim. Acta* Suppl. 2, Vol. 2, pp. 1773–1789. MIT Press.

Heydegger H. R. and Turkevich A. (1970). Radioactivity induced in Apollo 11 lunar-surface material by solar flare protons. *Science* **168,** 575–576.

Hubbard N. J. and Gast P. W. (1971) Chemical composition and origin of nonmare lunar basalts. *Proc. Second Lunar Sci. Conf., Geochim. Cosmochim. Acta* Suppl. 2, Vol. 2, pp. 999–1020. MIT Press.

Hubbard N. J., Meyer C., Gast P. W., and Wiesmann H. (1971). The composition and derivation of Apollo 12 soils. *Earth Planet. Sci. Lett* **10,** 341–350.

LSPET (Lunar Sample Preliminary Examination Team) (1970) Preliminary examination of lunar samples from Apollo 12. *Science* **167,** 1325–1339.

LSPET (Lunar Sample Preliminary Examination Team) (1971) Preliminary examination of lunar samples from Apollo 14. *Science* **173,** 681–693.

LSPET (Lunar Sample Preliminary Examination Team) (1972) The Apollo 15 lunar samples: A preliminary description. *Science* **175,** 363–375.

McKay D. S., Morrison D. A., Clanton U. S., Ladle G. H., and Lindsay J. T. (1971) Apollo 11 soil and breccias. *Proc. Second Lunar Sci. Conf., Geochim. Cosmochim. Acta* Suppl. 2, Vol. 1, pp. 755–773. MIT Press.

McLane J. C., King E. A., Flory D. A., Richardson K. A., Dawson J. P., Kemmerer W. W., and Wooley B. C. (1967) Lunar Receiving Laboratory. *Science* **155,** 525–529.

Meyer C. Jr., Brett R., Hubbard N. J., Morrison D. A., McKay D. S., Aitken F. K., Takeda H., and Schonfeld E. (1971) Mineralogy, chemistry, and the origin of the KREEP component in soil samples from the Ocean of Storms. *Proc. Second Lunar Sci. Conf., Geochim. Cosmochim. Acta* Suppl. 2, Vol. 1, pp. 393–411. MIT Press.

O'Kelley G. D., Eldridge J. S., Schonfeld E., and Bell P. R. (1970) Primordial radionuclide abundance, solar proton and cosmic-ray effects and ages of Apollo 11 lunar samples by nondestructive gamma-ray spectrometry. *Proc. Apollo 11 Lunar Sci. Conf., Geochim. Cosmochim. Acta* Suppl. 1, Vol. 2, pp. 1407–1423. Pergamon.

O'Kelley G. D., Eldridge J. S., Schonfeld E., and Bell P. R. (1971a) Abundances of the primordial radionuclides K, Th, and U in Apollo 12 lunar samples by nondestructive gamma-ray spectrometry: Implications for origin of lunar soils. *Proc. Second Lunar Sci. Conf., Geochim. Cosmochim. Acta* Suppl. 2, Vol. 2, pp. 1159–1168. MIT Press.

O'Kelley G. D., Eldridge J. S., Schonfeld E., and Bell P. R. (1971b) Cosmogenic radionuclide concentrations and exposure ages of lunar samples from Apollo 12. *Proc. Second Lunar Sci. Conf., Geochim. Cosmochim. Acta* Suppl. 2, Vol. 2, pp. 1747–1755. MIT Press.

O'Kelley G. D., Eldridge J. S., Schonfeld E., and Northcutt K. J. (1972). Concentrations of primordial radioelements and cosmogenic radionuclides in Apollo 15 samples by nondestructive gamma-ray spectroscopy (abstract). In *Lunar Science—III* (editor C. Watkins), pp. 581–583, Lunar Science Institute Contr. No. 88.

Perkins R. W., Rancitelli L. A., Cooper J. A., Kaye J. H., and Wogman N. A. (1970) Cosmogenic and primordial radionuclide measurements in Apollo 11 lunar samples by nondestructive analysis. *Proc. Apollo 11 Lunar Sci. Conf., Geochim. Cosmochim. Acta* Suppl. 1, Vol. 2, pp. 1455–1471. Pergamon.

Rancitelli L. A., Perkins R. W., Felix W. D., and Wogman N. A. (1971) Erosion and mixing of the lunar surface from cosmogenic and primordial and radionuclide measurements in Apollo 12 lunar samples. *Proc. Second Lunar Sci. Conf., Geochim. Cosmochim. Acta* Suppl. 2, Vol. 2, pp. 1757–1772. MIT Press.

Rancitelli L. A., Perkins R. W., Felix W. D., and Wogman N. A. (1972a) Cosmic ray flux and lunar surface processes characterized from radionuclide measurements in Apollo 14 and 15 lunar samples (abstract). In *Lunar Science—III* (editor C. Watkins), pp. 631–633, Lunar Science Institute Contr. No. 88.

Rancitelli L. A., Perkins R. W., Felix W. D., and Wogman N. A. (1972b) (to be published).

Swann G. A., Bailey N. G., Batson R. M., Eggleton R. E., Hait M. H., Holt H. E., Larson K. B., McEwen M. C., Mitchell E. D., Schaber G. G., Schafer J. P., Shepard A. B., Sutton R. L., Trask N. J., Ulrich G. E., Wilshire H. G., and Wolfe E. W. (1971a) *Preliminary Geologic Investigations of the Apollo 14 Landing Site*, Interagency Report: 29, U.S. Geological Survey.

Swann G. A., Hait M. H., Schaber G. G., Freeman V. L., Ulrich G. E., Wolfe E. W., Reed V. S., and Sutton R. L. (1971b) *Preliminary Description of Apollo 15 sample environments*, Interagency Report: 36, U.S. Geological Survey.

Warner J. (1971) *A Summary of Apollo 11 Chemical, Age, and Modal Data*. Curator's Office, Manned Spacecraft Center.

Wrigley R. C. (1971) Some cosmogenic and primordial radionuclides in Apollo 12 lunar surface materials. *Proc. Second Lunar Sci. Conf., Geochim. Cosmochim. Acta* Suppl. 2, Vol. 2, pp. 1791–1796. MIT Press.

Wrigley R. C. and Quaide W. L. (1970) Al^{26} and Na^{22} in lunar surface materials: Implications for depth distribution studies. *Proc. Apollo 11 Lunar Sci. Conf., Geochim. Cosmochim. Acta* Suppl. 1, Vol. 2, pp. 1751–1757. Pergamon.

Proceedings of the Third Lunar Science Conference
(Supplement 3, *Geochimica et Cosmochimica Acta*)
Vol. 2, pp. 1681–1691
The M.I.T. Press, 1972

Lunar surface processes and cosmic ray characterization from Apollo 12–15 lunar sample analyses*

L. A. RANCITELLI, R. W. PERKINS, W. D. FELIX, and N. A. WOGMAN

Battelle, Pacific Northwest Laboratories, Richland, Washington

Abstract—The Apollo 14 samples; 14310,187, 14321,0, and 14163,0 and the Apollo 15 samples 15205,0, 15206,0, 15211,2, 15221,2, 15231,1, 15091,15, 15261,15, 15271,19, 15031,14, 15041,14, 15501,2, 15505,0, 15535,0, 15557,1, and 15556,0 were analyzed for their cosmogenic and primordial radionuclide contents.

Samples from two stations at the Apollo 15 Hadley Apennine site were shown to have lunar surface exposure ages of less than one million years based on ^{26}Al undersaturation. Two chips, 15205 and 15206, from a meter-sized boulder at Station 2 indicated the boulder had been ejected during a cratering incident about three-fourths of a million years ago. A soil clod from a 15 meter diameter crater and a breccia at Station 9 showed similar short exposure ages. Measurements of ^{56}Co (77*d*) established that the proton flux above 10 MeV from the January 24, 1971 flare was about 1.4 $\times$ 10^9 protons per cm^2 while ^{48}V measurements indicated that the galactic flux is not significantly different between 1 and 2 AU. The solar flare proton energy distribution determined from the depth concentration gradients of both ^{26}Al and ^{22}Na is in accord, indicating constancy of the solar flare energy spectrum for the past few million years. The primordial radionuclide concentrations at the Apollo 15 site show a local range in concentrations comparable to the total concentration range from the previous Apollo landing sites.

INTRODUCTION

IN ADDITION to the obvious benefits of direct geological lunar exploration, the lunar samples from the Apollo missions are permitting a great deal to be learned concerning the history of both the moon and the sun. The cosmogenic radionuclides reflect both the recent and long-term character of the solar and galactic cosmic ray flux, while primordial radionuclides help to describe the magmatic differentiation processes at the lunar surface. The Apollo 11 lunar sample studies provided our first look at the cosmogenic radionuclide production rates on the moon and confirmed the fact that the top centimeter of the lunar surface receives a relatively intense solar proton bombardment with a smaller galactic cosmic ray contribution (Perkins *et al.*, 1970; Shedlovsky *et al.*, 1970; O'Kelley *et al.*, 1970). Lunar samples returned by the Apollo 12 mission included core tubes which have allowed the concentration of cosmogenic radionuclides ^{26}Al and ^{22}Na to be characterized to depths of 40 cm, and thus provide a record on solar and galactic cosmic ray flux. Measurements on these samples have provided the basis for estimating the erosion rate of rocks, the mixing of soil, the long-term average galactic cosmic ray flux at 1 A.U. (Rancitelli *et al.*, 1971) and the recent and ancient solar cosmic ray intensity and energy spectrum (Rancitelli *et al.*, 1971;

* This paper is based on work supported by the National Aeronautics and Space Administration, Manned Spacecraft Center, Houston, Texas under Contract NAS 9-11712.

Finkel *et al.*, 1971). The Apollo 14 samples have not yet been analyzed by our laboratory to the extent of those from other missions, but have helped to confirm observations of samples from the Apollo 11, 12, and 15 missions. The Apollo 15 mission provided a remarkable collection that contains numerous unique samples (LSPET, 1972). This is due in large part to the very excellent lunar surface sample documentation (Swann *et al.*, 1971) provided by the astronauts and the fortuitous collection of material that has been shown by this present work to have a very young lunar surface exposure age. Of particular interest to the study of the character of the galactic cosmic ray flux was the fact that the last major solar flare occurred seven months before the Apollo 15 landing. This, coupled with the revocation of the quarantine requirements, permitted the galactic cosmic ray production rates of short-lived radionuclides such as ^{48}V to be measured directly.

Apollo 15 samples were received within 6 days of splashdown and subjected to our nondestructive gamma ray analysis (Perkins *et al.*, 1970) for both short-lived and long-lived cosmogenic radionuclides. The high degree of accuracy and precision attained in our earlier studies (Perkins *et al.*, 1970; Rancitelli *et al.*, 1971) was maintained in these analyses to permit the observation of subtle differences in radionuclide concentrations. This high precision and accuracy has been extremely helpful as it has permitted small, but very meaningful, variations of ^{26}Al in soil and rocks to be observed.

PROCEDURE

The multiple gamma coincidence counting techniques (Perkins *et al.*, 1970; Rancitelli *et al.*, 1971) described in our earlier work were used to analyze the Apollo 14 and 15 samples. Briefly, the technique involves counting the sample for 8000 to 15,000 minutes on an anticoincidence shielded multidimensional gamma-ray spectrometer. A comparison of the observed concentrations after background subtraction with the count rate of a sample mockup containing known radionuclide additions provides the basis for determining the radionuclide concentrations. The mockups are prepared from a mixture of casting resin, iron powder, and aluminum oxide that contains a precisely known radionuclide addition. These mockups reproduce the precise shape, size, physical and electron densities (of the samples). In most cases, the uncertainties associated with counting statistics were on the order of 1–2% for ^{22}Na, ^{26}Al, K, Th, and U while the absolute errors for these radionuclides based on all analytical uncertainties including the error in radioisotope standards ranged from 3 to 8%. The errors associated with the other radionuclides such as ^{46}Sc, ^{48}V, ^{56}Co, and ^{60}Co are due predominantly to poor counting statistics.

RESULTS AND DISCUSSION

Radionuclide concentration and surface ages

The summary of radionuclide concentrations in the Apollo 15 samples is contained in Tables 1 and 2. Table 1 is devoted to the unique set of samples collected at Station 2 during the first EVA, while Table 2 summarizes the samples collected at Stations 2, 6, 8, 9, and 9a. The samples collected at Station 2 include chips (15205 and

Table 1. Radionuclide content of Apollo 15 lunar samples from near St. George Crater, Station 2 (dpm/kg except as noted).

	15205,0	15206,0	15211,2	15221,1	15231,1	15091,15
^{22}Na	48 ± 2	50 ± 4	64 ± 3	72 ± 3	44 ± 3	50 ± 3
^{26}Al	52 ± 2	46 ± 4	152 ± 4	169 ± 5	104 ± 3	166 ± 5
^{46}Sc	3.3 ± 1.6	<4	<2.1	1.9 ± 1.9	2.8 ± 2.0	5 ± 4
^{48}V	6.7 ± 2.9	—	—	6 ± 6	9 ± 5	—
^{54}Mn	17 ± 20	<30	12 ± 9	<19	9 ± 7	<40
^{56}Co	<8	<11	6 ± 6	5 ± 5	<8	<26
^{60}Co	<6	<3	—	<2.7	<3.1	<3
K (ppm)	4680 ± 200	4980 ± 200	1440 ± 60	1360 ± 70	1410 ± 70	1440 ± 80
Th (ppm)	12.6 ± 0.3	12.4 ± 0.2	3.95 ± 0.08	3.57 ± 0.18	3.59 ± 0.18	3.97 ± 0.06
U (ppm)	3.28 ± 0.10	3.22 ± 0.10	1.02 ± 0.03	0.97 ± 0.03	0.94 ± 0.03	0.93 ± 0.04
Sample weight (grams)	334	85.5	104	96	96	96
Sample type	Boulder-chips		Boulder fillet	Soil	Soil	Soil

15206) from the top of a meter size boulder, a soil sample from beneath the boulder (15231,1), a sample of soil adjacent to the boulder (15211,2) originally described by astronauts Scott and Irwin as a boulder fillet, and soil samples collected at about 0.5 m (15231,1) and 10 m (15091,15) from the boulder. The two boulder chips that were identified as breccias (lunar sample information catalog, Apollo 15) have high primordial radionuclide concentrations similar to the Apollo 14 breccias. The four soil samples collected at Station 2 showed little variation in their K, U, and Th concentrations, but contained only about one-third the primordial radionuclide contents of the boulder chips. The "soil fillet" (15211,2) adjacent to the boulder has primordial radionuclide concentrations which are essentially identical to the surrounding soil samples. This requires that the fillet sample originated almost entirely from soil rather than from erosion of the boulder.

The ^{22}Na content of the two boulder chips (15205 and 15206) is at equilibrium as can be verified by comparison with the ^{22}Na content of Apollo 11 (Perkins *et al.*, 1970), Apollo 12 (Rancitelli *et al.*, 1971) and Apollo 14 and 15 rocks. However, the ^{26}Al content of these chips (46 to 50 dpm/kg) is considerably lower than any previously observed in the Apollo 11, 12, and 14 suites of samples. The fact that the ^{22}Na is at saturation while the ^{26}Al is at one-half to two-thirds of the saturation value indicates that this boulder has been in its present position for less than one million years. While firm conclusions as to the precise exposure age of the rocks must await chemical analysis data, it can be shown that the low ^{26}Al content could not reasonably be the result of an artifact of the rock's composition. The range in ^{22}Na and ^{26}Al concentrations that could result from variations in chemical composition was determined by calculating production rates from solar protons using a model described in our earlier work (Rancitelli *et al.*, 1971). Basalts and breccias from the Apollo 11, 12, 14, and 15 collections with the highest and lowest reported Al, Na, Si, Ti, Fe, Mg, and Ca contents were chosen for the production rate calculations. The solar cosmic ray production rates were calculated for a sample integrated to a depth of 10 g/cm^2 (Rancitelli *et al.*, 1971), while galactic cosmic ray production rates through this depth were calculated by the method of Fuse and Anders (1969). These calculations show that

Table 2. Radionuclide content of Apollo 15 lunar samples from Stations 6, 8, 9, and 9a (dpm/kg except as noted).

	15261,15 (6)	15271,19 (6)	15031,14 (8)*	15041,14 (8)	15501,2 (9)	15505,0 (9)	15535,0 (9a)	15557,1 (9a)	15556,0 (9a)
^{22}Na	37 ± 3	50 ± 4	33 ± 2	65 ± 2	62 ± 3	44 ± 2	39 ± 2	39 ± 2	40 ± 2
^{26}Al	50 ± 4	136 ± 3	60 ± 2	123 ± 4	74 ± 2	44 ± 2	61 ± 2	75 ± 2	103 ± 6
^{46}Sc	—	—	6.3 ± 2.7	2.9 ± 1.6	7 ± 5	< 3.0	< 3.1	3.4 ± 1.7	6.5 ± 1.0
^{48}V	—	—	< 14	< 11	—	—	—	—	12 ± 4
^{54}Mn	—	—	24 ± 8	14 ± 8	< 20	42 ± 30	21 ± 5	34 ± 9	41 ± 12
^{56}Co	—	—	6 ± 6	27 ± 6	< 31	< 12	< 16	< 13	11 ± 4
^{60}Co	—	—	4.3 ± 2.8	< 1.5	< 3.6	< 1.2	< 1.2	< 0.8	< 1.7
K (ppm)	1670 ± 70	1620 ± 70	1780 ± 60	1640 ± 60	1250 ± 100	1550 ± 70	490 ± 50	340 ± 20	440 ± 30
Th (ppm)	4.64 ± 0.09	4.87 ± 0.10	4.74 ± 0.12	4.56 ± 0.14	4.15 ± 0.12	3.64 ± 0.07	0.45 ± 0.03	0.44 ± 0.02	0.56 ± 0.00
U (ppm)	1.18 ± 0.04	1.22 ± 0.06	1.33 ± 0.04	1.28 ± 0.04	1.03 ± 0.03	0.94 ± 0.02	0.104 ± 0.010	0.131 ± 0.008	0.15 ± 0.01
Sample weight (grams)	104	104	142	146	46.6	862	230	408	1514
Sample type	Trench soil	Soil	Trench soil	Trench soil	Soil clod	Breccia	Porphyritic basalt	Basalt	Basalt, vesicular

* Sampling station.

even where the major target elements Al and Mg vary in concentration by a factor of 3, the production rate and thus the equilibrium ratios of ^{26}Al and ^{22}Na can only vary from about 1.4 to 2.5. Thus, the ^{26}Al to ^{22}Na ratio of 1.0 in the boulder chips 15205 and 15206 represent undersaturation of ^{26}Al, even if the chemical composition proves to be as unusual as 12012 (low Si and high Mg), thus producing a low ^{26}Al to ^{22}Na ratio. The short exposure age of these boulder chips is further verified by comparing the ^{26}Al and ^{22}Na concentrations of the soil sample from beneath the boulder 15231,1 with those of soil samples adjacent to the boulders; 15211, 15221, and 15091. The ^{22}Na and ^{26}Al concentrations of sample 15231,1 are 44 dpm/kg and 104 dpm/kg, respectively, while those in the adjacent soil 15221 are on the order of 72 and 169 dpm/kg, respectively. Based upon the minimum shielding of 20 g/cm^2, subtended by the boulder over the sample 15231 (Swann *et al.*, 1971), we would expect both the ^{22}Na and the ^{26}Al concentrations to be about 45 dpm/kg. The excess ^{26}Al in this sample of about 60 dpm/kg would exist if the boulder had covered soil sample 15231 about three-fourths of a million years ago when the soil had a ^{26}Al content similar to that of the present-day nearby soil samples 15211 or 15221. During the last three-fourths million years, the ^{26}Al originally present would have decayed from 160 dpm/kg to 80 dpm/kg, while the galactic production of ^{26}Al would have reached one-half of the saturation value of 45 dpm/kg, producing a present-day total ^{26}Al content of about 105 dpm/kg. The short exposure age of this boulder is also supported by its physical appearance such as the sharp, well-defined features of its surface, including areas of bubbly glass. The origin of the boulder at Station 2 is evidently a fresh impact some distance from its final resting place. The region at Station 2 has been described in the Field Geology Report (Swann *et al.*, 1971) as being free of rock fragments larger than a few centimeters with the exception of two boulders. Large fragments without accompanying smaller debris are generally found beyond 30 crater diameters (Sutton, 1972). Thus, this young meter-sized boulder must be associated with a fresh crater at least a few hundred meters and more likely a kilometer or more from Station 2. A fresh crater that meets these requirements and may possibly be the source of the boulder is present on the northeast rim of St. George Crater, at a distance of about 1 kilometer from the boulder's location.

Samples collected from Station 9 (see Table 2) on the third EVA also proved to have a short exposure age as determined from ^{26}Al undersaturation. The soil clod 15501,2 was collected near the bench of a 15 m diameter crater which was described as having a very fresh appearance (Swann *et al.*, 1971). The rather high ^{22}Na content of 62 dpm/kg was consistent with that expected for a surface sample where the solar proton bombardment adds substantially to the total production of the cosmogenic radionuclides. On the basis of the ^{22}Na content of this soil clod, an ^{26}Al concentration of about 150 dpm/kg, which is similar to that in sample 15211 (see Table 1), would be predicted from our production rate model (Rancitelli *et al.*, 1971). The actual ^{26}Al content was only 74 dpm/kg, indicating that the sample has been exposed to solar protons for the past three-fourths million years. An alternate plausible explanation for the low ^{26}Al content is that this very soft soil clod was eroding at a relatively high rate. Our previous calculations (Rancitelli *et al.*, 1971) indicate that an erosion rate of greater than 3 cm per million years would be required to produce the observed

^{22}Na and ^{26}Al concentrations. Such a high erosion rate is not supported by the very blocky appearance of the crater ejecta (Swann *et al.*, 1971). Thus, the young age, on the order of three-fourths million years, is supported. A second sample collected at Station 9, breccia 15505, also has a low ^{26}Al content of 44 dpm/kg and a normal ^{22}Na content of 49 dpm/kg, indicating extreme undersaturation of ^{26}Al and thus a recent lunar surface exposure age on the order of a few hundred thousand years. Although chemical analyses of these samples will permit a more accurate estimate of exposure ages, this will not change the general observation. The arguments employed in the case of boulder chips 15205 and 15206 can again be used to show that the observed ^{26}Al to ^{22}Na ratios of about 1 can only be the result of ^{26}Al undersaturation. Thus, the samples 15501 and 15505 together with the observations described in Swann *et al.* (1971) indicate a very recent cratering event near Station 9.

Three samples collected at Station 9a, approximately 300 meters from Station 9, were also analyzed. These samples consisted of a highly vesicular basalt 15556,0, a porphyritic basalt 15535, and a light gray basalt 15557. All of these samples contained normal amounts of ^{22}Na and ^{26}Al, indicating surface exposure ages long compared with the ^{26}Al half-life. While the ^{22}Na content of all three basalt samples was essentially identical (39 dpm/kg), the highly vesicular basalt 15556,0 contained a 50% higher ^{26}Al concentration and an ^{26}Al to ^{22}Na ratio of 2.58. This ratio may be explained on the basis of the rock's chemical composition and the fact that it was only slightly recessed in the lunar soil with approximately 75% of its surface exposed to solar cosmic ray bombardment.

The radionuclide contents of two samples of soil collected from the top (15031,14) and bottom (15041,14) of a 35 cm deep trench at Station 8 are summarized in Table 2. The ^{26}Al and ^{22}Na contents of sample 15041 are compatible with an average sampling depth to 6 cm. Our previous observations of both rock and soil samples (Rancitelli *et al.*, 1971) have shown that where the chemical composition of the major target elements for ^{26}Al and ^{22}Na production are reasonably constant, the ^{26}Al to ^{22}Na ratio decreases by as much as twofold in the first 20 g/cm^2 of depth. The fact that the ^{26}Al to ^{22}Na ratio is the same at the surface as at the trench bottom requires either a very different chemical composition for the soil at the two levels, or that the soil at the top contains a very young component with an undersaturated ^{26}Al content. The latter hypothesis can be evaluated when the chemical analyses of these samples become available. The primordial radionuclide contents of the two soil samples are nearly identical; however, this does not insure the constancy of other elements. The approximate twofold increase in ^{54}Mn and ^{46}Sc concentrations with depth, and the fourfold decrease in the ^{56}Co with depth are in accord with the expected galactic cosmic ray buildup with depth and the solar cosmic ray attenuation with depth, respectively.

Two samples of soil were collected at Station 6: 15261,15 from a trench dug in a crater rim and 15271,19, a surface sample from the Lunar Rover track. Since the primordial radionuclide contents of these samples are nearly identical and they were collected in the same vicinity, it is not unreasonable to compare these samples in the same manner as the above trench samples from Station 8. The ^{26}Al to ^{22}Na ratio of the surface sample 15271 is 2.72, while the ^{26}Al to ^{22}Na ratio of the bottom trench sample 15261,15 is 1.73. This decrease in the ratio with depth is compatible with our

Table 3. Radionuclide content of Apollo 14 lunar samples (dpm/kg except as noted).

	14310,187	14321,40	14163,0
^{22}Na	63 ± 5	32 ± 2	44 ± 4
^{26}Al	165 ± 6	74 ± 4	89 ± 4
^{46}Sc	—	< 3.6	< 5.3
^{48}V	—	—	—
^{54}Mn	—	37 ± 19	< 38
^{56}Co	—	< 7	< 13
^{60}Co	—	< 1.3	—
K (ppm)	3490 ± 160	4080 ± 120	4390 ± 130
Th (ppm)	11.3 ± 0.2	13.3 ± 0.3	14.6 ± 0.3
U (ppm)	2.85 ± 0.06	3.42 ± 0.07	3.65 ± 0.11
Sample weight (grams)	10.9	72.0	300
Sample type	Rock slice	Rock	Soil

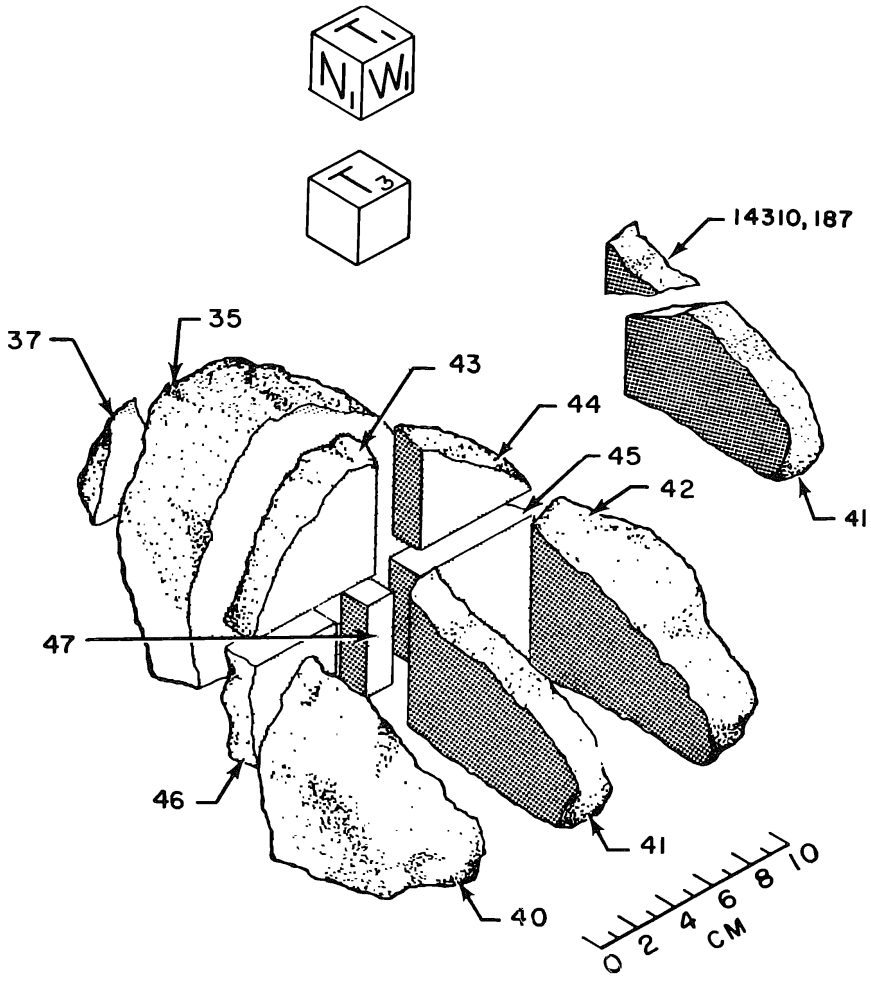

Fig. 1. Cutting diagram of rock 14310 showing the location of sample 14310,187.

observations in the Apollo 12 core tube and rock slices. The ^{26}Al content of 15261 is compatible with sampling depth to about 7 cm.

The radionuclide contents of three Apollo 14 samples are summarized in Table 3. Sample 14310,187 was a slice from the top surface of an igneous rock. The relationship of this sample to the original rock is presented in Fig. 1: Due to the small size of this sample the only radionuclides measured were the primordials K, U, and Th and the cosmogenics ^{22}Na and ^{26}Al. The high ^{26}Al (165 dpm/kg) and ^{22}Na contents (63 dpm/kg) are compatible with the relatively unshielded position of this sample (5 g/cm^2). A predicted ^{26}Al content of this rock slice of 145 dpm/kg is obtained using the model described by Rancitelli *et al.* (1970) that employs the rock's chemical composition, the ^{26}Al excitation function from major target elements, and the average incident solar proton flux. The excellent agreement between the observed and predicted ^{26}Al contents of this rock slice indicates a saturation concentration and hence the rock was at the surface for at least the last two or three million years. This is of particular interest since preliminary track measurements (Walker, 1972) suggested the rock might have had a relatively short lunar surface age. Rock sample 14321,40 is a 700 gram surface specimen of the 9 kilogram football sized breccia. The ^{22}Na and ^{26}Al concentrations in this section indicate saturation; however, the ^{26}Al is somewhat low and may be the result of losses of surface material which are known to have occurred during the cutting of this specimen. Soil sample 14163,0 has substantially lower ^{22}Na and ^{26}Al concentrations than are present in the top two or three centimeters of lunar soil. From previously established concentration gradients for ^{26}Al it can be shown that the average sampling depth for these specimens exist from the surface to approximately 16 centimeters.

Solar and galactic fluxes

The relatively short-lived cosmogenic radionuclides ^{48}V (16.1*d*) and ^{56}Co (77*d*) were measured in some of the Apollo 15 samples and provided a basis for determining the intensity of the January 24, 1971 solar flares and the relative galactic cosmic ray flux intensity at 1 AU compared with that at meteorite orbit distances. Cobalt-56 is produced in the first few centimeters of the lunar surface primarily from the interaction of solar protons on Fe. The galactic production rate of ^{56}Co has been estimated from meteorite data to be about 1 dpm/kg (Perkins *et al.*, 1970) while the solar proton produced ^{56}Co in lunar samples of a few grams per cm depth has been on the order of 20 to 50 dpm/kg. Since the last major solar flare prior to the Apollo 15 mission occurred January 24, 1971 seven months prior to the mission, the ^{56}Co (77*d*) produced by this flare had decayed through 2.5 half-lives by the time of collection, resulting in the low concentrations reported in Tables 1 and 2. In fact, the top section of trench soil sample 15041,14 was the only Apollo 15 sample which contained sufficient ^{56}Co (27 ± 6 dpm/kg) so it could be measured with a reasonable degree of accuracy. This, together with the fact that the average sampling depth of 6 cm was known from the ^{26}Al and ^{22}Na activities, permitted the recent solar flare intensity to be calculated. This ^{56}Co content was decay corrected to January 24, 1971, the time of the last major flare, and employed along with known excitation functions (Brodzinski *et al.*, 1971),

the iron content of soil sample 15021 (LSPET, 1972), and a kinetic power law form of the solar proton energy distribution with a shape function equal to 3.1, see equation (1), to estimate the flare intensity. These computations indicate that the January 1971 flare emitted 14 $\times$ 10^9 protons above 10 MeV to produce the observed ^{56}Co content of 15041 in a 2π bombardment. Some uncertainty exists in these calculations since the precise chemical composition of 15041 and the shape function of the January flare were unavailable. However, they do indicate that the January 1971 flare and the April 1969 flare were approximately equal in intensity.

Vanadium-48 is produced in lunar material by high energy spallation of iron and low energy proton reactions on Ti. Due to its short half-life, the ^{48}V produced by the January 1971 solar flare decayed to insignificant levels during the seven-month interval prior to the Apollo 15 landing. Thus, the ^{48}V present in the Apollo 15 samples (see Tables 1 and 2) is the result of the steady state galactic cosmic ray bombardment of the lunar surface. The ^{48}V content of the Apollo 15 samples 15205 and 15556 was measured with sufficient accuracy to permit an estimation of the galactic cosmic ray production rate. Based upon an iron content of 18%, we calculate a production rate of 52 $\pm$ 15 dpm/kg Fe. This can be compared with a predicted production rate of 50 $\pm$ 15 dpm/kg Fe based on observed ^{48}V in the Allende meteorite (Rancitelli *et al.*, 1969), with appropriate corrections for the 2π bombardment on the moon. While the uncertainties are significant, this accord between the ^{48}V galactic production rate from iron in lunar samples and in meteorites supports our previous observations that the galactic cosmic ray flux is not significantly different between 1 AU and 2 AU (Rancitelli *et al.*, 1971). These earlier observations indicated that the galactic cosmic ray production rate of ^{26}Al was comparable in meteorites with that in the lunar surface if the 2π lunar irradiation was considered.

In our previous work (Rancitelli *et al.*, 1971), we described a model for calculating the depth dependence of ^{26}Al and ^{22}Na production from a representative incident solar proton spectrum, the appropriate excitation functions and the sample's target element composition. This model employs the kinetic power law form:

$$\frac{dJ}{dE} = kE^{-\alpha} \tag{1}$$

to describe the incident proton spectrum, where J is the proton flux, E is the proton energy, α is a shape function, and k a constant related to the particle intensity. In this work on Apollo 12 samples, ^{26}Al and ^{22}Na concentrations as a function of depth were calculated for various lunar rock erosion rates. Concentrations versus depth were also calculated for lunar soil. The shape of the incident proton flux was chosen to conform with the average of the 1968–1969 solar flares measured by the IMP satellites (Simpson and Hsieh, 1970). These calculated gradients were then compared with measured gradients in lunar rocks and core tube materials to estimate the erosion rate of rocks and the mixing of soil.

In the present work, ^{26}Al and ^{22}Na concentration gradients were generated as a function of the incident proton spectrum shape while the erosion rates remained constant. The limits on the shape function (α) for the incident proton spectrum were varied from 2.5 to 3.5. The best fit of the calculated to observed ^{26}Al gradients occurred

for a shape function (α) equal to 3.1; this would require an average proton flux above 10 MeV for the last few million years of 60 p/cm^2-sec. For comparison, as stated above, the January 1971 flare emitted 1.4×10^9 protons of greater than 10 MeV. This is equivalent to a two-day average flux of 7900 p/cm^2-sec and would contribute 43 p/cm^2-sec to the 1971 Average Annual Solar proton flux. The fact that the observed ^{26}Al and ^{22}Na concentration depth gradients in lunar material can be produced by the same proton energy and intensity spectra supports the idea that the solar flare activity has remained relatively unchanged for the past million years.

Primordial radionuclides

The concentrations of K, U, and Th, the primordial radionuclides in lunar materials, are not only important to our understanding of the moon's geochemistry and its relationship to other objects in the solar system but can also serve as indicators of local mixing and transport of lunar soil. The primordial radionuclide contents of Apollo 15 soil samples fall in a range between those at the Apollo 11 and Apollo 12 sites (see Table 4). The K, U, and Th contents of the soil samples near Hadley Rille (Stations 2 and 9) are lower than those at the landing site (Station 9) and along the Apennine Front (Station 6) indicating that the wide differences in the primordial radionuclide contents of soil such as those between the Apollo 11 and 12 sites can also occur on a distance scale of a few kilometers. The K, U, and Th concentrations of the Apollo 14 soil sample (14163,0) are two- to fourfold higher than those of the Apollo 12 and 15 samples, while the K/U ratios (1200–1500) are comparable. The uniformity of K/U ratios for different lunar areas suggests that magnetic differentiation has not been sufficient to significantly alter their ratios over a large portion of the lunar surface.

The highest primordial radionuclide contents were found in the Apollo 14 rocks 14310,187 and 14321,40 and the Apollo 15 boulder chip 15205 and 15206. The K content (0.4 to 0.5%), the U content (2.8 to 3.4 ppm) and the Th content (11.3 to 13.3 ppm) were comparable to the Apollo 12 breccia 12034,9 (Rancitelli *et al.*, 1971). The three basalts from Apollo 15 sampling Station 9a had low K (0.034 to 0.049%), U (0.10 to 0.15 ppm), and Th (0.44 to 0.56 ppm) contents comparable to the Apollo 12 basalts. The low K basalts from Station 9a were also characterized by the highest K/U ratios (2600–4700) observed in the suite of Apollo 14 and 15 samples; generally

Table 4. Primordial radionuclide content of lunar soils.

	K (%)	Th (ppm)	U (ppm)	K/U
Apollo 11	0.11	2.3	0.55	2000
Apollo 12	0.20	6.7	1.7	1180
Apollo 14	0.44	14.6	3.6	1220
Apollo 15				
(2)*	0.14	3.8	0.94	1500
(6)	0.16	4.7	1.2	1330
(8)	0.17	4.6	1.3	1310
(9)	0.12	4.2	1.0	1200

* Sampling station.

the K/U ratios of Apollo 15 rocks and soils ranged from 1200 to 1600, lower than the range of K/U values (1800–3100) we reported for the Apollo 12 samples.

The average relative atomic abundances of Th/U is 4.05 ± 0.04 in the two Apollo 14 rocks and 3.97 ± 0.28 in the fifteen Apollo 15 samples. These Th/U ratios are in excellent agreement with our previous measurements in Apollo 11 rocks (3.8 ± 0.2), Apollo 12 rocks (3.8 ± 0.1), and the calculated value of 3.8 ± 0.3 for the present-day solar system (Fowler and Hoyle, 1960).

Acknowledgments—We wish to thank R. M. Campbell, D. R. Edwards, J. G. Pratt, and J. H. Reeves of this Laboratory for their aid in standards preparation and in data acquisition. The unique and sensitive instrumentation that made this work possible was developed during the past decade under sponsorship of the United States Atomic Energy Commission, Division of Biology and Medicine.

References

Brodzinski R. L., Rancitelli L. A., Cooper J. A., and Wogman N. A. (1971) High-energy proton spallation of iron. *Physical Review C.* **4,** 1257–1265.

Finkel R. C., Arnold J. R., Imamura M., Reedy R. C., Fruchter J. S., Loosli H. H., Evans J. C., and Delany A. C. (1971) Depth variation of cosmogenic nuclides in a lunar surface rock and lunar soil. *Proc. Second Lunar Sci. Conf., Geochim. Cosmochim. Acta* Suppl. 2, Vol. 2, pp. 1773–1789. MIT Press.

Fowler W. A. and Hoyle F. (1960) Nuclear cosmochronology. *Ann. Phys.* **10,** 280.

Fuse K. and Anders E. (1969) Aluminum-26 in meteorites—VI achondrites. *Geochim. Cosmochim. Acta* **33,** 653–670.

Lunar Sample Information Catalog, Apollo 15 (1971) National Aeronautics and Space Administration MSC 03209.

O'Kelley G. D., Eldridge J. S., Schonfeld E., and Bell P. R. (1970) Primordial radionuclide abundances, solar proton and cosmic-ray effects, and ages of Apollo lunar samples by nondestructive gamma ray spectrometry. *Proc. Apollo 11 Lunar Sci. Conf., Geochim. Cosmochim. Acta* Suppl. 1, Vol. 2, pp. 1407–1423. Pergamon.

Perkins R. W., Rancitelli L. A., Cooper J. A., Kaye J. H., and Wogman N. A. (1970) Cosmogenic and primordial radionuclide measurements in Apollo 11 lunar samples by nondestructive analysis. *Proc. Apollo 11 Lunar Sci. Conf., Geochim. Cosmochim. Acta* Suppl. 1, Vol. 2, pp. 1455–1469. Pergamon.

LSPET (Lunar Sample Preliminary Examination Team) (1972) Preliminary examination of lunar samples from Apollo 15. *Science* **175,** 363–375.

Rancitelli L. A., Perkins R. W., Cooper J. A., Kaye J. H., and Wogman N. A. (1969) Radionuclide composition of the Allende meteorite from nondestructive gamma-ray spectrometric analysis. *Science* **166,** 1269–1272.

Rancitelli L. A., Perkins R. W., Felix W. D., and Wogman N. A. (1971) Erosion and mixing of the lunar surface from cosmogenic and primordial radionuclide measurements in Apollo 12 lunar samples. *Proc. Second Lunar Sci. Conf., Geochim. Cosmochim. Acta* Suppl. 2, Vol. 2, pp. 1757–1772. MIT Press.

Shedlovsky J. P., Honda M., Reedy R. C., Evans J. C. Jr., Lal D., Lindstrom R. M., Delany A. C., Arnold J. R., Loosli H., Fruchter J. S., and Finkel R. C. (1970) *Proc. Apollo 11 Lunar Sci. Conf., Geochim. Cosmochim. Acta* Suppl. 1, Vol. 2, pp. 1503–1532. Pergamon.

Simpson J. and Hsieh J. (1970) Personal communication.

Sutton R. L. (1972) Personal communication.

Swann G. A., Hait M. H., Schaber G. G., Freeman V. L., Ulrich G. E., Wolfe E. W., Reed V. S., and Sutton R. L. (1971) Interagency Report: 36, Preliminary description of Apollo 15 sample environments. U.S. Department of the Interior Geological Survey, September.

Walker R. (1972) Personal communication.

Proceedings of the Third Lunar Science Conference
(Supplement 3, *Geochimica et Cosmochimica Acta*)
Vol. 2, pp. 1693–1702
The M.I.T. Press, 1972

Cosmic-ray produced radioisotopes in Apollo 12 and Apollo 14 samples

F. BEGEMANN, W. BORN, H. PALME, E. VILCSEK, and H. WÄNKE

Max-Planck-Institut für Chemie (Otto-Hahn-Institut),
Mainz, Germany

Abstract—Results are reported for the ^{14}C-, ^{22}Na-, ^{26}Al-, ^{36}Cl-, and ^{39}Ar-content of three lunar fines (12001, 14163, 14259) and three different depth regions in the igneous rock 12053.

^{22}Na and ^{26}Al show the expected solar proton induced excess over the galactic cosmic ray produced levels. For the soil samples they allow qualitative statements about the mean sampling depth.

The ^{14}C-data represent the first depth profile of this isotope in a lunar sample. The observed gradient is not reconcilable with a mean flux of 100 solar protons/cm^2 sec and $R_0 \approx 100$ MV. Instead, a 3–5 times higher flux is necessary or the presence of a surface correlated component. It is tentatively suggested that the required flux of 1×10^{-3} ^{14}C-atoms/cm^2 sec as well as the tritium flux of 5×10^{-3} ^3H/cm^2 sec discussed by D'Amico *et al.* is due to (*n*, *p*)-reactions of secondary neutrons on the surface of the sun.

Two grain size fractions of the 12001 soil were found to contain approximately equal amounts of ^{22}Na, ^{26}Al, and ^{36}Cl but grossly different ^{39}Ar-activities. The data point to an almost complete loss of ^{39}Ar from the Ca-containing phases in the fine-grained fraction.

The ^{36}Cl- and ^{39}Ar-data obtained on rock 12053 as well as all others on rock samples available in the literature are discussed. The discrepancies between the predicted depth profiles and the measured ones are ascribed to the small size of the rocks analyzed. Model calculations for infinite flat surfaces neglect the enhanced flux of solar protons with ranges comparable to the rock radii.

INTRODUCTION

THE CONTINUOUS BOMBARDMENT of the lunar surface by cosmic-ray particles produces a number of radioactive and stable isotopes. The measured amounts have been used with considerable success to unravel part of the history of the lunar surface and to derive the intensity as well as the energy and charge spectrum of the cosmic radiation in the near and distant past. In particular, these measurements have provided us with the first detailed information on the *mean solar* cosmic radiation, averaged over various time intervals. From these data it is apparent that in near-surface layers the production of a number of proton induced activities is dominated by low energy solar protons. Model calculations by Armstrong and Alsmiller, Rancitelli *et al.*, and Reedy and Arnold are indeed able to reproduce the steep gradients observed and, most important, such an analysis indicates the mean rigidity and intensity of the solar protons to have been the same during the past 10 yr as that during the last few million years.

As no data are available for intermediate time intervals of a few thousand years we continued our measurements of ^{14}C ($T_{1/2} = 5730$ yr). In addition, a number of samples has been analyzed for their content of ^{36}Cl and ^{39}Ar, two isotopes that are mainly due to secondary neutrons produced by the galactic cosmic radiation. Although results are available for a number of samples, the situation is still rather confusing.

So far, neither the absolute amounts of these isotopes nor the depth gradients—or their absence—has been explained satisfactorily

EXPERIMENTAL PROCEDURE AND RESULTS

Three samples of lunar fines (12001, 14163, 14259) and a 110 g slab of rock 12053 were available for the present investigation. Prior to any further treatment the γ-activity of sample 12001 was determined by means of a Ge (Li)-detector. (For specifications see Begemann *et al.*, 1970.) Subsequently, the sample was sieved into four grain size fractions (<44 μ, 44–75 μ, 75–150 μ, >150 μ). As the coarsest fraction consisted mostly of aggregates it was crushed gently in an agate mortar, and the resulting sieve fractions were combined with the ones obtained originally. Magnetic particles were separated by means of a hand magnet; for the <44 μ fraction, this was done by agitating the powder with ultrasound in ethanol.

The surface of the rock slab was inspected for the presence of microcraters in order to determine the original orientation of rock 12053 on the lunar surface. Craters were found on about half the circumference, with a rather narrow transition region. A 4–6 mm layer was then removed from the top with a diamond wheel attached to a dental drill. The remainder was divided into two more depth regions of about equal weight (Fig. 1). These three portions were crushed to <100 μ and the two deep samples were split into two portions each for the determination of ^{14}C–^{39}Ar and ^{22}Na–^{26}Al–^{36}Cl–^{39}Ar, respectively.

For the extraction of ^{14}C–^{39}Ar the same procedure was followed as for the Apollo 11 samples; when samples were dissolved this was performed in one step as described for the *residues* of the Apollo 11 samples (Begemann *et al.*, 1970. See this reference for details of the counting procedure).

Our counting results are listed in Table 1. Whenever the same samples—or such from similar positions like for rock 12053—have been analyzed by other investigators their data are included for comparison. In all cases the agreement is seen to be good.

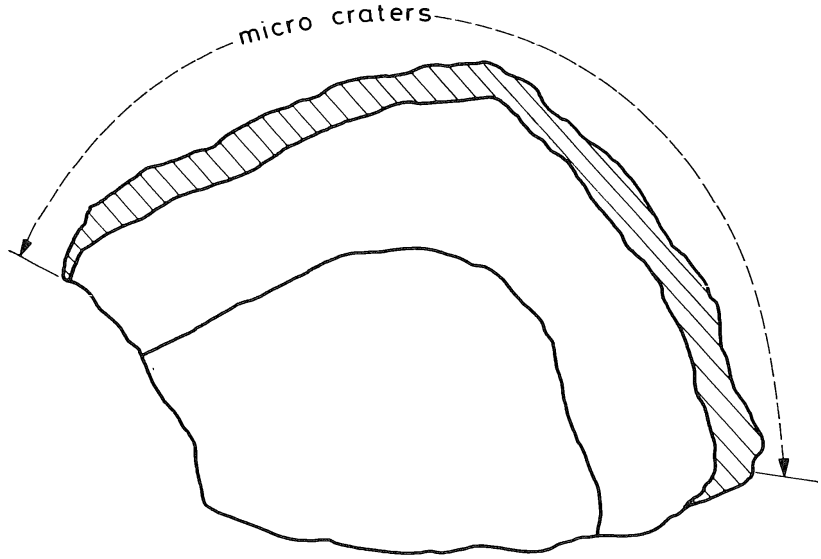

Fig. 1. Slab of rock 12053, showing the three depth regions analyzed.

Table 1. Specific activities determined in lunar soil and three depth regions in rock 12053. All activities are given in dpm/kg.

Sample	Weight (g)	Depth (cm)	^{14}C	^{22}Na	^{26}Al	^{36}Cl	^{39}Ar	^{54}Mn	Author*
Fines									
12001, bulk		—	—		128 ± 24	—	—	83 ± 25	—
< 44 μ	20.85	—	—	84 ± 8	109 ± 11	16.2 ± 0.8	2.4 ± 0.6		—
> 75 μ	22.98	—	—	78 ± 9	99 ± 12	13.4 ± 1.5	8.0 ± 0.6		—
14163	15.36	—	—	—	86 ± 11	25.0 ± 2.0	—	—	—
	—	—	—	45 ± 9	78 ± 16	—	—		(1)
	—	—	—	—	79 ± 6	—	—	—	(2)
	—	—	—	46 ± 5	79 ± 4	—	—	4 ± 7	(3)
14259	17.47	0–1	—	—	212 ± 25	16.5 ± 1.8	—	—	—
			—	84 ± 17	220 ± 40	—	—		(1)
	—		—	91 ± 8	222 ± 9	—	—	60 ± 20	(3)
	—		—	95 ± 15	176 ± 22	—	—	—	(4)
Rock									
12053	8.3	0–0.5	72.4 ± 7	—	—	—	10.0 ± 1.0		—
	15.0	0.5–2.0	32.8 ± 3	—	—	—	8.5 ± 0.7		—
	29.88		—	38 ± 6	69 ± 9	17.1 ± 0.8	7.7 ± 0.5		—
		≈1.5		45 ± 13	75 ± 14	—	—	—	(5)
	15.0	2.0–6.5	29.7 ± 3	—	—	—	8.6 ± 0.5		—
	27.72		—	34 ± 5	54 ± 6	15.7 ± 0.7	7.7 ± 0.5		—
	—	≈5.0	—	38 ± 8	58 ± 8	—	—	—	(5)

* For comparison the results obtained by other authors on the same samples are included. (1) LSPET (1971); (2) Wrigley (1972); (3) Keith *et al.* (1972); (4) Wahlen *et al.* (1972); (5) Rancitelli *et al.* (1971).

Table 2. Content of some relevant target elements in 12001 bulk soil and the two grain size fractions analyzed for activities. All entries are in weight percent.

	Mg	Al	Si	K	Ca	Fe	Ti
12001, bulk	5.92	6.65	21.6	0.210	6.1	12.9	1.6
12001, < 45 μ	5.8	7.4	21.8	0.221	7.4	11.7	1.7
75–150 μ	6.7	6.0	21.8	0.171	6.7	12.7	1.3

Table 2 gives the chemical composition of the different 12001 fractions measured. Although there are distinct differences—especially in the Mg, Al, and K-content—these are only minor. They can barely be expected to result in significant changes of the activities of the radioisotopes investigated. The more surprising is the large difference in the ^{39}Ar content of the two grain size fractions (see below).

Discussion

^{22}Na and ^{26}Al

These isotopes show the, by now, well-established strong dependance on mean sampling depth (Shrelldallf, 1970; Perkins *et al.*, 1970; Rancitelli *et al.*, 1971; Finkel *et al.*, 1971). Taking into account the different chemistry of 12001 and the Apollo 14 fines, we conclude that 14163 represents the thickest surface layer and 14259 the shallowest one, with 12001 somewhere in between. For 14259 this is in agreement with the LSPET (1971) according to which this sample was "skimmed from the upper 1 cm of the surface." Our data are not numerous enough to either support or contradict the conclusion of Wahlen *et al.* (1972) that the layer must have been twice as thick or that the exposure history of the top 1 cm was rather complicated.

^{14}C

According to the model calculations of Reedy and Arnold (1972) the concentration of ^{14}C should show a depth dependance similar to that of other proton induced

activities, i.e., a decrease in activity with depth superimposed on a slowly increasing contribution produced by galactic cosmic rays. Hence, the initial decrease or the integrated "excess" activity in the surface layers should again allow to determine the average flux of solar protons. Due to the half-life of ^{14}C the average flux thus determined would be that over the past 10^4 yr or so. This is an interesting time interval covered by no other isotopes.

The data obtained for rock 12053 are plotted in Fig. 2. The predicted decrease with depth of the activity is indeed observed. A quantitative analysis shows, however, that the results are not reconcilable with a 4π integral flux ($E > 10$ MeV) of 100 solar protons/cm^2 sec and a rigidity shape factor of $R_0 \approx 100$ MV as obatained from the analysis of various other isotopes (Finkel *et al.*, 1971). A rather good fit is obtained with $R_0 = 100$ MV and a three times higher flux, or $R_0 = 80$ MV and a five times higher flux. This, one could take to indicate that either the mean flux of solar protons over the past 10,000 yr has been 3–5 times higher than that averaged over the past 10 yr and the past million years, respectively, or that the cross sections used in the model calculations are completely wrong. Neither of these possibilities can be excluded with certainty. The fact, however, that the discrepancy between measured and calculated activities (with $R_0 = 100$ MV and a flux of 100 protons/cm^2 sec) is caused

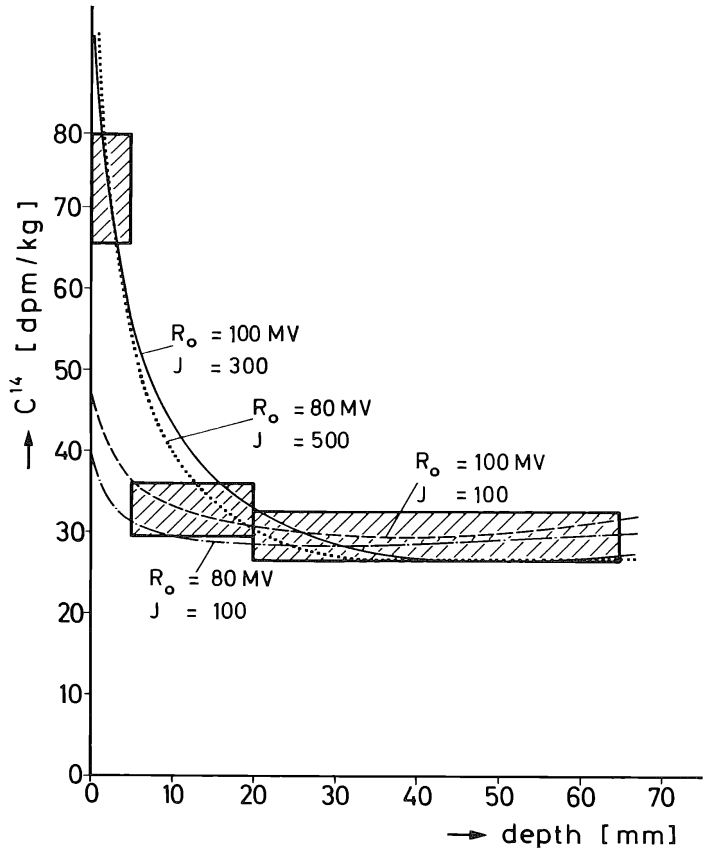

Fig. 2. ^{14}C activities measured in rock 12053. The curves are those predicted from the model calculations of Reedy and Arnold (1972) for different choices of R_0 and flux J [solar protons with $E > 10$ MeV/cm^2 sec and 4π irradiation].

by the high activity of the surface sample suggests that the excess ^{14}C might be surface correlated. For the geometry of our sample a mean ^{14}C flux of about 1×10^{-3} ^{14}C atoms/cm^2 sec would be required, assuming equilibrium conditions.

In this connection it is perhaps worth mentioning that D'Amico *et al.* (1971) suggested a ^3H flux of 5×10^{-3} tritium atoms/cm^2 sec to account for a surface correlated ^3H component in rock 12002. While this tritium might presumably be produced by the *direct* interaction of solar flare protons with the photosphere of the sun and subsequently be removed as flare particles (Fireman, 1962) and implanted into the lunar surface, there is no chance to produce the required amounts of ^{14}C by a similar process. There is the possibility, however, that both isotopes are produced on the sun by secondary neutrons via the exothermic (n, p)-reactions on ^3He and ^{14}N. If this were so the equilibrium ratio of the fluxes, barring any fractionation in the acceleration mechanism, would be

$$\frac{^3H}{^{14}C} = \left(\frac{^3He}{^{14}N}\right)_{sun} \times \frac{T(^3H)}{T(^{14}C)} \times \frac{\sigma(3)}{\sigma(14)}.$$

Inserting the values for the solar abundance ratio (Cameron, 1968), the half-lives of tritium and ^{14}C, and the ratio of the "thermal" cross sections yields a ratio of 1.6 as compared to the one of 5 deduced from the lunar samples.

We are aware, of course, that this close agreement is no proof for the processes suggested to take place on the required scale, especially since the assumption that equilibrium is established *at a rather high level of activity* needs special conditions. Vertical mixing rates on the solar surface are fast so that there is a huge dilution factor (mass in convective zone/mass in reaction zone). We understand, however, that solar physicists are discussing at present the possibility that following major solar flares the regions around the foot points are sucked up into the corona (Schmidt, private communication). Such a process would indeed obstruct the dilution and lead to conditions equivalent to equilibrium in the reaction zone.

^{36}Cl

In lunar samples this isotope is produced by spallation reactions on Fe, Ti, and Ca and by secondary neutrons from Ca, with the latter being most important target element. A contribution from K or from the ^{35}Cl (n, γ) reaction can only be expected for unusually high contents of K and Cl. This is shown in Fig. 3 for a sample with 25% (Fe + 4 Ti), 7% Ca, and 2000 ppm K. The differential energy spectra and fluxes of the nuclear active particles as well as the relevant cross sections used in this calculation are those of Reedy and Arnold (1972). From the computations of the same authors it is also apparent that *solar* protons contribute less then 1 dpm/kg even in the surface layer of <1 g/cm^2. Consequently, an increase in activity with depth must be expected.

Qualitatively, the soil samples listed in Table 1 conform to this expectation. The shallowest sample (14259) has an activity of (16.5 ± 1.8) dpm/kg, the deepest one (14163) (25 ± 2) dpm/kg. The intermediate sample 12001 (see above), corrected for its lower Ca content, falls into the same sequence. We do not believe, however, that

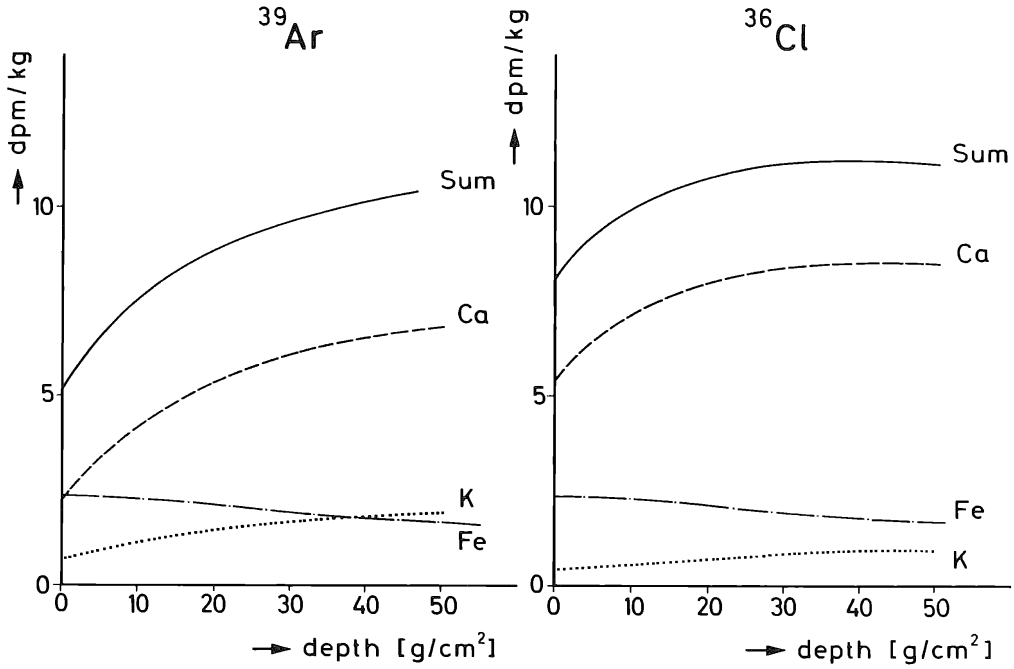

Fig. 3. Calculated ^{39}Ar and ^{36}Cl activities for a rock with 25% (Fe + 4 · Ti), 7% Ca, and 2000 ppm K.

the high activity of 14163 is entirely due to a greater mean depth. The only explanation we can put forward at the present time to account for the excess activity is that in this sample we have a major contribution of ^{35}Cl (n, γ)-produced ^{36}Cl. The Cl-content of an aliquot of this sample was found to be exceptionally high (280 ppm, Wänke *et al.*, 1972) and for this high Cl content a thermal neutron flux of about 1 neutron/cm^2 sec would be required to produce 10 dpm ^{36}Cl/kg. It is somewhat disturbing, however, that Brunfelt *et al.* (1971) and Reed *et al.* (1972) report for the 14163 fines Cl-contents of only 47 and 51 ppm, respectively, although there is the definite possibility of a very inhomogeneous distribution of trace elements like Cl.

The two samples of rock 12053 (Table 1, column 7) show a decrease or perhaps constant activity with depth, contrary to expectations. Furthermore, the absolute activity is considerably higher than expected from the chemistry of this rock and the curves in Fig. 3. If one looks at the ^{36}Cl data of all four rocks in which the activity has been measured for different layers (Shrelldallf, 1970; Finkel *et al.*, 1971; Wahlen *et al.*, 1972), it turns out that this is rather the rule (Fig. 4). Only for 14321 are the theoretical predictions in accord with the measurements although even here there might be an excess in the top layers. As the discrepancies appear to be the largest for the smallest rocks (10017, 0.98 kg; 12053, 0.88 kg) and smallest for 14321 (9.0 kg) we suggest that they might conceivably be due to applying a wrong model. Clearly, rocks with radii of only a few cm lying on top of the regolith do not have a 2π flat geometry for irradiation. Rather, the flux of solar protons with ranges comparable to the radii is considerably enhanced while the build-up of the secondary neutron flux is somewhat reduced.

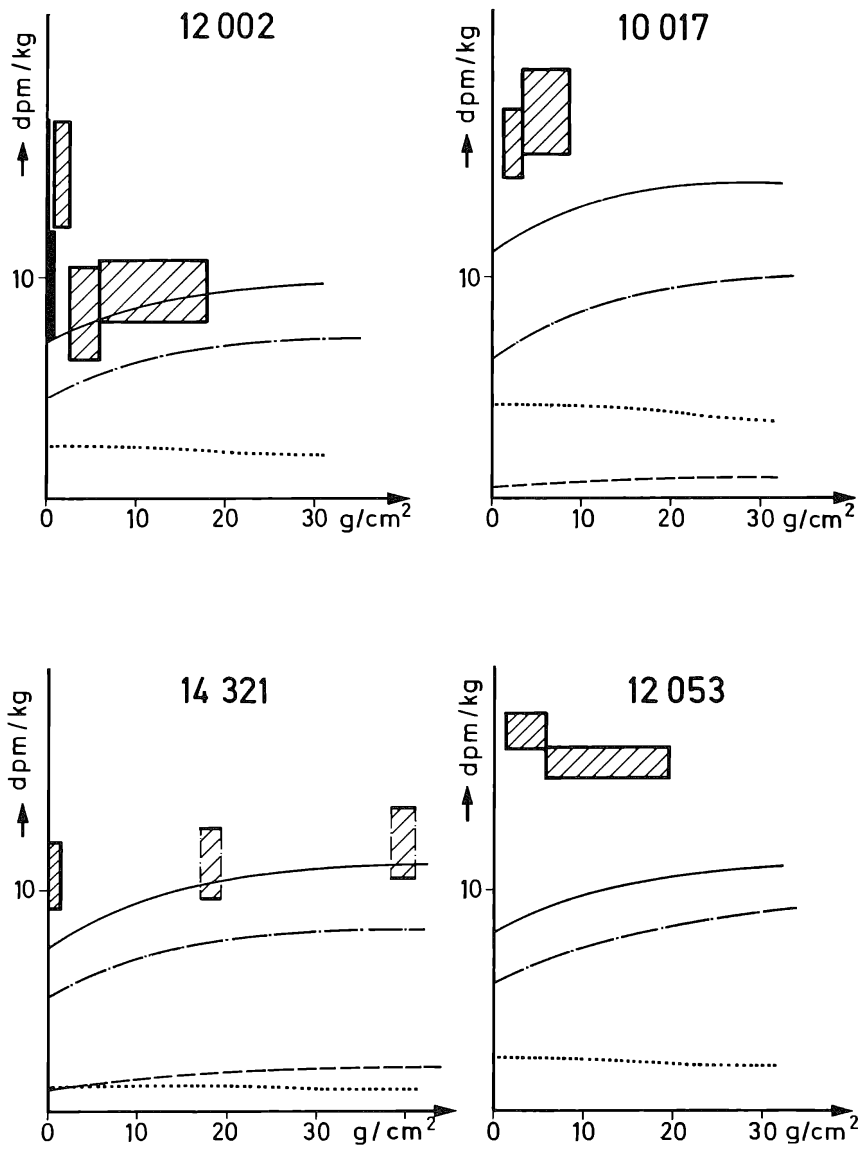

Fig. 4. Measured and predicted ^{36}Cl activities in 4 lunar rocks. —·—·: Contribution from Ca; ····· contribution from Fe + 4·Ti; — — —: contribution from K; —— sum.

^{39}Ar

In our first paper on the ^{39}Ar content of lunar samples (Begemann *et al.*, 1970) we were of the opinion that besides Fe and Ti, K is the most important target element. This conclusion was reached by estimating the contribution due to the ^{40}Ca (n, $2p$)-reaction from the measured (n, $2p$)- cross sections on neighboring nuclides. In the meantime the cross section for the production of ^{39}Ar from Ca has been measured with 14 MeV neutrons (Stoenner *et al.*, 1970) and Reedy and Arnold (1972) have constructed an excitation function for this reaction, with normalization at the one experimental point. Using these data it appears now that the contribution from Ca is dominant as the production per kg of K turns out to be only 10 times larger than that per kg Ca. This is somewhat surprising in view of the fact that for the enstatite

chondrite Abee we found a ratio of 120 instead (Begemann *et al.*, 1967). It does remove some of the inconsistencies mentioned in our first paper, however.

The most striking result obtained on the two grain size fractions of the 12001 fines is the large difference in their ^{39}Ar content that is clearly *not* due to a different chemical composition (Table 2). If anything, from these differences one would rather expect the activity in the finest fraction to be higher. Instead, the activity found can almost be accounted for by the production from Fe and Ti. This points to a more or less complete loss of ^{39}Ar from the Ca-containing phases. Whether this is solely a grain size effect or due to a higher relative abundance of Ca-rich *glass* in the finest fraction is not clear at present. That such diffusion loss of ^{39}Ar from lunar fines does

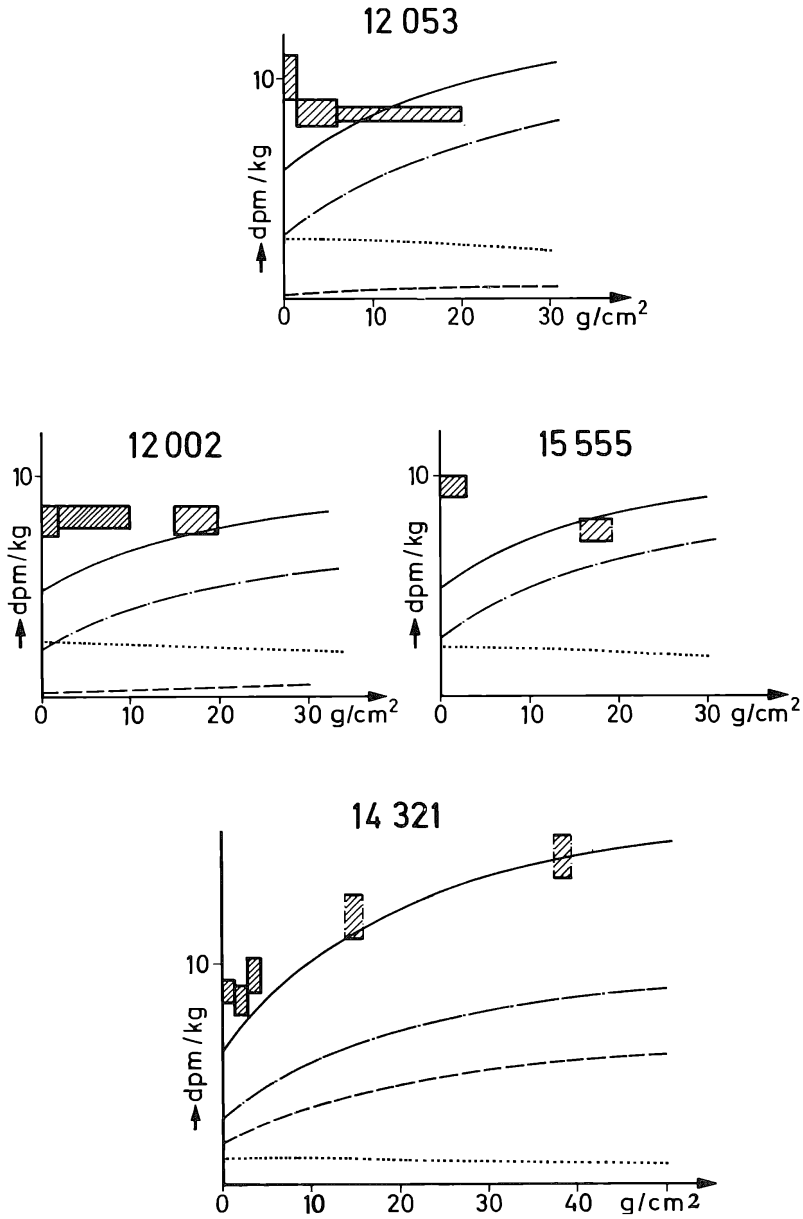

Fig. 5. Measured and predicted ^{39}Ar activities in 4 lunar rocks. For explanation of curves see legend to Fig. 4.

indeed occur has been shown by Stoenner *et al.* (1972) who report diffusion losses of 10^{-2}–10^{-3} %/day.

For the samples from the three layers of rock 12053 there is no increase with depth observed in the ^{39}Ar activity, again in contradiction to the prediction of the model calculations. As in the case of ^{36}Cl this is true for all lunar rocks analyzed so far, with the exception of 14321 (Fig. 5) (D'Amico *et al.*, 1971; Fireman *et al.*, 1972). Here, too, we suggest this to be due to the small size of the rocks analyzed. In the case of ^{39}Ar, however, the target element for the production of the excess activity by solar protons is probably Ti (not Ca or K) as protons of any energy can produce ^{39}Ar only from the rare isotopes of both elements.

Acknowledgments—We are grateful to NASA for making available the lunar material for this investigation. We wish to thank the staff of our Institute, in particular Miss G. Schmidt, Miss H. Prager and Mr. P. Keller. The financial support by the Bundesministerium für Bildung und Wissenschaft is gratefully acknowledged.

References

Armstrong T. W. and Alsmiller R. G. Jr. (1971) Calculation of cosmogenic radionuclides in the moon and comparison with Apollo measurements. *Proc. Second Lunar Sci. Conf., Geochim. Cosmochim. Acta* Suppl. 2, Vol. 2, pp. 1729–1745. MIT Press.

Begemann F., Vilcsek E., and Wänke H. (1967) The origin of the "excess" argon-39 in stone meteorites. *Earth Planet. Sci. Lett.* **3,** 207–212.

Begemann F., Vilcsek E., Rieder R., Born W., and Wänke H. (1970) Cosmic-ray produced radioisotopes in lunar samples from the Sea of Tranquility (Apollo 11). *Proc. Apollo 11 Lunar Sci. Conf., Geochim. Cosmochim. Acta* Suppl. 1, Vol. 2, pp. 995–1005. Pergamon.

Brunfelt A. O., Heier K. S., Steinnes E., and Sundvoll B. (1971) Determination of 36 elements in Apollo 14 bulk fines 14163 by activation analysis. *Earth Planet. Sci. Lett.* **11,** 351–353.

Cameron A. G. W. (1968) A new table of abundances of the elements in the solar system. In *Origin and Distribution of the Elements* (editor L. H. Ahrens), pp. 125–143, Pergamon.

D'Amico J., DeFelice J., Fireman E. L., Jones C., and Spannagel G. (1971) Tritium and argon radioactivities and their depth variations in Apollo 12 samples. *Proc. Second Lunar Sci. Conf., Geochim. Cosmochim. Acta* Suppl. 2, Vol. 2, pp. 1825–1839. MIT Press.

Finkel R. C., Arnold J. R., Imamura M., Reedy R. C., Fruchter J. S., Lossli H. H., Evans J. C., and Delany A. C. (1971) Depth variation of cosmogenic nuclides in a lunar surface rock and lunar soil. *Proc. Second Lunar Sci. Conf., Geochim. Cosmochim. Acta* Suppl. 2, Vol. 2, pp. 1773–1789. MIT Press.

Fireman E. L. (1962) Tritium in meteorites and in recovered satellite material. In *Tritium in the Physical and Biological Sciences*, Vol. 1, pp. 69–74, IAEA, Vienna.

Fireman E. L., D'Amico J., DeFelice J., and Spannagel G. (1972) Radioactivities in Apollo 14 and 15 materials (abstract). In *Lunar Science—III* (editor C. Watkins), pp. 262–264, Lunar Science Institute Contr. No. 88.

Keith J. E., Clark R. S., and Richardson K. A. (1972) Gamma ray measurements of Apollo 12, 14, and 15 lunar samples (abstract). In *Lunar Science—III* (editor C. Watkins), pp. 446–448, Lunar Science Institute Contr. No. 88.

LSPET (Lunar Sample Preliminary Examination Team) (1971) Preliminary examination of lunar samples from Apollo 14. *Science* **173,** 681–693.

Perkins R. W., Rancitelli L. A., Cooper J. A., Kaye J. H., and Wogman N. A. (1970) Cosmogenic and primordial radionuclide measurements in Apollo 11 lunar samples by nondestructive analysis. *Proc. Apollo 11 Lunar Sci. Conf., Geochim. Cosmochim. Acta* Suppl. 1, Vol. 2, pp. 1455–1469. Pergamon.

Rancitelli L. A., Perkins R. W., Felix W. D., and Wogman N. A. (1971) Erosion and mixing of the lunar surface from cosmogenic and primordial radionuclide measurements in Apollo 12 lunar samples. *Proc. Second Lunar Science Conf., Geochim. Cosmochim. Acta* Suppl. 2, Vol. 2, pp. 1757–1772. MIT Press.

Reed G. W. Jr., Jovanovic S., and Fuchs L. H. (1972) Concentrations and lability of the halogens, platinum metals and mercury in Apollo 14 and 15 samples (abstract). In *Lunar Science—III* (editor C. Watkins), pp. 637–639, Lunar Science Institute Contr. No. 88.

Reedy R. C. and Arnold J. R. (1972) Interaction of solar and galactic cosmic-ray particles with the moon. *J. Geophys. Res.* **77**, 537–555.

Shrelldalff: Shedlovsky J. P., Honda M., Reedy R. C., Evans J. C. Jr., Lal D., Lindstrom R. M., Delany A. C., Arnold J. R., Loosli H. H., Fruchter J. S., and Finkel R. C. (1970) Pattern of bombardment-produced radionuclides in rock 10017 and in lunar soil. *Proc. Apollo 11 Lunar Science Conf., Geochim. Cosmochim. Acta* Suppl. 1, Vol. 2, pp. 1503–1532. Pergamon.

Stoenner R. W., Lyman W. J., and Davis R. Jr. (1970) Cosmic-ray production of rare-gas radioactivities and tritium in lunar material. *Proc. Apollo 11 Lunar Sci. Conf., Geochim. Cosmochim. Acta* Suppl. 1, Vol. 2, pp. 1583–1594. Pergamon.

Stoenner R. W., Lindstrom R. M., Lyman W., and Davis R. Jr. (1972) Argon, radon, and tritium radioactivities in the sample return container and the lunar surface (abstract). In *Lunar Science—III* (editor C. Watkins), pp. 729–730, Lunar Science Institute Contr. No. 88.

Wahlen M., Honda M., Imamura M., Fruchter J., Finkel R., Kohl C., Arnold J., and Reedy R. (1972) Cosmogenic nuclides in football-sized lunar rocks (abstract). In *Lunar Science—III* (editor C. Watkins), pp. 764–766, Lunar Science Institute Contr. No. 88.

Wänke H., Baddenhausen H., Balacescu A., Teschke F., Spettel B., Dreibus G., Quijano-Rico M., Kruse H., Wlotzka F., and Begemann F. (1972) Multielement analyses of lunar samples (abstract). In *Lunar Science—III* (editor C. Watkins), pp. 779–781, Lunar Science Institute Contr. No. 88.

Wrigley R. C. (1972) Radionuclides at Fra Mauro (abstract). In *Lunar Science—III* (editor C. Watkins), pp. 814–815, Lunar Science Institute Contr. No. 88.

Proceedings of the Third Lunar Science Conference
(Supplement 3, *Geochimica et Cosmochimica Acta*)
Vol. 2, pp. 1703–1717
The M.I.T. Press, 1972

Argon, radon, and tritium radioactivities in the sample return container and the lunar surface

R. W. STOENNER, RICHARD M. LINDSTROM,
WARREN LYMAN,* and RAYMOND DAVIS, JR.

Chemistry Department, Brookhaven National Laboratory,
Upton, N.Y. 11973

Abstract—The radioactive rare gases ^{37}Ar (35 day), ^{39}Ar (269 yr), ^{222}Rn (3.8 day), and tritium (12.3 yr) were measured in the gas recovered from the Apollo 12, 14, and 15 sample return containers and in lunar rocks and soil. The activities observed in the sample return containers can be attributed to the diffusion of these activities from the fine material present in the box. An analysis of these results and the diffusion of argon activities and tritium from lunar fine material at various temperatures up to 900°C allows a determination of the heat of diffusion and the diffusion constant divided by the square of the mean grain size (D/a^2) for lunar material. An analysis is made of the loss of argon into the lunar atmosphere.

The cosmic ray production of ^{37}Ar, ^{39}Ar, and tritium in the lunar soil was measured in two deep samples, and in adjacent surface samples from the Apollo 15 mission. The ^{37}Ar activity was essentially the same at the surface and at depth (150 g/cm^2). This result is in accord with a 600-MeV proton bombardment of a thick target of lunar-like composition 100 g/cm^2 deep. Argon-37 activities from the Apollo 14 mission were high as a result of the January 1971 flare that occurred 12 days preceding the mission.

Measurements of the ^{222}Rn observed in the sample return container allow a determination of the ^{222}Rn emanation rate in lunar soil under conditions representative of the natural conditions on the moon. An analysis of the emanation rate permits an estimate of the amount of ^{222}Rn released to the lunar atmosphere.

INTRODUCTION

THE SAMPLE RETURN CONTAINER (SRC) when closed on the surface of the moon includes an 18-liter sample of the lunar atmosphere. In addition, it contains all gaseous products, both radioactive and stable, that have been released from the contents of the SRC, in particular from the lunar fine material. The lunar fines have unique adsorptive and emanation properties that are important to an understanding of the lunar atmosphere, properties that are essentially preserved in the SRC up to the time of opening at the Lunar Receiving Laboratory. The concentration of gas in the lunar atmosphere or the amounts of gas emanating from a kilogram of lunar fines is extremely small, too small to be observed with a conventional high-sensitivity mass spectrometer. However, one has a very high sensitivity for observing radioactive rare gas atoms and tritium, and also the background amounts of these atoms present as contamination are extremely small. The detection limits of the radioactivities reported in this work are: 20 atoms of ^{222}Rn ($t_{1/2}$ 3.8 days), 50 atoms of ^{37}Ar ($t_{1/2}$

* Present address: Department of Earth and Space Sciences, State University of New York, Stony Brook, N.Y. 11790.

35 days), 1.5×10^5 atoms of ^{39}Ar ($t_{1/2}$ 269 years), and 10^5 atoms of tritium ($t_{1/2}$ 12.3 years). In this paper we report measurements of the amounts of these radioactive gases present in the sample return container from the Apollo 12, 14, and 15 missions.

The results for argon and tritium will be interpreted in terms of the diffusion of these atoms from the fine material contained in the SRC. It will be shown that the loss of argon and tritium from the fines in the SRC at room temperature is quantitatively related to the loss of these gases from lunar fines heated to temperatures up to 1170°K, and also to the loss from bombarded simulated lunar fines over the temperature range 197 to 408°K. Combining these observations and the surface temperature of the moon, an estimate is made of the loss of argon and tritium to the lunar atmosphere.

The radon present in the lunar atmosphere and its daughter radioactivities have been the subject of direct observation from orbiting spacecraft and the Surveyor V landing spacecraft. It is of interest to measure the radon loss or emanating power of pristine lunar soil. The lunar fines present in the unopened SRC is the only available sample (the environmental sample is superior) of returned lunar material that approaches these requirements. The ^{222}Rn present in the SRC in the Apollo 12, 14, and 15 missions was measured, and the results are interpreted in terms of recoil processes and adsorption in the lunar soil. Using this measured emanating rate we estimate the amount of ^{222}Rn expected to appear in the lunar atmosphere.

After a brief description of our experimental procedures, we will discuss and interpret the results for individual radioactivities, argon, tritium, and radon in order.

EXPERIMENTAL

Sample return container

An effective seal was realized on one SRC from each of the Apollo 12, 14, and 15 missions, such that it was still under vacuum (30 to 70 μ Hg; see Table 1) upon arrival at the Lunar Receiving Laboratory. The second SRC returned from each of these missions could not be analyzed because the box was not properly closed on the lunar surface and therefore leaked to atmospheric pressure. The gas from the Apollo 15 SRC was removed in the same manner as described by Stoenner *et al.* (1971) except that to collect H_2 a trap with 10 g of activated powdered vanadium metal at room temperature was substituted for the liquid helium cooled charcoal trap used on Apollo missions 12 and 14. A liquid nitrogen cooled trap filled with 10 g of charcoal was used as before to collect all other gases. An absorption time of one hour was allowed in the box opening procedures, however this time was apparently sufficient to collect over 90% of the gases, as indicated by a thermocouple gauge on the pumping line between the SRC and the liquid nitrogen cooled charcoal trap. The argon, radon, and

Table 1. Argon and tritium radioactivities in the sample return container.*

Mission	SRC Pressure (Torr)	Wt. fines in SRC (kg)	Observed activity (dpm × 10^3)			Fraction of activity lost per day (× 10^5)		
			^{37}Ar	^{39}Ar	T	^{37}Ar	^{39}Ar	T
12	0.030	2.7	40 ± 2	2.3 ± 1.0	—	6	2	—
14	0.070	0.60	40 ± 2	0.8 ± 0.5	280 ± 20	18	2	40
15	0.032	2.30	106 ± 3	3.0 ± 1.2	550 ± 10	18	2	10

* Errors quoted throughout this paper, unless otherwise noted, are one standard deviation based on counting statistics.

hydrogen collected were separated from each other, purified, and counted in small low-level proportional counters to obtain the amounts of ^{37}Ar, ^{39}Ar, ^{222}Rn, and tritium activities. The separation procedures used are those described earlier (Stoenner *et al.*, 1970). In previous reports the counting efficiency for ^{222}Rn and its daughters was only estimated. In the present work the radon counters were standardized and the results applied to the earlier measurements. Radon-222 was swept from NBS standard radium solutions with helium gas and the ^{222}Rn trapped on charcoal. It was removed by heating to 250°C along with argon carrier gas and placed in the counter. Measured counting efficiencies were in the range of 1.9 counts per disintegration of ^{222}Rn.

The ^{37}Ar, ^{39}Ar, tritium, and ^{222}Rn observed in the Apollo 12, 14, and 15 missions is listed in Tables 1 and 2. The ^{37}Ar activity is corrected to the time of liftoff from the lunar surface. The ^{222}Rn activity given is the value at the time of box puncture corrected to an infinite accumulation time and therefore corresponds to the total equilibrium emanation rate for the mass of fine material in the container.

Argon and tritium activities in rocks and soils

Argon radioactivities and tritium in lunar rocks and soils were measured using the procedures previously given (Stoenner *et al.*, 1970). Most of the samples were either surface chips of rocks or surface soil samples, with an estimated depth of a few grams per cm^2. Two Apollo 15 samples at depth were measured: (1) 15031,16, the bottom of a trench 35 cm deep dug at station 8 at a distance of 80 m from the Lunar Module, and (2) 15231,18, a sample of soil below a boulder approximately 60 cm in diameter and 1 m long at station 2.

It was of interest to observe the rate of loss of these radioactivities with temperature from the fine material to determine the variation of the diffusion constant with temperature. An experiment of this nature was performed during the Apollo 11 mission under the biological quarantine restrictions that necessitated preheating the sample a day at 120°C for sterilization purposes. Since the effect of the preheating was not known, we heated the two Apollo 15 trench soil samples (15031,16 and 15041,16) stepwise to check the earlier results. The temperatures used were 300°C, 600°C, and 900°C, for periods of one to four days. The experiments were concluded by melting the samples. Table 3 summarizes the results.

A long delay in receipt of the trench samples, and the division of activity into several heating fractions, resulted in rather large counting errors, especially in the ^{39}Ar measurement. The fractions

Table 2. $^{222}Radon$ in the sample return container.

Mission	Total ^{238}U Disintegration Rate in Fines (dpm)	^{222}Rn in SRC Gas (Saturation dpm)	Fraction Emanated ($\times 10^3$)
12	3400	6.4 ± 0.4	1.9
14	1700	2.42 ± 0.03	1.4
15	1700	0.86 ± 0.05	0.50

Table 3. Thermal release of argon and tritium activities from lunar fines.

Temp. (°C)	Period (days)	Trench Top, 15041,16 Percent Released ^{37}Ar	^{39}Ar	T	Period (days)	Trench Bottom, 15031,16 Percent Released ^{37}Ar	^{39}Ar	T
300	0.85	7	2	5	0.93	0	5	13
600	1.2	1	21	56	4.0	10	17	66
900	2.0	40	15	37	0.97	79	36	21
Melt	—	52	62	2	—	12	41	0
Total dpm/kg		28.4 ± 3.6	12.9 ± 1.5	435 ± 8		24.9 ± 4.2	7.6 ± 1.5	202 ± 6

were later combined to reassay the ^{39}Ar activities; agreement was satisfactory. The temperature release of ^{37}Ar and tritium in the Apollo 15 trench samples agrees well with the earlier Apollo 11 results, and indicates that the amount of tritium released in the sterilization treatment was small.

Table 2 summarizes the ^{37}Ar, ^{39}Ar, and tritium values on all Apollo missions measured at this laboratory.

DISCUSSION

The production of argon and tritium radioactivities by cosmic rays

The argon radioactivities, ^{37}Ar and ^{39}Ar, are produced by high energy spallation processes on the abundant elements iron, titanium, calcium, and potassium. In addition, these activities are produced by the fast neutron reactions $^{40}Ca(n,\alpha)^{37}Ar$, $^{40}Ca(n,2p)^{39}Ar$, and $^{39}K(n,p)^{39}Ar$. In our previous reports the measured activities of lunar samples were compared to the 600-MeV proton thin target cross sections on iron, titanium, and calcium and fast neutron cross sections on potassium and calcium. Tritium is generally considered a high energy product because its production cross section increases with energy and target mass number. To obtain the relative production of these isotopes under more realistic conditions that would include the nucleon and meson cascade, a thick target (20 × 20 cm and 43 cm deep) of lunar-like material was irradiated with 600 MeV protons (Lyman, 1971). A detailed analysis of these results has not been made, but certain broad features of the results are clear. The total ^{37}Ar, ^{39}Ar, and tritium produced does not vary greatly with depth from 2 to 100 g/cm^2, and the activity ratio $^{37}Ar/^{39}Ar$ is 2.7 and the ratio $T/^{39}Ar$ is 20. The flat distribution with depth is a result of the nuclear cascade in the target; the target had lateral dimensions great enough to include about 80% of the cascade. The target contained 11.7% Fe, 3.9% Ti, 8.0% Ca, and 0.09% K, a composition similar to that of the lunar rocks and soils measured in this report. One might expect the $^{37}Ar/^{39}Ar$ ratios to depend somewhat on the composition, and also upon the bombarding energy. The target measurements do not show the increase of a factor of two in ^{37}Ar from the surface to a depth of 50 g/cm^2 expected in the calculations of Reedy and Arnold (1972). However, these calculations are based primarily on the $^{40}Ca(n,\alpha)^{37}Ar$ reaction as the ^{37}Ar production mechanism, and include a spectrum of cosmic ray particles interacting with the lunar surface with uniform angular distribution. These thick target results would indicate that lunar surface material under constant cosmic ray bombardment should exhibit little change in ^{37}Ar, ^{39}Ar, and tritium activity with depth, and the ratio $^{37}Ar/^{39}Ar$ should be approximately 2.7, and the ratio $T/^{39}Ar$ should be approximately 20.

It is clear that the surface of the moon is not subject to a constant bombardment but is exposed to periodic intense fluxes of solar flare particles. The ^{37}Ar activity will suddenly increase during a flare event whereas the long-lived ^{39}Ar will be little affected by any single event. These general features are seen in the argon activities observed in the four Apollo missions given in Table 2. Apollo 11 and 15 missions were relatively free of solar flare effects, and one observes that the ^{37}Ar activities are similar and show no change with depth, as for example the surface (15031,16) versus the bottom of the trench (15041,16), and the surface (15221,17) and under the boulder (15231,18). It can also be noted that the $^{37}Ar/^{39}Ar$ ratio in these samples varies

considerably over the range 1.6 to 6.1, thus showing poor agreement with the ratio of 2.7 obtained in the thick target bombardment. The largest variation is in the ^{39}Ar activities, and they appear to have lower values on the surface than at depth. This apparently anomalous result can be attributed to the loss of ^{39}Ar from surface fine material by diffusion. An analysis of this phenomenon will be given below. The Apollo 12 and 14 missions were preceded by solar flare events 17 and 12 days prior to the landing. Three of the four samples analyzed showed high ^{37}Ar levels. The value of 78 dpm/kg observed in the bulk fines sample 14259,84 is the highest ^{37}Ar observed in a lunar sample. It is interesting to note that at the time of the flare this sample would have contained 90 dpm ^{37}Ar/kg. The values reported by Fireman *et al.* (1972) for the Apollo 14 mission were also high (34 to 38 dpm ^{37}Ar/kg) but not as high as those reported here. The variations we observe are somewhat inconsistent with the more or less uniform production of ^{37}Ar expected from the target, consequently we can only attribute the variations observed to differences in chemical composition of the individual samples.

The tritium content in Apollo samples measured varies considerably. The Apollo 11 rock samples of all investigators appeared to be relatively uniform in tritium activity (Stoenner *et al.*, 1970; D'Amico *et al.*, 1970). If one takes an average of 226 dpm T/kg and an average of 10 dpm ^{39}Ar/kg for rock samples, the T/^{39}Ar ratio of 23 agrees rather well with the value of 20 obtained from the 600-MeV proton irradiation. However, there are some large variations in the tritium content of fine material. The two studies of presumably adjacent samples, one from the surface and one at depth, gave results that are difficult to explain. The soil sample from under the boulder (15231,18) and a surface sample a few meters away (15221,17) had very low tritium contents, only 56 dpm T/kg, whereas one would expect a tritium content for both of these samples in the range of 200–300 dpm T/kg. We attribute these low values to the escape of tritium. In the beginning of the extraction procedure these samples were placed in the vacuum system and allowed to stand at room temperature 16 hours. During this period the samples lost 4.9 $\pm$ 3.3 (15231,18) and 10.7 $\pm$ 3.2 (15221,17) dpm T/kg. These tritium losses were regarded as small, close to line backgrounds. Following this experiment the samples were heated for several days at 150°C to measure the ^{222}Rn emanation rate, but the tritium released during this period was not measured. It is entirely possible that these soil samples collected at Station 2 are not very retentive for hydrogen. It is interesting to note that Fireman *et al.* (1972) observed a 25% tritium loss in 3 months at room temperature in a sample of fines (15021,2). There apparently is a variation in the tritium retentivity of lunar fine samples, though the release patterns of the three fine samples that we studied in detail are very similar, as Table 4 shows.

The trench samples showed a higher tritium content at the bottom ($\sim$70 g/cm^2) of the trench, 435 dpm T/kg, than at the surface, 202 dpm T/kg. It is to be noted that the trench bottom sample (15031,16) did not release a measurable amount of tritium when retained in a vacuum at room temperature for 16 hours, 0.5 $\pm$ 2.5 dpm T/kg. The higher tritium content of the trench bottom sample can be explained by noting that a sample at a depth in the lunar soil is shielded from the solar diurnal heating and hence retains most of the tritium produced in it whereas a surface sample is

Table 4. Argon and tritium radioactivities from lunar rocks and soils.

Sample Information			Argon Radioactivities (dpm/Kg)				Composition (%)				
No.	Location	Depth (g/cm^2)	^{37}Ar	^{39}Ar	$^{37}Ar/^{39}Ar$	Tritium (dpm/Kg)	Fe	Ti	Ca	K	Ref.*
10002,6	Surface fines	Surface	18.7 ± 1.2	9.2 ± 0.4	2.0 ± 0.2	314 ± 13	12.4	4.2	8.6	0.10	
10057,3	Exterior chip	Surface	18.5 ± 0.9	11.2 ± 0.3	1.7 ± 0.1	224 ± 15	15.5	7.5	7.1	0.15	
10057,27	Interior chip	Surface	23.7 ± 4.1	14.8 ± 0.4	1.6 ± 0.3	214 ± 20					
12063,–	Exterior chip	Surface	27.8 ± 0.6	7.8 ± 0.6	3.6 ± 0.2	High on surface	16.7	3.1	7.9	0.065	
12065,–	Exterior chip	Surface	49.5 ± 0.6	7.8 ± 0.2	6.4 ± 0.2	High on surface	17.1	2.3	9.0	0.06	(1)
14259,84	Bulk fines	Surface	78.2 ± 3.4	9.1 ± 0.5	8.6 ± 0.6	203 ± 4	7.8	1.1	7.8	0.42	(2)
14163,116	Bulk fines	Surface	46.4 ± 3.4	10.2 ± 0.6	4.6 ± 0.4	—	—	—	—	—	
15221,17	Surface fines, near boulder	Surface	34 ± 4	5.6 ± 0.8	6.1 ± 1.1	56 ± 4	10.3	0.95	9.6	0.19	(3)
15231,18	Fines, under boulder	~150	35 ± 5	14 ± 1	2.6 ± 0.4	56 ± 4	10.3	0.95	9.6	0.19	
15031,16	Trench, surface	Surface	25 ± 4	5.9 ± 1.4	4.2 ± 1.2	202 ± 5	13.3	1.3	8.8	0.18	(4)
15041,16	Trench, bottom	~70	28 ± 4	14 ± 2	2.0 ± 0.4	435 ± 8	13.3	1.3	8.8	0.18	

* References for composition: (1) LSPET (1970); (2) LSPET (1971); (3) LSPET (1972), used 15101; (4) LSPET (1972), used 15021.

heated to 100 to 130°C during the lunar day. The diffusion loss will be discussed in a later section.

Thermal Release

We now turn to a consideration of the diffusion of gaseous radioactivity from minerals in order to explain some of the anomalies observed above. The topic has been reviewed by Fechtig and Kalbitzer (1966), from whom the equations below are taken. The fraction F of the total available gas diffusing from a mineral sample at absolute temperature T for a time t depends on the ratio D/a^2, where D is the diffusion constant and a is the mean grain size. For fractional losses $F < 0.9$,

$$\frac{D}{a^2} = \frac{2}{\pi t}\left(1 - \frac{\pi F}{6} - \sqrt{1 - \frac{\pi F}{3}}\right). \tag{1}$$

When $\ln (D/a^2)$ is plotted against $1/T$, a straight line is obtained if a single, simply activated, process is operating; the slope of the line is $-Q/R$, where Q is the heat of activation for diffusion and R the gas constant.

We have three separate experiments to consider on the rate of diffusion of ^{37}Ar, ^{39}Ar, and T from lunar soil: the heating curves for the two Apollo 15 soils, the room-temperature diffusion from the Apollo 15 SRC, and our previous laboratory bombardment of simulated lunar fines (Stoenner *et al.*, 1971). Data for T, F, and t from the trench fines are collected in Table 3. For the SRC we take $T = 25$°C, $t = 7.5d$ from box closure on the moon, and ^{37}Ar, ^{39}Ar, and T activities in the 2.3 kg of fines of 31.5, 9.9, and 192 dpm/kg, respectively. Data from the bombardment are given in Fig. 2 of Stoenner *et al.* (1971).

When we plot $\log (D/a^2)$ for each nuclide on a common graph against $1/T$ we find a straight line of surprisingly good quality considering the quite different nature of the three experiments and the wide range of temperatures examined. The plot for ^{39}Ar is given in Fig. 1; the other two are similar. Parameters obtained from least-squares fits for the three nuclides are collected in Table 5.

It is notable that the rate of diffusion loss of tritium into the Apollo 15 SRC is quite in line with the other points of the heating curve. If there were large amounts of loosely bound tritium in the Apollo 15 soil the SRC point would be high. We discuss the implications of this in the next section.

Table 5. Temperature release of Ar and T activities.

	^{37}Ar	^{39}Ar	T
Temperature range (°C)	−76 to 900	−76 to 900	−76 to 600
Number of points	13	13	11
Slope of log D/a^2 against $1/T$*	−3300 ± 230	−2240 ± 210	−2840 ± 280
Intercept*	−4.00 ± 0.66	−5.47 ± 0.60	−3.71 ± 0.88
Activation energy Q (kcal/mole)	15.1 ± 1.0	10.3 ± 1.0	13.0 ± 1.3

* Errors quoted for slope and intercept are standard deviations calculated from the fit, based on Williamson (1968).

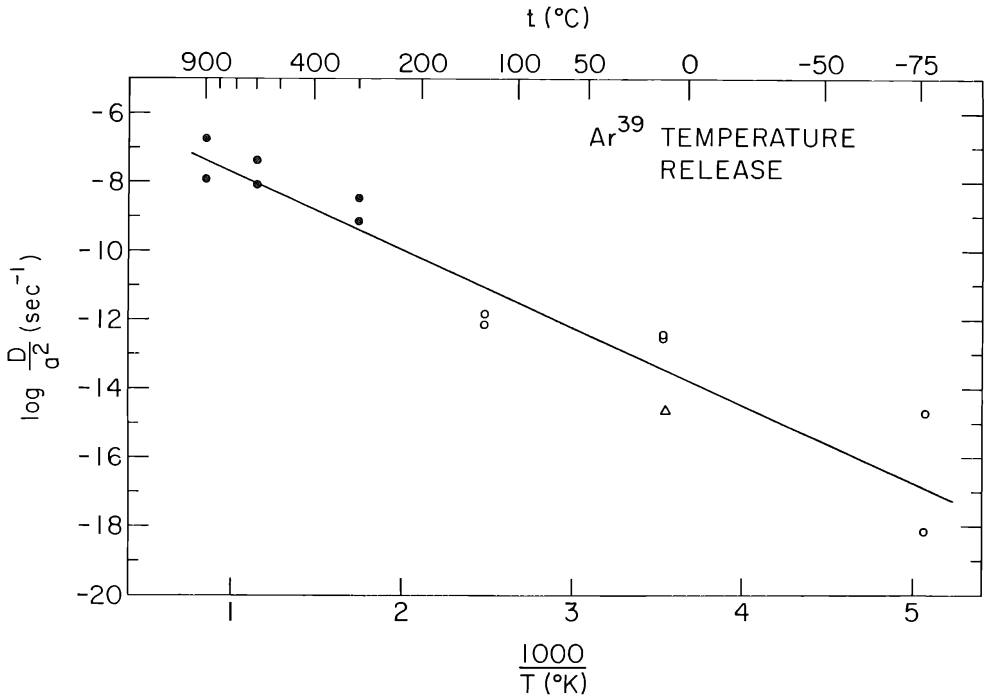

Fig. 1. Temperature release of ^{39}Ar from actual and simulated lunar fines. Solid points are the values obtained from stepwise heating of trench soils 15031,16 and 15041,16; open circles are the 600 MeV bombardment of minerals simulating lunar fines; and the open triangle is the Apollo 15 SRC. The vertical standard deviation of the points from the least-squares line is a factor 11.4.

The activation energies we give in Table 5 are twofold lower than the values found for the diffusion of Ar in meteorites (Fechtig and Kalbitzer, 1966) or hydrogen (Lord, 1967). There are several reasons for this.

At a given high temperature, particularly for the long heating times we employed, the finest particles may degas completely, with the result that as heating continues the gas is evolved from particles of larger a^2. There is independent evidence that the mean grain size in lunar soil is indeed very small. The surface area of 10087 fines has been measured to be 1 m^2/g by adsorption of nitrogen by the BET method (Fuller *et al.*, 1971). A sample of uniform spheres of this specific area and density 3 g/cm^3 would have a diameter of 2 μ, although the area obtained by summing over the sieve distribution determined by Heywood (1971) is 0.07 m^2/g. The difference is accounted for by adhesion of the finest particles to the surfaces of larger grains (McKay *et al.*, 1971; Arrhenius *et al.*, 1972).

A second reason for the low Q we find is an increase of D at low degassing rates by nonvolume diffusion along cracks and dislocations in the heavily shocked lunar soil. The curves in Fechtig and Kalbitzer (1966) clearly show this process overwhelming true volume diffusion at low temperatures. The coarse resolution of our experiments precludes separating the two components, with the result that we see a heat of activation for both volume and nonvolume diffusion.

Removal of rare gases and tritium by diffusion also takes place on the moon. An estimate of the loss of ^{39}Ar, the longest lived nuclide we measure, may be approached

by calculating an average lunar surface value of D/a^2. The exponential temperature dependence is given by the parameters in Table 5, and the variation of the lunar surface temperature with phase is approximated by a sine wave with minimum temperature 90°K and maximum 390°K. Then the average

$$\left(\frac{D}{a^2}\right)_{av} = \frac{1}{2\pi}\int_0^{2\pi} \exp\left[2.303\left(-5.47 - \frac{2240}{240 + 150\sin\phi}\right)\right] d\phi = 1.0 \times 10^{-12}\ \text{sec}^{-1}$$

for ^{39}Ar. The fractional gas loss F is then obtained from a rearrangement of equation (1). For $t = t_{1/2} = 269$ yr, $F_{39} = 0.29$. Similar calculations for ^{37}Ar and T give fractional losses in one halflife of 0.0013 and 0.083, respectively. Clearly diffusive loss is important only for gases of long halflife.

Because of the strong damping of the diurnal heat wave with depth in the regolith, the loss rate just calculated is an upper limit. If we consider that the temperature range is decreased to $1/e$ of the surface value in 4 cm (Hoyt *et al.*, 1971; Robie and Hemingway, 1971), then the ^{39}Ar deficiency we find is reasonably accounted for by a sampling depth comparable to the size of the scoop.

Reimplantation of escaping gas as a result of acceleration by the interplanetary electric field (Manka and Michel, 1970) and the temperate latitude of the Apollo 15 landing site both act further to reduce the importance of this degassing in our soil samples. The higher thermal conductivity and lower porosity of rocks reduce the effect still more, so that the observed ^{39}Ar activity in these samples more nearly reflects the production rate.

Tritium from the Sun

When surface lunar samples became available it was of great interest to search for tritium of solar origin. One recalls that Fireman and his associates (1961) observed excess amounts of tritium implanted in the Discoverer XVII satellite by the solar flare of November 12, 1960. Searches for implanted tritium in lunar materials have not revealed amounts in excess of that expected from cosmic ray interactions. One observation of extremely large amounts of lightly adsorbed tritium was reported by this laboratory on two Apollo 12 rocks, 12063 and 12065 (Stoenner *et al.*, 1971). This observation was made during the quarantine period, and unfortunately was not followed up immediately. The possibility of gross tritium contamination could not be eliminated at the time, and some additional searches for sources of tritium contamination will be described below.

If implanted, easily released, tritium is present in lunar samples, one might expect to find it present in the gas in the SRC. The Apollo 14 mission was the first opportunity to perform this measurement. In this mission a relatively small amount of charcoal was used as an adsorber. The stainless steel finger containing the charcoal and the valve assembly was sterilized at 160°C for 12 hours (a quarantine requirement) before removing the sample for counting. There was, of course, the possibility that tritium could be lost from the charcoal into the stainless steel during this heating. However, a test of this possibility was made at a later time with the trap assembly.

A known amount of hydrogen was adsorbed on the charcoal, the equivalent sterilization heating performed, and the hydrogen was recovered with greater than 90% yield. This experiment demonstrated that tritium losses during sterilization were small, and the measurements performed on the Apollo 14 SRC were valid. The measurements on Apollo 14 showed that very little tritium was present in the gas, even though the lunar surface was exposed to a solar flare 12 days prior to the mission. The small amount of tritium that was observed can easily be accounted for by diffusion from the fine material in the box. This was discussed quantitatively in an earlier section.

A second sample was obtained from the Apollo 15 SRC. In this experiment a larger amount of charcoal was used (10 g) and since there was no quarantine restriction, the assembly remained at room temperature (4 days) until the gas was removed. In addition, an activated vanadium metal hydrogen absorber (10 g) was used. This absorber will quantitatively absorb H_2 at room temperature. In this experiment 0.279 ± 0.005 dpm T was observed on the charcoal adsorber and 0.225 ± 0.007 dpm T was observed on the vanadium metal absorber. Again, it is clear that very little tritium is present in the gas phase of the sample return container. We can then safely conclude that there was little or no lightly adsorbed tritium present on the rock and soil samples returned by the Apollo 14 and 15 missions. Conditions for finding solar tritium were nearly ideal in the Apollo 14 mission. In the 12 days between a major flare and the landing, the sampling site was dark and cold, so tritium should have been retained well. We conclude that there was little or no tritium in the flare of January 24, 1971.

As mentioned earlier, large quantities of lightly adsorbed tritium was found on two rock samples measured during the Apollo 12 quarantine period. As much as 200 dpm of tritium was released at room temperature from a 10 g sample of rock, an enormous quantity. Because the amount of tritium was so large, we attributed it to gross surface contamination, though there was no obvious source of tritium in the spacecraft or at the Lunar Receiving Laboratory. Fireman and his associates (D'Amico *et al.*, 1971) examined one of these rocks (12065) for lightly adsorbed tritium 6 months later and found that no tritium was released from their sample at room temperature. This result could be explained easily if the tritium was only adsorbed on the surface. The question could be settled by finding a source of tritium contamination, but if none is found there is the real possibility that the large amount of tritium seen on these samples was of solar origin.

We would like now to describe some further efforts that were made to locate the sources of tritium contamination. Since these samples were returned from the lunar surface to the Lunar Receiving Laboratory not in a SRC but in the tote bag, the atmosphere inside the Command Module (CM) was considered as a possible source. A lithium hydroxide scrubber is used in the CM to remove carbon dioxide from the spacecraft atmosphere. Cosmic ray produced slow neutrons will yield tritium by the high cross section reaction $^6\mathrm{Li}(n,\alpha)T$. One would expect that the tritium so formed would be retained as water in the lithium hydroxide, and consequently would be released to the atmosphere of the CM at a very low rate.

Samples of the air inside the CM from Apollo 14 were taken immediately after opening the hatch upon its delivery to the Lunar Receiving Laboratory. The CM

had not been opened since the transfer of the astronauts to the Mobile Quarantine Facility aboard the recovery carrier, hence this should be a representative sample of the tritium level in the CM during the mission. Both tritium as hydrogen gas and tritium as water vapor were considered as possible chemical forms. Hydrogen gas was separated from the air by contacting with powdered vanadium metal at room temperature. The hydrogen was then evolved, diffused through hot palladium and counted. No tritium activity was observed in this fraction. The water vapor was separated from the air by freezing with liquid nitrogen and pumping away the air. The water was then treated with hot vanadium metal and the resulting hydrogen was purified and counted as above. The tritium activity in the CM was found to be 5.0 $\pm$ 0.3 dpm/liter of air, far too low to be considered a source of tritium contamination responsible for the large amount of tritium observed on rocks 12063 and 12065.

An additional sample was taken in the CM after the ventilation system had been started again, at a point near the lithium hydroxide cannister exhaust. Only the tritium in the water vapor was measured in this sample and it was found to be a little higher, 6.4 $\pm$ 0.2 dpm/liter, than the previous sample but still too low to contribute substantially to samples transported exposed in the CM. It should be remarked that the tritium levels observed in the water in these samples is very high compared to normal earth environmental samples. The T/H ratio corresponding to 5 dpm T per liter of air would be $50{,}000 \times 10^{-18}$, whereas terrestrial T/H ratios are from 20 to 50×10^{-18}. The CM levels are a factor of 1000 under maximum permissible concentrations for continuous exposure.

^{222}Radon in the Sample Return Container and on the Moon

Material in the SRC should be, for the reasons mentioned above, the best sample on which to determine the emanation rate of ^{222}Rn. Appreciable emanation should lead to an enrichment of daughter activities on the lunar surface. The topic has been widely studied (Yeh and Van Allen, 1969; Turkevich *et al.*, 1970; Economou and Turkevich, 1971; Stoenner *et al.*, 1971; Lindstrom *et al.*, 1971; Adams *et al.*, 1971; Yaniv and Heymann, 1972; Lambert *et al.*, 1972; Gorenstein and Bjorkholm, 1972) with considerable variation in the inferred flux of Rn into the lunar atmosphere. The present section is an attempt to rationalize this variation.

The ^{222}Rn observed in the SRC is attributed to radon loss from the fine material contained in the box (Stoenner *et al.*, 1971). The ^{222}Rn data from the Apollo 12, 14, and 15 missions are given in Table 2. To explain the quantities we observe, we discuss below the processes responsible for Rn emanation: recoil and stopping of daughter Rn from soil grains, and thermal diffusion through the pores of the soil.

Radon is first formed in the regolith by escape of recoil atoms resulting from α decay of ^{226}Ra. The fraction of decays recoiling from a grain of diameter a is

$$P = \frac{3}{2}\frac{L}{a} - \frac{1}{2}\left(\frac{L}{a}\right)^3$$

(Giletti and Kulp, 1955), where L is the recoil range. Combination of this relation with the particle size distribution of Heywood (1971) shows that recoil from 5–15 μ

grains accounts for nearly half the radon escape. For this size distribution the integrated escape is proportional to the range L, and $P = 1 \times 10^{-3}$ for $L = 200$ Å. This is indeed the fraction we find in the SRC (Table 2).

This calculation assumes that the size distribution of uranium-bearing phases is the same as that of the soil as a whole. In view of the observation of Burnett *et al.* (1971) and Haines *et al.* (1972) that U is concentrated in the finer grains of lunar rocks and soils, the calculation may be low and not all recoiling Rn atoms find their way into the atmosphere of the SRC.

The efficiency of release depends on thermalization and on diffusion of Rn atoms. The latter process is characterized by the diffusion constant D, which may be very different from values measured in terrestrial settings. In the absence of direct measurements we attempt to calculate D, following Friesen and Heymann (1972). From kinetic theory $D = x\bar{v}/3$, where x is the mean free path and $\bar{v}$ the mean velocity of Rn atoms. In turn, $\bar{v} = x/(t_f + t_a)$, where $t_f = x\sqrt{\pi m/8kT}$ is the flight time across a distance x for an atom of mass m at temperature T. The second term t_a is the time an atom spends adsorbed on a surface, and is given by $t_a = t_0 e^{Q/RT}$ (de Boer, 1953) where Q is the heat of adsorption.

Values of these parameters may be estimated. The mean free path x may be taken as $\bar{d}p$, where $\bar{d}$ is a typical grain size and p the porosity. Taking $\bar{d} = 3\ \mu$ as the number median diameter (Görz *et al.*, 1971) and $p = 0.5$, a reasonable $x = 1.5\ \mu$. The characteristic sticking time t_0 is estimated from de Boer's (1953) equation $t_0 = 4.75 \times 10^{13}\sqrt{M_s V^{2/3}/T_s}$. Using the mean molecular weight M and molar volume V of lunar soil calculated from Morrison's (1971) compilation for 12070, and the melting temperature T_s taken from Green *et al.* (1970), we calculate $t_0 = 1.1$–1.2×10^{-13} sec. For comparison, de Boer (1953) gives $t_0 = 0.75$, 0.95, and 0.67×10^{-13} sec for Al_2O_3, SiO_2, and MgO, respectively. We take $t_0 = 0.9 \times 10^{-13}$ sec as a fair average. The heat of adsorption Q of Rn on charcoal has been measured to be 7.51 kcal/mole from air (Gübeli and Störi, 1959) and estimated to be 13.5 ± 1.4 kcal/mole at low surface coverage in vacuum (Chackett and Tuck, 1957). In view of the low surface energy observed by Fuller *et al.* (1971) in adsorption of N_2 and CO on soil sample 10087, however, Q in lunar soil may not be so high. The lower limit is the heat of vaporization of liquid Rn, which is 4.3 kcal/mole. The most likely range is 10 ± 3 kcal/mole. Measurement of this quantity is in progress.

The diffusion constant calculated from these numbers is 4×10^{-1}, 4×10^{-3}, and 3×10^{-5} cm^2/sec for $T = 300$ K and $Q = 7$, 10, and 13 kcal/mole, respectively. These values are high enough that diffusion from the sample of soil in the rockbox is rapid during transport from the moon to the LRL. The exponential temperature dependence of the adsorption term, however, makes diffusion slow ($D = 10^{-5\pm3}$) at 225 K, the mean temperature of the regolith below a few decimeters in situ.

The flux J of Rn emanating from the lunar surface is, from a simple diffusion model (Wilkening and Hand, 1960; Schroeder *et al.*, 1965),

$$J = C_\infty \sqrt{\lambda D}$$

where C_∞ is the amount of Rn free to diffuse per unit volume of bulk soil, at a depth large compared to the diffusion length $\sqrt{2D/\lambda}$, and D is the diffusion constant, and λ is the decay constant of ^{222}Rn.

Taking 1 ppm U, an emanating power (the product of recoil and stopping efficiencies) of 10^{-3} from our SRC measurements, and $D = 10^{-5}$ cm^2/sec, we calculate $J = 3 \times 10^{-7}$ atoms/cm^2 sec. This is to be compared with the lowest observed upper limit of 2×10^{-5} alpha disintegrations/cm^2 sec (Lambert *et al.*, 1972). It should be clear that the present estimate is good to no better than an order of magnitude in J; the uncertainty in Q, and hence D, is the most important unknown at present.

Acknowledgments—We are indebted to the staff of the Lunar Receiving Laboratory, and especially the Gas Analysis Laboratory, for their assistance and the use of their facilities. The 600-MeV proton irradiation was performed by the staff of the NASA Space Radiation Effects Laboratory, Newport News, Va. We thank Don Bogard, Robert Reedy, and John Evans for useful discussions. This work was supported by NASA and the AEC.

References

Adams J. A. S., Barretto P. M., Clark R. B., and Duval J. S. (1971) Radon-222 emanation and the high apparent lead isotope ages in lunar dust. *Nature* **231,** 174–175.

Arrhenius G., Asunmaa S. K., and Fitzgerald R. W. (1972) Electrostatic properties of lunar regolith (abstract). In *Lunar Science—III* (editor C. Watkins), pp. 30–32, Lunar Science Institute Contr. No. 88.

Burnett D., Monnin M., Seitz M., Walker R., and Yuhas D. (1971) Lunar astrology—U–Th distributions and fission-track dating of lunar samples. *Proc. Second Lunar Sci. Conf., Geochim. Cosmochim. Acta* Suppl. 2, Vol. 2, pp. 1503–1519. MIT Press.

Chackett K. F. and Tuck D. G. (1957) The heats of adsorption of the inert gases on charcoal at low pressure. *Trans. Farad. Soc.* **53,** 1652–1658.

D'Amico J., De Felice J., and Fireman E. L. (1970) The cosmic-ray and solar-flare bombardment of the moon. *Proc. Apollo 11 Lunar Sci. Conf., Geochim. Cosmochim. Acta* Suppl. 1, Vol. 2, pp. 1029–1036. Pergamon.

D'Amico J., De Felice J., Fireman E. L., Jones C., and Spannagel G. (1971) Tritium and argon radioactivities and their depth variations in Apollo 12 samples. *Proc. Second Lunar Sci. Conf., Geochim. Cosmochim. Acta* Suppl. 2, Vol. 2, pp. 1825–1839. MIT Press.

de Boer J. H. (1953) *The Dynamical Character of Adsorption.* Oxford Press.

Economou T. E. and Turkevich A. L. (1971) Examination of returned Surveyor III camera for alpha radioactivity. *Proc. Second Lunar Sci. Conf., Geochim. Cosmochim. Acta* Suppl. 2, Vol. 3, pp. 2699–2703. MIT Press.

Fechtig H. and Kalbitzer S. (1966) The diffusion of argon in potassium-bearing solids. In *Potassium Argon Dating* (editors: O. A. Schaeffer and J. Zahringer), pp. 68–107. Springer-Verlag.

Fireman E. L., De Felice J., and Tilles D. (1961) Solar flare tritium in a recovered satellite. *Phys. Rev.* **123,** 1935–1936.

Fireman E. L., D'Amico J., De Felice J., and Spannagel G. (1972) Radioactivities in Apollo 14 and 15 materials (abstract). In *Lunar Science—III* (editor C. Watkins), pp. 262–264, Lunar Science Institute Contr. No. 88.

Friesen L. J. and Heymann D. (1972) Model for radon diffusion through the lunar regolith. Proc. Conf. on Lunar Geophysics, *The Moon* (in press).

Fuller E. L., Holmes H. F., Gammage R. B., and Becker K. (1971) Interaction of gases with lunar materials: Preliminary results. *Proc. Second Lunar Sci. Conf., Geochim. Cosmochim. Acta* Suppl. 2, Vol. 3, pp. 2009–2019. MIT Press.

Giletti B. J. and Kulp J. L. (1955) Radon leakage from radioactive minerals. *Amer. Mineral.* **40,** 481–496.

Gorenstein P. and Bjorkholm P. (1972) Results of the Apollo 15 alpha particle spectrometer experiment (abstract). In *Lunar Science—III* (editor C. Watkins), pp. 326–328, Lunar Science Institute Contr. No. 88.

Görz H., White E. W., Roy R., and Johnson G. G. (1971) Particle size and shape distributions by CESEMI. *Proc. Second Lunar Sci. Conf., Geochim. Cosmochim. Acta* Suppl. 2, Vol. 3, pp. 2021–2025. MIT Press.

Green D. H., Ringwood A. E., Ware N. G., Hibberson W. O., Major A., and Kiss E. (1971) Experimental petrology and petrogenesis of Apollo 12 basalts. *Proc. Second Lunar Sci. Conf., Geochim. Cosmochim. Acta* Suppl. 2, Vol. 1, pp. 601–615. MIT Press.

Gübeli O. and Störi M. (1954) Zur Mischadsorption von Radon an Aktivkohle mit verschiedenen Trägergasen. *Helv. Chim. Acta* **37,** 2224–2230.

Haines E. L., Gancarz A. J., Albee A. L., and Wasserburg G. J. (1972) The uranium distribution in lunar soils and rocks 12013 and 14310 (abstract). In *Lunar Science—III* (editor C. Watkins), pp. 350–352, Lunar Science Institute Contr. No. 88.

Heywood H. (1971) Particle size and shape distribution for lunar fines sample 12057,72. *Proc. Second Lunar Sci. Conf., Geochim. Cosmochim. Acta* Suppl. 2, Vol. 3, pp. 1989–2001. MIT Press.

Hoyt H. P., Miyajima M., Walker R. M., Zimmerman D. W., Zimmerman J., Britton D., and Kardos J. L. (1971) Radiation dose rates and thermal gradients in the lunar regolith: Thermoluminescence and DTA of Apollo 12 samples. *Proc. Second Lunar Sci. Conf., Geochim. Cosmochim. Acta* Suppl. 2, Vol. 3, pp. 2245–2263.

Lambert G., Grejebine T., Le Roulley J. C., and Bristeau P. (1972) Alpha spectrometry of a surface exposed lunar rock (abstract). In *Lunar Science—III* (editor C. Watkins), pp. 472–474, Lunar Science Institute Contr. No. 88.

Lindstrom R. M., Evans J. C., Finkel R. C., and Arnold J. R. (1971) Radon emanation from the lunar surface. *Earth Planet. Sci. Lett.* **11,** 254–256.

Lord H. C. (1967) Ph.D. Thesis, University of California, San Diego.

LSPET (Lunar Sample Preliminary Examination Team) (1970) Preliminary examination of lunar samples from Apollo 12. *Science* **167,** 1325–1339.

LSPET (Lunar Sample Preliminary Examination Team) (1971) Preliminary examination of lunar samples from Apollo 14. *Science* **173,** 681–693.

LSPET (Lunar Sample Preliminary Examination Team) (1972) The Apollo 15 lunar samples: A preliminary description. *Science* **175,** 363–375.

Lyman W. J. (1971) Production of ^{37}Ar, ^{39}Ar, ^{42}Ar, and T induced by 600-MeV proton bombardments on Ca, K, Ti and a simulated lunar target. BNL preliminary report, available on request from the author.

Manka R. H. and Michel F. C. (1970) Lunar atmosphere as a source of argon-40 and other lunar surface elements. *Science* **169,** 278–280.

McKay D. S., Morrison D. A., Clanton U. S., Ladle H. G., and Lindsay J. F. (1971) Apollo 12 soils and breccia. *Proc. Second Lunar Sci. Conf., Geochim. Cosmochim. Acta* Suppl. 2, Vol. 1, pp. 755–773. MIT Press.

Morrison G. H. (1971) Evaluation of lunar elemental analyses. *Anal. Chem.* **43** (7), 22A–31A.

Reedy R. C. and Arnold J. R. (1972) Interaction of solar and galactic cosmic-ray particles with the moon. *J. Geophys. Res.* **77,** 537–555.

Robie R. A. and Hemingway B. S. (1971) Specific heats of the lunar breccia (10021) and olivine dolerite (12018) between 90° and 350° Kelvin. *Proc. Second Lunar Sci. Conf., Geochim. Cosmochim. Acta* Suppl. 2, Vol. 3, pp. 2361–2365. MIT Press.

Schroeder G. L., Kraner H. W., and Evans R. D. (1965) Diffusion of radon in several naturally occurring soil types. *J. Geophys. Res.* **70,** 471–474.

Stoenner R. W., Lyman W. J., and Davis R. Jr. (1970) Cosmic-ray production of rare-gas radioactivities and tritium in lunar material. *Proc. Apollo 11 Lunar Sci. Conf., Geochim. Cosmochim. Acta* Suppl. 1, Vol. 2, pp. 1583–1594. Pergamon.

Stoenner R. W., Lyman W., and Davis R. Jr. (1971) Radioactive rare gases and tritium in lunar rocks

and in the sample return container. *Proc. Second Lunar Sci. Conf., Geochim. Cosmochim. Acta* Suppl. 2, Vol. 2, pp. 1813–1823. MIT Press.

Turkevich A. L., Patterson J. H., Franzgrote E. J., Sowinski K. P., and Economou T. E. (1970) Alpha radioactivity of the lunar surface at the landing sites of Surveyors 5, 6, and 7. *Science* **167,** 1722–1724.

Wilkening M. H. and Hand J. E. (1960) Radon flux at the earth–air interface. *J. Geophys. Res.* **65,** 3367–3370.

Williamson J. H. (1968) Least-squares fitting of a straight line. *Can. J. Phys.* **46,** 1845–1847.

Yaniv A. and Heymann D. (1972) Radon emanation from Apollo 11, 12, and 14 fines (abstract). In *Lunar Science—III* (editor C. Watkins), pp. 816–818, Lunar Science Institute Contr. No. 88.

Yeh R. S. and Van Allen J. A. (1969) Alpha-particle emissivity of the moon: An observed upper limit. *Science* **166,** 370–372.

Proceedings of the Third Lunar Science Conference
(Supplement 3, *Geochimica et Cosmochimica Acta*)
Vol. 2, pp. 1719–1732
The M.I.T. Press, 1972

Cosmogenic nuclides in football-sized rocks

M. WAHLEN, M. HONDA,* M. IMAMURA, J. S. FRUCHTER,† R. C. FINKEL,
C. P. KOHL, J. R. ARNOLD, and R. C. REEDY

Department of Chemistry, University of California,
San Diego, La Jolla, California

Abstract—Short- and long-lived radionuclides were measured in rock 14321 at depths of ~ 0.3 g/cm^2, ~ 1.1 g/cm^2, 18 g/cm^2, and 40 g/cm^2. The effects of solar cosmic rays are seen in the upper samples of 14321. After correcting for an attrition to the rock (loss of surface material in handling) of (0.4 ± 0.2) mm, the Co^{56} measurements imply, for the flare of January 24, 1971, a J (>10 MeV) of 200 protons/cm^2 sec (4π) averaged over the mean life of Co^{56} and an R_0 (exponential rigidity parameter) of 100 MV, in good agreement with satellite data (Bostrom *et al.*). The Fe^{55} and Na^{22} values, which average over many flares, are consistent with our rock 12002 measurements (Finkel *et al.*). The near surface profiles of the longer-lived isotopes, Mn^{53} and Al^{26}, suggest an erosion rate of about 2 mm/10^6 yr. Mn^{54}, Cl^{36}, and Be^{10} were also measured in 14321.

Fe^{55}, Be^{10}, and Mn^{53} were measured in a slice of rock 14310 from 24 g/cm^2 average depth. This sample was also separated into two density fractions enabling the production rates for Na^{22}, Cl^{36}, and Al^{26} from different target elements to be determined.

The activities in our sample of 14310 and in our deepest sample of 14321 have no contribution from solar cosmic rays and give the beginning of the galactic cosmic-ray depth profile. A brief comparison between the data and the Reedy–Arnold model (Reedy and Arnold) is discussed.

We also measured Co^{56}, Na^{22}, Al^{26}, and Mn^{53} in a sample of soil 14259. The observed solar cosmic ray produced activities are consistent with an average depth for the soil sample of 1 cm (1.8 g/cm^2).

INTRODUCTION

THE STUDY OF lunar surface samples from the Apollo 11 and Apollo 12 missions has shown that the production of cosmogenic nuclides can be accounted for by bombardment by two classes of high-energy particles. The solar cosmic rays (SCR) produce significant effects on a depth scale of a few g/cm^2, while the galactic cosmic rays (GCR) penetrate to greater depths (Finkel *et al.*, 1971; Rancitelli *et al.*, 1971; O'Kelley *et al.*, 1971).

Rock 14321, a 9 kg fragmental rock whose orientation was photographically documented on the lunar surface, provided an opportunity to extend our study of the variation of production of radionuclides with depth down to about 40 g/cm^2, a region where according to present ideas only GCR effects should be important. We therefore measured the activity of long- and short-lived isotopes in a series of samples from a vertical column through the center of this rock, 14321. Also investigated was a sample from the lower portion of rock 14310 where, in order to study target effects, two different density fractions (mineral separates) were analyzed. In addition we

* Present address: Institute for Solid State Physics, University of Tokyo, Tokyo, Japan.

† Present address: Center for Volcanology, Department of Geology, University of Oregon, Eugene, Oregon.

measured a few nuclides in a sample from the comprehensive fines 14259, material reported to have been collected largely from the top centimeter of the lunar soil.

The study of the deep samples of 14321 and 14310 provided us with values for the activity of isotopes at points where only GCR effects are significant. At the same time, the results obtained from the surface samples of 14321 confirm the effects of solar cosmic rays observed earlier.

EXPERIMENTAL TECHNIQUES

Sample description

Three categories of samples were used in this study. 14259,18 (FS) was a 5 g sample of lunar soil with a nominal depth of 0–1 cm (0–1.8 g/cm^2).

The second sample 14310,47 was a 5.5 cm long column taken from the bottom center of rock 14310. This rock is a fine grained igneous rock of density 2.9 g/cm^3 and weighs 3.4 kg. Its orientation on the lunar surface has been evaluated by counting in Houston (LSPET, 1971). The depth of our sample below the top of the rock was from 5.5–11 cm (Fig. 1).

Our most extensive set of samples was obtained from rock 14321, a complex fragmental rock of approximately 9 kg total mass and density 3.0 g/cm^3. The orientation of this "football-sized" rock on the lunar surface was documented photographically by the Apollo 14 astronauts. It was buried to ~4 cm in the lunar soil (cf. waterline Fig. 1). The three samples which we received (14321,91; 14321,92; 14321,123) were slices sawn from a large vertical column which was cut so that its base would be the most shielded position in the rock (cf. Fig. 1). The uppermost slice was further subdivided by grinding into samples of nominal depth 0–2 mm, FM-1, and 2–5 mm, FM-2, with an uncertainty of 0.5 mm. A large pit covered about 10% of the surface area. The middle sample, FM-3, has a mean

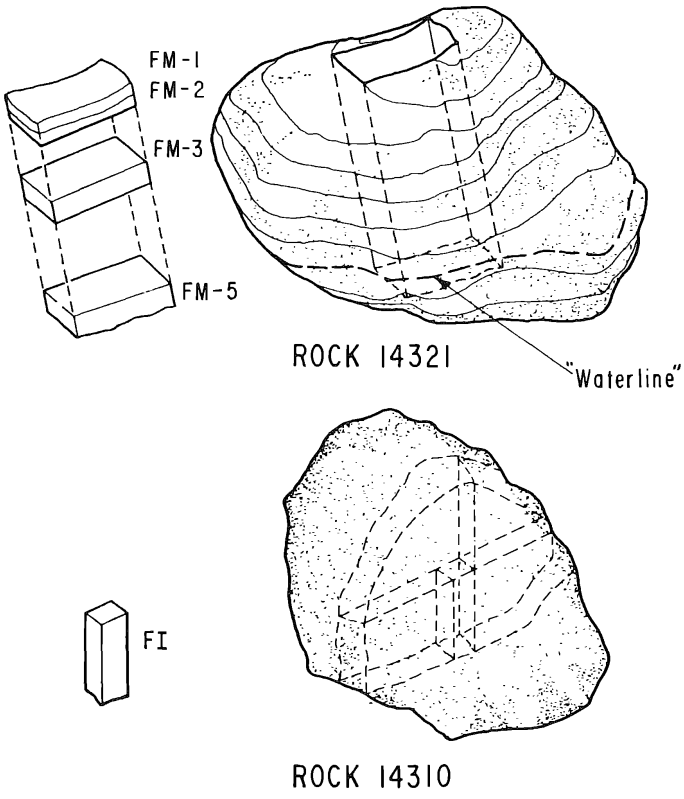

Sample		Depth (g/cm^2)
14321	FM-1	0-0.63
	FM-2	0.63 - 1.62
	FM-3	18
	FM-5	40
14310	FI	24

Fig. 1. Location of the samples from rocks 14321 and 14310.

depth of about 18 g/cm^2 and a thickness of ~3 g/cm^2; the bottom sample, FM-5, a mean depth of 40 g/cm^2 and a thickness of ~3 g/cm^2.

Chemical procedure

Some mineral grains were picked from each sample for track analysis (Arrhenius, priv. comm.), and samples were also taken for rare gas studies and Gd-isotope analysis (Lugmair and Marti, 1971; Lugmair and Marti, 1972). The rock slices were then ground to below 120 μ size under isopropyl alcohol. Grinding was difficult because of the mixture of hard and soft regions, which are characteristic of such a fragmental rock.

In order to get information on target effects in the galactic cosmic ray production of certain radionuclides, 27 g of the sample of 14310 was subjected to a mineral separation procedure. The sample, ground to finer than 120 μ size, was separated into 3 density fractions using aquaeous Tl-malonate-formate heavy liquid. The density fractions were selected with the goal of separating the two major mineral components, plagioclase ($\rho < 2.8$ g/cm^3) and clinopyroxene ($\rho > 3.2$ g/cm^3). The heavy density separate, FIH ($\rho > 3.22$), made up 36% of the total sample; the middle density separate, FIM ($3.0 \leq \rho \leq 3.22$), 14%; and the light density separate, FIL ($\rho < 3.0$), 50%. Only FIH and FIL were used, since the middle density fraction was regarded as a mixture of clinopyroxene and plagioclase. The separation of clinopyroxene and plagioclase obtained seemed to be satisfactory, as can be seen from the chemical compositions of FIH and FIL (Table 1). We were able to observe target effects in the induced activities of Al^{26}, Na^{22}, and Cl^{36}.

Table 1. Chemical composition of Apollo 14 samples determined by atomic absorption spectroscopy and colorimetry.

	14321				14259	14310		
	FM-1	FM-2	FM-3	FM-5	FS	FIH	FIL	FI (calc.)
Na (ppm)	4890	5260	5500	5330	4800	1540	7830	5560
Mg (%)	6.3	6.4	6.4		5.6	11.5	1.0	4.8
Al (%)	7.8	8.0	8.3	8.2	9.2	3.0	16.3	11.5
Si (%)			21.9		22.3	23.3	21.1	21.9
K (ppm)	3100	4000	4800	4000	4100	1580	5040	3800
Ca (%)	7.8	7.7	7.9	7.8	7.7	5.0	11.9	9.4
Ti (%)			1.4		1.0	1.7	0.42	0.87
Mn (ppm)	1460	1440	1210	1280	1050	1830	278	840
Fe (%)	10.9	10.9	9.5	10.5	8.0	13.6	2.4	6.4

About 0.25 g of each sample was used for the determination of the concentration of the chief target elements. For the soil, 14259, where the size of our sample did not permit us to take such an aliquot, the data were adopted from analyses by other investigators. Measurements were done by atomic absorption spectrometry for all elements except Ti, which was determined by colorimetry. For Si, $LiBO_2$ fusion followed by atomic absorption spectrometry was applied using a separate 50 mg aliquot (Ingamells, 1966). For Cl the results of Reed *et al.* (1972) were used.

The chemical separation procedure for the radionuclides was essentially the same as in Apollo 11 and Apollo 12 (Shrelldalff, 1970; Finkel *et al.*, 1971) with some small modification in the Co and Mn chemistries. Be, Ar, Cl, Co, and I carriers were added at the stage of the still chemistry and Be, Na, Al, Cl, Mn, Fe, and Co were then separated and purified.

The counting sample for Co^{56} was plated on a copper sample holder in an area of 1.8 cm × 3 cm from a plating solution of hydrazine sulfate (1 g/100 cc), ammonium tartrate (0.3 g/100 cc), and ammonium sulfate (5 g/100 cc). The *p*H was held between 5–7 with NH_4OH and an applied voltage of 2 V was used.

Mn^{53} was determined by neutron activation analysis following a procedure similar to that described in Finkel *et al.* (1971).

Counting

The counting was done with essentially the same detectors and equipment as previously reported (Shrelldalff, 1970; Finkel *et al.*, 1971), except for the modifications described below.

For isotopes such as Fe^{55}, which decay purely by electron capture, the method of pulse-rise-time discrimination has been applied (Davis *et al.*, priv. comm.) to the existing proportional counters in order to increase the precision of the measurements. This method makes use of the fact that in a given proportional counter the x-rays following an electron capture decay cause output signals different in rise-time from those triggered by "background events." X-rays of a few keV, because of their short ranged secondary ionization (interaction of the primary photo-electron with the counter gas) produce a response signal of short rise-time, typically ~10 nsec. On the other hand, "background events" (charged cosmic ray particles, Compton electrons, interactions in the ineffective volume) lead to longer-range ionization, thus producing signals with considerably longer rise-times, typically ~100 nsec. To take advantage of this difference the pulse-height analysis is performed in a two-parameter mode, using two separate amplifiers (with their differentiation-time-constants of about 10 nsec and 100 nsec, respectively) and two ADC's. In order to get sufficient resolution, a large memory array is necessary. This large memory has been obtained by interfacing the counter system on-line to an IBM-1800 computer (with large disc storage capacity) allowing us to obtain a maximum memory array of 256 × 256 channels. By this method the background was reduced in the case of Fe^{55} by a factor 4 to 5, to 0.016 cpm without a substantial loss of efficiency.

A 40 cc Ge-Li well-detector (diameter of the well = 5 mm) was used for the measurement of Mn^{54}. For the 835 keV line of Mn^{54} the resolution with this detector is 3.5 keV FWHM. The absolute total photopeak efficiency is 3.4%. The corresponding background, when operated in anticoincidence with a NaI guard annulus, is 0.07 cpm.

RESULTS

Counting

The concentrations of radioisotopes found in the samples of rock 14321 and 14310 (including separate phases) and in the soil sample 14259 are given in Table 2. The activities are corrected to 6 February 1971. The errors quoted include (quadratically added) a one-standard deviation counting error, a 5% error due to calibration standards used for the determination of the detector efficiencies, a 5 to 10% error in the self-absorption correction where applicable, and a 5% error for the chemical yield. In the case of Co^{56}, where three commercially available standard sources differed widely among themselves, we allowed for a 10% error in the absolute efficiency.

Background counting was performed using blank samples made from Indian Ocean basalts (with appropriate amounts of K, Th, and U mixed in), which underwent the same chemical treatment as the actual lunar samples. In the case of rock 14310 the results for Fe^{55}, Mn^{53}, and Be^{10} denoted as FI are from direct measurements of the combined elemental fractions of FIL and FIH, whereas those for Al^{26}, Na^{22}, and Cl^{36} are calculated from the measurements on the separate phases.

Keith *et al.* (1972) measured several cosmogenic radionuclides in soil sample 14259,18. Their results and ours are, respectively [Co^{56} (60 ± 30, 47 ± 24); Al^{26} (222 ± 9, 170 ± 21); Na^{22} (91 ± 8, 89 ± 14)]. The agreement is quite good except for Al^{26} where there seems to be some discrepancy. Several groups (Keith *et al.*, 1972; Rancitelli *et al.*, 1972; Eldridge *et al.*, 1972) made measurements of cosmogenic radionuclides similar to ours in rocks 14321 and 14310. The data available at present do not allow a detailed comparison with our measurements. The results, however, do seem to be in general agreement.

Table 2. Counting results (dpm/kg rock), corrected to February 6, 1971.

Sample			Isotope							
	Wt. (g)	Depth (g/cm^2)	Co^{56} (77 days)	Mn^{54} (303 days)	Fe^{55} (2.6 yr)	Na^{22} (2.6 yr)	Al^{26} (7.4×10^5 yr)	Mn^{53} (3.7×10^6 yr)	Cl^{36} (3.1×10^5 yr)	Be^{10} (2.5×10^6 yr)
14321,91										
FM-1	6.9	0.0–0.63*	220 ± 45	41 ± 11	310 ± 40	116 ± 13	148 ± 16	44 ± 3	10.7 ± 1.5	12.8 ± 2.3
FM-2	19.0	0.63–1.62*	78 ± 30		135 ± 20	71 ± 7	109 ± 13	36 ± 2		
14321,92										
FM-3	27.5	18		21 ± 6	26 ± 7	39 ± 5	57 ± 7	23 ± 2	11.2 ± 1.6	13.8 ± 2.0
14321,123										
FM-5	42	40		27 ± 5	34 ± 8	32 ± 4	54 ± 8	25 ± 2	12.1 ± 1.6	12.3 ± 2.0
14310,47										
FIL	11.6	24				28 ± 6	80 ± 13		15.9 ± 2.2	
FIH	8.7	24				38 ± 5	47 ± 7		7.3 ± 1.5	
Total										
FI		24			22 ± 6	32 ± 4 calc.	65 ± 9 calc.	16 ± 1	12.3 ± 2.0 calc.	13.1 ± 2.3
14259,18										
FS	4.4	0.0–1.8†	47 ± 24			89 ± 14	170 ± 21	44 ± 2		

* This number does not include an attrition of 0.12 g/cm^2.

† Reported depth LSPET (1971); most probable depth 0–3.6 g/cm^2 derived from our measurements.

Chemical composition

The chemical composition of each sample is shown in Table 1. That of 14259 was taken from the data of several authors (Schnetzler *et al.*, 1971; Wänke *et al.*, 1972; Jackson *et al.*, 1972; Klein *et al.*, 1972). The variation of the chemical composition of 14321 from sample to sample was small but not negligible.

DISCUSSION

Solar cosmic ray effects

The surface samples FM-1 and FM-2 (and FS) show the now familiar effects due to solar cosmic-ray bombardment.

Co^{56} in these samples is essentially produced only by SCR's. Because of its short half-life, Co^{56} production is dominated by recent solar flares. We know of only one flare of importance, that of 24 January 1971, that occurred close enough to the time of the Apollo 14 mission to have produced a significant amount of Co^{56}.

Comparison of the measured activities of Co^{56}, 220 $\pm$ 45 dpm/kg for FM-1 and 78 $\pm$ 30 dpm/kg for FM-2, with activities predicted by theoretical calculations based on satellite data (Bostrom *et al.*, 1971) for the January 1971 flare immediately implies that considerable attrition, i.e., loss of surface material due to handling and transit of the rock, has occurred. This fact is confirmed when one examines the activities observed for Fe^{55} and Na^{22}. The best estimate for the amount of attrition as derived from these three isotopes is (0.4 $\pm$ 0.2) mm. This estimate is in excellent agreement with an estimate derived from comparison with the Co^{56} measurements of Schonfeld (private communication) on rock 14310. After correction for the different Fe content, these measurements show a total activity (dpm/cm^2) about one-quarter greater in rock 14310 than in 14321. This excess is just what one would expect if rock 14321 had lost about 0.4 mm after its collection from the moon. Such a loss is very much in accord with the friability of 14321, a fragmental rock, as opposed to the strongly cohesive nature of 14310.

The best fit of our Co^{56} data to the calculated values is obtained if we use an exponential rigidity shape with an R_0 of 100 MV and an equivalent steady state flux of J ($E > 10$ MeV) = 200 protons/cm^2 sec (4π) for the spectral shape and the intensity of the 24 January flare. The values reported from the data obtained by the solar proton monitor experiment (Bostrom *et al.*, 1971) correspond to an R_0 of about 70 MV and J = 160 p/cm^2 sec (4π) [or J ($E > 10$ MeV) = 1.5×10^9 protons/cm^2 for the whole flare]. If we adopt the value of R_0 = 75 MV, to which our data also fit well within the limits of error, we find a J of 175 p/cm^2 sec (4π) in good agreement with the satellite data. This flare seems to have been approximately 50% more intense and perhaps somewhat harder than the November 1969 flare responsible for the Co^{56} production we observed in rock 12002.

In the light of this analysis the measurements of 35-day Ar^{37} (Fireman *et al.*, 1972) on surface samples of 14321 similar to ours are quite puzzling. We can correct for GCR production by using measurements of Ar^{37} in rock 15555 (Fireman *et al.*, 1972) which, because of the lack of flares immediately before the Apollo 15 mission, show

essentially no SCR effect. The net solar cosmic-ray production profile in 14321 is then seen to be relatively flat, indicating for the 24 January 1971 flare a spectral shape $R_0 > 150$ MV and an equivalent steady state flux $J < 100$ p/cm^2 sec (4π). These results are in disagreement with the Co^{56} data discussed above. At present the most likely reason for this discrepancy lies in the great uncertainty in the excitation functions for the production of Ar^{37} from Ca, which are required for deducing flare characteristics from activity measurements. A more detailed discussion of this problem is given in Fireman *et al.* (1972a).

The depth gradients of Fe^{55} and Na^{22} ($t_{1/2} = 2.6$ yr) allow us to derive the mean spectral shape and intensity of the solar flare particle flux to which this rock was exposed, weighted according to the mean life of these isotopes (3.7 yr). In order to determine the characteristics of the bombarding SCR's we must first subtract that portion of the activity produced by GCR bombardment. The GCR contribution to each sample was determined by normalizing the theoretical depth profile (Reedy and Arnold, 1972) to the activity measured in the FM-5 sample. At the depth of this sample (40 g/cm^2) there is no appreciable production by SCR's. The shape of the GCR-produced profile will be discussed in more detail in the next section.

From both isotopes, Fe^{55} and Na^{22}, we derive an $R_0 = 85$ MV for the spectral shape and a $J = 100$ p/cm^2 sec (4π) for the mean intensity of the solar flare particle flux responsible for the production of these nuclides. The loss of surface material by attrition was taken to be (0.4 ± 0.2) mm.

In order to extract the same information from the data on the long-lived nuclei, Al^{26} and Mn^{53}, one has to consider two additional parameters: the surface irradiation age, which will affect the extent to which activity values have reached equilibrium with production rates, and the rate of erosion while on the surface of the moon. Undersaturation can be excluded by the Kr–Kr age of 27×10^6 yr (Lugmair and Marti, 1972), the track age of (25 ± 3) $\times 10^6$ yr (Crozaz *et al.*, 1972), and the Ar^{38} spallation age of (24 ± 2) $\times 10^6$ yr (Burnett *et al.*, 1972). Using both Al^{26} and Mn^{53} one obtains, after correcting for attrition, the best fit to theoretical SCR produced activity gradients with a surface erosion rate of 1.5–3.0 mm/10^6 yr. The best fitting spectral shapes and intensities are then $R_0 = 85$–100 MV and $J = 70$ protons/cm^2 sec (4π) for Al^{26}, and $R_0 = 100$ MV and $J = 100$ protons/cm^2 sec (4π) for Mn^{53}. Figure 2 illustrates the range of values of R_0, J, and erosion rates which will fit the experimental profiles. The slight difference in the value of J derived from the two "profiles" is not significant considering the precision of the data.

It is logical to assume that the rocks 12002 and 14321 both experienced the same cosmic ray particle flux, because both have long surface exposure ages. We can therefore compare the solar produced activity profiles obtained from 14321 to those of rock 12002 (Finkel *et al.*, 1971). Using our newly measured values for pure galactic cosmic ray production we can reexamine the solar profiles of rock 12002. Such a recalculation shows that the galactic production within this rock has been overestimated in the deeper samples OP-4, OP-5, and OP-6. This led to an underestimation of the solar production. The increased net solar production in the deeper samples thus would seem to imply that for rock 12002 the R_0's should be higher than those given in Finkel *et al.* (1971). However, at least for Mn^{53}, this possibility is precluded

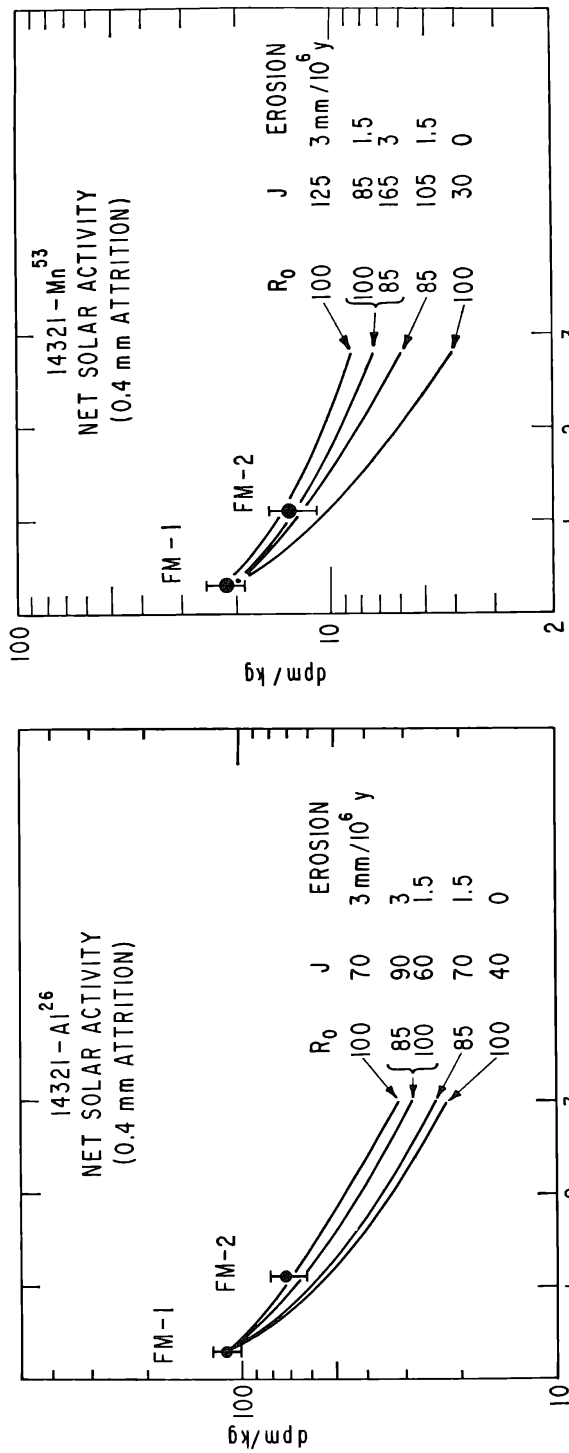

Fig. 2. Observed and calculated solar production for Al^{26} and Mn^{53}. Experimental points are given after galactic production has been subtracted. Solid lines are theoretical curves which have been normalized to the surface sample, FM-1. R_0 is the mean rigidity in units of MV, and J is the corresponding 4π integral flux above 10 MeV in units of protons/cm^2 sec. Erosion rates are given in units of mm/10^6 years.

by the Be^{10} results. The complete lack of any observed solar cosmic ray produced Be^{10} sets an upper limit for R_0 of about 150 MV for the average long-term parameter of the solar flare particle spectrum.

Therefore, a more likely explanation of the flat shape for both Mn^{53} and Al^{26}, as well as for other isotopes, is that the infinite plane geometry previously used for assessing solar cosmic ray produced activities underestimates production below 3 g/cm^2. If we instead use a more realistic hemispherical geometry with a radius of 21 g/cm^2 for the calculation of solar cosmic ray production profiles, the best fit to the higher net solar values mentioned above is then found (assuming erosion rates of 0.5 mm/10^6 yr for 12002 and 2 mm/10^6 yr for 14321) with the following R_0's and J's:

$$\begin{array}{lrlrl}
Na^{22} & R_0 = & 85 \text{ MV} & J(E > 10 \text{ MeV}) = & 110 \text{ protons/cm}^2 \text{ sec } (4\pi) \\
Fe^{55} & R_0 = & 100 \text{ MV} & J(E > 10 \text{ MeV}) = & 100 \text{ protons/cm}^2 \text{ sec } (4\pi) \\
Al^{26} & R_0 = & 100 \text{ MV} & J(E > 10 \text{ MeV}) = & 80 \text{ protons/cm}^2 \text{ sec } (4\pi) \\
Mn^{53} & R_0 = & 100 \text{ MV} & J(E > 10 \text{ MeV}) = & 90 \text{ protons/cm}^2 \text{ sec } (4\pi).
\end{array}$$

These values agree with those derived from 14321 above and are essentially the same as in Finkel *et al.* (1972).

Again one notices the striking fact that the fluxes and rigidities observed from Al^{26} and Mn^{53} are very similar to those obtained from the short-lived species. One exception to this conclusion is the C^{14} results of Begemann *et al.* (1972). These results, which are in general agreement with unpublished results of Suess and Boeckl (private communication) on rock 12002, indicate an increase in C^{14} production of about a factor of 4 over that predicted from a steady state solar activity as derived from other isotopic measurements. The meaning of this result is as yet uncertain. The result on another long-lived isotope, 24 my U^{236}, reported by Fields *et al.* (1972), may also be partially explained by cosmic ray bombardment.

The results on the soil sample 14259,18, which is reported to be material from the top centimeter of the surface LSPET (1971) look puzzling at first. The Co^{56}, Al^{26}, and Na^{22} activities are all in good agreement with values obtained in the same sample by other workers. The low Co^{56} value (although the error is quite large) together with the high Al^{26} and Mn^{53} activities could imply a rather complicated history for this sample. However, assuming an actual collection depth of 0 to about 2 cm (3.6 g/cm^2), the net solar activities for Co^{56} (if this is taken at the upper edge of its error range), Mn^{53}, Al^{26}, and Na^{22} are consistent with the results obtained from the surface samples of rock 14321 when corrected for the slightly different target chemistry.

Galactic cosmic ray effects

In contrast to the sharp decrease in activity between FM-1 ($\sim$0.3 g/cm^2) and FM-2 ($\sim$1.1 g/cm^2) which is evident in all isotopes except Cl^{36} and Be^{10}, the gradient between FM-3 and FM-5 is quite small. The overlying mass of the rock has nearly extinguished any solar cosmic ray contribution at these depths. We are thus seeing only the effects of the GCR's. The Reedy–Arnold model predicts that galactic cosmic rays will produce an activity level that in general is low at the surface, rises gradually

to a peak at about 40 to 70 g/cm^2 and then decreases exponentially with depth. However, in the case of FM-3, a small contribution of solar produced activities cannot be excluded. This would tend to obliterate any small positive gradient between FM-3 and FM-5 expected from GCR production. Table 3 shows the possible solar contribution to FM-3 calculated using two geometries: an infinite plane and a hemisphere with a radius R of 21 g/cm^2. The second geometry seems to be more realistic for the top part of the rock. Both sets of calculations used the model of Reedy and Arnold (1972). The calculated production rates are higher for the hemisphere because the mean path for solar protons to any depth is smaller than for an infinite plane.

In particular the Fe^{55} measurements (Fig. 3) illustrate a complete composite profile. Because of the short half-life, 2.6 yr, erosion and other peculiarities of a rock's

Table 3. Calculated solar cosmic ray production rates (dpm/kg rock) for sample FM-3 (18 g/cm^2 depth).

	Model			
	Infinite plane		Hemisphere with R = 21 g/cm^2	
Isotope	$J(>10$ MeV, $4\pi) = 100$ p/cm^2 sec $R_0 = 75$ MV	$R_0 = 100$ MV	$J(>10$ MeV, $4\pi) = 100$ p/cm^2 sec $R_0 = 75$ MV	$R_0 = 100$ MV
Fe^{55}	0.6	2.6	1.9	7
Mn^{53}	0.2	0.8	0.6	2.2
Na^{22}	0.5	2.6	1.8	7.5
Al^{26}	0.8	3.5	2.7	10.4

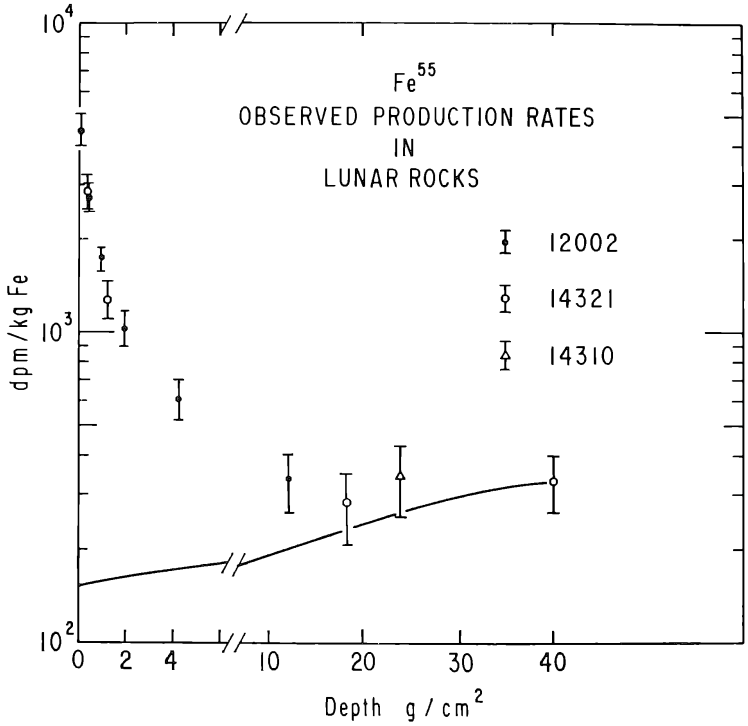

Fig. 3. Observed production rates (dpm/kg Fe) versus depth for Fe^{55} in lunar rocks. The solid line is the calculated production from galactic cosmic rays alone, normalized at the deepest sample.

history while on the moon have no effect on this isotope. On the other hand, the half-life is long enough that any given solar flare event will have only a small effect on the total activity. These simplifications, coupled with the fact that iron is the only target of importance, allow us to compare directly our Apollo 14 measurements with our Apollo 12 measurements. As can be seen, the agreement between the samples is quite good. The line in Fig. 3 is the calculated galactic shape normalized at FM-5. There is no indication of a solar contribution to the FI sample, which integrates over a broad depth range from 16.5 g/cm^2 to 33 g/cm^2. The maximum possible SCR contribution to FM-3 is about 65 dpm/kg Fe or 7 dpm/kg rock 14321 (Table 3).

In the case of Na^{22} the more complicated target chemistry makes direct intercomparison of samples more difficult. The FM-3 and FM-5 values of 39 $\pm$ 5 dpm/kg and 32 $\pm$ 4 dpm/kg do again show the expected flat gradient.

The interpretation of the Mn^{53} and Al^{26} measurements must take into account the fact that rock history (erosion, exhumation, etc.) can have an important effect. This is especially illustrated for Mn^{53} in Fig. 4, which presents measurements of the rocks 12002, 14321, and 14310, and Apollo 11 core samples 10004 and 10005. The lower values and flatter gradient of the 14321 surface samples compared with the 12002 measurements illustrate graphically the increased erosion which rock 14321 has experienced. The deeper samples, which are less affected by erosion, agree quite well in the different samples and again illustrate the flat nature of the galactic gradient in this region.

In the case of Al^{26} we cannot as easily compare samples of different chemistry because several targets are important. However, measurements discussed below allow us to normalize the FI value to the chemistry of FM-3 and FM-5. The values then are

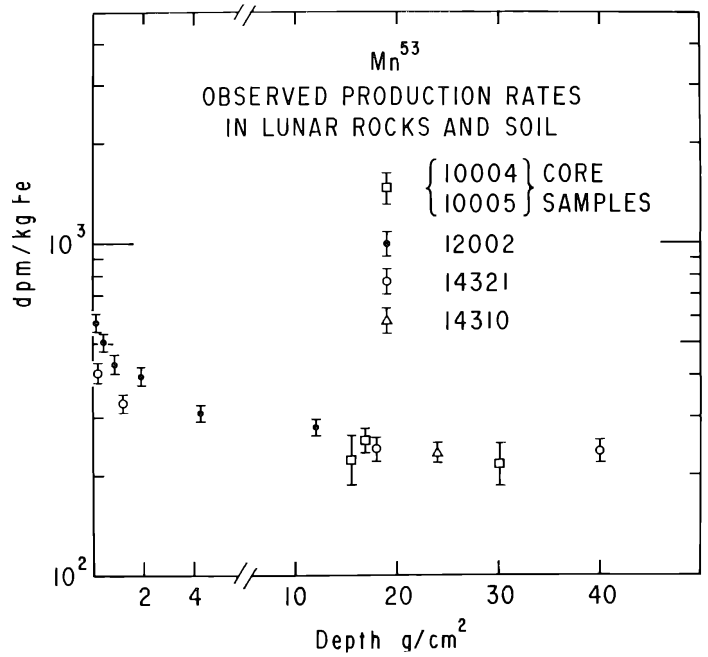

Fig. 4. Observed production rates (dpm/kg Fe) versus depth for Mn^{53} in lunar rocks and soil.

57 ± 7 dpm/kg, 60 ± 8 dpm/kg, and 54 ± 8 dpm/kg for FM-3, FI, and FM-5, respectively. Again we see a flat spectrum as predicted.

Our sample of rock 14310, denoted FI, came from a mean depth of 24 g/cm^2. The separation of plagioclase and pyroxene which we were able to obtain on this sample allowed us to observe target effects in the induced activities of Al^{26}, Na^{22}, and Cl^{36}. The counting data, along with the chemical compositions, are given in Table 4.

Al^{26} is the simplest case since production from only Al and Si is important. Production from Fe, Mg, and Ca is small enough to be ignored. A simple solution of the two equations involved give $P_{Al} = 270 \pm 60$ dpm/kg Al and $P_{Si} = 170 \pm 50$ dpm/kg Si. These values are in quite good agreement with the results calculated by Reedy and Arnold (1972) and with the values of Fuse and Anders (1969), obtained from studies of meteorites, after correcting for a 2π rather than a 4π bombardment. Also shown are values measured by Cressy (1971) in the meteorite Bruderheim and by Begemann *et al.* (1970) in lunar rocks.

In the case of Na^{22} the situation is complicated by the fact that four targets make important contributions: Na, Mg, Al, and Si. This complication coupled with the fact that neither laboratory nor geochemical processes give useful separations of these targets makes it very difficult to calculate production rates from individual targets. If, however, we look at the Reedy–Arnold calculation for a sample of FIH and FIL chemistry we find good agreement between the predicted FIL/FIH ratio and that actually measured.

For Cl^{36} we are in a somewhat better situation if we are willing to use measurements from meteorites and other lunar samples besides rock 14310. Using measurements from iron meteorites we can, after correcting for a 2π rather than a 4π

Table 4. Galactic cosmic ray production rates for Al^{26} and Cl^{36} from various targets in rock 14310.

	Al (%)	Si (%)	Al^{26} dpm/kg rock		
FIL	16.3	21.1	80 ± 13		
FIH	3.0	23.3	47 ± 7		
dpm/kg target	270 ± 60	170 ± 50	This work		
	540	170	(Lunar rock)[1]		
	476 ± 54	310 ± 10	(Meteorite)[2]		
	1130 ± 190	245 ± 31	(Meteorite)[3]		
	300	160	(Calculated)[4]		
	Ca (%)	K (%)	Ti (%)	Fe (%)	Cl^{36} dpm/kg rock
FIL	11.9	0.50	0.42	2.4	15.9 ± 2.2
FIH	5.0	0.16	1.7	13.6	7.3 ± 1.5
10017	7.8	0.24	7.1	15.3	16.5 ± 1.8
dpm/kg target	115 ± 25	—	80 ± 35	8 (set)	This work
	152				(Lunar rock)[1]
	112	420	65	7	(Calculated)[4]

[1] Begemann *et al.*, 1970.
[2] Fuse and Anders, 1969.
[3] Cressy, 1971.
[4] Reedy and Arnold, 1972.

bombardment, set the production $P_{Fe} = 8$ dpm/kg Fe. Then using Cl^{36} measurements from rock 10017 we can calculate $P_{Ti} = 80 \pm 35$ dpm/kg Ti and from the FIL and FIH determinations $P_{Ca} = 115 \pm 25$ dpm/kg Ca. Both numbers are in good agreement with Reedy–Arnold estimates.

Fe^{55} and Mn^{53} being produced from only one target can easily be compared with other samples as we have done above.

Acknowledgments—The authors have as always been helped by many persons. Norman Fong, Florence Kirchner and Lawrence Finnin supported our work in many ways. We have benefited from valuable discussions with Kurt Marti, Ernest Schonfeld, Edward Fireman, and other colleagues. We owe a special debt to the astronauts and others involved in collecting and documenting the large rocks which made this work possible. This research was supported by NASA Grant GNL 05-009-148.

References

Begemann F., Born W., Palme H., Vilcsek E., and Wänke H. (1972) Cosmic ray produced radioisotopes in Apollo 12 and Apollo 14 samples (abstract). In *Lunar Science—III* (editor C. Watkins), p. 53, Lunar Science Institute Contr. No. 88.

Begemann F., Vilcsek E., Rieder R., Born W., and Wänke H. (1970) Cosmic ray produced radioisotopes in lunar samples from the Sea of Tranquility (Apollo 11). *Proc. Apollo 11 Lunar Sci. Conf., Geochim. Cosmochim. Acta* Suppl. 1, Vol. 2, pp. 995–1005. Pergamon.

Bostrom C. O., Williams D. J., and Arens J. R. (1971) Solar proton monitor experiment. *Solar Geophysical Data*, No. 328, Part II.

Burnett D. S., Huneke J. C., Podosek F. A., Russ G. P. III, Turner G., and Wasserburg G. J. (1972) The irradiation history of lunar samples (abstract). In *Lunar Science—III* (editor C. Watkins), p. 105, Lunar Science Institute Contr. No. 88.

Cressy P. J. Jr. (1971) The production rate of Al^{26} from target elements in the Bruderheim chondrite. *Geochim. Cosmochim. Acta* **35,** 1283–1296.

Crozaz G., Drozd R., Hohenberg C. M., Hoyt H. P. Jr., Ragan D., Walker R. M., and Yuhas D. (1972) Solar flare and galactic cosmic ray studies of Apollo 14 samples (abstract). In *Lunar Science—III* (editor C. Watkins), p. 167, Lunar Science Institute Contr. No. 88.

Eldridge J. S., O'Kelley G. D., and Northcutt K. J. (1972) Abundances of primordial and cosmogenic radionuclides in Apollo 14 rocks and fines (abstract). In *Lunar Science—III* (editor C. Watkins), p. 221, Lunar Science Institute Contr. No. 88.

Fields P. R., Diamond H., Metta N. D., Rokop D. J., and Stevens C. M. (1972) Np^{237}, U^{236}, and other actinides on the moon (abstract). In *Lunar Science—III* (editor C. Watkins), p. 256, Lunar Science Institute Contr. No. 88.

Finkel R. C., Arnold J. R., Imamura M., Reedy R. C., Fruchter J. S., Loosli H. H., Evans J. C., Delany A. C., and Shedlovsky J. P. (1971) Depth variation of cosmogenic nuclides in a lunar surface rock and lunar soil. *Proc. Second Lunar Sci. Conf., Geochim. Cosmochim. Acta* Suppl. 2, Vol. 2, pp. 1773–1789. MIT Press.

Fireman E. L., D'Amico J., Defelice J., and Spannagel G. (1972) Radioactivities in Apollo 14 and 15 materials (abstract). In *Lunar Science—III* (editor C. Watkins), p. 262, Lunar Science Institute Contr. No. 88.

Fireman E. L., D'Amico J., Defelice J., and Spannagel G. (1972a) Radioactivities in returned lunar materials. *Proc. Third Lunar Sci. Conf., Geochim. Cosmochim. Acta* Suppl. 3, Vol. 2. MIT Press.

Fuse K. and Anders E. (1969) Al^{26} in meteorites—VI. Achondrites. *Geochim. Cosmochim. Acta* **33,** 653–670.

Ingamells C. O. (1966) Absorptiometric methods in rapid silicate analysis. *Anal. Chem.* **38,** 1228.

Jackson P. F. S., Coetzee J. H. J., Strasheim A., Strelow F. W. E., Gricius A. J., Wybenga F., and Kokot M. L. (1972) The analysis of lunar material returned by Apollo 14 (abstract). In *Lunar Science—III* (editor C. Watkins), p. 424, Lunar Science Institute Contr. No. 88.

Keith J. E., Clark R. S., and Richardson K. A. (1972) Gamma ray measurements of Apollo 12, 14. and 15 lunar samples (abstract). In *Lunar Science—III* (editor C. Watkins), p. 446, Lunar Science Institute Contr. No. 88.

Klein C. Jr., Drake J. C., Frondel C., and Ito J. (1972) Mineralogy and petrology of several Apollo 14 rock types and chemistry of the soil (abstract). In *Lunar Science—III* (editor C. Watkins), p. 455, Lunar Science Institute Contr. No. 88.

LSPET (Lunar Sample Preliminary Examination Team) (1971) Preliminary examination of lunar samples from Apollo 14. *Science* **173,** 681–693.

Lugmair G. W. and Marti K. (1971) Neutron capture effects in lunar gadolinium and the irradiation histories of some lunar rocks. *Earth Planet. Sci. Lett.* **13,** 32.

Lugmair G. W. and Marti K. (1972) Neutron and spallation effects in Fra Mauro regolith (abstract). In *Lunar Science—III* (editor C. Watkins), p. 495, Lunar Science Institute Contr. No. 88.

O'Kelley G. D., Eldridge J. S., Schonfeld E., and Bell P. R. (1971) Cosmogenic radionuclide concentrations and exposure ages of lunar samples from Apollo 12. *Proc. Second Lunar Sci. Conf., Geochim. Cosmochim. Acta* Suppl. 2, Vol. 2, pp. 1747–1755. MIT Press.

Rancitelli L. A., Perkins R. W., Felix W. D., and Wogman N. A. (1971) Erosion and mixing of the lunar surface from cosmogenic and primordial radionuclide measurements in Apollo 12 lunar samples. *Proc. Second Lunar Sci. Conf., Geochim. Cosmochim. Acta* Suppl. 2, Vol. 2, pp. 1757–1772. MIT Press.

Rancitelli L. A., Perkins R. W., Felix W. D., and Wogman N. A. (1972) Cosmic ray flux and lunar surface processes characterized from radionuclide measurements in Apollo 14 and 15 lunar samples (abstract). In *Lunar Science—III* (editor C. Watkins), p. 630, Lunar Science Institute Contr. No. 88.

Reed G. W. Jr., Jovanovic S., and Fuchs L. H. (1972) Concentrations and lability of the halogens, platinum metals and mercury in Apollo 14 and Apollo 15 samples (abstract). In *Lunar Science—III* (editor C. Watkins), p. 637, Lunar Science Institute Contr. No. 88.

Reedy R. C. and Arnold J. R. (1972) Interaction of solar and galactic cosmic ray particles with the moon. *J. Geophys. Res.* **77,** No. 4, 537–555.

Schnetzler C. C. and Nava D. F. (1971) Chemical composition of Apollo 14 soils 14163 and 14259. *Earth Planet. Sci. Lett.* **11,** 345.

Shrelldalff: Shedlovsky J. P., Honda M., Reedy R. C., Evans J. C., Lal, D., Lindstrom R. M., Delany A. C., Arnold J. R., Loosli H. H., Fruchter J. S., and Finkel R. C. (1970) Pattern of bombardmentproduced radionuclides in rock 10017 and in lunar soil. *Proc. Apollo 11 Lunar Sci. Conf., Geochim. Cosmochim. Acta* Suppl. 1, Vol. 2, 1503–1532. Pergamon.

Wänke H., Baddenhausen H., Balacescu A., Teschke F., Spettel B., Dreibus G., Quijano-Rico M., Kruse H., Wlotzka F., and Begemann F. (1972) Multielement analyses of lunar samples (abstract). In *Lunar Science—III* (editor C. Watkins), p. 779, Lunar Science Institute Contr. No. 88.

Proceedings of the Third Lunar Science Conference
(Supplement 3, *Geochimica et Cosmochimica Acta*)
Vol. 2, pp. 1733–1746
The M.I.T. Press, 1972

Cosmonuclides in lunar rocks

Y. YOKOYAMA, R. AUGER, R. BIBRON, R. CHESSELET, F. GUICHARD,
C. LEGER, H. MABUCHI,* J. L. REYSS, and J. SATO*

Centre des Faibles Radioactivités, C.N.R.S., 91-Gif-sur-Yvette, France

Abstract—The rates of production of cosmonuclides as a function of depth in the moon are calculated with a simplified method. The differential spectra of particles due to galactic cosmic ray and of solar protons are calculated as a function of depth. For solar protons, the range-energy relation of Wilson is used. For galactic cosmic rays, a three-steps cascade model is used. Integration as a function of incident angle is simplified by dividing zenith angles to have an equal solid angle. The calculated production rates are compared with experimental results and with the earlier calculations. Th, U, ^{26}Al, and ^{55}Fe are measured in lunar rock 14305.

INTRODUCTION

LUNAR SAMPLES bear fossil records of cosmic radiation. From studies of Apollo 11 samples, clear evidence was obtained for the long term bombardment by solar particles in the region of tens of MeV per nucleon (Shrelldalff, 1970; O'Kelley *et al.*, 1970; Marti *et al.*, 1970; Crozaz *et al.*, 1970; Fleischer *et al.*, 1970; Lal *et al.*, 1970; Price and O'Sullivan, 1970). Studies of Apollo 12 samples (Finkel *et al.*, 1971) showed a similarity of the depth profile of 7.16×10^5 yr ^{26}Al to that of 2.6 yr ^{22}Na. Thus the flux of the solar particles averaged over 10^6 yr has been similar to that observed recently. The profile for 3.7×10^6 yr ^{53}Mn suggests a possibility of either an erosion rate of 0.2 mm per m.y. or the variation of the solar cosmic flux (Finkel *et al.*, 1971).

The aim of the work reported here comprises experimental measurements of the depth variation of radionuclides, theoretical calculations of the expected profiles, and comparison of these results. We report here mainly the results of the theoretical calculation which have been obtained by somewhat different approach using different input data from the previous work of Shrelldalff (1970), Armstrong and Alsmiller (1971), Reedy and Arnold (1971), and Tanaka *et al.* (1971).

SOLAR PRODUCTION

We consider here only the interactions of the primary protons. The production by α-particles will be reported later. The spectrum of incident solar protons is assumed to decrease exponentially with their rigidity:

$$N(R)\,dR = k \exp\left(-\frac{R}{R_0}\right) dR \qquad (1)$$

* Present address: Department of chemistry, Faculty of Science, University of Tokyo, Tokyo, Japan.

where $N(R)\,dR$ is the number of particles having rigidities between R and $R + dR$, and R_0 is the characteristic slope (MV). By using the relation between the rigidity and the energy,

$$R^2 = E^2 + 1876E \tag{2}$$

the rigidity spectrum is converted in the energy spectrum:

$$N(E)\,dE = \frac{k(E + 938)}{R} \exp\left(-\frac{R}{R_0}\right) dE \tag{3}$$

where $N(E)\,dE$ is the number of particles having energies between E and $E + dE$ (MeV), and 938 is the rest mass of the proton in MeV.

To calculate the depth variation of the proton flux, we have used a simplified relationship between range and energy, proposed by Wilson and Brobeck (Wilson, 1947):

$$P = \frac{2.21}{S} E^{1.8} \tag{4}$$

where P is the range (mg/cm^2) of a proton of energy E (MeV) and S is the relative mass stopping power which depends on the chemical composition of the material and is 1 for air, 0.91 for the rock 14305, and 0.88 for the rock 12002. The relative mass stopping power was calculated by the equations (7-1, 7-2) of Friedlander and Kennedy (1955). The equation (4) is valid in the energy domain of about 10 to 200 MeV.

The incident energy E of the particle coming with a zenith angle θ and having an energy E_D at a given depth D (mg/cm^2) is calculated by

$$E = \left(\frac{SD}{2.21 \cos\theta} + E_D{}^{1.8}\right)^{1/1.8} \tag{5}$$

The incident flux is assumed to be isotropic. Incident angles are divided in ten parts, of which the cos θ are comprised between 0 to 0.1, 0.1, to 0.2 and so on, in order that each part has equal solid angle. Then each part is represented by its mean cos θ, namely cos θ = 0.05, 0.15, and so on.

The differential flux of particles having energy E_D at a given depth D is then obtained by integrating the flux of particles having initial energy E (E being a function of cos θ) over all angles:

$$N(E_D)\,dE_D = N(E)\,dE = N(E)\frac{dE}{dE_D}\,dE_D = N(E)\left(\frac{E_D}{E}\right)^{0.8} dE_D$$

$$= \frac{k}{20}\sum_{\cos\theta}\frac{E + 938}{R}\exp\left(-\frac{R}{R_0}\right)\left(\frac{E_D}{E}\right)^{0.8} dE_D \tag{6}$$

where E should be determined by the equation (5) as the function of E_D, D, cos θ; R does by the equation (2) from E, and summation should be done for cos θ = 0.05, 0.15, . . . , to 0.95.

The depth variation of the proton flux thus calculated for several values of R_0 is shown in Fig. 1.

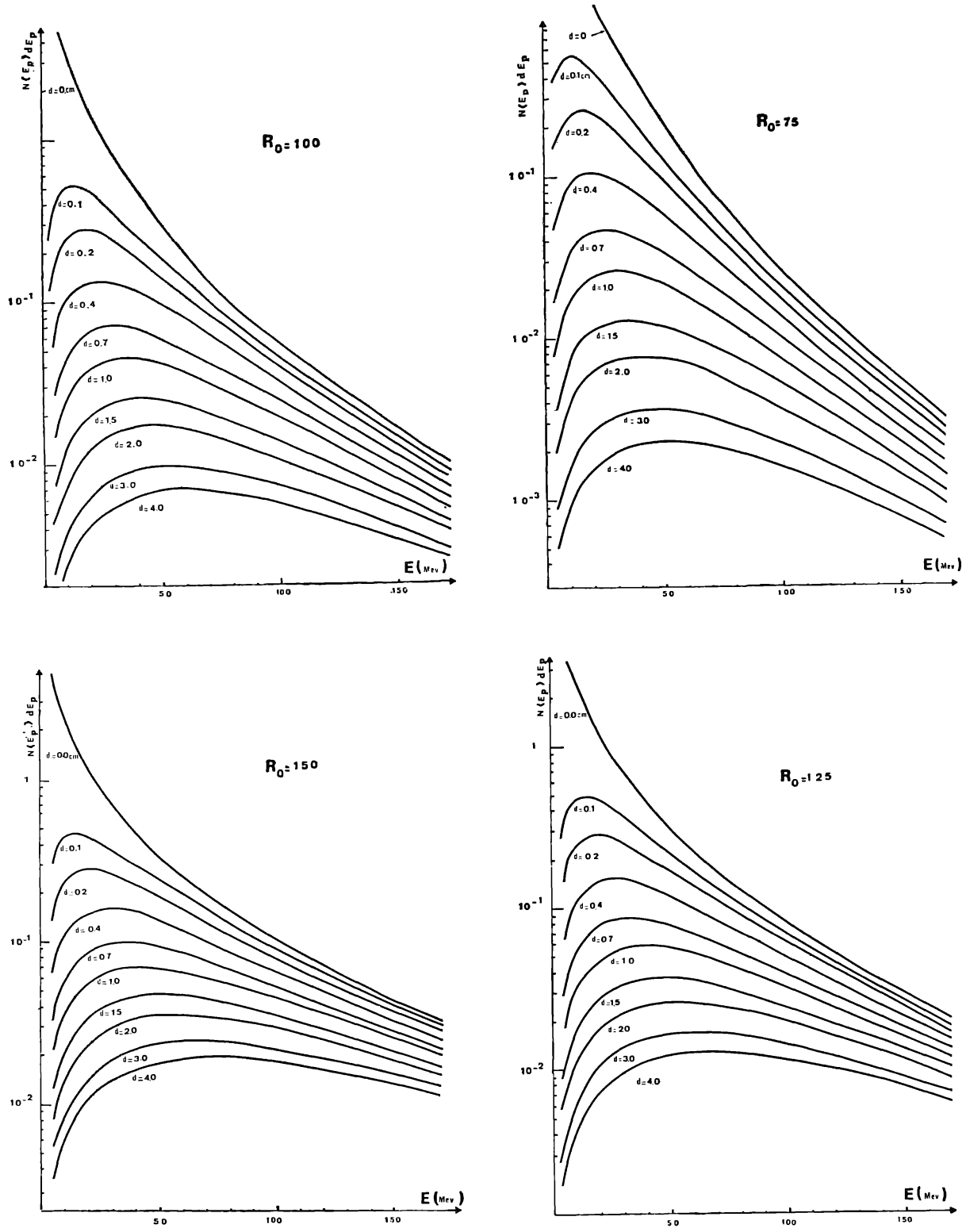

Fig. 1. Differential energy spectra of solar protons at various depth (d) in the moon (in units of proton/cm^2-sec-MeV). Here J (4π integral flux above 10 MeV in units of protons/cm^2-sec) is taken to be 100. R_0 is the mean rigidity in units of MV. The density of rock is taken to be 3.

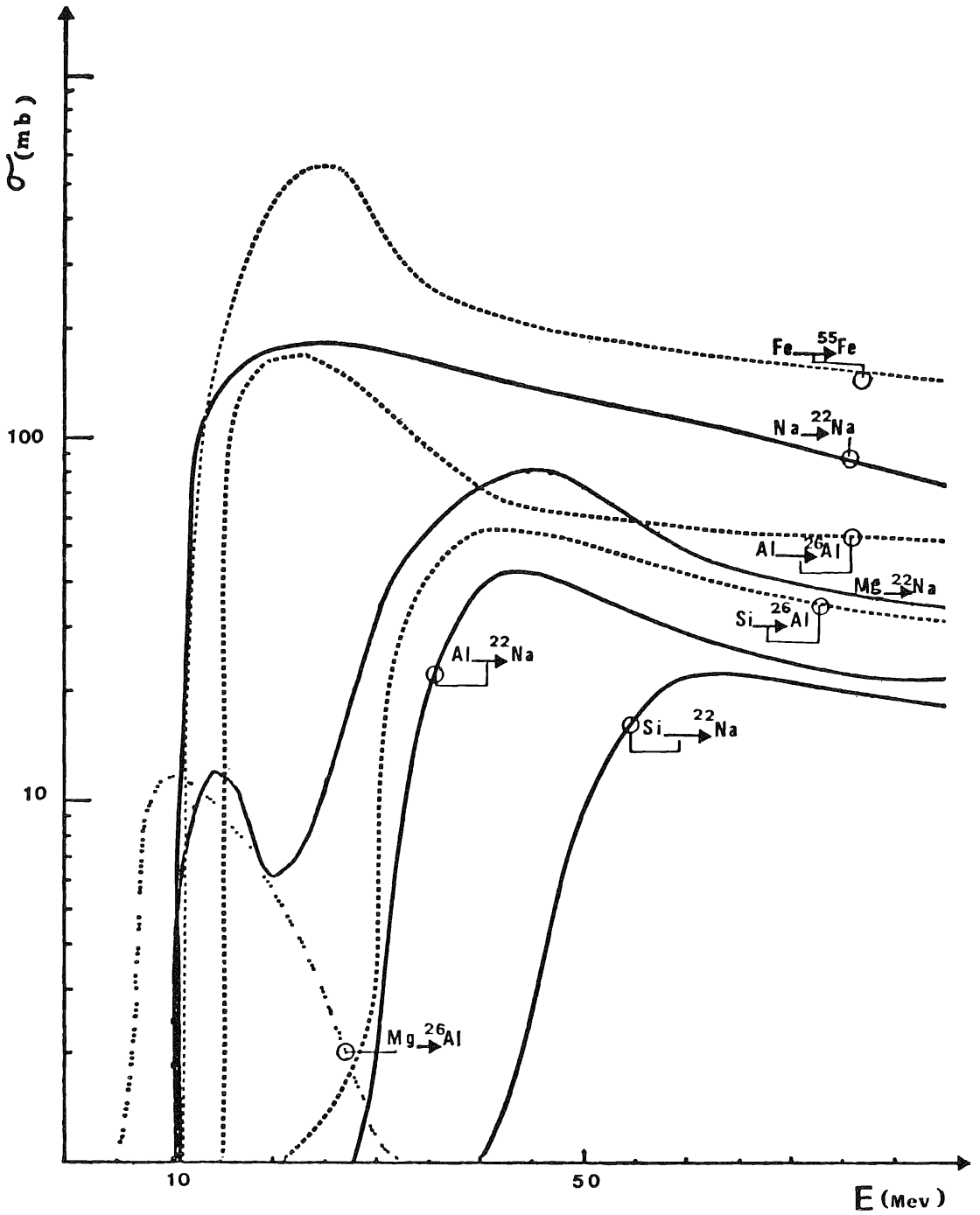

Fig. 2. Adopted excitation functions for the production of various radionuclides. The functions are for the proton reactions.

The production rates of nuclides are calculated by integrating $nN(E_D)\mathfrak{S}(E_D)\,dE_D$ for all energies, where n is the number of target nuclei per kg, $\mathfrak{S}(E_D)$ is the excitation function of a given reaction. We have used the excitation functions selected from experiments, corrected for the adopted values of the monitor reactions, of decay schemes, and synthesized by Tobailem and de Lassus St-Genies (1971, 1972). The excitation functions of main reactions are shown in Fig. 2. For the productions of

^{53}Mn and ^{54}Mn, we have adopted the excitation functions of Reedy and Arnold (1971).

Galactic Production

The depth variation of the particle flux due to galactic cosmic rays is estimated in the following way.

We divide particles in three components. The first component is the energetic incident particles. We assumed an exponential decrease of the flux of this component with the traversed length L:

$$N_1 = N_{1,0} \exp(-\mu_1 L) \tag{7}$$

where $N_{1,0}$ is the incident flux, N_1 is the flux at L (cm), and μ_1 is the attenuation coefficient (cm^{-1}).

The second component is the medium energy particles formed by the interaction of the first component with matter. Assuming $dN_2 = (m_1\mu_1 N_1 - \mu_2 N_2)\, dL$, we obtained

$$N_2 = C_1 N_{1,0}(e^{-\mu_1 L} - e^{-\mu_2 L}) \tag{8}$$

where N_2 is the flux of the second component at L, μ_2 is the attenuation length of this component, m_1 is the multiplication factor (a primary particle producing m_1 secondary particles), and C_1 is a constant equal to $m_1\mu_1/(\mu_2 - \mu_1)$.

The third component is the low energy particles (mainly neutrons) formed from the second component. The flux N_3 of the third component is obtained by assuming $dN_3 = (m_2\mu_2 N_2 - \mu_3 N_3)\, dL$,

$$N_3 = C_2 N_{1,0}[e^{-\mu_1 L} - e^{-\mu_2 L} - (\mu_2 - \mu_1)Le^{-\mu_2 L}] \tag{9}$$

where m_2 is the multiplication factor for the production of the third component and C_2 is a constant equal to $m_1 m_2 \mu_1 \mu_2/(\mu_2 - \mu_1)^2$. We have assumed that the attenuation length of the third component μ_3 is equal to μ_2.

We have adopted five particles (nucleons)/cm^2/sec/4π for $N_{1,0}$, and 0.02 and 0.08 cm^{-1} for μ_1 and μ_2, respectively. The energy domains of the three components are assumed somewhat arbitrarily to be $E > 1$ BeV, 1 BeV $> E >$ 200 MeV, 200 MeV $> E >$ 2 MeV. The values of 3.3 and 13.3 were adopted for C_1 and C_2, respectively.

The incident flux is assumed to be isotropic. The effect of the incident angle was calculated in a similar way as that of solar production: by substituting L in the equations (7, 8, 9) by $D/\cos\theta$, the fluxes N_1, N_2, N_3 are numerically integrated over 2π. We assumed $L = 7$ cm if L exceeds 7 cm, in order to fit approximately the shape of the rock 14305 (this was done also for the calculation of solar production, but the difference from the case of infinite plane was negligible).

The cross section in the energy domain over more than 200 MeV is approximately constant for a given reaction, if the difference of mass is small between target and product. We express this mean cross section by $\mathfrak{S}_H$.

On the other hand, if we assume the differential spectrum of the third component (2 to 200 MeV) to have a form of E^{-1}, we can calculate the mean cross section in this domain by an arithmetic mean of the cross sections corresponding to the

energies taken as a geometric progression, such as 2, 2.8, 4, 5.7, 8, 11, 16, . . . , 128, 181 MeV. We express this mean by $\mathfrak{S}_L$, namely $\mathfrak{S}_L = (\mathfrak{S}_2 + \mathfrak{S}_{2.8} + \mathfrak{S}_4 + \cdots + \mathfrak{S}_{181})/14$ where $\mathfrak{S}_2$ is the cross section for 2 MeV and so on.

Then the production rate A is calculated by

$$A = n[(N_{1,D} + N_{2,D})\mathfrak{S}_H + N_{3,D}\mathfrak{S}_L] \tag{10}$$

where $N_{1,D}$ is the flux of the first component at the depth D, $N_{2,D}$, that of the second and so on.

RESULTS AND DISCUSSION

Figure 3 shows the calculated profiles for ^{26}Al and the preliminary observed value obtained by us with nondestructive gamma-gamma coincidence spectrometry on the rock 14305 (Table 1). This rock was thought to have been turned recently,

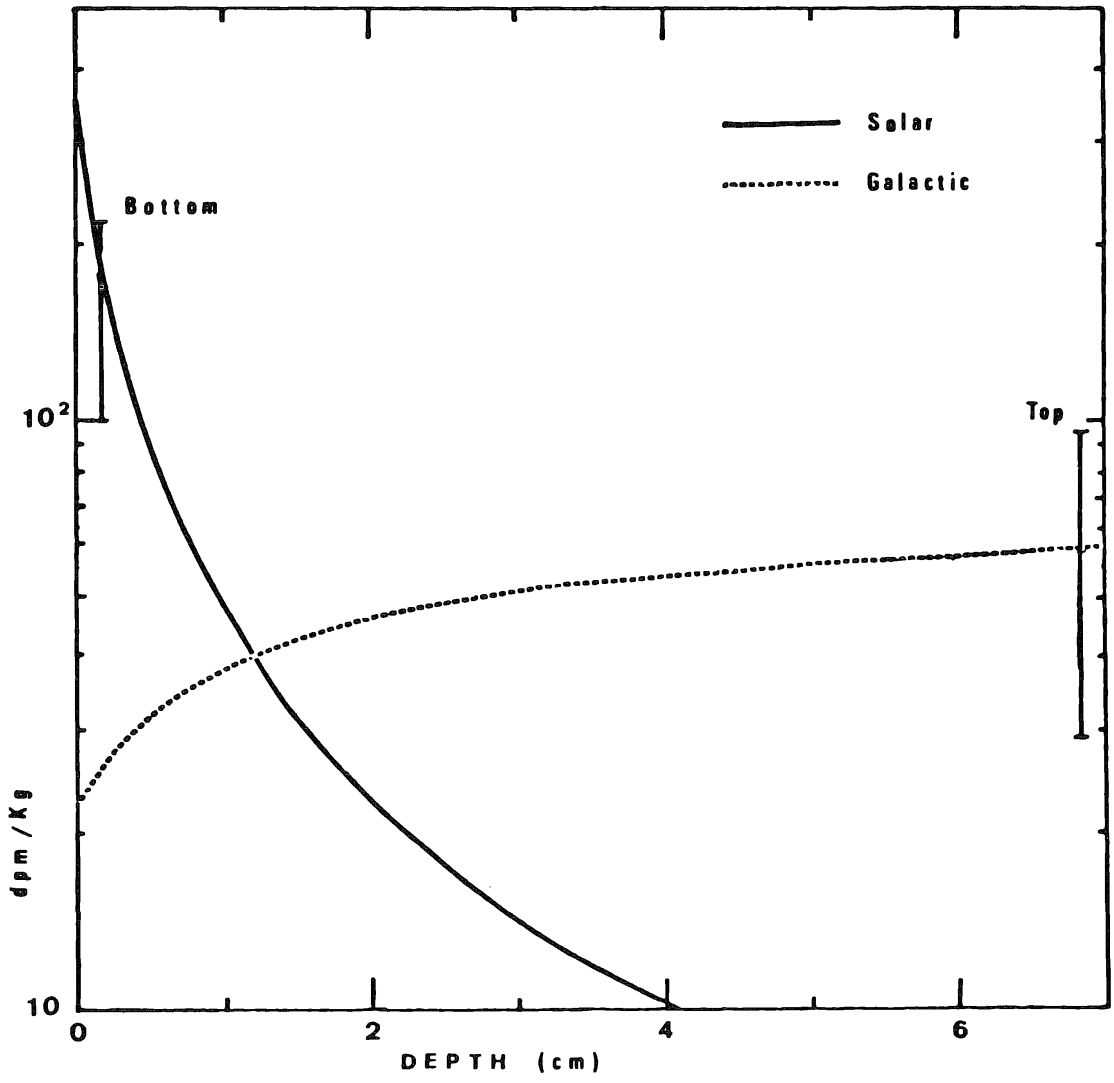

Fig. 3. Depth variation of ^{26}Al in the lunar rock 14305. The calculated solar production is based on the values of $R_0 = 100$ and $J = 70$. Galactic contribution is not subtracted from experimental points.

Table 1. Nondestructive gamma-ray measurements of rocks 14305 and 14302.

Samples	Weight (g)	Th (ppm)	U (ppm)	^{26}Al (dpm/kg)
This work 14305				
Top (0–3 mm)	2.7	14.6 ± 0.9	3.8 ± 0.4	63 ± 34
Bottom (0–3 mm)	1.45	13.3 ± 0.9	3.8 ± 0.5	160 ± 60
LSPET (1971) 14302*	381	14.3 ± 1.4	3.8 ± 0.6	85 ± 17

* 14302 was a part of 14305 at the lunar surface.

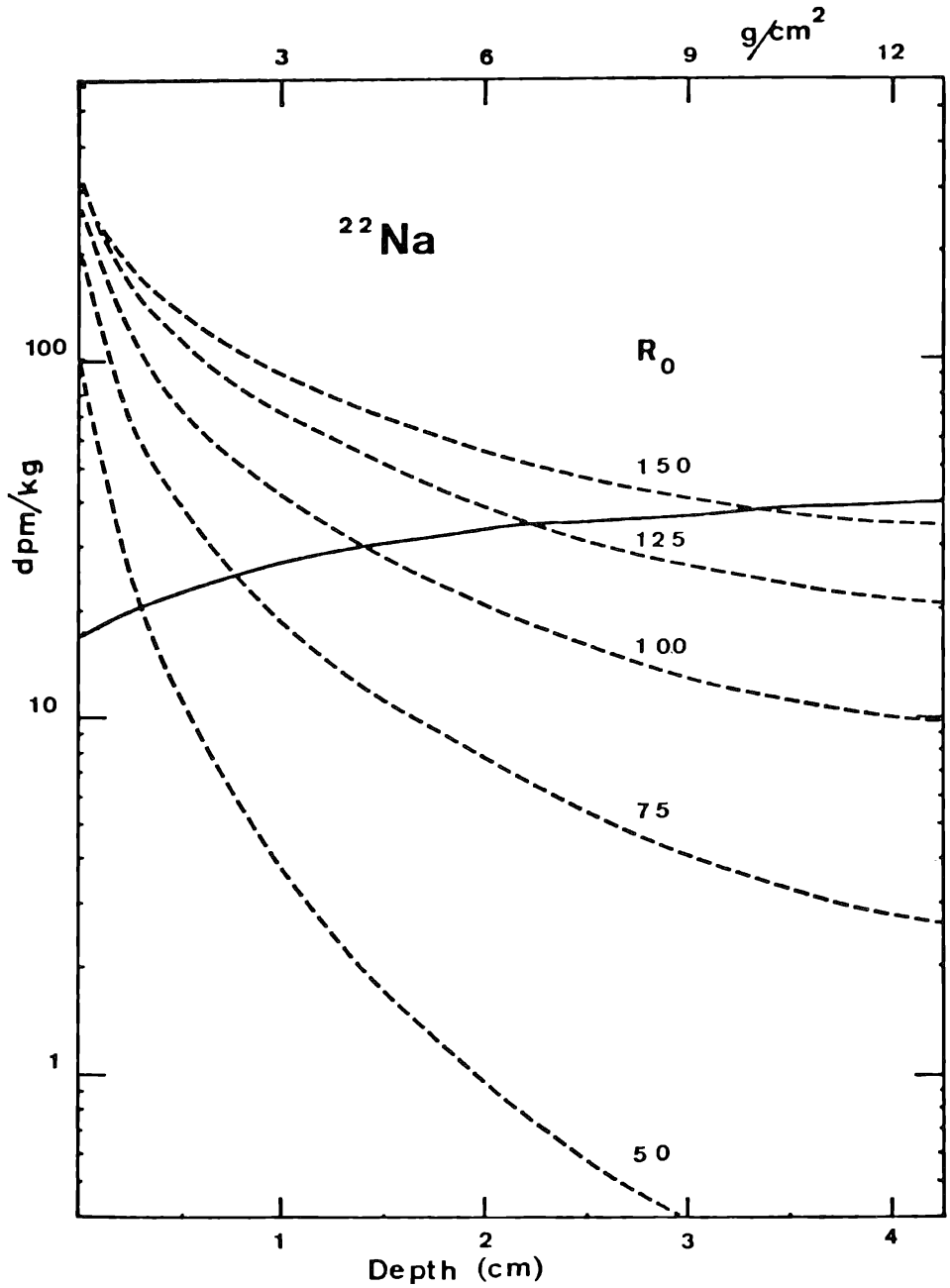

Figs. 4 to 8. Calculated depth variations of various radionuclides in the lunar rock 14305. The broken curves represent the solar production (J = 100) and the full curves, the galactic production. Adopted contents of Si, Al, Mg, Fe, and Na are 23.0, 8.5, 7.8, 7.4, and 0.63%, respectively (LSPET, 1971).

from the photographic studies of its situation on the lunar surface and from the pits counting. This was confirmed by our results, showing more activities of ^{26}Al at the bottom than at the top. The calculated profiles of ^{22}Na, ^{26}Al, ^{53}Mn, ^{54}Mn, and ^{55}Fe are shown in Figs. 4 to 8. A preliminary result of the measurement of ^{55}Fe of the rock 14305 is shown in Fig. 9.

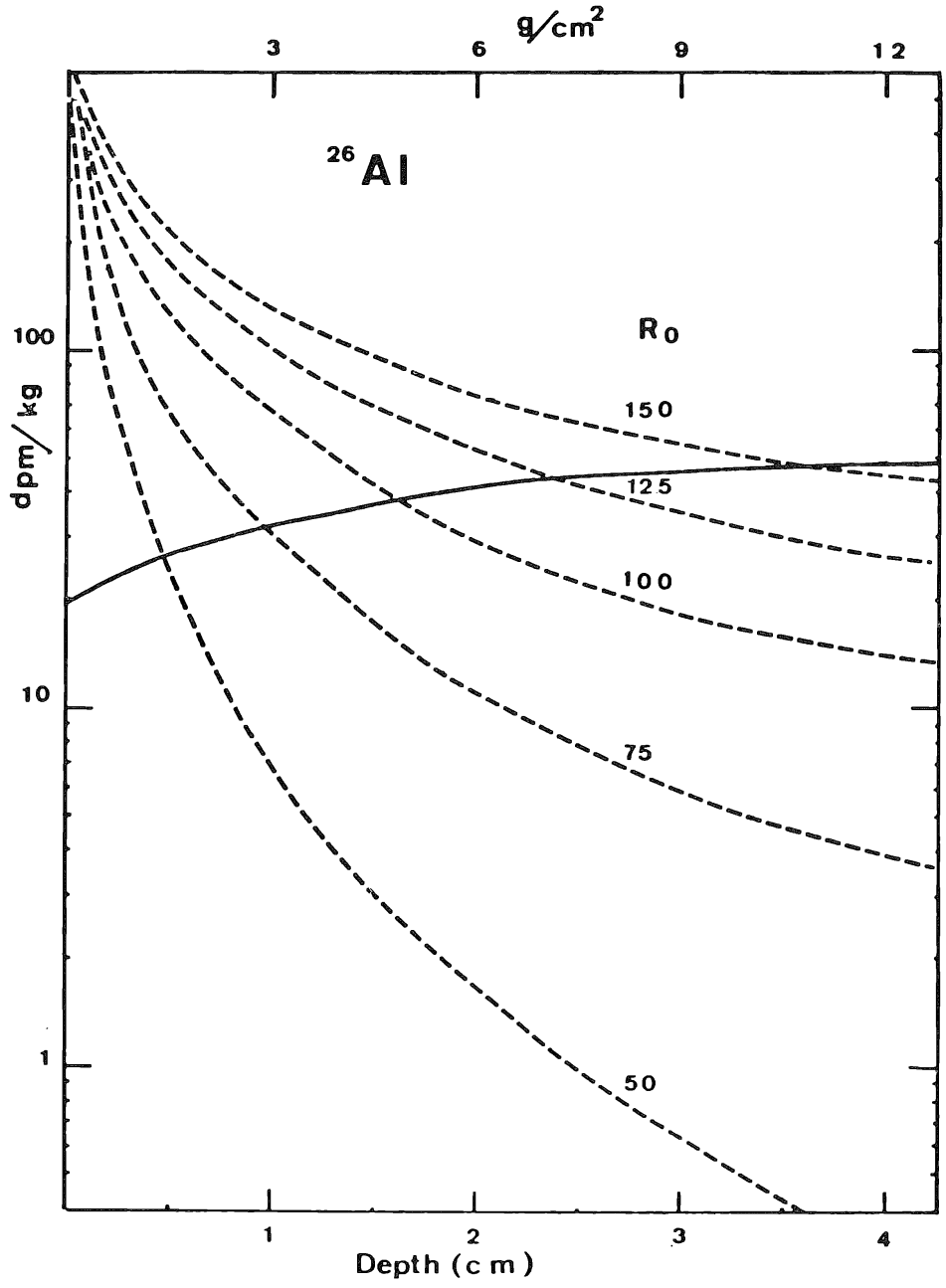

Fig. 5.

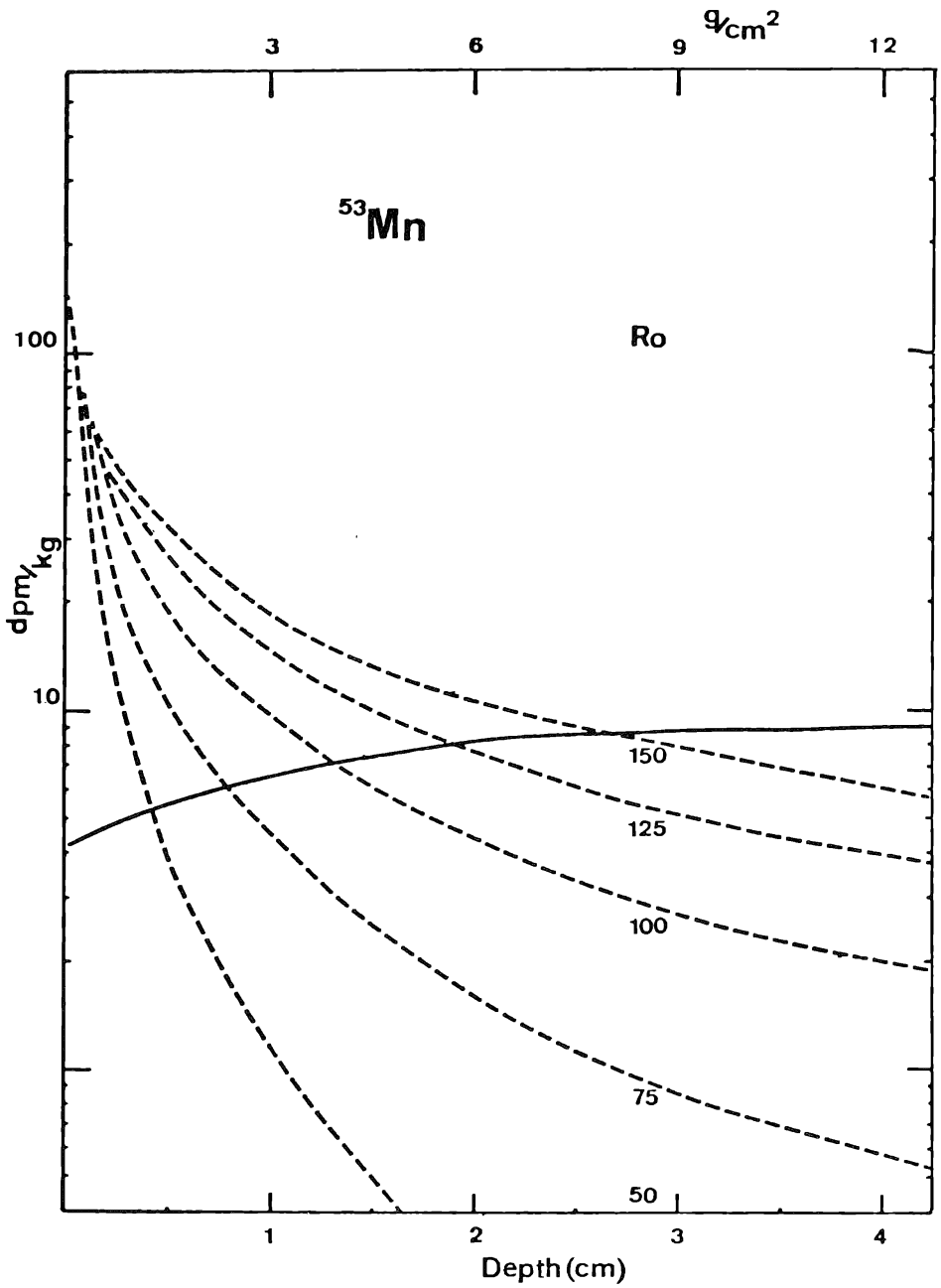

Fig. 6.

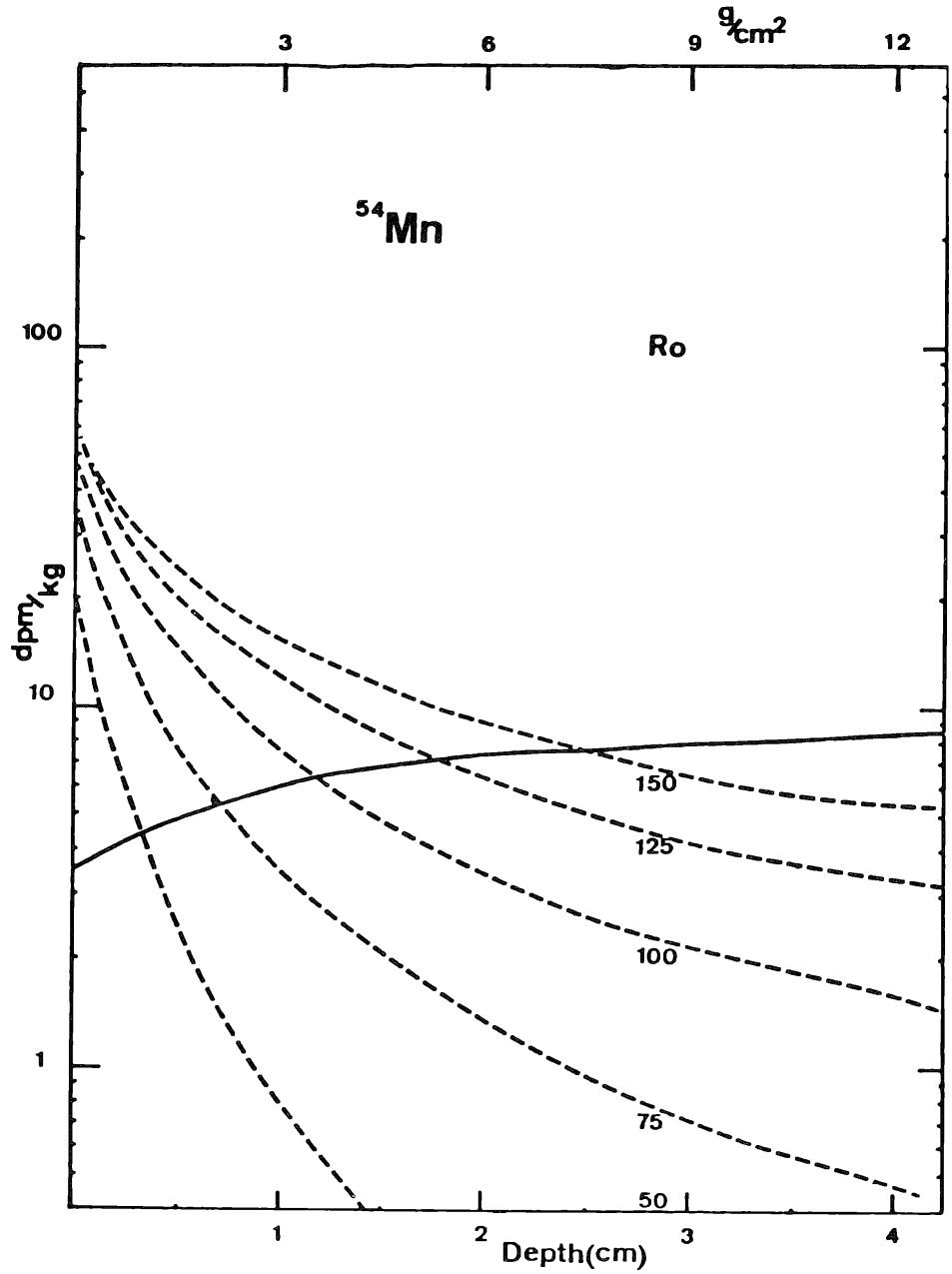

Fig. 7.

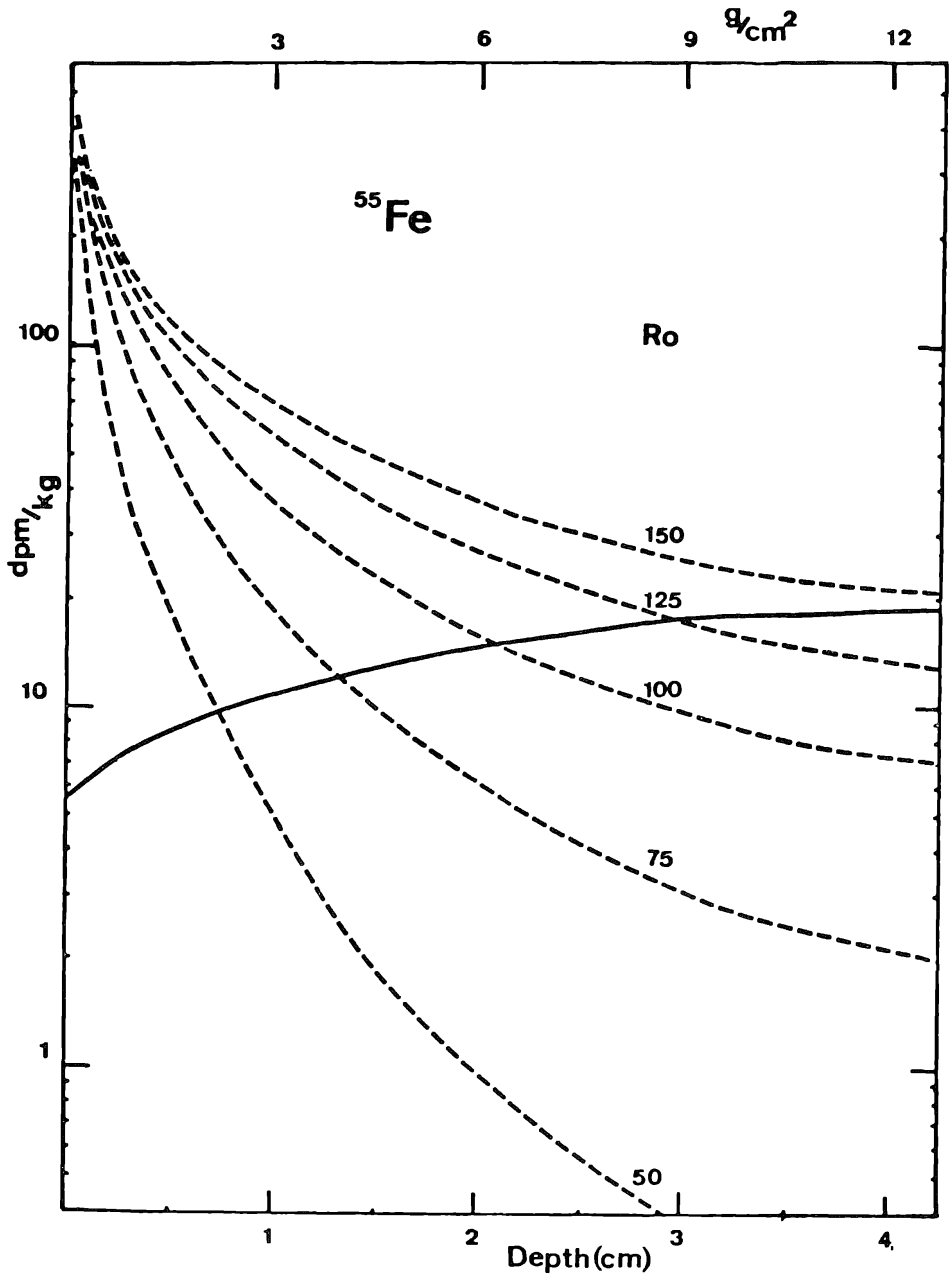

Fig. 8.

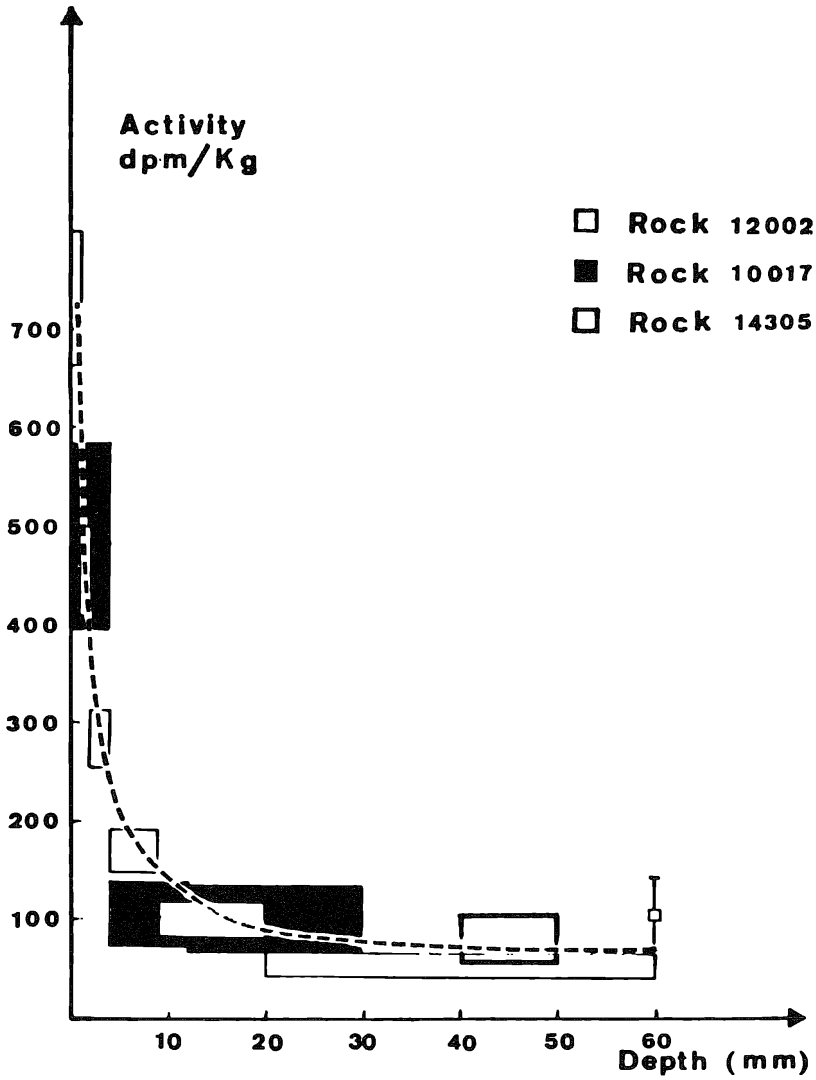

Fig. 9. Measurements of ^{55}Fe in the lunar rocks 14305 (this work), 12002 (Finkel *et al.*, 1971) and 10017 (Shrelldalff, 1970). Iron contents are normalized to 16.8%.

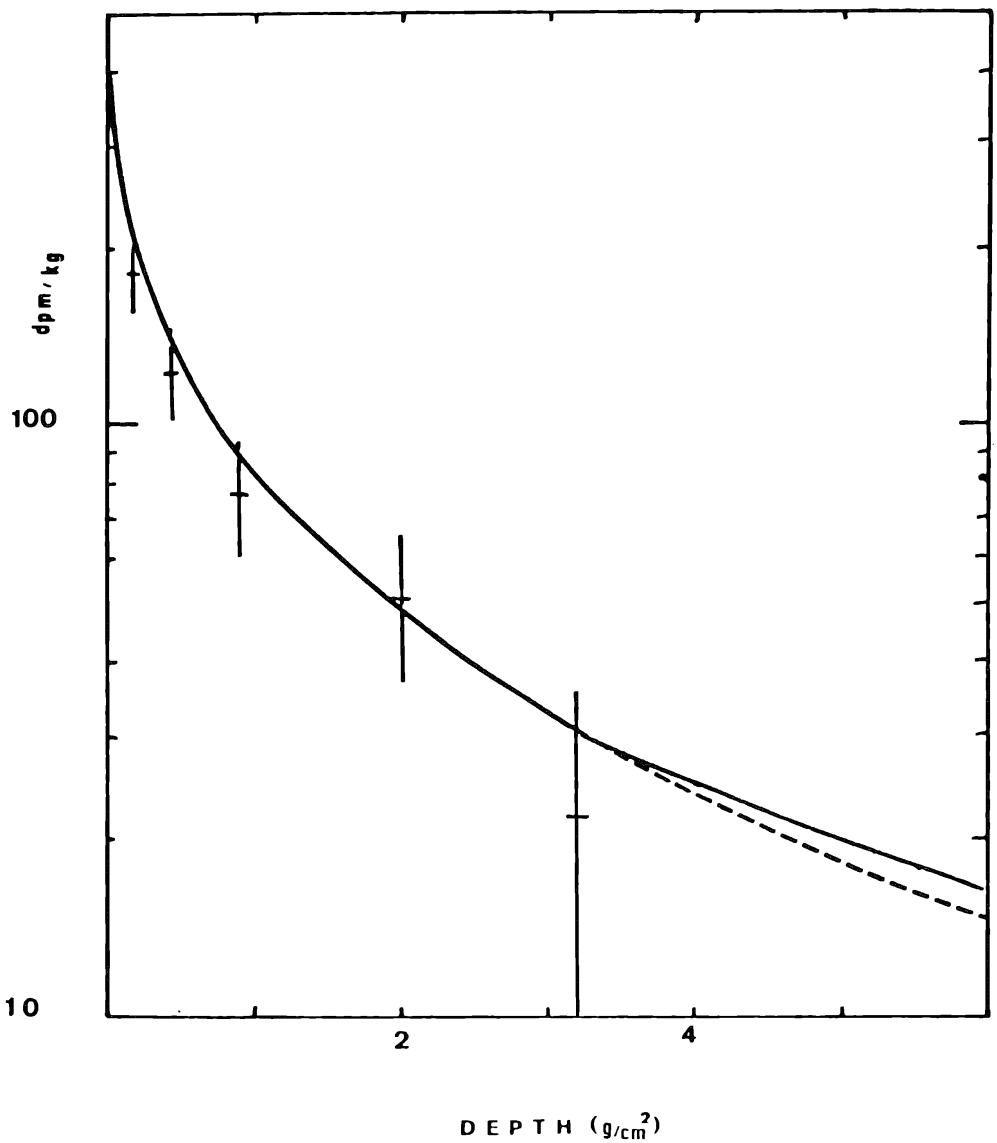

Fig. 10. Depth variation of ^{26}Al produced by solar protons in the lunar rock 12002. The full curve represents the calculated production rate by this work, and the broken curve, that of Reedy and Arnold (1971) for $R_0 = 100$ and $J = 70$. Experimental points are those of Finkel *et al.* (1971), and are given after subtracted for the galactic contributions calculated by this work.

The result of our calculation for the rock 12002 is in good agreement with that of Reedy and Arnold (1971) as shown in Fig. 10. It indicates the validity of our simplified method.

Natural radioactive elements, Th and U were also measured by nondestructive gamma-gamma coincidence spectrometry (Table 1). Our results are in good agreement with the results of LSPET (1971). It shows a possibility of measurement of these elements of small samples (of the order of grams) with a good precision by this method.

Acknowledgments—We are grateful to Dr. J. Labeyrie for his encouragement and helpful discussions. This work is done in the Consortium of rock 14305. We wish to thank Dr. J. Geiss, consortium leader and Dr. N. Grögler for their helpful discussions and their kindness of sawing and preparing of samples. We are also indebted to Drs. J. Tobailem and C. H. de Lassus St-Genies for their kindness of providing the cross-section data prior to publication.

REFERENCES

Armstrong T. W. and Alsmiller R. G. (1971) Calculation of cosmogenic radionuclides in the moon and comparison with Apollo measurements. *Proc. Second Lunar Sci. Conf., Geochim. Cosmochim. Acta* Suppl. 2, Vol. 2. M.I.T. Press.

Crozaz G., Haack U., Hair M., Maurette M., Walker R., and Woolum D. (1970) Nuclear track studies of ancient solar radiations and dynamic lunar surface processes. *Proc. Apollo 11 Lunar Sci. Conf., Geochim. Cosmochim. Acta* Suppl. 1, Vol. 3, pp. 2051–2080. Pergamon.

Finkel R. C., Arnold J. R., Reedy R. C., Fruchter J. S., Loosli H. H., Evans J. C., Shedlovsky J. P., Imamura M., and Delany A. C. (1971) Depth variation of cosmogenic nuclides in a lunar surface rock. *Proc. Second Lunar Sci. Conf., Geochim. Cosmochim. Acta* Suppl. 2, Vol. 2, p. 1773. M.I.T. Press.

Fleischer R. L., Haines E. L., Hart H. R., Woods R. T., and Comstock G. M. (1970) The particle track record of the Sea of Tranquility. *Proc. Apollo 11 Lunar Sci. Conf., Geochim. Cosmochim. Acta* Suppl. 1, Vol. 3, pp. 2103–2120. Pergamon.

Friedlander G. and Kennedy J. W. (1955) *Nuclear and Radiochemistry*, p. 190. John Wiley.

Lal D., MacDougall D., Wilkening L., and Arrhenius G. (1970) Mixing of the lunar regolith and cosmic ray spectra: Evidence from particle track studies. *Proc. Apollo 11 Lunar Sci. Conf., Geochim. Cosmochim. Acta* Suppl. 1, Vol. 3, pp. 2295–2303. Pergamon.

LSPET (1971) (Lunar Sample Preliminary Examination Team) Preliminary examination of lunar samples from Apollo 14. *Science* **173,** 681–693.

Marti K., Lugmair G. W., and Urey H. C. (1970) Solar wind gases, cosmic ray spallation products, and the irradiation history of Apollo 11 samples. *Proc. Apollo 11 Lunar Sci. Conf., Geochim. Cosmochim. Acta* Suppl. 1, Vol. 2, pp. 1357–1367. Pergamon.

O'Kelley G. D., Eldridge J. S., Schofeld E., and Bell P. R. (1970) Primordial radionuclide abundances, solar proton and cosmic ray effects and ages Apollo 11 lunar samples by non-destructive gamma ray spectrometry. *Proc. Apollo 11 Lunar Sci. Conf., Geochim. Cosmochim. Acta* Suppl. 1, Vol. 2, pp. 1407–1422. Pergamon.

Price P. B. and O'Sullivan D. (1970) Lunar erosion rate and solar flare paleontology. *Proc. Apollo 11 Lunar Sci. Conf., Geochim. Cosmochim. Acta* Suppl. 1, Vol. 3, pp. 2351–2359. Pergamon.

Reedy R. C. and Arnold J. R. (1971) Interaction of solar and galactic cosmic ray particles with the moon. To be published in *J. Geophys. Res.*

Shrelldalff (Shedlovsky J. P., Honda M., Reedy R. C., Evans J. C., Lal D., Lindstrom R. M., Delany A. C., Arnold J. R., Loosli H. H., Fruchter J. S., and Finkel R. C.) (1970) Pattern of bombardment produced radionuclides in rock 10017 and in lunar soil. *Proc. Apollo 11 Lunar Sci. Conf., Geochim. Cosmochim. Acta* Suppl. 1, Vol. 2, pp. 1503–1532. Pergamon.

Tanaka S., Sakamoto K., and Komura K. (1971) Al^{26} and Mn^{53} production by solar flare particles in lunar rock and cosmic dust. To be published.

Tobailem J., de Lassus St-Genies C. H., and Leveque L. (1971) Sections efficaces des réactions nucléaires induites par protons, deutons, particules alpha, I. Réaction nucléaires moniteurs. Note CEA-N-1466(1) Commissariat à l'Energie Atomique, France.

Tobailem J. and de Lassus St-Genies C. H. (1972) Sections efficaces des réactions nucléaires induites par protons, deutons, particules alpha, II, III. In preparation.

Wilson R. R. (1947) Range, straggling, and multiple scattering of fast protons. *Phys. Rev.* **71,** 385–386.

Proceedings of the Third Lunar Science Conference
(Supplement 3, *Geochimica et Cosmochimica Acta*)
Vol. 2, pp. 1747–1762
The M.I.T. Press, 1972

Radioactivities in returned lunar materials

E. L. FIREMAN, J. D'AMICO, J. DEFELICE, and G. SPANNAGEL

Smithsonian Institution, Astrophysical Observatory,
Cambridge, Massachusetts 02138

Abstract—The H^3, Ar^{37}, and Ar^{39} radioactivities were measured at several depths in the large documented lunar rocks 14321 and 15555. The comparison of the Ar^{37} activities from similar locations in rocks 12002, 14321, and 15555 gives direct measures of the amounts of Ar^{37} produced by the 2 November 1969 and 24 January 1971 solar flares. From the Ar^{37} measurements, the intensities of the 2 November 1969 and 24 January 1971 solar flares were estimated to be $(5.1 \pm 1.2) \times 10^6$ and $(5.9 \pm 1.0) \times 10^6$ protons $(>50$ MeV)/cm^2 sr, respectively. Because of the large differences in the K and Fe contents of the documented rocks, the Ar^{39} produced from the separate target elements, Fe + Ti, K, and Ca, at 1-, 5-, and 12-cm depths was obtained from the Ar^{39} measurements. The high-energy proton flux (>200 MeV) averaged over 1000 yr was obtained from the Fe + Ti $\rightarrow$ Ar^{39}; the neutron flux ($\gtrsim 1$ MeV) averaged over 1000 yr was obtained from the K $\rightarrow$ Ar^{39}; and the neutron flux ($\gtrsim 10$ MeV) averaged over 1000 yr was obtained from the Ca $\rightarrow$ Ar^{39}. From the depth dependence of Ar^{39}, the intensity of solar-flare protons (>50 MeV) averaged over the past 1000 yr was estimated to be 7×10^8/cm^2 yr. The tritium contents in the documented rocks decreased with increasing depth. The solar-flare intensity averaged over 30 yr obtained from the tritium depth dependence was approximately the same as the flare intensity averaged over 1000 yr obtained from the Ar^{39} measurements. Radioactivities in two Apollo 15 soil samples, H^3 in several Surveyor 3 samples, and tritium and radon weepage were also measured.

INTRODUCTION

THE RADIOACTIVITIES OF Ar^{37}, Ar^{39}, and H^3 were measured in a number of Apollo 11 and 12 samples (Fireman *et al.*, 1970; D'Amico *et al.*, 1970, 1971; Stoenner *et al.*, 1970a, b, 1971; Begemann *et al.*, 1970; Bochsler *et al.*, 1971). In the main, the measurements from different laboratories agree. D'Amico *et al.* (1971) measured the depth variation of Ar^{37}, Ar^{39}, and H^3 in rock 12002, a 6.4-cm-thick crystalline rock.

With samples from known locations in the large documented rocks, 14321 and 15555, we extended the Ar^{37}, Ar^{39}, and H^3 in a number of important ways. Apollo 14 material was subjected to a large solar flare on 24 January 1971, two weeks before sample recovery. No large solar flares occurred for several months before the Apollo 15 mission. The difference between the Ar^{37} activities from similar locations in 12002 and 15555 gives direct measures of the Ar^{37} activities produced by the 2 November 1969 flare, and the difference between the Ar^{37} activities in 14321 and 15555 gives the Ar^{37} activities produced by the 24 January 1971 flare. By use of measured Ar^{37} cross sections in simulated lunar material, the intensities of these flares were determined.

The target elements important for Ar^{39} production are Fe, Ti, K, and Ca. Rock 14321 is a breccia with low Fe and high K contents; rocks 12002 and 15555 have high Fe and low K contents; the Ca and Ti contents of the rocks differ only slightly. Since Ar^{39} is produced by the action of high-energy protons (>200 MeV) on Fe and Ti, by low-energy neutrons ($\lesssim 1$ MeV) on K, and by intermediate-energy neutrons ($\lesssim 10$

MeV) on Ca, the Ar^{39} measurements from similar depths in the rocks determine the Ar^{39} from the separate target elements and the fluxes of the corresponding particles that interact with the separate target elements. The Ar^{39} has a 270-yr half-life so that the fluxes integrated over approximately 1000 yr are obtained from these determinations. The average high-energy proton flux for 1000 yr can be compared with measurements of the galactic rays; the neutron fluxes averaged over 1000 yr can be compared with the neutron fluxes that are obtained from Ar^{37} measurements.

The tritium was released in a two-step heating process, 3-hour heating at 275°C and melting, in the Apollo 14 and 15 and Surveyor 3 materials. The tritium released at 275°C may be either tritium implanted by the solar wind as suggested by D'Amico *et al.* (1971) or terrestrial contamination as suggested by Bochsler *et al.* (1971). The tritium released at high temperatures is mainly caused by solar-flare and galactic cosmic-ray interactions. The depth dependence of the tritium in rocks 14321 and 15555, Apollo 15 soil samples, and Surveyor 3 samples and its temperature-release pattern give information about the sources of the tritium and information about the intensity of solar flares integrated over the past 30 yr.

SAMPLE DESCRIPTION

Both brecciated rock 14321 and crystalline rock 15555 are documented rocks, which means that their position and orientation on the lunar surface were determined from photographs taken by an astronaut on the lunar surface. We received samples 14321,81,* 14321,267,† and 14321,95 from rock 14321. A drawing of 14321, together with a slice taken from the center of the rock showing the locations of the samples, is given in Fig. 1. Sample 14321,81 extended from the top surface to 1.5-cm depth; the material from this sample was broken into three 0.5-cm-thick sections for separate analysis. The orientations of the sections were approximately preserved. Sample 14321,95 was from the bottom of the rock at approximately 12 cm or 40 g/cm^2 depth.

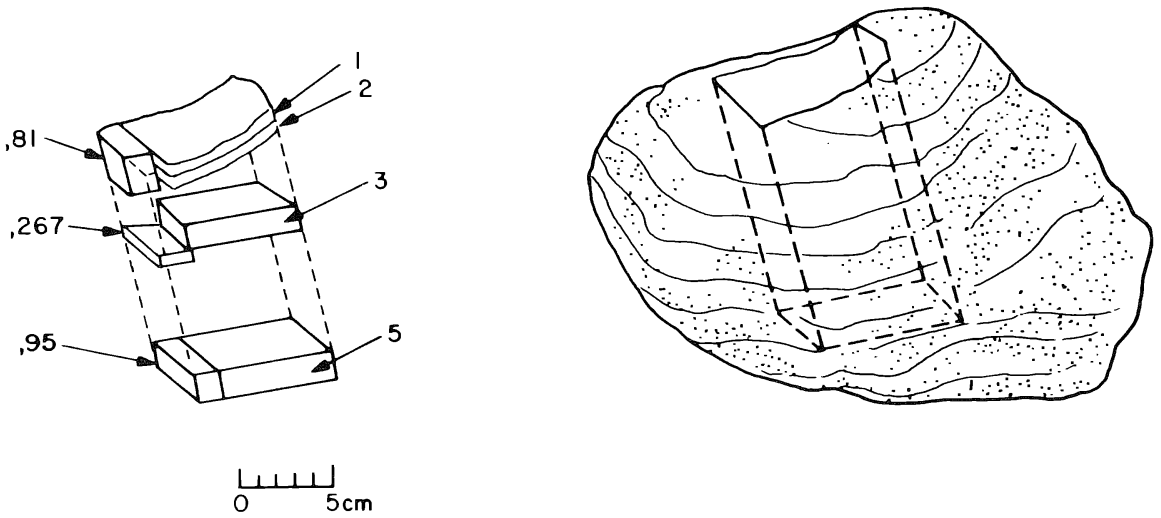

Fig. 1. Lunar rock 14321 and sample locations.

* Samples 14321,81 and 14321,83 were combined and called sample 14321,81.
† Samples 14321,261; 14321,262; and 14321,267 were combined and called 14321,267.

Sample 14321,267 was from 5-cm depth. Although samples 14321,81 and 14321,95 were received 78 days after the Apollo 14 mission, sample 14321,267 was received more than six months after the mission. Nearby samples of 14321 labeled 1, 2, 3, and 5 were analyzed by Wahlen *et al.* (1972) for a number of radioactive nuclides. Figure 1 was obtained from Wahlen *et al.* (1972). Rock 14321 was very fragile, so that samples could be broken with small hand tweezers without much difficulty.

Our samples of 15555 were taken from slice 15555,57 shown by solid lines in Fig. 2,

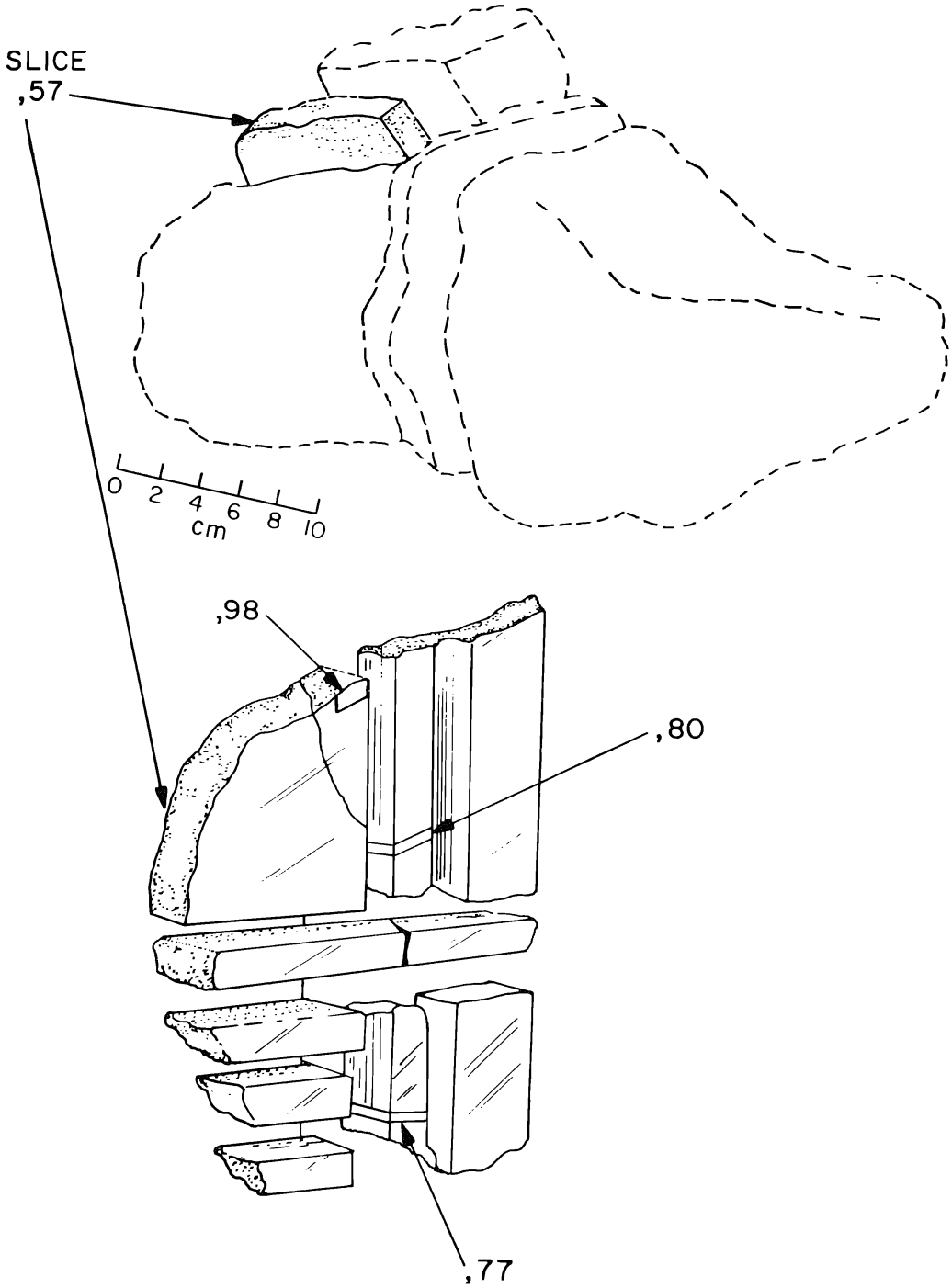

Fig. 2. Lunar rock 15555 and sample locations.

where the outline of rock 15555 is shown by dashed lines. This drawing was made by members of the Lunar Receiving Laboratory. Sample 15555,98 was a top-surface sample approximately 0.8-cm thick. Sample 15555,80 was from near the middle of an adjacent column cut from slice 15555,57 at approximately 6-cm depth, and sample 15555,77 was from near the bottom of the same column at approximately 14-cm depth. These samples were received 119 days after the Apollo 15 mission. Two soil samples, 15271,17 and 15261,14, of 1.97- and 2.04-g weight were received 51 days after the mission; their Ar^{37} activities could be measured more accurately than those in the larger 15555 rock samples. Soil 15271,17 was taken from the compressed wheel track of the lunar rover, and soil 15261,14 was collected from a trench dug into the rim of a 12-m-diameter crater. The depth of the trench was estimated at approximately 30 cm.

EXPERIMENTAL PROCEDURE

Since Ar^{37} decays with a 35-day half-life, we measured the argon radioactivities as rapidly as possible and stored the tritium, except for that from the remelting of the samples, for later analysis. The tritium from the remelt was measured before proceeding to the next sample to ascertain that all tritium had been removed from the sample. The gamma-ray analysis of Apollo 14 samples done at LRL indicated that their uranium and thorium contents were ten-fold higher than those in most previous samples. We therefore put an additional charcoal trap in the purification system to ensure the complete removal of the larger amounts of radon expected from 14321 samples. Otherwise, the extraction and purification procedures for the gases from the 14321 samples were identical to those used for most previous lunar samples (D'Amico *et al.*, 1971). The additional charcoal trap was not used in the processing of the Apollo 15 samples.

The gas was removed in three heatings. After the sample had been placed in a molybdenum crucible that had been previously outgassed, the extraction system was pumped down to a pressure of several Torrs. Hydrogen carrier was added, and the sample was heated to 275°C with a resistance heater for 2 hr. The gases were removed with an automatic toepler pump and stored in a glass bulb for later purification and tritium analysis. The sample was then melted by induction heating in the presence of argon and hydrogen carrier. The gases from the molten Apollo 14 samples were collected on charcoal at liquid-nitrogen temperature and removed at dry-ice temperature, and then transferred to finely divided vanadium powder at 800°C. The gases from the molten Apollo 15 samples were transferred to the vanadium directly. The hot vanadium removed the chemically active constituents; the vanadium was then slowly cooled to room temperature to absorb hydrogen as vanadium hydride. The remaining gas was then removed from the cool vanadium, and its volume measured. If the volume of gas was larger than the amount of argon carrier used, the gas was repurified over vanadium. This procedure was repeated until the volume of gas did not change. At this stage, the volume was the same (within several percent) as that of the argon carrier used. This gas was repurified over hot titanium and condensed on charcoal at liquid-nitrogen temperature. The argon was removed from the charcoal at dry-ice temperature and placed in the same small low-level proportional counters used for Apollo 11 and 12 samples (Fireman *et al.*, 1970; D'Amico *et al.*, 1970, 1971). Methane (10%) was added to the argon. The counter was removed from the purification system and counted in the low-level system, where the counts between 0.4 and 8.0 keV were recorded on a 100-channel analyzer, and those above 7.4 keV, on scalers. Fig. 3 is a plot of the argon counting data for sample 14321,95 for an 8-day period from 27 April to 6 May 1971. Figure 4 is a plot of the argon counting data for 15555,80 for a 22-day period from 6 to 28 December 1971.

The hydrogen was recovered from the vanadium by reheating the vanadium to 800°C and pumping the released hydrogen into a storage bulb.

The sample was then remelted by induction heating, and wall deposits were heated with a torch in the presence of hydrogen carrier. The gas was transferred to finely divided vanadium power at

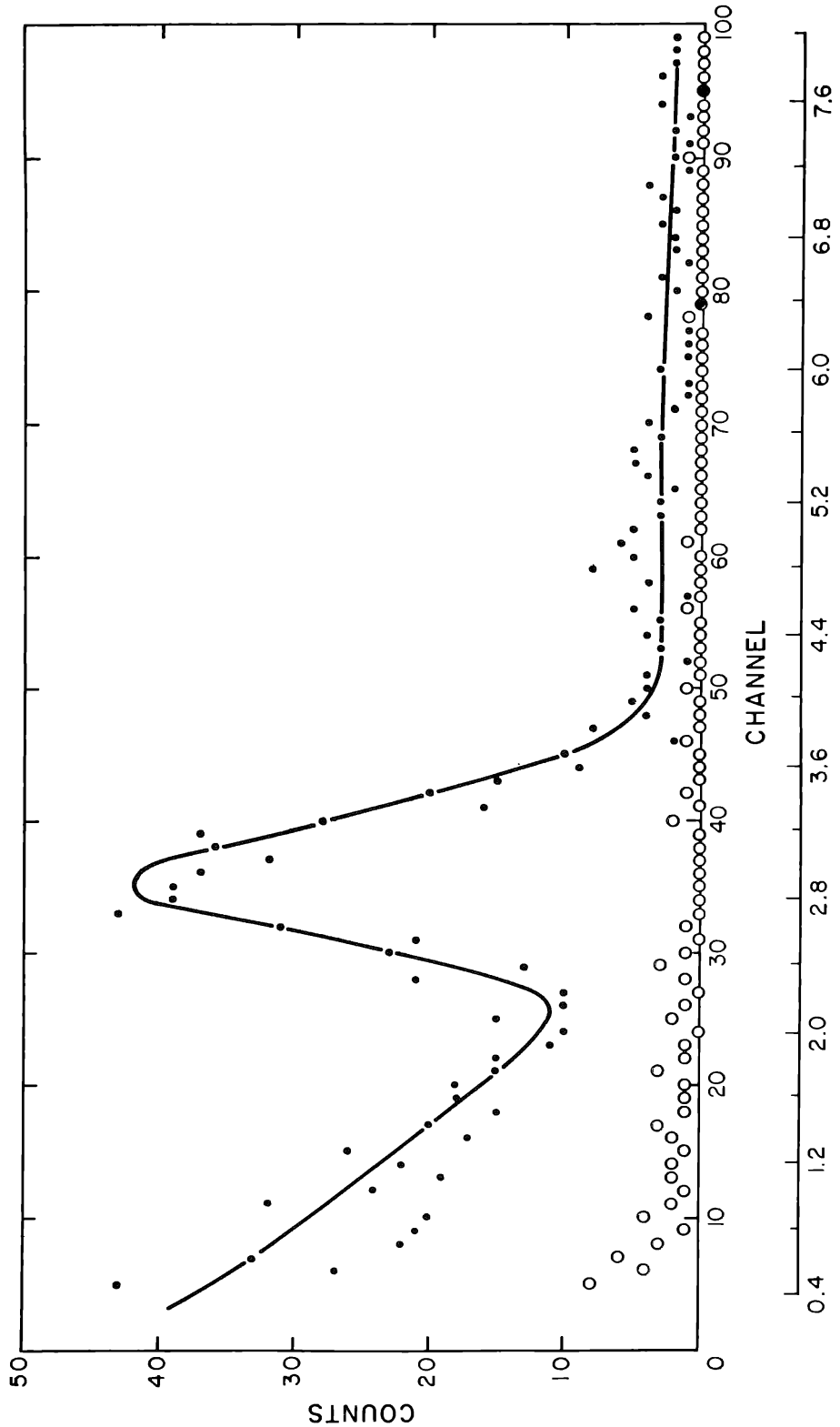

Fig. 3. Argon radioactivities for 10.26 g of lunar rock sample 14321,95. Curve is from calibrations with Ar^{39} = 14.8 ± 1.1 dpm/kg and Ar^{37} = 32.6 dpm/kg. ● = counts/channel, 12158 min, 80 to 88 days after collection on 6 February 1971; ○ = background counts/channel, 11426 min; counts beyond channel 90 = 11. counts beyond channel 99 = 157.

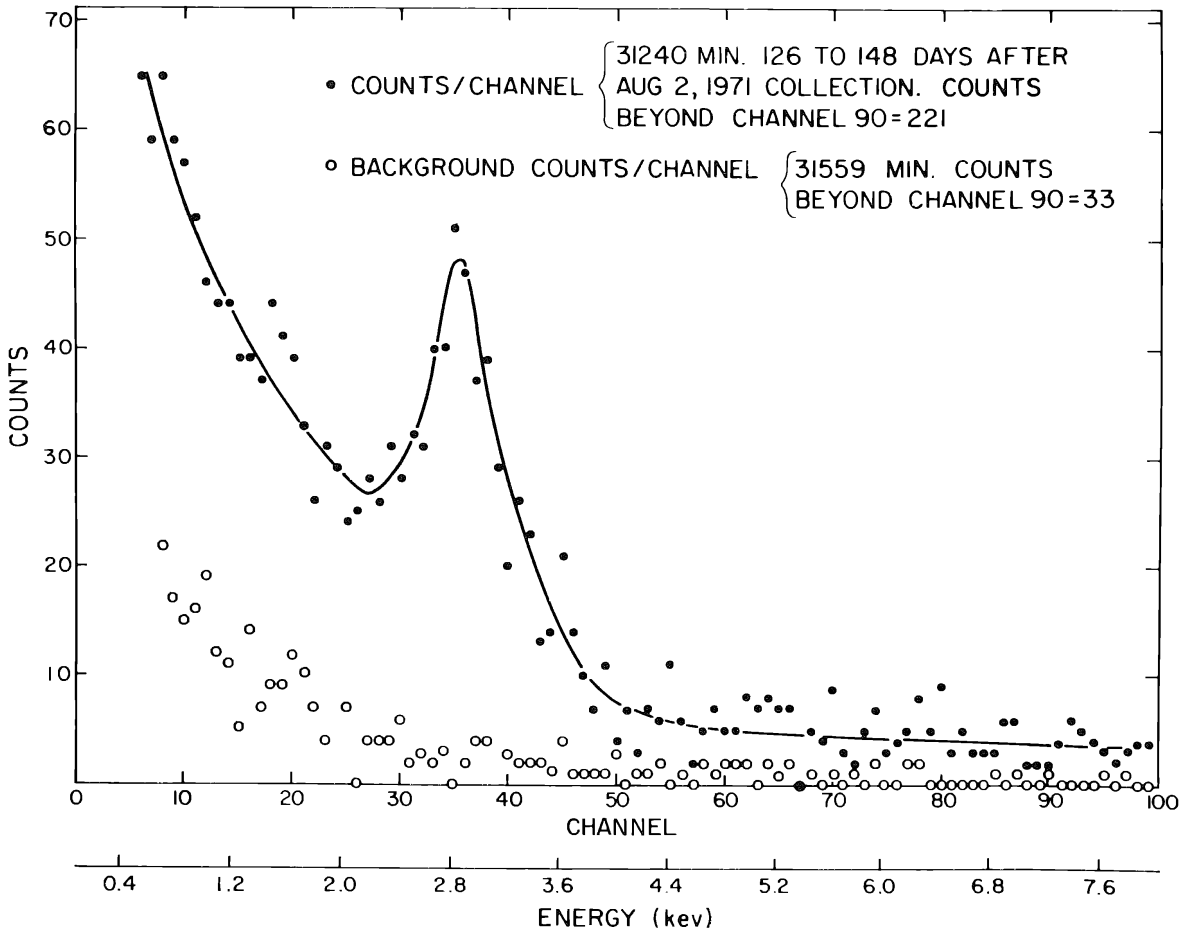

Fig. 4. Argon radioactivity for lunar rock sample 15555,80 (10.25 g).

800°C, which was slowly cooled to room temperature until no gas remained. The hydrogen was removed from the vanadium by reheating and passed through a charcoal trap at dry-ice temperature to remove any possible radon. After its volume had been measured, the hydrogen was added to a low-level proportional counter that contained 400-Torr pressure of P-10 gas. The resolution of the counter was checked with an Fe^{55} source, and the counting was done in a low-level system.

RESULTS

Table 1 gives the Ar^{37} activities that we have measured and the dates of large solar flares that occurred within four months before the missions. Apollo 15 samples were not exposed to any such flares; Apollo 14 samples were exposed to the 24 January 1971 flare 13 days before recovery; and Apollo 12 samples were exposed to the 2 November 1969 flare 21 days before recovery. The Ar^{37} activity in the top sample of 15555, 15.8 $\pm$ 3.0 dpm/kg is a factor of 2.5 lower than in the top sample of 14321 and a factor of 2 lower than in the top sample of 12002. The Ar^{37} activities in 15555 are produced solely by galactic cosmic rays; those in 14321 and 12002 are produced by both galactic cosmic rays and a solar flare. Ar^{37} activity is produced mainly by the action of protons and neutrons on Ca. The Ar^{37} activity per kg of Ca in the top sample of 15555 is slightly lower than in soils 15271, 10017, and 10084, showing that

1972LPSC....3.1637F

Table 1. Ar^{37} activities and solar flares within 4 months of mission.

Sample	Depth (cm)	Recovery date	Flare date	Ar^{37}* (dpm/kg)	Ca (%)	Ar^{37} (dpm/kg Ca)	ΔAr^{37}† (dpm/kg Ca)	Solar-proton flux ($1/cm^2$ sr)	Solar-proton energies
15555,98	0–0.8	2 August 1971	none	15.8 ± 2.8	6.7	236 ± 42	—	—	—
15555,80	~6	2 August 1971	none	31.2 ± 3.3	6.7	465 ± 49	—	—	—
15555,77	~14	2 August 1971	none	35.0 ± 6.5	6.7	520 ± 97	—	—	—
14321,81,83	0–0.5	6 February 1971	24 January 1971	38.5 ± 2.5	6.4	600 ± 39	364 ± 60	$(5.9 \pm 1.0) \times 10^6$	(> 50 MeV)
14321,81,83	0.5–1.0	6 February 1971	24 January 1971	37.6 ± 2.5	6.4	590 ± 39	354 ± 60	—	—
14321,81,83	1.0–1.5	6 February 1971	24 January 1971	35.0 ± 4.0	6.4	550 ± 63	324 ± 75	—	—
14321,95	~12	6 February 1971	24 January 1971	34.0 ± 2.7	6.4	530 ± 42	≤100	$(< 1.6) \times 10^6$	(> 200 MeV)
12002,57	0–0.8	23 November 1969	2 November 1969	30.0 ± 4.0	5.4	556 ± 65	320 ± 70	$(5.1 \pm 1.2) \times 10^6$	(> 50 MeV)
12002,57	0.8–3.1	23 November 1969	2 November 1969	25.0 ± 1.5	5.4	463 ± 28	160 ± 50	$(2.6 \pm 0.9) \times 10^6$	(> 70 MeV)
12002,59	4.9–6.4	23 November 1969	2 November 1969	27.5 ± 2.5	5.4	510 ± 46	55 ± 65	$(0.9 \pm 1.1) \times 10^6$	(> 100 MeV)
Soil 15271,17	0–5	2 August 1971	none	21.4 ± 2.0	8.1	264 ± 25	—	—	—
Soil 15261,14	~30	2 August 1971	none	26.4 ± 3.0	—	—	—	—	—
Soil 10017,14	0–5	21 July 1969	none	21.0 ± 2.0	7.4	284 ± 27	20 ± 37	—	—
Soil 10084,24	0–5	21 July 1969	none	27.2 ± 2.2	8.8	309 ± 25	45 ± 35	—	—

* Activity at time of recovery.

† Solar-flare-produced Ar^{37} from calcium, $\Delta Ar^{37} = (Ar^{37}/\%\ Ca) - [Ar^{37}(15)/\%\ Ca]$, where $Ar^{37}(15)$ is the Ar^{37} in an Apollo 15 sample at a comparable depth.

these soil samples, although not affected by solar flares, were taken from slightly larger average depths than sample 15555,98 was. The solar-flare-produced Ar^{37} in the top samples of 14321 and 12002 were 364 ± 60 dpm/kg Ca and 324 ± 70 dpm/kg Ca, respectively; however, at approximately 6-cm depth, the solar-flare-produced Ar^{37} is only 55 ± 65 dpm/kg Ca.

Reedy and Arnold (1972) calculated the Ar^{37} activities as a function of depth by galactic cosmic rays on lunar material. The Ar^{37} activity measured at three depths in rock 15555 agrees quite well with Reedy and Arnold's calculations. It is not necessary to use Reedy and Arnold's calculations to obtain the intensities of the 24 January 1971 and the 2 November 1969 flares from the Ar^{37} measurements. D'Amico *et al.* (1971) measured the Ar^{37} production cross sections in a series of targets of simulated lunar material containing 6.7% Ca bombarded by 158-MeV protons. Interspersed between the lunar-type targets were iron absorbers so that the Ar^{37} production cross sections for 50-, 85-, and 158-MeV protons could be determined. The protons of these energies in the flares should contribute more Ar^{37} than those of higher energies if the differential energy spectrum varies as E^{-3}; the Ar^{37} production cross section, $\sigma_{Ca}(Ar^{37})$, is 60 ± 3 mb for 158- and 85-MeV protons and 10.8 ± 1.0 mb for 50-MeV protons. The cross section falls steeply between 85 and 50 MeV; below 50 MeV, the cross section probably falls even more steeply. On the basis of these cross sections and the solar-flare-produced Ar^{37} from calcium, ΔAr^{37}, which is defined in Table 1, we estimate the solar-flare-proton fluxes given in Table 1. The 24 January 1971 flare intensity is estimated to be $(5.9 \pm 1.0) \times 10^6$ protons/cm^2 sr greater than 50-MeV energy; the 2 November 1969 flare intensity is estimated to be $(5.1 \pm 1.2) \times 10^6$ protons/cm^2 sr (>50 MeV). These flare intensities obtained from lunar rocks can be compared with satellite measurements. From the Explorer 35 satellite, Van Allen (private communication, 1972) obtained 4.9×10^6 protons (>55 MeV/cm^2 sr) for the 24 January 1971 flare and 3.2×10^6 protons (>55 MeV/cm^2 sr) for the 2 November 1969 flare with 20% uncertainty. The intensities of the flares obtained from the Ar^{37} activities in lunar rocks are slightly higher than those obtained by Van Allen from his Explorer 35 counters.

Table 2 gives the Ar^{39} activities at several depths in three oriented lunar rocks and in four soil samples. An interesting feature of the Ar^{39} activities is that the Ar^{39} increases with depth in 14321, a high K rock, but is approximately constant with depth in low K rocks 15555 and 12002. Ar^{39} is produced by high-energy protons on Fe (>300 MeV) and on Ti ($\gtrsim$200 MeV); on the other hand, Ar^{39} is produced from K and Ca by the action of neutrons through the K^{39} (n, p) and Ca^{40} $(n, 2p)$ reactions. The K^{39} reaction is exothermic; the Ca^{40} reaction has an 8.1-MeV threshold energy. The Ar^{39} production rates for four individual target elements can be calculated from Ar^{39} measurements in four lunar samples at the same depth; however, such calculated rates would have considerable error and there would be no consistency checks. If the Ar^{39} production rates from Fe and Ti are lumped together and the Fe + Ti → Ar^{39} production rate is estimated theoretically, then the K → Ar^{39} and Ca → Ar^{39} production rates are obtained from the data with relatively small errors and there are six samples that remain for consistency checks. We have therefore adopted this procedure for obtaining the Ar^{39} production rates in K and Ca.

Table 2. Ar^{39} activities, estimated productions from target elements with and without energetic solar flares, and neutron fluxes.

							Situation 1 No solar-flare protons (>200 MeV) past 1000 yr			Situation 2 Solar-flare protons (>200 MeV) past 1000 yr equal galactic cosmic rays			Neutrons/cm² sec	
Sample	Depth (cm)	K (%)*	Fe (%)*	Ti (%)*	Ca (%)*	Ar^{39} (dpm/kg)	Fe + Ti → Ar^{39} (dpm/kg)†	K → Ar^{39} (dpm/kg)	Ca → Ar^{39} (dpm/kg)	Fe + Ti → Ar^{39} (dpm/kg)‡	K → Ar^{39} (dpm/kg)	Ca → Ar^{39} (dpm/kg)	>1 MeV**	>10 MeV††
15555,98	0–0.8	0.025	17.5	1.36	6.7	8.4 ± 0.5	1.8	0.13	6.5	3.6	0.17	4.7		
15555,80	~6	0.025	17.5	1.36	6.7	7.5 ± 0.5	1.7	0.3	5.5	3.4	0.5	3.7		
15555,77	~14	0.025	17.5	1.36	6.7	9.8 ± 0.8	1.4	0.4	8.0	2.8	0.6	6.3		
14321,81	0–0.5	0.37	8.6	1.2	6.4	8.8 ± 0.5	1.0	2.0 ± 0.6	5.8 ± 0.7	2.0	2.6 ± 0.6	4.2 ± 0.6	3.7	2.0
14321,81	0.5–1.0	0.37	8.6	1.2	6.4	8.3 ± 0.7	1.0	2.0 ± 0.6	5.8 ± 0.7	2.0	2.6 ± 0.6	4.2 ± 0.6	3.7	2.0
14321,81	1.0–1.5	0.37	8.6	1.2	6.4	9.5 ± 0.8	1.0	2.0 ± 0.6	5.8 ± 0.7	2.0	2.6 ± 0.6	4.2 ± 0.6	3.7	2.0
14321,267	~5	0.37	8.6	1.2	6.4	12.1 ± 1.0	0.95	6.2 ± 1.1	5.0 ± 0.7	1.9	7.0 ± 1.2	3.2 ± 0.5	10.6	1.6
14321,95	~12	0.37	8.6	1.2	6.4	14.8 ± 1.0	0.84	6.8 ± 1.2	7.2 ± 0.9	1.7	7.5 ± 1.3	5.7 ± 0.8	12	2.7
12002,57	0–0.8	0.045	16.5	1.5	5.4	8.0 ± 0.7	1.8	0.3	5.2	3.6	0.4	3.7		
12002,57	0.8–3.1	0.045	16.5	1.5	5.4	8.2 ± 0.5	1.8	0.4	5.2	3.5	0.5	3.7		
12002,59	4.9–6.4	0.045	16.5	1.5	5.4	8.0 ± 0.6	1.7	0.7	4.4	3.4	0.9	3.0		
Soil:														
15271,17	0–5	0.17	9.5	0.88	8.1	10.0 ± 1.5	1.0	0.9	7.7	2.0	1.2	5.6		
15261,14	~30	—	—	—	—	7.1 ± 1.0	—	—	—	—	—	—		
10017,14	0–5	0.24	15.3	7.1	7.4	16.4 ± 0.9	3.0	1.3	7.2	6.0	1.8	5.2		
10084,24	0–5	0.11	12.3	4.4	8.8	12.1 ± 0.7	2.0	0.6	8.4	4.0	0.8	6.2		

* A weight percent obtained from various publications of chemical composition of lunar material.
† Reedy and Arnold's calculated galactic cosmic-ray production rate of Ar^{39} from Fe + Ti (private communication, 1972).
‡ Twice calculated galactic cosmic-ray production rate of Ar^{39} from Fe + Ti.
** Based on Ar^{39} from K^{39} with $\sigma(n,p) = 200$ mb.
‡‡ Based on Ar^{39} from Ca^{40} with $\sigma(n,2p) = 40$ mb.

In Table 2, two situations are represented: (1) the Ar^{39} from Fe + Ti is produced solely by galactic cosmic rays of the present average intensity and is given by Reedy and Arnold's calculation (private communication, 1972); and (2) extremely energetic solar flares have occurred during the past 1000 yr, which raised the cosmic-ray intensity to twice the present average, so that the Ar^{39} from Fe + Ti is twice the Reedy and Arnold value.

The calculation proceeds by subtracting the Ar^{39} produced from Fe + Ti from the measured Ar^{39} to give the Ar^{39} from Ca + K. The Ar^{39} produced from Ca and the Ar^{39} from K are regarded as unknowns, and a pair of simultaneous equations is set up with 14321 and 15555 data. These equations are solved for each depth. The results are given in Table 2. Because 15555 and 14321 samples differ by a factor of 15 in K contents, the procedure gives the Ar^{39} produced from Ca and from K with errors of the same magnitude as the error in the Ar^{39} measurement. Ar^{39} from K for situation (1) is approximately 15% lower than from situation (2); the Ar^{39} from Ca for situation (1) is 40% higher than from situation (2). With these production rates, the Ar^{39} production rates from K and from Ca for rock 12002 samples and the soil samples are calculated. The sum of the productions from the individual target elements agrees fairly well with the measured Ar^{39} activities for most cases. In soil 10017 the measured Ar^{39} activity is too high. Situation (2) gives a better approximation to the measured activities for the six samples that serve as consistency checks than does situation (1). The K $\rightarrow$ Ar^{39} production rate for the top of 14321 is lower than estimated by Begemann *et al.* (1970) for Apollo 11 fines.

The question arises as to how large can the Fe + Ti $\rightarrow$ Ar^{39} rate be made before inconsistencies arise. The Ar^{39} measured activity in sample 15555,80 limits the Fe + Ti $\rightarrow$ Ar^{39} production rate to less than four times the Reedy and Arnold calculated rates. Therefore, the intensity of solar-flare protons of energy greater than $\sim$200 MeV averaged over the past 1000 yr must be less than four times the intensity of the recent galactic cosmic rays if galactic cosmic rays have remained unchanged over 1000 yr.

The next question is whether or not there is any positive evidence from the Ar^{39} measurements for the presence of lower energy protons (<200 MeV) from solar flares during the past 1000 yr. The depth variation of Ca $\rightarrow$ Ar^{39} does provide positive evidence for low-energy solar flares. The Ca $\rightarrow$ Ar^{39} production rates for all cases decrease slightly with increasing depth from 0 to 5 cm and then increase with increasing depth from 5 to 14 cm. Such a depth dependence is different than that expected for galactic cosmic rays. For example, Reedy and Arnold (1972) calculate that the Ca $\rightarrow$ Ar^{39} from galactic cosmic rays should increase by a factor of 2 in the first 5-cm depth. A direct determination of the intensity of <200-MeV solar-flare protons averaged over 1000 yr from the Ca $\rightarrow$ Ar^{39} production rates requires knowledge of the Ar^{39} production cross section in thick Ca targets bombarded by protons of less than 200-MeV energy. These cross sections have not been measured. Since neutron-production cross sections for Ar^{39} from K^{39} and from Ca^{40} are known, the neutron fluxes from the K $\rightarrow$ Ar^{39} and Ca $\rightarrow$ Ar^{39} determinations can be obtained and the neutron fluxes can be used to estimate the flux of solar-flare protons.

The $\sigma(n, p)$ cross section in K^{39} decreases from 350 $\pm$ 50 mb for 14-MeV neutrons, to 270 $\pm$ 40 mb for 4-MeV neutrons, and to approximately 50 mb for 1.5-MeV

neutrons (Stehn *et al.*, 1964). Although neutrons of lower energies produce Ar^{39} from K^{39}, we call the neutron flux obtained from the $K^{39} \rightarrow Ar^{39}$ reaction the (>1 MeV) neutron flux in Table 2, because of energy dependence of the cross section. This flux is 3.7, 10.6, and 12/cm^2 sec at 1-, 5-, and 12-cm depths, respectively, with a $\sigma(n, p)$ cross section of 200 mb. The (>1-MeV) neutron flux increases with increasing depth. The $K \rightarrow Ar^{39}$ production rates in 14321 are almost twice the rates calculated by Reedy and Arnold for galactic cosmic-ray production (private communication, 1972).

The $\sigma(n, 2p)$ on Ca^{40} has an 8.1-MeV threshold and is 35 mb for 14-MeV neutrons (Stoenner *et al.*, 1971). The contribution of Ca^{42} to Ar^{39} is small because of its low natural abundance, 0.6%, if the (n, α) Ca^{42} cross section is similar to the (n, α) Ca^{40} cross section. The Ar^{39} from Ca is therefore mainly produced by greater than 10-MeV neutrons on Ca^{40} with approximately a 40-mb cross section. The (>10 MeV) neutron fluxes obtained from the $Ca \rightarrow Ar^{39}$ column in Table 2 are 2.0, 1.6, and 2.7/cm^2 sec at approximately 1-, 5-, and 12-cm depths, respectively. The action of galactic cosmic rays on lunar material should produce a neutron flux (>10 MeV) that increases with increasing depth for the first 14 cm. Evidently, solar flares during the past 1000 yr have increased the >10-MeV neutron flux in the top centimeter of material by approximately one neutron per cm^2 sec relative to the flux at 5-cm depth. We shall assume that neutrons of greater than 10-MeV energy are produced by solar-flare protons of greater than 50-MeV energy with a cross section of 0.5 b; then 25 protons of (>50 MeV) energy are required to produce one neutron of (>10 MeV) energy in the top centimeter. With this estimate, a solar-flare-proton flux (>50 MeV) of 25/cm^2 sec or 7×10^8/cm^2 yr averaged over the past 1000 yr is obtained from $Ca \rightarrow Ar^{39}$ values in Table 2. On the bases of the Ar^{37} depth dependence after the 24 January 1971 and 2 November 1969 flares, we estimated that approximately 6×10^6/cm^2 sr or 4×10^7/cm^2 of protons >50 MeV were in each of these flares. From the Ar^{39} depth dependence, we estimate that during the past 1000 yr, the flare flux was equivalent to 15 such flares per year.

The measured tritium radioactivities from the samples of 14321 and 15555 and two Apollo 15 soil samples with their approximate depths are given in Table 3. Very little tritium was released at 275°C from the 14321 and 15555 samples. From soil 15271,17, 15% of the tritium was released at 275°C and from soil 15261,14, 8% of the tritium was released at 275°C. If the low-temperature tritium observed from the top of rock 12002 (D'Amico *et al.*, 1971) and from soil 15271 is caused by solar-wind implantation of tritium, then the top surface material from our 14321 and 15555 samples, which should contain solar wind, was lost during the sawings and handlings. This is quite likely for 14321, which was a fragile breccia. Rock 15555 is a crystalline rock; our top sample, 15555,98, was from a broken sloped section (see Fig. 2) and could also have had its surface material removed in handling and sawing; however, this is less likely. In both rocks 15555 and 14321, the tritium decreased with increasing depth; however, the decrease was quite small from 6- to 14-cm depth in rock 15555. The decrease of tritium contents with depth is evidence for tritium produced by solar-flare interactions. Figure 5 gives the H^3 depth dependence in the three rocks. The top samples of 15555 and of 14321 had 280 ± 14 dpm/kg compared to 392 ± 11 dpm/kg of tritium in the top of 12002. Differences in the topographies of the rocks probably

Table 3. Tritium activities in Apollo 15 and 14 samples.

Sample	Wt (g)	Depth (cm)	Temperature (°C)	H^3 (dpm/kg)	Total H^3 (dpm/kg)	Extraction date
15555,98	10.65	0–1	275	< 3		
		surface	Melt	260 ± 9	281 ± 11	12/10/71
			Remelt	21 ± 5		
15555,80	10.25	~6	275	11 ± 3		
			Melt	146 ± 6	171 ± 8	12/2/71
			Remelt	14 ± 3		
15555,77	8.44	~14	275	< 3		
			Melt	141 ± 5	166 ± 8	12/23/71
			Remelt	25 ± 5		
14321,81	10.08	0–0.5	275	< 3		
		surface	Melt	270 ± 12	280 ± 14	5/10/71
			Remelt	10 ± 2		
14321,81	8.49	0.5–1.0	275	5 ± 3		
			Melt	197 ± 6	208 ± 8	5/3/71
			Remelt	6 ± 3		
14321,81	9.46	1.0–1.5	275	6 ± 3		
			Melt	164 ± 8	198 ± 11	4/28/71
			Remelt	28 ± 5		
14321,267	4.7	~5	275	15 ± 5		
			Melt	161 ± 7	176 ± 11	7/20/71
			Remelt	< 7		
14321,95	10.08	~12	275	3 ± 3		
			Melt	133 ± 5	145 ± 8	5/25/71
			Remelt	9 ± 4		
Soil 15271,17	1.97	0–5	275	45 ± 7		
			Melt	255 ± 10	300 ± 15	10/7/71
			Remelt	< 7		
Soil 15261,14	2.03	~30	275	20 ± 5		
			Melt	220 ± 15	240 ± 15	9/24/71
			Remelt	< 4		

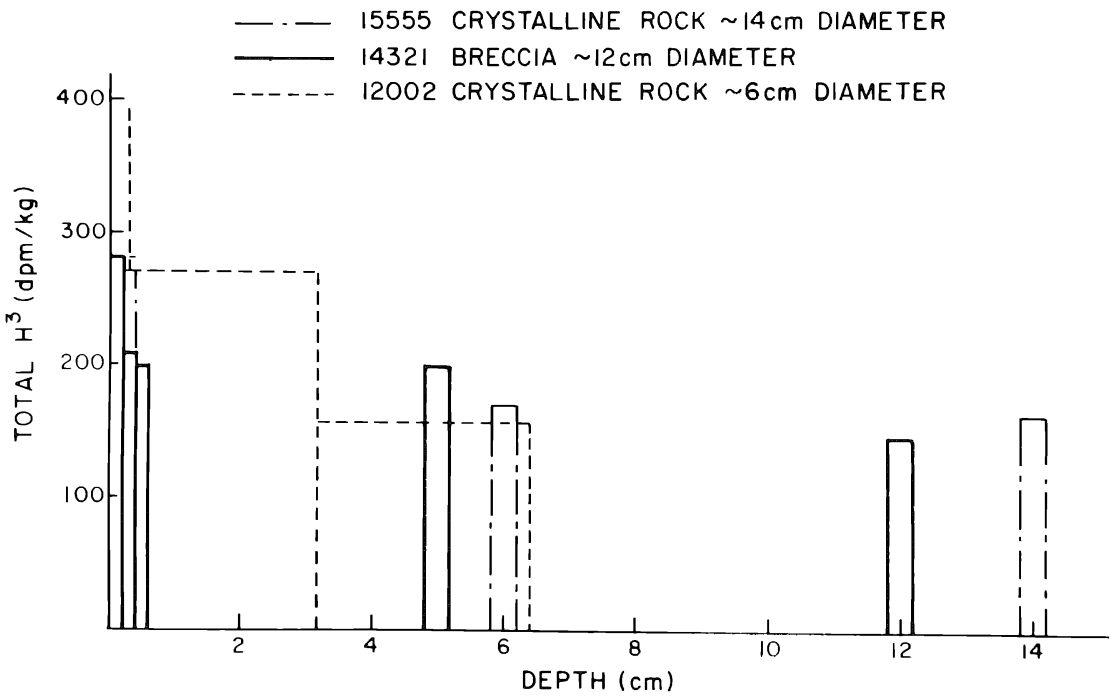

Fig. 5. Depth variation of tritium.

account for most of tritium differences between the samples at similar depths. We do not consider the differences in tritium contents between samples from 15555, 14321, and 12002 to indicate any serious discrepancies, except possibly for the high tritium in the top sample of 12002. Soil sample 15271,17 had 300 ± 15 dpm/kg, and soil 15261,14 had 240 ± 15 dpm/kg of tritium. An estimated 150 dpm/kg of tritium were produced by the action of solar flares in the top centimeter of 14321 and 15555, based on the tritium depth dependences. The solar-flare intensity calculated with this tritium excess is 1.7×10^9 protons (>30 MeV)/cm^2 yr or 6×10^8 (>50 MeV)/cm^2 yr with an E^{-3} differential energy spectrum. The cross sections for this calculation are given by D'Amico *et al.* (1970). This intensity, which represents an average over the past 30 yr, is nearly the same as that obtained from the Ar^{39}.

The gases from the Apollo 15 soil samples were extracted approximately two months after recovery; the gases from rock 15555 samples were extracted 4 to 4½ months after recovery. During most of these times, the samples were stored at room temperature with an atmosphere of either air or dry nitrogen. To examine whether or not this type of storage had any effect on the tritium contents, samples of an Apollo 15 soil, crystalline rock, and breccia were sealed in closed containers with air and hydrogen carrier on 9 August 1971, shortly after the returned sample box was opened. After approximately three months' storage at room temperature, the tritium and radon radioactivities in the gas were measured. The results are given in Table 5, where the tritium in the gas of the sealed container is called tritium weepage. No tritium weeped from the crystalline rock sample, which was a sample of 15555. We therefore conclude that the tritium activities measured in 15555 were actually the activities at the time of sample return. The amount tritium weeped from breccia 15565 was only 12.8 ± 1.0 dpm/kg, which is between 5 and 10% of the amounts observed in breccia 14321. If breccia 14321 is similar to breccia 15565 with regard to tritium weepage, then three months of storage only reduced its tritium contents by 5 to 10%. However, the tritium weepage from soil 15021, 51 ± 4 dpm/kg, was 20% of the amount observed in soil 15271. If the tritium content of 15271 soil is raised by 20%, its total tritium content is higher than in the top samples from rocks 14321 and 15555 and quite close to the tritium content observed in the top sample of 12002. This may add some support to the suggestion made by D'Amico *et al.* (1971) that the low-temperature tritium from the top of rock 12002 was solar-wind-implanted tritium.

Table 4 gives the hydrogen and tritium data from Surveyor 3 samples. Although most lunar samples were analyzed with the counter of 42-cm^3 volume and a background of 0.140 ± 0.005 count/min, most Surveyor 3 samples, because of their smaller hydrogen contents, were analyzed with the counter of 7-cm^3 volume and background of 0.0261 ± 0.0014 count/min. The Surveyor samples are very thin, ~0.2 g/cm^2 thick. Two of the Surveyor samples were exposed to sunlight while on the moon; these released tritium at 270°C. One of the Surveyor samples was facing the soil and protected from sunlight; it released no tritium at 270°C. This sample has 198 ± 25 dpm/kg of tritium. Since 198 ± 25 dpm/kg of the tritium were produced during 2.4 yr, the tritium activity at saturation is 1580 ± 150 dpm/kg. The higher tritium contents in Surveyor 3 material exposed to sunlight than in lunar material indicates that those samples were either contaminated with terrestrial tritium or contain loosely bound tritium that was implanted at the surface by solar wind. Even the

Table 4. Tritium and hydrogen data from Surveyor 3 samples.

Sample	Wt. (g)	Area (cm^2)	Extraction	Hydrogen (ccSTP)	Counter volume (efficiency)	Background (count/min)	Sample (count/min)	H^3 (dpm)	H^3 (dpm/kg)	H^3 (dpm/cm^2)	H^3 (sat.) (dpm/kg)
Painted aluminum blank	0.320	1.3	Melt	0.45	42 cm^3 (62%)	0.140 ± 0.005	0.139 ± 0.005	< 0.012			
Painted aluminum blank	0.255	1.0	Melt	0.47	14 cm^3 (55%)	0.048 ± 0.003	0.042 ± 0.003	< 0.008			
Painted aluminum blank	0.335	1.3	20–270°C	0.09	7 cm^3 (50%)	0.0261 ± 0.0014	0.0269 ± 0.0017	< 0.005			
			270°C-melt	0.30							
Surveyor 1011,2	0.335	1.3	20–270°C	0.62	7 cm^3 (50%)	0.0261 ± 0.0014	0.0353 ± 0.0016	0.018 ± 0.004	54 ± 12	0.014 ± 0.003	430 ± 95
Some sunlight		—	270°C-melt	0.82	7 cm^3 (50%)	0.0261 ± 0.0014	0.0375 ± 0.0016	0.022 ± 0.004	66 ± 12	0.017 ± 0.003	530 ± 95
		—	Wall heating and remelt	0.70	7 cm^3 (50%)	0.0261 ± 0.0014	0.0383 ± 0.0016	0.023 ± 0.004	68 ± 12	0.018 ± 0.003	545 ± 96
		—	2nd wall heating and remelt	0.09	7 cm^3 (50%)	0.0261 ± 0.0014	0.0252 ± 0.0016	< 0.004	< 12	< 0.003	< 95
Total								0.063 ± 0.007	188 ± 21	0.049 ± 0.005	1505 ± 170
Surveyor 1002	0.243	1.86	20–270°C	with H_2 carrier	7 cm^3 (50%)	0.0261 ± 0.0014	0.0270 ± 0.0016	< 0.004	< 16	< 0.002	
No sunlight			270°C-melt	with H_2 carrier	7 cm^3 (50%)	0.0261 ± 0.0014	0.0432 ± 0.0016	0.034 ± 0.004	140 ± 16	0.018 ± 0.002	1120 ± 130
			Wall heating and remelt	with H_2 carrier	0.5 cm^3 (68%)	0.0070 ± 0.0010	0.0166 ± 0.0014	0.014 ± 0.002	58 ± 8	0.008 ± 0.001	466 ± 50
			2nd wall heating and remelt	with H_2 carrier	7 cm^3 (50%)	0.0261 ± 0.0014	0.0284 ± 0.0016	< 0.005	< 20	< 0.003	< 150
Total								0.048 ± 0.005	198 ± 25	0.026 ± 0.003	1580 ± 150
Surveyor 1015	0.394	1.67	20–270°C	with H_2 carrier	7 cm^3 (50%)	0.0261 ± 0.0014	0.0651 ± 0.0044	0.078 ± 0.009	198 ± 23	0.047 ± 0.005	1580 ± 185
Most sunlight			270°C-melt	with H_2 carrier	7 cm^3 (50%)	0.0261 ± 0.0014	0.0515 ± 0.0028	0.051 ± 0.006	130 ± 15	0.030 ± 0.004	1040 ± 120
			Remelt	with H_2 carrier	42 cm^3 (62%)	0.140 ± 0.004	0.147 ± 0.004	0.011 ± 0.009	28 ± 23	0.006 ± 0.005	210 ± 185
Total								0.129 ± 0.014	328 ± 36	0.077 ± 0.009	2620 ± 240

Table 5. Tritium and radon weepage from Apollo 15 samples packaged with air on 9 August 1971.

Sample	Type	Wt (g)	Extraction date	H^3 (dpm/kg)	Rn^{222*} (dpm/kg)
15555,1	Crystalline rock	18.7	23 November 1971	< 3	—
15565	Breccia	9.7	28 October 1971	12.8 ± 1.0	25 ± 5
15021	Soil	10.0	2 November 1971	51 ± 4	5 ± 1
					2.5 ± 1†

* Counter efficiency for Rn^{222} is estimated to be 2.
† Under vacuum conditions.

Surveyor 3 sample that was not exposed to sunlight had a higher saturation H^3 content than the lunar samples did, which is somewhat of a mystery.

The radon emanation from the sealed containers was also measured. The soil under vacuum conditions had a radon emanation rate similar to that observed in the sample container (Stoenner *et al.*, 1971). The samples sealed with air had a higher rate of radon emanation.

Acknowledgment—This research was supported in part by Grant NGR 09-015-145 from the National Aeronautics and Space Administration.

References

Begemann F., Vilcsek E., Rieder R., Born W., and Wänke H. (1970) Cosmic-ray produced radioisotopes in lunar samples from the Sea of Tranquility. *Proc. Apollo 11 Lunar Sci. Conf., Geochim. Cosmochim. Acta* Suppl. 1, Vol. 2, pp. 995–1007. Pergamon.

Bochsler P., Wahlen M., Eberhardt P., Geiss J., and Oeschger H. (1971) Tritium measurements of lunar material (fines 10084 and breccia 10046) from Apollo 11. *Proc. Second Lunar Sci. Conf., Geochim. Cosmochim. Acta* Suppl. 2, Vol. 2, pp. 1803–1812. MIT Press.

D'Amico J., DeFelice J., and Fireman E. L. (1970) The cosmic-ray and solar flare bombardment of the moon. *Proc. Apollo 11 Lunar Sci. Conf., Geochim. Cosmochim. Acta* Suppl. 1, Vol. 2, pp. 1029–1036. Pergamon.

D'Amico J., DeFelice J., Fireman E. L., Jones C., and Spannagel G. (1971) Tritium and argon radioactivities and their depth variations in Apollo 12 samples. *Proc. Second Lunar Sci. Conf., Geochim. Cosmochim. Acta* Suppl. 2, Vol. 2, pp. 1825–1839. MIT Press.

Fireman E. L., D'Amico J., and DeFelice J. (1970) Tritium and argon radioactivities in lunar material. *Science* **167,** 566–568.

Reedy R. C. and Arnold J. R. (1972) Interaction of solar and galactic cosmic-ray particles with the moon. *J. Geophys. Res.* **77,** 537–555.

Stehn J. R., Goldberg M. D., Magurno B. A., and Wiener-Chasman R. (1964) Neutron cross sections. Brookhaven Nat. Lab. Rep. 325, 2nd ed., Suppl. No. 2.

Stoenner R. W., Lyman W. J., and Davis R. Jr. (1970a) Cosmic-ray production of rare gas radioactivities and tritium in lunar material *Science* **167,** 553–555.

Stoenner R. W., Lyman W. J., and Davis R. Jr. (1970b) Cosmic-ray production of rare gas radioactivities and tritium in lunar material. *Proc. Apollo 11 Lunar Sci. Conf., Geochim. Cosmochim. Acta* Suppl. 1, Vol. 2, pp. 1029–1036. Pergamon.

Stoenner R. W., Lyman W. J., and Davis R. Jr. (1971) Radioactive rare gases in lunar rocks and in the lunar atmosphere. *Proc. Second Lunar Sci. Conf., Geochim. Cosmochim. Acta* Suppl. 2, Vol. 2, pp. 1813–1823. MIT Press.

Wahlen M., Honda M., Imamura M., Fruchter J., Finkel R., Kohl C., Arnold J., and Reedy R. (1972) Cosmogenic nuclides in football-sized lunar rocks (abstract). In *Lunar Science—III* (editor C. Watkins), pp. 764–766, Lunar Science Institute Contr. No. 88.

Proceedings of the Third Lunar Science Conference
(Supplement 3, *Geochimica et Cosmochimica Acta*)
Vol. 2, pp. 1763–1769
The M.I.T. Press, 1972

Study on the cosmic ray produced long-lived Mn-53 in Apollo 14 samples

W. HERR and U. HERPERS
Institut für Kernchemie der Universitaet Köln
and
R. WOELFLE
Institut für Radiochemie der KFA Juelich, Germany

Abstract—Accurate determinations of long-lived spallation nuclides, are of current interest for the estimation of "radiation ages," depth profiles, and for the detection of possible variations in the cosmic flux. With respect to the previous unsatisfactorily known ^{53}Mn half-life, we have performed a redetermination of the ^{53}Mn-neutron cross section. Having irradiated meteoritic Mn for 392 days in a high neutron flux we find $\sigma_{therm} = 66 \pm 7$ barns. Based on the "Peace River" chondrite, the ^{53}Mn content of which is well known, a product of $T \times \sigma = (260 \pm 32) \times 10^6$ barns × years is derived, thus leading to a ^{53}Mn half-life of $(3.9 \pm 0.6) \times 10^6$ years. On the basis of this figure a number of Apollo 11 to 14 soil and rock samples are analyzed by neutron activation techniques for their ^{53}Mn contents. The K-emitter ^{53}Mn is converted by neutron capture to the γ-emitting ^{54}Mn, which is sensitively detected by a 75 cc Ge(Li) well-type detector. The surface soil 14259 (comprehensive) with 644 dpm/kg Fe is found to be twice as high in ^{53}Mn as the bulk soils. The ^{53}Mn-depth effect on rock 10017 was reestablished. From the respective low value of the microbreccia 14305 (interior), pointing out that "saturation" activity is not reached, a remarkable short exposure age in the order of $\sim$6 million years is concluded.

INTRODUCTION

SINCE THE FIRST OBSERVATION of the existence of a long-lived manganese isotope in nature by Shedlovsky (1960), the interest in this spallation produced nuclide has steadily grown. It offers a possibility to get additional information about the complex radiation history of meteorites and of cosmic ray exposed matter. A supplement to ^{26}Al, ^{36}Cl, etc., ^{53}Mn can be useful to reach back into the past, at least to $\sim$10–15 m.y. Obviously, the large production cross section (its main source is iron) and the high sensitivity in detection are of great importance. With respect to the latter the K-emitting nuclide can be transformed by neutron capture into the γ-emitting ^{54}Mn isotope, raising the activity ratio by a factor of up to $>10^4$ (Millard, 1965, Herpers *et al.*, 1967). We have developed this activation technique and shown on a larger number of iron meteorites that there are considerable advantages, as high accuracy and economy of sample need (Herpers *et al.*, 1969, Herr *et al.*, 1969). ^{53}Mn depth profiles of lunar rocks were recently presented by Shedlovsky *et al.* (1970), Finkel *et al.* (1971), Wahlen *et al.* (1972) and also by our group (Herr *et al.*, 1971, 1972).

However, the decay constant of ^{53}Mn was until recently not very well known, and more precise information was highly desirable, for being the basis of any dating work in cosmochemistry. Earlier attempts to establish the half-life were made on several

approaches. On considerations of spin and nuclear reaction yields Sheline and Hooper (1957) came to $T = 2 \times 10^6$ yr. Kaye and Cressy (1965) estimated $T = (1.9 \pm 0.5) \times 10^6$ yr, based on counting meteoritic Mn. The latter value was considered the best for a long time. Matsuda *et al.* (1971) reported $T = (2.9 \pm 1.2) \times 10^6$ yr working with accelerator produced ^{53}Mn and ^{54}Mn. Then mass-spectrometry on meteoritic Mn (Cañon Diablo) resulted in a figure of $T = (10.8 \pm 4.5) \times 10^6$ yr (Hohlfelder, 1969), pointing out the enormous technical difficulties. Obviously, more weight has the recent work of Honda and Imamura (1971) succeeding in a measurement of the specific activity and the abundance of naturally and artificially produced ^{53}Mn. Their value is $T = (3.7 \pm 0.4) \times 10^6$ yr.

In view of the importance of this constant, we started independently three years ago an experiment, in order to establish the half-life via the ^{53}Mn$(n, \gamma)^{54}$Mn thermal neutron cross section (σ_{53}) (Herpers *et al.*, 1969). The principle is as follows: ~2 mg of Mn from the Duchesne meteorite (activity of ^{53}Mn = 412 ± 34 dpm/kg) were activated in a high flux reactor ($\Phi = 10^{14}$n cm^{-2} s^{-1}), one aliquot was irradiated only for a "short" period (20*d*), the other for a "long" period (392*d*) together with suitable flux monitors (Fe, ^{55}Mn, ^{54}Mn, and Cu etc. standards). From the systematics of the activation process the thermal neutron capture cross section σ_{53} was determined as 66 ± 7 *barns*.

The next step is the determination of the ^{53}Mn half-life. By courtesy of J. R. Arnold we received a sample of the meteorite "Peace River" having a well-known ^{53}Mn decay rate (measured by direct counting). With the "Peace River" manganese we performed an activation experiment and obtained a product of $T \times \sigma = (260 \pm 32) \times 10^6$ barns × yr.

On the basis of the above established $\sigma_{53} = 66 \pm 7$ b and the product $T \times \sigma$ we derived a ^{53}Mn half-life of $T = (3.9 \pm 0.6) \times 10^6$ yr. Obviously, this value is in excellent agreement with that published quite recently by Honda and Imamura (1971).

Experimental (Analysis of Lunar Material)

Amounts of 200–500 mg powdered Apollo 14 samples were fused in NaOH + Na_2O_2 and the Mn isolated and purified by ion exchange techniques as described earlier (Herr *et al.*, 1970, 1971). The MnO_2 probes were brought into an Al-foil sandwich and irradiated for 31 days (FRJ-2) at Juelich. $\Phi_{therm} = 5 \times 10^{12}$ n cm^{-2} s^{-1}, $\Phi_{fast}/\Phi_{therm} \leq 0.001$. The latter ratio was measured by ^{31}P (n, p) ^{31}Si and ^{59}Co (n, γ) ^{60}Co. Postirradiation treatment consisted of an $HMnO_4$ distillation followed by ion exchange separation. The radiometric essay was very much improved by a 75 cc Ge(Li) detector (well-type), kindly supplied by J. Eberth, Institut für Kernphysik, Köln. Resolution: 3.8 keV at 1.33 MeV and an efficiency of 1.4% at the ^{54}Mn 835 keV peak. By heavy shielding (Pb + Hg) the background was lowered to 0.3 cpm under the total line of ^{54}Mn at 835 ± 15.3 keV. No other interfering radioactivities were observed near, or at, the ^{54}Mn photo peak. Absolute neutron flux calibration was done by an internal Zn standard (^{65}Zn) against a standardized ^{22}Na sample on the basis of their annihilation radiation.

Results and Discussion

The importance of the knowledge of the ^{53}Mn half-life for precise estimations of exposure ages, sedimentation rates, and for the discovery of possible variations in the

solar and cosmic fluxes is evident. Following these intentions, we have analyzed two Apollo 14 soils, 14163 (bulk) and 14259 (comprehensive soil) and also the interior part of rock 14305 (microbreccia) for their ^{53}Mn contents. Based on our new half-life $T = 3.9 \times 10^6$ yr a number of Apollo 12 samples were also redetermined.

It has been already reported that the Fe and Mn contents of the minerals from the Apollo 14 landing site were lower by a factor of ~ 2 than those of the earlier missions (Waenke *et al.*, 1972) and others. Our Fe and Mn contents of the respective lunar samples are presented in Table 1. The Fe and Mn contents of the "Peace River" chondrite are given for comparison. They are by a factor of ~ 2.5 higher than the Apollo 14 samples. The results of our ^{53}Mn determinations are listed in Table 2. The given errors include all systematic and counting (1σ) errors in the procedure. However, not included is the still remaining uncertainty in the product of the ^{53}Mn half-life times cross section.

In the course of our work we were able to measure an aliquot of the ^{53}Mn "Tokyo"-standard, kindly provided by Prof. M. Honda. A very good agreement was reached on this man-made sample.

It should be mentioned also that the Apollo 12 samples were recalculated. The results in the last column are given in dpm/kg iron. Most of the soil samples are in the range of 340–380 dpm/kg Fe, with the only exception of the comprehensive soil 14259 (~ 1 cm below surface), which is higher nearly by a factor of 2. Evidently, this extremely high value of 644 ± 21 dpm/kg Fe (the error presented corresponds to one standard deviation of counting) is due to a contribution of solar protons. This value is in concordance with that of J. R. Arnold and coworkers, presented at the Third

Table 1. Mn and Fe contents of Apollo 14 samples.

Sample no.	Type	Mn (ppm)	Fe (%)
14163	Soil	1117 ± 34	7.50
14259	Soil	1103 ± 33	7.74
14305,BD1 (interior)	Breccia	1059 ± 31	7.91
Peace River (chondrite)		2544 ± 52	21.35

Table 2. ^{53}Mn content of lunar material.

Sample no.	Type	Sample weight (mg)	^{54}Mn (total) (cpm)	Contribution of $(n,2n)$ plus (n,p) (%)	^{53}Mn (dpm/kg)	Fe (%)	^{53}Mn (dpm/kg Fe)
14163	Soil	248	0.377 ± 0.008	27.8	28 ± 3	7.5	372 ± 34
14259	Soil	231	0.563 ± 0.012	17.5	50 ± 5	7.7	644 ± 58
12070	Soil	501	14.1 ± 0.2	25.8	50 ± 4	13.2	380 ± 27
10084	Soil	990	17.7 ± 3.2	30.2	41 ± 7	12.0	341 ± 58
14305,BD1 (interior)	Breccia	504	0.389 ± 0.007	49.4	13 ± 1	7.9	169 ± 16
12021	Rock	842	25.4 ± 0.3	38.8	33 ± 4	14.2	232 ± 28
12022	Rock	1038	35.7 ± 0.4	36.6	38 ± 4	16.4	232 ± 24
12053	Rock	1070	41.2 ± 0.4	34.1	41 ± 3	15.3	268 ± 20
^{53}Mn* Tokyo—std.	0.5 n HCl solution	1000	16.89 ± 0.39	0.26	(dpm/g sol) 0.392 ± 0.059		

* ^{53}Mn standard solution supplied by courtesy of Prof. M. Honda with a value of 0.395 dpm/g solution (private communication).

Lunar Science Conference (Wahlen *et al.*, 1972). Their figure of 44 ± 2 dpm/kg material corresponds with a value of 572 ± 27 dpm/kg Fe. It is notable, that in the comprehensive soil also the ^{22}Na and ^{26}Al contents are a factor of 1.9, respectively, 2.8 higher (LSPET, 1971, Rancitelli *et al.*, 1972) than those of the bulk soils (10084, 12070, and 14163). Since the latter are undefined in their depth position and may have suffered some "gardening," it is hard to estimate their former depth.

From earlier studies on Apollo 11 and 12 samples, clear evidence was obtained of a long-term bombardment of solar (wind) particles in the ~10 MeV per nucleon range (Finkel *et al.*, 1971). A certain similarity of the depth profile of ^{26}Al ($T = 7.5 \times 10^5$ yr) to that of ^{22}Na ($T = 2.6$ yr) was also observed, whereas the respective ^{53}Mn profile seemed less steep. Evidently, from these measurements it followed that the solar particles, averaged over some 10^6 yr, has been in the same range as those measured today. Furthermore, the precise estimation of activity profiles from short and longlived activities, especially ^{53}Mn has led to the discussion of the still open question: Should there have happened (possible) variations in the solar and cosmic flux in the last 10^6 yr, or is there either a rather large corrosion rate (of ~0.2 mm/10^6 yr) responsible for differences in the respective activity ratios? One has to work further on this problem. (We received the 14 material only very late in November 1971.)

In the diagram of Fig. 1, the depth dependence of ^{53}Mn in rock 10017 together with data of Apollo 11 to 14 samples are shown. The rock 14305, a fist-sized micro-

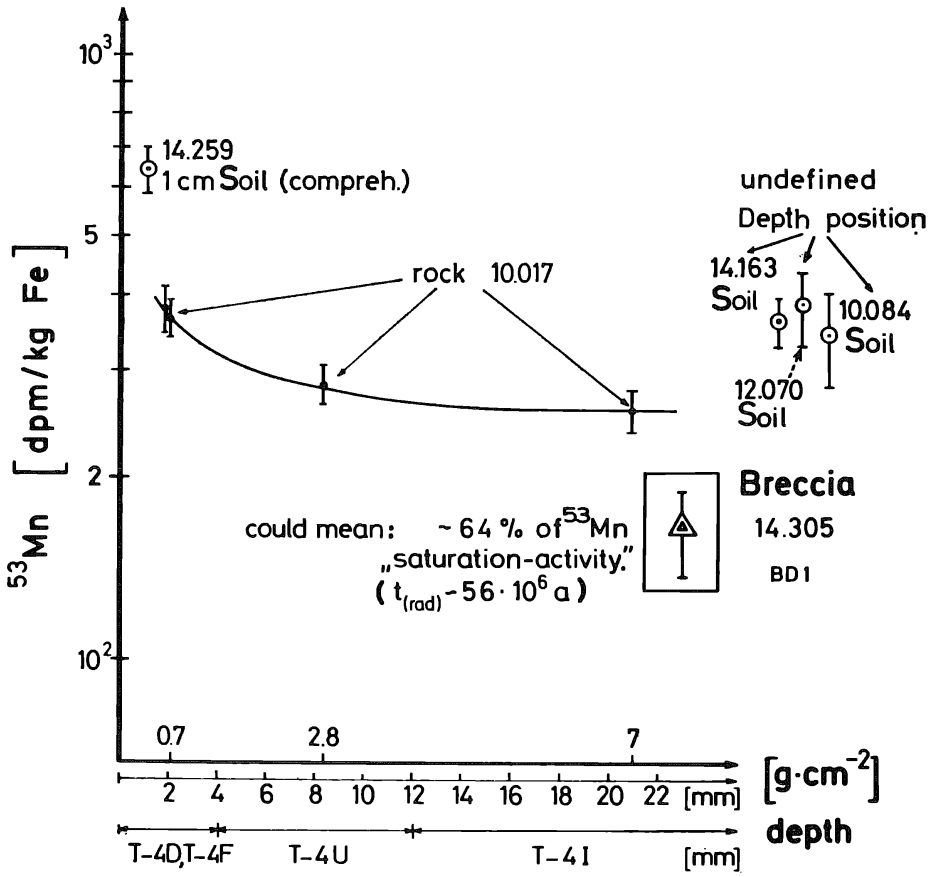

Fig. 1. ^{53}Mn values in relation to the depth.

breccia, is thought to have had irradiations from the top and the bottom. There is evidence from photographic studies and also from the number of the microcraters on the surfaces that in this case we probably are dealing with a "moving" rock. The ^{26}Al data from the top and the bottom recently published by Yokoyama *et al.* (1972) do support this view.

Some remarks to the ^{53}Mn results on rock 10017, having a radiation age of $\sim 300 \times 10^6$ yr (D'Amico *et al.*, 1970, Marti *et al.*, 1970). Thus, it may be sure that its ^{53}Mn concentration has reached "saturation," and only the depth effect reflects the differences in the specific activity. If we take this fact into consideration and transfer this model to the interior sample of breccia 14305 (taken from ~ 2.5 cm below the top surface), we see that this sample has not yet reached the respective "saturation activity." However, we are simplifying and also neglecting the fact that this object may have "turned" around during its stay on the lunar surface. So, the assumed depth cannot be well defined.

Nevertheless, we conclude that the ^{53}Mn radiation age of 14305 must be comparatively short and should be in the range of $T_{rad} \sim 6 \times 10^6$ yr only. This would mean an extraordinarily short irradiation period, but unless other detailed information on its ^{53}Mn profile are available a more precise statement cannot be made. It appears that the breccia 14305 was buried on the average more deeply than the neighboring rocks, which give the 20–25 $\times 10^6$ yr radiation age.

There are some other independent investigations on the same microbreccia that strengthen our view that we are here really dealing with one of the youngest ejecta found in the Apollo 14 landing site. The rare gases were studied in these microbreccias and Bogard and Nyquist (1972) concluded that this material (it was recovered very near the Cone Crater), has a rare gas exposure age of max $T_{rad} \sim 20 \times 10^6$yr, which may reflect the age of the Cone Crater itself. This is also pointed out by Lugmair and Marti (1972). Independently, the group of Hart *et al.* (1972) came to comparable results by recording particle tracks. For a similar microbreccia from the rim of the Cone Crater, they evaluated a maximum surface age of 8×10^6 yr. It is, however, clear that these breccias have a very complicated history, at least compared with the basaltic rocks. The possibility that the major surface exposure occurred for a longer time (e.g., in the interior of a considerably larger rock or below the surface) cannot be excluded. It is noteworthy that the Apollo 14 breccias are by a factor of 10 to 20 shorter "exposed" compared with the basalts of Apollo 11 and 12. This may be also one of the results of the more friable nature of these 14—rocks that will allow even a more rapid and larger erosion and also a promoted catastrophic break up by nearby impacts.

Acknowledgments—We express our thanks to Prof. J. R. Arnold, La Jolla, for having forwarded a sample of the Peace River chondrite and to Prof. M. Honda, Tokyo, for sending his ^{53}Mn standard. We are also indebted to Mr. J. Eberth, Köln, for placing the 75 cc Ge(Li) detector at our disposal. Our thanks are also due to NASA for supplying lunar material.

References

Bogard D. D. and Nyquist L. E. (1972) Noble gas studies on regolith materials from Apollo 14 and 15 (abstract). In *Lunar Science—III* (editor C. Watkins), pp. 89–91, Lunar Science Institute Contr. No. 88.

D'Amico J., De Felice J., and Fireman E. L. (1970) The cosmic-ray and solar-flare bombardment of the moon. *Proc. Apollo 11 Lunar Sci. Conf., Geochim. Cosmochim. Acta* Suppl. 1, Vol. 2, pp. 1029–1036. Pergamon.

Finkel R. C., Arnold J. R., Imamura M., Reedy R. C., Fruchter J. S., Loosli H. H., Evans J. C., Delany A. C., and Shedlovsky J. P. (1971) Depth variation of cosmogenic nuclides in a lunar surface rock and lunar soil. *Proc. Second Lunar Sci. Conf., Geochim. Cosmochim. Acta* Suppl. 2. Vol. 2, pp. 1773–1789. MIT Press.

Hart H. R. Jr., Comstock G. M., and Fleischer R. L. (1972) The particle track record of Fra Mauro (abstract). In *Lunar Science—III* (editor C. Watkins), pp. 360–362, Lunar Science Institute Contr. No. 88.

Herpers U., Herr W., and Woelfle R. (1967) Determination of cosmic ray produced nuclides ^{53}Mn, ^{45}Sc, and ^{26}Al in meteorites by neutron activation and gamma coincidence spectroscopy. In *Radioactive Dating and Methods of Low-Level Counting*, pp. 199–205, International Atomic Energy Agency, Vienna.

Herpers U., Herr W., and Woelfle R. (1969) Evaluation of ^{53}Mn by (n, γ) activation, ^{26}Al, and special trace elements in meteorites by γ-coincidence techniques. In *Meteorite Research*, pp. 387–396, International Atomic Energy Agency, Vienna.

Herr W., Herpers U., and Woelfle R. (1969) Die Bestimmung von ^{53}Mn, welches in meteoritischem Material durch kosmische Strahlung erzeugt wurde, mit Hilfe der Neutronenaktivierung. *J. Radioanal. Chem.* **2,** 197–203.

Herr W., Herpers U., Hess B., Skerra B., and Woelfle R. (1970) Determination of manganese-53 by neutron activation and other miscellaneous studies on lunar dust. *Proc. Apollo 11 Lunar Sci. Conf., Geochim. Cosmochim. Acta* Suppl. 1, Vol. 2, pp. 1233–1238. Pergamon.

Herr W., Herpers U., and Woelfle R. (1971) Spallogenic ^{53}Mn ($T \sim 2 \times 10^6$ y) in lunar surface material by neutron activation. *Proc. Second Lunar Sci. Conf., Geochim. Cosmochim. Acta* Suppl. 2, Vol. 2, pp. 1797–1802. MIT Press.

Herr W., Herpers U., and Woelfle R. (1972) Study on the cosmic ray produced longlived Mn-53 in Apollo 14 samples (abstract). In *Lunar Science—III* (editor C. Watkins), pp. 373–375, Lunar Science Institute Contr. No. 88.

Hohlfelder J. J. (1969) Half-life of ^{53}Mn. *Phys. Rev.* **186,** 1126–1131.

Honda M. and Imamura M. (1971) Half-life of ^{53}Mn. *Phys. Rev.* C. **4,** 1182–1188.

Kaye J. H. and Cressy P. J. (1965) Half-life of manganese-53 from meteorite observations. *J. Inorg. Nucl. Chem.* **27,** 1889–1892.

LSPET (Lunar Sample Preliminary Examination Team) (1971) Apollo 14 Preliminary Science Report. NASA SP-272.

Lugmair G. W. and Marti K. (1972) Neutron and spallation effects in Fra Mauro regolith (abstract). In *Lunar Science—III* (editor C. Watkins), pp. 495–497, Lunar Science Institute Contr. No. 88.

Marti K., Lugmair G. W., and Urey H. C. (1970) Solar wind gases, cosmic-ray spallation products, and the irradiation history of Apollo 11 samples. *Proc. Apollo 11 Lunar Sci. Conf., Geochim. Cosmochim. Acta* Suppl. 1, Vol. 2, pp. 1357–1367. Pergamon.

Matsuda H., Umemoto S., and Honda M. (1971) Manganese-53 produced by 730 MeV proton bombardment of iron. *Radiochim. Acta* **15,** 51–53.

Millard H. T. Jr. (1965) Thermal neutron activation: Measurement of cross section for manganese-53. *Science* **147,** 503–504.

Rancitelli L. A., Perkins R. W., Felix W. D., and Wogman N. A. (1972) Cosmic ray flux and lunar surface processes characterized from radionuclide measurements in Apollo 14 and 15 lunar samples (abstract). In *Lunar Science—III* (editor C. Watkins), pp. 630–632, Lunar Science Institute Contr. No. 88.

Shedlovsky J. P. (1960) Cosmic-ray produced manganese-53 in iron meteorites. *Geochim. Cosmochim. Acta* **21,** 156–158.

Shedlovsky J. P., Honda M., Reedy R. C., Evans J. C. Jr., Lal D., Lindstrom R. M., Delany A. C., Arnold J. R., Loosli H. H., Fruchter J. S., and Finkel R. C. (1970) Pattern of bombardment-produced radionuclides in rock 10017 and in lunar soil. *Science* **167,** 574–576.

Shedlovsky J. P., Honda M., Reedy R. C., Evans J. C. Jr., Lal D., Lindstrom R. M., Delany A. C.,

Arnold J. R., Loosli H. H., Fruchter J. S., and Finkel R. C. (1970) Pattern of bombardment-produced radionuclides in rock 10017 and in lunar soil. *Proc. Apollo 11 Lunar Sci. Conf., Geochim. Cosmochim. Acta* Suppl. 1, Vol. 2, pp. 1503–1532. Pergamon.

Sheline R. K. and Hooper J. E. (1957) Probable existence of radioactive manganese-53 in iron meteorites. *Nature* **179,** 85–87.

Waenke H., Baddenhausen H., Balacescu A., Teschke F., Spettel B., Dreibus G., Quijano M., Kruse H., Wlotzka F., and Begemann F. (1972) Multielement analyses of lunar samples (abstract). In *Lunar Science—III* (editor C. Watkins), pp. 779–781, Lunar Science Institute Contr. No. 88.

Wahlen M., Honda M., Imamura M., Fruchter J., Finkel R., Kohl C., Arnold J., and Reedy R. (1972) Cosmogenic nuclides in football-sized lunar rocks (abstract). In *Lunar Science—III* (editor C. Watkins), pp. 764–766, Lunar Science Institute Contr. No. 88.

Yokoyama Y., Auger R., Bibron R., Chesselet R., Guichard F., Léger C., Mabuchi H., Reyss J. L., and Sato J. (1972) Cosmonuclides in lunar rocks (abstract). In *Lunar Science—III* (editor C. Watkins), pp. 819–821, Lunar Science Institute Contr. No. 88.

Proceedings of the Third Lunar Science Conference
(Supplement 3, *Geochimica et Cosmochimica Acta*)
Vol. 2, pp. 1771–1777
The M.I.T. Press, 1972

Alpha spectrometry of a surface exposed lunar rock

GÉRARD LAMBERT, TOVY GRJEBINE, JEAN CLAUDE LE ROULLEY,
and PIERRE BRISTEAU

Centre des Faibles Radioactivités, CNRS,
Gif-sur-Yvette (91), France

Abstract—The α activity of the top surface of a moon rock has been measured in order to detect an eventual layer of lead 210 and polonium 210 that could be designated as descendant of the radon escaping from the lunar soil. The limit for this activity is proposed as 2.10^{-5} dis/sec/cm². The possibility for the existence of this process was meanwhile shown in a simulating experiment. The absence of the activity can be attributed to an apparently very low transmission coefficient of fines. This is also seen in another simulation experiment where a source emanating radon is covered with increasing layers of basalt powder.

INTRODUCTION

ON EARTH, an average concentration of 4 ppm of uranium in the soil gives rise to an outgassing flux of radon 222 of 0.7 atoms per second and cm². If a layer of 7 cm of terrestrial soil were entirely degassed, it should produce such a flux. Therefore, if all processes involved were similar on the moon, an average concentration of 1 ppm of uranium would produce a flux in the range of 0.1 to 1 atoms of radon per second and cm². Kraner *et al.* (1966) have shown that, even with the day time heating of the moon's surface, the atoms do not have enough energy to leave the moon. It should be pointed out that, during the lunar night, the temperature reaches 90°K, i.e., a lower temperature than the melting point of radon (202°K).

After the α disintegration of radon 222 (energy 5.5 MeV) the residual nucleus of polonium 218 (RaA) has a recoil energy of about 100 keV. If the α particle were emitted toward the soil, this recoil energy would be sufficient to overcome the lunar gravity and the RaA would be able to leave the moon. If, on the contrary, the α particle were directed toward the outside, the RaA would be projected toward the lunar soil and become embedded in the external surface layer. Taking into account the mass and the recoil energy of the RaA, it may be assumed that its range is approximately 20.10^{-6} g/cm² (Domeij *et al.*, 1963). The effect of this depth is almost negligible for the α particles emitted by the further disintegrations.

Thus, we have the formation of a thin layer of lead 210 (half-life 20 yr) in equilibrium with the decay products bismuth 210 and polonium 210. This layer produces an α emission of definite energy, 5.30 MeV, but this is in contrast to the continuous spectrum of α radioactive decay products of uranium and thorium, which are directly yielded inside the rock.

EXPERIMENTAL

In order to investigate the formation of such a layer of polonium 218 and its daughter products, several flat rocks were laid on a bed of pulverized sand mixed with 1 microcurie of radium 226.

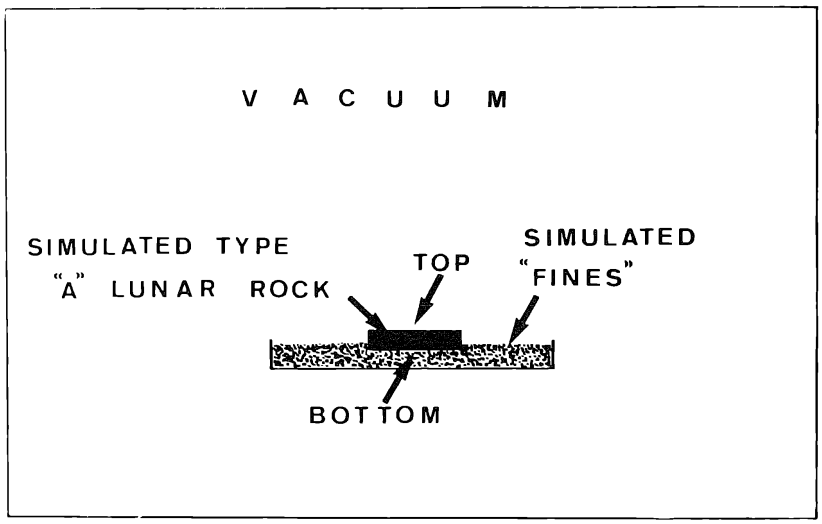

Fig. 1. Experimental device for simulating the embedding process of a recoiling atom, after an α disintegration.

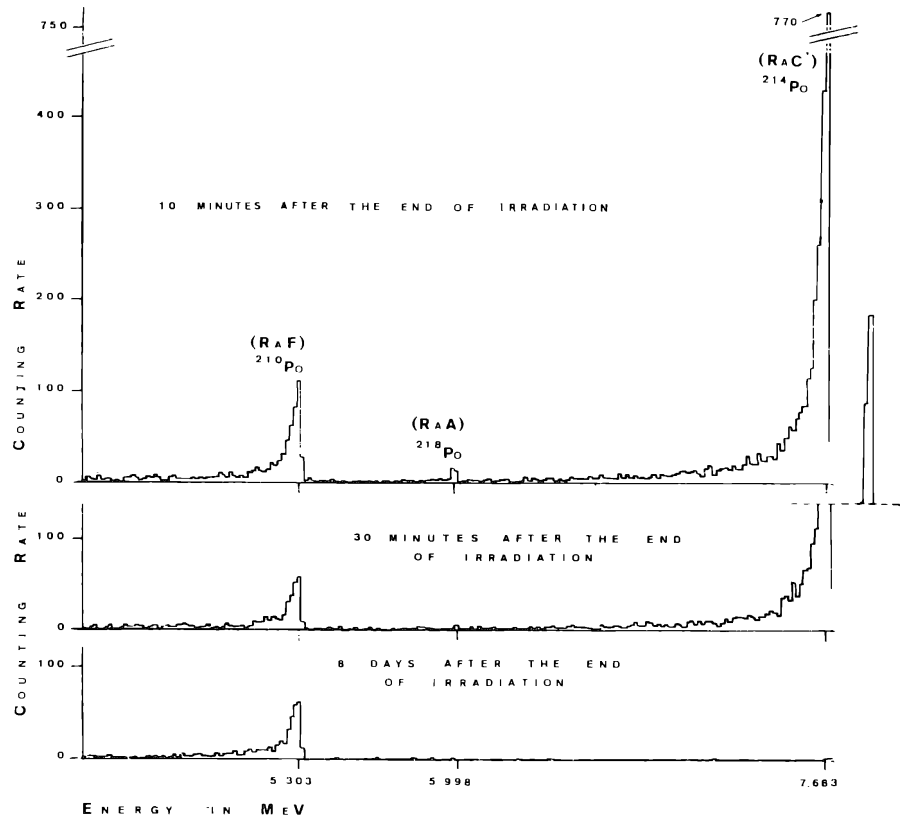

Fig. 2. α spectrum of the top face of a rock in a simulating experiment. Curve A: 10 minutes after removing from the vessel; Curve B: 30 minutes after removing from the vessel; Curve C: 8 days later after removing from the vessel.

This material was put in a vessel which was brought to a primary vacuum (Fig. 1). After 8 months, the rocks were removed and measured with an α spectrometer.

The α spectrum of the top face of a rock, 10 min after its removing from the vessel, is shown on Fig. 2, curve a. Characteristic peaks of polonium 218, 214, and 210 (RaA, C′, and F) are visible. Since there is no contamination by radium 226 or radon 222, this demonstrates that polonium 218 and its decay products were effectively embedded in the top face by the disintegration of the gaseous radon present in the vessel. Thirty minutes later, the polonium 218 peak disappeared (curve b). One day later, only the polonium 210 peak remained visible (curve c).

Results and Discussion

Therefore, according to the theory proposed by Kraner *et al.* (1966) and to the results above, it seems possible to measure the flux of radon outgassing from the moon soil, by measuring the lead 210 deposited in the top layer of lunar rocks. Lunar sample 14321,212 provided by NASA was measured with an α semiconductor spectrometer. This sample was cut off the top of a rock. Two faces were measured: The first face was identified as an external face from the presence of a large meteoritic pit and available documentation. The second face was irregular, without any pits or erosion features.

The α spectrometer was comprised of a surface barrier detector (ORTEC 2 cm^2) connected to a linear amplifier and a 200 channel analyzer. It was located in an air conditioned room and fed with a battery stabilized power supply. The measurements were made on the external face for one and a half months (i.e., 1176 hours of effective counting) without changing the position of the sample. The apparatus was checked for stability every week by feeding calibrated pulses into the amplifier: no shift was noted.

The low activity of the sample suggested the regrouping of the channels four by four (100 keV intervals) in order to diminish the statistical fluctuations (Fig. 3). The negligible background, on the order of 2 counts per 100 keV in 1176 hours, was not subtracted. The smooth-curve can be interpreted as a spectrum of a powder. Uranium

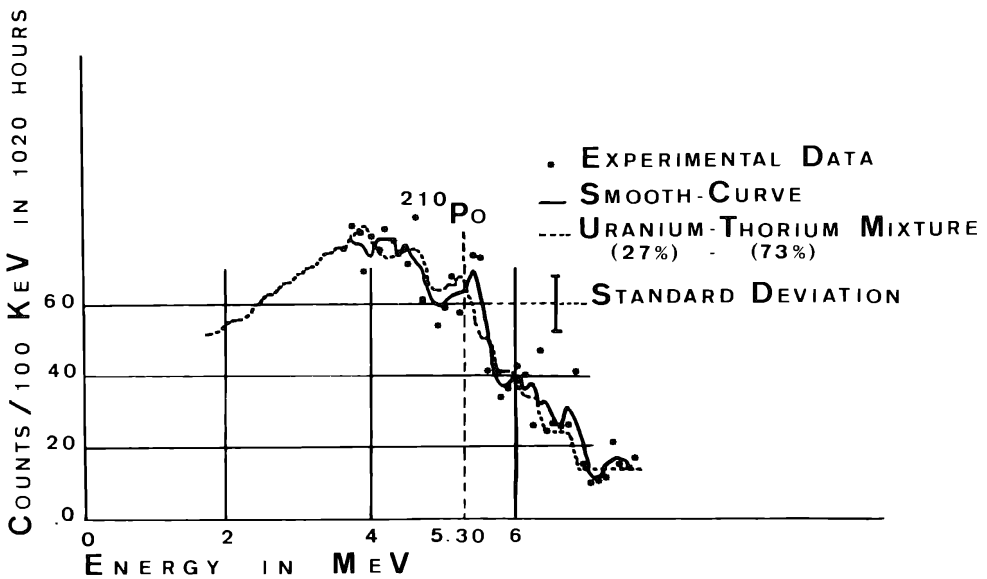

Fig. 3. The α spectrum of the top of the lunar rock 14321,212.

238 could account for 51% and thorium 232 for 49% of this activity, also keeping in secular equilibrium all their daughter products. Activities such as these are in agreement with the usually observed concentrations (LSPET, 1971). The observed data between 5.10 and 5.30 MeV show no significant activity above the continuous spectrum that could be attributed to excess polonium 210. The spectrum obtained with the internal face presents effectively the same features (Fig. 4). In the spectrum

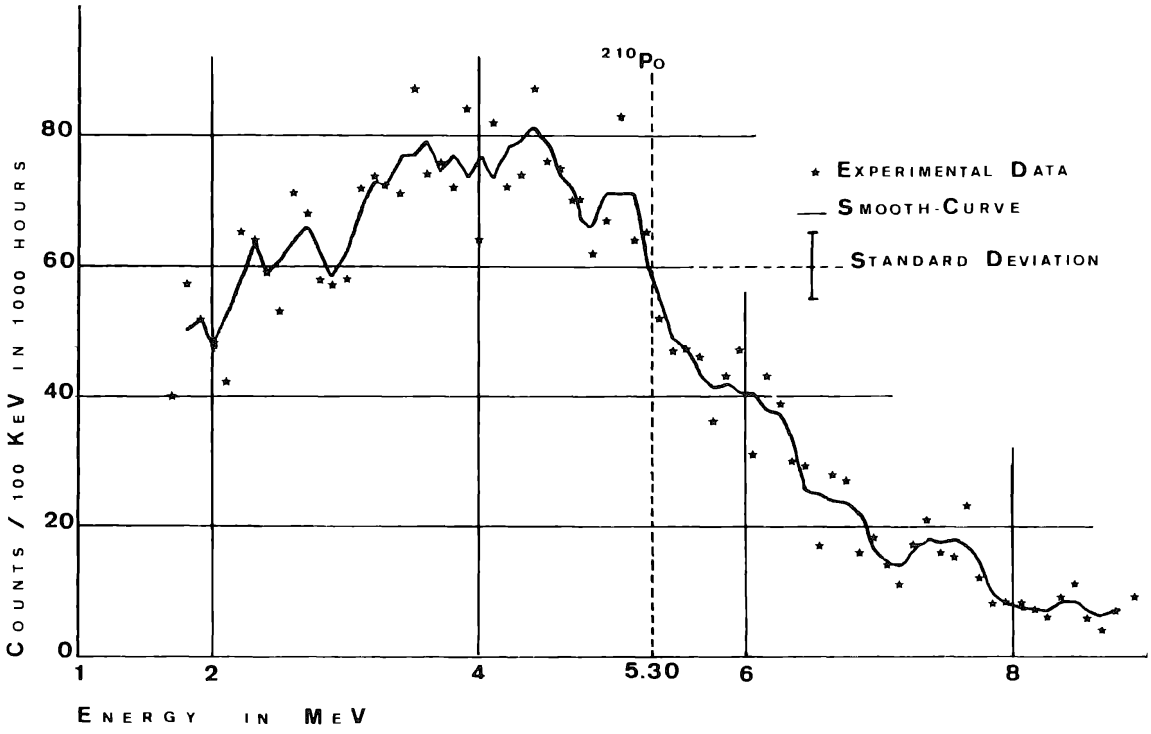

Fig. 4. The α spectrum of an internal face of lunar rock 14321,212.

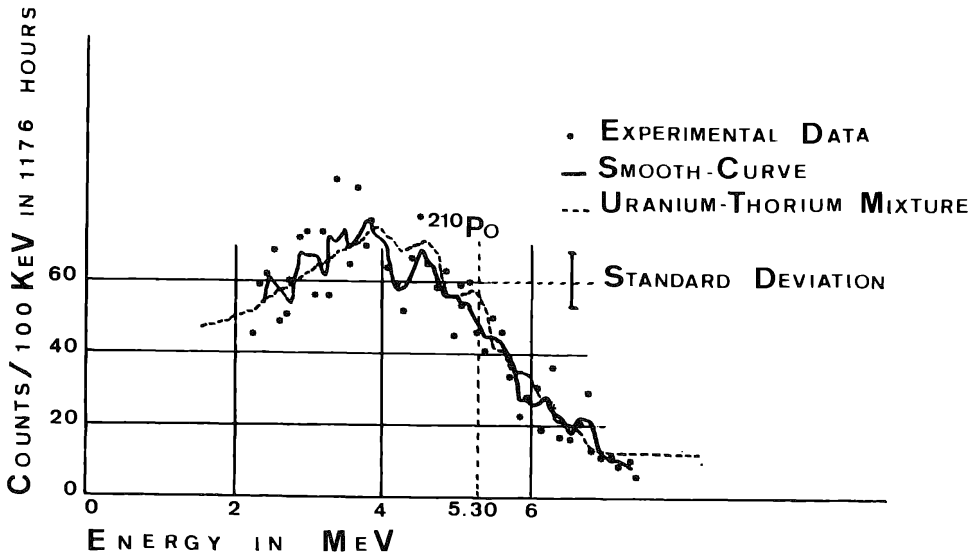

Fig. 5. The α spectrum of lunar fines 14163,92.

for the external face, the total number of counts between 5.10 and 5.30 MeV was $N = 124$ for 1776 hours. Setting as a detection limit 2 standard deviations of this rate ($2\sqrt{N} = 22.3$), and a counting efficiency of 13%, it is possible to assume that an excess of this rate would be detected. The upper limit is 4.10^{-5} dis/sec for the total sample. The measured surface of the sample was approximately 2 cm^2 therefore; the upper limit for a deposit of polonium 210 on the moon surface was 2.10^{-5} dis/sec/cm^2. A similar result obtained with fines sample 14163,92 (Fig. 5) confirms the extreme weakness of a possible excess of polonium 210 in the superficial lunar soil.

This result is in agreement with the measurements made by Economou and Turkevitch (1971) who found an upper limit of 5.10^{-3} dis/sec/cm^2 on the filter of the Surveyor 3 television camera, and of Lindstrom *et al.* (1971) who found 4.5 10^{-4} dis/sec/cm^2 in Apollo 11 fines. All these limits are in agreement with the results obtained from Lunar orbiters by Yeh and Van Allen (1965) and Gorenstein and Bjokholm (1972). They did not detect any surplus in the lunar α activity. Only one experiment has shown different results: Turkevitch *et al.* (1970) using the Surveyor α spectrometer have reported at the Surveyor 5 landing site (Mare Tranquilitatis) an α activity that was described as polonium 210.

The lunar fines when brought to terrestrial conditions, on the other hand, apparently behave the same way as terrestrial soil. Adams *et al.* (1971) have found that 40% of the radon produced in 0.473 g of lunar fines was outgassed. This experiment was performed at room temperature and pressure. Yaniv and Heymann (1972), using a similar technique working in a moderate vacuum have lowered this emanating-to-production ratio between 2.10^{-3} and 5.10^{-3} for Rn^{222} and 3.10^{-3} to 5.10^{-3} for Rn^{220} in Apollo 14 fines. They did not observe any outgassing in Apollo 11 and Apollo 12 fines. Yaniv and Heymann (1972) have not therefore reached the same results as Adams *et al.* (1971). This suggests that the pressure may be of great importance. The absence of interstitial gas between the grains of the regolith may influence the outgassing in two different ways. First, Lindstrom *et al.* (1971) have suggested that, in the lunar soil, after the α emission of radium 226 the recoiling atom of radon 222 is not slowed down in the vacuum space between grains and therefore is reembedded in the next crystal.

In the previously described simulation experiment where the rocks were placed on the mixture of sand and radium 226, this effect may be seen on the bottom face. The α spectrum of this face shows (Fig. 6) although there is no contamination by radium 226 but the α peaks of radon 222 and daughter products are clearly apparent. Since the α spectrum remains almost unchanged after heating 15 min at 500°C, these atoms are strongly bound to the rock. These results can be interpreted as the reembedding process of radon atoms recoiling after the α disintegration of radium 226.

Grjebine *et al.* have calculated that, at a depth of a few centimeters, the temperature of the lunar soil is leveled to about 210°K. This calculation is in agreement with the measurements made during the Apollo 15 mission (Langseth *et al.*, 1972). These very low temperatures could mean that the adsorption possibilities of the lunar soil are very large for radon.

The combined effects of the reembedding and adsorption processes in fines

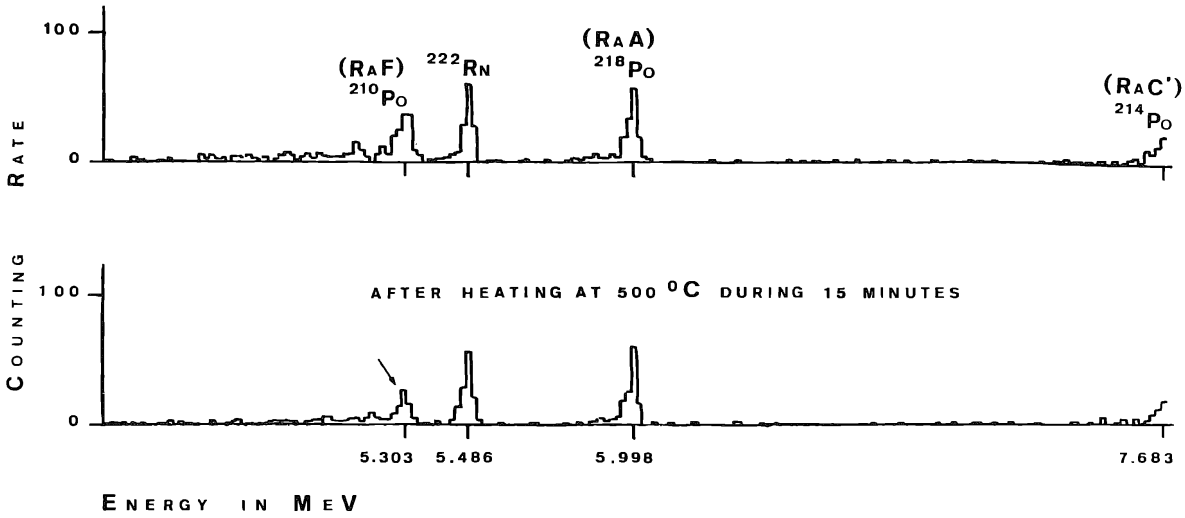

Fig. 6. The α spectrum of the bottom face of a rock in simulating experiment.

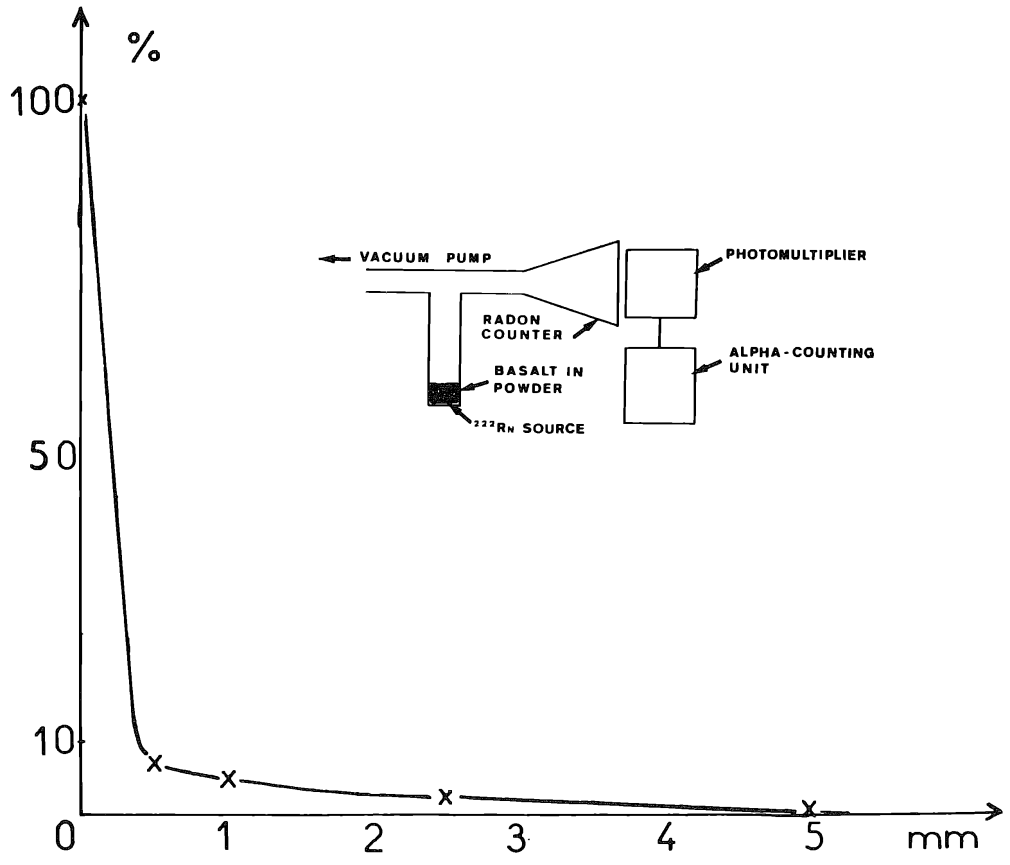

Fig. 7. Transmission of radon through basalt powder.

have been studied in the following experiment. A very thin source of radon was made by depositing radium on a platine plate. One sees in the α spectrum of this source that it loses half of its radon. This source was put in the bottom of a vessel connected to a scintillating bottle outside the view of the source (Fig. 7). The vessel was continuously pumped to maintain a primary vacuum. The radon emitted by the bare

source was measured. Then the source was covered with successive layers of fine basalt powder (grain diameter $<50\mu$). It may be seen that the counting rate in the radon counter is lowered to 7% with half a mm of powder and to 1% with one cm. One sees the great importance of the first layers from the slope of the curve. This layer most probably combines the adsorption and reembedding processes.

The experimental result obtained in this work shows that there is $\leq 2.10^{-5}$ dis/sec/cm^2 lead 210 deposited layer on the moon surface. The measurement of the emanation-to-production ratio performed by Yaniv and Heymann (1972) do not support our simulation experiment of adsorption of radon. However, up to this point, there have been no experiments performed under exact lunar conditions. We must consider, in addition, other possible effects such as the partial erosion of volatile elements by solar winds.

References

Adams J. A. S., Barretto M., Clark R. B., and Duvoljun J. S. (1971) Radon 222 emanation and the high apparent lead isotope ages in lunar dust. *Nature* **231,** 174–175.

Domeij I., Bergstrom I., Davies J. A., and Uhler J. (1963) A method of determining heavy ion range by analysis of α-line shapes. *Arkiv Fysik* **24,** 399–411.

Economou T. E. and Turkevitch A. L. (1971) Examination of returned Surveyor 3 camera visor for α radioactivity. Houston Conference.

Gorenstein P. and Bjokholm P. (1972) Results of the Apollo 15 α particle spectrometer experiment (abstract). In *Lunar Science—III* (editor C. Watkins), pp. 326–328, Lunar Science Institute Contr. No. 88.

Grjebine T., Lambert G., and Le Roulley J. C. (1972) α Spectrum of a surface exposed lunar rock. *Earth Planet. Sci. Lett.* **14,** 3, 322–324.

Kraner H. W., Schroeder G. L., Davidson G., and Carpentier J. W. (1966) Radioactivity of the lunar surface. *Science* **152,** 1235.

Langseth M. G. Jr., Clark S. P. Jr., Chute J. Jr., and Keihm S. (1972) The Apollo 15 lunar heat flow measurement (abstract). In *Lunar Science—III* (editor C. Watkins), pp. 475–477, Lunar Science Institute Contr. No. 88.

Lindstrom R. M., Evans J. C. Jr., Finkel R. C., and Arnold J. R. (1971) Radon emanations from the lunar surface. *Earth Planet. Sci. Lett.* **11,** 254.

LSPET (Lunar Sample Preliminary Examination Team) (1971) Apollo 14 Preliminary Science Report. NASA SP-272, pp. 123.

Turkevitch A. L., Patterson J. H., Franzgrote E. J., Sowinski K. P., and Economou T. E. (1970) Alpha radioactivity of the lunar surface at the landing sites of Surveyors 5, 6, and 7. *Science* **167,** 1722–1724.

Yaniv A. and Heymann D. (1972) Radon emanation from Apollo 11, 12, and 14 fines (abstract). In *Lunar Science—III* (editor C. Watkins), pp. 816–818, Lunar Science Institute Contr. No. 88.

Yeh R. S. and Van Allen J. A. (1969) Alpha particle emissivity of the moon: An observed upper limit. *Science* **166,** 370.

Proceedings of the Third Lunar Science Conference
(Supplement 3, *Geochimica et Cosmochimica Acta*)
Vol. 2, pp. 1779–1786
The M.I.T. Press, 1972

Vanadium isotopic composition and the concentrations of it and ferromagnesian elements in lunar material

P. REY

Department of Chemistry, Purdue University,
Lafayette, Ind. 47907, U.S.A.

H. BALSIGER

Physikalisches Institut der Universität, Bern, Switzerland

and

M. E. LIPSCHUTZ

Departments of Chemistry and Geosciences, Purdue University and
Department of Physics and Astronomy, Tel-Aviv University,
Ramat Aviv, Tel-Aviv, Israel

Abstract—The isotopic composition of vanadium from three Apollo 14 samples, an Apollo 11 sample, the dark portion of a gas-rich chondrite and a standard rock are the same as that of previous lunar, meteoritic, and terrestrial samples within the limits of error. The maximum difference possible between the mean isotopic composition in lunar and meteoritic material is about 1‰. The concentrations of iron, magnesium, titanium, chromium, and vanadium and the weight ratios of the first four of these elements to vanadium in Apollo 12 and 14 lunar materials suggest different primary source materials for different inclusions in rock 14321.

INTRODUCTION

DURING THE LAST several hundred million years lunar surface material and meteorites have been irradiated by energetic charged particles and the radiation history of these extraterrestrial samples has been investigated extensively by studies of a variety of monitors including a number of highly sensitive noble gas nuclides and radionuclides and tracks. Such monitors are not suitable for searches for the effects of a similar bombardment postulated to have taken place early in the history of the solar system (Fowler *et al.*, 1962; Bernas *et al.*, 1967) since this irradiation could have occurred under conditions such that these monitors would not be retained or would later be lost. The nongaseous elements provide several suitable radiation monitors, among the most sensitive of which is the vanadium isotopic composition (Shima and Honda, 1963; Burnett *et al.*, 1966; Balsiger *et al.*, 1969). An early charged particle irradiation should be revealed by comparison of the $^{50}V/^{51}V$ ratios in terrestrial, meteoritic and lunar samples unless either (a) there was thorough mixing of all matter now constituting these different objects, or (b) the integrated particle fluxes and the ratios of irradiated to shielded material were virtually identical in those parts of the solar system where these objects were formed (cf. Burnett *et al.*, 1965, 1966).

In previous studies (Balsiger *et al.*, 1969; Pelly *et al.*, 1970; Lipschutz *et al.*, 1971), we found that the vanadium isotopic composition in terrestrial, meteoritic and lunar samples was the same within the error limits (about 1%) and Albee *et al.* (1970) noted that the $^{50}V/^{51}V$ ratios in two Apollo 11 samples were the same as that of terrestrial vanadium to within 2 and 3%. However, our results showed that the $^{50}V/^{51}V$ ratios in lunar samples tended to be systematically higher than those in meteorites, the difference in the mean ratios lying just at the limits of confidence. We felt it worthwhile therefore to investigate additional samples to determine whether this difference persisted and, if so, the probable cause for this. Here we report results for four additional lunar samples, a chondrite and standard rock W-1. We also report determinations of some ferromagnesian elements (iron, magnesium, titanium, chromium) and vanadium in standard rocks and in these lunar samples and two others studied previously (Lipschutz *et al.*, 1971) which were undertaken to provide further information on the selenochemistry of vanadium.

EXPERIMENTAL

The lunar materials, whose vanadium isotopic composition was studied here, included samples of 10084,247 (studied previously by Albee *et al.*, 1970) and <1 mm lunar fines 14163,129 and two portions of the football-sized rock 14321,184. This rock is quite complex petrographically as it consists of a variety of crystalline (lunar basaltic) and fragmental (microbreccia) fragments in a lighter-colored matrix (Grieve *et al.*, 1972). Inasmuch as we were particularly interested in determining the $^{50}V/^{51}V$ ratios in more primitive material we studied samples of the two inclusion types but not the matrix. These 1.5 g subsamples (1c and 20/22, respectively) were excavated from the interior of the rock with vanadium-free WC or TaC tools by A. R. Duncan (personal communication) and, like the fines samples and standard rock, were not etched prior to their solution. The chondrite (Leighton), whose vanadium isotopic composition is reported here, is one of six being studied concurrently, and is the only one for which we have data as yet. This H5 chondrite is a typical gas-rich meteorite with a light-dark structure and only the dark portion (which was etched briefly with 1:1 HNO_3 to remove surface contamination) was taken for analysis.

Each lunar sample was dissolved (Pelly *et al.*, 1970) and after centrifugation to remove insoluble material (i.e., sulfates, etc.) the supernate was divided into three aliquots. Vanadium was extracted from the largest (60–70%) of these aliquots by the chemical separation technique described by Pelly *et al.* (1970) and its isotopic composition was determined mass-spectrometrically by the surface-ionization technique described by Balsiger *et al.* (1969). We used the same chemical and mass-spectrometric techniques to determine the vanadium concentration by isotope dilution (Lipschutz *et al.*, 1971) in the second aliquot (20–33%) of this solution. The third aliquot (10–14%) was diluted to 25 ml with 2N H_2SO_4 containing 2% NH_4Cl and portions of this solution were further diluted with appropriate reagents for determination of iron, magnesium, titanium, and chromium by atomic absorption spectroscopy (Slavin, 1968). Half-gram samples of standard rocks W-1 and BCR-1 and the 2 g sample of Leighton were treated similarly except that the sample solutions were each divided into only two aliquots, for determination of the vanadium isotopic composition and total vanadium concentration. Since we had not reserved appropriate aliquots of the Apollo 12 samples studied previously (Lipschutz *et al.*, 1971), 100–200 mg chips of two of the crystalline rocks (12021,49 and 12038,43) were processed chemically only for determination of iron, magnesium, titanium, and chromium. We also prepared separate stock solutions of standard rocks BCR-1 (for analysis of iron, magnesium, and titanium) and DTS-1 (for chromium), which for these elements have compositions similar to lunar samples, and we analyzed aliquots of these stock solutions whenever we determined these elements in lunar samples. The replicate analyses for each element in these aliquots differed by much less than 1%. We also attempted to determine the concentrations of these four elements in the precipitates removed prior to division of the lunar sample solutions, and we found only negligible

quantities ($\ll 0.1\%$) of these elements in all cases save for magnesium in 12021,49 where the amount measured in the precipitate corresponded to $\sim 2\%$ of the total magnesium in the sample.

Results and Discussion

The vanadium isotopic ratios for the samples included in this study are listed in Table 1 together with the uncertainty (the sum of the statistical error [three estimated standard errors] and those errors arising from correction of the mass-50 peak for contributions by ^{50}Ti and ^{50}Cr) associated with each measurement (Lipschutz *et al.*, 1971). Unfortunately the uncertainties associated with the measurements of lunar fines 10084,247 and 14163,129 were unusually large due to a substantial ($\sim 37\%$) correction for ^{50}Cr in the former sample and low beam intensity in the latter. The remaining uncertainties are more in accord with our previous results. As before, the ^{50}V/^{51}V ratios were not corrected for source or multiplier discrimination nor do the uncertainties listed include the error due to a possible variation in mass discrimination from one run to another.

The vanadium isotopic ratios and associated uncertainties listed in Table 1 are plotted in Fig. 1 together with our previous results (Pelly *et al.*, 1970; Lipschutz *et al.*, 1971). Within the uncertainty limits assigned to each of the ^{50}V/^{51}V ratios none of the individual isotopic ratios differs from those of the other samples or from the mean isotopic ratio, 2.455×10^{-3} (Table 2), for all samples. However the isotopic ratios for lunar samples still tend to be higher than those in meteoritic samples (Fig. 1) and the difference in the weighted means (obtained by inversely weighting each measurement by the square of its assigned uncertainty) for the two

Table 1. Vanadium isotopic ratios in samples investigated in this study.

Material	Lunar Sample No. or Sample Name	Type	^{50}V/^{51}V*
Lunar	10084,247	fines	$(2.474 \pm 0.064) \times 10^{-3}$
Lunar	14163,129	fines (< 1 mm)	$(2.477 \pm 0.065) \times 10^{-3}$
Lunar	14321,184(1c)	lunar basaltic inclusion	$(2.456 \pm 0.015) \times 10^{-3}$
Lunar	14321,184(20/22)	microbreccia inclusion	$(2.483 \pm 0.047) \times 10^{-3}$
Terrestrial	W–1	diabase	$(2.469 \pm 0.042) \times 10^{-3}$
Meteoritic	Leighton	H5 (dark portion)	$(2.471 \pm 0.028) \times 10^{-3}$

* The uncertainty listed for each sample includes a statistical error (three estimated standard errors) as well as those errors arising from correction of the mass-50 peak (see text).

Table 2. Vanadium isotopic ratios in terrestrial, meteoritic, and lunar samples.

Material	No. Investigated	Weighted ^{50}V/^{51}V*
Lunar	8	$(2.461 \pm 0.002) \times 10^{-3}$
Terrestrial	4	$(2.458 \pm 0.004) \times 10^{-3}$
Meteoritic	10	$(2.449 \pm 0.004) \times 10^{-3}$
All	22	$(2.455 \pm 0.002) \times 10^{-3}$

* The uncertainty listed for each group is the estimated weighted standard deviation of the mean calculated from the dispersions of the measurements of the individual samples.

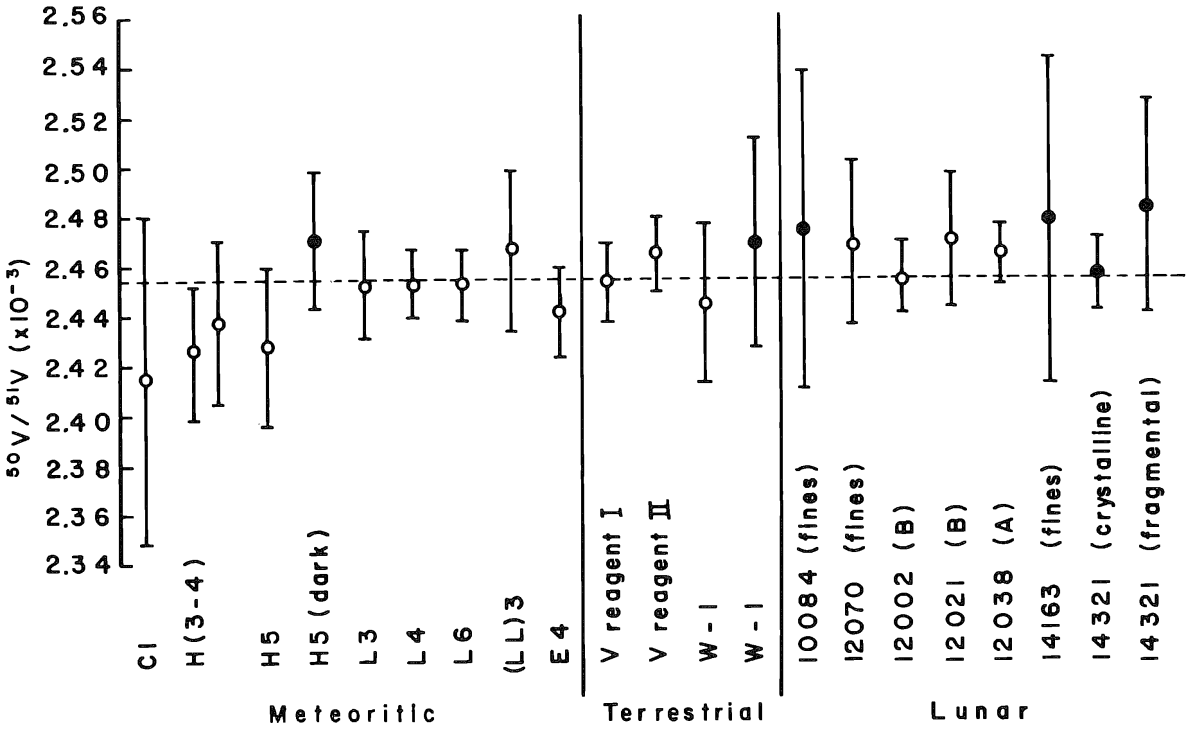

Fig. 1. $^{50}V/^{51}V$ ratios measured in this study (filled circles) compared with those measured in previous studies (open circles) of lunar samples, terrestrial diabase W-1 and reagent vanadium (I, II) and chondrites (uncertain classifications in parentheses). The weighted mean ratio of all samples is indicated by the dashed line.

groups persists (Table 2). The same weighting factors were used in calculating the estimated standard deviations of the group means (Table 2) from the dispersions of the measurements of the relevant individual samples, the standard deviation for the lunar-meteoritic difference, 0.013×10^{-3}, being $\pm 0.005 \times 10^{-3}$. It appears that the lunar-meteoritic difference may be marginally significant since it slightly exceeds two estimated standard deviations, whereas by the same criterion the terrestrial-meteoritic and lunar-terrestrial differences are not statistically significant.

If we treat the lunar-meteoritic difference as reflecting an irradiation effect, it cannot be ascribed to recent cosmic-ray or energetic solar particle bombardment since these should each alter the meteoritic and lunar $^{50}V/^{51}V$ ratios by less than 0.1% over times greater than the exposure ages of these materials (cf., Lipschutz *et al.*, 1971; Crozaz *et al.*, 1972). Since the bulk of the measurements of the lunar samples were made after the measurements of the meteorites and terrestrial samples it may well be that the lunar-meteoritic difference in the $^{50}V/^{51}V$ ratios merely reflects a long-term variation in mass-discrimination. Indeed the measurements of this ratio in Leighton and W-1 reported here tend to be higher than those of other meteoritic and terrestrial samples that we determined previously (Fig. 1). It will be necessary to carry out additional measurements, particularly of meteorites, to determine whether this tendency persists.

At this stage it seems safest to continue to assume that the samples constituting each of the groups in Table 2 have the same vanadium isotopic composition and that

the lunar-meteoritic difference plus two estimated standard deviations, $(0.013 \pm 2 \times 0.005) \times 10^{-3}$, corresponds to the maximum difference possible between these two sample groups (Lipschutz *et al.*, 1971). This maximum difference of about 1% can be used to calculate upper limits for the possible integrated flux ($\Delta\phi$) differences experienced by these materials for two types of proton spectra (Balsiger *et al.*, 1969). The resulting $\Delta\phi$ limits are similar to those calculated by Lipschutz *et al.* (1971), i.e., 1.6×10^{18} "hard" protons/cm^2 (cosmic-ray spectrum, $E > 30$ MeV) and 8×10^{19} "soft" protons/cm^2 (solar flare spectrum, $E > 10$ MeV).

The concentrations of iron and vanadium in the samples studied must be utilized in calculating these $\Delta\phi$ limits, and we determined these concentrations as well as those of other elements expected to provide clues to the selenochemistry of vanadium. Our analyses for the ferromagnesian elements iron, magnesium, titanium, and chromium agree very well ($\leq 1\%$) with mean values for homogeneous standard rocks and the mutual agreement of the vanadium data is nearly as satisfactory (Table 3) especially when due regard is taken of the scatter of the data summarized by Fleischer (1969) and Flanagan (1969). Chemical inhomogeneities in 0.1–0.2 g lunar rock samples would be expected to result in less good agreement and indeed our analyses of these five elements in rocks 12021 and 12038 differ from the mean values reported by others by somewhat greater amounts, typically 5–10% (Table 3). Some results (notably iron, titanium and chromium in 10084 and chromium in 12021) exhibit even greater differences which may also be due to sample inhomogeneity. Our sample of fines 10084 was allocated after the Apollo 12 mission and quite possibly is not representative of samples prepared during the original allocation of these Apollo 11 fines. Indeed our results for fines 14163 are in much better agreement (generally $\sim 5\%$) with the results of other investigations of this material (cf., Table 3 for references). We are at a loss to explain the unusually large discrepancy in the case of chromium in 12021 although it should be noted that this element appears to present serious analytical difficulties at lunar concentration levels, the wet chemical analyses (with which we generally agree) being markedly different in DTS-1 from those

Table 3. Concentrations of ferromagnesian elements in standard rocks and lunar samples.

	Fe (%)		Mg (%)		Ti (%)		Cr (%)		V (ppm)	
Sample	This Study	Others*	This Study	Others*	This Study	Others*	This Study	Others*	This Study	Others*
BCR–1	9.48‡	*9.45*(a)	1.99‡	*1.98*(a)	1.35‡	*1.34*(a)	—	*0.0016*(a)	393	*384*(a) 395(c)
DTS–1	—	*6.19*(a)	—	*30.04*(a)	—	*0.014*(a)	0.370	*0.374*(a)	—	*19*(a)
W–1	—	**7.76**(b)	—	**3.99**(b)	—	**0.641**(b)	—	**0.120**(b)	259	**240**(b) 256(c)
10084,247	13.98	*12.3*(d)	4.96	*4.73*(d)	5.05	*4.36*(d)	0.255	*0.20*(d)	†	—
12021,49	15.71	*15.0*(e)	5.14	*4.48*(e)	2.08	*2.01*(e)	0.391	*0.26*(e)	160(e)	*175*(e)
12038,43	13.09	*13.8*(e)	4.41	4.10(e)	2.06	*1.95*(e)	0.219	*0.20*(e)	126(e)	*123*(e)
14163,129	8.22	*8.04*(f,g, h,j)	5.77	*5.58*(f,g, h,j)	1.08	*1.04*(f,g, h,j)	0.153	*0.13*(f,g, h,j)	43	*47*(h,l)
14321,184(1c)	12.07	*12.8*(i,k)	5.68	5.37(k)	1.55	1.26(i)	0.342	*0.309*(i,k)	133	96(i)
14321,184 (20/22)	7.75	*8.8*(i,k)	7.03	6.80(k)	1.25	1.07(i)	0.158	*0.131*(i,k)	44	48(i)

* References: (a) Flanagan (1969); (b) Fleischer (1969); (c) Wyttenbach (1970); (d) Wänke *et al.* (1970) and references cited by them; (e) Lipschutz *et al.* (1971) and references cited by them; (f) Compston *et al.* (1972); (g) Hubbard *et al.* (1972); (h) Jackson *et al.* (1972); (i) Lindstrom and Duncan (personal communication); (j) Scoon (1972); (k) Wänke *et al.* (1972); (l) LSPET (1971). Entries in italics are mean values of different investigators, those in boldface are values recommended for standard rock W–1.

† Sample lost in laboratory mishap.

‡ Mean values of at least 6 replicate analyses.

obtained using other techniques (cf., Flanagan, 1969). Our results for the crystalline basaltic and fragmental microbreccia subsamples from rock 14321 generally agree quite well with the mean values listed in Table 3 (which were obtained from analyses only of similar type inclusions in this rock). In view of the heterogeneous nature of rock 14321 and, indeed, of the inclusions within it (Grieve *et al.*, 1972), those differences that do exist between our results and others may be easily ascribed to sample

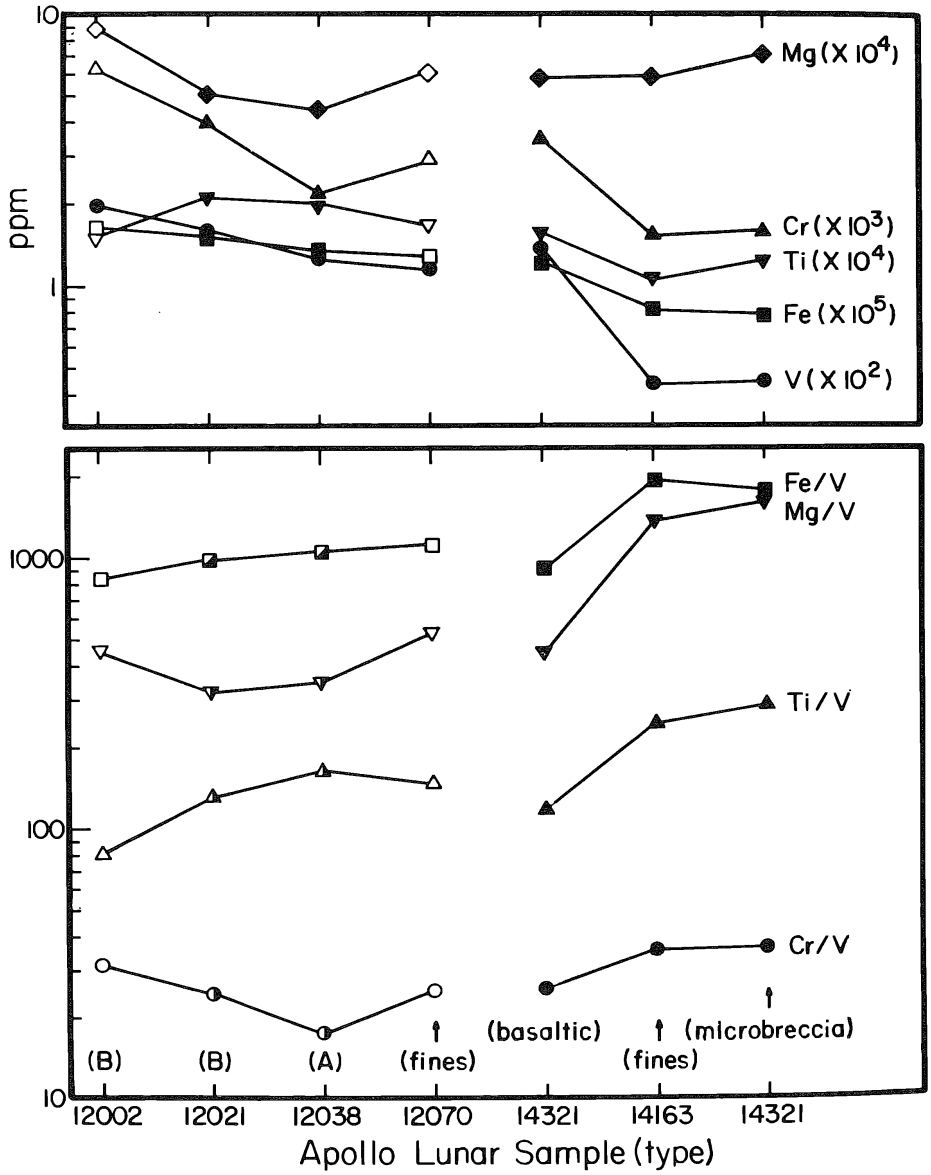

Fig. 2. Concentrations of four major and minor ferromagnesian elements and vanadium, and the weight ratios of these four elements relative to vanadium in Apollo 12 and 14 lunar samples. Filled and half-filled symbols represent our results (the former obtained from aliquots of the same sample solution, the latter obtained from different chips of the same subsample), and open symbols represent the average of other determinations of ferromagnesian elements (cf. Lipschutz *et al.* [1971] for references). For these elements the basaltic inclusion in rock 14321 resembles Apollo 12 crystalline rocks and fines and the microbreccia resembles fines 14163.

inhomogeneities. We should note that, overall, application of the Student's t test shows that our data for each of the elements studied do not differ significantly from those reported by other investigators of the same samples.

Our results for the Apollo 12 and 14 lunar samples listed in Table 3, together with previous results for rock 12002 and fines 12070 (cf., Lipschutz *et al.*, 1971), are plotted in Fig. 2 in decreasing order of iron concentration. Even our very limited sampling yields results exhibiting the same gross trends noted by LSPET (1971), i.e., that iron, titanium, chromium and vanadium are less abundant in Apollo 14 than in Apollo 12 material whereas the amounts of magnesium are generally similar. Interestingly, the basaltic inclusion 184 (1c) in rock 14321 contains these five elements in amounts similar to those in 12070 fines. The contents of iron, chromium and vanadium in the microbreccia subsample 184 (20/22) are lower than those in the basaltic inclusion and are quite similar to those in the fines 14163 whereas magnesium exhibits the opposite trend, its concentrations in the basaltic inclusion and fines 14163 being quite similar. The titanium concentration in the basaltic inclusion is higher than that in the microbreccia, the latter having a content closer to that of fines 14163.

The trends exhibited by the concentrations of these five elements as well as the Fe/V, Mg/V, Ti/V and Cr/V concentration ratios illustrated in the bottom portion of Fig. 2 seemingly indicate that vanadium follows chromium in fines 14163 and rock 14321 rather than iron as in Apollo 12 fines and crystalline rocks (Lipschutz *et al.*, 1971). However, this conclusion contains the implicit assumption that the Apollo 14 material studied was largely, if not entirely, derived from a single source material. The mineralogy of rock 14321 (Grieve *et al.*, 1972) indicates a more likely alternative, i.e., that various subsamples of rock 14321 were derived from different source materials. In this event the concentrations and ratios illustrated in Fig. 2 suggest that basaltic inclusion 184 (1c) was derived primarily from mare basalt material similar in composition to fines 12070 and/or a mixture of Apollo 12 crystalline rocks whereas the primary source material for the microbreccia subsample 184 (20/22) may well have had a composition similar to that of fines 14163.

Acknowledgments—This research was supported by the U.S. National Aeronautics and Space Administration (Grant NGR-134) and the Swiss National Science Foundation (Grant 2-213-69). We thank Professor J. Geiss for his continuing aid and encouragement.

References

Albee A. L., Burnett D. S., Chodos A. A., Eugster O. J., Huneke J. C., Papanastassiou D. A., Podosek F. A., Russ G. P. II, Sanz H. G., Tera F., and Wasserburg G. J. (1970) Ages, irradiation history, and chemical composition of lunar rocks from the Sea of Tranquillity. *Science* **167,** 463–466.

Balsiger H., Geiss J., and Lipschutz M. E. (1969) Vanadium isotopic composition in meteoritic and terrestrial matter. *Earth Planet. Sci. Lett.* **6,** 117–122.

Barnes I. L., Carpenter B. S., Garner E. L., Gramlich J. W., Kuehner E. C., Machlan L. A., Mainethal E. J., Moody J. R., Moore L. J., Murphy T. J., Paulsen P. J., Sappenfield K. M., and Shields W. R. (1972) The isotopic abundance ratio and assay analysis of selected elements in Apollo 14 samples (abstract). In *Lunar Science—III* (editor C. Watkins), pp. 41–43, Lunar Science Institute Contr. No. 88.

Bernas R., Gradsztajn E., Reeves H., and Schatzmann E. (1967) On the nucleosynthesis of lithium, beryllium and boron. *Ann. Phys.* **44,** 462–478.

Burnett D. S., Fowler W. A., and Hoyle F. (1965) Nucleosynthesis in the early history of the solar system. *Geochim. Cosmochim. Acta* **29,** 1209–1241.

Burnett D. S., Lippolt H. J., and Wasserburg G. J. (1966) The relative isotopic abundance of K^{40} in terrestrial and meteoritic samples. *J. Geophys. Res.* **71,** 1249–1269, 3609.

Compston W., Vernon M. J., Berry H., Rudowski R., Gray C. M., Ware N., Chappell B. W., and Kaye M. (1972) Age and petrogenesis of Apollo 14 basalts (abstract). In *Lunar Science—III* (editor C. Watkins), pp. 151–153, Lunar Science Institute Contr. No. 88.

Crozaz G., Drozd R., Hohenberg C. M., Hoyt H. P. Jr., Ragan D., Walker R. M., and Yuhas D. (1972) Solar flare and galactic cosmic ray studies of Apollo 14 samples (abstract). In *Lunar Science—III* (editor C. Watkins), p. 165, Lunar Science Institute Contr. No. 88.

Flanagan F. J. (1969) U.S. Geological Survey Standards—II. First compilation of data for the new U.S.G.S. rocks. *Geochim. Cosmochim. Acta* **33,** 81–120.

Fleischer M. (1969) U.S. Geological Survey Standards—I. Additional data on rocks G-1 and W-1, 1965–1967. *Geochim. Cosmochim. Acta* **33,** 65–79.

Fowler W. A., Greenstein J. L., and Hoyle F. (1962) Nucleosynthesis during the early history of the solar system. *Geophys. J.* **6,** 148–220.

Grieve R., McKay G., Smith H., Weill D., and McCallum J. (1972) Mineralogy and petrology of polymict breccia 14321 (abstract). In *Lunar Science—III* (editor C. Watkins), pp. 338–340, Lunar Science Institute Contr. No. 88.

Hubbard N. J., Gast P. W., Rhodes M., and Wiesmann H. (1972) Chemical composition of Apollo 14 materials and evidence for alkali volatilization (abstract). In *Lunar Science—III* (editor C. Watkins), pp. 407–409, Lunar Science Institute Contr. No. 88.

Jackson P. F. S., Coetzee J. H. J., Strasheim A., Strelow F. W. E., Gricius A. J., Wybenga F., and Kokot M. L. (1972) The analysis of lunar material returned by Apollo 14 (abstract). In *Lunar Science—III* (editor C. Watkins), pp. 424–426, Lunar Science Institute Contr. No. 88.

Lipschutz M. E., Balsiger H., and Pelly I. Z. (1971) Vanadium isotopic composition and contents in lunar rocks and dust from the Ocean of Storms. *Proc. Second Lunar Sci. Conf., Geochim. Cosmochim. Acta* Suppl. 2, Vol. 2, pp. 1443–1450. M.I.T. Press.

LSPET (1971) (Lunar Sample Preliminary Examination Team) Preliminary examination of lunar samples from Apollo 14. *Science* **173,** 681–693.

Pelly I. Z., Lipschutz M. E., and Balsiger H. (1970) Vanadium isotopic composition and contents in chondrites. *Geochim. Cosmochim. Acta* **34,** 1033–1036.

Scoon J. H. (1972) Chemical analysis of lunar samples 14003, 14311, and 14321 (abstract). In *Lunar Science—III* (editor C. Watkins), pp. 690–691, Lunar Science Institute Contr. No. 88.

Shima M., and Honda M. (1963) Isotopic abundance of meteoritic lithium. *J. Geophys. Res.* **68,** 2844–2854.

Slavin W. (1968) *Atomic Absorption Spectroscopy*, Interscience.

Wänke H., Baddenhausen H., Balacescu A., Teschke F., Spettel B., Dreibus G., Quijano-Rico M., Kruse H., Wlotzka F., and Begemann F. (1972) Multielement analyses of lunar samples (abstract). In *Lunar Science—III* (editor C. Watkins), pp. 779–781, Lunar Science Institute Contr. No. 88.

Wänke H., Rieder R., Baddenhausen H., Spettel B., Teschke F., Quijano-Rico M., and Balacescu A. (1970) Major and trace elements in lunar material. *Proc. Apollo 11 Lunar Sci. Conf., Geochim. Cosmochim. Acta* Suppl. 1, Vol. 2, pp. 1719–1727.

Wyttenbach A. (1970) Die zerstörungsfreie Aktivierungsanalytische Bestimmung von Na, Mg, Al, Ca, V, und Mn in Gesteinen und Steinmeteoriten. Habilitationsschrift, EIR Bericht Nr. 177.

Proceedings of the Third Lunar Science Conference
(Supplement 3, *Geochimica et Cosmochimica Acta*)
Vol. 2, pp. 1787–1795
The M.I.T. Press, 1972

Rare-gas analyses on neutron irradiated Apollo 12 samples

E. C. ALEXANDER, JR., P. K. DAVIS, and J. H. REYNOLDS

Department of Physics, University of California,
Berkeley, California 94720

Abstract—Argon, krypton, and xenon from stepwise heating of five Apollo 12 rocks that had been irradiated to a neutron fluence of $\sim 10^{19}$ neutrons/cm^2 were analyzed mass-spectrometrically. The ^{40}Ar–^{39}Ar ages were determined and range from $3.18 \pm 0.06 \times 10^9$ years to $3.32 \pm 0.06 \times 10^9$ years. Trace elements Ba, Br, I, and U were measured via the neutron induced reactions that produce isotopes of krypton and xenon. The following concentration ranges were observed: Ba, 46 to 70 ppm; Br, 48 to 146 ppb; I, 16 to 73 ppb; and U, 170 to 247 ppb.

INTRODUCTION

THIS WORK REPRESENTS a continuation of our previous study (Davis *et al.*, 1971) of rare gases from neutron irradiated lunar samples. Five Apollo 12 crystalline rocks were analyzed: 12002,83; 12020,36; 12022,52; 12051,12; and 12065,33. The objectives are to obtain simultaneously K–Ar ages, via the ^{40}Ar–^{39}Ar technique (Merrihue and Turner, 1966) and concentrations of the trace elements Ba, Br, I, and U from each sample. Subtle changes in trace element concentrations with age (which normally would be obscured by sample inhomogeneity, interlaboratory biases, etc.) thus may be examined. Only those trace elements that produce rare-gas isotopes by neutron induced reaction are determinable, but both the volatile (Br and I) and refractory (U and Ba) elements are represented.

EXPERIMENTAL TECHNIQUE

Experimental procedures for the Apollo 12 samples were modified from those used in our Apollo 11 work (Davis *et al.*, 1971). The samples, weighing about 90 mg, were sealed in evacuated quartz break-seal capsules for irradiation. This permitted the analysis of low temperature fractions, which previously were lost.

The neutron irradiation was carried out in the pool of the General Electric Test Reactor, Vallecitos Nuclear Center, Pleasanton, California, and is designated Vallecitos four. The Vallecitos center indicated the samples received the following fluence:

Thermal ($E < 0.17$ eV)	1.34×10^{19} neutrons/cm^2
Epithermal (0.17 eV $< E <$ 0.18 MeV)	4.21×10^{18} neutrons/cm^2
Fast ($E >$ 0.18 MeV)	1.16×10^{18} neutrons/cm^2

Crystalline KI was irradiated with the samples to monitor the fluence. Isotope dilution of the ^{128}*Xe extracted from part of the KI gave ^{128}*Xe/^{127}I $= (1.210 \pm 0.014) \times 10^{-4}$, which corresponds to a fluence of 1.92×10^{19} neutrons/cm^2 using $\sigma_{127} = 6.3$ barns. This value, which is the value used in subsequent calculations, is larger than the thermal fluence indicated by the Vallecitos Center but agrees well with their total fluence. Fluence variations within the irradiation can were monitored by placing a Co-doped Al wire inside each quartz capsule. The maximum correction for fluence inhomogeneity was 3%.

After irradiation and cooling, the capsules were glass-blown to an extraction system. Any gases lost by the sample during or after the irradiation were measured as part of the 80°C fraction. This fraction and the 350°C fraction were obtained using an external resistance heater. After completion of the 350°C gas extraction, the samples were removed from the quartz capsules and placed in an induction heater extraction system for the high temperature analyses. All of the high temperature Kr and Xe fractions were accumulated and analyzed as a single total fraction after the Ar analyses were completed.

Details of data reduction are discussed in Alexander *et al.* (1972) and Podosek and Lewis (1972).

^{40}Ar–^{39}Ar AGES

Table 1 lists the $^{37}Ar/^{39}Ar$, $^{40*}Ar/^{39}Ar$, and the concentration of $^{39*}Ar$ for the Apollo 12 rocks we analyzed. Complete sets of the isotopic data on which Table 1 is based have been prepared and are available on request from the authors. Data in the first two columns of Table 1 were used to construct $^{40*}Ar/^{39}Ar$ versus $^{37}Ar/^{39}Ar$ plots for each rock. Figure 1 shows a typical plot for sample 12051. Turner (1970b) has discussed the use and meaning of such plots, and Alexander *et al.* (1972) explain in detail our use of the plots. The "intercept" values listed in Table 1 are from cubic-least-squares fits (York, 1966) for all temperatures >800°C for each sample. The horizontal intercept is $(^{37}Ar/^{39}Ar)_{Ca}$ or calcium-derived argon, and the vertical intercept is $(^{40*}Ar/^{39}Ar)_{K}$ or potassium-derived argon. The latter values were used, after

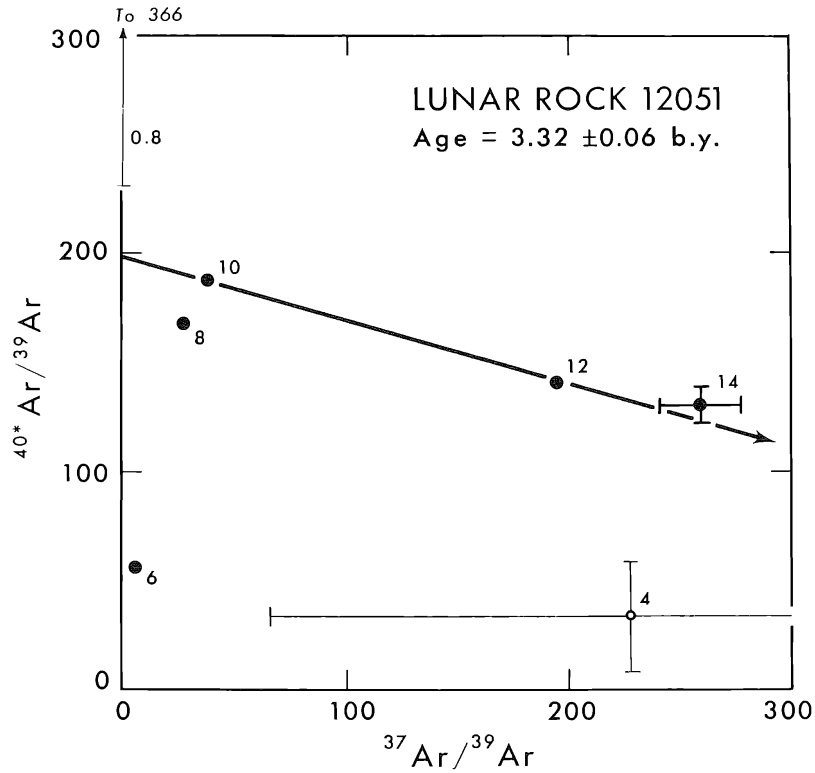

Fig. 1. Argon from neutron irradiated lunar rock 12051. The other rocks yield similar graphs. Errors of 1σ are either indicated or are smaller than the points. The number by each point is the temperature of that fraction in hundreds of degrees Celsius. Low temperature points indicated in light symbols are included for completeness but represent negligible fractions of the gas. The figure is discussed more fully in the text.

Table 1. Argon data for five neutron irradiated Apollo 12 rocks.

Temperature (°C)	$^{37}Ar/^{39}Ar$	$^{40*}Ar/^{39}Ar$	$^{39*}Ar$ ($\times 10^{-8}$ ccSTP/gm)
	Lunar rock 12002 (0.968 ± 0.0025)†		
400	—	—	0.55
600	9.1 ± 2.6	38.69 ± 0.85	4.48
800	36.0 ± 1.9	137.8 ± 1.1	6.30
1000	68.0 ± 1.8	177.3 ± 1.3	4.20
1200	243.2 ± 5.7	136.5 ± 2.7	2.21
1400	400 ± 112	57 ± 20	0.13
Intercept	811 ± 91	193.7 ± 3.7	
	Lunar rock 12020 (0.991 ± 0.0026)†		
400	—	5.4 ± 3.4	0.52
600	9.0 ± 4.5	39.41 ± 0.40	5.13
800	28.1 ± 1.8	127.9 ± 1.9	6.57
1000	57.4 ± 2.0	166.5 ± 1.7	4.00
1200	191.6 ± 2.6	138.1 ± 1.5	3.43
1400	347 ± 17	106.1 ± 5.5	0.43
Intercept	848 ± 52	178.5 ± 2.4	
	Lunar rock 12022 (0.989 ± 0.0026)†		
80	—	240 ± 73	0.11
350	—	200 ± 62	0.14
400	—	8.9 ± 4.3	0.78
600	—	46.45 ± 0.83	5.37
800	26.9 ± 2.4	151.2 ± 1.8	5.95
1000	42.8 ± 2.1	166.4 ± 1.1	6.11
1200	180.6 ± 2.3	134.0 ± 3.0	5.53
1400	325 ± 37	76 ± 13	0.15
Intercept	715 ± 99	177.1 ± 3.0	
	Lunar rock 12051 (0.969 ± 0.0025)†		
80	—	366 ± 137	0.06
400	227 ± 160	33 ± 25	0.12
600	5.9 ± 3.3	59.4 ± 2.6	2.49
800	28.1 ± 1.3	167.7 ± 1.6	8.56
1000	38.8 ± 2.0	186.9 ± 2.6	9.60
1200	196.4 ± 2.8	140.6 ± 2.8	5.17
1400	261 ± 17	130.9 ± 7.9	0.45
Intercept	693 ± 64	197.7 ± 4.4	
	Lunar rock 12065 (0.989 ± 0.0026)†		
350	—	271 ± 96	0.09
400	—	6.3 ± 4.0	0.69
600	14.1 ± 1.6	65.90 ± 0.71	4.50
800	29.0 ± 1.7	169.09 ± 0.87	7.18
1000	50.1 ± 2.7	171.5 ± 1.2	6.97
1200	224.7 ± 5.6	129.9 ± 3.1	3.40
1400	518 ± 69	84 ± 15	0.10
Intercept	791 ± 84	183.0 ± 2.7	

† Fluence corrections (normalized to one of the monitors). These factors are to be applied to the "intercept" values before the age calculation.

The tabulated amounts of ^{37}Ar and ^{39}Ar are corrected for radioactive decay that took place both during and after the irradiation. The additional error of 1.5% that this introduces into the $^{37}Ar/^{39}Ar$ ratio does not affect the age calculation and has not been included in the tabulated values.

Fractions in which there was no measurable ^{39}Ar have been omitted.

application of the fluence corrections listed in Table 1, to calculate the sample ages. The $(^{40*}Ar/^{39}Ar)_K$ intercepts (fluence corrected) for the monitors are 419.6 ± 2.8 and 410.1 ± 2.1 for an average of 414.8 ± 6.9.

Ages were calculated for the Apollo 12 samples using the equation:

$$T_s = (1/\lambda) \ln [1 + R(e^{\lambda T_m} - 1)], \quad (1)$$

where T_s is the age of the sample, λ is the total decay probability of ^{40}K, T_m is the age of the monitor, and $R = (^{40*}Ar/^{39}Ar)_K$ sample/$(^{40*}Ar/^{39}Ar)_K$ monitor. The age of the monitor is assumed to be 4.56 ± 0.05 b.y., based on Goplan and Wetherill's (1969) Rb–Sr age of the amphoterite chondrites. Any change in the age assigned to the monitor will propagate to the sample ages by a factor of $\delta T_s/\delta T_m = 0.914$.

Ages listed in the second column of Table 2 were calculated using $\lambda = 5.480 \times 10^{-10}$ yr^{-1} from Beckinsale and Gale's (1969) summary of physical determinations of the ^{40}K decay parameters. Ages listed in the third column were calculated using $\lambda = 5.304 \times 10^{-10}$ yr^{-1}, which is the geochronological value (Smith, 1964) used by most laboratories. The former are our preferred values, and the values in the third column are included only to facilitate interlaboratory comparisons. Our results agree satisfactorily with those of other workers (Turner, 1971; Stettler *et al.*, 1972).

Figure 2 is a conventional "plateau plot" of $^{40*}Ar/^{39*}Ar$ and apparent age versus the fraction of ^{39}Ar released for sample 12051. This particular method of data display was first used by Podosek *et al.* (1972). The $^{39*}Ar$ is the ^{39}Ar derived from potassium and is given by:

$$^{39*}Ar = {}^{39}Ar - (^{39}Ar/^{37}Ar)_{Ca}\,{}^{37}Ar, \quad (2)$$

where $(^{39}Ar/^{37}Ar)_{Ca}$ is the inverse of the horizontal intercept in Fig. 1. Figure 2 is typical of the plots for the other samples.

TRACE ELEMENTS

Krypton and xenon isotopic data for each of the temperature fractions are available on request from the authors. The complex Kr and Xe spectra were decomposed

Table 2. ^{40}Ar–^{39}Ar ages of Apollo 12 crystalline rocks.

Sample	Age (in units of 10^9 yr)		
	Preferred values* (this work)	Comparison values† (this work)	Other workers‡
12002	3.29 ± 0.04 (±0.06)	3.26 ± 0.06	3.24 ± 0.05[a]
12020	3.20 ± 0.03 (±0.06)	3.17 ± 0.06	
12022	3.18 ± 0.04 (±0.06)	3.15 ± 0.06	
12051	3.32 ± 0.04 (±0.06)	3.29 ± 0.06	3.27 ± 0.05[a] 3.15, 3.19[b]
12065	3.23 ± 0.03 (±0.06)	3.20 ± 0.06	3.24 ± 0.05[a]

* Preferred values are calculated using $\lambda = 5.48 \times 10^{-10}$ yr^{-1} (Beckinsale and Gale, 1969) and are relative to an assumed monitor age of 4.56 ± 0.05 × 10^9 yr for St. Severin. The first error listed does not include the monitor error and is for internal comparison. The second error is the total error and is for interlaboratory comparisons.

† Comparison values are calculated using $\lambda = 5.304 \times 10^{-10}$ yr^{-1} (Smith, 1964), which is the value used by the other workers.

‡ References: [a] Turner (1971), [b] Stettler *et al.* (1972).

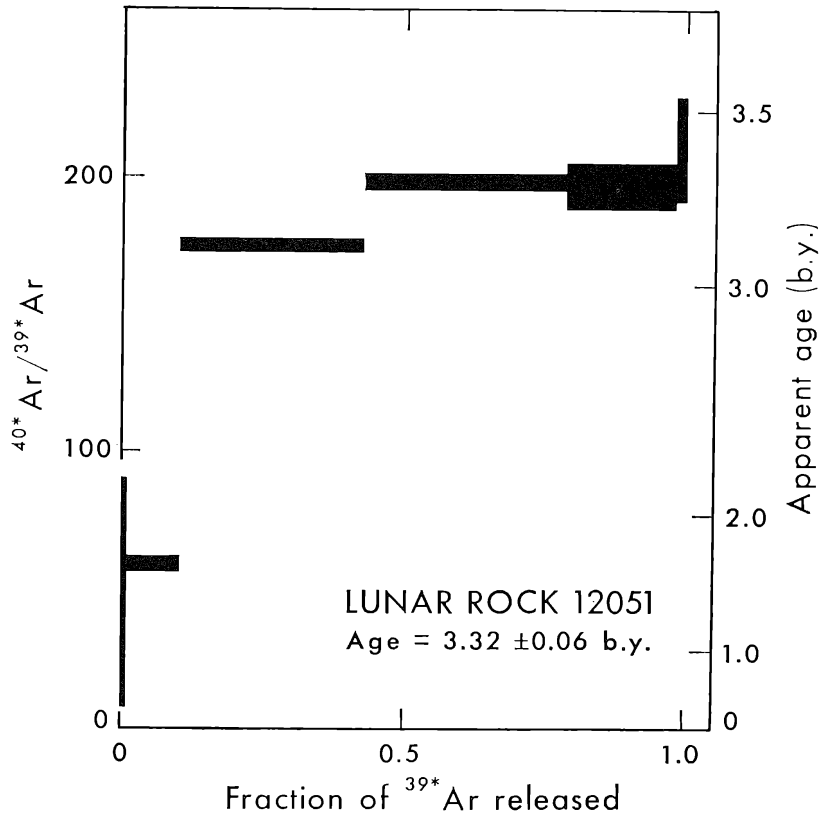

Fig. 2. The ^{40}Ar–^{39}Ar release pattern for lunar rock 12051. The other rocks yield similar patterns. This particular form of data display was developed by Podosek *et al.* (1972). For each temperature fraction the calculated $^{40*}Ar/^{39*}Ar$ ratio is at the center of a box the length of which is the fraction of $^{39*}Ar$ released at that temperature. The height of the box is the statistical error associated with the $^{40*}Ar/^{39*}Ar$ ratio.

into their various components using a multidimensioned matrix method outlined by Davis *et al.* (1971). The concentrations of I represented by the amount of $^{128*}Xe$ in each temperature fraction were calculated using the $^{128*}Xe/^{127}I$ ratio measured in a KI monitor. Br, Ba, and U concentrations were calculated using the KI monitor data, the ratios of $\sigma^{n,\gamma}_{80,82}$, $\sigma^{n,\gamma}_{130}$, and $\sigma^{n,f}_{235}$ to $\sigma^{n,\gamma}_{127}$, and the measured amounts of $^{80+82*}Kr$, $^{131*}Xe$, and $^{131-136f}Xe$. Table 3 lists the results of the calculations. The low temperature data in Table 3 were corrected for the contribution of the quartz capsule and aluminum foil to the observed neutron induced Kr and Xe isotopes. This correction was based on a "blank" quartz capsule, which contained only aluminum foil. An error equal to the size of this correction was applied to the data. Errors listed in Table 3 are the 1σ quadratic sum of all known sources of error, including sensitivity errors in the amount of rare gas.

Our Ba and U concentrations compare favorably with those measured for Apollo 12 rocks by many other workers. Our Br value for sample 12022, 48 ± 17 ppb, agrees well with that obtained by Reed and Jovanovic (1971), 43 ppb. Anders *et al.* (1971) reported Br values for samples 12002, 12020, and 12051 of 10, 16, and 16 ppb, respectively, while we observe values of 127 ± 23, 121 ± 20, and 146 ± 25 ppb, respectively. The reason for this (roughly order-of-magnitude) difference with Anders

Table 3. Trace element concentrations in Apollo 12 crystalline rocks.

Sample	Temperature (°C)	Br (ppb)	Ba (ppm)	I (ppb)	U (ppb)
12002	80	96 ± 23	0.08 ± 0.02	52.0 ± 7.8	0.8 ± 0.3
	350	20.2 ± 3.6	< 0.03	1.9 ± 0.3	< 1.0
	1730	11.7 ± 1.9	47.6 ± 5.7	0.6 ± 0.1	174 ± 21
	Total	127 ± 23	47.8 ± 5.7	54.5 ± 7.8	176 ± 21
12020	80	111 ± 20	0.18 ± 0.02	30.1 ± 4.3	< 1.6
	350	5.1 ± 1.1	< 0.04	0.8 ± 0.2	< 0.6
	1730	5.7 ± 0.9	45.4 ± 5.4	0.4 ± 0.2	168 ± 21
	Total	121 ± 20	45.7 ± 5.4	31.3 ± 4.3	170 ± 21
12022	80	35 ± 17	0.17 ± 0.02	69.0 ± 9.4	< 0.9
	350	6.1 ± 1.8	< 0.2	3.2 ± 0.4	< 4.0
	1730	7.6 ± 1.2	57.6 ± 6.9	0.4 ± 0.2	204 ± 25
	Total	48 ± 17	58.0 ± 6.9	72.6 ± 9.4	209 ± 26
12051	80	104 ± 24	0.08 ± 0.02	14.6 ± 5.1	0.3 ± 0.1
	350	27.6 ± 4.7	0.03 ± 0.02	1.0 ± 0.3	< 1.5
	1730	14.0 ± 2.2	69.5 ± 8.3	0.7 ± 0.1	245 ± 30
	Total	146 ± 25	69.6 ± 8.3	16.3 ± 5.1	247 ± 30
12065	80	†	†	†	†
	350	~8.7 ± 1.8	< 0.03	~0.4 ± 0.2	< 1.2
	1730	8.3 ± 1.3	51.1 ± 6.1	0.5 ± 0.1	201 ± 24
	Total	†	51.2 ± 6.1	†	203 ± 24

† The 80° fraction of 12065 was lost because the "break seal" apparently was not gas tight. Some of the 350° fraction may have been lost, also.

et al.'s (1971) work is not clear, but we are encouraged by our agreement with Reed and Jovanovic's (1971) results. We conclude that the Br content of Apollo 12 crystalline rocks is higher than the average value of 13 ppb calculated by Anders *et al.* (1971).

The value of this unique (and laborious) method of trace element determination is particularly evident for I determinations. Reed and Jovanovic (1971) are the only other group to determine I in lunar samples, and their radiochemical method yields extremely variable results. Our I value for 12022, 72.6 ± 9.4 ppb, falls between the values reported by Reed and Jovanovic (1971) of 14 ppb (water extractable) and 508 ppb (total sample) for two samples of 12022. The rare gas I measurements show a smaller range of values than the radiochemical determinations and agree well with the range, 10 to 60 ppb, quoted by Reed and Jovanovic (1971) as their most reliable results.

Release patterns of the rare gases produced from each element are very similar for all five rocks but vary drastically from element to element. Figure 3 shows the release patterns for each of the elements in rock 12022. Gases derived from Ba and U are almost completely contained in the high temperature fractions. The ^{128*}Xe from I is almost entirely contained in the low temperature fractions, and Br derived Kr isotopes, while mainly in the low temperature fractions, have a small but significant high temperature component. Similar release patterns for neutron irradiated meteorites have been inferred by Hohenberg (1968).

DISCUSSION

Davis *et al.* (1971), in a comparison of the ^{40}Ar release patterns from irradiated and unirradiated samples of 10044 and 10057, found that the release patterns were

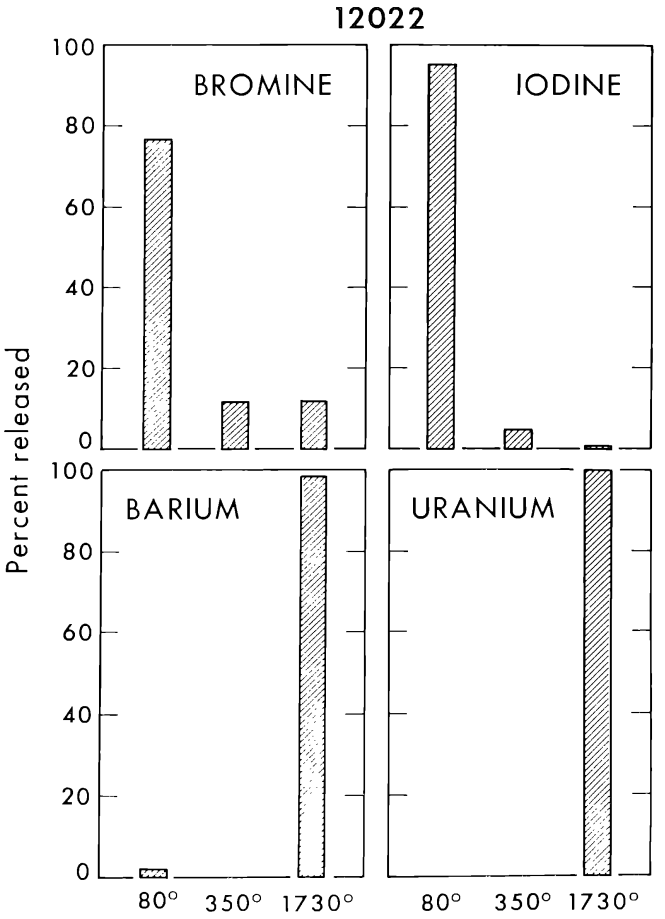

Fig. 3. Release patterns of neutron capture (or fission) rare gases from trace elements in lunar rock 12022. The other rocks have very similar release patterns. Bromine has a small but distinct high temperature component, while iodine does not.

clearly altered by the irradiation. One of the purposes of this work was to check for selective loss of ^{39}Ar (due perhaps to recoil effects of the ^{39}K (n, p) ^{39}Ar reaction) in lunar samples. The low temperature data indicate that loss of ^{39}Ar was not a significant problem for the Apollo 12 samples. Potassium is apparently located in retentive sites in these samples. In this context it is interesting to note that all five Apollo 12 crystalline rocks yield high temperature plateaus and are datable using the ^{40}Ar–^{39}Ar method. In contrast, three of the eight Apollo 11 crystalline rocks analyzed by the ^{40}Ar–^{39}Ar method did not yield meaningful ages (Turner, 1970a, 1970b; Davis *et al.*, 1971). It will be interesting to see if ^{39}Ar loss is significant in samples from other missions.

Figure 4 is a plot of trace element concentration versus age for the five Apollo 12 rocks. The spread in ages confirms the observation of Papanastassiou and Wasserburg (1971) that small but real differences exist in the ages of the Apollo 12 rocks. There appears to be significant variation of the I and Br concentrations with age. Although both I and Br are considered volatile elements, their trends are opposite. The Br increases with age, while the I decreases. The data for Ba and U do not define trends, but the oldest rock, 12051, is the highest in Ba and U.

The difference in the release patterns of Br and I described in the previous section

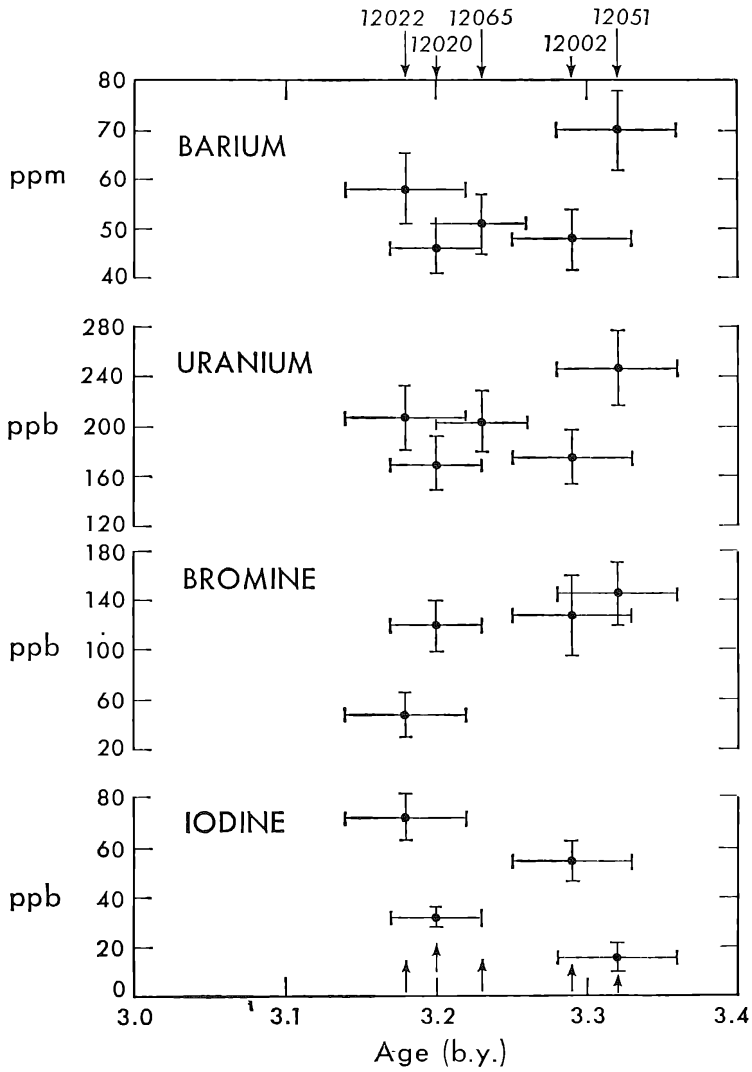

Fig. 4. Trace element content versus age for Apollo 12 samples. Bromine tends to increase with age, while iodine tends to decrease.

is relevant to the recent discovery of Br neutron capture anomalies in Apollo 14 rock 14310 (Lugmair and Marti, 1971). The high temperature fraction of the neutron capture Kr represents only about 10% of the total produced. As the low temperature fractions would be lost in the lunar surface environment, any attempt to calculate the lunar neutron fluence from the Br content and ^{80}Kr and ^{82}Kr excesses in unirradiated Apollo 14 samples will yield fluences that are an order of magnitude too low. The almost total absence of a high temperature ^{128*}Xe component from neutron capture on ^{127}I observed in the Apollo 12 samples probably explains why no neutron capture ^{128}Xe was observed in those Apollo 14 samples that contained the Kr neutron capture anomalies. While most of the neutron capture Kr was lost on the lunar surface, all of the neutron capture ^{128}Xe was lost.

Acknowledgments—We acknowledge many stimulating discussions of this data with Drs. R. S. Lewis, W. A. Kaiser, and B. Srinivasan. G. A. McCrory contributed invaluable assistance in maintaining the equipment. This work was supported by NASA under grant NGL 05-003-409.

References

Alexander E. C. Jr., Davis P. K., and Lewis R. S. (1972) Argon 40–argon 39 dating of Apollo sample 15555. *Science* **175,** 417–419.

Anders E., Ganapathy R., Keays R. R., Laul J. C., and Morgan J. W. (1971) Volatile and siderophile elements in lunar rocks: Comparison with terrestrial and meteoric basalts. *Proc. Second Lunar Conf., Geochim. Cosmochim. Acta* Suppl. 2, Vol. 2, pp. 1021–1036. MIT Press.

Beckinsale R. D. and Gale N. H. (1969) A reappraisal of the decay constants and branching ratio of ^{40}K. *Earth Planet. Sci. Lett.* **6,** 289.

Davis P. K., Lewis R. S., and Reynolds J. H. (1971) Stepwise heating analyses of rare gases from pile-irradiated rocks 10044 and 10057. *Proc. Second Lunar Sci. Conf., Geochim. Cosmochim. Acta* Suppl. 2, Vol. 2, pp. 1693–1703. MIT Press.

Goplan K. and Wetherill G. W. (1969) Rubidium–strontium age of amphoterite (LL) chondrites. *J. Geophys. Res.* **74,** 4349–4358.

Hohenberg C. A. (1968) Extinct radioactivities in meteorites. Unpublished paper written for the "Nininger Meteorite Award" competition.

Lugmair G. W. and Marti K. (1971) Neutron capture effects in lunar gadolinium and the irradiation histories of some lunar rocks. *Earth Planet. Sci. Lett.* **13,** 32–42.

Merrihue C. M. and Turner G. (1966) Potassium–argon dating by activation with fast neutrons. *J. Geophys. Res.* **71,** 2852–2857.

Papanastassiou D. A. and Wasserburg G. J. (1971) Lunar chronology and evolution from Rb–Sr studies of Apollo 11 and Apollo 12 samples. *Earth Planet. Sci. Lett.* **11,** 37–62.

Podosek F. A., Huneke J. C., and Wasserburg G. J. (1972) Gas-retention and cosmic ray exposure ages of lunar rock 15555. *Science* **175,** 423.

Podosek F. A. and Lewis R. S. (1972) ^{129}I and ^{244}Pu abundances in white inclusions of the Allende meteorite. *Earth Planet. Sci. Lett.*, in press.

Reed G. W. and Jovanovic S. (1971) The halogens and other trace elements in Apollo 12 samples and the implications of halides, platinum metals, and mercury on surfaces. *Proc. Second Lunar Sci. Conf., Geochim. Cosmochim. Acta* Suppl. 2, Vol. 2, pp. 1261–1276. MIT Press.

Smith A. G. (1964) Potassium–argon decay constants and age tables. *Quart. J. Geol. Soc. London* **120s,** 129.

Stettler A., Eberhardt P., Geiss J., and Grögler N. (1972) Ar^{39}/Ar^{40} ages of Apollo 11, 12, 14, and 15 rocks (abstract). In *Lunar Science—III* (editor C. Watkins), p. 724, Lunar Science Institute Contr. No. 88.

Turner G. (1970a) Argon-40/argon-39 dating of lunar rock samples. *Science* **167,** 466–468.

Turner G. (1970b) Argon-40/argon-39 dating of lunar rock samples. *Proc. Apollo 11 Lunar Sci. Conf., Geochim. Cosmochim. Acta* Suppl. 1, Vol. 2, pp. 1665–1684. Pergamon.

Turner G. (1971) ^{40}Ar–^{39}Ar ages from the lunar maria. *Earth Planet. Sci. Lett.* **11,** 169.

York D. (1966) Least-square fitting of a straight line. *Can. J. Phys.* **44,** 1079.

Proceedings of the Third Lunar Science Conference
(Supplement 3, *Geochimica et Cosmochimica Acta*)
Vol. 2, pp. 1797–1819
The M.I.T. Press, 1972

Noble gas studies on regolith materials from Apollo 14 and 15

D. D. BOGARD and L. E. NYQUIST

NASA Manned Spacecraft Center,
Houston, Texas 77058

Abstract—Abundances and isotopic compositions of He, Ne, Ar, Kr, and Xe have been determined in a number of Apollo 14 and 15 samples, including bulk analyses on soils and breccias, a range of depths in a trench and a core, and grain size separates and stepwise temperature releases of Apollo 14 bulk fines. Several samples exhibit measured values of $^{84}Kr/^{36}Ar \simeq 3 \times 10^{-4}$ and $^{132}Xe/^{36}Ar \simeq 0.4 \times 10^{-4}$, and set new upper limits for these ratios in the solar wind. A few samples indicate a trapped Ne other than solar wind Ne with $^{20}Ne/^{22}Ne \leq 11.4$. Trapped solar wind, $^{20}Ne/^{22}Ne$ (12.65 ± 0.10), and $^{36}Ar/^{38}Ar$ (5.36 ± 0.03) obtained from grain size separates and stepwise temperature release data are identical to values found for Apollo 11 and 12; $^{4}He/^{3}He$ is variable (2000–2800). Both He and Ne exhibit a low-temperature enhancement of $^{3}He/^{4}He$ and $^{20}Ne/^{22}Ne$ which may be due to a lunar atmosphere implanted component. Trapped $^{40}Ar/^{36}Ar$ is variable among a number of samples. Low-temperature releases reveal a Kr component distinct from the cosmic ray spallation component defined by high temperature releases and grain size separates, and for which $^{82}Kr/^{86}Kr$, $^{83}Kr/^{86}Kr$, and $^{84}Kr/^{86}Kr$ are enriched over typical trapped values by up to 29%, 21%, and 3%, respectively. This low-temperature component is apparently not due to implantation of lunar atmosphere Kr, but may result from solar flare reactions on Rb. Xe isotope correlation diagrams for stepwise temperature releases and grain size separates exhibit linear correlations of slightly different slope, which apparently are not caused by mass fractionation during the stepwise heating. For both Kr and Xe, grain size separates and temperature releases above 900°C indicate different trapped components, which may be related as mixtures of trapped solar wind and other low temperature components. Spallation $^{131}Xe/^{126}Xe$ in many fines and gas-rich breccias varies by a factor of two, while $^{124}Xe/^{126}Xe$ is essentially constant at 0.53 ± 0.02. If much of the excess ^{131}Xe is due to neutron capture on Ba, the variations in spallation $^{131}Xe/^{126}Xe$ possibly indicate differences in average shielding. By this criterion, samples from core 14230 and the Apollo 14 trench samples show nearly the same average burial depth during cosmic ray exposure, the topmost samples having marginally greater $^{131}Xe/^{126}Xe$. A number of soils and breccia show differences in spallation xenon of ≥ a factor of three. indicating variable exposure times.

INTRODUCTION AND TECHNIQUES

THE PURPOSE OF THE PRESENT investigation is to determine the nature of the various noble gas components in a number of lunar regolith samples in order to define solar wind implanted abundances of these elements, and to interpret lunar surface processes and history. Thus, we have determined abundances and isotopic compositions of the five stable noble gases, He, Ne, Ar, Kr, and Xe in soils and breccia from Apollo 14 and 15, including samples from a range of depths in a trench and a core tube, and grain size separates and stepwise temperature releases of the Apollo 14 bulk soil. Noble gas determinations were performed in a 6-inch all-metal mass spectrometer of high sensitivity (Bogard *et al.*, 1971a). Analog signal output was integrally digitized, and computations were performed on programmable calculators.

Table 1. Measured noble gas abundances.

Sample	Weight (mg)	$\times 10^{-6}$ ccSTP/g				$\times 10^{-9}$ ccSTP/g					
		^{3}He	^{4}He	^{22}Ne	^{36}Ar	^{84}Kr	^{132}Xe	$^{20}Ne/^{22}Ne$	$^{22}Ne/^{21}Ne$	$^{36}Ar/^{38}Ar$	$^{40}Ar/^{36}Ar$
I. *Bulk samples*											
14148,27 (trench top)	5.31	22.7	55,040	74.6	267	170	20.1	12.52 ± 0.05	26.64 ± 0.21	5.32 ± 0.01	2.03 ± 0.02
14156,27 (trench middle)	6.66	21.6	52,000	79.0	321	113	22.5	12.54 ± 0.05	27.27 ± 0.36	5.34 ± 0.01	1.77 ± 0.02
14149,43 (trench bottom)	5.52	21.2	50,950	77.5	239	93	25.7	12.41 ± 0.04	26.42 ± 0.14	5.33 ± 0.02	3.12 ± 0.01
14003,6 (fines)	9.32	25.5	62,560	84.0	253	159	13.8	12.60 ± 0.04	28.80 ± 0.16	5.38 ± 0.02	1.68 ± 0.01
14301,48 (breccia)	28.78	2.98	9,260	11.3	3.51	0.17	0.098	12.39 ± 0.14	28.5 ± 0.7	5.54 ± 0.04	15.1 ± 0.1
14307,26,2 (breccia–dark)	19.32	26.0	70,740	108	311	59	12.9	12.24 ± 0.04	29.4 ± 1.2	5.38 ± 0.02	5.67 ± 0.02
14307,26,2 (repeat–dark)	10.76	16.3	42,020	101	83	36	8.7	12.38 ± 0.04	29.1 ± 0.9	5.38 ± 0.02	5.86 ± 0.02
14307,26 (light)	35.62	1.0	1,240	0.26	≤0.12*	0.33	0.33	2.73 ± 0.01	1.331 ± 0.002	1.45*	109*
14006,3	20.05	1.99	3,080	0.76	1.56	0.45	0.33	7.33 ± 0.08	2.74 ± 0.03	2.75	88
14068,3 (breccia)	11.3	0.23	1,450	0.63	0.68	2	0.7	12.15 ± 0.03	13.70 ± 0.16	5.15 ± 0.05	41.7 ± 0.7
14230,113 (core–4 cm)	16.65	15.3	35,110	47.4	136	66	6.85	12.57 ± 0.02	25.54 ± 0.27	5.37 ± 0.01	2.18 ± 0.01
14230,130 (core–8 cm)	17.30	11.7	29,000	39.1	57	12	1.6	12.72 ± 0.04	25.3 ± 0.2	5.45 ± 0.02	2.48 ± 0.02
14230,121 (core–12 cm)	9.85	16.4	40,730	61.1	170	72	10.2	12.69 ± 0.03	27.1 ± 0.2	5.37 ± 0.02	2.09 ± 0.02
II. *Grain size separates*											
14161,35 (2–4 mm)	33.63	0.98	213	0.57	0.32	0.61	0.13	5.39 ± 0.03	2.00 ± 0.01	2.42	64
14162,22 (1–2 mm) (G)	32.02	20.7	43,070	11.7	39.4	26	6.2	12.36 ± 0.04	19.17 ± 0.15	5.23 ± 0.03	4.50 ± 0.03
14163,97											
1000–250 μ (F)	2.02	2.07	3,030	4.43	23.3	16*	10*	11.04 ± 0.05	8.70 ± 0.09	4.73 ± 0.02	32.6 ± 0.2
250–90 μ (E)	1.33	7.02	14,200	22.7	94	45	15	12.11 ± 0.10	17.80 ± 0.11	5.15 ± 0.03	3.37 ± 0.2
90–60 μ (D)	1.13	11.2	26,300	37.6	164	100	33	12.24 ± 0.04	22.82 ± 0.10	5.24 ± 0.03	2.94 ± 0.01
60–30 μ (C)	1.97	19.5	49,200	63.3	285	130	25	12.8 ± 0.1	26.4 ± 0.1	5.32 ± 0.02	2.49 ± 0.03
30–20 μ (B)	1.98	51.4	133,000	164	519	244	60	12.64 ± 0.10	29.17 ± 0.11	5.33 ± 0.01	2.39 ± 0.10
20 μ (A)	2.54	62.6	166,500	187	533	170	41	12.64 ± 0.05	29.78 ± 0.11	5.33 ± 0.01	2.40 ± 0.05

Based on variations in machine sensitivity, abundances have an estimated uncertainty of ±5–10%, except for Kr which is ±15%. Blank corrections were usually small and have been applied. Values marked with an * possessed large blank corrections and are less accurate. Uncertainties for isotopic ratios are one sigma for multiple measurements. The $^{3}He/^{4}He$ was not measured directly, but can be obtained from the abundances with an uncertainty of about 2%. Letter codes listed for the grain size separates are for identification in Figs. 3 and 6 to 10.

Table 2. Measured noble gas isotopic composition for 14163,97 temperature release.

Temperature (°C)	$^4He/^3He$	$^{20}Ne/^{22}Ne$	$^{21}Ne/^{22}Ne$	$^{38}Ar/^{36}Ar$	$^{40}Ar/^{36}Ar$
150	1720	14.46 ± 0.18	—	—	—
225	1770	14.30 ± 0.05	0.0365 ± 0.0006	0.180 ± 0.011	25.2 ± 1.5
275	1780	14.03 ± 0.03	0.0418 ± 0.0005	0.1818 ± 0.0006	28.9 ± 0.7
325	1900	13.30 ± 0.05	0.0462 ± 0.0005	0.1811 ± 0.0026	28.7 ± 0.8
400	2080	12.88 ± 0.05	0.0450 ± 0.0002	0.1836 ± 0.0013	30.2 ± 0.4
500	2165	12.71 ± 0.04	0.0354 ± 0.0004	0.1832 ± 0.0010	20.0 ± 0.1
600	2240	12.59 ± 0.02	0.0321 ± 0.0007	0.1812 ± 0.0007	10.40 ± 0.09
700	2365	12.79 ± 0.02	0.0341 ± 0.0002	0.1802 ± 0.0004	5.57 ± 0.03
800	2325	12.58 ± 0.03	0.0342 ± 0.0002	0.1858 ± 0.0004	2.32 ± 0.05
900	2675	12.61 ± 0.03	0.0348 ± 0.0001	0.1874 ± 0.0003	1.59 ± 0.01
1000	2570	12.58 ± 0.02	0.0388 ± 0.0004	0.1896 ± 0.0004	1.70 ± 0.01
1000	3105	12.31 ± 0.07	0.0418 ± 0.0002	0.1928 ± 0.0002	2.09 ± 0.01
1200	2555	11.91 ± 0.03	0.0452 ± 0.0006	0.1927 ± 0.0006	1.99 ± 0.01
1400	1305	10.81 ± 0.04	0.0797 ± 0.0008	0.1986 ± 0.0007	1.90 ± 0.07
1600	1175	12.0 ± 1.0	0.084 ± 0.02	0.208 ± 0.004	4.3 ± 0.1

Table 3. Measured krypton isotopic composition (relative to ^{86}Kr).

Sample	78	80	82	83	84
I. *Bulk samples*					
14148,27	0.033 ± 0.003	0.164 ± 0.003	0.715 ± 0.006	0.721 ± 0.008	3.279 ± 0.021
14156,27	0.023 ± 0.003	0.152 ± 0.004	0.696 ± 0.012	0.703 ± 0.012	3.30 ± 0.05
14149,43	0.026 ± 0.003	0.151 ± 0.004	0.697 ± 0.008	0.701 ± 0.008	3.289 ± 0.032
14003,6	0.026 ± 0.003	0.148 ± 0.003	0.685 ± 0.006	0.692 ± 0.006	3.279 ± 0.021
14301,48	0.340 ± 0.032	0.182 ± 0.024	0.737 ± 0.073	0.741 ± 0.028	3.37 ± 0.09
14307,26,2 (dark)	0.030 ± 0.003	0.163 ± 0.003	0.716 ± 0.004	0.716 ± 0.004	3.331 ± 0.009
14307,26 (light)	1.18	3.22	4.99	6.34	4.44
14006,3	0.20 ± 0.02	0.572 ± 0.065	1.33 ± 0.12	1.53 ± 0.14	3.51 ± 0.09
14068,3	0.0328 ± 0.0033	0.162 ± 0.003	0.723 ± 0.005	0.720 ± 0.006	3.347 ± 0.020
14230,113,2	0.305 ± 0.0013	0.1553 ± 0.0010	0.703 ± 0.006	0.709 ± 0.006	3.311 ± 0.022
14230,130,2	0.044	0.179 ± 0.002	0.749 ± 0.009	0.757 ± 0.009	3.369 ± 0.034
14230,112,2	0.0303 ± 0.0006	0.1525 ± 0.0017	0.696 ± 0.003	0.701 ± 0.003	3.293 ± 0.009
15301,1 (fines)	0.022 ± 0.002	0.135 ± 0.002	0.671 ± 0.009	0.670 ± 0.008	3.282 ± 0.024
15021,4 (fines)	0.023 ± 0.007	0.138 ± 0.002	0.678 ± 0.008	0.678 ± 0.009	3.30 ± 0.03
15101,2 (fines)	0.022 ± 0.001	0.139 ± 0.002	0.679 ± 0.007	0.679 ± 0.007	3.29 ± 0.03
15298,3 (breccia)	0.028 ± 0.002	0.137 ± 0.002	0.675 ± 0.012	0.677 ± 0.013	3.28 ± 0.04
15558,3 (breccia)	0.027 ± 0.002	0.146 ± 0.003	0.690 ± 0.006	0.693 ± 0.007	3.304 ± 0.025
15923,2 (matrix)	0.017 ± 0.004	0.139 ± 0.007	0.692 ± 0.019	0.700 ± 0.020	3.280 ± 0.012
15923,2 (glass)	—	—	0.712 ± 0.026	0.754 ± 0.028	3.35 ± 0.06
15498 (breccia)	0.033 ± 0.003	0.155 ± 0.004	0.710 ± 0.008	0.711 ± 0.009	3.330 ± 0.017
15265 (breccia)	0.031 ± 0.003	0.152 ± 0.003	0.696 ± 0.009	0.700 ± 0.008	3.306 ± 0.029
15601 (fines)	0.026 ± 0.002	0.137 ± 0.002	0.674 ± 0.007	0.676 ± 0.008	3.284 ± 0.025
II. *Grain size separates*					
14161,35,7 (2–4 mm)	0.45 ± 0.03	0.768 ± 0.028	1.53 ± 0.03	1.71 ± 0.03	3.62 ± 0.05
14162,22 (1–2 mm)	0.042 ± 0.001	0.174 ± 0.002	0.725 ± 0.005	0.737 ± 0.004	3.291 ± 0.014
14163,97					
1000–250 μ	0.050 ± 0.013	0.217 ± 0.004	0.793 ± 0.004	0.824 ± 0.004	3.338 ± 0.006
250–90 μ	0.044 ± 0.003	0.183 ± 0.002	0.739 ± 0.007	0.760 ± 0.006	3.300 ± 0.019
90–60 μ	0.036 ± 0.004	0.168 ± 0.001	0.714 ± 0.003	0.729 ± 0.003	3.287 ± 0.012
60–30 μ	0.028 ± 0.002	0.149 ± 0.003	0.692 ± 0.012	0.697 ± 0.012	3.298 ± 0.045
30–20 μ	0.043 ± 0.011	0.181 ± 0.004	0.797 ± 0.005	0.776 ± 0.003	3.537 ± 0.008
30–20 (repeat)	0.041 ± 0.005	0.171 ± 0.004	0.729 ± 0.013	0.744 ± 0.014	3.31 ± 0.05
III. *Stepwise temperature extractions*					
14163,97					
325°C	—	—	0.849 ± 0.035	0.800 ± 0.032	3.28 ± 0.09
500°C	—	—	0.744 ± 0.027	0.712 ± 0.024	3.165 ± 0.040
700°C	0.033 ± 0.013	0.187 ± 0.017	0.716 ± 0.008	0.699 ± 0.015	3.344 ± 0.034
800°C	0.022 ± 0.003	0.134 ± 0.007	0.698 ± 0.019	0.689 ± 0.021	3.279 ± 0.064
900°C	0.020 ± 0.007	0.139 ± 0.007	0.677 ± 0.004	0.673 ± 0.004	3.300 ± 0.011
1000°C	0.023 ± 0.002	0.139 ± 0.002	0.670 ± 0.004	0.673 ± 0.004	3.268 ± 0.012
1100°C	0.029 ± 0.002	0.152 ± 0.002	0.689 ± 0.003	0.701 ± 0.002	3.252 ± 0.004
1200°C	0.032 ± 0.002	0.159 ± 0.002	0.704 ± 0.006	0.713 ± 0.006	3.257 ± 0.021
1400°C	0.042 ± 0.002	0.183 ± 0.001	0.734 ± 0.004	0.761 ± 0.004	3.279 ± 0.011
1600°C	0.08 ± 0.01	0.234 ± 0.004	0.828 ± 0.007	0.881 ± 0.004	3.300 ± 0.011

Uncertainties are one sigma for multiple measurements, except for ^{78}Kr and ^{80}Kr, which include an additional uncertainty due to hydrocarbon corrections.

Table 4. Measured xenon isotopic compositions (relative to ^{136}Xe).

Sample	124	126	128	129	130	131	132	134
I. *Bulk samples*								
14148,27	0.075 ± 0.003	0.123 ± 0.003	0.458 ± 0.009	3.66 ± 0.08	0.658 ± 0.011	3.339 ± 0.065	3.390 ± 0.045	1.233 ± 0.019
14156,27	0.0532 ± 0.0014	0.084 ± 0.004	0.385 ± 0.003	3.56 ± 0.03	0.606 ± 0.010	3.067 ± 0.033	3.326 ± 0.022	1.224 ± 0.008
14149,43	0.0491 ± 0.0020	0.0776 ± 0.0011	0.371 ± 0.006	3.53 ± 0.03	0.595 ± 0.005	3.014 ± 0.025	3.317 ± 0.022	1.228 ± 0.009
14003,6	0.044 ± 0.002	0.065 ± 0.002	0.364 ± 0.004	3.59 ± 0.04	0.596 ± 0.010	3.002 ± 0.034	3.362 ± 0 033	1 234 ± 0.019
14301,48	—	—	0.380 ± 0.023	3.27 ± 0.13	0.567 ± 0.029	2.85 ± 0.12	3.10 ± 0.12	1.19 ± 0.07
14307,26,2 (dark)	0.0327 ± 0.0010	0.0469 ± 0.0007	0.342 ± 0.005	3.75 ± 0.03	0.590 ± 0.004	2.960 ± 0.024	3.37 ± 0.02	1 236 ± 0.009
14307,26,2 (light)	1.154 ± 0.014	2.163 ± 0.033	3.59 ± 0.05	5.06 ± 0.07	2.70 ± 0.03	17.05 ± 0.20	3.782 ± 0.024	1.43 ± 0.03
14006,3	0.375 ± 0.026	0.648 ± 0.039	1.307 ± 0.059	4.37 ± 0.17	1.20 ± 0.05	6.47 ± 0.26	3.75 ± 0.14	1.29 ± 0.06
14068,3	0.0314 ± 0.0011	0.0456 ± 0.0015	0.332 ± 0.005	3.65 ± 0.04	0.575 ± 0.007	2.90 ± 0.03	3.34 ± 0.04	1.234 ± 0.013
14230,113,2	0.0595 ± 0.0027	0.0930 ± 0.0024	0 408 ± 0.004	3.65 ± 0.03	0.628 ± 0.007	3.154 ± 0.023	3.38 ± 0.02	1.238 ± 0.120
14230,130,2	0.088 ± 0.015	0.135 ± 0.013	0.478 ± 0.016	3.73 ± 0.08	0.684 ± 0.017	3.34 ± 0.08	3.42 ± 0.07	1.24 ± 0.04
14230,121,2	0.0476 ± 0.0014	0.0773 ± 0.0024	0.370 ± 0.007	3.54 ± 0.04	0.600 ± 0.009	3.01 ± 0.04	3.33 ± 0.04	1.23 ± 0.02
15301,1	0.0211 ± 0.0010	0.0241 ± 0.0013	0.290 ± 0.003	3.47 ± 0.03	0.548 ± 0.011	2.745 ± 0.025	3.30 ± 0.02	1.23 ± 0.01
15021,4	0.0278 ± 0.0004	0.0356 ± 0.0008	0.316 ± 0.005	3.57 ± 0.04	0.575 ± 0.007	2.87 ± 0.04	3.39 ± 0.04	1.243 ± 0.015
15101,2	0.0270 ± 0.0010	0.0347 ± 0.0010	0.309 ± 0.009	3.51 ± 0.03	0.567 ± 0.006	2.83 ± 0.03	3.34 ± 0.03	1.233 ± 0.012
15298,3	0.0256 ± 0.0013	0.0338 ± 0.0010	0.300 ± 0.006	3.40 ± 0.03	0.551 ± 0.009	2.75 ± 0.03	3.28 ± 0.03	1.218 ± 0.012
15558,3	0.0287 ± 0.0010	0.0393 ± 0.0016	0.314 ± 0.003	3.50 ± 0.03	0.567 ± 0.008	2.831 ± 0.017	3.300 ± 0.014	1 220 ± 0.007
15923,2 (matrix)	—	—	0.307 ± 0.015	3.51 ± 0.08	0.551 ± 0.016	2.80 ± 0.06	3.30 ± 0.07	1.19 ± 0.03
15923,2 (glass)	0.050 ± 0.018	0.076 ± 0.009	0.395 ± 0.013	3.41 ± 0.13	0.610 ± 0.012	3.09 ± 0.06	3.32 ± 0.04	1.23 ± 0.04
15498,2	0.037 ± 0 003	0.052 ± 0.003	0.348 ± 0.007	3.63 ± 0.06	0.594 ± 0.012	2.92 ± 0.14	3.35 ± 0.04	1.24 ± 0.02
15265,3	0.045 ± 0.003	0.069 ± 0.006	0.361 ± 0.009	3.48 ± 0.07	0.595 ± 0.012	3.00 ± 0.05	3.32 ± 0.05	1.225 ± 0.023
15601,3	0.024 ± 0.003	0.0325 ± 0.0023	0.301 ± 0.005	3.48 ± 0.03	0.563 ± 0.014	2.78 ± 0.02	3.32 ± 0.02	1.224 ± 0.012
II. *Grain size separates*								
14161,35,7 (2–4 mm)	0.59 ± 0.05	1.06 ± 0.11	1.93 ± 0.14	4.82 ± 0.32	1.46 ± 0.09	7.19 ± 0.47	3.80 ± 0.23	1.28 ± 0.09
14162,22 (1–2 mm)	0.0589 ± 0.0014	0.0927 ± 0.0022	0.372 ± 0.003	3.33 ± 0.02	0.575 ± 0.003	2.961 ± 0.021	3.200 ± 0.011	1.201 ± 0.007
14163,97								
1000–250 μ	0.1623 ± 0.0034	0.279 ± 0.004	0.710 ± 0.007	3.98 ± 0.03	0.826 ± 0.010	4.153 ± 0.047	3.545 ± 0.023	1.251 ± 0.010
250–90 μ	0.0956 ± 0.0044	0.164 ± 0.003	0.517 ± 0.010	3.76 ± 0.06	0.699 ± 0.012	3.52 ± 0.06	3.44 ± 0.05	1.246 ± 0.022
90–60 μ	0.0742 ± 0.0013	0.1226 ± 0.0010	0.451 ± 0.004	3.66 ± 0.03	0.651 ± 0.005	3.278 ± 0.026	3.38 ± 0.02	1.230 ± 0.010
60–30 μ	0.0482 ± 0.0004	0.0747 ± 0.0007	0.375 ± 0.003	3.57 ± 0.02	0.601 ± 0.010	3.015 ± 0.016	3.321 ± 0.015	1.230 ± 0.008
30–20 μ	0.058 ± 0.003	0.0862 ± 0.0024	0.423 ± 0.005	3.92 ± 0.02	0.651 ± 0.010	3.216 ± 0.018	3.519 ± 0.012	1.256 ± 0.019
30–20 (repeat)	0.059 ± 0.003	0.0944 ± 0.0035	0.404 ± 0.007	3.62 ± 0.04	0.617 ± 0.010	3.114 ± 0.036	3.37 ± 0.03	1.228 ± 0.015

Sample	124	126	128	129	130	131	132	134
III. *Stepwise temperature releases*								
14163,97								
325°C	—	—	0.271 ± 0.010	3.02 ± 0.08	0.473 ± 0.026	2.49 ± 0.05	3.05 ± 0.07	1.16 ± 0.04
525°C	—	—	0.346 ± 0.004	3.30 ± 0.05	0.517 ± 0.013	2.64 ± 0.06	3.12 ± 0.03	1.171 ± 0.024
700°C	0.025	0.044	0.324 ± 0.019	3.30 ± 0.19	0.53 ± 0.03	2.68 ± 0.15	3.14 ± 0.18	1.21 ± 0.07
800°C	0.025	0.034	0.313 ± 0.007	3.48 ± 0.05	0.551 ± 0.008	2.76 ± 0.04	3.28 ± 0.04	1.23 ± 0.02
900°C	0.0240 ± 0.0004	0.0297 ± 0.0007	0.307 ± 0.004	3.53 ± 0.04	0.563 ± 0.005	2.81 ± 0.03	3.33 ± 0.02	1.23 ± 0.01
1000°C	0.0269 ± 0 0003	0.0359 ± 0.0004	0.314 ± 0.002	3.52 ± 0.03	0.568 ± 0.007	2.846 ± 0.016	3.324 ± 0.011	1.230 ± 0.007
1100°C	0.0423 ± 0.0010	0.0650 ± 0.0010	0.356 ± 0.004	3.540 ± 0.023	0.593 ± 0.004	2.973 ± 0.019	3.333 ± 0.011	1.230 ± 0.005
1200°C	0.0595 ± 0.0007	0.0953 ± 0.0014	0.406 ± 0.005	3.58 ± 0.04	0.620 ± 0.007	3.120 ± 0.035	3.344 ± 0.034	1.231 ± 0.016
1400°C	0.0788 ± 0.0004	0.1290 ± 0.0014	0.454 ± 0.003	3.64 ± 0.02	0.653 ± 0.004	3.269 ± 0.015	3.367 ± 0.011	1.229 ± 0.005
1600°C	0.086 ± 0.010	0.147 ± 0.011	0.493 ± 0.012	3.73 ± 0.09	0.685 ± 0.013	3.42 ± 0.08	3.42 ± 0.08	1.25 ± 0.03

RESULTS

Measured concentrations of all noble gases and isotopic abundances of He, Ne, and Ar in Apollo 14 bulk samples and grain size separates are given in Table 1. Isotopic compositions of He, Ne, and Ar from the stepwise temperature release of fines 14163,97 (30–60 microns) are given in Table 2. Tables 3 and 4 present the isotopic compositions of Kr and of Xe, respectively, for many of these samples and a number of Apollo 15 samples. Noble gas data on additional Apollo 14 samples were given in the PET report (LSPET, 1971); He, Ne, and Ar data and Kr and Xe concentrations for the Apollo 15 samples listed in Tables 3 and 4 were presented in the Apollo 15 PET report (LSPET, 1972). In the following figures and discussion use is made of these previously published data as well as those contained in Tables 1–4. Throughout much of the discussion we shall be especially interested in a comparison of the grain-size separates and stepwise heating data of 14163. In several important respects, the grain size separates and stepwise heating experimental methods give results that supplement each other, an informative approach which has been very little used.

SOLAR WIND DERIVED NOBLE GAS CONCENTRATIONS AND ELEMENTAL RATIOS

Most of the Apollo 14 and 15 soils analyzed exhibit elemental noble gas ratios which agree to within a factor of two, and show typical values of $^{4}He/^{36}Ar = 250$, $^{22}Ne/^{36}Ar = 0.30$, and $^{132}Xe/^{36}Ar = 0.5 \times 10^{-4}$. Previous work has shown the relative abundances of the lighter elements, He, Ne, and possibly Ar in bulk samples, to be mass fractionated compared to gases observed in ilmenite and the assumed solar wind abundances. However, relative abundances of the heavier noble gases are generally the same in silicate and ilmenite fractions, and upper limits to solar wind ratios have been given as $^{84}Kr/^{36}Ar \leq 4.3 \times 10^{-4}$ and $^{132}Xe/^{36}Ar \leq 0.62 \times 10^{-4}$ (Eberhardt *et al.*, 1970).

Figure 1 presents relative abundances for a number of the Apollo 14 and 15 sample analyses reported here and in LSPET (1972). Also given are the theoretical solar abundances of Aller (1961) and Cameron (1968), and the limits of the lowest measured $^{84}Kr/^{36}Ar$ and $^{132}Xe/^{36}Ar$ values in lunar soils by Eberhardt *et al.* (1970). Essentially all Ar, Kr, and Xe measurements by various laboratories on Apollo 11 and 12 materials fall above and to the right of this lower limit. Mass fractionation processes affecting the noble gases in these samples would tend to move the plotted points to the upper right. This is exemplified by the connected small points that represent the total gas content (T) and the gas remaining in fines 10084 during the early stages of a stepwise temperature release conducted on this sample (Pepin *et al.*, 1970). Several samples analyzed by us plot below the Bern limit, and establish new upper limits to the solar $^{84}Kr/^{36}Ar$ and $^{132}Xe/^{36}Ar$ ratios a factor of two below those quoted above. These limits are, however, still greater than the theoretical values by factors of two ($^{84}Kr/^{36}Ar$) and four ($^{132}Xe/^{36}Ar$). Likewise, measured $^{132}Xe/^{84}Kr$ ratios are variable in the range 0.1–0.5, and are all greater than the theoretical solar values by at least a factor of two.

Large relative fractionations in Ar, Kr, and Xe exhibited by these samples is

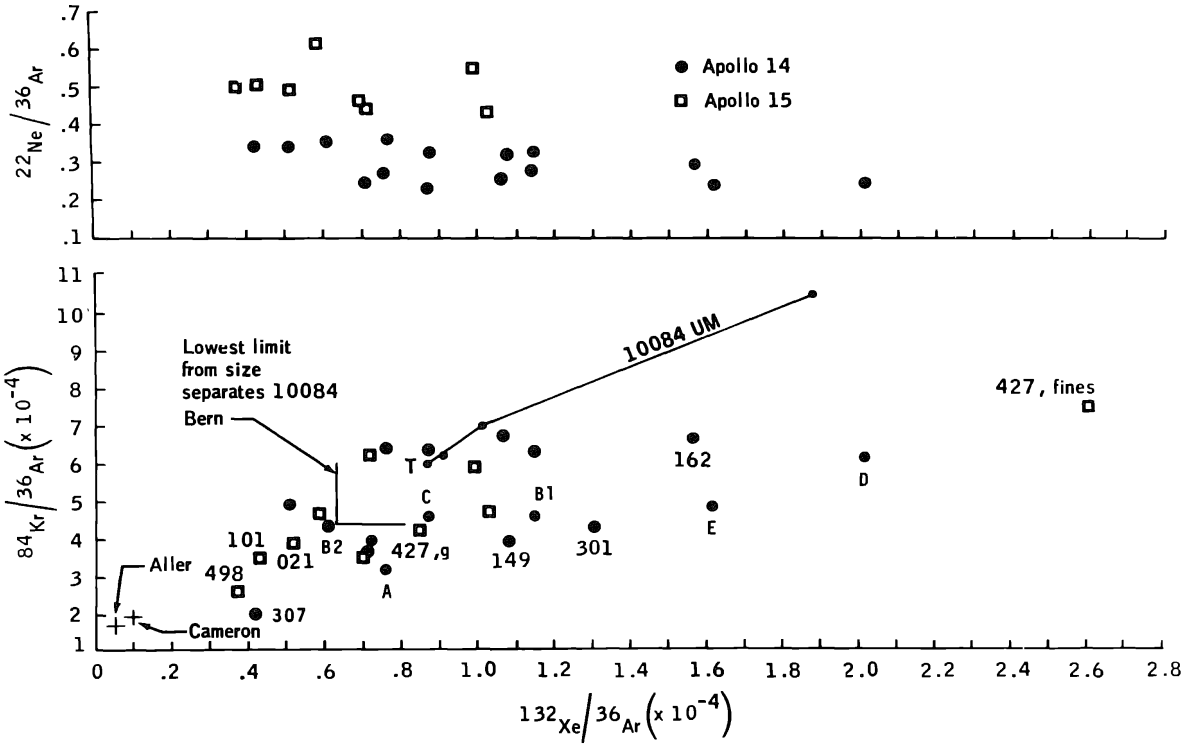

Fig. 1. Elemental abundance ratios for several Apollo 14 and 15 soils and gas rich breccia. Letters denote various grain size fractions of Table 1.

inconsistent with the much smaller variations in $^{22}Ne/^{36}Ar$ shown in the upper portion of Fig. 1. Note that most samples from a given landing site show $^{22}Ne/^{36}Ar$ ratios within a factor of two, with an obvious difference between Apollo 14 and 15, while $^{132}Xe/^{36}Ar$ varies by nearly a factor of ten. (One depth of core 14230 and fines 15427 gave much higher $^{22}Ne/^{36}Ar$ values of 0.68 and 2.45, respectively, and are not plotted.) Large fractionation for the heavier gases are also inconsistent with ilmenite results. Therefore, it appears that the relative noble gas abundances exhibited by many samples in Fig. 1 are inconsistent with simple, equilibrium fractionation processes. These samples showing the largest apparent fractionation in $^{132}Xe/^{36}Ar$ may represent mixtures of two trapped noble gas components, one representing severely fractionated solar gases for which Ne and Ar have been largely lost and the $^{132}Xe/^{84}Kr$ ratio increased to ≥ 0.5. The second component represents much less fractionated trapped solar gas for which Ne and Ar are in equilibrium relative to one another and dominate the total concentrations in the sample. These two components may occur in separate soil particles, or alternatively may be produced in the same particles by severe outgassing followed by later gas loading.

Figure 2 presents the ^{4}He, ^{22}Ne, ^{36}Ar, and ^{132}Xe abundances measured in size separates of soil 14163-14161, plotted against grain size (as separated by dry sieving). A straight line relationship of slope $-n$ results if $C \propto d^{-n}$ where $C \equiv$ gas concentration; $d \equiv$ grain diameter (Eberhardt *et al.*, 1970). Generally, Figure 2 shows well-defined linear relationships. The lower gas abundances at the smallest grain sizes have been noted on previous relationships of this type (Hintenberger *et al.*, 1971) and may

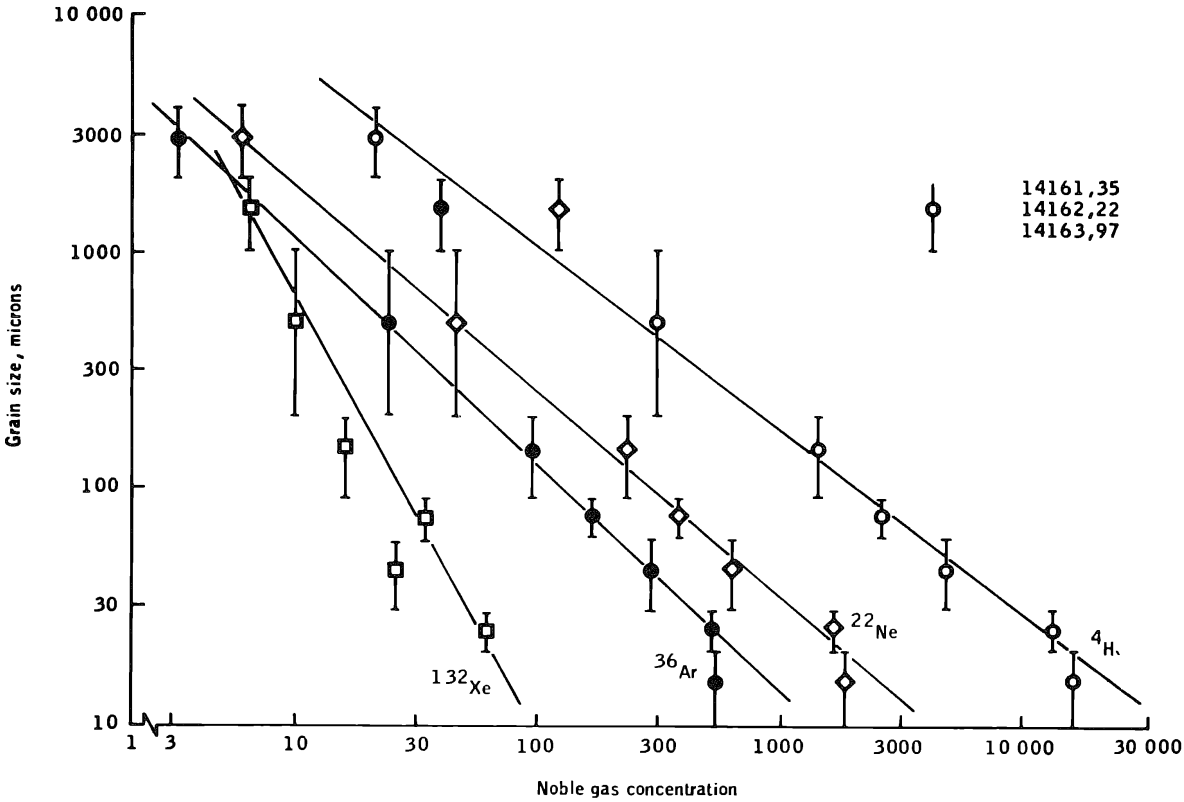

Fig. 2. Grain size effect on noble gas abundances for soil 14161 (2–4 mm), 14162 (1–2 mm), and 14163 (<1 mm). Linear relationships indicate log gas concentration is proportional to log grain diameter. Grain sizes plotted are the median of sieve sizes.

be due to gas loss or different proportions of breccia particles. The 1–2 mm fraction possesses much higher He, Ne, and Ar contents than the simple grain size relationship allows, and is probably due to the presence of breccia particles with trapped interior gases. This size fraction also shows considerable relative enhancement of the lighter gases over the heavier (e.g., $^{4}He/^{22}Ne$, $^{22}Ne/^{38}Ar$) compared to the other size separates; however, these elemental ratios are still below those measured in ilmenite (Eberhardt *et al.*, 1970). While previous work has given nearly constant slopes for all the noble gases of about -0.6 for bulk samples and about -1 for ilmenite separates (Eberhardt *et al.*, 1970; Kirsten *et al.*, 1970; Hintenberger *et al.*, 1971; Kirsten *et al.*, 1971), the slopes in Figure 2 are variable and are: $^{4}He = -1.27$, $^{22}Ne = -1.13$, $^{36}Ar = -1.02$, and $^{132}Xe = -0.6$. A slope greater than -1 implies a higher gas concentration per unit surface area for the smaller grain sizes and may arise from longer irradiation times for smaller particles; a slope less than -1 probably indicates diffusion losses (Eberhardt *et al.*, 1965). If this explanation applies, the Xe grain size correlation is more suggestive of diffusion losses than the correlations for the lighter gases, implying a multistage irradiation of the type discussed in connection with Figure 1. We note that the grain size separates show a variation of a factor $2\frac{1}{2}$ in $^{132}Xe/^{36}Ar$ and trend between the theoretical values and the 15427 point in Fig. 1. Alternatively, the pattern shown by Fig. 2 may arise from differences in the grain surface characteristics of the sized fractions resulting in a grain size dependency of

the relative saturation concentrations for the various gases. In any case, we emphasize that elemental ratios can be grain size dependent.

Isotopic Compositions of He, Ne, and Ar in the Bulk Samples, Grain Size Separates, and Stepwise Temperature Releases

Helium

For most of these Apollo 14 and 15 fines and breccias which contain appreciable amounts of solar wind He, the measured $^4He/^3He$ ratio falls in the range 2000–2800 (Table 1; LSPET, 1971; LSPET, 1972). Many of the variations in $^4He/^3He$ among these samples can undoubtedly be explained by differences in radiogenic ^4He (about 10% of the ^4He in Apollo 14 fines and breccia is radiogenic, less in Apollo 15), and by differences in spallogenic ^3He (about 10% of the ^3He is probably spallogenic). However, as $^4He/^3He$ has been found to be quite variable in the solar wind (Geiss *et al.*, 1970; Bühler *et al.*, 1972) the possibility exists that this cause is also a major factor in the $^4He/^3He$ variations measured in these bulk samples. A plot (not shown) of $^3He/^4He$ vs. the inverse of the measured ^4He concentration for grain size separates of 14163 gives essentially a straight line for the five finer grain size fractions. From the ordinate intercept and the slope we obtain for 14163, $(^4He/^3He)$ trapped $= 2750 \pm 75$ and (^3He) spallation $= 1.7 \times 10^{-6}$ cc/g. However, as spallation Xe is apparently grain size dependent in these separates (discussed later), spallation ^3He may be also, and thus the applicability of this technique is questionable.

Neon

The isotopic composition of Ne for most bulk analyses is consistent with a two-component mixture of solar wind Ne and spallation Ne with a composition similar to that commonly found in meteorites. For the grain size separates of 14163, an ordinate-intercept plot of $^{22}Ne/^{21}Ne$ vs. the inverse of the ^{21}Ne concentration showed apparent scatter, due either to variations in abundances of the major target elements, Mg and Si, or to grain size differences in exposure age. However, the four finest grain size fractions define a straight line which gives $(^{22}Ne/^{21}Ne)$ trapped $= 31.8 \pm 0.5$ and (^{21}Ne) spallation $= 5 \times 10^{-7}$ cc/g. This trapped $^{22}Ne/^{21}Ne$ is essentially identical with that obtained for other lunar fines (Eberhardt *et al.*, 1970; Kirsten *et al.*, 1970; Pepin *et al.*, 1970; Hintenberger *et al.*, 1971).

Several bulk analyses as well as the stepwise temperature release of 14163 reveal Ne components other than the simple trapped solar plus spallation mixture. Figure 3 is a neon isotope correlation diagram for these samples and omits other analyses which exhibit only two neon components and thus fall along the solar plus spallation mixing line. The 150–400°C temperature releases of 14163 show an enhancement in the $^{20}Ne/^{22}Ne$ and a structure in $^{21}Ne/^{22}Ne$ which has been seen in temperature releases on previous lunar samples (Pepin *et al.*, 1970; Hohenberg *et al.*, 1970; Kaiser, 1972). We interpret this as a lightly bound neon component arising from the lunar atmosphere and will discuss the phenomenon later in this paper. The 500–1000°C temperature releases and the finest grain size fractions cluster in a small region of Fig. 3,

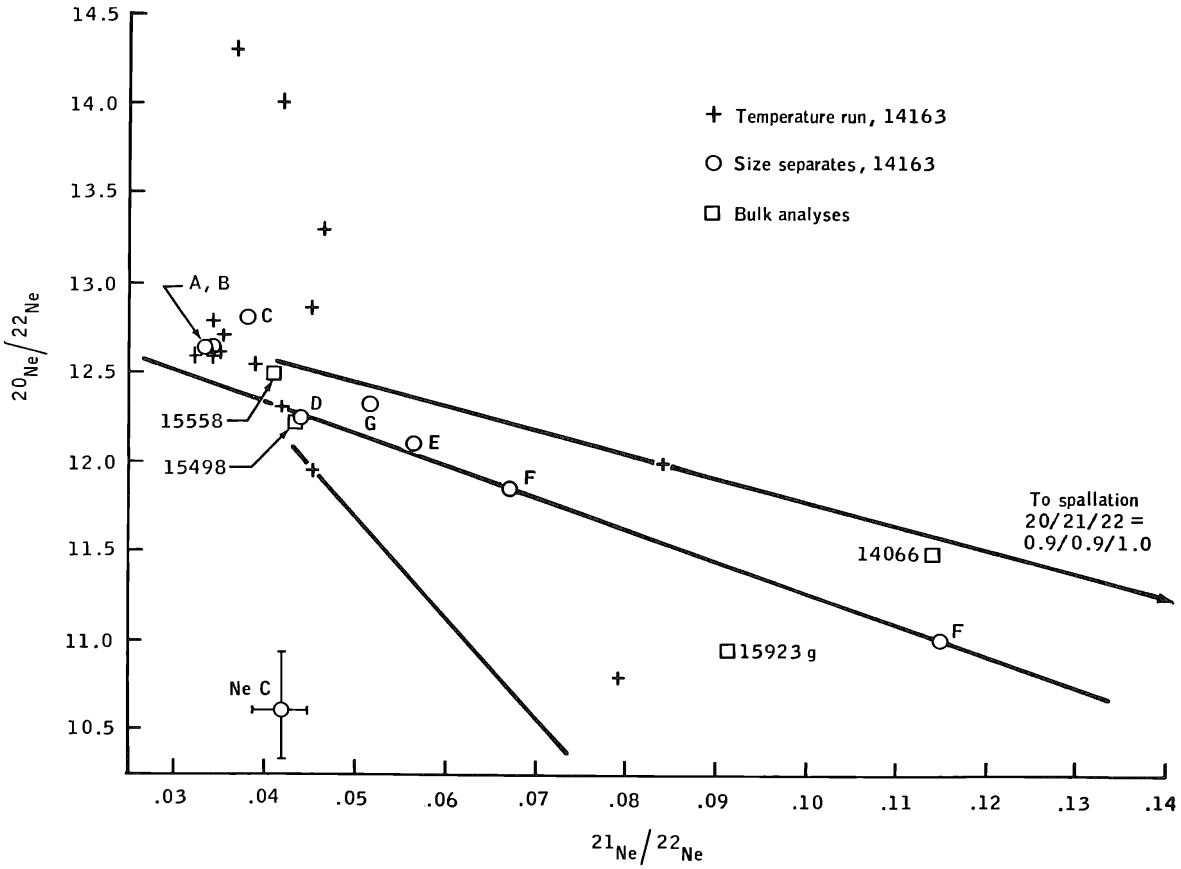

Fig. 3. Neon isotope correlation plot for grain size separates and stepwise temperature analyses of 14163,97 and bulk analyses of a few other fines and breccia. Letters denote various grain size fractions of Table 1.

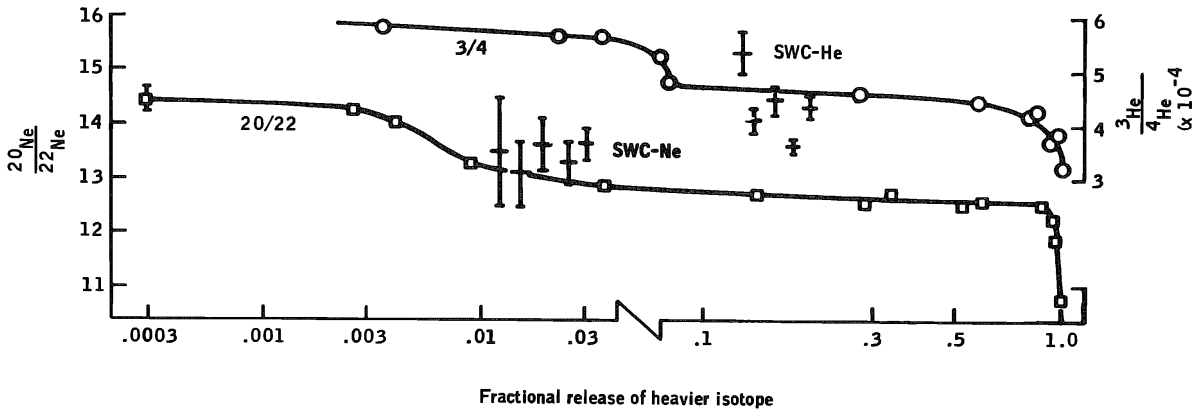

Fig. 4. Measured isotopic ratios of $^{3}He/^{4}He$ and $^{20}Ne/^{22}Ne$ as a function of fractional release of the heavier isotope for stepwise heating of fines 14163. Measured $^{3}He/^{4}He$ and $^{20}Ne/^{22}Ne$ ratios obtained from the Solar Wind Composition Experiment (SWC) from (plotted from left to right) Apollo 11, Apollo 12, Apollo 14, Surveyor, and Apollo 15 are shown (Eberhardt *et al.*, 1972; Bühler *et al.*, 1971).

and substantiate trapped solar $^{20}Ne/^{22}Ne = 12.65 \pm 0.10$ (also see Fig. 4). Bulk analyses of Apollo 14 and 15 samples not plotted on Fig. 3 show trapped Ne consistent with this $^{20}Ne/^{22}Ne$ ratio. Coarser grain size separates, the 1100–1400°C temperature releases, and bulk analyses on 15498 and the glass phase of 15923 all reveal the presence of either a trapped neon component with lower $^{20}Ne/^{22}Ne$ or a spallation neon with lower $^{21}Ne/^{22}Ne$. The line arbitrarily drawn through the grain size separates on Fig. 3 also passes very near the measured Ne isotopic compositions in two coarse-grained soils and a breccia from Apollo 12 (Nyquist and Pepin, unpublished data) and an amber glass soil fragment (Yaniv *et al.*, 1971). Neon from three high-temperature releases of Luna 16 soil (Kaiser, 1972a) would be essentially consistent with a line drawn through the trapped solar component and 15923. Thus, a variety of samples from at least four lunar sites display the existence of an additional neon component, which may also be present in minor amounts in other samples. The 1200°C and 1400°C neon data of 14163 establish an upper limit for any possible second spallation component as $^{21}Ne/^{22}Ne \leq 0.5$ (assuming spallation $^{20}Ne/^{22}Ne = 1$). However, there is no direct evidence for such a spallation Ne component in either meteorites or lunar samples. The second alternative, a trapped component with $^{20}Ne/^{22}Ne \leq 11.4$ (the limit set by our 1400°C point) is consistent with trapped Ne in several gas-rich meteorites. Black (1972) presents evidence for the existence in gas rich meteorites and lunar fines of Ne with $^{20}Ne/^{22}Ne = 10.6 \pm 0.3$ (Ne C in Figure 3), and infers this to be directly implanted solar flare Ne.

Argon

An ordinate-intercept plot of $^{36}Ar/^{38}Ar$ vs. the inverse of the ^{38}Ar content for size separates of 14163 yields a trapped $^{36}Ar/^{38}Ar$ value of 5.36 ± 0.03, in agreement with previous determinations of this ratio (Eberhardt *et al.*, 1970; Kirsten *et al.*, 1970; Hintenberger *et al.*, 1971). Measured values of $^{40}Ar/^{36}Ar$ in various Apollo 14 and 15 fines and gas-rich breccia commonly range 0.7–3 (Table 1; LSPET, 1971; LSPET, 1972). Neither in situ decay of ^{40}K nor solar wind ^{40}Ar can account for $^{40}Ar/^{36}Ar$ ratios this large, and therefore much of the ^{40}Ar present in apparently orphan argon (Heymann and Yaniv, 1970; Manka and Michel, 1970; Manka and Michel, 1971; Baur *et al.*, 1972). Apollo 14 fines show larger $^{40}Ar/^{36}Ar$ ratios than Apollo 11 or 12 fines, but similar to those of Apollo 11 breccias. An $^{40}Ar/^{36}Ar$ ordinate-intercept plot (not shown) for the five finest grain size separates of 14163 form an essentially linear correlation whose ordinate intercept defines the trapped (surface correlated) $^{40}Ar/^{36}Ar = 2.16 \pm 0.08$ and whose slope defines the radiogenic (volume-correlated) ^{40}Ar (Eberhardt *et al.*, 1970; Heymann and Yaniv, 1970). Three different depths in core 14230 form a different linear relation with an intercept of $^{40}Ar/^{36}Ar = 1.9$ and a slope corresponding to the very low radiogenic ^{40}Ar value of 0.32×10^{-4}. The three trench samples 14149, 14148, and 14156 form a linear array which does not have a positive $^{40}Ar/^{36}Ar$ intercept, as is also the case for the fines samples 15301, 15101, and 15021. As measured K abundances are nearly identical for the trench samples (LSPET, 1971) and similar for the three Apollo 15 soils (LSPET, 1972), *differences in trapped* $^{40}Ar/^{36}Ar$ must produce this effect. Correcting for

radiogenic ^{40}Ar that would accumulate in these trench samples for 3.9×10^9 yr yields trapped $^{40}Ar/^{36}Ar$ ratios of about 1.2 for 14148 and 14156 and 2.2 for 14149. Likewise, correcting 15021, 15101, and 15301 for radiogenic ^{40}Ar that would accumulate in 3.5×10^9 yr yields trapped $^{40}Ar/^{36}Ar$ ratios varying from 0.4 to 1.5. Thus, for both Apollo 14 and 15 samples there exist large variations in trapped $^{40}Ar/^{36}Ar$, even for samples collected in close proximity as were the trench fines. The explanation for these $^{40}Ar/^{36}Ar$ variations apparently goes beyond lunar latitude effects on fluxes of lunar atmosphere ^{40}Ar, and probably includes local shielding factors, chemical and mineralogical effects on trapping efficiencies, and possibly surface exposure histories.

The five grain size fractions of 14163 yield a radiogenic ^{40}Ar content of 1.16×10^{-4} cc/g, which with the measured K content of 0.48% (LSPET, 1971) gives the low K–Ar age of 2.7×10^9 yr. This age is essentially identical to the K–Ar age derived in the same manner for soil 14259 (Pepin *et al.*, 1972; Kirsten *et al.*, 1972) and is somewhat higher than the 2.0×10^9 yr event inferred from Pb–U data on these soils (Tatsumoto *et al.*, 1972).

Stepwise temperature release of 14163. Figure 4 shows $^3He/^4He$ and $^{20}Ne/^{22}Ne$ as a function of the fractional gas release during stepwise heating of the 30-60 micron fraction of fines 14163. Real variations also exist for $^{36}Ar/^{38}Ar$, $^{40}Ar/^{36}Ar$, and $^{83}Kr/^{86}Kr$ (Tables 2 and 3). All of these ratios show sizeable changes above 80% gas release which is largely due to spallation-produced isotopes. The $^{40}Ar/^{36}Ar$ ratio changes during gas release from a high of 30 to less than 2 above 70% argon release, presumably as a result of differential release of lunar atmosphere ^{40}Ar and solar wind implanted ^{36}Ar. Several ratios also show an enhancement of the lighter isotope over the heavier at very low fractional release. The maximum low-temperature enrichment of the lighter isotope compared to the ratios of 50% gas release are: $^3He/^4He$, 28%; $^{20}Ne/^{22}Ne$, 14%; $^{36}Ar/^{38}Ar$, 4%; $^{83}Kr/^{86}Kr$, 18% (also see Figs. 3 and 5). Similar low-temperature enrichments of $^3He/^4He$ and $^{20}Ne/^{22}Ne$ have been observed previously. In addition, stepwise heating and bulk analysis data from several laboratories show a correlation between high $^{20}Ne/^{22}Ne$ and high $^{36}Ar/^{38}Ar$ (this work; Pepin *et al.*, 1970; Hintenberger *et al.*, 1971; Yaniv *et al.*, 1971). These isotope enrichments have been variously attributed to mass fractionation during the heating experiment, a mass fractionation during solar wind implantation or subsequent gas loss, and a low-energy, directly implanted lunar atmosphere component (Hohenberg *et al.*, 1970; Pepin *et al.*, 1970; Black, 1972; Kaiser, 1972).

Simple models of laboratory-induced fractionation cannot explain the He and Ne release patterns of Fig. 4. For a gas initially uniformly distributed throughout a volume V of surface area S, the fractional gas release F as a function of time t is given by

$$F = (2/\pi)(S/V)\sqrt{Dt}, \qquad (F \leq 0.25)$$

where D is the diffusion coefficient (Lagerwall and Zimen, 1964). This equation approximates the solutions of Fick's law for small gas release. Although the exact solutions of Fick's law depend on the geometry of the reservoir, they are in general smooth functions. Thus it is difficult to see how the "break-over" at 7% of the ^4He

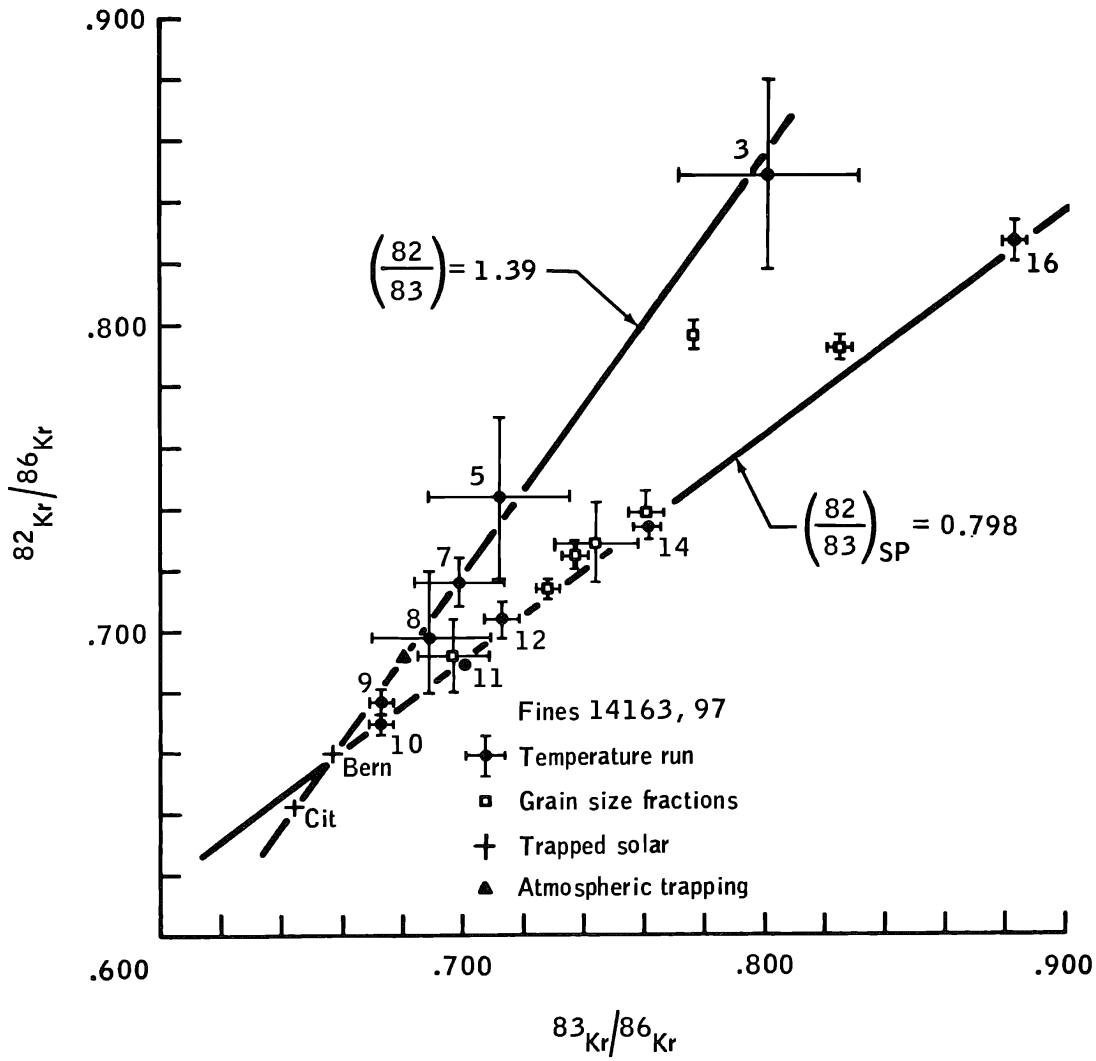

Fig. 5. $^{82}Kr/^{86}Kr$–$^{83}Kr/^{86}Kr$ isotope correlation plot for grain size separates and stepwise temperature release of 14163. Trapped solar compositions shown are from Eberhardt *et al.*, (1970) and Podosek *et al.* (1971). Letters denote various grain size fractions of Table 1. In addition to trapped solar Kr, a high temperature spallation component ($^{82}Kr/^{83}Kr$ = 0.80) and a distinct low temperature component ($^{82}Kr/^{83}Kr$ = 1.39) are apparent.

release and 0.6% of ^{22}Ne can occur. Assumption of gas release from multiple reservoirs would not materially affect this conclusion. One would expect the fractionation to persist at least until 25% of the "larger" reservoirs had been depleted. A possible mechanism might be fractionation during early gas release from radiation-damaged areas (P. Signer, pers. comm.); the break-over would then correspond to annealing at 300–400°C, a temperature at which gas release rates from various lunar mineral separates decrease (Baur *et al.*, 1972). It is nevertheless difficult to account for the magnitude of the sudden decrease in fractionation. The strongest reasonable mass dependence of the diffusion mechanism is $D \propto m^{-\frac{1}{2}}$, which produces fractionation proportional to $(m_2/m_1)^{1/4}$. Larger fractionations could be attributed to variations in

the effective volume of diffusion for the two isotopes (Hohenberg *et al.*, 1970). While changes in the mass dependence of D during annealing seem possible, changes in the relative concentration profiles of the isotopes do not. Thus we prefer the release of a low-energy trapped atmosphere component as the simplest explanation for the He and Ne release patterns of Fig. 4. As will be discussed later however, the low-temperature Kr component may have another origin.

Krypton

Isotope correlation plots of krypton measured in grain size separates and stepwise temperature extractions of 14163 are presented in Figs. 5 and 6. A two-component mixture of solar wind Kr and spallation-produced Kr will define a straight line, and deviations from this line will indicate other Kr components. Figure 5 clearly indicates that data from grain size separates and extraction temperatures above 900°C define a single spallation Kr with $^{82}Kr/^{83}Kr = 0.80$ (assuming ^{86}Kr spallation = 0), and the 300–900°C data define a distinct component with $^{82}Kr/^{83}Kr = 1.39$. Although less pronounced, there also appear to be a high-temperature $^{84}Kr/^{83}Kr$ component and a low-temperature $^{84}Kr/^{83}Kr$ component (Fig. 6).* A correlation plot of $^{80}Kr/^{86}Kr$ vs. $^{83}Kr/^{86}Kr$ (not shown) exhibits only one spallation $^{80}Kr/^{83}Kr$ component for both grain sizes and temperature releases and with a value of 0.49. Kr correlation plots for a number of bulk analyses of Apollo 14 and 15 fines and gas-rich breccia (Tables 3 and 4) tend to fall along two component straight lines with spallation $^{80}Kr/^{83}Kr = 0.51$ and $^{82}Kr/^{83}Kr = 0.79$. These ratios are identified as the galactic cosmic ray spallation Kr component in these samples and are similar to values found for Apollo 11 and 12 fines (Pepin *et al.*, 1970; Nyquist and Pepin, 1971; Podosek *et al.*, 1971). The similarity of the isotopic composition of this component in a number of samples indicates that no major shielding differences existed for many lunar soils and breccia.

Low-temperature Kr data of fines 10084 and 12028 (Pepin *et al.*, 1970; Nyquist and Pepin, 1971) also showed a third component for ^{82}Kr, ^{83}Kr, and ^{84}Kr, but not ^{80}Kr, with $^{82}Kr/^{83}Kr = 1.3$ and $^{84}Kr/^{83}Kr = 3.4$ (Fig. 6). The data presented here on 14163 have a factor of three greater measured enrichment of ^{82}Kr and ^{83}Kr than these previous measurements, and substantiate the occurrence of a lightly bound Kr component distinct from the typical cosmic ray spallation Kr. Podosek *et al.* (1971) have argued that the low-temperature Kr observed by the Minnesota laboratory is probably not due to neutron capture on bromine or to solar flare reactions, mainly because of the absence of any low-temperature ^{80}Kr. A possible origin not considered by these workers is a lightly bound Kr component arising from low-energy implantation of lunar atmosphere Kr (Manka and Michel, 1971). The triangular point in Figs.

* The first analyses of the 20–30 μ fraction (B1) also shows the presence of this low-temperature component, as well as anomalous Xe isotopic ratios shown later. A second analysis of this grain size fraction (B2) performed much later possessed lower Kr and Xe contents by a factor of two and showed no evidence of anomalous Kr or Xe compared to other grain size fractions. As we have no reason to suspect the B1 analysis, we have included it in the figures.

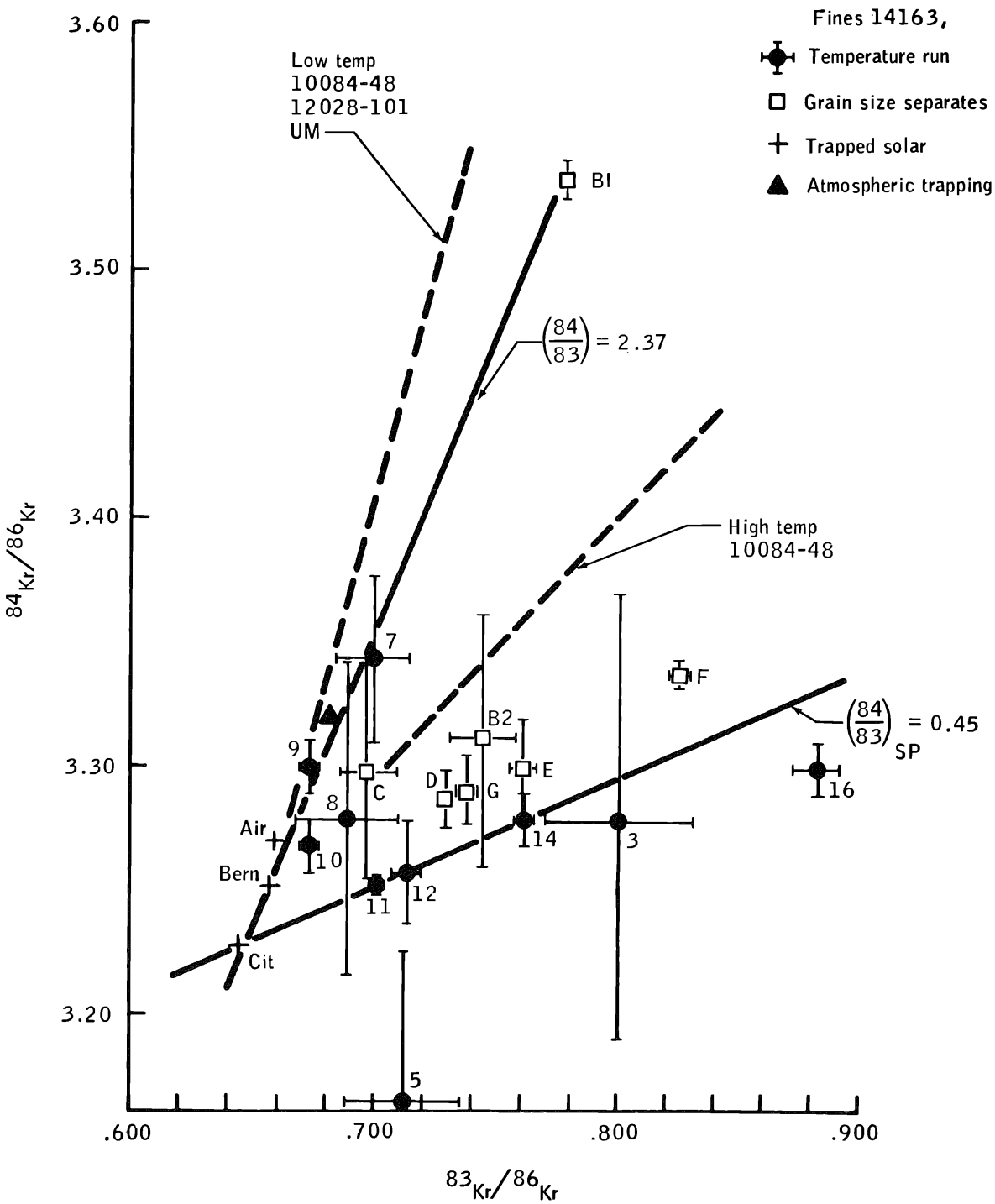

Fig. 6. $^{84}Kr/^{86}Kr$–$^{83}Kr/^{86}Kr$ isotope correlation plot for grain size separates and stepwise temperature release of 14163. Dotted lines are extrapolations of trends found by Pepin *et al.* (1970) and Nyquist and Pepin (1971).

5 and 6 represents the predicted simple mass-fractionated composition of this lunar atmosphere Kr, and in both figures falls on the lines defined by the low-temperature data. Lunar atmosphere ^{80}Kr would not be apparent in the correlation plot mentioned earlier because mass fractionated lunar atmosphere ^{80}Kr/^{83}Kr falls so close to the trapped solar plus spallation mixing line that it is not distinguishable from it. However, the Kr data for 14163 (Fig. 5) shows much greater ^{82}Kr/^{86}Kr and ^{83}Kr/^{86}Kr low temperature enrichments than predicted by the Manka and Michel model, while the ^{82}Kr/^{83}Kr is the same. Thus the lunar atmosphere does not seem a probable source for this low-temperature Kr, as not even a multistage mass fractionation model would fractionate ^{82}Kr/^{86}Kr and ^{83}Kr/^{86}Kr to such a large extent compared to the ^{82}Kr/^{83}Kr and ^{80}Kr/^{83}Kr.

We believe the low-temperature Kr data could result from variations in the spallation spectra among different target elements. Spallation Kr ought to be produced in relatively large amounts from Rb by lower energy nuclear reactions. Only three common reactions are possible: (p, α) reactions on ^{85}Rb and ^{87}Rb to yield ^{82}Kr and ^{84}Kr and (p, pn) reactions on ^{85}Rb to yield ^{84}Kr; reactions on Rb leading to ^{80}Kr, ^{83}Kr, and ^{86}Kr are much less probable. After allowing for ^{84}Kr and ^{82}Kr produced by spallation reactions on Sr + Y + Zr, the remaining excess Kr in the low temperature fractions possesses a ratio ^{84}Kr/^{82}Kr = 3. If (p, α) reactions leading to ^{82}Kr and ^{84}Kr possess roughly equal cross sections, then the (p, pn) reaction on ^{85}Rb would have to be roughly three times as probable as the (p, α) reaction on ^{87}Rb. This cross-section ratio is quite reasonable in view of the uncertainty of the proton energies involved. To produce spallation ^{83}Kr at low extraction temperatures, the ^{82}Kr and ^{84}Kr arising from Rb would have to be accompanied by spallation Kr from Sr. Thus, the low-temperature Kr may arise from the high Rb and K phases known to occur in Apollo 14 samples and where Rb/Sr can be increased by an order of magnitude (Papanastassiou and Wasserburg, 1971). Argon-39 dating has indicated that these phases lose argon at lower temperatures than other phases (Turner *et al.*, 1971). The excess ^{82}Kr and ^{84}Kr may also be produced from Rb on grain surfaces by solar flares of insufficient energy to produce normal amounts of spallation Kr from Sr. In this case the low-temperature Kr component would be characteristic of lunar soils but not of crystalline rocks.

Figures 5 and 6 also allow some distinction to be made as to the isotopic composition of trapped solar Kr in 14163 and the solar compositions reported by Eberhardt *et al.* (1970) and Podosek *et al.* (1971). The ^{82}Kr/^{83}Kr mixing line for high temperature and grain size data and the ^{84}Kr/^{83}Kr mixing line for grain size data tend to extrapolate through the Bern composition, while the ^{84}Kr/^{83}Kr high temperature data extrapolate through the CIT composition. The low-temperature data extrapolates through both the Bern and CIT compositions. This suggests that Kr from bulk analyses may not extrapolate to the same trapped composition as temperature data, and that the Bern trapped component may be related to the CIT trapped Kr by the addition of a small amount of the low-temperature, lightly bound Kr. Isotope correlation plots for Xe discussed next also show a difference in trapped composition between grain size data and temperature data.

Xenon

Xenon isotope correlation plots for the 14163 grain size separates and stepwise temperature release are presented in Figs. 7 and 8. As no ^{124}Xe and ^{126}Xe data was obtained below 700°C, low-temperature ratios are not plotted for other isotopes. For temperatures above 700°C the data are consistent with a mixture of solar Xe plus spallation Xe. Correlation plots relative to $^{130}Xe/^{136}Xe$ (not shown) reveal a low-temperature third component, which is displaced in the direction of atmospheric Xe (also note the 700°C point of Figs. 7 and 8), and it may represent small amounts of adsorbed atmospheric Xe on our samples. As the presence of a fission Xe component would produce displacements in the same general direction on the Xe correlation diagrams, this may also be a source of the low-temperature Xe. Fission Xe is undoubtedly the explanation for similar displacements for Xe on bulk sample analyses (Table 4) which show 14301, 14307, and 14162 (G on Figs. 7, 8) to contain appreciable amounts of fission Xe (LSPET, 1971). As Crozaz *et al.* (1972) have recently attributed this fission Xe in 14301 partially to spontaneous fission of the extinct isotope ^{244}Pu, the possibility exists of fission Xe of this type existing in these other samples and in the low-temperature release of 14163.

From Figs. 7 and 8 it can be seen that the 900–1400°C Xe data (containing 94% of the total Xe released) define a solar plus spallation mixing line which is slightly different in slope from the solar plus spallation mixing line defined by the grain size separates. (Analyses for B1 and G were not considered for reasons already given.) The fact that each set of data define a straight line indicates a single spallation component for the grain size separates lying on the line and for the temperature data. If we assume the CIT-trapped component, the derived spallation Xe for the 1400°C point and grain size fraction F are given in Table 5. For those isotopes showing large spallation enrichments the two spallation spectra are essentially the same. Differences in relative spallation yields for ^{129}Xe, ^{131}Xe, and ^{132}Xe are probably due to our choice of a single trapped solar Xe for these two samples. For the $^{131}Xe/^{136}Xe$, $^{130}Xe/^{136}Xe$, and $^{128}Xe/^{136}Xe$ correlation plots the 900–1400°C data extrapolate through the CIT-trapped solar composition, and the grain size separates extrapolate through the Bern trapped solar composition. This difference in slopes cannot be due to mass fractionation during the stepwise temperature release, for the high-temperature data (1400°C) show enrichment of the lighter Xe isotopes over the heavier, while the 900 and 1000°C data show depletion of the lighter Xe isotopes over the heavier. This is the opposite of the effect to be expected from mass fractionation during stepwise heating. Thus it appears that the grain size separates contain a sufficient

Table 5. Spallation Xe spectra for 14163.

	124	126	128	129	130	131	132
1400°C	0.550	1.00	1.53	1.30	1.01	4.69	0.41
±	0.008		0.03	0.14	0.04	0.14	0.10
250–1000 μ	0.553		1.63	1.87	1.05	5.37	0.85
±	0.015	1.00	0.03	0.12	0.04	0.20	0.10

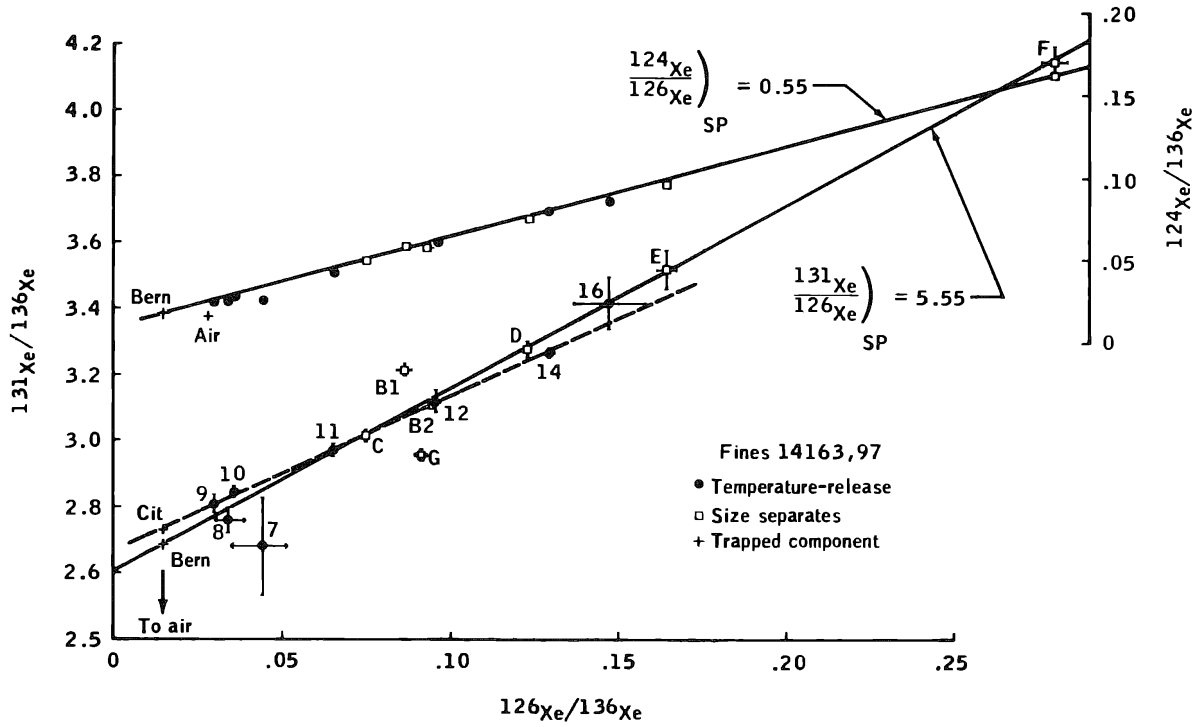

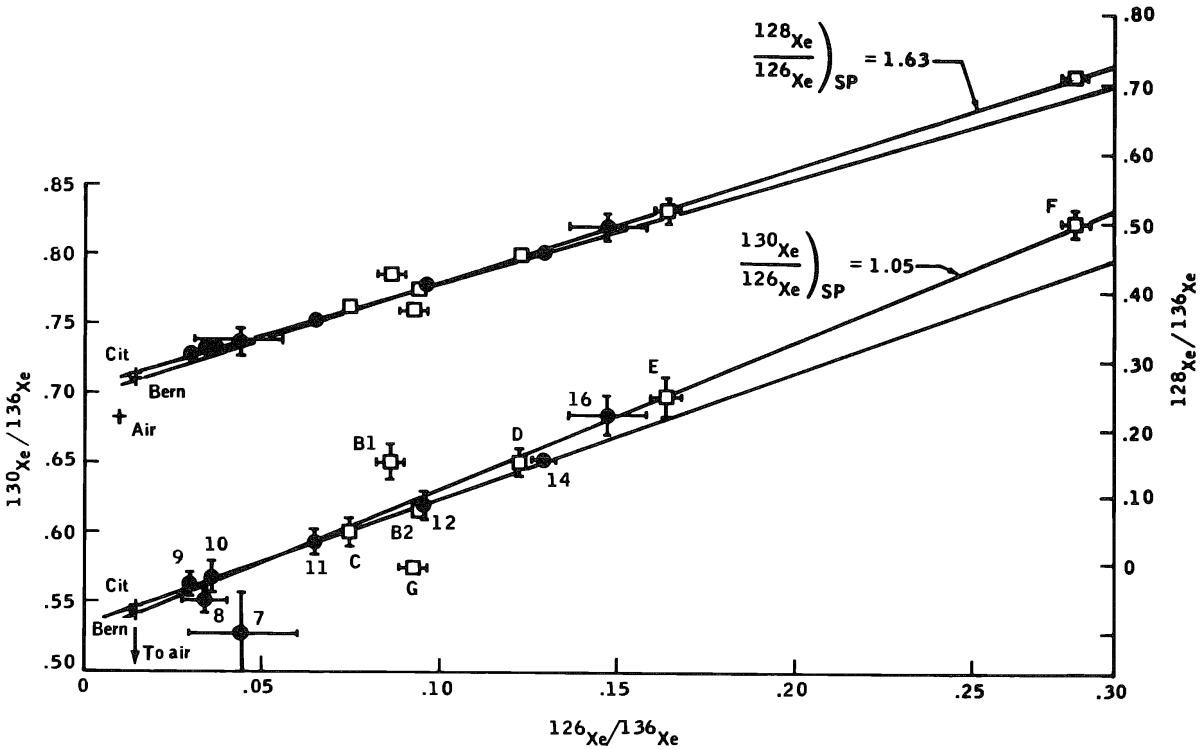

Fig. 7 and 8. Isotope correlation plots for $^{124}Xe/^{136}Xe$, $^{131}Xe/^{136}Xe$, $^{128}Xe/^{136}Xe$, and $^{130}Xe/^{136}Xe$ against $^{126}Xe/^{136}Xe$ for grain size separates and stepwise temperature release of fines 14163. Letters denote various grain size fractions of Table 1.

amount of Xe similar to the Xe released at low extraction temperatures to alter slightly the trapped Xe component. The trapped Xe composition given by CIT would then represent the more tightly bound solar wind component, while the Xe composition given by Bern would contain an additional small amount of the low temperature Xe component. This situation is analogous to the Kr correlation plots where the Bern trapped Kr composition appeared to be a mixture of the CIT high-temperature component and Kr released at low extraction temperatures.

Figures 5–8 demonstrate that grain size separates and stepwise heating of a lunar sample give nearly the same results for the isotopic composition of the spallation component. There is no evidence for a mass fractionation during the stepwise heating altering the spallation spectrum obtained. However, it is apparent that Kr and Xe in lunar fines are not simple mixtures of components, but that the trapped solar and spallation Kr and Xe components may vary in composition (also see Burnett *et al.*, 1971). The techniques used to obtain both the CIT and the Bern trapped Kr and Xe compositions (Podosek *et al.*, 1971; Eberhardt *et al.*, 1970) assume that Kr and Xe can be described as a two-component system for which the composition of the two components and the amounts of the spallation component are the same for all samples. The techniques for deriving the composition of the trapped component are thus sensitive to the types of isotope correlation variations seen for fines 14163.

Figure 9 presents the same Xe correlation diagram as Fig. 7 for a large number of

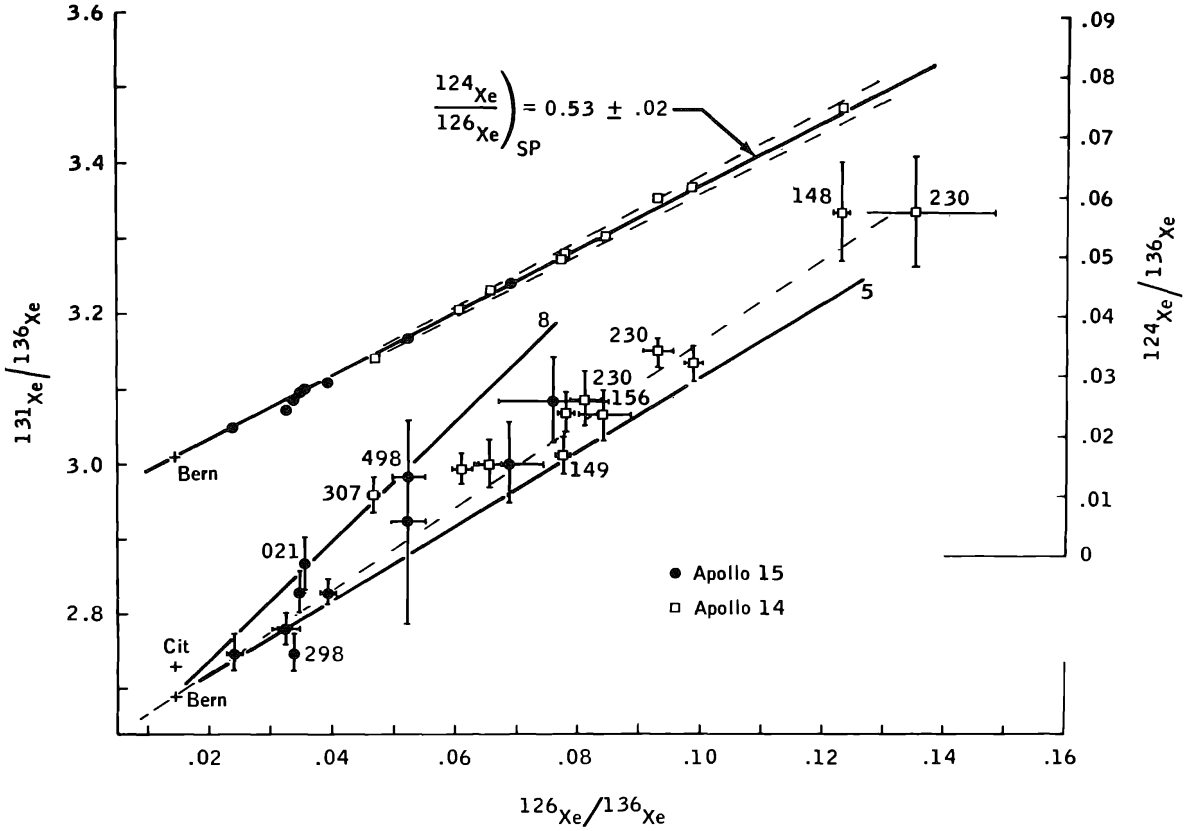

Fig. 9. Xenon isotope correlation plot for a number of Apollo 14 and 15 fines and gas rich breccia. The two solid lines represent spallation $^{131}Xe/^{126}Xe$ ratios of 5 and 8; the dashed line represents spallation $^{131}Xe/^{126}Xe$ determined for 14163 (Fig. 8).

Apollo 14 and 15 fines and gas-rich breccia. The spallation $^{124}Xe/^{126}Xe$ is essentially constant at 0.53 ± 0.02. This value contrasts with the range of $^{124}Xe/^{126}Xe$ spallation ratios found in meteorites of 0.52–0.65 (see Bogard *et al.*, 1971b, for references), and indicates that these particular lunar samples have not experienced major energy differences in the higher-energy cosmic-ray component that produces the light spallation isotopes of Xe. However, the spallation $^{131}Xe/^{126}Xe$ vary by a factor of two and possess values considerably higher than those commonly found for spallation Xe in meteorites. These high values for spallation $^{131}Xe/^{126}Xe$ have also been found to be typical of lunar crystalline rocks, and apparently are not due to chemical differences (Hohenberg *et al.*, 1970; Marti *et al.*, 1970; Pepin *et al.*, 1970; Bogard *et al.*, 1971a; Marti and Lugmair, 1971; Alexander, 1971; Huneke *et al.*, 1972). Recent target irradiation experiments (Eberhardt *et al.*, 1971; Kaiser, 1972b) have shown that this excess ^{131}Xe above what is expected from cosmic ray spallation is probably due to epithermal neutron capture on ^{130}Ba. Thus, the spallation excess ^{126}Xe allows a quantitative determination of the integrated cosmic ray exposure, while the excess ^{131}Xe allows a qualitative determination of the integrated energy of that exposure (shielding). Samples which were physically associated on the lunar surface (e.g., core samples), but which do not exhibit the same spallation $^{131}Xe/^{126}Xe$ ratio on Figure 9 would have had different average burial depths in the regolith. Thus fines 15021 and breccia 15498 and 14307 possess excess $^{131}Xe/^{126}Xe = 8$, and should exhibit considerable evidence of low-energy neutron fluxes. By the same criterion, breccia 15298 must have existed on the surface for most of its exposure. The excess $^{131}Xe/^{126}Xe$ also allows examination of the various samples collected at depth. Three different depths of core 14230 and the three different trench samples show small apparent variations in this ratio. Trench sample 14148 and core 14230,113 both appear to have higher excess $^{131}Xe/^{126}Xe$, implying greater average shielding.

Calculated concentrations of spallation ^{126}Xe in many of these fines and gas-rich breccia are given in Table 6. Spallation gases in a number of gas-poor Apollo 14 breccia have been discussed elsewhere (Bogard and Nyquist, 1972; LSPET, 1971), and indicate that a number of these rocks were excavated by Cone Crater approximately 20×10^6 yr ago. The difference in ^{126}Xe concentrations between Apollo 14 and 15 fines and gas-rich breccia is largely due to differences in abundance of the main target element Ba. However, the differences in ^{126}Xe (>factor of three) which exist among the Apollo 14 samples apparently are not due to target element variations, but rather to real differences in cosmic ray exposure times. Ba concentrations in most Apollo 14 fines and gas-rich breccias are constant within ±20% (LSPET, 1971; Hubbard *et al.*, 1972, and personal comm.; Schnetzler and Nova, 1972; Wakita *et al.*, 1972). Utilizing ^{126}Xe production rates previously reported (Bogard *et al.*, 1971a; Huneke *et al.*, 1972) gives typical exposure times of Apollo 14 soils ranging from 200–500 $\times 10^6$ yr. Very little Ba and rare earth data on Apollo 15 fines and breccia have been reported, and the factor of three variation in spallation ^{126}Xe for these samples may be due to either differences in target elements or integrated exposure times. Utilizing measured Ba contents of soils 15301, 15021, and 15101 (Hubbard, personal comm.) gives exposure ages of 190, 200, and 200 $\times 10^6$ yr, respectively. The Apollo 14 bulk soil 14161-14163 shows an inverse correlation of spallation ^{126}Xe

Table 6. Abundances of spallation ^{126}Xe in Apollo 14 and 15 fines and gas rich breccia (10^{-10} cc/g).

Sample	^{126}Xe	Sample	^{126}Xe
14259,10	12.5 ± 1.7	14163	
14003,6	2.06 ± 0.29	1000–250 μ	2.49 ± 0.29
14047,2	4.31 ± 0.52	250–90 μ	4.07 ± 0.49
14049,3	5.31 ± 0.62	90–60 μ	3.52 ± 0.38
14301,48*	0.022 ± 0.007	60–30 μ	5.56 ± 0.62
14307,26 (dark)	1.25 ± 0.15	30–20 μ	0.47 ± 0.06
14307,26 (light)	1.83 ± 0.21	30–20 (repeat)	0.45 ± 0.07
14230,113	1.57 ± 0.12	15301	0.47 ± 0.11
14230,130	0.56 ± 0.12	15021	0.73 ± 0.10
14230,121	1.93 ± 0.27	15101	0.53 ± 0.08
14148 (T)	6.54 ± 0.84	15601	0.30 ± 0.07
14156 (M)	4.71 ± 0.74	15298	0.85 ± 0.13
14149 (B)	4.89 ± 0.58	15558	1.00 ± 0.17
14161 (2–4 mm)	0.34 ± 0.07	15498	0.37 ± 0.07
14162 (1–2 mm)	1.51 ± 0.19	15265	0.81 ± 0.17
		15923 (matrix)*	0.10 ± 0.06
		15923 (glass)	0.065 ± 0.016

Spallation abundances calculated from the data in Tables 1 and 4 and in LSPET (1971) and (1972) assuming the trapped solar composition given by Eberhardt *et al.* (1970). Uncertainties listed are 10% plus the fractional value given by the one sigma uncertainty in measured $^{126}Xe/^{136}Xe$ divided by the difference in this ratio between measured and trapped values, and thus seem conservatively estimated.

* Calculated on basis of (128/126) spallation = 1.55.

with grain size. Even after considering target element differences (Hubbard *et al.*, 1972, and personal comm.), at least a factor of five difference in exposure time remains between the largest grain size and the finer fractions. The reason for the abrupt drop in ^{126}Xe for the 30–20 μ fraction is not known. As the Ba content for this fraction was not measured, this decrease may reflect a gross chemical change for the smallest grain sizes. Alternatively, if the Ba content of this smallest grain size is the same as the bulk soil, the exposure time of this component would be $\sim 40 \times 10^6$ yr. The large differences in spallation gases shown by various soil and breccia samples and by grain sizes of the same soil are important considerations in the derivation of isotopic composition of the various trapped noble gas components.

Acknowledgments—We acknowledge the competent technical support of the following persons of the Brown and Root-Northrop support staff: W. Hart, W. Hirsch, C. Polo, and R. Wilkin.

References

Alexander E. C. Jr. (1971) Spallogenic Ne, Kr, and Xe from a depth study of 12022. *Proc. Second Lunar Sci. Conf., Geochim. Cosmochim. Acta* Suppl. 2, Vol. 0, pp. 1643–1650. MIT Press.

Aller L. H. (1961) *The Abundance of the Elements.* Interscience.

Baur H., Frick U., Funk H., Schultz L., and Signer P. (1972) On the question of retrapped 40-Ar in lunar fines (abstract). In *Lunar Science—III* (editor C. Watkins), pp. 47–49, Lunar Science Institute Contr. No. 88.

Black D. C. (1972) On the origins of trapped He, Ne, and Ar isotopic variations in meteorites—I. Gas rich meteorites, lunar soil, and breccia. *Geochim. Cosmochim. Acta* **36,** 347–376.

Bogard D. D., Funkhouser J. G., Schaeffer O. A., and Zahringer J. (1971a) Noble gas abundances in lunar material—cosmic ray spallation products and radiation ages from the Sea of Tranquility and the Ocean of Storms. *J. Geophys. Res.* **76,** 2757–2779.

Bogard D. D., Huneke J. C., Burnett D. S., and Wasserburg G. J. (1971b) Xe and Kr analyses of silicate inclusions from iron meteorites. *Geochim. Cosmochim. Acta* **35,** 1231–1254.

Bogard D. D. and Nyquist L. E. (1972) Noble gas studies on regolith materials from Apollo 14 and 15 (abstract). In *Lunar Science—III* (editor C. Watkins), pp. 89–91, Lunar Science Institute Contr. No. 88.

Bühler F., Eberhardt P., Geiss J., and Schwarzmüller J. (1971) Trapped solar wind He and Ne in Surveyor 3 material. *Earth Planet. Sci. Lett.* **10,** 297–306.

Bühler F., Cerutti H., Eberhardt P., and Geiss J. (1972) Results of the Apollo 14 and 15 solar wind composition experiments (abstract). In *Lunar Science—III* (editor C. Watkins), pp. 102–104, Lunar Science Institute Contr. No. 88.

Burnett D. S., Huneke J. C., Podosek F. A., Russ G. P. III, and Wasserburg G. J. (1972) The irradiation history of lunar samples (abstract). In *Lunar Science—III* (editor C. Watkins), pp. 105–107, Lunar Science Institute Contr. No. 88.

Cameron A. G. W. (1968) A new table of abundances of the elements in the solar system. In *Origin and Distribution of the Elements*, pp. 125–143, Pergamon.

Crozaz G., Drozd H., Graf H., Hohenberg C. M., Mannin M., Rogan D., Ralston C., Seitz M., Shirck J., Walker R. M., and Zimmerman J. (1972) Evidence for extinct Pu^{244}: Implications for the age of the pre-Imbrium crust (abstract). In *Lunar Science—III* (editor C. Watkins), pp. 164–166, Lunar Science Institute Contr. No. 88.

Eberhardt P., Geiss J., and Grögler N. (1965) Über die Verteilung der Uredelgase in Meteoriten Khor Temiki. *Tschermaks Mineral. Petrogr. Mitt.* **10,** 535–551.

Eberhardt P., Geiss J., Graf H., Grögler N., Krähenbühl U., Schwaller H., Schwarzmüller J., and Stettler A. (1970) Trapped solar wind noble gases, exposure age and K/Ar age in Apollo 11 lunar fine material. *Proc. Apollo 11 Lunar Sci. Conf., Geochim. Cosmochim. Acta* Suppl. 1, Vol. 1, pp. 1037–1070. Pergamon.

Eberhardt P., Geiss J., and Graf H. (1971) On the origin of excess ^{131}Xe in lunar rocks. *Earth Planet. Sci. Lett.* **12,** 260–262.

Geiss J., Eberhardt P., Bühler F., Meister J., and Signer P. (1970) Apollo 11 and 12 solar wind composition experiments: Fluxes of He and Ne isotopes. *J. Geophys. Res.* **75,** 5972–5979.

Heymann D. and Yaniv A. (1970) Ar^{40} anomaly in lunar samples from Apollo 11. *Proc. Apollo 11 Lunar Sci. Conf., Geochim. Cosmochim. Acta* Suppl. 1, Vol. 2, pp. 1261–1268. Pergamon.

Hintenberger H., Weber H. W., and Takaoka N. (1971) Concentrations and isotopic abundances of the rare gases in lunar matter. *Proc. Second Lunar Sci. Conf., Geochim. Cosmochim. Acta* Suppl. 2, Vol. 2, pp. 1607–1626. MIT Press.

Hohenberg C. M., Davis P. K., Kaiser W. A., Lewis R. S., and Reynolds J. H. (1970) Trapped and cosmogenic rare gases from stepwise heating of Apollo 11 samples. *Proc. Apollo 11 Lunar Sci. Conf., Geochim. Cosmochim. Acta* Suppl. 1, Vol. 2, pp. 1283–1310. Pergamon.

Hubbard N. J., Gast P. W., Rhodes M., and Wiesmann H. (1972) Chemical composition of Apollo 14 materials and evidence for alkali volatilization (abstract). In *Lunar Science—III* (editor C. Watkins), pp. 407–409, Lunar Science Institute Contr. No. 88.

Huneke J. C., Podosek F. A., Burnett D. S., and Wasserburg G. J. (1972) Rare gas studies of the galactic cosmic ray irradiation history of lunar rocks. *Geochim. Cosmochim. Acta* **36,** 269–302.

Kaiser W. A. (1972a) Rare gas studies in Luna 16 G-7 fines by stepwise heating technique. *Earth Planet. Sci. Lett.* **13,** 387–399.

Kaiser W. A. (1972b) The average ^{130}Ba (n, γ) cross section and the origin of ^{131}Xe on the moon (abstract). In *Lunar Science—III* (editor C. Watkins), p. 44, Lunar Science Institute Contr. No. 88.

Kirsten T., Müller O., Steinbrum F., and Zähringer J. (1970) Study of distribution and variations of rare gases in lunar material by a microprobe technique. *Proc. Apollo 11 Lunar Sci. Conf., Geochim. Cosmochim. Acta* Suppl. 1, Vol. 2, pp. 1331–1344. Pergamon.

Kirsten T., Steinbrum F., and Zähringer J. (1971) Location and variation of trapped rare gases in Apollo 12 lunar samples. *Proc. Second Lunar Sci. Conf., Geochim. Cosmochim. Acta* Suppl. 2, Vol. 2, pp. 1651–1670. MIT Press.

Kirsten T., Deubner J., Ducati H., Gentner W., Horn P., Jessberger E., Kalbitzer S., Kaneoka I., Kiko J., Krätschmer W., Müller H., Plieninger T., and Thio S. (1972) Rare gases and ion tracks in individual components and bulk samples of Apollo 14 and 15 fines and fragmental rocks (abstract). In *Lunar Science—III* (editor C. Watkins), pp. 452–454, Lunar Science Institute Contr. No. 88.

Lagerwall T. and Zimen K. E. (1964) The kinetics of rare gas diffusion in solids. EURACE Report No. 772, Hahn-Meitner Institut für Kernforschung, Berlin.

LSPET (Lunar Sample Preliminary Examination Team) (1971) Preliminary examination of lunar samples from Apollo 14. *Science* **173,** 681–693.

LSPET (Lunar Sample Preliminary Examination Team) (1972) Preliminary examination of lunar samples from Apollo 15. *Science* **175,** 363–374.

Manka R. H. and Michel F. C. (1970) Lunar atmosphere as a source of argon-40 and other lunar surface elements. *Science* **169,** 278–280.

Manka R. H. and Michel F. C. (1971) Lunar atmosphere as a source of lunar surface elements. *Proc. Second Lunar Sci. Conf., Geochim. Cosmochim. Acta* Suppl. 2, Vol. 2, pp. 278–280. MIT Press.

Marti K., Lugmair G. W., and Urey H. C. (1970) Solar wind gases, cosmic-ray spallation products, and the irradiation history of Apollo 11 samples. *Proc. Apollo 11 Lunar Sci. Conf., Geochim. Cosmochim. Acta* Suppl. 1, Vol. 2, pp. 1357–1368. Pergamon.

Marti K. and Lugmair G. W. (1971) Kr^{81}–Kr and K–Ar^{40} ages, cosmic ray spallation products, and neutron effects in lunar samples from Oceanus Procellarum. *Proc. Second Lunar Sci. Conf., Geochim. Cosmochim. Acta* Suppl. 2, Vol. 2, pp. 1591–1606. MIT Press.

Nyquist L. E. and Pepin R. O. (1971) Rare gases in Apollo 12 lunar materials. *Abstrs. Second Lunar Sci. Conf.* and unpublished data.

Papanastassiou D. A. and Wasserburg G. J. (1971) Rb–Sr ages of igneous rocks from the Apollo 14 mission and the age of the Fra Mauro formation. *Earth Planet. Sci. Lett.* **12,** 36–48.

Pepin R. O., Nyquist L. E., Phinney D., and Black D. C. (1970) Rare gases in Apollo 11 lunar material. *Proc. Apollo 11 Lunar Sci. Conf., Geochim. Cosmochim. Acta* Suppl. 1, Vol. 2, pp. 1435–1454. Pergamon.

Pepin R. O., Bradley J. G., Dragon J. C., and Nyquist L. E. (1972) K–Ar dating of lunar soils: Apollo 12, Apollo 14, and Luna 16 (abstract). In *Lunar Science—III* (editor C. Watkins), pp. 602–604, Lunar Science Institute Contr. No. 88.

Podosek F. A., Huneke J. C., Burnett D. S., and Wasserburg G. J. (1971) Isotopic composition of Xe and Kr in the lunar soil and in the solar wind. *Earth Planet. Sci. Lett.* **10,** 199–216.

Schnetzler C. C. and Nava D. F. (1971) Chemical composition of Apollo 14 soils. *Earth Planet. Sci. Lett.* **11,** 345–350.

Tatsumoto M., Hedge C. E., Doe B. R., and Unruh D. (1972) U–Th–Pb and Rb–Sr measurements on some Apollo 14 lunar samples (abstract). In *Lunar Science—III* (editor C. Watkins), pp. 741–743, Lunar Science Institute Contr. No. 88.

Turner G., Huneke J. C., Podosek F. A., and Wasserburg G. J. (1971) ^{40}Ar–^{39}Ar ages and cosmic ray exposure ages of Apollo 14 samples. *Earth Planet. Sci. Lett.* **12,** 19–36.

Wakita H., Showalter D. L., and Schmitt R. A. (1972) Bulk, REE, and other abundances in Apollo 14 soils (abstract). In *Lunar Science—III* (editor C. Watkins), pp. 767–769, Lunar Science Institute Contr. No. 88.

Yaniv A., Taylor G. J., Allen S., and Heymann D. (1971) Stable rare gas isotopes produced by solar flares in single particles of Apollo 11 and Apollo 12 fines. *Proc. Second Lunar Sci. Conf., Geochim. Cosmochim. Acta* Suppl. 2, Vol. 2, pp. 1705–1716. MIT Press.

Proceedings of the Third Lunar Science Conference
(Supplement 3, *Geochimica et Cosmochimica Acta*)
Vol. 2, pp. 1821–1856
The M.I.T. Press, 1972

Trapped solar wind noble gases in Apollo 12 lunar fines 12001 and Apollo 11 breccia 10046

P. EBERHARDT, J. GEISS, H. GRAF,* N. GRÖGLER, M. D. MENDIA,†
M. MÖRGELI, H. SCHWALLER, and A. STETTLER

Physikalisches Institut, University of Bern,
Sidlerstrasse 5, 3012 Bern, Switzerland

and

U. KRÄHENBÜHL‡ and H. R. VON GUNTEN

Institut für anorganische, analytische und physikalische Chemie,
University of Bern, Freiestrasse 3,
3012 Bern, Switzerland

Abstract—We have measured the concentrations and isotopic composition of the five noble gases in an unseparated bulk sample of the Apollo 12 fines 12001, in seven bulk and five ilmenite grain size fractions from 12001 and in four ilmenite grain size fractions separated from the Apollo 11 breccia 10046. In addition, we determined Sr, Zr, Ba, La, Ce, Sm, and Eu in several bulk grain size fractions from 12001.

Similar to previous investigations, a well defined anticorrelation between the concentration $C(Y, d)$ of trapped solar wind noble gases Y and the grain size d is found. The experimental data can be represented by a power law of the form $C(Y, d) = S_y (d/d_0)^{-n_y}$. For the ilmenite grain size fractions from soils 10084 (Eberhardt *et al.*, 1970) and 12001 the exponents n_y are close to one, which is the value expected for solar wind implanted ions. Absolute gas concentrations (S_y) are also very similar in the two soil ilmenites. The 10084 and 12001 bulk grain size fractions have exponents $n_y \approx 0.6$. Several possible explanations for these low n values are discussed, the most likely explanation being contamination of the coarser fractions with microbreccias or a similar volume correlated noble gas component. The He and Ne in the 10046 ilmenites show virtually the same grain size dependency as the two soil ilmenites. The grain size dependency of the heavier noble gases, especially of Ar, is considerably less steep, with exponents $n \approx 0.7$. The most probable explanation of this lower exponent is a volume correlated Ar, Kr, and Xe component, which probably originated during the compaction of the breccia from loose soil material.

$(Ar^{36}/Kr^{86})_{tr}$ and $(Kr^{86}/Xe^{132})_{tr}$ ratios are similar in the 10084 and 12001 bulk and ilmenite grain size fractions and also in the 10046 ilmenites. The average values are 5000 and 1.8, respectively. The $(He^4/Ne^{20})_{tr}$ is very similar in the 10084, 12001, and 10046 ilmenites with average values between 218 and 253. In the bulk samples from both soils this ratio is a factor 2 to 5 lower. Similarly, the $(Ne^{20}/Ar^{36})_{tr}$ ratio in the bulk samples is a factor of 5 lower than in the two soil ilmenites which gave an average value of 27. The $(Ne^{20}/Ar^{36})_{tr}$ ratio in the 10046 ilmenite is grain size dependent, which can be explained in terms of the volume component of trapped Ar, Kr, and Xe in the 10046 ilmenites.

The exposure ages for the 12001 soil are between 300×10^6 yr (ilmenite) and 440×10^6 yr (bulk grain size fractions). These ages are similar to the ones obtained for the 10084 soil. The ilmenite of breccia 10046 has a distinctly higher exposure age of 800×10^6 yr.

---

* Present address: Washington University, Laboratory for Space Physics, St. Louis, Mo. 63130.
† ESRO fellow, on leave from the University of Zaragoza, Spain.
‡ Present address: Enrico Fermi Institute, University of Chicago, Chicago, Ill. 60637.

The considerably lower $(He^4/Ne^{20})_{tr}$ and $(Ne^{20}/Ar^{36})_{tr}$ ratios of the bulks relative to the ilmenites show, that an evaluation of the isotopic composition of trapped He and Ne in the bulk is rather futile, as these ratios are certainly affected by the heavy diffusion loss. The 10084 and 12001 soil ilmenites have identical $(He^3/He^4)_{tr}$ ratios of 3.7×10^{-4}. This value, which corresponds to recent solar wind, is in basic agreement with the present solar wind He^3/He^4 ratio measured by the SWC experiment (Geiss *et al.*, 1971a). The breccia ilmenite, containing older solar wind, has a 10% lower (He^3/He^4) ratio than the soil ilmenites. This result supports the proposed secular variation of the He^3/He^4 ratio in the solar wind and in the sun.

The isotopic composition of surface correlated trapped Ne is essentially identical in the 10084, 12001, and 10046 ilmenites. The average $(Ne^{20}/Ne^{22})_{sc} = 12.8$ is approximately 5% lower than the ratio measured in the present day solar wind. This difference might be the result of unequal trapping probabilities for the two Ne isotopes, of saturation effects and of diffusion losses.

The $(Ar^{36}/Ar^{38})_{sc}$ ratio in all investigated samples is identical and agrees excellently with the terrestrial value. The $(Ar^{40}/Ar^{36})_{sc}$ ratio is different in the five samples varying from 0.37 to 1.35. Differences between bulk samples could be explained in terms of differences in the mineralogy. The variability between ilmenites from different samples, however, must represent genuine variations of the Ar^{40}/Ar^{36} ratio in the source of the surface correlated gas. It is well known that the trapped Ar^{40} is not of direct solar wind origin but represents retrapped Ar^{40} from a transient lunar atmosphere. We thus interpret the variability of the $(Ar^{40}/Ar^{36})_{sc}$ ratio in different ilmenites by time variations in the Ar^{40} outgassing of the moon.

The isotopic composition of surface correlated Kr in the 12001 bulk grain size fractions (BEOC 12001) is intermediate between AVCC and atmospheric Kr and essentially related to these by a simple mass fractionation. However, to fully explain the difference, an excess Kr^{86} component in atmospheric and AVCC Kr would be required. Such a 1.1% Kr^{86} excess in the terrestrial atmosphere might be identified as a fission component, which however could not have originated from known terrestrial sources. Further experimental evidence seems necessary to establish the presence of excess Kr^{86} in the terrestrial atmosphere.

The Xe^{124}/Xe^{130}, Xe^{126}/Xe^{130}, and Xe^{128}/Xe^{130} ratios of the surface correlated Xe in the 12001 bulk grain size fractions (BEOC 12001) are identical within 1.5% with the isotopic composition of AVCC Xe. The well known excess in the heavy isotopes of AVCC Xe is also observed relative to BEOC 12001 Xe. The AVCC fission, derived from the comparison with BEOC 12001 Xe, is—within the rather large error limits—compatible with Pu^{244} spontaneous fission Xe. BEOC 12001 and atmospheric Xe are not related by a mass fractionation process depending linearly on the mass difference. Our $Xe^{124,126,128}$ BEOC 12001 data are also not compatible with the 41‰ per mass unit fractionation proposed by Kaiser (1972).

INTRODUCTION AND RESULTS

THE LUNAR SURFACE is directly exposed to the solar wind and a considerable fraction of the impinging solar wind particles is trapped in the surface of the exposed lunar material (typical ranges of solar wind ions in solids are a few hundred to two thousand Å). These trapped solar wind atoms can be detected in the lunar surface material for elements with low intrinsic abundance in lunar material, e.g., hydrogen, the noble gases and some other elements.

In this paper we report and discuss our investigations of trapped solar wind noble gases in the Apollo 12 fines 12001,38 and the Apollo 11 breccia 10046,45. The main aims of the present investigation were:

(1) To study the elemental and isotopic composition of the trapped solar wind particles in a soil sample from a locality of the moon different from Mare Tranquillitatis and to compare the results obtained at the two places.

(2) To establish the isotopic composition of trapped Kr and Xe with improved accuracy.

(3) To investigate possible time variations in the elemental and isotopic composition of the solar wind.

A single analysis of a bulk soil or breccia sample can give only limited and inconclusive evidence on the elemental and isotopic composition of the trapped solar wind particles. Interference from spallation produced isotopes and erratic diffusion losses of the lighter noble gases must be considered and corrected for, in order to obtain meaningful results. To date, the best experimental approach to solve these problems consists in measuring the noble gases in grain size fractions of the bulk material and of mineral separates, notably ilmenite. We have therefore prepared the following bulk and mineral grain size fractions and analyzed all noble gases therein:

An unseparated sample from 12001.
Seven bulk grain size fractions from 12001.
Five ilmenite grain size fractions from 12001.
Four ilmenite grain size fractions from 10046.

For a thorough evaluation of the data it is necessary to know the concentration of the relevant target elements for the production of spallation isotopes. Therefore, the elements Sr, Zr, Ba, La, Ce, Sm, and Eu were determined in aliquots of several bulk grain size fractions from 12001.

The experimental technique used for the mineral and grain size separation and the noble gas determinations has been previously described (cf. Eberhardt *et al.*, 1970). The mineralogical purity of the ilmenite fractions was estimated to be better than 90–95% (X-ray diffraction patterns and optical microscopy). Sr, Zr, and Ba were determined with the isotopic dilution technique, La, Ce, Sm, and Eu by neutron activation (cf. Krähenbühl *et al.*, 1972). All results are given in Tables 1 to 4.

Grain Size Dependency of Trapped Gases

The Ne^{20}, Ar^{36}, Kr^{86}, and Xe^{132} present in all investigated fractions is at least 99% trapped gas.* Corrections for spallation and other components can thus be neglected for the discussion of the elemental abundances of these isotopes. For He^4 a correction for radiogenic He^4 had to be applied in the coarser bulk grain size fractions ($He^4_r = 110{,}000 \times 10^{-8}$ cm^3 STP/g, correction always smaller than 5%, see discussion of isotopic ratios). A distinct anticorrelation between trapped gas content and grain size down to 1μ is evident (Figs. 1 to 3). The trapped gas in the Apollo 12 fines 12001 and the ilmenite of breccia 11046 is thus surface correlated and represents most likely implanted low energy particles, such as solar wind ions. The 36μ ilmenite grain size fraction bb-51 does not fit onto the corresponding grain size-trapped gas correlation line. This is especially apparent for the heavier noble gases Ar, Kr, and

* As customary, we use the term trapped gas for the noble gas component that did not originate by *in situ* nuclear reactions (radioactive decay, spallation reactions, etc.). The following indices will be used to define different components: c: cosmogenic (includes spallation and low energy neutron reactions); f: fission; fs: spontaneous fission; fn: neutron induced fission; m: measured; n: produced by thermal or epithermal neutron capture; r: radiogenic, i.e., decay product of primordial nuclei; sc: surface correlated; sp: spallation; tr: trapped; vc: volume correlated.

Table 1. Results of He, Ne, and Ar measurements on an unseparated sample of Apollo 12 soil 12001, on bulk and ilmenite grain size fractions separated from 12001 and on ilmenite grain size fractions separated from Apollo 11 breccia 10046.

Sample no.	Grain size (μ)	Weight of analyzed sample (mg)	He^4	Ne^{20}	Ar^{36}	He^4/He^3	Ne^{20}/Ne^{22}	Ne^{22}/Ne^{21}	Ar^{36}/Ar^{38}	Ar^{40}/Ar^{36}
			(10^{-8} cm^3 STP/g)							
Unseparated sample from 12001										
A-12	—	11.2	9,250,000 ± 320,000	129,000 ± 4,500	24,500 ± 2,000	2,315 ± 70	12.37 ± 0.20	29.0 ± 0.5	5.23 ± 0.06	0.57 ± 0.01
Bulk grain size fractions from 12001										
bb-12	151	10.4	2,270,000 ± 80,000	43,700 ± 1,800	9,300 ± 700	2,350 ± 70	12.37 ± 0.20	23.0 ± 0.4	5.18 ± 0.08	0.86 ± 0.01
bb-13	82	9.5	2,930,000 ± 100,000	55,200 ± 2,000	13,300 ± 1,000	2,280 ± 70	12.17 ± 0.20	21.4 ± 0.4	5.20 ± 0.06	0.68 ± 0.01
bb-14	44	6.3	4,270,000 ± 150,000	80,800 ± 3,000	16,800 ± 1,300	2,520 ± 70	12.42 ± 0.20	26.2 ± 0.3	5.14 ± 0.10	0.62 ± 0.01
bb-15	20	5.3	9,970,000 ± 360,000	149,300 ± 5,500	23,500 ± 1,800	2,350 ± 80	12.33 ± 0.20	26.7 ± 0.8	5.20 ± 0.08	0.55 ± 0.01
bb-16	10.4	4.4	16,900,000 ± 600,000	244,000 ± 9,000	48,000 ± 3,500	2,600 ± 70	12.52 ± 0.20	30.2 ± 0.6	5.29 ± 0.06	0.50 ± 0.01
bb-17	2.0	3.0	44,100,000 ± 1,600,000	504,000 ± 30,000	89,000 ± 7,000	2,310 ± 70	12.52 ± 0.25	30.2 ± 0.6	5.28 ± 0.06	0.48 ± 0.01
bb-18	1.3	2.0	58,000,000 ± 2,000,000	720,000 ± 25,000	142,000 ± 11,000	2,400 ± 70	12.66 ± 0.20	31.4 ± 1.0	5.31 ± 0.07	0.48 ± 0.01
Ilmenite grain size fractions from 12001										
bb-26	125	5.2	10,400,000 ± 400,000	40,800 ± 1,500	2,000 ± 170	2,600 ± 70	12.62 ± 0.30	29.3 ± 1.2	5.06 ± 0.07	0.88 ± 0.03
bb-37	75	6.7	21,300,000 ± 2,300,000	89,000 ± 9,000	3,400 ± 250	2,600 ± 110	12.70 ± 0.45	30.0 ± 1.5	5.13 ± 0.06	0.57 ± 0.01
bb-51	36	6.3	18,900,000 ± 700,000	105,700 ± 4,000	1,400 ± 130	2,615 ± 80	12.83 ± 0.20	30.8 ± 0.7	5.44 ± 0.06	0.83 ± 0.04
bb-52	17.2	5.6	79,000,000 ± 3,000,000	309,000 ± 11,000	11,500 ± 900	2,590 ± 70	12.90 ± 0.20	31.6 ± 1.0	5.31 ± 0.06	0.45 ± 0.01
bb-57	10.9	4.3	200,000,000 ± 8,000,000	760,000 ± 30,000	22,500 ± 1,800	2,700 ± 80	13.00 ± 0.20	32.2 ± 0.7	5.30 ± 0.06	0.44 ± 0.01
Ilmenite grain size fractions from 10046										
DA-14	114	1.6	13,900,000 ± 900,000	65,000 ± 3,500	6,700 ± 600	2,810 ± 80	12.61 ± 0.30	28.85 ± 0.8	5.07 ± 0.13	2.40 ± 0.09
DA-15	78	4.8	31,000,000 ± 1,800,000	129,000 ± 6,000	8,800 ± 800	2,830 ± 70	12.54 ± 0.15	30.55 ± 0.6	5.18 ± 0.08	1.94 ± 0.05
DA-16	28	5.0	66,000,000 ± 3,500,000	290,000 ± 16,000	15,100 ± 1,500	2,810 ± 100	12.49 ± 0.25	31.05 ± 0.8	5.21 ± 0.08	1.78 ± 0 .05
DA-17	14	5.4	200,000,000 ± 10,000,000	825,000 ± 40,000	28,900 ± 3,000	3,010 ± 70	12.81 ± 0.15	30.85 ± 0.6	5.28 ± 0.08	1.61 ± 0.05

Grain size determined according to equation (4) of Eberhardt *et al.* (1965). The uncertainty in the average grain size is estimated to be always smaller than ±20%.

Table 2. Results of Kr measurements on an unseparated sample of Apollo 12 soil 12001, on bulk and ilmenite grain size fractions separated from 12001 and on ilmenite grain size fractions separated from Apollo 11 breccia 10046.

Sample no.	Kr^{86} (10^{-8} cm^3 STP/g)	Kr^{78}/Kr^{86}	Kr^{80}/Kr^{86}	Kr^{82}/Kr^{86}	Kr^{83}/Kr^{86}	Kr^{84}/Kr^{86}
		× 100				
Unseparated sample from 12001						
ba-2	6.0 ± 1.2	2.180 ± 0.07	13.38 ± 0.2	66.55 ± 0.7	66.95 ± 0.5	326.8 ± 1.7
Bulk grain size fractions from 12001						
bb-12	2.0 ± 0.4	2.510 ± 0.06	14.23 ± 0.18	67.20 ± 0.7	68.35 ± 0.6	325.6 ± 3
bb-13	2.7 ± 0.9	2.440 ± 0.05	14.16 ± 0.18	67.45 ± 0.6	67.75 ± 0.6	324.5 ± 2.5
bb-14	3.7 ± 0.7	2.295 ± 0.045	13.62 ± 0.18	66.45 ± 0.6	67.00 ± 0.45	324.9 ± 1.9
bb-15	5.3 ± 1	2.205 ± 0.05	13.39 ± 0.2	66.25 ± 0.7	66.90 ± 0.45	325.4 ± 2
bb-16	9.9 ± 2	2.095 ± 0.04	13.06 ± 0.17	65.80 ± 0.6	66.20 ± 0.4	325.3 ± 1.8
bb-17	21 ± 4	2.040 ± 0.045	13.02 ± 0.2	66.20 ± 0.5	66.30 ± 0.4	328.1 ± 2
bb-18	33 ± 6	1.970 ± 0.04	12.80 ± 0.14	65.65 ± 0.5	65.90 ± 0.45	327.3 ± 1.6
Ilmenite grain size fractions from 12001						
bb-26	0.39 ± 0.08	5.695 ± 0.09	21.44 ± 0.35	77.95 ± 0.9	84.30 ± 0.5	326.7 ± 3
bb-37	0.59 ± 0.12	8.44 ± 0.3	27.06 ± 0.5	86.30 ± 0.9	93.45 ± 0.8	329.3 ± 3
bb-51	0.099 ± 0.02	11.33 ± 0.25	34.20 ± 0.8	100.1 ± 1.7	108.9 ± 0.9	337.1 ± 4.5
bb-52	2.3 ± 0.4	4.495 ± 0.1	18.54 ± 0.18	74.25 ± 0.7	76.80 ± 0.7	326.8 ± 1.7
bb-57	4.8 ± 0.9	3.010 ± 0.035	15.26 ± 0.2	69.05 ± 0.6	70.80 ± 0.5	326.6 ± 1.8
Ilmenite grain size fractions from 10046						
DA-14	0.95 ± 0.20	3.90 ± 0.16	17.85 ± 0.40	74.8 ± 1.1	76.2 ± 0.9	329.0 ± 2.3
DA-15	1.5 ± 0.3	3.69 ± 0.07	17.30 ± 0.25	73.9 ± 0.8	75.95 ± 0.8	330.0 ± 2.5
DA-16	2.8 ± 0.5	2.93 ± 0.08	15.25 ± 0.25	70.35 ± 0.65	71.05 ± 0.65	328.6 ± 1.9
DA-17	4.8 ± 0.9	2.57 ± 0.05	14.45 ± 0.20	69.1 ± 0.9	69.85 ± 0.75	329.9 ± 3

For grain sizes see Table 1.

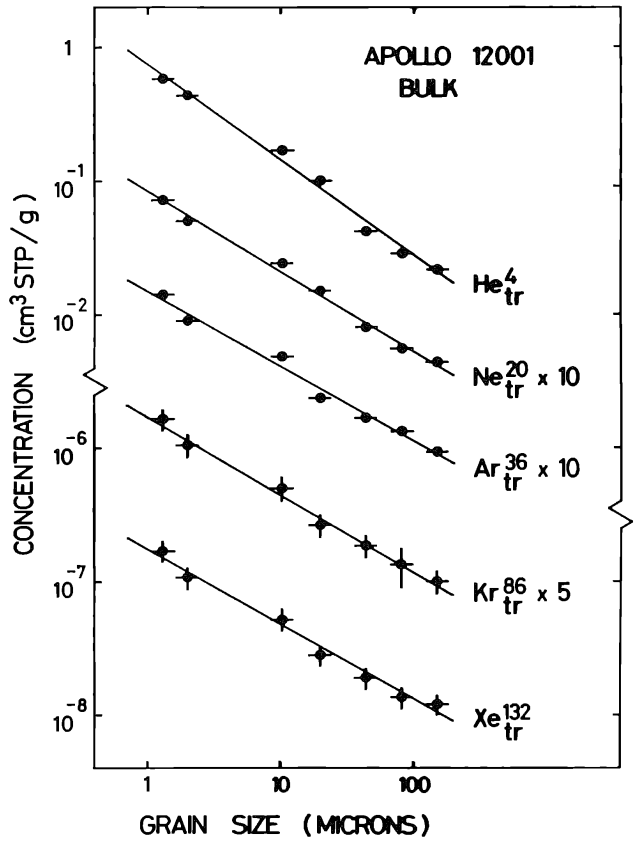

Fig. 1. Grain size dependency of the trapped He^4, Ne^{20}, Ar^{36}, Kr^{86}, and Xe^{132} concentrations in unseparated Apollo 12 lunar fine material 12001.

1972LPSC....3.1637F

Table 3. Results of Xe measurements on an unseparated sample of Apollo 12 soil 12001, on bulk and ilmenite grain size fractions separated from 12001 and on ilmenite grain size fractions separated from Apollo 11 soil 10046.

Sample no.	Xe^{132} (10^{-8} cm³ STP/g)	Xe^{124}/Xe^{132}	Xe^{126}/Xe^{132}	Xe^{128}/Xe^{132}	Xe^{129}/Xe^{132}	Xe^{130}/Xe^{132}	Xe^{131}/Xe^{132}	Xe^{134}/Xe^{132}	Xe^{136}/Xe^{132}
		× 100							
Unseparated sample from 12001									
ba-2	2.6 ± 0.5	0.862 ± 0.025	1.126 ± 0.025	9.50 ± 0.1	106.3 ± 1.1	16.96 ± 0.13	85.06 ± 0.7	36.91 ± 0.25	29.21 ± 0.3
Bulk grain size fractions from 12001									
bb-12	1.21 ± 0.2	1.234 ± 0.05	1.810 ± 0.06	10.38 ± 0.16	106.3 ± 1.4	17.72 ± 0.3	88.35 ± 1.4	36.48 ± 0.4	29.80 ± 0.6
bb-13	1.35 ± 0.25	1.073 ± 0.05	1.492 ± 0.05	9.85 ± 0.19	104.4 ± 1.8	17.23 ± 0.2	86.79 ± 0.35	37.00 ± 0.35	30.44 ± 0.6
bb-14	1.91 ± 0.35	0.958 ± 0.025	1.355 ± 0.035	9.73 ± 0.2	105.1 ± 1.2	17.21 ± 0.15	86.23 ± 0.3	36.81 ± 0.35	30.01 ± 0.45
bb-15	2.8 ± 0.5	0.832 ± 0.02	1.103 ± 0.045	9.33 ± 0.14	105.1 ± 1.2	17.09 ± 0.25	85.16 ± 0.9	36.90 ± 0.3	30.16 ± 0.45
bb-16	5.2 ± 1	0.723 ± 0.02	0.892 ± 0.02	8.99 ± 0.16	104.5 ± 1.1	16.83 ± 0.25	83.92 ± 0.9	37.05 ± 0.45	30.12 ± 0.5
bb-17	10.7 ± 2	0.625 ± 0.019	0.703 ± 0.02	8.78 ± 0.18	105.0 ± 1.2	16.70 ± 0.13	83.42 ± 0.5	36.88 ± 0.3	29.91 ± 0.45
bb-18	17.1 ± 3	0.576 ± 0.025	0.625 ± 0.02	8.59 ± 0.12	105.0 ± 1.3	16.67 ± 0.17	83.30 ± 0.5	36.86 ± 0.3	30.04 ± 0.45
Ilmenite grain size fractions from 12001									
bb-26	0.17 ± 0.03	1.564 ± 0.05	2.412 ± 0.09	11.00 ± 0.35	102.4 ± 2.2	17.46 ± 0.5	89.34 ± 1.4	36.94 ± 0.8	30.24 ± 0.7
bb-37	0.22 ± 0.04	0.998 ± 0.045	1.409 ± 0.09	9.46 ± 0.35	103.5 ± 2.5	17.22 ± 0.45	85.17 ± 0.9	37.18 ± 0.45	30.18 ± 0.5
bb-51	0.034 ± 0.007	0.796 ± 0.09	1.005 ± 0.1	8.76 ± 0.7	101.9 ± 4.5	17.34 ± 0.9	82.60 ± 0.6	37.69 ± 2	32.22 ± 2
bb-52	0.96 ± 0.18	0.599 ± 0.018	0.626 ± 0.02	8.46 ± 0.45	104.2 ± 1.3	16.69 ± 0.45	82.49 ± 1	37.33 ± 0.35	30.54 ± 0.5
bb-57	2.1 ± 0.4	0.524 ± 0.009	0.531 ± 0.02	8.00 ± 0.35	103.9 ± 0.9	16.35 ± 0.25	81.75 ± 0.9	37.10 ± 0.5	30.45 ± 0.3
Ilmenite grain size fractions from 10046									
DA-14	0.60 ± 0.12	0.840 ± 0.050	1.082 ± 0.085	9.42 ± 0.30	104.8 ± 1.3	16.96 ± 0.1	84.85 ± 1.2	37.00 ± 0.45	30.98 ± 0.4
DA-15	0.90 ± 0.18	0.695 ± 0.030	0.819 ± 0.050	8.90 ± 0.13	104.4 ± 2.2	16.88 ± 0.4	83.2 ± 1.2	37.30 ± 0.55	30.66 ± 0.5
DA-16	2.1 ± 0.4	0.591 ± 0.025	0.633 ± 0.030	8.52 ± 0.13	103.8 ± 1.3	16.50 ± 0.2	82.55 ± 0.5	37.39 ± 0.3	30.87 ± 0.4
DA-17	4.0 ± 0.8	0.5005 ± 0.015	0.494 ± 0.018	8.32 ± 0.11	104.1 ± 0.8	16.34 ± 0.2	81.85 ± 0.5	37.58 ± 0.25	30.78 ± 0.3

For grain sizes see Table 1.

Table 4. Results of Sr, Zr, Ba, La, Ce, Sm, and Eu determinations in bulk grain size fractions separated from Apollo 12 fines 12001.

Sample no.	Sr	Zr	Ba	La	Ce	Sm	Eu
	(ppm)						
bb-14	134 ± 7	405 ± 40	305 ± 20	22 ± 2	77 ± 5	10 ± 1	1.2 ± 0.1
bb-15	141 ± 7	410 ± 40	315 ± 20	—	—	—	—
bb-16	175 ± 9	460 ± 45	400 ± 25	38 ± 3	130 ± 8	18 ± 2	2.4 ± 0.2
bb-17	182 ± 9	440 ± 45	490 ± 30	—	—	—	—
bb-18	214 ± 11	400 ± 40	630 ± 40	53 ± 4	167 ± 10	28 ± 2	3.1 ± 0.3
12001 (a)	145.5	—	370	—	87.2	16.1	1.78
bulk (b)	130	—	460	32.4	87	15.0	1.80

Measurements were done on aliquots of the samples used for the noble gas analyses. Sample sizes analyzed: 9 to 13 mg. For grain sizes see Table 1. Data for 12001 bulk sample from: (a) Schnetzler and Philpotts (1971); (b) Wänke *et al.* (1971).

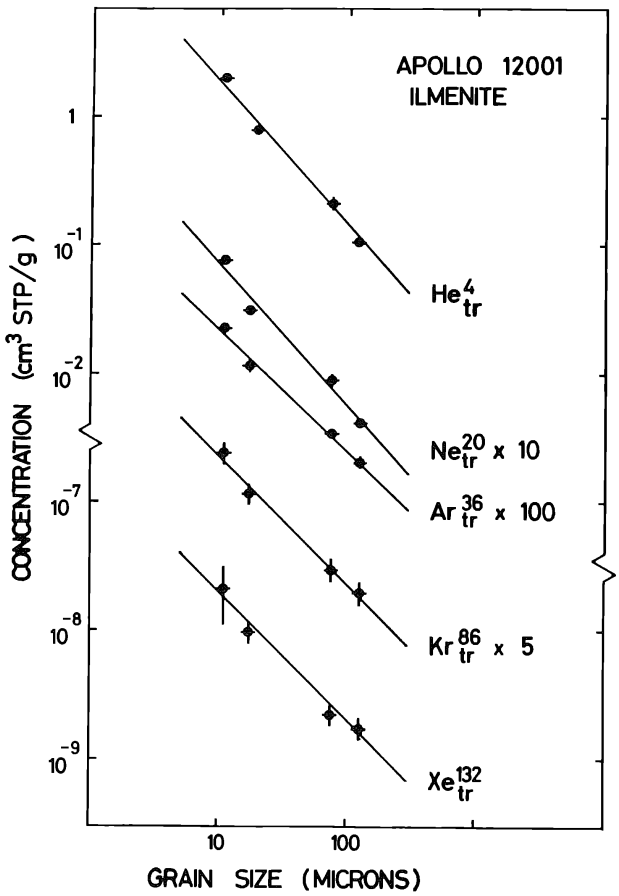

Fig. 2. Grain size dependency of the trapped He^4, Ne^{20}, Ar^{36}, Kr^{86}, and Xe^{132} concentrations in ilmenite separated from the Apollo 12 lunar fine material 12001.

Xe. Not enough material was available to make a duplicate analysis and we can thus not decide whether this discrepancy is due to an analytical error or whether this peculiarity is inherent to this grain size fraction. Therefore, the results from this fraction will be disregarded in our further discussion.

Within the experimental uncertainties and limitations, the different grain size fractions fall on straight lines in the log grain size versus log concentration plots

(Figs. 1 to 3). The concentration $C(Y, d)$ of the trapped noble gas Y in the grain size d can be expressed as

$$C(Y, d) = S_y \left(\frac{d}{d_0}\right)^{-n_y} \tag{1}$$

where d_0 is an arbitrary reference grain size, S_y the noble gas concentration in the grain size d_0, and n_y the exponent defining the slope of the correlation line in the log-log plot. The S_y and n_y values obtained by a least square fit are given in Table 5. As reference grain size $d_0 = 10\ \mu$ was chosen.

For the ilmenite grain size fractions separated from the Apollo 11 and 12 fines, virtually identical values for the noble gas concentrations and the exponent n are found. For He^4_{tr} and Ne^{20}_{tr} the ilmenite separated from breccia 10046 shows similar exponents and only slightly higher gas concentrations. The exponent n for Ar^{36}_{tr} and Kr^{86}_{tr} is, however, distinctly smaller than for the other two ilmenites. This is also evident from Figs. 2 and 3. For strongly differing n values the comparison of the reference trapped gas concentrations is not any more appropriate. The low n_{36} value for the 10046 ilmenites will be discussed in more detail in a later section.

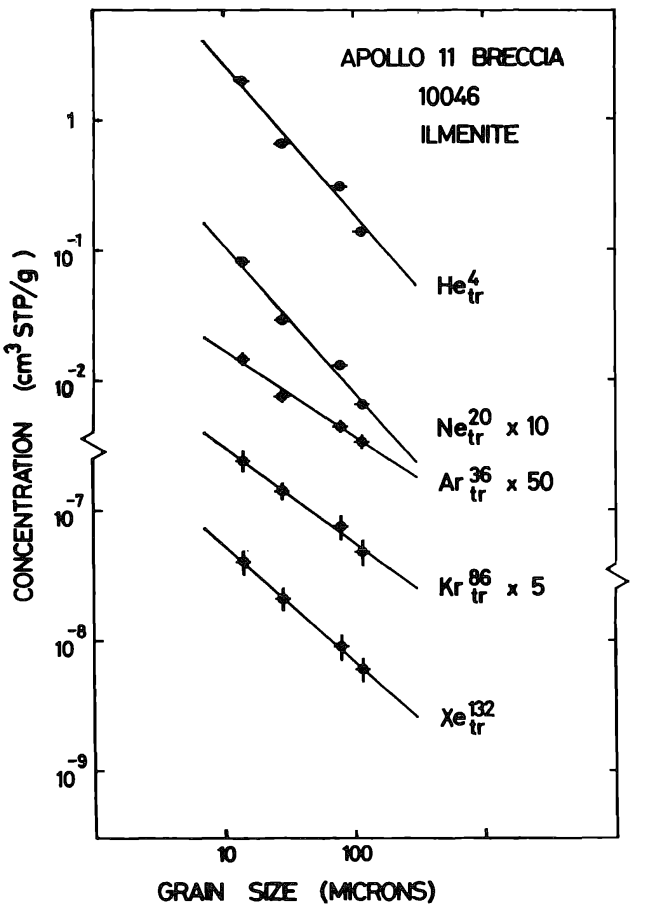

Fig. 3. Grain size dependency of the trapped He^4, Ne^{20}, Ar^{36}, Kr^{86}, and Xe^{132} concentrations in ilmenite separated from the Apollo 11 breccia 10046.

Table 5. Best fit of the measured concentrations $C(Y,d)$ in the different grain sizes d to the equation $C(Y,d) = S_y(d/d_0)^{-n_y}$ ($d_0 = 10\ \mu$).

Samples	S_y: trapped gas concentration in 10 μ fraction					n_y				
	He^4	Ne^{20}	Ar^{36}	Kr^{86}	Xe^{132}	He^4	Ne^{20}	Ar^{36}	Kr^{86}	Xe^{132}
	(10^{-3} cm^3 STP/g)			(10^{-8} cm^3 STP/g)						
Bulk grain size fractions										
10084	305 ± 15	3.15 ± 0.25	0.48 ± 0.05	9.5	5.7	0.64 ± 0.03	0.59 ± 0.04	0.60 ± 0.05	0.55 ± 0.06	0.56 ± 0.04
12001	145 ± 8	2.1 ± 0.1	0.41 ± 0.03	9.1	4.8	0.71 ± 0.03	0.60 ± 0.02	0.56 ± 0.03	0.58 ± 0.02	0.56 ± 0.03
Ilmenite grain size fractions										
10084	1700 ± 170	7.3 ± 0.6	0.21 ± 0.06	4.8	2.1	1.15 ± 0.06	1.11 ± 0.04	0.96 ± 0.15	0.98 ± 0.11	0.82 ± 0.13
12001	1850 ± 350	7.1 ± 1.5	0.22 ± 0.02	4.6	1.95	1.12 ± 0.11	1.10 ± 0.12	0.95 ± 0.06	1.00 ± 0.07	1.02 ± 0.1
10046	2700 ± 700	11.1 ± 2.5	0.35 ± 0.03	6.1	5.3	1.16 ± 0.15	1.13 ± 0.12	0.67 ± 0.06	0.74 ± 0.06	0.89 ± 0.04

S_y represents the trapped gas concentration in a (hypothetical) 10 μ grain size fraction; $-n_y$ the slope of the correlation lines in Figs. 1 to 3.

The bulk grain size fractions separated from 10084 and 12001 show remarkably similar grain size dependencies. However, the n values are nearly a factor of 2 smaller than for the corresponding ilmenites. For the heavy noble gases the reference gas concentrations S_y are similar in the two bulk samples, while for Ne^{20} and especially for He^4 they are higher in 10084 than in 12001. For He and Ne the trapped gas concentrations in the bulk material are up to an order of magnitude lower than in the ilmenite for a grain size of 10 μ. On the other hand, at $d = 10\,\mu$, the bulk material has twice as high Ar, Kr, and Xe concentrations as the ilmenite.

Presuming ideal conditions (e.g., no broken grains, no microbreccia, etc.) the exponent n should be equal to unity for surface correlated gases. This holds quite well for all noble gases in the 10084 and 12001 ilmenite and for He and Ne in the 10046 ilmenite. The bulk samples have n values considerably lower than one. Several explanations are possible:

(1) A systematically increasing dilution of the finer grain size fractions with broken larger grains or grains containing no trapped gases.
(2) A contamination of the coarser grain size fractions with microbreccias.
(3) The presence of a volume correlated component.
(4) A grain size dependent noble gas loss.

The ilmenite grain size fractions were prepared from the corresponding bulk grain size fractions. It is thus improbable that during our sample preparation a contamination of the finer bulk grain size fractions with fragmented grains occurred, without leading to a similar contamination in the ilmenite fractions. The same argument holds for the lunar surface. "Rapid" reworking of the regolith and breaking-up of the larger crystal should influence both the bulk grain size fractions and the ilmenite. A certain discrimination could occur if the ilmenite were more resistant than the bulk material against the specific break-up process. The exposure age of the ilmenite is then expected to be higher than that of the bulk material, which is not in agreement with our measurements (cf. Table 7). A continuous dilution of the lunar regolith by fine, fresh, ilmenite-poor dust can also be considered. No possible source and transport mechanism for such a virgin dust component is, however, apparent, especially considering the time scales involved. An exposure of a thousand years would already saturate the grain surface with trapped solar wind gases and rapid transport and burial (a few microns) of this virgin dust would be necessary.

Equivalent to a dilution of the finer grain sizes with a component free of trapped gases would be a contamination of the coarser grain size fractions with small grains, either adhering to larger grains or as microbreccias. The latter would essentially correspond to a volume correlated component. The coarser grain size fractions indeed contained some composite grains, whereas the finer fractions consisted essentially of single grains. We thus cannot exclude this contamination effect.

If a volume correlated component is present equation (1) must be replaced by:

$$C(Y, d) = S_y \left(\frac{d}{d_0}\right)^{-n_y} + V_y. \qquad (2)$$

V_y is the concentration of the grain size independent volume correlated component. In a log C–log d plot equation (2) is not any more a straight line. The deviation from a straight line in a limited d range is, however, relatively small. Figure 4 shows a best fit of the experimental data for Ar^{36}_{tr} in the 10084 bulk grain size fractions both with equation (1) and (2). For equation (2) $n = 1$ was assumed. It is evident that equation (2), e.g., the assumption of a volume correlated component, gives at least as good a fit to the measured concentrations as the straight line of equation (1). Ar^{36}_{tr} is a typical case for all the bulk grain size fractions since the value of $n_{36} = 0.6$ is very close to the n values of all the other gases.

In analogy to the Ar^{36}_{tr} in 10084 also the other noble gases in the bulk material of 10084 and 12001 could be explained as a mixture of a volume and a surface correlated ($n = 1$) component. A similarly satisfactory agreement of equation (2) with the observed grain size dependence as for Ar^{36} in 10084 can be obtained. As the exponents n_y of equation (1) are approximately identical for all the noble gases the volume correlated component would have to have similar relative abundance ratios as the surface correlated gas. A contamination by microbreccia, as discussed above, would satisfy this requirement.

A grain size dependent diffusion loss seems to us an unlikely explanation of the low n values for the bulk grain size fractions. The similarity of the n for all noble gases requires the same relative gas loss for all noble gases for any given grain size. All the available evidence on the diffusion behavior of the trapped noble gases in lunar material shows that the lighter noble gases have much higher diffusion constants than the heavier ones (Hohenberg *et al.*, 1970; Pepin *et al.*, 1970; Baur *et al.*, 1972). Diffusion loss by thermal heating will thus always give a strong mass fractionation. The loss pattern could, however, be changed if solar wind irradiation and

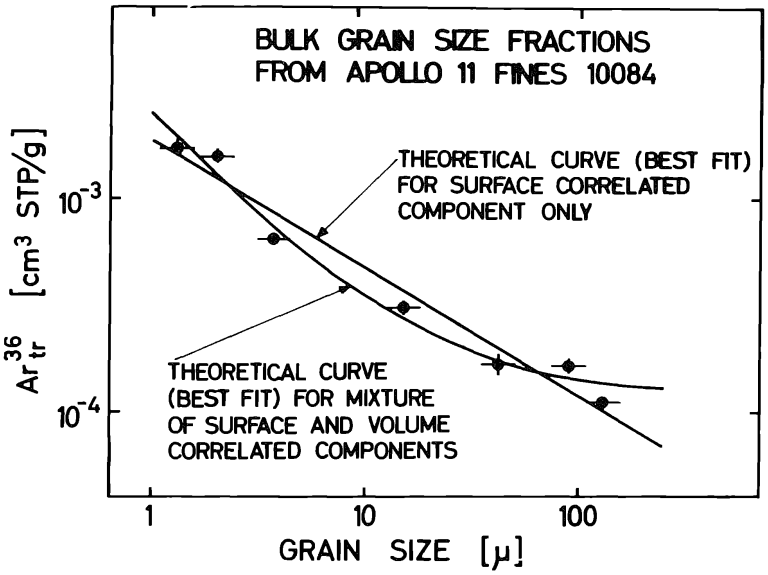

Fig. 4 Comparison of measured grain size dependency for Ar^{36}_{tr} with the theoretical curves expected for purely surface correlated gas ($Ar^{36}_{tr} \propto (d/d_0)^{-0.6}$) and for a mixture of surface and volume correlated gas ($Ar^{36}_{tr} \propto 240\,(d/d_0)^{-1} + 12$). Experimental data from Eberhardt *et al.* (1970).

diffusion loss occurred simultaneously or alternately or if the loss is induced by saturation/sputtering effects.

Flaking-off of the amorphous surface layer (Borg *et al.*, 1971), saturated with trapped solar wind noble gases, could lead to a trapped gas loss independent of mass. If this flaking-off is grain size dependent, then such a process might be a possible explanation for the low n values.

With the present available evidence we cannot decide which of the discussed processes is mainly responsible for making the trapped gas concentration less grain size dependent in the bulk fractions than in the ilmenites. It may well be that several of the above mentioned mechanisms, and perhaps some yet unrecognized ones, have contributed to the decrease in the slope of the grain size dependency curves.

ELEMENTAL ABUNDANCE RATIOS OF TRAPPED GASES

In Table 6 the elemental abundance ratios—averaged over the grain size fractions—are given for the investigated samples (bulk and ilmenite). In two cases a systematic trend of the ratios with grain size is observed. Accordingly, no average value is then given, but the range of observed ratios is indicated in Table 6. In one case [$(Ne^{20}/Ar^{36})_{tr}$ for 12001 ilmenite] a weak grain size dependency may exist (cf. Fig. 5).

The abundance ratios between trapped Ar, Kr, and Xe are quite similar in all five investigated bulk and ilmenite samples. The $(Ar^{36}/Kr^{86})_{tr}$ agree within $\pm 15\%$, the $(Kr^{86}/Xe^{132})_{tr}$ within $\pm 30\%$. The trapping and diffusion behavior of the heavy noble gases in the different minerals must thus be fairly similar. Measurements on bulk grain size fractions ought to be no less reliable than measurements on separated minerals (e.g., ilmenite) for deriving the "true" isotopic and elemental abundances in the heavy trapped gases.

The $(He^4/Ne^{20})_{tr}$ and especially the $(Ne^{20}/Ar^{36})_{tr}$ ratios in the bulk material are 2 to 5 times lower than in the ilmenites. However, for the same type of material (bulk, ilmenite) the elemental abundances are remarkably similar (excluding the two cases of clear grain size dependency). Heavy diffusion loss of trapped He and Ne in the less retentive minerals of the bulk material must have occurred. Normalized to Ar, the bulk material has lost 90% of the trapped He and 80% of the trapped Ne if compared

Table 6. Average elemental abundance ratios of the trapped noble gases in different lunar grain size fractions.

Sample	He^4/Ne^{20}	Ne^{20}/Ar^{36}	Ar^{36}/Kr^{86}	Kr^{86}/Xe^{132}
	($\times 10^3$)			
Bulk grain size fractions				
10084	96 ± 18	6.8 ± 2.0	5.1 ± 1.2	1.65 ± 0.55
12001	49 – 87	5.1 ± 0.7	4.5 ± 0.3	1.9 ± 0.1
Ilmenite grain size fractions				
10084	218 ± 8	27.4 ± 4.3	4.7 ± 0.9	1.8 ± 0.25
12001	253 ± 10	26.8 ± 5.4	5.2 ± 0.5	2.4 ± 0.2
10046	231 ± 13	9.7 – 28.5	6.1 ± 0.7	1.45 ± 0.2

The errors are standard deviations and are thus a direct measure for the scattering of the measured ratios within the individual grain size fractions relative to the average value. A range of values indicates a systematic trend with grain size.

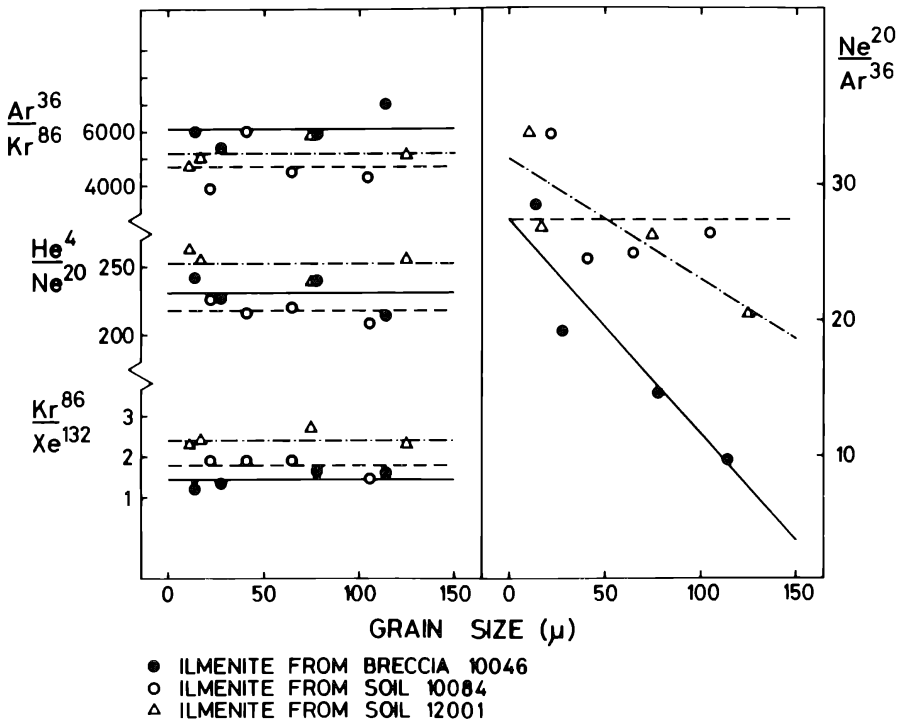

Fig. 5. Elemental abundance ratios of the trapped noble gases in the 10084, 12001, and 10046 ilmenite fractions as function of the grain size. For error see Table 1 to 3.

with the ilmenite. The ilmenite itself has probably also lost some He and perhaps Ne (see subsequent discussion). The heavy He and Ne diffusion loss in the bulk material is also evident when absolute gas concentrations in the same grain size of bulk and ilmenite are compared (cf. Table 5). It has to be expected that the large diffusion losses have altered the isotopic composition of trapped He and Ne in the bulk material. Thus data obtained on bulk lunar fine material are not representative for the elemental and isotopic composition of the light noble gases which were originally trapped in the lunar material.

$(He^4/Ne^{20})_{tr}$ *variation in 12001 bulk grain size fractions*

A volume correlated component of trapped Ne, Ar, Kr, and Xe could explain the systematic decrease of $(He^4/Ne^{20})_{tr}$ with grain size.

More severe He diffusion loss in the larger grain sizes is the other possible explanation. The grain size dependent He loss does not require a grain size dependent thermal history. A more or less systematic change in the mineralogical composition or the glass content in the bulk grain size fractions bb-12 to bb-18 could lead to systematically varying loss factors.

$(Ne^{20}/Ar^{36})_{tr}$ *variation in the 10046 ilmenite grain size fractions*

In Fig. 5 the grain size dependency of the trapped gas elemental abundance ratios in the investigated ilmenite fractions are shown. It is evident that these ratios, except

for $(Ne^{20}/Ar^{36})_{tr}$, are essentially independent of grain size. The $(Ne^{20}/Ar^{36})_{tr}$ ratio in the 10046 ilmenite is strongly grain size dependent, increasing systematically by a factor of 3 from the coarsest to the finest fraction. A weaker grain size dependency is also present for the 12001 ilmenite. The 10084 ilmenite shows no systematic trend in the $(Ne^{20}/Ar^{36})_{tr}$ ratio, except that the finest fraction has a somewhat higher ratio. Two different models could explain the systematic trend in these elemental abundance ratios, and we would like to discuss them specifically for the 10046 ilmenite:

Model A: A volume correlated Ar, Kr, *and* Xe *component*

The trapped gas concentration in the different grain sizes is described by equation (2). The $(He^4/Ne^{20})_{tr}$ ratio is constant within $\pm 7\%$ and shows no grain size dependency, and thus no volume correlated He_{tr} and Ne_{tr} components are present ($V_4 = V_{20} = 0$). The constancy of the $(He^4/Ne^{20})_{tr}$ ratio also indicates that the grain size dependency of the surface correlated component is identical for He^4_{tr} and Ne^{20}_{tr} ($n_4 = n_{20}$, cf. Table 5). If we assume that the surface correlated component of Ar^{36}_{tr}, Kr^{86}_{tr}, and Xe^{132}_{tr} have the same grain size dependency ($n_{36} = n_{86} = n_{132} = n_4 = n_{20}$), we obtain

$$\frac{C(Y, d)}{C(X, d)} = \frac{S_y}{S_x} + \frac{V_y}{C(X, d)}, \tag{3}$$

where X is He^4_{tr} or Ne^{20}_{tr} and Y is Ar^{36}_{tr}, Kr^{86}_{tr} or Xe^{132}_{tr}. Equation (3) represents a straight line if $C(Y, d)/C(X, d)$ is plotted versus $1/C(X, d)$. The ratio S_y/S_x is the ratio of the surface correlated component. For $X = Ne^{20}_{tr}$ and $Y = Ar^{36}_{tr}$ equation (3) reads:

$$\left(\frac{Ar^{36}}{Ne^{20}}\right)_{tr} = \left(\frac{Ar^{36}}{Ne^{20}}\right)_{sc} + \frac{V_{36}}{Ne^{20}_{tr}} \tag{4}$$

Figure 6 shows the corresponding correlation diagram. The experimental points define indeed a straight line within the experimental uncertainties. From Fig. 6 and the corresponding correlations for Kr^{86}_{tr} and Xe^{132}_{tr} the concentration of the volume correlated component and the elemental abundance ratios in the surface correlated component can be calculated.

Model B: All trapped gases are surface correlated, but constant amounts of trapped He *and* Ne *were lost*

In this model it is assumed that in all ilmenite fractions of rock 10046 a constant amount per unit weight of He^4_{tr} and Ne^{20}_{tr} was lost. Then the remaining concentration of a noble gas can be written as:

$$C(Y, d) = S_y \left(\frac{d}{d_0}\right)^{-n_y} - L_y. \tag{5}$$

The first term in equation (5) represents the surface correlated gas originally present, the second term, L_y, represents the lost gas. Since $(Ar^{36}/Kr^{86})_{tr}$ and $(Kr^{86}/Xe^{132})_{tr}$

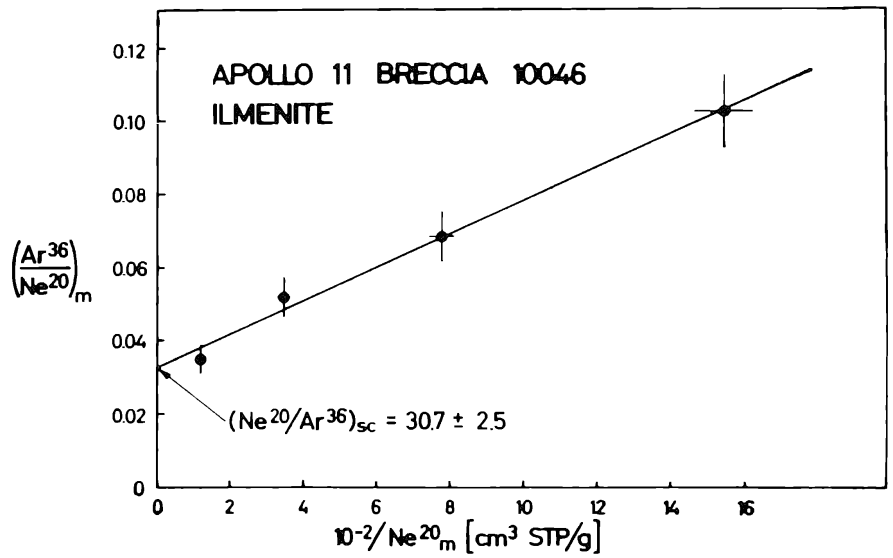

Fig. 6. Correlation between the $(Ar^{36}/Ne^{20})_m$ ratio and $1/Ne^{20}_m$ in the 10046 ilmenite grain size fractions. The excellent correlation proves that the grain size dependent $(Ne^{20}/Ar^{36})_{tr}$ ratio in these samples can be explained by the presence of a volume correlated Ar^{36}_{tr} component.

are approximately constant, we take $L_{36} = L_{86} = L_{132} = 0$. We assume again that all n_y are equal and obtain

$$\frac{C(X, d)}{C(Y, d)} = \frac{S_x}{S_y} - \frac{L_x}{C(Y, d)} . \tag{6}$$

Here X is He^4_{tr} or Ne^{20}_{tr} and Y is Ar^{36}_{tr}, Kr^{86}_{tr} or Xe^{132}_{tr}. Equation (6) represents again a straight line if $C(X, d)/C(Y, d)$ is plotted versus $1/C(Y, d)$ and S_x/S_y is the isotopic ratio of the surface correlated component. A detailed analyses of the data shows that also this model could give a satisfactory explanation of the experimental data.

Discussion

The two models mentioned and the assumptions made have to be considered as limiting cases. Some assumptions, such as the absence of a He and Ne volume component, could be relaxed to some extent. Also, a mixture of the two models would equally well represent the experimental data.

Model B requires a constant He and Ne loss in all fractions. This gas loss could have occurred during the compaction process leading from the loose soil to the breccia. The surface correlated gases are concentrated in a layer approximately 1000 Å thick below the surface of the individual grains (Eberhardt *et al.*, 1970). The diffusion path is thus *not* grain size dependent, except for submicron sized grains. As Eberhardt *et al.* (1970) have shown, heavy saturation occurs in the regolith. The gas concentration in the surface layer is then not grain size dependent. A constant gas

loss per gram of material would thus imply that the larger grains lost relatively more gas from the saturated surface layer than the smaller ones. Such a grain size dependent loss requires a grain size dependent temperature history, the larger grains having been subjected to a higher temperature or heated for a longer time.

Model B leads to an exponent $n \approx 0.65$ for the surface correlated gas, whereas model A gives $n \approx 1.15$ which is much closer to the expected value of 1, and very similar to the values observed in the ilmenite grain size fractions of the lunar fine material. Additional assumptions for explaining the low n values of model B would be required. This is a serious drawback inherent to model B which does not arise with model A.

The Ar, Kr, and Xe volume component, required by model A, could be explained in several ways. The volume component could have originated during the crystallization and cooling or a later reheating of the ilmenite, provided a sufficient partial pressure of Ar, Kr, and Xe was present. Solar wind particles implanted at elevated temperatures, or alternating cycles of bombardment and heating might also lead to a volume component of the heavier noble gases. He and Ne diffuses much easier and could have been completely lost. The loss of the heavier noble gases will be less complete and part of the gases trapped at the surface will diffuse into the interior of the grains, slowly building up a volume component. Channeling effects (Piercy *et al.*, 1964), leading to much longer ranges for a very small fraction of the impinging solar wind ions, could also contribute to the build up of a volume component. Solar flare particles are another possible source for a volume component in millimeter and submillimeter sized lunar regolith particles. The present day average solar flare flux of 100 cm^{-2} sec^{-1} (Finkel *et al.*, 1971) would lead, if quantitatively retained, to an Ar^{36}_{tr} volume component of only 0.5×10^{-8} cm^3 STP/g (8×10^8 yr exposure age, 20 cm average shielding, cf. discussion of $(Xe^{131}/Xe^{126})_{sp}$ ratios). This amount is 4 orders of magnitude smaller than the required volume component for 10046.

If we assume a genetic relationship between the regolith material and the breccia, then all the above discussed processes would also predict a volume correlated component in the regolith. No such component is evident in the 10084 ilmenite.

We must also consider the possibility that the volume correlated Ar, Kr, and Xe component is not contained in the ilmenite but associated with an impurity in our mineral separates. Our 10046 ilmenite fractions are at least 95% pure and this associated component would thus have to have at least concentrations of $90{,}000 \times 10^{-8}$ cm^3 STP Ar^{36}/g, 13×10^{-8} cm^3 STP Kr^{86}/g and 6×10^{-8} cm^3 STP Xe^{132}/g. Much higher trapped gas concentrations are found in the micron sized lunar fine material, but of course together with correspondingly higher trapped He and Ne concentrations. Unaltered, micron or submicron sized lunar fine material attached to the ilmenite grains could thus not explain the volume component. However, if some heating of this fine accessory material occurred most of the He and Ne might have been lost. A difference in the diffusion coefficients between the ilmenite and the accessory material would be required to explain the absence of diffusion loss in the ilmenite. This requirement would be fulfilled if this accessory phase consisted of glassy lunar material which shows much poorer gas retention properties.

Exposure Ages and Spallation Produced Noble Gases

The calculation of the concentration and isotopic composition of the spallation produced noble gases and the exposure ages is hampered by the required large corrections for the trapped gas. Furthermore, for some isotopes the target element concentrations are not known. Our best estimates for the average exposure ages are given in Table 7. These exposure ages were calculated as follows:

12001, unseparated sample

Assuming $(Xe^{126}/Xe^{136})_{tr} = 0.0141$ (this paper) and $Xe^{136}_{sp} \equiv 0$ we calculate $Xe^{126}_{sp} = 185 \times 10^{-12}$ cm³ STP/g. From rocks 10017 and 10071 Eberhardt *et al.* (1972) obtained a production rate of 1.3×10^{-21} cm³ STP Xe^{126}_{sp}/yr "ppm Ba." This production rate includes the contribution from all target elements, i.e., Ba and the REE. For convenience, normalization to Ba alone was used. We denote this by writing ppm Ba in quotation marks. The REE contribute only approximately 25% of the total Xe^{126}_{sp} (Eberhardt *et al.*, 1970a) and the production rate given above is valid within ±10% as long as the Ba/REE ratio is the same as in rocks 10017 and 10071 to within ±40%. In rocks 10017 and 10071 the Ba/Ce ratios are 4.0 and 3.9, respectively (Gast *et al.*, 1970). In 12001 this ratio is 4.2 (Schnetzler and Philpotts, 1971). With a Ba content of 370 ppm (Schnetzler and Philpotts, 1971) we obtain for the 12001 bulk sample an exposure age of 390×10^6 yr.

12001, bulk grain size fractions

From the $(Xe^{126}/Xe^{130})_m$ versus "Ba"/Xe^{130}_m correlation (cf. Fig. 8) we obtain Xe^{126}_{sp}/"Ba" = $(0.57 \pm 0.015) \times 10^{-12}$ cm³ STP/ppm. The average Ba/Ce ratio in the bulk grain size fractions is 3.6, again very similar to rocks 10017 and 10071. With the production rate given above we obtain $T_E = 440 \times 10^6$ yr.

12001, ilmenite grain size fractions

From the slope of the correlation line in the $(Ar^{36}/Ar^{38})_m$ versus $1/Ar^{38}_m$ correlation diagram we obtain $Ar^{38}_{sp} = (24 \pm 4) \times 10^{-8}$ cm³ STP/g. With an Ar^{38}_{sp} production rate of 8.1×10^{-16} cm³ STP/yr g ilmenite (Eberhardt *et al.*, 1972) an exposure age of 300×10^6 yr is calculated.

10046, ilmenite grain size fractions

From the slope of the correlation line in the $(Ar^{36}/Ar^{38})_m$ versus $1/Ar^{38}_m$ correlation diagram we obtain $Ar^{38}_{sp} = (70 \pm 15) \times 10^{-8}$ cm³ STP/g and exposure age of 860×10^6 yr results.

An average Kr^{83}_{sp} content of 1450×10^{-12} cm³ STP/g is obtained if the measured $(Kr^{83}/Kr^{86})_m$ ratios are individually corrected for trapped gas. The isotopic composition for trapped Kr as derived in this paper was used. With the average production rate of 1.95×10^{-18} cm³ Kr^{83}_{sp}/yr g ilmenite

Table 7. Average exposure ages (in million years) of the investigated fractions.

	10084		12001			10046
	Bulk grain size fractions	Ilmenite grain size fractions	Unseparated sample	Bulk grain size fractions	Ilmenite grain size fractions	Ilmenite grain size fractions
Average exposure age (m.y.)	520	380	390	440	300	800

The exposure ages for the fractions separated from the Apollo 11 fines 10084 are from Eberhardt *et al.* (1970) (see also discussion in text). We estimate that the exposure ages are accurate within ±20% (neglecting the uncertainties in the production rates).

measured in ilmenite concentrates of rocks 10003 and 10017 (Eberhardt *et al.*, 1972 and yet unpublished results) we estimate from the average Kr^{83}_{sp} content an exposure age of 740 × 10^6 yr. The exposure ages derived from Ar^{38}_{sp} and Kr^{83}_{sp} agree fairly well. We adopt an exposure age of 800 × 10^6 yr for breccia 10046.

10084, ilmenite grain size fractions

The Ar^{38}_{sp} content given in Table 9 of Eberhardt *et al.* (1970) for the ilmenite separated from the Apollo 11 fines 10084 is incorrect. From the slope of the correlation line in Fig. 8 of Eberhardt *et al.* (1970) we calculate an Ar^{38}_{sp} content of (31 ± 7) × 10^{-8} cm^3 STP/g ilmenite for the sample 10084. This corresponds to an exposure age of 380 × 10^6 yr.

The exposure ages of the two soil samples are similar, with an indication that soil 12001 was, on the average, irradiated for a somewhat shorter time. Both ilmenite fractions have consistently lower exposure ages than the bulk fractions.

The ilmenite from breccia 10046 is older by a factor of more than two than the soil ilmenites. Assuming that the parent material of the breccia had a similar irradiation history as the 10084 and 12001 samples we can conclude that the compaction of breccia 10046 from loose soil material must have occurred at least 400 to 500 m.y. ago. Consequently, we estimate that the trapped solar wind particles are, on the average, at least 400 to 500 m.y. older than in the two soil samples.

Concentrations of spallation noble gases and the relative isotopic abundances of the spallation components are compiled in Table 8. Spallation concentrations were derived from the correlation between isotopic ratios and inverse concentrations. All isotopic compositions are derived from the slope of the correlation line in the usual two isotope ratio correlation diagrams [e.g., $(Xe^{124}/Xe^{126})_{sp}$ from the correlation between $(Xe^{124}/Xe^{132})_m$ and $(Xe^{126}/Xe^{132})_m$]. For error definition see next chapter.

The Kr spallation yields are similar to those observed in lunar rocks (Marti *et al.*, 1970; Pepin *et al.*, 1970; Hohenberg *et al.*, 1970; Eberhardt *et al.*, 1972). The observed variations are probably due to differences in the irradiation hardness and the Sr/Zr ratio (Eberhardt *et al.*, 1970a; Schwaller *et al.*, 1971). The $(Kr^{80}/Kr^{78})_c$ ratio could also be influenced by epithermal neutron capture on Br (Marti *et al.*, 1966; Eugster *et al.*, 1969; Lugmair and Marti, 1972).

Table 8. Concentrations and isotopic composition of the cosmogenic components in the investigated samples.

	12001		10046
	Bulk grain size fractions	Ilmenite grain size fractions	Ilmenite grain size fractions
Ne^{21}_{sp}	51 ± 10	11 ± 3	14 ± 4
Ar^{38}_{sp}	58 ± 20	24 ± 4	70 ± 15
$(Kr^{80}/Kr^{78})_c$	2.75 ± 0.15	2.18 ± 0.05	2.59 ± 0.06
$(Kr^{82}/Kr^{78})_c$	3.1 ± 0.6	3.16 ± 0.08	4.4 ± 0.2
$(Kr^{83}/Kr^{78})_{sp}$	4.3 ± 0.4	4.2 ± 0.4	5.2 ± 0.5
$(Xe^{124}/Xe^{126})_{sp}$	0.556 ± 0.012	0.548 ± 0.01	0.575 ± 0.014
$(Xe^{128}/Xe^{126})_c$	1.54 ± 0.04	1.58 ± 0.10	1.96 ± 0.08
$(Xe^{130}/Xe^{126})_{sp}$	0.96 ± 0.09	0.66 ± 0.15	1.23 ± 0.27
$(Xe^{131}/Xe^{126})_c$	5.0 ± 0.2	4.6 ± 0.2	5.6 ± 0.4

All concentrations in units of 10^{-8} cm^3 STP/g. For spallation Kr and Xe concentrations in some of the fractions see text.

The isotopic composition of the spallation Xe is in good agreement with the spectra observed in corresponding lunar rocks (Marti *et al.*, 1970; Pepin *et al.*, 1970; Hohenberg *et al.*, 1970; Eberhardt *et al.*, 1972). From the observed $(Xe^{131}/Xe^{126})_c$ ratio of approximately 5 it follows that these samples were not irradiated at the surface for most of their exposure time (cf. Eberhardt *et al.*, 1970a; Schwaller *et al.*, 1971; Eberhardt *et al.*, 1971). For surface irradiation a $(Xe^{131}/Xe^{126})_c$ ratio of 3 or below would be expected, for irradiation at considerable depth the ratio could be as high as 9. The intermediate ratio of 5 corresponds to an average shielding of approximately 20 g cm^{-2} or an average burial depth in the regolith of approximately 10 cm.

Isotopic Composition of Trapped Gases

Basically the same approach as used by Eberhardt *et al.* (1970) is utilized to make the necessary corrections in the measured isotope ratios in order to obtain the true trapped gas isotopic compositions. A more detailed discussion of the methods can be found in the above mentioned paper and only a short summary of the necessary corrections will be given here. If not otherwise stated, spallation isotope production rates used are from Eberhardt *et al.* (1972).

It is important to point out that the two basic approaches used by Eberhardt *et al.* (1970) are not completely equivalent. Correcting measured isotopic ratios individually for the cosmogenic, radiogenic, and fission components will give the isotopic composition of the total trapped component; i.e., the weighted average of the isotopic composition of the surface correlated and the volume correlated components. On the other hand the use of a correlation diagram, as introduced by Eberhardt *et al.* (1970), will give the isotopic composition of the surface correlated component. The two approaches are equivalent if no volume correlated trapped component is present ($n \approx 1$, i.e., ilmenite grain size fractions) or if the isotopic composition of the volume correlated and the surface correlated trapped gas are the same.

The errors given for a trapped gas isotopic composition obtained by individually correcting measured isotope ratios is the standard deviation of the individually corrected values, as determined from their distribution about the average. For the isotopic composition of the surface correlated gas derived by extrapolation, the standard deviation of the ordinate intercept is given as error. The same error definition was used in the case of spallation gas concentrations determined from the slope of the correlation diagrams. With this error definition the individual experimental errors are automatically taken into account, with the possible exception of systematic errors in the measured ratios or concentrations (possible systematic errors are, however, included in the errors given in Tables 1 to 3). As we mainly compare results obtained at Bern with identical experimental techniques, such systematic errors will essentially cancel out. Our error definition does not include possible uncertainties in the necessary assumptions, and this point will have to be discussed specifically for each result.

Helium

12001, unseparated sample. With an exposure age of 390 × 10^6 yr and a production rate of 10^{-14} cm^3 STP He^3/g yr we calculate He^3_{sp} = 390 × 10^{-8} cm^3 STP/g. However, He^3_{sp} diffusion loss is frequent in lunar material (Hintenberger *et al.*, 1971; Eberhardt *et al.*, 1972) and this concentration

must be considered as an upper limit for the true He^3_{sp} content. We estimate $He^4_r = 110{,}000 \times 10^{-8}$ cm³ STP/g, corresponding to an "age" of 2.5×10^9 yr (U and Th concentrations from Wänke *et al.*, 1971). With these assumptions we obtain $2290 \leq (He^3/He^4)_{tr} \leq 2630$.

12001, bulk grain size fractions. Similar to the unseparated sample we can only give an upper limit of 440×10^{-8} cm³ STP/g for the spallation He^3 content. This uncertainty makes an evaluation of the $(He^4/He^3)_{tr}$ ratio in the coarser grain size fractions impossible. For the two finest fractions bb-17 and bb-18 the correction for He^3_{sp} is small ($He^3_{sp}/He^3_m < 2.5\%$) and we estimate $2210 \leq (He^4/He^3)_{tr} \leq 2540$.

12001, ilmenite grain size fractions. With an exposure age of 300×10^6 yr and a He^3_{sp} production rate of 0.9×10^{-14} cm³ STP/yr g ilmenite we obtain $He^3_{sp} = 270 \times 10^{-8}$ cm³ STP/g ilmenite. From the measurements on ilmenite separated from rocks 10071 and 10003 (Eberhardt *et al.*, 1972, and yet unpublished results) it is evident that He^4_r is $<1\%$ even for the coarsest ilmenite fraction and can be neglected. After correcting for spallation He^3 we obtain for the bb-26, bb-37, bb-52, and bb-57 grain size fractions $(He^4/He^3)_{tr}$ ratios of 2790; 2700; 2610; and 2710, respectively, and an average value of 2700 ± 70.

10046, ilmenite grain size fractions. The exposure age of 800×10^6 yr corresponds to $He^3_{sp} = 720 \times 10^{-8}$ cm³ STP/g ilmenite. Again He^4_r can be neglected. After correcting for the spallation He^3 we obtain for the four grain size fractions DA-14, DA-15, DA-16, and DA-17 ratios $(He^4/He^3)_{tr}$ of 3280; 3020; 2890; and 3040, respectively. The average value is 3060 ± 160.

Neon

12001, unseparated sample. The exposure age of the unseparated 12001 sample is 10% lower than the average age of the bulk grain size fractions (cf. Table 7). Thus we expect in the 12001 unseparated sample a 10% lower Ne^{21}_{sp} content than in the grain size fractions. With $Ne^{21}_{sp} = 45 \times 10^{-8}$ cm³ STP/g we obtain $(Ne^{20}/Ne^{22})_{tr} = 12.43$ and $(Ne^{22}/Ne^{21})_{tr} = 33.0$.

12001, bulk grain size fractions. From the correlation between $(Ne^{22}/Ne^{21})_m$ and $1/Ne^{21}_m$, we obtain $(Ne^{22}/Ne^{21})_{sc} = 31.5 \pm 1.1$.

From the same correlation diagram an average Ne^{21}_{sp} content of $(51 \pm 10) \times 10^{-8}$ cm³ STP/g is calculated. Correcting for the corresponding amount of Ne^{22}_{sp} we calculate in the fractions bb-12 to bb-18 ratios $(Ne^{20}/Ne^{22})_{tr}$ of 12.56; 12.31; 12.52; 12.38; 12.55; 12.54; and 12.67, respectively. The correction is always smaller than 1.6% and less than 0.3% for the three finest fractions. From all fractions we obtain an average $(Ne^{20}/Ne^{22})_{tr} = 12.50 \pm 0.12$.

12001, ilmenite grain size fractions. From the correlation between $(Ne^{22}/Ne^{21})_m$ and $1/Ne^{21}_m$, we obtain $(Ne^{22}/Ne^{21})_{sc} = 32.0 \pm 0.4$. This value is in good agreement with the measured ratio in the two finest grain size fractions which contain negligible amounts of Ne^{21}_{sp}. From the slope of the correlation line $Ne^{21}_{sp} = 11 \times 10^{-8}$ cm³ STP/g is calculated. Correcting for the corresponding amounts of Ne^{22}_{sp} we obtain for bb-26, bb-37, bb-52, and bb-57 ratios $(Ne^{20}/Ne^{22})_{tr}$ of 12.67; 12.72; 12.91; and 13.00, respectively. The average of 12.83 ± 0.16 is slightly lower than the value of $(Ne^{20}/Ne^{22})_{sc} = 12.96 \pm 0.06$ calculated from the correlation between $(Ne^{20}/Ne^{22})_m$ and $1/Ne^{22}_m$.

10046, ilmenite grain size fractions. From the correlation between $(Ne^{22}/Ne^{21})_m$ and $1/Ne^{21}_m$, we obtain $(Ne^{22}/Ne^{21})_{sc} = 31.4 \pm 0.4$. This is again in good agreement with the measured ratios of the finest two fractions which contain negligible amounts of Ne^{21}_{sp}. The slope of the correlation lines gives $Ne^{21}_{sp} = 14 \times 10^{-8}$ cm³ STP/g. Correcting for the corresponding amounts of Ne^{22}_{sp} we obtain for DA-14 to DA-17 ratios $(Ne^{20}/Ne^{22})_{tr}$ of 12.64; 12.56; 12.50; and 12.81, respectively. The average is 12.63 ± 0.13.

Argon

12001, bulk grain size fractions. From the $(Ar^{36}/Ar^{38})_m$ versus $1/Ar^{38}_m$ correlation diagram, we obtain $(Ar^{36}/Ar^{38})_{sc} = 5.29 \pm 0.03$. From the correlation between $(Ar^{40}/Ar^{36})_m$ and $1/Ar^{36}_m$, a value of $(Ar^{40}/Ar^{36})_{sc} = 0.42 \pm 0.02$ is derived.

12001, ilmenite grain size fractions. From the $(Ar^{36}/Ar^{38})_m$ versus $1/Ar^{38}_m$ correlation diagram, we obtain $(Ar^{36}/Ar^{38})_{sc} = 5.33 \pm 0.03$. The correlation between $(Ar^{40}/Ar^{36})_m$ and $1/Ar^{36}_m$ gives $(Ar^{40}/Ar^{36})_{sc} = 0.37 \pm 0.05$.

10046, ilmenite grain size fractions. From the two corresponding correlations, we obtain $(Ar^{36}/Ar^{38})_{sc} = 5.33 \pm 0.03$ and $(Ar^{40}/Ar^{36})_{sc} = 1.35 \pm 0.14$.

Krypton

12001, bulk grain size fractions. The use of a correlation diagram, such as $(Kr^{78}/Kr^{86})_m$ versus $1/Kr^{86}_m$ for deducing the $(Kr^{78}/Kr^{86})_{sc}$ ratio, implies that the nontrapped Kr^{78} and Kr^{86} concentrations (e.g., Kr^{78}_{sp}) are the same in all grain size fractions. A necessary condition is thus the equality of the target element concentrations in all grain size fractions. This assumption is certainly valid for spallation argon in the ilmenites, as the important target elements Ti and Fe are main constituents. If trace elements are the major target elements, possible systematic or random variations with grain size must be considered.

In the five finest bulk grain size fractions we have measured the Sr and Zr concentrations. If [Sr] is the Sr abundance and [Zr] the Zr abundance, then we estimate from spallation theory (Geiss *et al.*, 1962; $n = 2$) that the concentration of a spallation Kr isotope is proportional to [Sr] + 0.8 [Zr] [assuming $Y/Zr = 0.3$; cf. Morrison *et al.* (1971); Wänke *et al.* (1971)]. A correlation diagram between a measured Kr isotope ratio $(Kr^M/Kr^{86})_m$ and ([Sr] + 0.8 [Zr])/Kr^{86}_m will then give a straight line even if the target element concentration is different in different grain sizes. The ordinate intercept gives the isotopic composition of the surface correlated gas and the slope of the correlation line essentially the exposure age. This is true if two assumptions are fulfilled: (1) The gases in all fractions

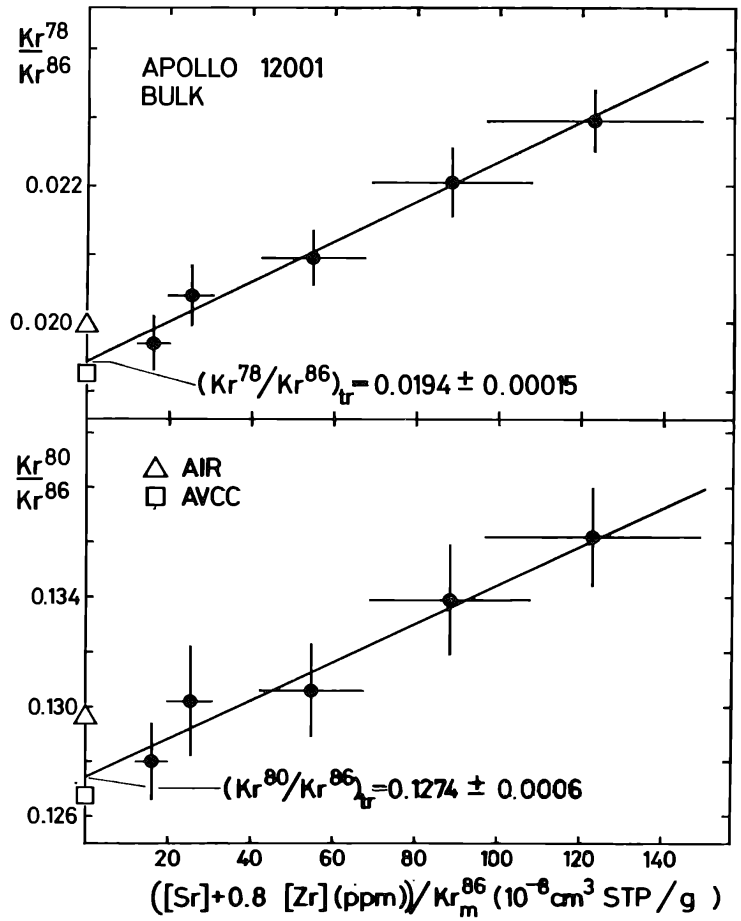

Fig. 7. Correlation between the measured Kr^{78}/Kr^{86} and Kr^{80}/Kr^{86} ratios for the 12001 bulk grain size samples bb-14 to bb-18 and ([Sr] + 0.8 [Zr])/Kr^{86}_m. The factor [Sr] + 0.8 [Zr] compensates the variable chemical composition in the different grain size fractions.

are a mixture with different mixing ratios of the same two components (trapped and "spallation"). (2) The exposure age of all fractions is the same.

Figure 7 shows the correlation diagram for the evaluation of the $(Kr^{78}/Kr^{86})_{sc}$ and $(Kr^{80}/Kr^{86})_{sc}$ ratios. The isotopic composition of the trapped Kr, as derived from such diagrams, is given in Table 11. It is important to point out that the factor 0.8 for the relative production cross section of Zr does not enter critically in the calculation for the trapped ratios. Assuming $Kr_{sp} \propto [Sr] + 1.6[Zr]$ would change the $(Kr^{78}/Kr^{86})_{sc}$ ratio by less than 0.2% and all other ratios by less than 0.1%.

Xenon

12001, bulk grain size fractions. The isotopic composition of surface correlated Xe is obtained from correlation diagrams. Similar to the case of krypton, variations in the target element concentrations are taken into account by correlating the measured isotopic ratios with the Ba/Xe_m^{130} ratio. Ba and the REE are the main target elements for the production of spallation Xe. The Ba/Ce ratio is the same within ±15% in the three fractions bb-14, bb-16, and bb-18. The Ba concentration is thus representative for the target element concentration (cf. discussion on exposure age of 12001 bulk sample).

The correction for the variability in the target element abundances is important for the 12001 bulk grain size fractions. This is evident from Fig. 8 where the correlations of the measured $(Xe^{126}/Xe^{130})_m$ ratio both with $1/Xe_m^{130}$ and with Ba/Xe_m^{130} are shown. The two correlation lines are different and the use of the $(Xe^{126}/Xe^{130})_m$ versus $1/Xe_m^{130}$ correlation line would give a 30% higher $(Xe^{126}/Xe^{130})_{sc}$ ratio than the barium corrected diagram. The variable chemistry is of similar importance for the evaluation of $(Xe^{124}/Xe^{130})_{sc}$ and $(Xe^{128}/Xe^{130})_{sc}$. In Table 12 the isotopic composition of the trapped Xe in the 12001 bulk grain size fractions are compiled. All ratios were calculated from correlation with the Ba/Xe_m^{130} ratio.

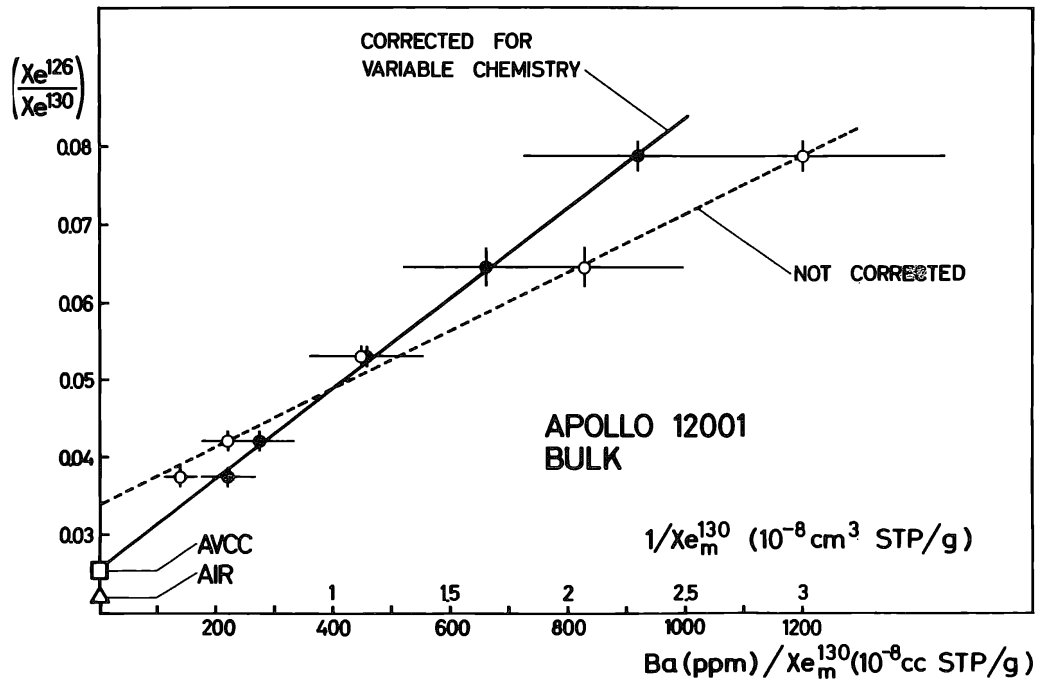

Fig. 8. Correlation between the measured Xe^{126}/Xe^{130} ratios and $1/Xe_m^{130}$ (dashed line) and $[Ba]/Xe_m^{130}$ (solid line). The variable target element concentration in the different grain sizes is automatically compensated for by correlating the $(Xe^{126}/Xe^{130})_m$ ratio with the $[Ba]/Xe_m^{130}$ ratio. The importance of using this refined evaluation method for obtaining the isotopic composition of the surface correlated trapped gas from the measurements on the 12001 bulk grain size fractions is evident from this figure.

Discussion of Isotopic Composition of Trapped Gases

Helium

There is an excellent agreement between the $(He^3/He^4)_{tr}$ ratios in the 10084 and 12001 ilmenites (Table 9) (in this discussion we shall preferably use ratios with the heavier isotope in the denominator). The ilmenite of breccia 10046 shows a distinctly lower ratio. This systematic difference is also apparent if the measured ratios are directly compared. The $(He^4/Ne^{20})_{tr}$ ratio of 10046 is intermediate between the two soils. Therefore, helium diffusion losses, if any, must be similar in all three ilmenites. It is thus very unlikely that the low $(He^3/He^4)_{tr}$ ratio in 10046 is due to a different diffusion history of the trapped solar wind particles in this sample.

The He^3/He^4 ratio in the solar wind is variable (Bame *et al.*, 1968; Geiss *et al.*, 1970, 1971a). The most reliable estimate for the average ratio in the present day solar wind can be obtained from the observed correlation between the He^3/He^4 ratio and the magnetic index K_p (Geiss *et al.*, 1971a). The soil ilmenite $(He^3/He^4)_{tr}$ is slightly lower than the solar wind value, but, within the experimental uncertainty, they would still agree. However, this comparison is rather futile as the influence of the unknown trapping probability of ilmenite for the solar wind ions, of the heavy saturation and of the possible He diffusion loss on the $(He^3/He^4)_{tr}$ ratio in the ilmenite has not yet been investigated. The low $(He^4/Ne^{20})_{tr}$ ratio in the ilmenite, as compared with the present day solar wind value, must be taken as an indication that the $(He^3/He^4)_{tr}$ ratio in the ilmenite might have been lowered by the same processes which changed the $(He^4/Ne^{20})_{tr}$ ratio. If such processes are taken into account, a still better agreement between the present day solar wind He^3/He^4 and the $(He^3/He^4)_{tr}$ in the ilmenite might result.

The trapped gases in aubritic meteorites are also surface correlated and located at the surface of the individual grains (Eberhardt *et al.*, 1965, 1965a). They most likely represent trapped old solar wind particles or similar low energy ions. The $(He^3/He^4)_{tr}$ ratio in the aubrites is distinctly higher than in the lunar ilmenites. The $(He^4/Ne^{20})_{tr}$ ratio is intermediate between the ilmenite and present day solar wind

Table 9. Comparison of elemental and isotopic abundance ratios in different reservoirs of trapped solar wind particles with average composition in present day solar wind (Geiss *et al.*, 1971a).

Reservoir	He^4/Ne^{20}	Ne^{20}/Ar^{36}	He^3/He^4 ($\times 10^{-4}$)	Ne^{20}/Ne^{22}	Ne^{21}/Ne^{22} ($\times 10^{-2}$)
Trapped solar wind in					
10084 ilmenite	218 ± 8	27.4 ± 4	3.68 ± 0.12	12.85 ± 0.1	3.22 ± 0.08
12001 ilmenite	253 ± 10	26.8 ± 5	3.70 ± 0.1	12.9 ± 0.1	3.13 ± 0.04
10046 ilmenite	231 ± 13	—	3.27 ± 0.17	12.65 ± 0.15	3.18 ± 0.04
Aubritic meteorites	380 ± 70	~22	2.50 ± 0.30	12.5 ± 0.6	—
For comparison					
Present day solar wind	600 ± 150	37^{+10}_{-5}*	4.00 ± 0.45	13.6 ± 0.3	3.23 ± 0.4
Terrestrial atmosphere	n.r.	0.5	n.r.	9.80 ± 0.08	2.90 ± 0.08

Data for aubritic meteorites from Zähringer (1962) and Eberhardt *et al.* (1965); data for 10084 ilmenite from Eberhardt *et al.* (1970).

* Preliminary value from Apollo 14 SWC experiment only (Geiss *et al.*, 1971).

n.r. = not relevant.

values. In other meteorites, particularly in chondrites, trapped gases with low $(He^3/He^4)_{tr}$ ratios have been found (Hintenberger *et al.*, 1965). Strong evidence exists, that in these meteorites at least two components with different $(He^3/He^4)_{tr}$ ratio are present (Anders *et al.*, 1970; Black, 1970; Jeffery and Anders, 1970), a planetary component with a low $(He^3/He^4)_{tr}$ ratio and a solar component with a high ratio.

These at present available data on the $(He^3/He^4)_{tr}$ ratio in different reservoirs of trapped solar wind particles strongly suggests a secular variation of this ratio in the solar wind and probably also in the sun (Schatzman, 1970; Eberhardt *et al.*, 1970; Geiss *et al.*, 1970). Present day solar wind as directly measured or approximately preserved in the soil ilmenite shows the highest He^3 abundances. The solar wind particles in the breccia ilmenite are at least 500×10^6 yr older and have a He^3 abundance approximately 10% lower than in the soil ilmenite. A similar trend is also apparent in the measurements on bulk soil and breccia samples of Hintenberger *et al.* (1971). The trapped gas in aubrites would then represent perhaps the oldest solar wind reservoir, having a He^3 abundance which is nearly 40% lower. In our opinion the presently available data do not establish the secular increase of the He^3/He^4 ratio in the solar wind beyond doubt. However, our data from the 10084, 12001, and 10046 ilmenites clearly support a long-time variation. It will be most important to substantiate the He^3/He^4 secular trend as the solar He^3/He^4 ratio prevailing shortly after the formation of the solar system is an important parameter for deducing the D/H ratio in the solar nebula (Black, 1972; Geiss and Reeves, 1972).

Neon

The isotopic composition of surface correlated Ne is very similar in the three ilmenites. The $(Ne^{20}/Ne^{22})_{sc}$ ratios are consistently lower than the ratio measured in the present day solar wind (Geiss *et al.*, 1970, 1971, 1971a) (cf. Table 9). The difference is small ($\approx 5\%$) and could well be due to fractionation in the trapping process of solar wind Ne ions or to the heavy saturation of the surface layer with solar wind particles. In the ilmenite there is no evidence for a large diffusion loss of trapped Ne. The $(Ne^{20}/Ar^{36})_{tr}$ ratio in the ilmenite is only 30% lower than the ratio measured in the solar wind during the Apollo 14 mission (Geiss *et al.*, 1971).

The systematic difference between the isotopic composition of terrestrial Ne and trapped lunar or solar wind Ne has already been discussed earlier (Eberhardt *et al.*, 1970).

Argon

The surface correlated Ar^{36}/Ar^{38} ratio is identical in the 12001 bulk and the three ilmenite samples (Table 10). The ratio agrees very well with the terrestrial Ar^{36}/Ar^{38} abundance.

The $(Ar^{40}/Ar^{36})_{sc}$ ratio is different in all five samples. It has already been established that the Ar^{40}_{sc} in lunar fine material is not of direct solar wind origin, but that it represents retrapped lunar Ar^{40} from the decay of K^{40} in lunar rocks (Heymann *et al.*, 1970; Heymann and Yaniv, 1970; Eberhardt *et al.*, 1970). Escaping Ar^{40} atoms form a transient lunar atmosphere, which is ionized by solar uv or charge exchange with

Table 10. Comparison of argon isotopic composition in different reservoirs of trapped solar wind particles.

Reservoir	Ar^{36}/Ar^{38}	Ar^{40}/Ar^{36}
Trapped solar wind in		
10084 bulk	—	0.95 ± 0.06
12001 bulk	5.29 ± 0.03	0.42 ± 0.02
10084 ilmenite	5.32 ± 0.08	0.67 ± 0.06
12001 ilmenite	5.33 ± 0.03	0.37 ± 0.05
10046 ilmenite	5.33 ± 0.03	1.35 ± 0.14
For comparison		
Terrestrial atmosphere	5.32 ± 0.01	n.r.

Error definition for 10084 is different from the one used in present paper (cf. Eberhardt *et al.*, 1970).
n.r. = not relevant.

the solar wind and subsequently accelerated. A fraction of these accelerated ions is trapped along with the solar wind particles in the surface of the regolith grains (cf. Manka and Michel, 1971). The $(Ar^{40}/Ar^{36})_{sc}$ ratio is thus a complicated function depending on the Ar^{40} outgassing rate of the moon, the Ar^{36} flux in the solar wind, the interplanetary magnetic field, the local lunar magnetic field, the lunar latitude and longitude of the sample and other parameters. Trapping probabilities, saturation and diffusion effects will also influence the $(Ar^{40}/Ar^{36})_{sc}$ ratio as the average energy and direction of the solar wind ions and the secondary ions from the lunar neutral atmosphere are significantly different. The observed variability in the $(Ar^{40}/Ar^{36})_{sc}$ ratio in the different grain size fractions is thus not unexpected and can have resulted from one or from a combination of any of the above mentioned factors. The variability of the $(Ar^{40}/Ar^{36})_{sc}$ ratio between different bulk samples has also been found and discussed by other investigator teams (LSPET, 1970; Heymann and Yaniv, 1971; Heymann *et al.*, 1972). For the three ilmenite fractions the influence of trapping probability, saturation, etc., should be relatively similar and we could interpret the lower $(Ar^{40}/Ar^{36})_{sc}$ ratio in the 12001 ilmenite relative to the 10084 ilmenite as a longitude effect. Similarly, the high $(Ar^{40}/Ar^{36})_{sc}$ ratio in the 10046 ilmenite may reflect a long time variation in the Ar^{40} outgassing rate of the moon. About twice the present outgassing rate would be required 500×10^6 yr or longer ago.

Along with radiogenic Ar^{40}, the moon will loose other noble gases or volatiles by outgassing. These should be mainly radiogenic He^4, Rn, Xe^{129}, fission Kr and Xe, primordial trapped noble gases, volatile elements, and also trapped solar wind gases. For the lighter elements, the thermal escape from the lunar atmosphere will be fast compared with the lifetime for ionization. For heavier or less volatile elements the retrapping from the temporary lunar atmosphere may become of importance. As already discussed (Eberhardt *et al.*, 1970; Podosek *et al.*, 1971), this retrapping of outgassing products of the moon could have influenced the abundance and isotopic composition of the surface correlated heavier noble gases in lunar material.

Krypton and Xenon

The isotopic composition of surface correlated trapped Kr and Xe derived from the 12001 bulk grain size fractions is compared in Tables 11 and 12 with other de-

Table 11. Isotopic composition of surface correlated trapped Kr in lunar fine material.

	Kr^{78}/Kr^{86}	Kr^{80}/Kr^{86}	Kr^{82}/Kr^{86}	Kr^{83}/Kr^{86}	Kr^{84}/Kr^{86}
			× 100		
BEOC 12001 (this paper)	1.945 ± 0.015	12.74 ± 0.06	65.73 ± 0.2	65.86 ± 0.17	327.9 ± 0.7
BEOC 10084 (Eberhardt *et al.*, 1970)	2.00 ± 0.035	12.90 ± 0.2	66.0 ± 0.3	65.75 ± 0.3	325.2 ± 1.8
SUCOR (Podosek *et al.*, 1971)	—	12.42 ± 0.08	64.25 ± 0.26	64.55 ± 0.27	322.8 ± 0.8
AVCC (Eugster *et al.*, 1967a)	1.927 ± 0.014	12.65 ± 0.09	65.04 ± 0.2	65.11 ± 0.2	322.8 ± 0.8
Atmosphere (Nief 1960; Eugster *et al.*, 1967)	1.995 ± 0.008	12.96 ± 0.04	66.17 ± 0.16	66.00 ± 0.14	327.3 ± 0.7

The error definitions are not necessarily equivalent, see original papers.

terminations of the isotopic composition of surface correlated Kr and Xe in lunar material. Other authors have also published isotopic compositions of trapped lunar Kr and Xe (Hohenberg *et al.*, 1970; Marti *et al.*, 1970; Pepin *et al.*, 1970; Kaiser, 1972). However, all these authors had to assume at least one isotopic ratio in the trapped Kr in order to make the necessary corrections for spallation Kr and Xe.

In order to facilitate the following discussion we shall designate the determinations

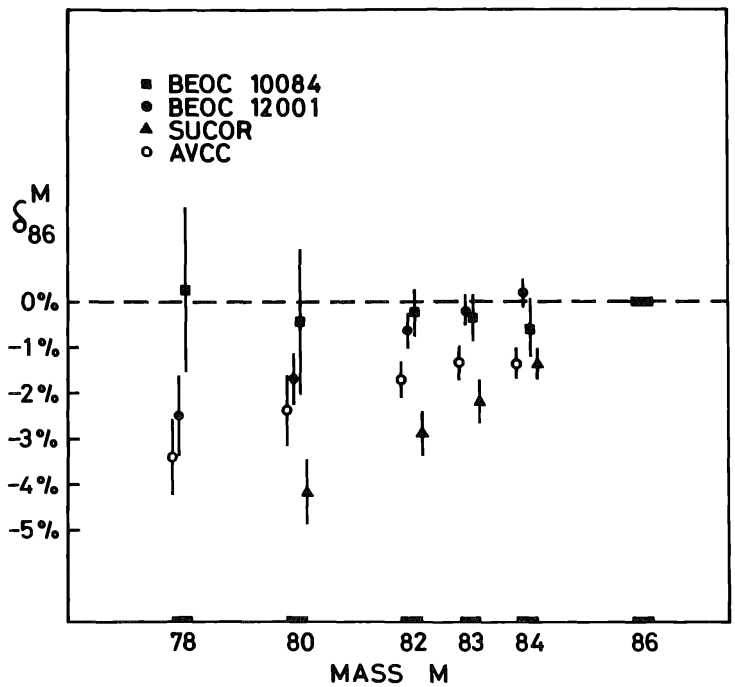

Fig. 9. Comparison between different determinations of the isotopic composition of surface correlated trapped Kr in lunar samples. Shown are the relative deviations from the composition of atmospheric Kr:

$$\delta^M_{86} = [(Kr^M/Kr^{86})_{sc}/(Kr^M/Kr^{86})_{atm} - 1].$$

Data from: BEOC 10084: Eberhardt *et al.* (1970); SUCOR: Podosek *et al.* (1971); BEOC 12001: this paper. The average isotopic composition of trapped Kr in carbonaceous chondrites (AVCC) is from Eugster *et al.* (1967a).

Table 12. Isotopic composition of surface correlated trapped Xe in lunar fine material.

	Xe^{124}/Xe^{130}	Xe^{126}/Xe^{130}	Xe^{128}/Xe^{130}	Xe^{129}/Xe^{130}	Xe^{131}/Xe^{130}	Xe^{132}/Xe^{130}	Xe^{134}/Xe^{130}	Xe^{136}/Xe^{130}
	× 100							
BEOC 12001 (this paper)	2.90 ± 0.07	2.59 ± 0.09	50.38 ± 0.28	635.4 ± 1.7	498.8 ± 1.1	606.2 ± 1.6	223.9 ± 0.8	181.8 ± 0.6
BEOC 10084 (Eberhardt *et al.*, 1970)	2.99 ± 0.18	2.67 ± 0.2	50.45 ± 0.8	634.5 ± 3.5	495.5 ± 3	607 ± 5	225.8 ± 3.5	184.2 ± 3
SUCOR (Podosek *et al.*, 1971)	2.89 ± 0.04	2.63 ± 0.06	50.9 ± 0.3	637.1 ± 1.8	499.0 ± 2.2	606.6 ± 2.1	225.2 ± 0.9	182.7 ± 0.6
Luna 16 (Kaiser, 1972)	—	—	—	633.8 ± 6.5	494.7 ± 3	600.6 ± 3	220.1 ± 1.8	176.0 ± 2
Pesyanoe 1000°C (Marti, 1969)*	—	—	—	633.1 ± 9.5	495.0 ± 6.5	608 ± 7	222.2 ± 3.2	179.6 ± 2.8
AVCC (Eugster *et al.*, 1967b)	2.854 ± 0.065	2.550 ± 0.03	51.0 ± 0.45	634.4 ± 4†	508.1 ± 3.9	621.9 ± 4.2	237.6 ± 2	199.6 ± 1.8
Atmosphere (Nier, 1950; Podosek *et al.*, 1971)	2.335 ± 0.014	2.176 ± 0.014	47.08 ± 0.17	650.5 ± 1.5	522.4 ± 1.2	661.4 ± 1.2	256.7 ± 0.7	218.2 ± 0.6

For Luna 16 and Pesyanoe no abundance data for the less abundant isotopes $Xe^{124-128}$ are given, as these depend critically on the spallation correction. The error definition for the different determinations are not equivalent, see original papers.

* The Xe in Pesyanoe is believed to be mainly trapped solar wind or low energy particles. For the discussion of the necessary spallation correction for Pesyanoe see Eberhardt *et al.* (1970).

† Abundance from Novo Urei (Marti, 1967).

made at Bern of the isotopic composition of the surface correlated trapped noble gases in the bulk material as BEOC 10084 and BEOC 12001 (BEOC = Bern Oberflächen-Correliert).

BEOC 10084, BEOC 12001, and SUCOR Kr do not agree within the error limits assigned by the respective authors. The deviations are however small and show a fairly systematic trend with the mass number (Fig. 9). For the BEOC 10084 and the SUCOR determinations the possibility of a variable target element composition in the different grain sizes was not investigated. Our experience with the BEOC 12001 evaluation has shown that a systematic variation of the spallation gas content with grain size can indeed lead to a nonnegligible shift of the ordinate intercept in the extrapolation method used in determining the BEOC 10084 and SUCOR isotopic compositions. Furthermore, mineral dependent mass fractionation could occur in the trapping of the solar wind particles in the lunar dust grains. The gas losses associated with the heavy saturation and the subsequent structural changes which occur at the surface of the grains (Borg *et al.*, 1971) and also possible thermal diffusion losses could give an additional mass fractionation. We may thus expect small differences in the isotopic composition of surface correlated trapped gases between lunar samples of different mineralogy, thermal history and solar wind irradiation history.

Figure 10 shows the isotopic composition of atmospheric Kr and AVCC Kr (AVCC = average carbonaceous chondrites) relative to BEOC 12001. All η values, except for the reference isotope Kr^{86}, fall on straight lines. Our conclusions are:

(1) AVCC and BEOC 12001 Kr have identical isotopic composition except for a Kr^{86} excess with $Kr^{86}_{excess}/Kr^{86} = 1.5\%$ in AVCC Kr and a very small mass fractionation of $\sim 1‰$ per mass unit.

(2) ATM Kr and BEOC 12001 Kr are related by a mass dependent fractionation process with a fractionation factor of $4.7‰$ per mass unit (light isotopes enriched in atmospheric Kr). In addition, a Kr^{86} excess with $Kr^{86}_{excess}/Kr^{86} = 1.1\%$ is present in atmospheric Kr.

The mass dependent fractionation between atmospheric and BEOC 12001 Kr could easily have occurred at the lunar surface (see above discussion). In our opinion no definite conclusion that solar wind Kr or solar Kr have an overall isotopic composition different from terrestrial Kr can be drawn with the presently available data.

Excess Kr^{86} in the terrestrial atmosphere and in AVCC Kr could be interpreted as fission Kr. The presence of fission Kr in AVCC krypton has already been discussed (Eugster *et al.*, 1967). For the terrestrial atmosphere the required $Kr^{86}_f/Kr^{86} = 1.1\%$ corresponds to $Kr^{86}_f = 1.7 \times 10^{-3}$ cm^3 STP/cm^2 earth surface. The K abundance in the crust as given by Wasserburg *et al.* (1964) accounts for the production of atmospheric Ar^{40}. With the average U concentration of 9 g/cm^2 in the crust (Wasserburg *et al.*, 1964) a Kr^{86}_f/U ratio of 2×10^{-6} results. This ratio is much too high for spontaneous fission. For thermal neutron fission an integrated thermal flux of 3×10^{17} to 2×10^{19} neutrons cm^{-2} would be necessary to give the required Kr^{86}_f/U ratio. The lower flux corresponds to an irradiation early in the earth's history, the higher flux to a recent irradiation. Other neutron induced reactions, including some leading to noble gas isotopes, should also occur and at these high flux levels measurable effects should result. We estimate that with Cl/U and Br/U atomic ratios of 500

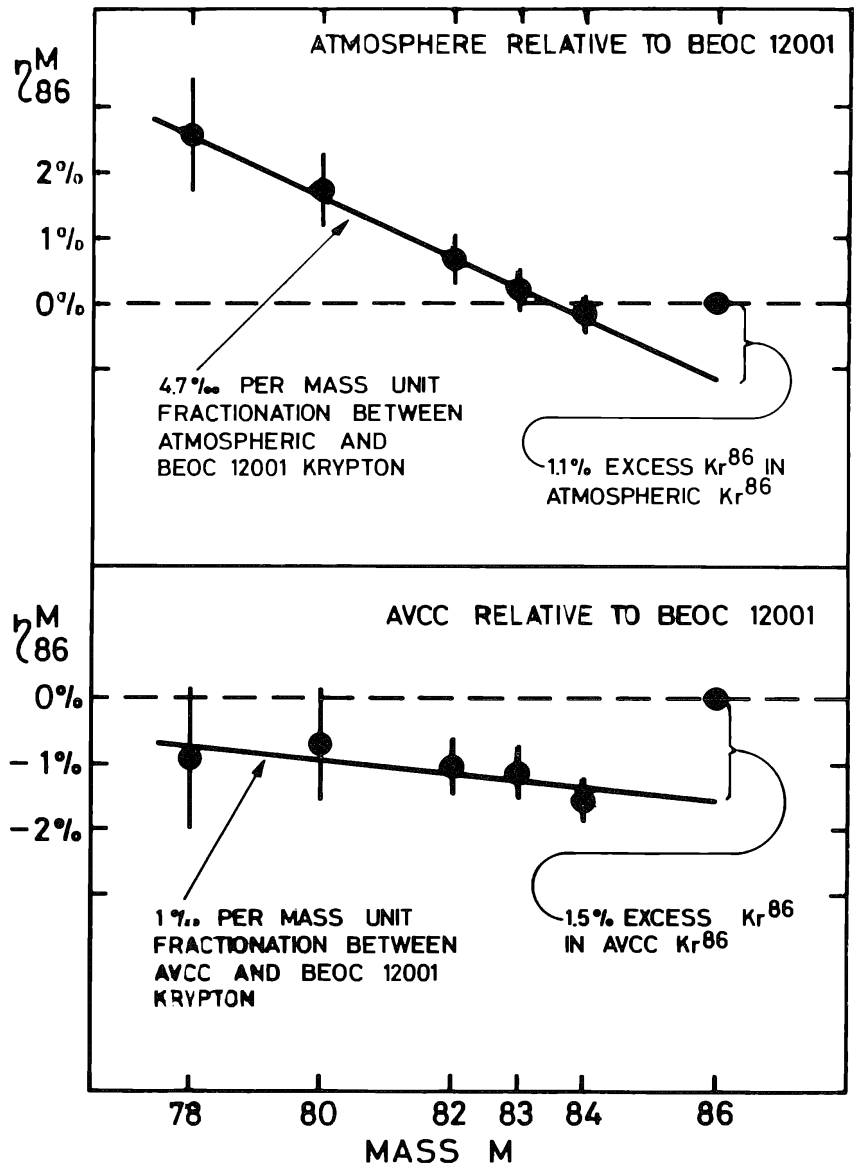

Fig. 10. Comparison of the isotopic composition of atmospheric Kr and average carbonaceous chondrite Kr (AVCC) with surface correlated (solar) trapped Kr in lunar material (BEOC 12001). Shown are the relative deviations

$$\eta^M_{86} = [(Kr^M/Kr^{86})_{sample}/(Kr^M/Kr^{86})_{BEOC\ 12001} - 1].$$

and 4 respectively, as are typical for the earth's crust (Mason, 1966), neutron capture on Cl and Br should produce between 4 and 300 cm^3 STP Ar^{36}/cm^2 and at least 0.05 cm^3 STP Kr^{80}/cm^2. These contributions would drastically alter the isotopic composition of atmospheric Ar and Kr. Fission Xe must be associated with fission Kr^{86}. Even the low $(Xe^{136}/Kr^{86})_f$ ratio of U^{235}_{fn} would imply that 90% of the atmospheric Xe^{136} is of fission origin, if Kr^{86}_f is 1.1% of the Kr^{86} in the atmosphere. For spontaneous fissions, with the correspondingly higher $(Xe^{136}/Kr^{86})_f$ ratios the resulting Xe^{136}_f/Xe^{136} would be considerably greater than one. This problem could, however, be alleviated by either assuming incomplete Xe outgassing of the Kr^{86}_f reservoir or by assuming

completely different origins or histories for terrestrial Kr and Xe. The latter possibility is of course strongly supported by the large isotopic anomalies observed between terrestrial Xe and xenon present in other reservoirs of the solar system.

Our conclusion, that excess Kr^{86} is present in the terrestrial atmosphere, hinges critically on the BEOC 12001 $(Kr^{84}/Kr^{86})_{sc}$ ratio. If this ratio would be in error by $\sim 1\%$, i.e., if it would be ~ 324 instead of 327.9, then the difference between BEOC 12001 and atmospheric Kr could be explained by a simple mass fractionation. As the data in Table 2 show, the Kr^{84}/Kr^{86} ratio increases with decreasing grain size. This is contrary to what would be expected from the spallation contribution and the negative slope in the $(Kr^{84}/Kr^{86})_m$ versus $([Sr] + 0.8[Zr])/Kr_m^{86}$ correlation diagram can only be explained by a volume component of Kr^{86}, i.e., a possible fission component in lunar krypton. A weak negative correlation is also indicated in the 10084 grain size data of Eberhardt *et al.* (1970). The amount of this volume component in the 12001 bulk grain size fractions is approximately 400×10^{-12} cm^3 STP Kr_{ff}^{86}/g. An *in situ* origin of this fission Kr is not compatible with the U and Th abundances and estimated neutron fluxes. The small meteoritic component in the lunar fine material (Ganapathy *et al.*, 1970; Laul *et al.*, 1971) also cannot provide the necessary Kr_f^{86} as in carbonaceous chondrites Kr_f^{86} is only of the order of 20×10^{-12} cm^3 STP/g (Eugster *et al.*, 1967). If this volume correlated Kr^{86} component in the bulk 12001 grain size fractions is neglected, i.e., if the measured Kr^{84}/Kr^{86} ratios are directly corrected for spallation Kr^{84} only, an approximately 0.7% lower $(Kr^{84}/Kr^{86})_{tr}$ ratio would result.

We may summarize our conclusion regarding the presence of excess Kr^{86} in atmospheric Kr as follows: With the presently available data we do not consider the presence of an excess Kr^{86} component in the terrestrial atmosphere, presumably fission Kr^{86}, as firmly established. It cannot be fully excluded that the deduced excess is an artifact of spurious analytical uncertainties and/or of an oversimplified data treatment. It is mandatory to further study the isotopic composition of trapped Kr in lunar material in order to obtain firm conclusions.

BEOC 10084, BEOC 12001, and SUCOR xenon agree within the errors assigned by the respective authors. In our opinion, the BEOC 12001 data ought to be the most reliable of the three determinations, because the variable target element chemistry was taken into account in correcting for spallation. We shall therefore base our further discussion on the BEOC 12001 data.

In Fig. 11 the isotopic composition of BEOC 12001 is compared with AVCC-Xe (Eugster *et al.*, 1967). Excellent agreement in the abundance of the fission shielded isotopes is observed. For $Xe^{131-136}$ an excess is present in the AVCC-Xe. This excess relative to trapped solar wind has already been observed by many investigators (Hohenberg *et al.*, 1970; Marti *et al.*, 1970; Pepin *et al.*, 1970; Eberhardt *et al.*, 1970; Podosek *et al.*, 1971). Mass spectra of this presumed fission component in AVCC-Xe are compiled in Table 13. The presence of a fission component in AVCC xenon had already been recognized by several investigator teams before lunar samples were analyzed, either on the basis of temperature release experiments (Reynolds and Turner, 1964; Pepin, 1968) or from the direct comparison of fractionated terrestrial Xe with AVCC-Xe (Krummenacher *et al.*, 1962; Eugster *et al.*, 1967; Marti, 1967; Podosek *et al.*, 1971). These spectra are also compiled in Table 13 and compared with

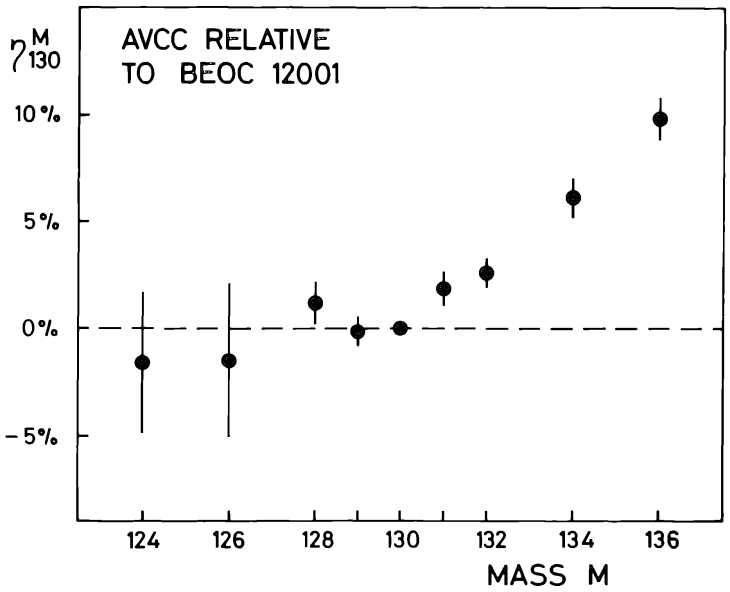

Fig. 11. Comparison of the isotopic composition of average carbonaceous chondrite Xe (AVCC) with surface correlated (solar) trapped Xe in lunar material (BEOC 12001). Shown are the relative deviations

$$\eta^{M}_{130} = [(Xe^{M}/Xe^{130})_{AVCC}/(Xe^{M}/Xe^{130})_{BEOC\ 12001} - 1].$$

Table 13. Isotopic composition of excess $Xe^{131-136}$ in AVCC Xenon. Results obtained by different experimental approaches are compared.

Method	Xe^{131}/Xe^{136}	Xe^{132}/Xe^{136}	Xe^{134}/Xe^{136}
Temperature release experiment			
Reynolds and Turner (1964)	0.13 ± 0.1	0.16 ± 0.1	0.72 ± 0.04
Pepin (1968)	0.17 ± 0.08	0.33 ± 0.06	0.70 ± 0.03
AVCC-fractionated atmospheric Xe			
Krummenacher *et al.* (1962)	0.31	0.46	0.67
Eugster *et al.* (1967)	0.25 ± 0.15	0.38 ± 0.21	0.64 ± 0.1
Marti (1967)	0.12 ± 0.12	0.17 ± 0.17	0.57 ± 0.07
Podosek *et al.* (1971) (Murray)	0.19 ± 0.1	0.21 ± 0.18	0.62 ± 0.08
AVCC-surface correlated trapped Xe			
Marti (1969) (Pesyanoe 1000° Xe)*	0.65 ± 0.39	0.69 ± 0.42	0.77 ± 0.22
Eberhardt *et al.* (1970) (BEOC 10084)	0.80 ± 0.35	0.95 ± 0.45	0.75 ± 0.3
Podosek *et al.* (1971) (SUCOR)	0.38 ± 0.18	0.66 ± 0.21	0.66 ± 0.1
Present results (BEOC 12001)	0.52 ± 0.25	0.88 ± 0.33	0.77 ± 0.19
Kaiser (1972)†	0.57 ± 0.22	0.90 ± 0.24	0.74 ± 0.14
Known fission spectra			
U^{235} thermal neutron	0.45	0.67	1.25
U^{238} spontaneous fission	0.08 ± 0.01	0.60 ± 0.01	0.83 ± 0.01
Pu^{244} spontaneous fission	0.25 ± 0.02	0.88 ± 0.03	0.92 ± 0.03

Known fission spectra from Hyde (1964) (U^{235}_{fn}), Wetherill (1953) (U^{238}_{fs}) and Alexander *et al.* (1971) (Pu^{244}_{fs}).

* Calculated using the data of Marti (1969), making the appropriate spallation correction (cf. Eberhardt *et al.*, 1970) and using the AVCC composition given by Eugster *et al.* (1967a).

† Calculated using AVCC composition given by Eugster *et al.* (1967a).

known fission spectra. It is apparent from this Table that the AVCC-fission spectra derived from temperature release experiments and from the direct comparison of fractionated atmospheric Xe with AVCC-Xe are quite similar. The comparison of AVCC-Xe with surface correlated Xe gives systematically higher Xe^{131} and $X^{132}e$ yields. The dissimilarity of the fission spectra obtained from the comparison of AVCC-Xe with surface correlated Xe, and from the comparison of AVCC-Xe with fractionated terrestrial Xe is not necessarily surprising. Terrestrial Xe and BEOC 12001 xenon are most likely not related by a simple, linear mass fractionation (cf. Fig. 12). The two calculation methods are thus not equivalent. In our opinion, the comparison of the AVCC-Xe with the surface correlated Xe is preferable and more reasonable than the comparison with the hypothetical fractionated atmospheric Xe.

The discrepancy between the AVCC fission spectra derived from temperature release experiments and from the direct comparison of AVCC xenon with surface correlated Xe is difficult to understand. Either the surface correlated trapped Xe—even Kaiser's (1972) "low fission Xe"—is not representative for the nonfission Xe in carbonaceous chondrites or the difference results, at least partly, from the special conditions of the temperature release technique. The general agreement observed for the light Xe isotopes between AVCC and BEOC 12001 seems to rule out the first of the two possible explanations.

In Fig. 12 the isotopic composition of atmospheric Xe is compared with BEOC 12001 xenon. A very systematic trend of the η values with the mass difference is

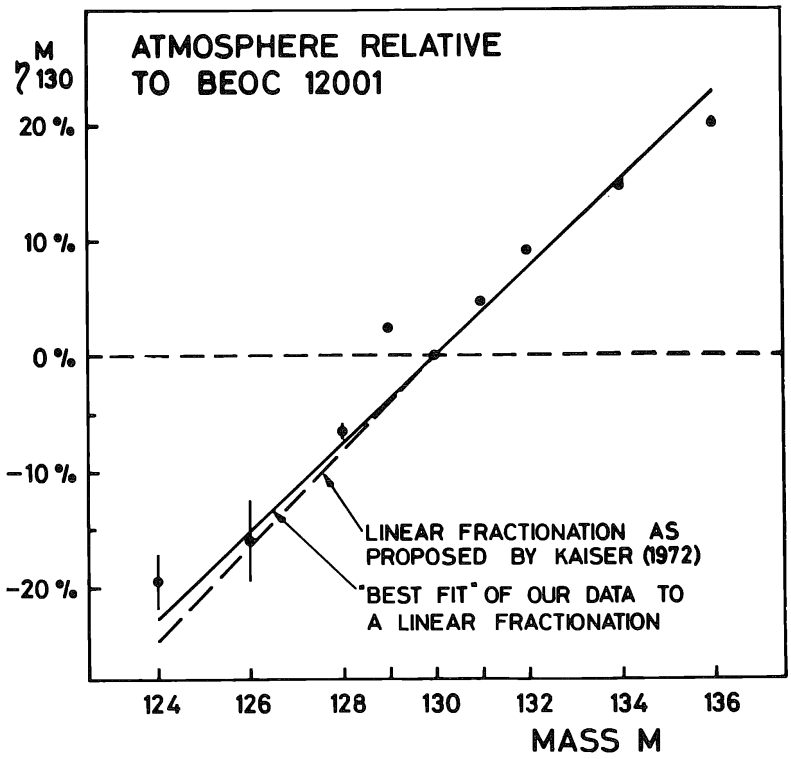

Fig. 12. Comparison of the isotopic composition of atmospheric Xe with surface correlated (solar) trapped Xe in lunar material (BEOC 12001). Shown are the relative deviations

$$\eta^{M}_{130} = [(Xe^{M}/Xe^{130})_{ATM}/(Xe^{M}/Xe^{130})_{BEOC\ 12001} - 1].$$

obvious. However, even pushing the error limits to the extreme, it is not possible to explain the difference between atmospheric and BEOC 12001 xenon by a simple, linear mass fractionation alone.

Recently, Kaiser (1972) observed Xe with somewhat lower $Xe^{131-136}$ abundances than BEOC 12001 in the stepwise degassing of a Luna 16 sample. He concludes that atmospheric Xe and his Luna 16 trapped Xe are related by a linear mass fractionation with a 4.1% per mass unit fractionation factor. Our BEOC 12001 data on the low mass Xe isotopes are not in agreement with Kaiser's suggestion (cf. Fig. 12).

A satisfactory explanation of the observed overall differences in the isotopic composition of xenon in the different reservoirs of the solar system (terrestrial atmosphere; surface correlated lunar Xe, e.g., solar Xe) is still lacking. A simple mass dependent fractionation as the sole source of the differences seems to be ruled out by our BEOC 12001 data. However, the question remains if BEOC 12001 corresponds indeed to the true solar Xe isotopic composition, or if secondary processes on the lunar surface could have significantly changed the isotopic composition of the trapped solar wind Xe.

Acknowledgments—We would like to thank the National Aeronautics and Space Administration for generously supplying the necessary lunar samples for this investigation. We would like to acknowledge stimulating discussions with Drs. E. Anders and O. Eugster. We are grateful to Carmen Geiss, Madeleine Thönen, W. Fahrer, V. Horvath, E. Lenggenhager, A. Schaller, and F. Schweizer for their help during the measurements and the preparation of the manuscript.

This research was supported by the Swiss National Science Foundation (grants NF 2.213.69, 2.190.69, 2.405.70, and 2.592.71).

References

Alexander E. C. Jr. (1971) Spallogenic Ne, Kr, and Xe from a depth study of 12002. *Proc. Second Lunar Sci. Conf., Geochim. Cosmochim. Acta* Suppl. 2, Vol. 2, pp. 1643–1650. MIT Press.

Anders E., Heymann D., and Mazor E. (1970) Isotopic composition of primordial helium in carbonaceous chondrites. *Geochim. Cosmochim. Acta* **34,** 127–132.

Bame S. J., Hundhausen A. J., Asbridge J. R., and Strong I. B. (1968) Solar wind ion composition. *Phys. Rev. Lett.* **20,** 393–395.

Baur H., Frick U., Funk H., Schultz L., and Signer P. (1972) On the thermal release of helium, neon, and argon from lunar fines (abstract). In *Lunar Science*—III (editor C. Watkins), pp. 47–49, Lunar Science Institute Contr. No. 88.

Black D. C. (1970) Trapped helium-neon isotopic correlations in gas-rich meteorites and carbonaceous chondrites. *Geochim. Cosmochim. Acta* **34,** 132–140.

Black D. C. (1972) On the origins of trapped helium, neon, and argon isotopic variations in meteorites —I. Gas rich meteorites, lunar soil, and breccia. *Geochim. Cosmochim. Acta* **36,** 347–375.

Borg J., Maurette M., Durrieu L., and Jouret C. (1971) Ultramicroscopic features in micron-sized lunar dust grains and cosmophysics. *Proc. Second Lunar Sci. Conf., Geochim. Cosmochim. Acta* Suppl. 2, Vol. 3, pp. 2027–2040. MIT Press.

Eberhardt P., Geiss J., and Grögler N. (1965) Ueber die Verteilung der Uredelgase im Meteoriten Khor Temiki. *Tschermaks Mineral. Petrogr. Mitt.* **10,** 535–551.

Eberhardt P., Geiss J., and Grögler N. (1965a) Further evidence on the origin of trapped gases in the meteorite Khor Temiki. *J. Geophys. Res.* **70,** 4375–4378.

Eberhardt P., Geiss J., Graf H., Grögler N., Krähenbühl U., Schwaller H., Schwarzmüller J., and Stettler A. (1970) Trapped solar wind noble gases, exposure age and K/Ar-age in Apollo 11 lunar fine material. *Proc. Apollo 11 Lunar Sci. Conf., Geochim. Cosmochim. Acta* Suppl. 1, Vol. 2, pp. 1037–1070. Pergamon.

Eberhardt P., Geiss J., Graf H., Grögler N., Krähenbühl U., Schwaller H., Schwarzmüller J., and Stettler A. (1970a) Correlation between rock type and irradiation history of Apollo 11 igneous rocks. *Earth Planet. Sci. Lett.* **10,** 67–72.

Eberhardt P., Geiss J., Graf H., and Schwaller H. (1971) On the origin of excess ^{131}Xe in lunar rocks. *Earth Planet. Sci. Lett.* **12,** 260–262.

Eberhardt P., Geiss J., Graf H., Grögler N., Krähenbühl U., Schwaller H., and Stettler A. (1972) Noble gas investigations of lunar rocks 10017 and 10071. *Geochim. Cosmochim. Acta* (to be submitted).

Eugster O., Eberhardt P., and Geiss J. (1967) The isotopic composition of krypton in unequilibrated and gas rich chondrites. *Earth Planet. Sci. Lett.* **2,** 385–393.

Eugster O., Eberhardt P., and Geiss J. (1967a) Krypton and xenon isotopic composition in three carbonaceous chondrites. *Earth Planet. Sci. Lett.* **3,** 249–257.

Eugster O., Eberhardt P., and Geiss J. (1969) Isotopic analysis of krypton and xenon in fourteen stone meteorites. *J. Geophys. Res.* **74,** 3874–3896.

Finkel R. C., Arnold J. R., Imamura M., Reedy R. C., Fruchter J. S., Loosli H. H., Evans J. C., Delany A. C., and Shedlovsky J. P. (1971) Depth variation of cosmogenic nuclides in a lunar surface rock and lunar soil. *Proc. Second Lunar Sci. Conf., Geochim. Cosmochim. Acta* Suppl. 2, Vol. 2, pp. 1773–1789. MIT Press.

Ganapathy R., Keays R. R., Laul J. C., and Anders E. (1970) Trace elements in Apollo 11 lunar rocks: Implications for meteorite influx and origin of moon. *Proc. Apollo 11 Lunar Sci. Conf., Geochim. Cosmochim. Acta* Suppl. 1, Vol. 2, pp. 1117–1142. Pergamon.

Gast P. W., Hubbard N. J., and Wiesman H. (1970) Chemical composition and petrogenesis of basalts from Tranquillity Base. *Proc. Apollo 11 Lunar Sci. Conf., Geochim. Cosmochim. Acta* Suppl. 1, Vol. 2, pp. 1143–1163. Pergamon.

Geiss J., Oeschger H., and Schwarz U. (1962) The history of cosmic radiation as revealed by isotopic changes in the meteorites and on the earth. *Space Sci. Rev.* **1,** 197–223.

Geiss J., Eberhardt P., Bühler F., Meister J., and Signer P. (1970) Apollo 11 and Apollo 12 solar wind composition experiments: Fluxes of He and Ne isotopes. *J. Geophys. Res.* **75,** 5972–5978.

Geiss J., Bühler F., Cerutti H., Eberhardt P., and Meister J. (1971) Solar wind composition experiment. *Apollo 14 Preliminary Science Report*, NASA SP-272, pp. 221–226.

Geiss J., Bühler F., Cerutti H., and Eberhardt P. (1971a) The solar wind composition experiment. *Apollo 15 Preliminary Science Report*, NASA SP, in press.

Geiss J. and Reeves H. (1972) Cosmic and solar system abundances of deuterium and helium-3. *Astron. Astrophys.*, in press.

Heymann D. and Yaniv A. (1970) Ar^{40} anomaly in lunar samples from Apollo 11. *Proc. Apollo 11 Lunar Sci. Conf., Geochim. Cosmochim. Acta* Suppl. 1, Vol. 2, pp. 1261–1267. Pergamon.

Heymann D., Yaniv A., Adams J. A. S., and Fryer G. E. (1970) Inert gases in lunar samples. *Science* **167,** 555–558.

Heymann D. and Yaniv A. (1971) Ar^{40} in meteorites, fines and breccias from the moon. *Chem. Erde.* **30,** 175–189.

Heymann D., Yaniv A., and Walton J. (1972) Inert gases in Apollo 14 fines and the case of parentless Ar^{40} (abstract). In *Lunar Science—III* (editor C. Watkins), pp. 376–378, Lunar Science Institute Contr. No. 88.

Hintenberger H., Vilcsek E., and Wänke H. (1965) Ueber die Isotopenzusammensetzung und über den Sitz der leichten Uredelgase in Steinmeteoriten. *Z. Naturforsch.* **20a,** 939–945.

Hintenberger H., Weber H. W., and Takaoka N. (1971) Concentrations and isotopic abundances of the rare gases in lunar matter. *Proc. Second Lunar Sci. Conf., Geochim. Cosmochim. Acta* Suppl. 2, Vol. 2, pp. 1607–1625. MIT Press.

Hohenberg C. M., Davis P. K., Kaiser W. A., Lewis R. S., and Reynolds J. H. (1970) Trapped and cosmogenic rare gases from stepwise heating of Apollo 11 samples. *Proc. Apollo 11 Lunar Sci. Conf., Geochim. Cosmochim. Acta* Suppl. 1, Vol. 2, pp. 1283–1309. Pergamon.

Hyde E. K. (1964) The nuclear properties of heavy elements. In *Fission Phenomena*, Vol. 3, Prentice Hall.

Jeffery P. M. and Anders E. (1970) Primordial noble gases in separated meteoritic minerals—I. *Geochim. Cosmochim. Acta* **34,** 1175–1198.

Kaiser W. A. (1972) Rare gas studies in Luna 16 G-7 fines by stepwise heating technique. A low fission solar wind Xe. *Earth Planet. Sci. Lett.* **13,** 387–399.

Krähenbühl U., Rolli H. P., and von Gunten H. R. (1972) Aktivierungsanalytische Bestimmung von seltenen Erden in Gesteinsstandards und in Mondproben. *Helv. Chim. Acta* (submitted).

Krummenacher D., Merrihue C. M., Pepin R. O., and Reynolds J. H. (1962). Meteoritic krypton and barium versus the general isotopic anomalies in meteoritic xenon. *Geochim. Cosmochim. Acta* **26,** 231–249.

Laul J. C., Morgan J. W., Ganapathy R., and Anders E. (1971) Meteoritic material in lunar samples: Characterization from trace elements. *Proc. Second Lunar Sci. Conf., Geochim. Cosmochim. Acta* Suppl. 2, Vol. 2, pp. 1139–1158. MIT Press.

LSPET (Lunar Sample Preliminary Examination Team) (1970) Preliminary examination of the lunar samples from Apollo 12. *Science* **167,** 1325–1339.

Lugmair G. W. and Marti K. (1972) Neutron and spallation effects in Fra Mauro regolith (abstract). In *Lunar Science—III* (editor C. Watkins), pp. 495–497, Lunar Science Institute Contr. No. 88.

Manka R. H. and Michel F. C. (1971) Lunar atmosphere as a source of lunar surface elements. *Proc. Second Lunar Sci. Conf., Geochim. Cosmochim. Acta* Suppl. 2, Vol. 2, pp. 1717–1728. MIT Press.

Marti K. (1967) Isotopic composition of trapped krypton and xenon in chondrites. *Earth Planet. Sci. Lett.* **3,** 243–248.

Marti K. (1969) Solar-type xenon: A new isotopic composition of xenon in the Pesyanoe meteorite. *Science* **166,** 1263–1265.

Marti K., Eberhardt P., and Geiss J. (1966) Spallation, fission, and neutron capture anomalies in meteoritic krypton and xenon. *Z. Naturforsch.* **21a,** 398–413.

Marti K., Lugmair G. W., and Urey H. C. (1970) Solar wind gases, cosmic-ray spallation products, and the irradiation history of Apollo 11 samples. *Proc. Apollo 11 Lunar Sci. Conf., Geochim. Cosmochim. Acta* Suppl. 1, Vol. 2, pp. 1357–1367. Pergamon.

Mason B. (1966) *Principles of Geochemistry*, third edition. John Wiley.

Morrison G. H., Gerard J. T., Potter N. M., Gangadharam E. V., Rothenberg A. M., and Burdo R. A. (1971) Elemental abundances of lunar soil and rocks from Apollo 12. *Proc. Second Lunar Sci. Conf., Geochim. Cosmochim. Acta* Suppl. 2, Vol. 2, pp. 1169–1185. MIT Press.

Nief G. (1960) As reported in isotopic abundance ratios reported for reference samples stocked by the National Bureau of Standards, ed. Mohler F. (NBS Techn. Note 51).

Nier A. O. (1950) A redetermination of the relative abundances of the isotopes of neon, krypton, rubidium, xenon and mercury. Phys. Rev. **79,** 450–454.

Pepin R. O. (1968) Neon and xenon in carbonaceous chondrites. In *Origin and Distribution of the Elements* (editor L. H. Ahrens), pp. 379–386, Pergamon.

Pepin R. O., Nyquist L. E., Phinney D., and Black D. C. (1970) Rare gases in Apollo 11 lunar material. *Proc. Apollo 11 Lunar Sci. Conf., Geochim. Cosmochim. Acta* Suppl. 1, Vol. 2, pp. 1435–1454. Pergamon.

Piercy G. R., McCargo M., Brown F., and Davies D. A. (1964) Experimental evidence for the channeling of heavy ions in monocristalline aluminum. *Can. J. Phys.* **42,** 1116–1134.

Podosek F. A., Huneke J. C., Burnett D. S., and Wasserburg G. J. (1971) Isotopic composition of xenon and krypton in the lunar soil and in the solar wind. *Earth Planet. Sci. Lett.* **10,** 199–216.

Reynolds J. H. and Turner G. (1964) Rare gases in the chondrite Renazzo. *J. Geophys. Res.* **69,** 3263–3281.

Schatzmann E. (1970) CERN Lecture Notes.

Schnetzler C. C. and Philpotts J. A. (1971) Alkali, alkaline earth, and rare-earth element concentrations in some Apollo 12 soils, rocks, and separated phases. *Proc. Second Lunar Sci. Conf., Geochim. Cosmochim. Acta* Suppl. 2, Vol. 2, pp. 1101–1122. MIT Press.

Schwaller H., Eberhardt P., Geiss J., Graf H., and Grögler N. (1971) The $(^{78}Kr/^{83}Kr)_{sp}$–$(^{131}Xe/^{126}Xe)_{sp}$ correlation in Apollo 12 rocks. *Earth Planet. Sci. Lett.* **12,** 167–169.

Wänke H., Wlotzka F., Baddenhausen H., Balacescu A., Spettel B., Teschke F., Jagoutz E., Kruse H., Quijano-Rico M., and Rieder R. (1971) Apollo 12 samples: Chemical composition and its relation to sample locations and exposure ages, the two-component origin of the various soil samples and studies on lunar metallic particles. *Proc. Second Lunar Sci. Conf., Geochim. Cosmochim. Acta* Suppl. 2, Vol. 2, pp. 1187–1208. MIT Press.

Wasserburg G. J., MacDonald G. J. F., Hoyle F., and Fowler W. A. (1964) Relative contributions of uranium, thorium, and potassium to heat production in the earth. *Science* **143,** 465–467.

Wetherill G. W. (1953) Spontaneous fission yields from uranium and thorium. *Phys. Rev.* **92,** 907–912.

Zähringer J. (1962) Ueber die Uredelgase in den Achondriten Kapoeta und Staroe Pesyanoe. *Geochim. Cosmochim. Acta* **26,** 665–680.

Proceedings of the Third Lunar Science Conference
(Supplement 3, *Geochimica et Cosmochimica Acta*)
Vol. 2, pp. 1857–1863
The M.I.T. Press, 1972

Inert gases from Apollo 12, 14, and 15 fines

D. HEYMANN, A. YANIV,* and S. LAKATOS
Departments of Geology and Space Science,
Rice University, Houston, Texas 77001

Abstract—He and Ne contents have been determined in five Apollo 14, five Apollo 12, and two Apollo 15 samples (Ar data are presented in the following paper). Kr and Xe contents were measured in all but the two Apollo 15 samples. The two "mini-rocks" from 14166 and 14167 contain radiogenic He^3_R. Their apparent U, Th–He^4 age, and in fact that of all the Apollo 14 fines is 3700 ± 800 m.y. If this age is real then it follows that either the (< 1 mm) ejecta from Cone Crater (about 1 km away) lost little if any He^4_R during the formation of the crater, or that these ejecta constitute only a small proportion in the bulk, contingency, and comprehensive fines. The He^3_C radiation ages of 14003, 14163, and 14259 are about 300 m.y.; the Ne^{21}_C ages are about 400, 400, and 300 m.y., respectively. The Ne^{21}_C age of 15601 is about 350 m.y.

INTRODUCTION

IN THIS PAPER we report the results of our continuing studies of inert gases in lunar fines, i.e., from the Apollo 12, 14, and 15 missions. The inert gases are important geochemical tracers of the solar wind, the cosmic rays, and of the evolution of the regolith. The Apollo 15 fines are of particular interest in this respect because of the presence in them of significant amounts of green glass of high iron content. Because of our special interest in the Ar^{40} problem, we will discuss it in a separate paper.

Our measurements were done by mass spectrometry; the details of which have been published elsewhere (Heymann and Yaniv, 1970a) hence need not be repeated here. Results are given in Table 1.

RESULTS AND DISCUSSION

(*1*) *Radiogenic He^4 and Ar^{40}*

Inert gases in lunar fines consist of the following principal constituents: trapped gases of solar wind origin, cosmogenic gases produced by galactic and solar cosmic rays, and radiogenic He^4_R and Ar^{40}_R. He^4_R, if any is present, is difficult to detect in fines in general, because it is normally wholly masked by the solar wind component in these samples. However, samples 14166 and 14167 (1–2 mm and 2–4 mm fines, respectively) clearly contain He^4_R. These "mini-rocks" have He^4/He^3 ratios of 5500 and 8700, far greater than the largest directly measured solar-wind value of 2600 (Geiss *et al.*, 1970) or typical values seen in bulk fines, which are usually smaller than 3000. In addition, the He^4/Ne^{20} ratios in 14166 and 14167, 160 and 390 respectively are far greater than the typical value of about 50 in the bulk Apollo 14 fines.

* On leave from the Department of Physics and Astronomy, Tel Aviv University, Ramat Aviv, Israel.

Table 1. Inert gas contents of Apollo 12, 14, and 15 samples.

Sample	He^3 10^{-5}	He^4 10^{-3}	Ne^{20} 10^{-3}	Ne^{21} 10^{-6}	Ne^{22} 10^{-4}	Kr^{84} 10^{-8}	Xe^{132} 10^{-8}
14003 (bulk)	2.95	84.3	1.31	3.64	1.01	19.0	4.6
14163 (bulk)	3.20	80.6	1.40	4.06	1.08	20.0	3.8
14166 (1 fragment) ~1 mm	0.0617	3.37	0.0207	0.201	0.0173	—	—
14167 (1 fragment) ~3 mm	0.0372	3.25	0.0083	0.048	0.00656	—	—
14259 (bulk)	3.48	85.7	1.52	4.16	1.15	18.9	3.6
14163 (< 37 μ)	4.41	108	2.02	5.58	1.56	20.1	5.2
14163 (37–63 μ)	1.01	22.4	0.482	1.79	0.386	6.3	1.6
14163 (63–74 μ)	0.693	15.4	0.312	1.31	0.251	4.9	1.4
14163 (74–88 μ)	0.940	20.2	0.404	1.66	0.319	6.0	1.6
14163 (88–105 μ)	0.798	17.3	0.332	1.44	0.264	5.6	1.5
14163 (105–250 μ)	0.818	17.5	0.352	1.57	0.281	5.0	1.3
14163 (250–354 μ)	0.599	12.3	0.293	1.20	0.178	4.2	0.93
14163 (354–500 μ)	0.998	21.1	0.381	1.61	0.299	3.7	1.1
14163 (500–700 μ)	0.369	5.49	0.0607	0.691	0.0553	0.86	0.36
14163 (700–1000 μ)	0.281	3.96	0.0408	0.534	0.0361	0.82	0.35
14259 (< 37 μ)	4.83	123	2.13	5.61	1.65	26.1	5.8
14259 (37–53 μ)	1.56	47.6	0.731	2.41	0.597	10.6	2.3
14259 (53–63 μ)	1.94	44.9	0.852	2.40	0.651	12.2	2.6
14259 (63–74 μ)	1.10	25.1	0.495	1.68	0.384	7.5	1.9
14259 (74–88 μ)	1.05	27.0	0.504	1.70	0.390	9.6	3.1
14259 (88–105 μ)	0.889	21.0	0.450	1.50	0.350	8.8	2.0
14259 (105–250 μ)	0.757	16.6	0.322	1.25	0.254	6.5	2.2
14259 (250–354 μ)	1.07	25.5	0.525	1.85	0.412	8.1	1.8
14259 (354–500 μ)	0.616	12.1	0.205	0.988	0.162	3.3	0.91
14259 (500–700 μ)	0.627	13.0	0.235	0.938	0.184	2.8	0.83
14259 (700–1000 μ)	0.427	6.90	0.152	0.870	0.122	3.8	1.2
12042 (bulk)	3.40	97.6	1.56	4.27	1.21	12.5	2.4
12073 (interior chip)	1.10	27.7	0.494	1.67	0.383	4.2	1.0
12030 (bulk)	16.0	382	6.14	16.8	4.76	4.2	1.2
12044 (bulk)	3.27	84.2	1.49	4.06	1.14	11.5	1.9
12033 (> 250 μ)	0.0946	0.512	0.0197	0.315	0.0188	0.41	0.18
12033 (105–250 μ) strongly magnetic	0.290	5.43	0.109	0.942	0.0882	1.2	0.33
12033 (105–250 μ) weakly magnetic	0.117	0.786	0.0498	0.821	0.0463	0.31	0.089
12033 (< 105 μ)	0.303	—	0.164	0.786	0.134	1.6	0.55
12033 (< 105 μ)	0.197	3.59	0.0808	0.848	0.0658	—	—
15601 (bulk)	2.59	61.9	1.33	3.88	1.04		
15601 (500–700 μ)	0.457	6.67	0.152	0.805	0.122		
15601 (354–500 μ)	0.594	7.75	0.162	1.06	0.132		
15601 (250–354 μ)	0.634	9.29	0.238	1.16	0.189		
15601 (105–250 μ)	0.859	—	0.324	1.29	0.257		
15601 (88–105 μ)	0.970	19.3	0.494	1.78	0.385		
15601 (74–88 μ)	1.06	22.1	0.588	2.03	0.444		
15601 (63–74 μ)	1.10	26.8	0.601	2.05	0.461		
15601 (53–63 μ)	0.702	15.6	0.552	1.84	0.431		
15601 (44–53 μ)	1.38	22.9	0.789	2.60	0.627		
15601 (< 44 μ)	4.67	118	2.36	9.37	1.83		
15091 (bulk)	2.36	60.6	1.38	3.82	1.07		

Sample	4/3	20/22	21/22	4/20	20/36	36/84	84/132
14003 (bulk)	2900	13.0	0.036	64	3.7	1900	4.1
14163 (bulk)	2500	12.9	0.038	58	4.0	1700	3.8
14166 (1 fragment) ~1 mm	5500	11.9	0.116	160	3.0	—	—
14167 (1 fragment) ~3 mm	8700	12.6	0.073	390	2.3	—	—
14259 (bulk)	2500	13.2	0.036	56	3.5	2300	5.3
14163 (< 37 μ)	2400	13.0	0.036	54	4.0	2500	3.9
14163 (37–63 μ)	2210	12.5	0.047	47	3.2	2400	3.9
14163 (63–74 μ)	2200	12.4	0.052	49	3.0	2100	3.5
14163 (74–88 μ)	2100	12.7	0.052	50	2.9	2400	3.8
14163 (88–105 μ)	2200	12.6	0.055	52	2.4	2500	3.8
14163 (105–250 μ)	2100	12.5	0.056	50	3.0	2400	3.9
14163 (250–354 μ)	2100	13.5	0.068	52	2.4	2300	4.6
14163 (354–500 μ)	2100	12.7	0.054	55	4.0	2600	3.2
14163 (500–700 μ)	1500	11.0	0.125	90	3.7	1900	2.4
14163 (700–1000 μ)	1400	11.3	0.148	97	3.9	1300	2.4
14259 (< 37 μ)	2500	13.0	0.034	58	3.6	2300	4.5
14259 (37–53 μ)	3100	13.1	0.040	65	2.7	2600	4.5
14259 (53–63 μ)	2300	13.1	0.037	53	2.9	2400	4.6
14259 (63–74 μ)	2300	12.9	0.044	51	2.9	2300	3.9
14259 (74–88 μ)	2600	12.9	0.044	54	2.5	2100	3.1
14259 (88–105 μ)	2400	12.9	0.043	47	2.4	2100	4.4
14259 (105–250 μ)	2200	12.7	0.049	52	2.6	1900	3.0
14259 (250–354 μ)	2400	12.7	0.045	49	2.9	2200	4.6
14259 (354–500 μ)	2000	12.7	0.061	59	3.2	2000	3.6
14259 (500–700 μ)	2100	12.8	0.051	55	3.5	2400	3.3
14259 (700–1000 μ)	1600	12.5	0.071	45	1.9	2100	3.2
12042 (bulk)	2900	12.9	0.035	63	5.2	2400	5.3
12073 (interior chip)	2500	12.9	0.044	56	4.9	2400	4.2
12030 (bulk)	2400	12.9	0.039	63	4.9	3000	3.5
12044 (bulk)	2600	13.1	0.036	57	4.9	2700	6.1
12033 (> 250 μ)	540	10.6	0.167	26	4.06	1200	2.3
12033 (105–250 μ) strongly magnetic	1900	12.4	0.070	50	4.29	2000	3.7
12033 (105–250 μ) weakly magnetic	670	10.8	0.177	16	5.64	1400	3.5
12033 (< 105 μ)	—	12.3	0.059	—	5.63	1800	2.9
12033 (< 105 μ)	1822	12.3	0.129	44	4.56	—	—
15601 (bulk)	2390	12.85	0.035	47	6.33		
15601 (500–700 μ)	1370	12.44	0.066	44	5.26		
15601 (354–500 μ)	1220	12.26	0.080	48	5.70		
15601 (250–354 μ)	1470	12.60	0.061	39	6.15		
15601 (105–250 μ)	—	12.63	0.050	—	6.49		
15601 (88–105 μ)	1990	12.72	0.046	39	6.41		
15601 (74–88 μ)	1950	12.75	0.044	38	6.69		
15601 (63–74 μ)	2440	13.56	0.046	45	5.72		
15601 (53–63 μ)	2220	12.80	0.043	28	5.52		
15601 (44–53 μ)	1660	12.57	0.041	29	6.98		
15601 (< 44 μ)	2530	12.88	0.039	50	7.11		
15091 (bulk)	2670	12.91	0.036	44	4.92		

Notes: (1) Ar^{36}, Ar^{38}, and Ar^{40} results are reported in the companion paper.
(2) Errors in absolute amounts are usually less than ±5%.
(3) Typical system blanks were: $He^4 = 8 \times 10^{-8}$ cm³ STP; $Ne^{20} = 7 \times 10^{-10}$ cm³ STP; $Ar^{40} = 10^{-8}$ cm³ STP.
(4) Sample weights ranged from about 0.1–1 mg.

When we plot He^4 versus Ne^{20} for all the Apollo 14 samples in Table 1, we find that most points fall close to a curve with $He^4/Ne^{20} \sim 50$ and a positive He^4 intercept of $(3 \pm 1) \times 10^{-3}$ cm^3 STP/g. We have assumed that *all* of the Apollo 14 samples in Table 1 contain this amount of He^4 and have assumed that it is, in fact, *in situ* produced radiogenic He^4_R from U and Th decay. The average U and Th contents of Apollo 14 fines are 3.9 ppm and 13.7 ppm, respectively (LSPET, 1971). With these values we calculate an apparent U, Th-He^4 age of 3700 ± 800 m.y. This result is somewhat surprising in view of the fact that Cone Crater is located only a little more than 1 km to the east of the sites from which all five Apollo 14 fines were collected. The formation of Cone Crater has now been dated at 20–27 m.y. (Bogard and Nyquist, 1972; Lugmair and Marti, 1972). This means that either our assumptions are wrong, or that the Cone Crater materials lost little if any He^4_R when they were ejected, or that these ejecta constitute only a relatively small proportion of the fines only 1 km away.

The Ar^{40} intercepts from Ar^{40}–Ar^{36} correlation plots have been used to obtain apparent K–Ar^{40} ages of fines or certain constituents in fines (Heymann *et al.*, 1970; Pepin *et al.*, 1972). The Ar^{40} intercepts of 14163 and 14259 (see companion paper) combined with K contents taken from LSPET (1971) give apparent K–Ar^{40} ages of 3690 and 3630 m.y., respectively. These numbers seem to imply that the fines in question were not substantially heated since about 3600 m.y. ago, but this statement must be qualified in the light of our own Luna 16 results (Heymann *et al.*, 1972). We have found that breccia fragments in the Luna 16 soil contain "excess" Ar^{40} of unknown origin. The breccia from Apollo 11 are exceedingly rich in Ar^{40} (Funkhouser *et al.*, 1970). Certain Apollo 14 breccia rocks are also gas-rich (Bogard and Nyquist, 1972). Hence one must suspect that fines from nearly everywhere on the lunar surface contain variable proportions of gas-rich breccia fragments, whose Ar^{40} consists in part of a component which cannot be accurately estimated from gas measurements on bulk fines.

(2) *Cosmogenic gases*

For the Apollo 14 fines we have already made the assumption that these contain $(3 \pm 1) \times 10^{-3}$ cm^3 STP/g of He^4_R. Accordingly we have corrected all the He^4 measurements for this component. The corrected He^4/He^3 ratios range from 342 to 2860; the small values reflecting the presence of substantial quantities of cosmogenic He^3_C. For the Apollo 12 and 15 samples we could not make any correction for He^4_R; hence we have used the He^4/He^3 ratios as measured. We have further assumed that the trapped $(He^4/He^3)_T$ ratio in all of the samples is 2700 ± 100; i.e., we have calculated He^3_C only when $(He^4/He^3)_T$ is less than 2600. The results are shown in Table 2. Perhaps the most striking result is that the amount of He^3_C varies so little, and is typically around 0.3×10^{-5} cm^3 STP/g, which corresponds to an apparent He^3_C exposure age of about 300 m.y. For the few cases where He^3_C exposure ages of fines in different locations on the moon can be directly compared, one finds that these ages are roughly the same: 300 m.y. for 10084 (Kirsten *et al.*, 1970); 150 m.y. for 12070 (Hintenberger *et al.*, 1971). But it is also known that ages determined via Ne^{21}_C, or $Kr^{81}_C - Kr^{83}_C$, or $Ba - Xe^{126}_C$ are nearly always considerably older than He^3_C ages (Bogard *et al.*, 1971;

Table 2. Cosmogenic He^3_C and Ne^{21}_C.

Sample	$He^3_C(10^{-5}$ cm^3 STP/g)	$Ne^{21}(10^{-6}$ cm^3 STP/g)
14003 (bulk)	—	0.48
14163 (bulk)	0.33	0.68
14166 (1 fragment)	—	0.15
14167 (1 fragment)	—	0.028
14259 (bulk)	0.42	0.49
14259 (< 37 μ)	0.39	0.45
14259 (37–53 μ)	—	0.64
14259 (53–63 μ)	0.39	0.34
14259 (63–74 μ)	0.28	0.48
14259 (74–88 μ)	0.16	0.48
14259 (88–105 μ)	0.22	0.41
14259 (105–250 μ)	0.25	0.47
14259 (250–354 μ)	0.24	0.58
14259 (354–500 μ)	0.28	0.49
14259 (500–700 μ)	0.26	0.37
14259 (700–1000 μ)	0.28	0.50
14163 (< 37 μ)	0.52	0.72
14163 (37–63 μ)	0.29	0.63
14163 (63–74 μ)	0.23	0.56
14163 (74–88 μ)	0.30	0.69
14163 (88–105 μ)	0.27	0.64
14163 (105–250 μ)	0.28	0.72
14163 (250–354 μ)	0.25	0.50
14163 (354–500 μ)	0.33	0.69
14163 (500–700 μ)	0.28	0.55
14163 (700–1000 μ)	0.25	0.44
12042 (bulk)	—	0.47
12073 (interior chip)	0.08	0.47
12030 (bulk)	1.8	1.8
12044 (bulk)	0.13	0.43
12033 (> 250 μ)	0.08	0.03
12033 (105–250 μ) strongly magnetic	0.08	0.68
12033 (105–250 μ) weakly magnetic	0.09	0.70
12033 (< 105 μ)	—	0.39
12033 (< 105 μ)	0.06	0.65
15601 (bulk)	0.30	0.44
15091 (bulk)	—	0.45
15601 (500–700 μ)	0.24	0.43
15601 (354–500 μ)	0.35	0.67
15601 (250–354 μ)	0.29	0.58
15601 (105–250 μ)	—	0.50
15601 (88–105 μ)	0.26	0.58
15601 (74–88 μ)	0.32	0.60
15601 (63–74 μ)	0.11	0.58
15601 (53–63 μ)	0.12	0.49
15601 (44–53 μ)	0.53	0.68
15601 (< 44 μ)	0.30	3.61

Eberhardt *et al.*, 1970; Marti *et al.*, 1970). Apparently the He^3_C ages are false, reflecting as they perhaps do a steady state between the production of He^3_C by cosmic rays and diffusion losses from minerals of poor He retentivity, such as Ca-rich plagioclase.

The isotopic relationships of trapped neon (Ne^{20}/Ne^{22}; $Ne^{22}/Ne^{21})_T$ were obtained for 14163 and 14259 by the method first used by Eberhardt *et al.* (1970). We obtained $(Ne^{22}/Ne^{21})_T = 31.1 \pm 1.0$ and $(Ne^{20}/Ne^{21})_T = 410 \pm 30$ for both fines.

This means that $(Ne^{20}/Ne^{22})_T = 13.2$. We have used the $(Ne^{20}/Ne^{21})_T$ ratio to calculate Ne_C^{21}, with the simple assumption that all Ne^{20} is of the trapped variety. The results are given in Table 2. Again, the most salient result is that the amounts of Ne_C^{21} are rather constant, e.g., 37 of 45 values (14166 and 14167 excluded) fall between 0.4 and 0.7×10^{-6} cm^3 STP/g. The average Ne_C^{21} contents of 14163 and 14259 (size fractions plus bulk) are 0.64×10^{-6} and 0.47×10^{-6} cm^3 STP/g, respectively. The Ne_C^{21} production rate was calculated from the assumed He_C^3 rate of 1.0×10^{-8} cm^3 STP/g per m.y. with the correlation of Bogard *et al.* (1971) for He_C^3/Ne_C^{21} as a function of composition and the average composition of Apollo 14 fines as reported by LSPET (1971). We have thus calculated a production rate of 0.16×10^{-8} cm^3 STP/g per m.y. with this value the Ne_C^{21} exposure ages of 14163 and 14259 are 400 and 300 m.y., respectively. The average Ne_C^{21} content of 15601 is 0.55×10^{-6} cm^3 STP/g, which corresponds to an exposure age of 350 m.y.

The following results in Table 2 call for comments:

(1) The Ne_C^{21} ages of the 14166 and 14167 fragments are well below the ages of the fines. But this probably reflects merely a statistical effect of ages determined on single particles as against ages determined on a large number of particles.

(2) He_C^3 contents of all 12033 samples are far below those of typical bulk fines; they correspond to an apparent exposure age of only about 80 m.y. Four of the five Ne_C^{21} values on the other hand are in the same range as most of the values seen in the fines samples; i.e., the former correspond to ages of some 250–400 m.y. We think that the small He_C^3 in 12033 are indicative of substantial He diffusion losses from this sample.

(3) Both He_C^3 and Ne_C^{21} in 12030 are unusually large, but this sample is also the most gas-rich in Table 1. The large numbers may well be an artifact because of our choice of $(He^4/He^3)_T = 2700$ and $(Ne^{20}/Ne^{21})_T = 410$. Sample 12030 is apparently not a genuine sample of fines but comes from glass covered fragments at the bottom of a 1-m diameter crater, which "don't seem to hold together very well" according to the astronaut's comments (Shoemaker *et al.*, 1970). From this we infer that 12030 is a loosely consolidated soil breccia. If the He_C^3 and Ne_C^{21} shown in Table 2 are real, they may imply that this breccia was formed from pre-irradiated fines, which had been very near the top of the regolith for about 1800 m.y. (He_C^3 age), or that the crater itself was formed about 1800 m.y. ago. In the second case one must assume that the glass covered soil clod was produced by the impact, and was not covered since by a substantial amount of regolith to shield it from cosmic ray bombardment.

Acknowledgment—This work was supported by NASA Grant NGL 44-006-127.

REFERENCES

Bogard D. D., Funkhouser J. G., Schaeffer O. A., and Zähringer J. (1971) Noble gas abundances in lunar material-cosmic ray spallation products and radiation ages from the Sea of Tranquility and the Ocean of Storms. *J. Geophys. Res.* **76,** 2757–2779.

Bogard D. D. and Nyquist L. E. (1972) Noble gas studies on regolith materials from Apollo 14 and 15 (abstract). In *Lunar Science—III* (editor C. Watkins), pp. 89–91, Lunar Science Institute Contr. No. 88.

Eberhardt P., Geiss J., Graf H., Grögler N., Krähenbühl U., Schwaller H., Schwarzmüller J., and Stettler A. (1970) Trapped solar wind noble gases, exposure age and K/Ar-age in Apollo 11 lunar fine material. *Proc. Apollo 11 Lunar Sci. Conf., Geochim. Cosmochim. Acta* Suppl. 1, Vol. 2, pp. 1037–1070. Pergamon.

Funkhouser J. G., Schaeffer O. A., Bogard D. D., and Zähringer J. (1970) Gas analysis of the lunar surface. *Proc. Apollo 11 Lunar Sci. Conf., Geochim. Cosmochim. Acta* Suppl. 1, Vol. 2, pp. 1111–1116. Pergamon.

Geiss J., Eberhardt P., Signer P., Buehler F., and Meister J. (1970) The solar wind composition experiment. *Apollo 12 Preliminary Science Report*, NASA SP-235, pp. 99–102.

Heymann D., Yaniv A., Adams J. A. S., and Fryer G. E. (1970) Inert gases in lunar samples. *Science* **167,** 555–558.

Heymann D. and Yaniv A. (1970a) Inert gases in the fines from the Sea of Tranquility. *Proc. Apollo 11 Lunar Sci. Conf., Geochim. Cosmochim. Acta* Suppl. 1, Vol. 2, pp. 1247–1259. Pergamon.

Heymann D., Yaniv A., and Lakatos S. (1972) Inert gases in twelve particles and one "dust" sample from Luna 16. *Earth Planet. Sci. Lett.* **13,** 400–406.

Hintenberger H., Weber H. W., and Takaoka N. (1971) Concentrations and isotopic abundances of the rare gases in lunar matter. *Proc. Second Lunar Sci. Conf., Geochim. Cosmochim. Acta* Suppl. 2, Vol. 2, pp. 1607–1626. MIT Press.

LSPET (Lunar Sample Preliminary Examination Team) (1971) Preliminary examination of lunar samples. *Apollo 14 Preliminary Science Report*, NASA SP-272, pp. 109–132.

Lugmair G. W. and Marti K. (1972) Neutron and spallation effects in Fra Mauro regolith (abstract). In *Lunar Science—III* (editor C. Watkins), pp. 495–497, Lunar Science Institute Contr. No. 88.

Marti K., Lugmair G. W., and Urey H. C. (1970) Solar wind gases, cosmic ray spallation products and the irradiation history of Apollo 11 samples. *Apollo 11 Lunar Sci. Conf., Geochim. Cosmochim. Acta* Suppl. 1, Vol. 2, pp. 1357–1367. Pergamon.

Pepin R. O., Bradley J. G., Dragon J. C., and Nyquist R. E. (1972) K–Ar dating of lunar soils: Apollo 12, Apollo 14, and Luna 16 (abstract). In *Lunar Science—III* (editor C. Watkins), pp. 602–604, Lunar Science Institute Contr. No. 88.

Shoemaker E. M., Batson R. M., Bean A. L., Conrad C. Jr., Dahlem D. H., Goddard E. N., Hait M. H., Larson K. B., Schaber G. G., Schleicher D. L., Sutton R. L., Swann G. A., and Waters A. C. (1970) Preliminary geologic investigation of the Apollo 12 landing site. *Apollo 12 Preliminary Science Report*, NASA SP-235, pp. 113–156.

Proceedings of the Third Lunar Science Conference
(Supplement 3, *Geochimica et Cosmochimica Acta*)
Vol. 2, pp. 1865–1889
The M.I.T. Press, 1972

The rare gas record of Apollo 14 and 15 samples

T. KIRSTEN, J. DEUBNER, P. HORN, I. KANEOKA, J. KIKO,
O. A. SCHAEFFER, and S. K. THIO

Max-Planck-Institut für Kernphysik,
Heidelberg, Germany

Abstract—Rare gases have been measured in numerous samples from Apollo 14 and 15 returns including bulk soils, individual soil grains, 10–50 mg rock fragments from the soil, clasts, pieces of breccia, and pieces of large crystalline rocks. Some of the samples were irradiated with fast neutrons before analysis, allowing a determination of ^{39}Ar–^{40}Ar crystallization ages and ^{37}Ar–^{38}Ar cosmic ray exposure ages. The ages show that the Fra Mauro formation at the Apollo 14 landing site contains mainly debris from the pre-Mare Imbrium terrain, with some fragments from neighboring maria and that there has been igneous activity at the pre-Mare Imbrium site for over 200 m.y. from 3.8 to 4.0×10^9 years ago. Exposure ages are found to lie between 15 m.y. and 770 m.y. for the rocks. Individual soil grains give ages as high as 1700 m.y. These ages reflect the gardening of the lunar soil. As the solar wind component in the soil is similar at all sites, it is inferred that the retained solar wind may be very ancient, possibly up to 4.0×10^9 years. Some single grains contain solar wind very little changed by diffusion. Several anomalies exist, the Ne is enriched in 15421 soil from near Spur Crater and the abundance ratio of "parentless" ^{40}Ar relative to implanted ^{36}Ar is variable and can be as high as 8.

INTRODUCTION

THE RARE GAS CONTENTS of lunar samples provide a comprehensive record of their evolution. Radiogenic, cosmogenic, trapped, and dissolved rare gases have been used extensively to study formation ages, stratigraphic relationships, exposure ages, regolith formation, transport processes, and solar wind abundances.

Age determinations have shown that lunar rocks crystallized between 3.2×10^9 and 3.9×10^9 yr ago, except for rocks 12013 (Husain *et al.*, 1972) and 15415 (Turner, 1971) which show slightly older crystallization ages. Major events dated are one of the latest mare fillings at Oceanus Procellarum 3.3×10^9 yr ago, Mare Tranquilitatis 3.7×10^9 yr ago, and Imbrium Basin excavation 3.8×10^9 yr ago. Here we report on further age measurements using the ^{39}Ar–^{40}Ar method, shown by Turner (1970) to be particularly applicable to lunar rocks. Rock fragments from the soil and from clasts in 14303 have been studied. In addition, conventional K–Ar dating has been applied to determine model ages for lunar soils.

The time spent by rock fragments at the top layer of the regolith can be estimated from the amount of accumulated spallation products. In this paper we report particularly on spallation products in various lunar soils. Such data provide mean turnover rates for the sampled regolith sites. In addition, a search for extremely high exposure ages was performed by analyzing single soil particles. This could narrow the gap of recordable time between $\sim 1 \times 10^9$ and 3×10^9 yr.

The solar wind implanted gases in lunar soils and breccias are of interest with regard to elemental and isotopic solar abundances at present and in the past; they

are, however, sensitive to the various temperatures within the lunar regolith. Apart from bulk soil analyses, we have therefore analyzed implanted gases in single Apollo 14 soil particles. This is a continuation of previous studies for Apollo 12 soil (Kirsten *et al.*, 1971). It is hoped then to find a particular specimen in which implanted gases display minimal alteration by solid state diffusion. Results on diffusion studies in single soil particles reported at the Third Lunar Science Conference (Kirsten *et al.*, 1972) will be published in Ducati *et al.*, 1972.

Sample Description and Preparation

Bulk soils were measured in mg-sized samples from aliquots as obtained. Sieve fractions were prepared by wet sieving using anhydrous ethanol. Etched samples were exposed for 10 sec to a solution of 1 part H_2SO_4, 1 part HF, and 2 parts H_2O. Single soil particles were handpicked from the coarser sieve fractions under the microscope. They were identified by standard mineralogic techniques, occasionally controlled by XRD methods.

Single rock fragments from coarse fines were ultrasonically cleaned in ethanol. The fragmental rock 14303,13 was cut dry into slices of $\sim 20 \times 30 \times 2$ mm, using a wire saw. Two slices were gently crushed into fragments ≤ 4 mm, the size of the largest clasts. Igneous and brecciated clasts were handpicked under the binocular, liberated from adhering ground mass particles, and ultrasonically cleaned. Different clast types were selected according to color, crystallinity, homogeneity, etc. Before analysis, small chips were broken off to prepare polished sections. A similar treatment was given to basalts handpicked from coarse fines 14161. The small chips used for polished sections may not always be representative of the whole sample. Occasionally very fine grained patches of mesostasis with a "sieve structure" enriched in K according to microprobe analysis (El Goresy, 1972) occur. In judging shock effects, the presence of milky white plagioclases, cataclastic deformations, and fragmentations in the minerals and planar elements in plagioclase were taken as indications. Local melting due to shock and subsequent recrystallization is rare.

Sample description

14001,5	contingency soil, 2–4 mm, near LM
14003,24	contingency soil, <1 mm, near LM
14161,26 + 34	coarse fines, composed of lithic clasts, pyroxene, plagioclase, glass, and opaques, 2–4 mm, near LM
14257,9	comprehensive soil, 2–4 mm, 100 m NW of LM
14303,13	fragmental rock, highly metamorphosed, group 6 of the classification by Warner (1972), 100 m NW of LM
15021,94	contingency soil <1 mm, near LM
15101,59	soil <1 mm from Apennine front (St. George Crater)
15301,79	soil <1 mm, rich in green glass, rim of Spur Crater
15421,21	soil <1 mm, very rich in green glass, rim of Spur Crater
15556,25	vesicular basalt, 60 m from the rim of Hadley Rille
15601,63	comprehensive soil <1 mm, 20 m NE of rim of Hadley Rille, matured surface

Subsamples used for ^{39}Ar–^{40}Ar dating

14161,34,2	ophitic basalt, shocked, interlocking plagioclase laths enclosed in pyroxenes; ilmenite, iron, chromite, ulvöspinel, troilite, very little tridymite; fine grained ($<100\ \mu$); local patches of K-rich mesostasis
14161,34,5	intergranular basalt, rounded pyroxene grains in a matrix of plagioclase; ilmenite, iron, troilite, spinel, tridymite; relatively coarse grained ($\sim 100\ \mu$)
14161,34,4	vuggy intergranular basalt, shocked, plagioclase intergrown with pyroxenes; olivine; ilmenite, iron, chromite, troilite; little tridymite; troilite in microcracks of pyroxenes; coarse grained ($\sim 100\ \mu$); local patches of K-rich mesostasis
14161,34,6	basalt with cognate basalt inclusion, shocked, composed of two types of basaltic rocks, one being coarser grained than the other; both composed of pyroxene and plagioclase, laths of ilmenite, iron, large spinels, troilite, baddeleyite; resembling rock 14310
14303,13,R5,1	intergranular basalt, shocked, plagioclase intergrown with pyroxenes; much tridymite and iron, little ilmenite, troilite and spinel; coarse grained ($\geq 100\ \mu$)
14303,13,R5,21	coarse grained annealed basaltic microbreccia, shocked, angular fragments of plagioclases ($\sim 100\ \mu$) in a fine grained matrix ($<20\ \mu$) of plagioclase and pyroxene; ilmenite extremely fine grained and dispersed, iron, troilite, spinel; holocrystalline
14303,13,R5,22	fine grained annealed basaltic microbreccia, shocked as R5,21, finer grained; glass probably present
14161,34,3	feldspathic accumulate + pyroxene, shocked, very coarse grained plagioclases ($\sim 90\%$) and small aggregates of pyroxenes ($\sim 10\%$); no opaques
14161,26,11	intergranular basalt, pyroxenes intergrown with plagioclases; troilite, spinel, iron, ilmenite; ore content is small; coarse grained ($\geq 100\ \mu$)
14161,26,12	intergranular basalt, as 26,11, coarser

Subsamples used for rare gas analysis

14001,5,1 + 2	lithic clasts
14003,24,1 + 2	inhomogeneous sieve fraction $>300\ \mu$
14161,26,1	fine grained, coherent microbreccia
14161,34,8	"sintered soil"
14161,34,9	friable microbreccia, glass rich
14161,34,10	friable ground mass
14257,9,1	lithic clast
14303,13,6	annealed breccia, fine grained dark lithic clast
14303,13,7	coarse grained basaltic rock
14303,13,8	matrix material
14303,13,9	fine grained black basaltic rock
14303,13,12	anorthositic fragment

Experimental Procedures and Results

^{39}Ar–^{40}Ar dating

Lunar samples (ranging from 10 to 60 mg) and terrestrial hornblende monitors were wrapped in aluminum foil, stacked alternatingly in quartz ampoules and vacuum-sealed together with a nickel wire to check the uniformity of the neutron flux from the induced ^{58}Co activity. Samples marked "K" in Table 1 were irradiated for 14 days in the core of the Karlsruhe FR2 reactor behind Cd-shielding. The integrated fast neutron flux was $\sim 2.7 \times 10^{18}$ n/cm^2. The neutron flux gradient along the length of the ampoule (4.5 cm) was $<2\%$. The "M" samples received a 10 days irradiation in the core of the BR-2 reactor at Mol, Belgium. Here, the integrated fast neutron flux

Table 1. Summary of ^{39}Ar–^{40}Ar ages and exposure ages.

Sample	J value used	K (%)	Ca (%)	Total argon age ($\times 10^9$ yr)	High-temperature age ($\times 10^9$ yr)	Plateau age ($\times 10^9$ yr)	Exposure age ^{38}Ar–Ca ($\times 10^6$ yr)
14161,34,2	0.01610 K	0.61	7.1	3.83 ± 0.08	3.85 ± 0.08	4.03 ± 0.08	380
14161,34,5	0.01610 K	0.73	7.6	3.92 ± 0.08	3.93 ± 0.08	4.01 ± 0.06	430
14161,34,4	0.01610 K	0.55	7.9	3.91 ± 0.06	3.96 ± 0.06	3.99 ± 0.04	300
14161,34,6	0.01740 K	0.76	7.8	3.74 ± 0.04	3.86 ± 0.04	3.90 ± 0.04	390
14303,13,R5,1	0.01740 K	1.10	7.1	3.75 ± 0.02	3.89 ± 0.04	3.91 ± 0.04	29
14303,13,R5,21	0.1502 M	0.69	8.3	3.44 ± 0.08	3.45 ± 0.08	(3.78 ± 0.14)	—
14303,13,R5,22	0.1502 M	0.0057	7.9	(5.69 ± 0.08)	—	—	—
14161,34,3	0.1502 M	0.46	13.4	3.62 ± 0.08	3.63 ± 0.10	3.63 ± 0.10	—
14161,26,11	0.01740 K	0.53	6.4	3.58 ± 0.04	3.59 ± 0.04	3.59 ± 0.04	360
14161,26,12	0.01740 K	0.062	8.5	3.54 ± 0.04	3.52 ± 0.04	3.54 ± 0.02	320

Error figures indicate 2σ standard deviation. Errors for K and Ca $\leq 5\%$, for exposure ages $\leq 10\%$.
K = Karlsruhe irradiation.
M = Mol (Belgium) irradiation (see text).

was 2.1×10^{19} n/cm^2. In this case, shielding from thermal neutrons turned out to be incomplete.

The irradiated samples were loaded into the high-vacuum, on-line extraction system of a high-sensitivity Nier-type mass spectrometer. Samples were inductively heated in a molybdenum crucible for periods of 1 hour, at successively higher temperatures ranging from 600°C to 1500°C, determined by a W–Re-alloy-thermocouple directly attached to the crucible. Temperature fluctuations were less than ±5°C.

After the purified gas was introduced into the spectrometer, the extraction furnace was isolated for the next extraction. Blanks determined after each sample ranged from 5×10^{-10} cc STP ^{40}Ar at low temperatures to 10^{-8} cc STP ^{40}Ar at 1500°C.

$^{40}Ar/^{39}Ar$ ratios were determined from 15–20 recordings, other Ar-isotopes from three recordings, taking into account linear zero-time extrapolations. Errors given for the $^{40}Ar/^{39}Ar$ ratio are 2σ standard deviations, errors of other isotopes are estimated from the general spectrometer characteristics and reproducibility considerations. The following corrections were applied to the measured values:

(a) Blank corrections.
(b) ^{37}Ar decay between time of bombardment and time of measurement.
(c) ^{39}Ar produced from Ca, with $(^{39}Ar/^{37}Ar)_{Ca} = 0.001$.
(d) ^{40}Ar trapped, with $(^{40}Ar/^{36}Ar)_{tr} = 1$.

Using production ratios given by Brereton (1970), we corrected for:

(e) ^{40}Ar produced from K, with $(^{40}Ar/^{39}Ar)_K = (1.23 \pm 0.24) \times 10^{-2}$.
(f) ^{38}Ar produced from K, with $(^{38}Ar/^{39}Ar)_K = (1.14 \pm 0.03) \times 10^{-2}$.
(g) ^{38}Ar produced from Ca, with $(^{38}Ar/^{37}Ar)_{Ca} = (1.39 \pm 0.26) \times 10^{-4}$.
(h) ^{36}Ar produced from Ca, with $(^{36}Ar/^{37}Ar)_{Ca} = (2.47 \pm 0.09) \times 10^{-4}$.

K and Ca contents are determined from ^{39}Ar and ^{37}Ar in sample and monitor and the K and Ca content of the monitor (see Table 1).

A hornblende separate from the Northern Light Gneiss of Northern Minnesota was used as monitor. Its K–Ar age was found to be $2.60 \pm 0.04 \times 10^9$ yr (K content by neutron activation 3030 ± 30 ppm; $^{40}Ar_{rad}$ $(6.7 \pm 0.2) \times 10^{-5}$ cc STP/g; $\lambda_\beta = 4.72 \times 10^{-10}$ yr^{-1}; $\lambda_\kappa = 0.585 \times 10^{-10}$ yr^{-1}; $^{40}K/K = 1.19 \times 10^{-4}$). Atomic

absorption analysis gave a Ca content of (8.00 ± 0.05)%. The J values (Grasty and Mitchell, 1966) needed to convert the measured $^{40}Ar/^{39}Ar$ ratios into ages, are listed in Table 1.

The release patterns of all Ar isotopes for all samples and temperature steps will be presented in a more detailed discussion (Kaneoka, 1972). However, the corrected total Ar isotope concentrations are given in Table 2. Figures 1–5 show the radiogenic

Table 2. Total amount of argon isotopes.

Sample	$^{40}Ar^*$	$^{39}Ar_K$	10^{-8}ccSTP/g $^{38}Ar_{corr}$	$^{37}Ar_{corr}$	$^{36}Ar_{corr}$	$^{38}Ar_{sp}$
14161,34,2	30150	73.2	66.2	543	153	42.5
14161,34,5	38490	88.5	59.4	577	93.5	47.6
14161,34,4	29000	67.0	56.1	605	136	34.7
14161,34,6	35670	99.4	52.3	694	51.2	48.4
14303,13,R5,1	52400	144	4.20	629	6.69	3.34
14303,13,R5,21	27030	783	108†	5090	3.91	—
14303,13,R5,22	539.9	4.18	40.3†	3130	25.0	—
14161,34,3	20020	518	109†	8170	6.10	—
14161,26,11	22770	69.6	49.8	572	72.8	41.0
14161,26,12	2591	8.10	51.6	755	40.7	49.9

† Partly due to improper shielding from thermal neutrons.
^{36}Ar corrected for reactor produced ^{36}Ar from Ca.
^{37}Ar corrected for decay after irradiation.
^{38}Ar corrected for reactor produced ^{38}Ar from K and Ca.

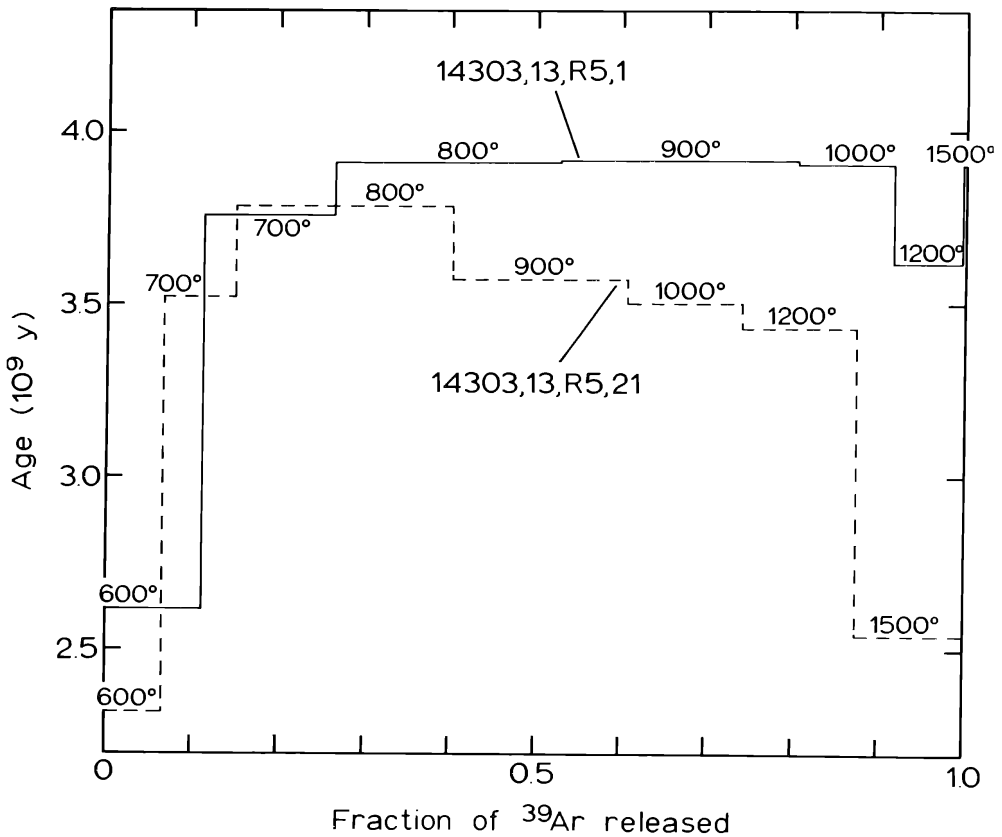

Fig. 1. ^{39}Ar–^{40}Ar age release patterns for basaltic fragment 14303,13,R5,1 showing a good plateau, and microbreccia 14303,13,R5,21 showing a steady decrease at higher temperatures.

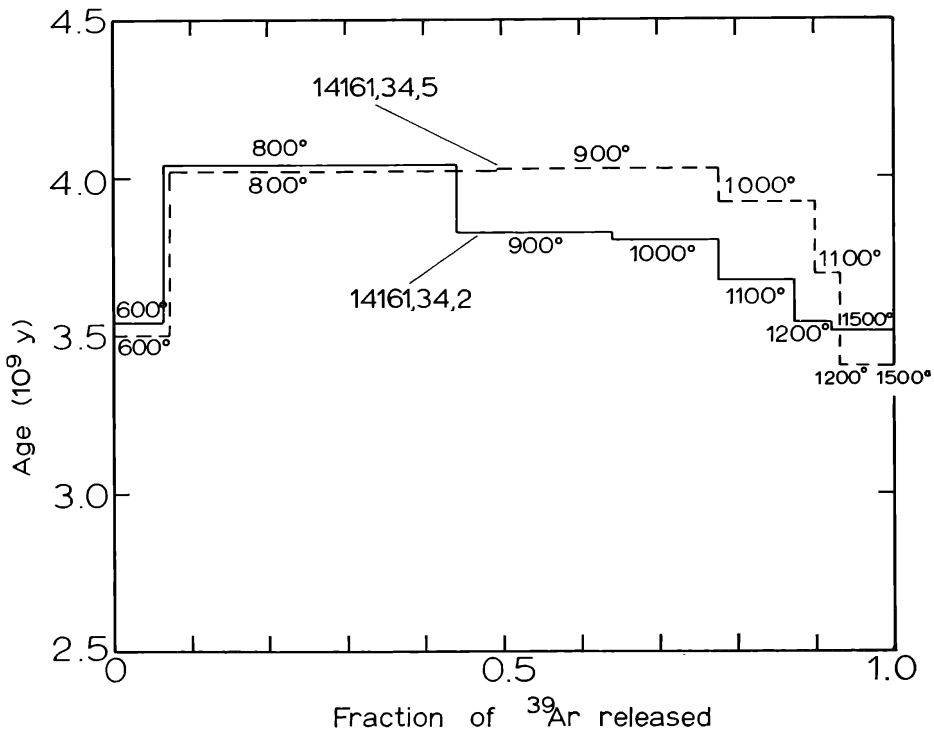

Fig. 2. ^{39}Ar–^{40}Ar age release patterns for basaltic fragments 14161,34,2 and 14161,34,5 with decrease in apparent ages at higher temperatures.

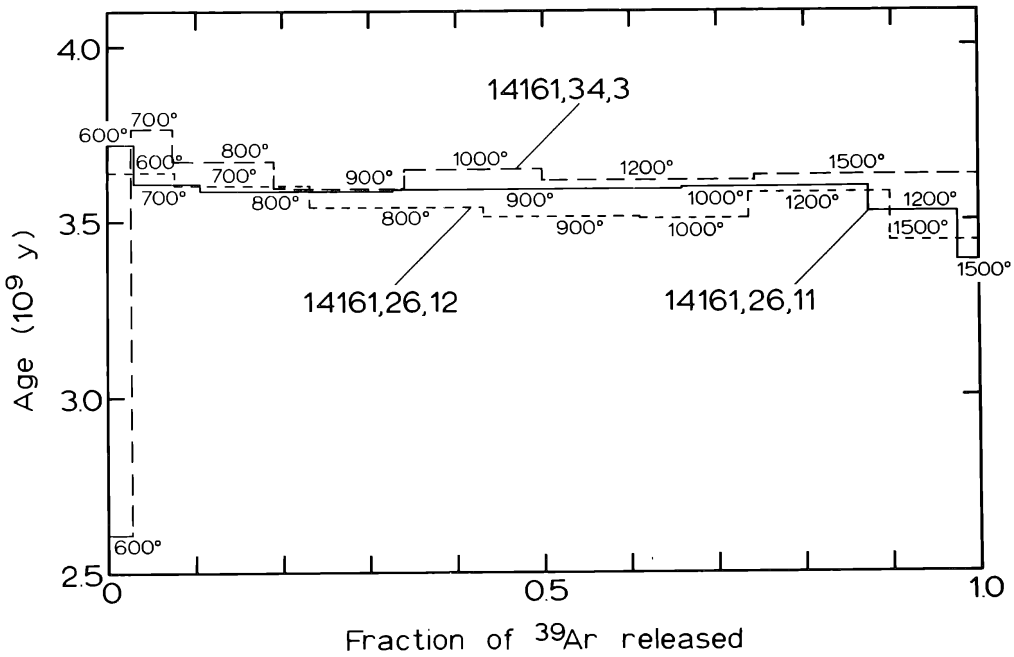

Fig. 3. ^{39}Ar–^{40}Ar age release patterns for basaltic fragments 14161,26,11 and 14161,26,12 and feldspathic accumulate, 14161,34,3 with very little loss of radiogenic argon and well defined plateaus.

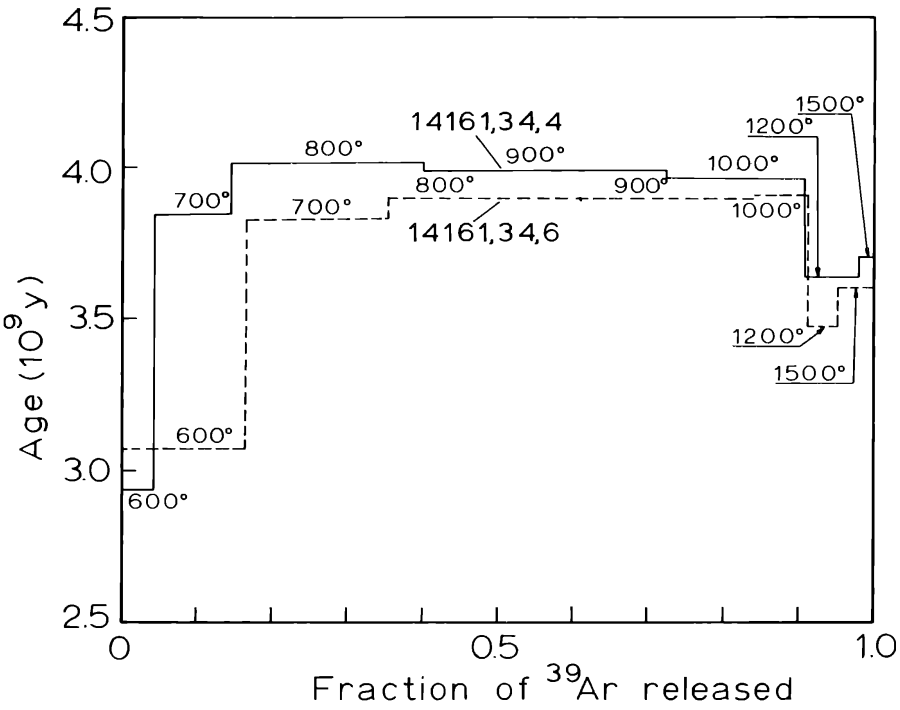

Fig. 4. ^{39}Ar–^{40}Ar age release patterns for basaltic fragments 14161,34,4 and 14161,34,6 with well-defined plateaus, but decrease at lower and higher temperatures.

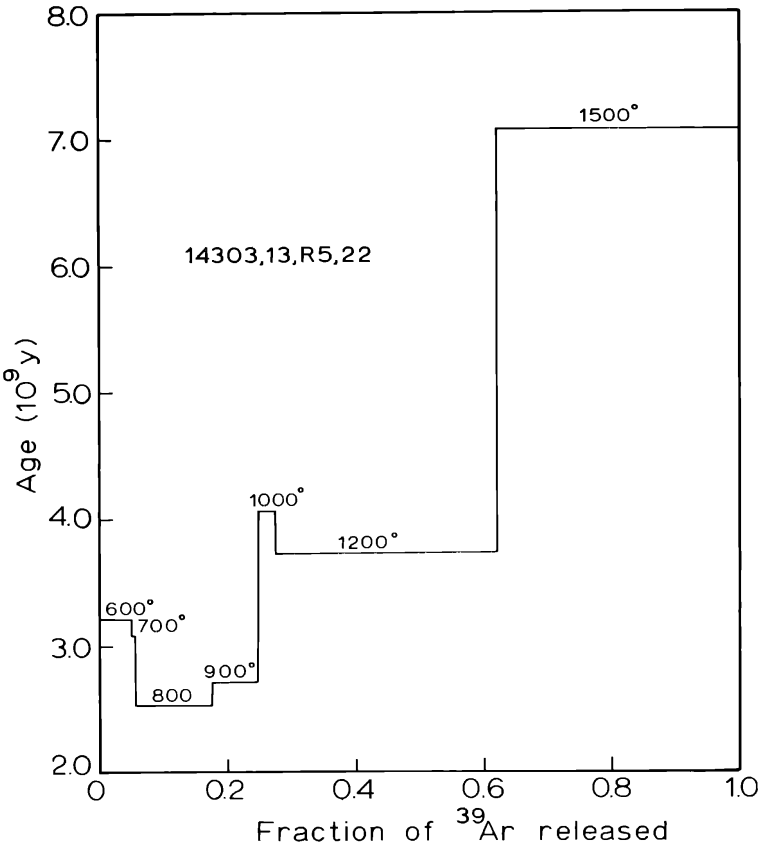

Fig. 5. ^{39}Ar–^{40}Ar age release pattern for microbreccia 14303,13,R5,22 with evidence for excess argon (even the total argon age is 5.7×10^9 yr).

gas release patterns converted into ages. As also observed by other authors (Turner *et al.*, 1971; Schaeffer *et al.*, 1972), the $^{40}Ar/^{39}Ar$ ratio in Apollo 14 rocks frequently decreases from the plateau value at the highest temperatures (e.g., Figs. 1, 2, and 4). Hence, we distinguish between total argon ages, plateau ages, and high-temperature ages. They are calculated from the Ar released between 600–1500°C, $T_{\text{Plateau, start}}$ to $T_{\text{Plateau, end}}$, and $T_{\text{Plateau, start}}$ to 1500°C, respectively. Table 1 is a summary of all ages so obtained. Error progression was calculated following Dalrymple and Lanphere (1971). Errors given are 2σ standard deviations. To calculate exposure ages from neutron-irradiated samples the corrected ^{38}Ar of each temperature fraction was split into a spallogenic and a trapped component assuming $(^{36}Ar/^{38}Ar)_{sp} = 0.63$; $(^{36}Ar/^{38}Ar)_{tr} = 5.35$. As shown in Figs. 6 and 7, the release pattern of ^{38}Ar is similar to that of Ca-derived ^{37}Ar, especially at higher temperatures, indicating that spallogenic ^{38}Ar is mainly produced from Ca. Particularly, the lowest $^{38}Ar_{sp}/^{37}Ar$ ratio should represent spallogenic ^{38}Ar from Ca alone and is therefore used to determine the total Ca-derived $^{38}Ar_{sp}$. Since Ca contents are also known, ^{38}Ar–Ca exposure ages can be calculated, adopting a production rate of 1.4×10^{-8} cc STP/g Ca, m.y. (Turner *et al.*, 1971). Results are given in Table 6.

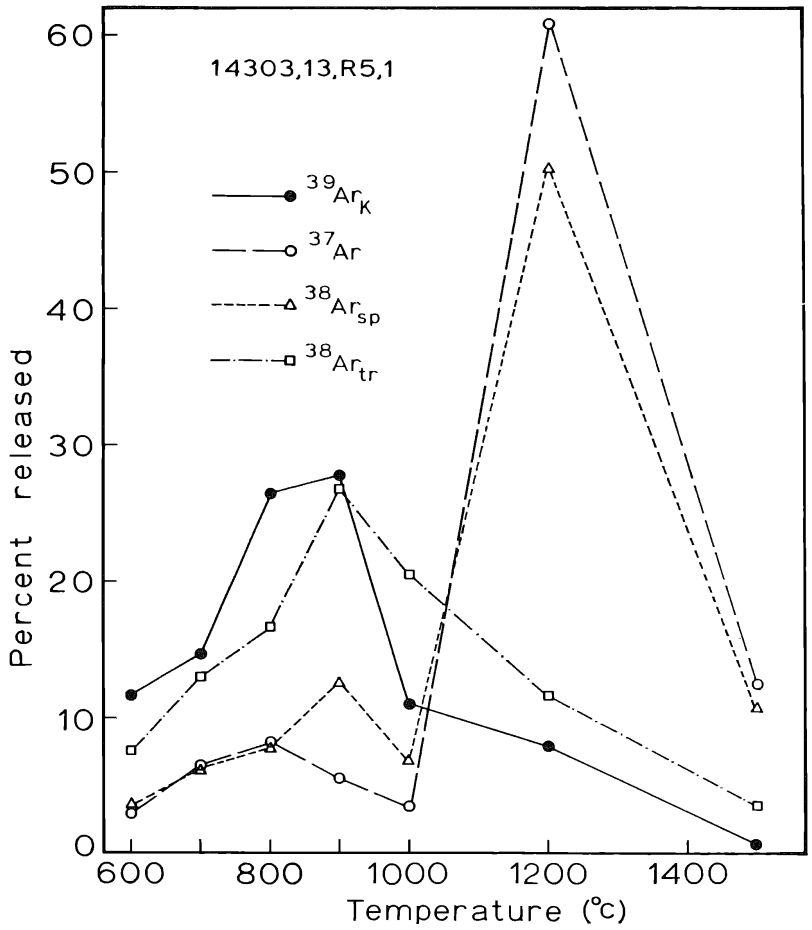

Fig. 6. Release pattern of different argon isotopes from basaltic fragment 14303,13,R5,1. Note correlation between ^{37}Ar and $^{38}Ar_{sp}$.

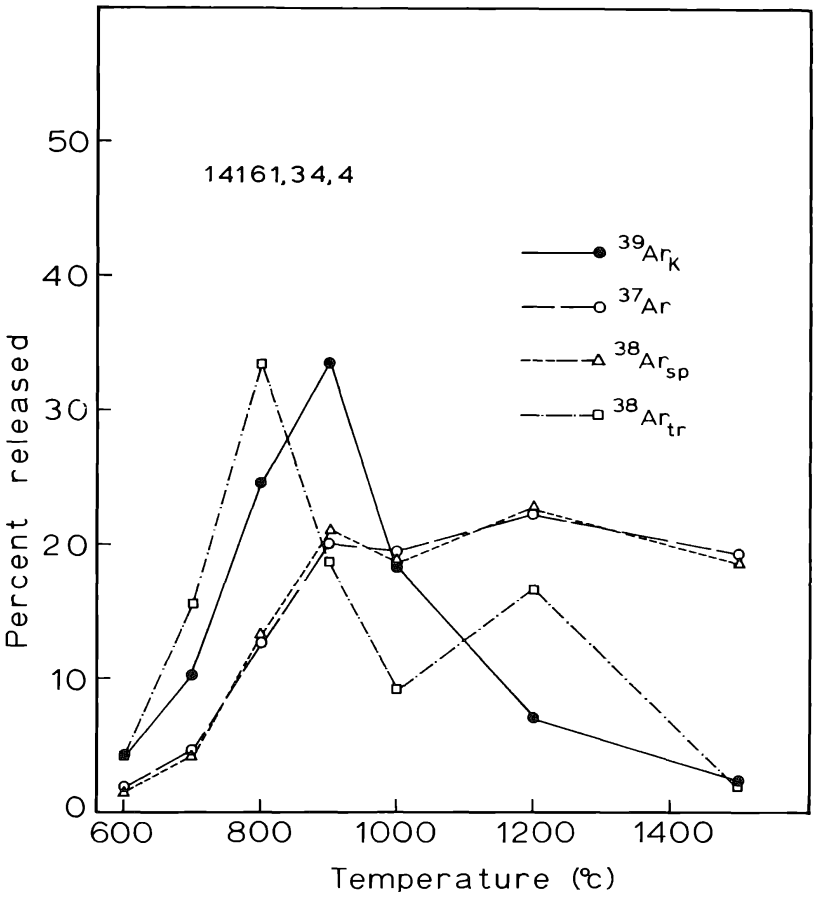

Fig. 7. Release pattern of each argon isotope for basaltic fragment 14161,34,4.

Rare gas analysis of bulk samples

Standard procedures were applied in the mass spectrometric rare gas analysis of bulk samples. Blank values were (in 10^{-10} cc STP) $^{3}He \sim 1$, $^{4}He \sim 40$; $^{20}Ne \sim 3$, $^{21}Ne \sim 0.5$, $^{22}Ne \sim 2$, $^{36}Ar \sim 0.1$, $^{38}Ar \sim 0.1$, $^{40}Ar \sim 150$, $^{84}Kr \sim 0.01$, $^{132}Xe \sim 0.01$. Samples were predegassed for 6 hours at 180°C.

In performing conventional K–Ar dating of soils, aliquots of ~100 mg were split into two parts. One part was used to determine K and U by neutron activation, the other was slightly etched in a diluted HF/H_2SO_4 solution to reduce the concentration of surface correlated gases. Afterwards mg-sized samples were taken for the mass spectrometric analysis.

Table 3 contains the results for bulk soils, sieve-fractions of 14003, and etched sieve-fractions of 14003 and 15101. All these data are based on duplicate or triplicate analyses.

Results from the analysis of coarse fines and rocks are given in Table 4. Small sample weights (generally $\lesssim 1$ mg) were chosen for accurate He, Ne, and Ar determinations to avoid errors caused by volume dilutions. As a consequence, the less abundant Kr and Xe isotopes were determined only for the various fractions of soil 14003. These data are listed in Table 5.

Absolute errors for He, Ne, and Ar are estimated to be less than $\pm 6\%$ from the

1972LPSC....3.1637F

Table 3. Rare gas concentrations in Apollo 14 and 15 soils (in 10^{-8} ccSTP/g).

Sample	^{3}He	^{4}He	^{20}Ne	^{21}Ne	^{22}Ne	^{36}Ar	^{38}Ar	^{40}Ar	^{84}Kr	^{132}Xe	K (ppm)	U (ppm)
Bulk fines												
14003	3150	8880000	160000	448	12100	43300	7940	67800	24.3	3.9	4360	3.3
15021	2890	8942000	186000	497	13700	40500	7450	29800	23.7	3.15	1610*	1.3*
15101	3030	7900000	168000	456	12850	34600	6450	40800	12.0	1.8	1430	0.91
15601	2610	7633000	159000	452	12270	24400	4600	21100	8.3	1.4	820	0.51
15301	1820	5614000	183300	486	13620	31600	5850	52700	13	2.3	1220*	0.8*
15421	900	2540000	125000	368	9290	15130	2810	54800	5.5	1.6	940†	
Sieve fractions												
14003 < 25 μ	5350	15340000	285000	753	21560	78200	14370	112900	53	7.3		
25–60 μ	1235	3700000	79500	240	5980	22700	4295	37740	16.2	2.0		
60–109 μ	990	2660000	55500	190	4250	20640	3805	39200	11.3	1.75		
109–272 μ	710	2092000	40900	147	3180	13540	2590	32800	9.7	1.65		
Etched fines												
14003 60–109 μ	300	820000	10750	87	905	2790	569	14200	2.33	0.44	3780	
109–272 μ	282	752000	15850	90	1290	7100	1375	23300	5.65	0.91	4240	
15101,59,1,3												
60–109 μ	334	572000	9900	87.2	830	2320	470	5800	—	—	1280	0.81
15101,59,1,2												
109–272 μ	298	548000	14000	90.3	1136	4200	800	7200	—	—	1190	0.74

* Keith *et al.* (1972). † LSPET (1972). Absolute errors < ±6%, for Kr and Xe < ±20%.

Table 4. Rare gas concentrations in coarse fragments, breccias and rocks (in 10^{-8} cc STP/g).

Sample	^{3}He	^{4}He	^{20}Ne	^{21}Ne	^{22}Ne	^{36}Ar	^{38}Ar	^{40}Ar	^{84}Kr	^{132}Xe	K (ppm)	U (ppm)
Coarse fines												
14003,24,1 > 300 μ	890	2500000	53000	177	4110	17200	3230	35000	19	4		
14003,24,2 > 300 μ	1200	4150000	60100	186	4640	10540	1990	86700	6.4	0.84		
14001,5,1	510	504000	2045	109	278	482	161	28000	0.60	0.24		
14001,5,2	490	420000	1200	144	199	240	114	28000	0.38	0.19		
14257,9,1	66	262000	990	16.4	87	211	52.5	27600	0.18	0.1		
14161,26,breccia	1310	4720000	96000	283	7000	13540	2560	160000	6.4	1.3	4500*	
14161,26,1	160	129000	309	40.8	66.7	78.9	51.1	31300			for range of varia-	
14161,34,8	228	351000	2520	42.7	247	640	157	22700			tions see Table 1,	
14161,34,9	3300	10900000	210000	632	15800	46000	8500	127000	27.7	5.7	and Hubbard *et al.*	
14161,34,10	2915	9700000	150000	409	11100	39000	7300	84700	24.8	4.4	(1972).	
											620–7600	3.3–5
Clastic rock fragments												
14303, saw dust	13.4	250000		2.6		9.4	3.66	24400	0.1	0.07	7450	4.0
14303,13,6	16.2	328000	≤4.7	2.65	3.18	13.6	4.4	40700				
14303,13,7	16.8	78900		3.0	3.8	9.9	5.5	64700				
14303,13,8	10.2	246000		2.3	4.2	11.4	4.3	58600				
14303,13,9		22700				13.1	5.8	33500			10430	
14303,13,12	7.4	10680		1.8		6.9	3.9	2435				
Crystalline rock												
15556	490	24400	238	77.6	99	72.5	72	1030			255†	

* Keith *et al.* (1972). † LSPET (1972). Absolute errors ≤ ±6%, for Kr and Xe ≤ ±20%.

Table 5. Isotopic composition of Kr and Xe in 14003 samples.

Sample	Normalized for $^{84}Kr = 100$ and $^{136}Xe = 30$												
	^{82}Kr	^{83}Kr	^{84}Kr	^{86}Kr	^{124}Xe	^{126}Xe	^{128}Xe	^{129}Xe	^{130}Xe	^{131}Xe	^{132}Xe	^{134}Xe	^{136}Xe
14003 bulk	21	21	= 100	30.5	1.23	1.62	10.5	108	17.7	93	101	38	= 30
< 25 μ	20	21	= 100	30.5	1.20	1.40	10.0	107	17.9	89	101	37	= 30
25–60 μ	20	21	= 100	30			14.8	114	21.6	99	104	37.8	= 30
60–109 μ	22	22	= 100	31			15.4	114	21.8	100	104	36.7	= 30
109–272 μ	21	21	= 100	30			13.9	112	22.4	101	103	36	= 30
14003,24,2 > 300 μ	21	21	= 100	30			18	117	21	92	105	38	= 30
Etched 60–109 μ	22	24	= 100	30			24	126	26.4	129	108.5	37	= 30
Etched 109–272 μ	22	24	= 100	30			18.1	122	23.7	116	105.5	36	= 30
Solar*	20	20	= 100	31	0.49	0.44	8.3	10.4	16.5	82	100	37	= 30
Spallogenic†	75	= 100	38	—	35	64	= 100	110	64	390	58	—	—

For absolute amounts, see Tables 3 and 4. Errors 0.1–2% depending on abundance.
Ba-content of 14003,24 aliquot was measured to be 825 ppm.
* Eberhardt *et al.* (1970). † Bogard *et al.* (1971).

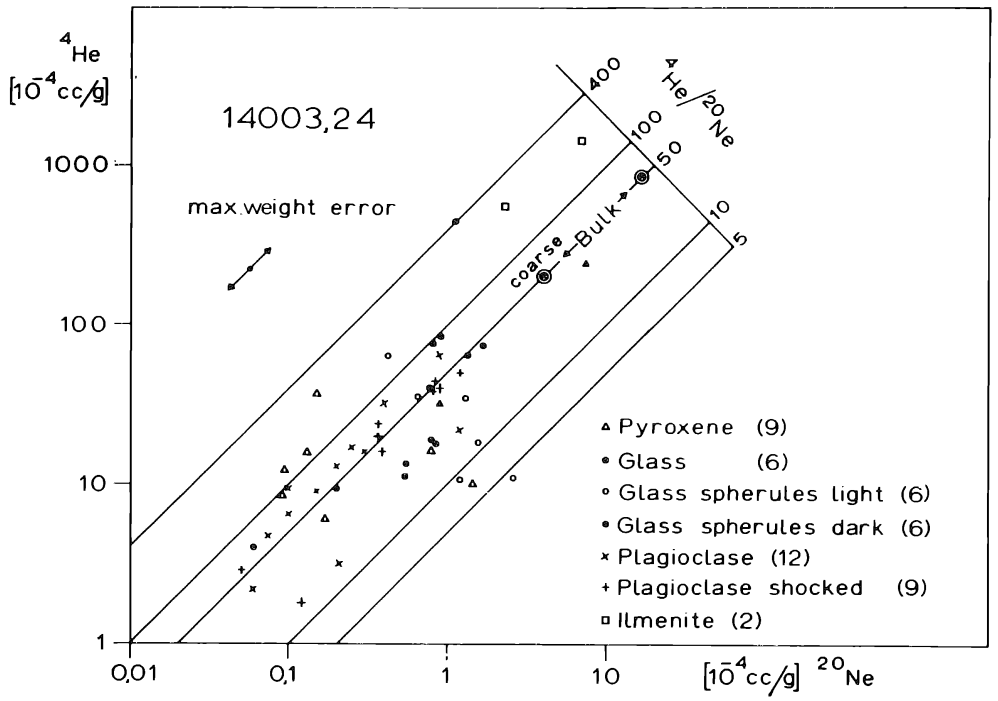

Fig. 8. ^{4}He, ^{20}Ne, and (^{4}He/^{20}Ne) in single grains of 14003,24 fines.

internal agreement of duplicate analyses and comparisons of the calibration standards with terrestrial and meteoritic interlaboratory standards. To calibrate Kr and Xe, Abee-meteorite standards were used instead of air spikes. In this case, absolute errors may be as large as 20%. Isotopic ratios have errors <2% for all gases.

K and U data required for the age determination are included in Tables 3 and 4. Their determination will be described in more detail by Müller (1972). Where comparisons are possible, our rare gas data compare favorably with those by Heyman *et al.* (1972) but tend to be generally higher than those reported by LSPET (1971, 1972). Sampling may account for some of the differences.

Single grain analysis

Single minerals and glasses were handpicked from 14003 soil and identified by optical and x-ray methods. Fifty specimens were then weighed on a microbalance

(range 10–300 μg) and measured in the Nier-type spectrometer, applying the single grain technique already described (Kirsten *et al.*, 1971). The results for ^{4}He, ^{20}Ne, and ^{36}Ar are given in Figs. 8 and 9. The isotopic composition of these gases corresponds in general to the known ratios for solar wind implanted gases as measured in the bulk. Due to the high K content of Apollo 14 fines, individual ^{40}Ar/^{36}Ar ratios are relatively high. They range from 0.4 to 20 and are centered around ~1.5. In 15 cases it was possible to determine the spallogenic contributions from the isotopic composition of Ne and Ar and to calculate the individual exposure ages given in Fig. 10.

For a survey of the variation of implanted ^{4}He concentrations in a larger number of single grains we have applied the He-microprobe technique (for details, see Kirsten *et al.*, 1970) to 153 individual specimens with emphasis on differently colored glass spherules. The resulting ^{4}He concentrations per cm^3 and per cm^2 surface area are given in Figs. 11 and 12. Grain surface areas were estimated by microscopic evaluation of shape parameters.

Discussion

Radiogenic, spallogenic, and trapped components contribute to the rare gases in lunar samples. In general, they can be distinguished from each other on the basis of their isotopic composition, especially if data for grain size fractions and etched samples are also available. For bulk soils the $(^4\text{He}/^3\text{He})_{tr}$ ratio is little affected by radiogenic ^{4}He and spallogenic ^{3}He. A plot of ^{4}He versus ^{3}He for all 14003 samples listed in Table 3 reveals that these contributions by chance compensate each other approximately. This prevents an exact determination of each component; however, an iteration which also involves the ^{4}He/^{20}Ne ratio allows an estimate of the components.

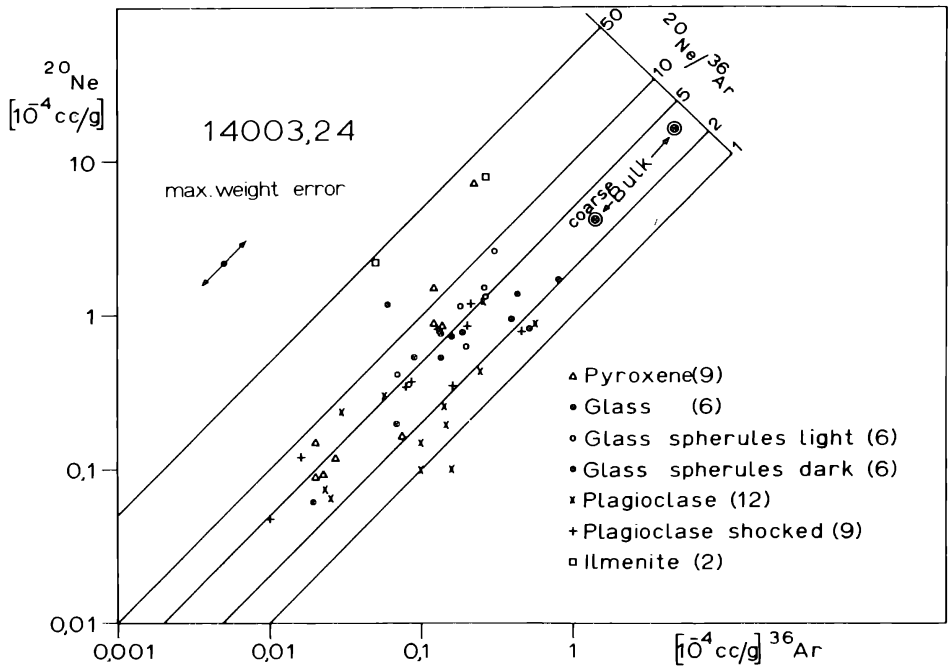

Fig. 9. ^{20}Ne, ^{36}Ar, and (^{20}Ne/^{36}Ar) in single grains of 14003,24 fines.

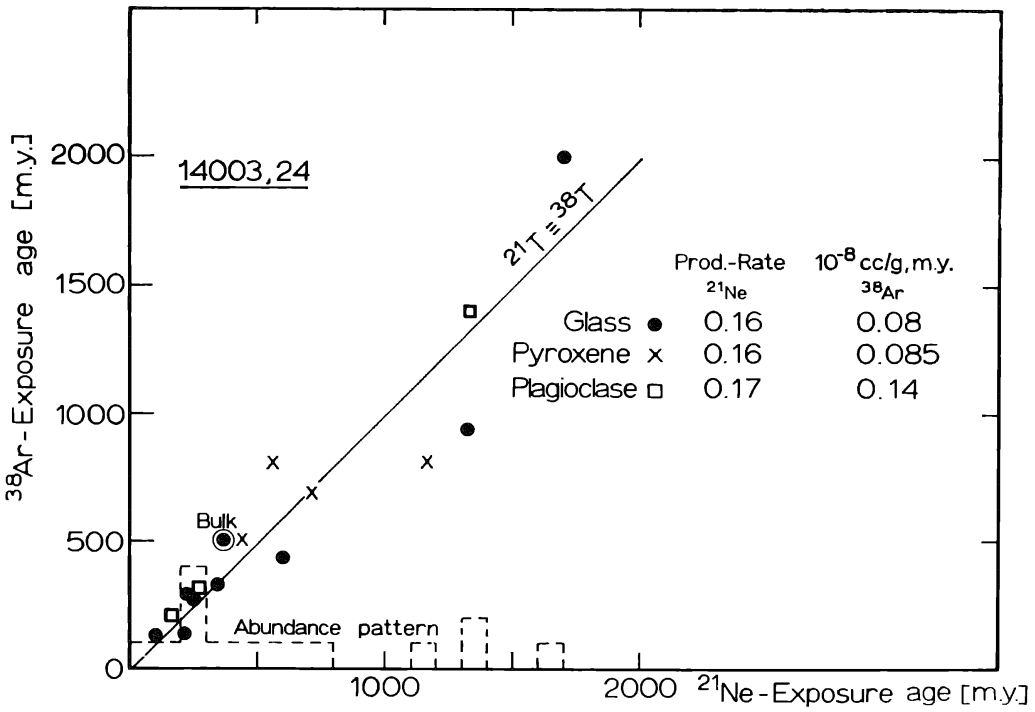

Fig. 10. ^{21}Ne and ^{38}Ar exposure ages of single particles from 14003,24 fines.

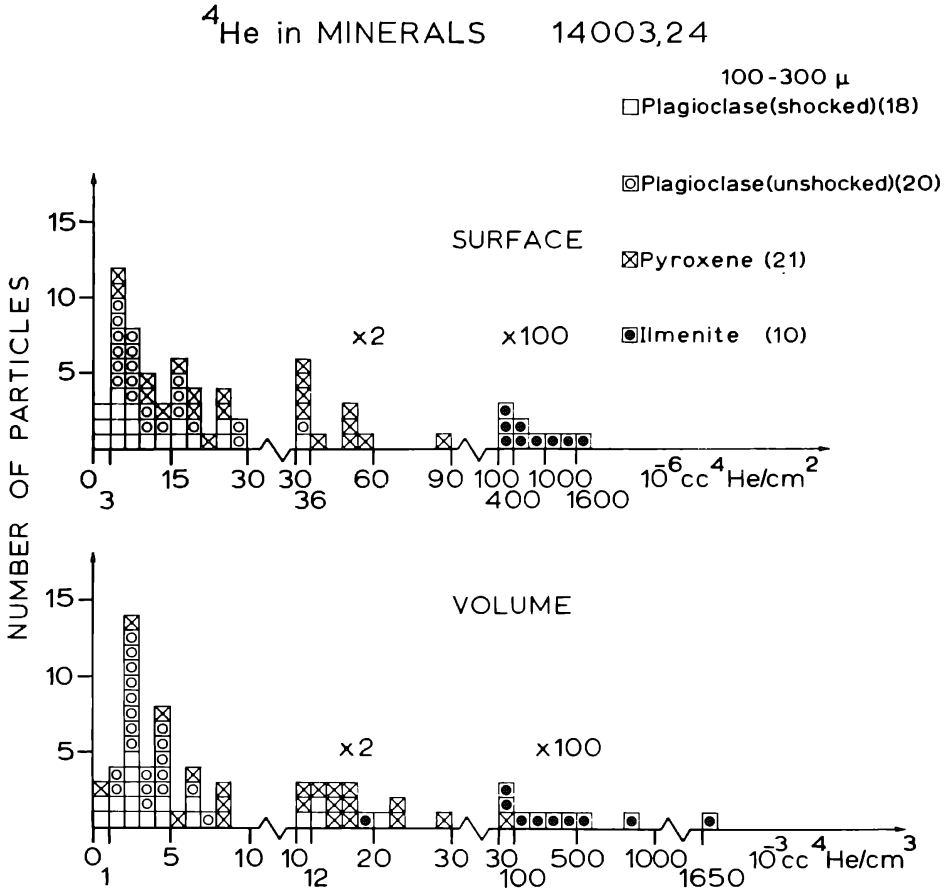

Fig. 11. ^{4}He concentrations in single mineral grains of 14003,24 fines. Micro-He-probe analysis.

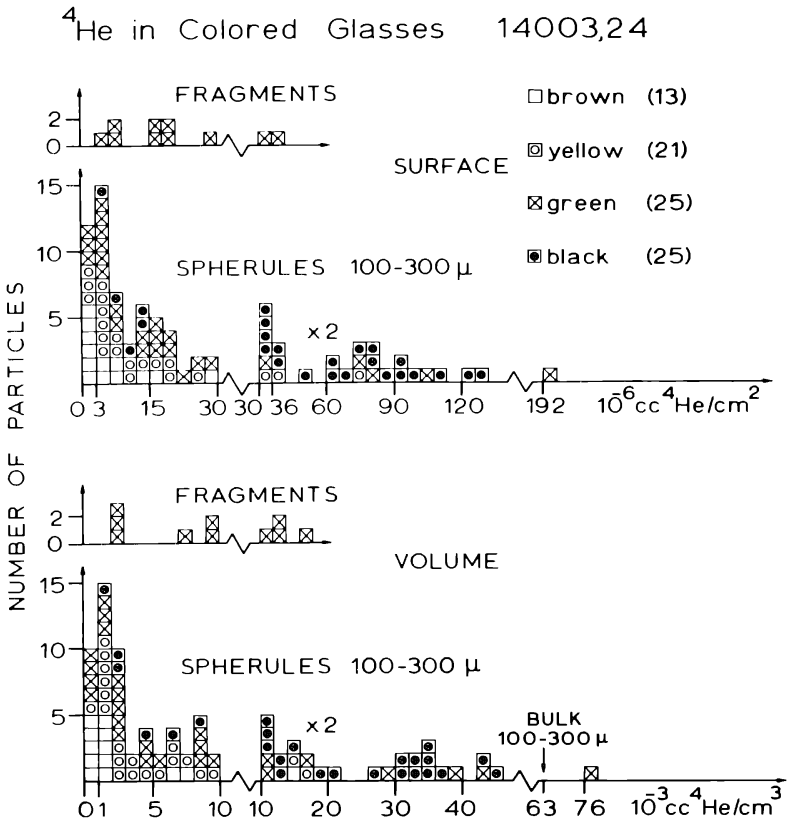

Fig. 12. ^{4}He concentrations in single glass spherules and fragments of different color. Micro-He-probe analysis.

For 15101, the known U content limits the maximum contribution of radiogenic ^{4}He. Similarly, spallogenic ^{3}He could be estimated for some of the coarse fines listed in Table 4.

The Ne isotopes were divided into spallogenic and trapped components adopting a ratio of $(^{20}Ne/^{21}Ne/^{22}Ne)_{sp} = 0.95 : 1 : 1.05$ by an iteration which corresponds to the application of a two-isotope plot as introduced by Eberhardt *et al.* (1970). The spallogenic Ne, which is used to calculate the exposure ages (Table 6), is then subtracted to calculate the trapped component. A similar treatment was given to the Ar isotopes adopting $(^{36}Ar/^{38}Ar)_{sp} = 0.63$. A plot of ^{40}Ar versus ^{36}Ar allows a separation in favorable cases of the radiogenic ^{40}Ar from the implanted ^{40}Ar and a calculation of characteristic $(^{40}Ar/^{36}Ar)_{tr}$ ratios as well as total K–Ar model ages (Table 6). The Xe isotopic composition of 14003 samples (Table 5) is normalized to $^{136}Xe = 30$, since this corresponds approximately to the abundance of ^{136}Xe relative to $^{132}Xe = 100$ in the trapped component and since there is no spallogenic ^{136}Xe. Then, spallogenic Xe is derived by subtracting the next-to-last line of Table 5 from each sample.

Trapped gases

The major source of the rare gases observed in lunar fines is solar wind implantation (e.g., Eberhardt *et al.*, 1970; Heymann *et al.*, 1970; Hintenberger *et al.*, 1970; Kirsten *et al.*, 1970). The absolute amounts of implanted solar wind gases turn out to

be remarkably similar for the soils of all landing sites. Total He, Ne, and Ar concentrations of the analyzed Apollo 14 and 15 bulk soils differ only by a factor of 2, except for 15421 (Table 3), and are not too distinct from Apollo 11 and 12 soils.

Solar wind is surface correlated because of its low initial implantation depth ($\sim$400 Å). Our data on grain size fractions and etched samples support this result; however, it is also apparent that about 5 to 10% of these gases are related to the volume rather than to the surface. This is explained by solid state diffusion (Kirsten *et al.*, 1971). Other sources for this component may be stopped solar flare particles (Poupeau *et al.*, 1972) or inclusion of ancient solar wind gases during remelting (Megrue and Steinbrunn, 1972; Roedder and Weiblen, 1972).

The relatively uniform surface loading of different soils is mainly due to saturation effects. This is illustrated by the absence of single soil particles without implanted gases. According to micrometeorite influx data and present-day erosion rates, 3–4 $\times$ 10^9 yr were required to form the lunar regolith. Sampling near medium-sized craters guarantees sampling from all regolith depths (e.g., Spur Crater, soil 15301). The rather uniform rare gas concentrations lead then to the conclusion that solar wind irradiation took place for at least 3 $\times$ 10^9 yr with relatively little change.

On the other hand, large differences of solar wind concentrations are observed among individual soil particles (Figs. 8, 9, 11, and 12). They are best explained by subsequent diffusion loss at or near the lunar surface.

The relative diffusion losses are governed by the crystal lattice parameters of the various minerals. The lowest concentrations are observed in plagioclases (Fig. 11) in agreement with diffusion studies by Baur *et al.* (1972). Shock effects seem to have little influence on the diffusion parameters. The distributions for shocked and unshocked plagioclases are quite similar.

Ilmenites have the highest retentivity (Fig. 11), resulting in 10 to 100 times higher ^{4}He concentrations. For a given mineral type, trapped gas concentrations vary by an order of magnitude since each grain has experienced its individual thermal history after it became saturated with solar wind.

Figure 12 exhibits a correlation between the solar wind content and the color of glass spherules. Mean concentrations increase in the order brown, yellow, green, black by a factor of about 10. Glass colors are due to different chemical composition (see, e.g., Bell and Mao, 1972) which may cause differences in retentivity. The color effect can be explained by glass production from different source materials (Giles and Nicholls, 1972). Darkening along with higher retentivity could also be due to opaque microcrystals within the glasses. Each black glass spherule we have looked at so far in polished sections contained fragments of ilmenite or newly crystallized phases (Ni–Fe and others).

Elemental ratios. We have measured $(^4\text{He}/^{20}\text{Ne})_{tr}$ ratios between 47 and 65 for Apollo 14 fines and between 20 and 48 for Apollo 15 fines. For soils from Apollo 11 and 12 this ratio varies between 30 and 120 (Bogard *et al.*, 1971). The large difference with the ^{4}He/^{20}Ne ratios directly observed in the present-day solar wind (430–620, Bühler *et al.*, 1972) indicates loss of implanted ^{4}He rather than a change of solar ratios. Similarly, $(^{20}\text{Ne}/^{36}\text{Ar})_{tr}$ ratios range from 3.7 to 8.3, much lower than the expected value of at least 43 which is observed in one single particle (see also Aller,

1961). The (^{36}Ar : ^{84}Kr : ^{132}Xe) ratios of the analyzed soils fall in the range previously observed for Apollo 11 and 12 soils but are also lower by factors of 3 to 5 than the expected solar abundances (Aller, 1961). Secondary fractionation of the lighter gases rather than solar abundance changes must be responsible.

Soil 15421, rich in green glass, is peculiar in its apparent Ne excess with ratios $(^4He/^{20}Ne)_{tr} = 20$ and $(^{20}Ne/^{36}Ar)_{tr} = 8.3$. Even higher $(^{20}Ne/^{36}Ar)_{tr}$ ratios are given by LSPET (1972) for fines and glass from soil 15923,2 which is derived from the same bulk sample as 15421. Apparently different portions of a particularly Ne-rich component (Bogard and Nyquist, 1972) are admixed to the samples. Single grain analysis will be performed to localize this component.

The basic uniformity of the composition of solar wind gases at various landing sites does not contradict the order of magnitude variations of elemental ratios observed in individual soil particles (Figs. 8 and 9). Similar results were obtained by Megrue and Steinbrunn (1972). In general, the depletion of light rare gases is enhanced for glasses and plagioclases compared to pyroxenes and ilmenites. The least fractionated gases are found in a dark glass spherule $(^4He/^{20}Ne)_{tr} = 400$ and in ilmenites $(^4He/^{20}Ne)_{tr} = 240$; $(^{20}Ne/^{36}Ar)_{tr} = 43$. Presumably, these particles were recently loaded with solar wind and suffered little subsequent diffusion. The $(^4He/^{20}Ne)_{tr}$ ratio of 400 is already close to the expected solar value. It is then indicated that with even better statistics, the maximum ratios obtained do closely represent the solar wind ratios.

The fragmental rock 14303 is almost free of solar wind. It has been almost completely outgassed during extensive metamorphism. It contains only traces of heavily fractionated gases [$8 \pm 3 \times 10^{-8}$ cc STP/g ^{36}Ar; $(^{20}Ne/^{36}Ar) < 1$], which are probably remainders of ancient solar wind dissolved during the formation or subsequent annealing of this fragmental rock.

Isotopic ratios. ^{4}He/^{3}He ratios in the trapped component are 2850 ± 100 for 14003 and 2750 ± 100 for 15101. For the other fines radiogenic ^{4}He prevents an exact determination. U and age data (Tables 3 and 6) yield estimated values between 2600 and 3000. The present-day ^{4}He/^{3}He ratio in the solar wind falls distinctly below the observed ratios and ranges from 1860 to 2450 (Bühler *et al.*, 1972). It is probably not by chance that the only isotopic ratio for which a distinct deviation is observed is the one that is most sensitive to the evolution of the sun. Geiss *et al.* (1970) conclude a true change in the solar wind ^{4}He/^{3}He ratio. If this is true it would suggest that most of the solar wind collected in the lunar regolith is very ancient since it displays ^{4}He/^{3}He ratios higher than at present. The Ne-isotopic ratios measured in Apollo 14 and 15 soils range from 13 to 13.6 for $(^{20}Ne/^{22}Ne)_{tr}$ and from 30 to 32 for $(^{22}Ne/^{21}Ne)_{tr}$. This is similar to the ratios observed in the solar wind composition experiment (Bühler *et al.*, 1972). We observed that $(^{36}Ar/^{38}Ar)_{tr}$ ratios are ~ 5.45, except for 15601. This is slightly above the ratio observed by us in Apollo 11 and 12 samples and in 15601. Since LSPET (1972) reports normal ratios, it may be too early to assign significance to this deviation.

The so-called parentless ^{40}Ar (Heymann and Yaniv, 1970) is also observed in Apollo 14 and 15 fines. This component is surface related and correlated with the solar wind; however, variable ^{40}Ar/^{36}Ar ratios and nuclear abundance considerations

exclude a solar wind origin. Heymann and Yaniv (1970) have proposed reimplantation of a latent lunar atmosphere by the solar wind. It is then interesting to compare the $(^{40}Ar/^{36}Ar)_{tr}$ ratios of different soils, since they may reflect the igneous outgassing processes in the early lunar history. In favorable cases (14003, 15101) a plot of ^{40}Ar versus ^{36}Ar allows one to distinguish in situ-radiogenic ^{40}Ar from the implanted ^{40}Ar (Table 6). For the other samples we have estimated the probable radiogenic contributions from the K concentrations and the K–Ar ages of Table 6 in order to calculate the $(^{40}Ar/^{36}Ar)_{tr}$ ratios given in Table 6.

Table 6. Ages and $(^{40}Ar/^{36}Ar)_{tr}$-ratios in Apollo 14 and 15 fines and rocks.

Sample	Exposure ages (m.y.)				Gas retention ages (10^9 yr)		$R = (^{40}Ar/^{36}Ar)_{tr}$
	^{3}He	^{21}Ne	^{38}Ar	^{128}Xe	U/Th–He	Total K–Ar	
Soils < 1 mm							
14003	90 ± 30	350 ± 40	470 ± 80	580 ± 150	2.5 ± 0.2	3.1 ± 0.15	1.24 ± 0.04
15101	150 ± 50	390 ± 30	330 ± 50			2.6 ± 0.15	1.08 ± 0.04
15021		370 ± 50					0.65 ± 0.08
15601		380 ± 50					0.78 ± 0.08
15301		310 ± 40					1.55 ± 0.1
15421		460 ± 60					3.4 ± 0.2
Coarse fines							
14003 > 300 μ		250 ± 40		(470)			14003,24,2: $4 < R < 8$
14001	360 ± 40	700 ± 50	570 ± 30			(~4)	
Various 14161	170 ± 30	300 ± 60	300 ± 40				Breccia: $9 < R < 12$
do, irrad. samples			300–430			3.54–3.92 (Table 1)	
14161,34,9		770 ± 100	610 ± 150				$1.9 < R < 2.8$
14257	50 ± 10	90 ± 10	110 ± 10			(~4)	
Rocks							
14303	15 ± 2	17 ± 2	22 ± 7		2.25 ± 0.15	3.15 ± 0.1	
do, irrad. samples			29 ± 4			3.44–3.75 (Table 1)	
15556	490 ± 50	525 ± 40	490 ± 50			3.4 ± 0.1	
Production rate* in 10^{-8} cc/g (m.y.)	1.0	0.154	0.14	0.000165			

* Based on chemical composition and specific production rates given by Bogard *et al.* (1971).

Variations between 0.65 and 3.4 exist for the various soils (<1 mm) even within one landing site. A soil breccia from coarse fines 14161 has a ratio $\gtrsim 8$, even after allowance is made for radiogenic ^{40}Ar produced from twice the maximum K amount observed in any of many investigated 14161 fragments (Tables 1 and 4, Hubbard *et al.* (1972)). A similar situation is encountered for 14003,24,2 with a minimum $(^{40}Ar/^{36}Ar)_{tr}$ ratio of 4.

The observed variations could be explained by a lunar atmosphere variable with time and incomplete mixing during transport of regolith material from various sites (Heymann *et al.*, 1972). However, it must be explained how *mean* differences persist within a relatively small, smooth area, while, on the other hand, a thorough mixing is required to explain the large variation of $^{40}Ar/^{36}Ar$ ratios in individual grains of one soil sample (Kirsten *et al.*, 1971) by a variable lunar atmosphere. The total $^{40}Ar/^{36}Ar$ ratios of the individual grains analyzed in this work vary from 0.4 to 20 and are centered around unity.

Poupeau *et al.* (1972) propose an early solar flare irradiation of Ca in highland materials as a source of the excess ^{40}Ar. One could also consider direct adsorption of ascendent ^{40}Ar in the overlaying regolith. The loose correlation between ^{40}Ar and ^{36}Ar could be related to enhanced adsorption capability of material heavily

damaged by solar wind irradiation. However, in diffusion experiments, Baur *et al.* (1972) have found little evidence for ^{40}Ar from a reimplanted lunar atmosphere. They consider adsorption of ^{40}Ar and subsequent migration caused by solar wind via a knock-on process or coatings of volatilized potassium as alternative explanations. Volatilization of K in crystallized material is likely to have occurred (Hubbard *et al.*, 1972; Biggar *et al.*, 1972; Nyquist *et al.*, 1972).

Exposure ages

The cosmic ray exposure ages given in Table 6 are based on the (relatively uniform) chemical composition of all analyzed samples and the production rates given by Bogard *et al.* (1971). It is known that ^{3}He exposure ages are often lowered by diffusion loss of spallogenic ^{3}He. Most reliable are the ^{21}Ne ages, while ^{38}Ar ages are less accurate. Nevertheless, ^{21}Ne and ^{38}Ar ages mostly agree within the limits of error. The slightly higher ^{128}Xe–Ba age of 14003 is not taken as indication for ^{21}Ne or ^{38}Ar losses.

Now that exposure ages for fines from four landing sites have been measured (for Apollo 11 and 12, see Kirsten *et al.*, 1970, 1971), it is remarkable that they are all around 400 m.y. This age probably reflects gardening in the regolith and indicates a relatively uniform mixing rate of ~ 2 mm/m.y. for the whole moon. Contrary to this uniformity, particular fragments of coarse fines exhibit individual exposure histories and have exposure ages between 100 and 770 m.y. The ^{38}Ar–Ca exposure ages derived from neutron irradiated 14161-fragments (300–430 m.y.) are similar to those of other 14161 samples. However, rock fragment 14161,9 has an exposure age of 770 m.y. The individual behavior of each fragment within the regolith is further illustrated by the exposure ages obtained for single soil fragments (Fig. 10). They range from <100 m.y. up to nearly 2×10^9 yr. This again is a proof for a regolith much older than 10^9 yr. The exposure age of fragmental rock 14303 from the rim of Cone Crater is ~ 25 m.y. This age is believed to be the age of Cone Crater (Bogard and Nyquist, 1972; Burnett *et al.*, 1972). Rock 15556 from the rim of Hadley Rille has an exposure age of ~ 500 m.y.

Total gas-retention ages

Total K–Ar and U–He model ages for soil 14003 and the K–Ar age for soil 15101 have been calculated (Table 6).

According to soil mixing models (Hubbard *et al.*, 1972; Birck *et al.*, 1972; Wänke *et al.*, 1972; Schonfeld, 1972), soils are composed of at least three components with different ages and K contents. Apart from diffusion losses, the measured K–Ar ages of 3.1 and 2.6×10^9 yr. may reflect the mixing ratio of these components (Pepin *et al.*, 1972). A comparison of the K–Ar and the U–He ages of 14003 indicates only moderate He losses. The similarity of both K–Ar and U–He ages for 14003 and saw dust of fragmental rock 14303 seems to indicate that Apollo 14 soil is made of essentially the same material as the local clastic rocks with little gas loss during the grinding process. The crystalline fragment 14161,34,9 has a total K–Ar age near 4×19^9 yr and corresponds to samples 14161,34,4 and 14161,34,5 discussed in the next section.

The 15556 mare basalt gives an age of 3.4×10^9 yr and corresponds to the age obtained by other authors for mare flows at Imbrium basin near Hadley Rille (Schaeffer *et al.*, 1972; Cliff *et al.*, 1972).

Crystallization ages

The ^{39}Ar–^{40}Ar method of age determination has been very successful for lunar samples (Alexander *et al.*, 1972; Husain *et al.*, 1971; Turner, 1970, 1971; Turner *et al.*, 1971). In general, the gas release pattern obtained for measured $^{40}Ar/^{39}Ar$ ratios at different temperatures shows several features: (1) a plateau of high $^{40}Ar/^{39}Ar$ value which is ascribed to the gas release from the retentive minerals and from which an age is obtained; (2) lower $^{40}Ar/^{39}Ar$ values at the lower temperature which is ascribed to the gas released from less retentive minerals and from which the diffusion loss of Ar is obtained; and (3) lower $^{40}Ar/^{39}Ar$ values at the highest temperatures for which there is no clear explanation. For certain rocks (1) and/or (3) are of little importance (see, for example, Fig. 3), while in a number of cases, as seen in Figs. 1 and 2, the interpretation of the drop-off in the $^{40}Ar/^{39}Ar$ ratio is of importance in establishing a precise age. Several suggestions have been advanced (Huneke *et al.*, 1972; Turner *et al.*, 1971) to explain the low $^{40}Ar/^{39}Ar$ values at high temperature releases. One is that the high temperature minerals, such as the pyroxenes, do not retain their argon as well as feldspars. There is experimental evidence to show that in separated mineral phases plagioclase gave an age agreeing with the Rb–Sr age, while the pyroxene fraction gave a low age. The same authors suggest, in cases where the plateau age is apparently too high and the drop off in age is large at the high temperatures, that the rock represents a case where the K and/or the Ar have been redistributed. Assuming a closed system, the age then is given by the average over the high temperature release.

We should like to suggest as an alternative explanation the slow devitrification of a minor K-rich glass phase. The fall-off in age at high temperatures was not seen for Apollo 11 or 12 basalts but seems to be related to the explosive origin of the Fra Mauro formation. Although there is no observable glass present in the samples, there is petrological evidence that the Fra Mauro rocks contain a fine grained phase which crystallized from a glass. If this took place slowly, then that phase could exhibit a much younger age and at present be very retentive with high temperature melting minerals (see also Turner, 1971). This removes the burden of explaining gas loss from pyroxenes without corroborating evidence for diffusion loss, and with the uncertainty as to why Fra Mauro pyroxenes are different from those from Apollo 11 or 12 basalts.

At the present time, when none of the explanations is established, it may be better to calculate gas retention ages based both on the plateau and the whole high temperature portion. In cases where these ages agree, there is no uncertainty, while in cases where there is a discrepancy one should increase the error in the age.

In seven cases listed in Table 1 and shown in Figs. 1, 2, 3, and 4, the difference between the two ages is small, while in two cases (14161,34,2 and 14303,13,R5,21, Figs. 1 and 2), the difference between the two ages is larger.

For two basaltic samples (14161,26,11 and 14161,26,12) and a feldspathic ac-

cumulation (14161,34,3) the two ages are in perfect agreement, but much lower than those of the other fragments. From microscopic examination it was expected that this sample is anorthositic in composition as it is composed of ~90% plagioclase and ~10% pyroxene. The high Ca content (13.4%) is in accordance with a mainly feldspathic composition. But as the potassium content is rather high (0.46%), a K-feldspar phase may also be present. The age measured on this sample is very well defined at $3.63 \pm 0.05 \times 10^9$ yr total argon age, high temperature age, and the plateau age. The total argon loss is 2.4%. The slight shock effects observed in this sample evidently did not affect the ages.

The two basaltic rocks show equally well-defined ages of $3.59 \pm 0.02 \times 10^9$ yr (14161,26,11) and $3.54 \pm 0.01 \times 10^9$ yr (14161,26,12)—the argon losses being well below 1% (Table 1). These two basalts are different from the other basalts analyzed by their extremely low opaque mineral content and their relatively high pyroxene-to-feldspar ratio.

The ages of all three rocks are unusual for Apollo 14 samples. As mare material is rare (but present) in the Apollo 14 soils (Adams and McCord, 1972; Powell and Weiblein, 1972), it follows that we have measured three mare-derived rocks with a mean age of $3.58 \pm 0.05 \times 10^9$ yr. These ages are typically found for Mare Tranquilitatis basalts (Papanastassiou and Wasserburg, 1971; Turner, 1971). Therefore the question arises where these samples from the Apollo 14 soils originate.

As judged from crater counts, Sinus Medii is the nearest mare surface about equal in age to Mare Tranquilitatis (Gault, 1972). It is located at the geographical center of the moon's surface, about 500 km ENE from the Apollo 14 landing site. This distance is rather large. Therefore, our rocks more plausibly might be ejecta material from a crater in the nearby mare basalts of the Imbrium or Erathosthenian formation. There is no reason to doubt the existence of older lava flows below the surface flows which show ages from 3.36 to 3.16×10^9 yr (Papanastassiou and Wasserburg, 1971). We assume that such older material impacted at the Fra Mauro formation, contributing to the regolith but contributing very little to the total amount of material there. Probably the cosmic ray exposure ages of the two young basalt samples which are 320 m.y. and 360 m.y. approximately date such a secondary event. The ages listed in Table 1 fall into two classes, one group at 3.5 to 3.6×10^9 yr, presumably material not originating in the Imbrium event as discussed above, and another group at 3.7 to 4.0×10^9 yr, if we include all other ages (Cliff *et al.*, 1972; Compston *et al.*, 1972; Huneke *et al.*, 1972; Husain *et al.*, 1971, 1972; Papanastassiou and Wasserburg, 1971; Murthy *et al.*, 1972; Schaeffer *et al.*, 1972; Stettler *et al.*, 1972; Sutter *et al.*, 1971; Turner, 1970; Turner *et al.*, 1971; York *et al.*, 1972). Rocks of these ages are probably all derived from the Imbrium event.

Petrologic observations show that these basaltic rocks must have been crystallized within the lunar crust before they were excavated during the Imbrium impact event and embedded into the pyroclastic ejecta material. They were not even affected thermally or chemically to an extent which would have disturbed the Rb/Sr isotopic systems (Papanastassiou and Wasserburg, 1971). It seems likely that the Imbrium event did little in the way of releasing radiogenic ^{40}Ar so that the crystallization ages measured represent the times of crystallization of these rocks in the crust of the moon

where Mare Imbrium is at present. In this case the event forming the Mare Imbrium basin is younger than the lowest age observed so far, $3.75 \pm 0.05 \times 10^9$ yr. On the other hand, as there is no evidence for pre-Mare Imbrium site ejecta on Mare Tranquilitatis, it is clear that Mare Tranquilitatis is younger than the Imbrium event. This, then, closely brackets the Imbrium event as being between 3.7×10^9 and 3.8×10^9 yr ago. As the rim of the Imbrium basin is penetrated by some craters which were flooded with basalts simultaneously with the mare one can assume that there is a time gap between basin formation and filling with basalts. The density of such craters is too small to allow an estimate for this time gap by crater counts (Gault, 1972).

In this respect the measurements on microbreccias 14303,R5,21 and 22 are probably meaningful (Table 1). The microbreccia-clast R5,21 shows a very badly defined "plateau age" of 3.78×10^9 yr (see Fig. 1). The ^{39}Ar–^{40}Ar release pattern gives an indication of the K/Ar system having been disturbed at 3.78×10^9 yr ago. The large argon loss of the sample (19.5%) indicates the formation of phases with poor Ar retentivities. The formation of this breccia is probably close to 3.78×10^9 yr ago. Sample R5,22 which also is a microbreccia but finer grained than R5,21 seems to be totally disturbed in respect of both K and Ar but not degassed. It therefore shows a large amount of excess argon in the high temperature range, possibly shock-implanted excess argon. It is interesting that this sample shows the smallest K content ever reported for a lunar rock. This low K content (57 ppm) most probably is due to potassium volatilization during the thermal spike caused by the large impact. A comparably low potassium content has recently been reported for the shock-molten gabbroic anorthosite 15418 (86 ppm, LSPET, Apollo 15, 1972).

In summary then, the upper crust of the moon at the pre-Mare Imbrium site was built up by an already complex sequence of rocks such as norite, granites, and anorthosites overlain by different basaltic lava flows. These were locally brecciated by impacts of meteorites—sometimes multiply. Multiple basalt flows or sills with distinct crystallization ages of 4.00 to 3.75×10^9 yr have been recognized. This complex was ejected at the time a large impact event formed the Mare Imbrium basin. The time of this event was between 3.70 and 3.80×10^9 yr ago. The ejecta material was deposited forming the Fra Mauro formation which was subsequently bombarded by meteorites leading to the formation of the regolith and impact craters.

Filling of the maria occurred some time after the Imbrium basin was excavated, starting with that of Mare Tranquilitatis at some time more than 3.70×10^9 yr ago and ending with the surface flows in the Oceanus Procellarum and the Mare Imbrium about 3.20×10^9 yr ago. Further bombardment of these surfaces led to cross contaminations of material from one place to the other over large areas and distances.

From this model it is expected that with increasing number of age determinations and refinements in their interpretation the clustering of ages for rocks from mare areas as it appears now to exist will disappear and continuous mare-filling processes will be recognized; these might vary in intensity within the time interval of 3.8 to 3.2×10^9 yr.

Acknowledgments—We are grateful to NASA for providing us with lunar samples. The skillful operation of the mass spectrometer by H. Richter is gratefully acknowledged. Thanks are given to Dr. O. Müller for making unpublished data available and for help in monitoring the neutron irradia-

tions. The technical assistance of D. Dörflinger, W. Ehrhardt, R. Schwan, H. Urmitzer, and H. Weber is appreciated. Discussions with Drs. D. Gault, A. El Goresy, S. Kalbitzer, J. F. Lovering, and with Professor W. Gentner have substantially contributed to the interpretations. We appreciate valuable comments by Professor F. Begemann.

References

Adams J. B. and McCord T. B. (1972) Optical evidence for regional cross-contamination of highland and mare-soils (abstract). In *Lunar Science—III* (editor C. Watkins), p. 1, Lunar Science Institute Contr. No. 88.

Alexander E. C. Jr., Davis P. K., and Lewis R. S. (1972) Argon-40–argon-39 dating of Apollo sample 15555. *Science* **175,** 417–419.

Aller L. H. (1961) *The Abundance of the Elements.* Interscience, New York.

Baur H., Frick U., Funk H., Schultz L., and Signer P. (1972) On the question of retrapped 40-Ar in lunar fines (abstract). In *Lunar Science—III* (editor C. Watkins), p. 47, Lunar Science Institute Contr. No. 88.

Bell P. M. and Mao H. K. (1972) Initial findings of a study of chemical composition and crystal field spectra of selected grains from Apollo 14 and 15 rocks, glasses and fine fractions (less than 1 mm) (abstract). In *Lunar Science—III* (editor C. Watkins), p. 55, Lunar Science Institute Contr. No. 88.

Biggar G. M., Ford C. E., Humphries D. J., Wilson G., and O'Hara M. J. (1972) Melting relations of more primitive mare-type basalt 14053 and of breccia 14321 and soil 14162 (average lunar crust?) (abstract). In *Lunar Science—III* (editor C. Watkins), p. 74, Lunar Science Institute Contr. No. 88.

Birck J. L., Loubet M., Manhes G., Provost A., Tatsumoto M., and Allegre C. J. (1972) Age and origin of lunar soils (abstract). In *Lunar Science—III* (editor C. Watkins), pp. 80–81, Lunar Science Institute Contr. No. 88.

Bogard D. D., Funkhouser J. G., Schaeffer O. A., and Zähringer J. (1971) Noble gas abundances in lunar material-cosmic-ray spallation products and radiation ages from the Sea of Tranquility and the Ocean of Storms. *J. Geophys. Res.* **76,** 2757–2779.

Bogard D. D. and Nyquist L. E. (1972) Noble gas studies on regolith materials from Apollo 14 and 15 (abstract). In *Lunar Science—III* (editor C. Watkins), pp. 89–91, Lunar Science Institute Contr. No. 88.

Brereton N. R. (1970) Corrections for interfering isotopes in the $^{40}Ar/^{39}Ar$ dating method. *Earth Planet. Sci. Lett.* **8,** 427–433.

Bühler F., Cerutti H., Eberhardt P., and Geiss J. (1972) Results of the Apollo 14 and 15 solar wind composition experiments (abstract). In *Lunar Science—III* (editor C. Watkins), pp. 102–104, Lunar Science Institute Contr. No. 88.

Burnett D. S., Huneke J. C., Podosek F. A., Russ G. P., Turner G., and Wasserburg G. J. (1972) The irradiation history of lunar samples (abstract). In *Lunar Science—III* (editor C. Watkins), pp. 105–107, Lunar Science Institute Contr. No. 88.

Cliff R. A., Lee-Hu C., and Wetherill G. W. (1972) K, Rb, and Sr measurements in Apollo 14 and 15 material (abstract). In *Lunar Science—III* (editor C. Watkins), pp. 146–147, Lunar Science Institute Contr. No. 88.

Compston W., Vernon M. J., Berry H., Rudowski R., Gray C. M., Ware N., Chappell B. W., and Kaye M. (1972) Age and petrogenesis of Apollo 14 basalts (abstract). In *Lunar Science—III* (editor C. Watkins), pp. 151–153, Lunar Science Institute Contr. No. 88.

Dalrymple G. B. and Lanphere M. A. (1971) $^{40}Ar/^{39}Ar$ technique of K–Ar dating: a comparison with the conventional technique. *Earth Planet. Sci. Lett.* **12,** 300–308.

Ducati H., Kalbitzer S., Kiko J., and Kirsten T. (1972) Rare gas diffusion studies in individual lunar soil particles. To be published.

Eberhardt P., Geiss J., Graf H., Grögler N., Krähenbühl U., Schwaller H., Schwarzmüller J., and Stettler A. (1970) Trapped solar wind noble gases, exposure age, and K/Ar-age in Apollo 11 lunar fine material. *Proc. Apollo 11 Lunar Sci. Conf., Geochim. Cosmochim. Acta* Suppl. 1, Vol. 2, pp. 1037–1070. Pergamon.

El Goresy A. (1972) Private communication.

Gault D. E. (1972) Private communication.
Geiss J., Eberhardt P., Bühler F., Meister J., and Signer P. (1970) Apollo 11 and Apollo 12 solar wind composition experiments: fluxes of He and Ne isotopes. *J. Geophys. Res.* **75,** 5972–5979.
Giles H. N. and Nicholls G. D. (1972) Preliminary results of mass spectrometric analysis of individual grains from lunar samples (abstract). In *Lunar Science—III* (editor C. Watkins), pp. 306–308, Lunar Science Institute Contr. No. 88.
Grasty R. L. and Mitchell J. G. (1966) Single sample potassium-argon ages using the omegatron. *Earth Planet. Sci. Lett.* **1,** 121–122.
Heymann D. and Yaniv A. (1970) Ar^{40} anomaly in lunar samples from Apollo 11. *Proc. Apollo 11 Lunar Sci. Conf., Geochim. Cosmochim. Acta* Suppl. 1, Vol. 2, pp. 1261–1267. Pergamon.
Heymann D., Yaniv A., Adams J. A., and Fryer G. (1970) Inert gases in lunar samples. *Science* **167,** 555–558.
Heymann D., Yaniv A., and Walton J. (1972) Inert gases in Apollo 14 fines and the case of parentless Ar^{40} (abstract). In *Lunar Science—III* (editor C. Watkins), pp. 376–378, Lunar Science Institute Contr. No. 88.
Hintenberger H., Weber H. W., Voshage H., Wänke H., Begemann F., Vilcsek E., and Wlotzka F. (1970) Rare gases, hydrogen, and nitrogen: Concentrations and isotopic composition in lunar material. *Science* **167,** 543–545.
Hubbard N. J., Gast P. W., Rhodes M., and Wiesmann H. (1972) Chemical composition of Apollo 14 materials and evidence for alkali volatilization (abstract). In *Lunar Science—III* (editor C. Watkins), pp. 407–409, Lunar Science Institute Contr. No. 88.
Huneke J. C., Podosek F. A., Turner G., and Wasserburg G. J. (1972) ^{40}Ar–^{39}Ar systematics in lunar rocks and separated minerals of lunar rocks from Apollo 14 and 15 (abstract). In *Lunar Science—III* (editor C. Watkins), pp. 413–414, Lunar Science Institute Contr. No. 88.
Husain L., Sutter J. F., and Schaeffer O. A. (1971) Ages of crystalline rocks from Fra Mauro. *Science* **173,** 1235–1236.
Husain L., Schaeffer O. A., and Sutter J. F. (1972) Age of a lunar anorthosite. *Science* **175,** 428–430.
Kaneoka I. (1972) $^{40}Ar/^{39}Ar$ age studies of Apollo 14 samples. To be published.
Keith J. E., Clark R. S., and Richardson K. A. (1972) Gamma ray measurements of Apollo 12, 14, and 15 lunar samples (abstract). In *Lunar Science—III* (editor C. Watkins), pp. 446–448, Lunar Science Institute Contr. No. 88.
Kirsten T., Müller O., Steinbrunn F., and Zähringer J. (1970) Study of distribution and variations of rare gases in lunar material by a microprobe technique. *Proc. Apollo 11 Lunar Sci. Conf., Geochim. Cosmochim. Acta* Suppl. 1, Vol. 2, pp. 1331–1343. Pergamon.
Kirsten T., Steinbrunn F., and Zähringer J. (1971) Location and variation of trapped rare gases in Apollo 12 lunar samples. *Proc. Second Lunar Sci. Conf., Geochim. Cosmochim. Acta* Suppl. 2, Vol. 2, pp. 1651–1669. MIT Press.
Kirsten T., Deubner J., Ducati H., Gentner W., Horn P., Jessberger E., Kalbitzer S., Kaneoka I., Kiko J., Krätschmer W., Müller H. W., Plieninger T., and Thio S. K. (1972) Rare gases and ion tracks in individual components and bulk samples of Apollo 14 and 15 fines and fragmental rocks (abstract). In *Lunar Science—III* (editor C. Watkins), pp. 452–454, Lunar Science Institute Contr. No. 88.
LSPET (Lunar Sample Preliminary Examination Team) (1971) Preliminary examination of lunar samples from Apollo 14. *Science* **173,** 681–693.
LSPET (Lunar Sample Preliminary Examination Team) (1972) The Apollo 15 lunar samples: A preliminary description. *Science* **175,** 363–375.
Megrue G. H. and Steinbrunn F. (1972) Classification and source of lunar soils; clastic rocks; and individual mineral, rock, and glass fragments from Apollo 12 and 14 samples as determined by the concentration gradients of the helium, neon, and argon isotopes (abstract). In *Lunar Science—III* (editor C. Watkins), pp. 532–534, Lunar Science Institute Contr. No. 88.
Müller O. (1972) Alkali and alkaline earth elements, La and U in Apollo 14 and Apollo 15 samples. To be published.
Murthy Rama V., Evensen N. M., Bor-ming Jahn, and Coscio M. R. (1972) Rb–Sr ages, trace elements, and speculations on lunar differentiation (abstract). In *Lunar Science—III* (editor C. Watkins), pp. 571–572, Lunar Science Institute Contr. No. 88.

Nyquist L. E., Hubbard N. J., Gast P. W., Wiesmann H., and Church S. E. (1972) Rb–Sr relationships for some chemically defined lunar materials (abstract). In *Lunar Science—III* (editor C. Watkins), pp. 584–586, Lunar Science Institute Contr. No. 88.

Papanastassiou D. A. and Wasserburg G. J. (1971) Lunar chronology and evolution from Rb–Sr studies of Apollo 11 and 12 samples. *Earth Planet Sci. Lett.* **11,** 37.

Papanastassiou D. A. and Wasserburg G. J. (1971) Rb–Sr ages of igneous rocks from the Apollo 14 mission and the age of the Fra Mauro formation. *Earth Planet. Sci. Lett.* **12,** 36–48.

Pepin R. O., Bradley J. G., Dragon J. C., and Nyquist L. E. (1972) K–Ar dating of lunar soils: Apollo 12, Apollo 14, and Luna 16 (abstract). In *Lunar Science—III* (editor C. Watkins), pp. 602–604, Lunar Science Institute Contr. No. 88.

Poupeau G., Berdot J. L., Chetrit G. C., and Pellas P. (1972) Predominant trapping of solar-flare gases in lunar soils (abstract). In *Lunar Science—III* (editor C. Watkins), pp. 613–615, Lunar Science Institute Contr. No. 88.

Powell B. N. and Weiblen P. W. (1972) Petrology and origin of rocks in the Fra Mauro formation (abstract). In *Lunar Science—III* (editor C. Watkins), pp. 616–618, Lunar Science Institute Contr. No. 88.

Roedder E. and Weiblen P. W. (1972) Petrographic and petrologic features of Apollo 14, 15, and Luna 16 samples (abstract). In *Lunar Science—III* (editor C. Watkins), pp. 657–659, Lunar Science Institute Contr. No. 88.

Schaeffer O. A., Husain L., Sutter J., Funkhouser J. G., Kirsten T., and Kaneoka I. (1972) The ages of lunar material from Fra Mauro and the Hadley Rille-Apennine front area (abstract). In *Lunar Science—III* (editor C. Watkins), pp. 675–677, Lunar Science Institute Contr. No. 88.

Schönfeld E. (1972) Component abundance and ages in soils and breccia (abstract). In *Lunar Science—III* (editor C. Watkins), pp. 683–685, Lunar Science Institute Contr. No. 88.

Stettler A., Eberhardt P., Geiss J., and Grögler N. (1972) Ar^{39}/Ar^{40} ages of Apollo 11, 12, 14, and 15 rocks (abstract). In *Lunar Science—III* (editor C. Watkins), pp. 724–725, Lunar Science Institute Contr. No. 88.

Sutter J. F., Husain L., and Schaeffer O. A. (1971) $^{40}Ar/^{39}Ar$ ages from Fra Mauro. *Earth Planet. Sci. Lett.* **11,** 249–253.

Turner G. (1970) Argon-40/argon-39 dating of lunar rock samples. *Proc. Apollo 11 Lunar Sci. Conf., Geochim. Cosmochim. Acta* Suppl. 1, Vol. 2, pp. 1665–1684. Pergamon.

Turner G. (1971) $^{40}Ar/^{39}Ar$ ages from the lunar maria. *Earth Planet. Sci. Lett.* **11,** 169–191.

Turner G., Huneke J. C., Podosek F. A., and Wasserburg G. J. (1971) ^{40}Ar–^{39}Ar ages and cosmic ray exposure ages of Apollo 14 samples. *Earth Planet. Sci. Lett.* **12,** 19–35.

Wänke H., Baddenhausen H., Balacescu A., Teschke F., Spettel B., Dreibus G., Quijano M., Kruse H., Wlotzka F., and Begemann F. (1972) Multielement analyses of lunar samples (abstract). In *Lunar Science—III* (editor C. Watkins), pp. 779–781, Lunar Science Institute Contr. No. 88.

Warner J. L. (1972) Apollo 14 breccias: Metamorphic origin and classification (abstract). In *Lunar Science—III* (editor C. Watkins), pp. 782–784, Lunar Science Institute Contr. No. 88.

York D., Kenyon W. J., and Doyle R. J. (1972) $^{40}Ar/^{39}Ar$ ages of Apollo 14 and 15 samples (abstract). In *Lunar Science—III* (editor C. Watkins), pp. 822–824, Lunar Science Institute Contr. No. 88.

Proceedings of the Third Lunar Science Conference
(Supplement 3, *Geochimica et Cosmochimica Acta*)
Vol. 2, pp. 1891–1897
The M.I.T. Press, 1972

Exposure ages and neutron capture record in lunar samples from Fra Mauro

G. W. LUGMAIR and KURT MARTI

University of California, San Diego Chemistry Department,
La Jolla, California 92037

Abstract—Cosmic-ray exposure ages of Apollo 14 rocks and rock fragments obtained by the ^{81}Kr–^{83}Kr method range from 27 to 700 million years. Rock 14321, collected near the Cone crater rim, is one of the many ~27 m.y. old ejecta which were reported at the Third Lunar Science Conference. All the other rocks have considerably higher exposure ages. Isotopic anomalies from neutron capture in gadolinium, in bromine and in barium are used to obtain information on the lunar neutron spectrum at various depths below the lunar surface. The flux ratio of resonance and slow (< 0.3 eV) neutrons is found to be nearly constant in the topmost ~100 g/cm^2.

INTRODUCTION

COSMIC RAYS AND SOLAR WIND are continuously bombarding the lunar surface. Nuclear transformation induced by primary or secondary particles yield information on surface processes and the time of exposure to cosmic rays. Information on the average irradiation depth of a sample can be obtained from measurements of spallogenic noble gases and neutron produced isotopic anomalies in gadolinium (Eugster *et al.*, 1970; Burnett *et al.*, 1971; Marti and Lugmair, 1971; Lugmair and Marti, 1971; Burnett *et al.*, 1972; Lugmair and Marti, 1972). Neutron capture anomalies were recently found in lunar Sm (Russ *et al.*, 1971), as well as in Kr from neutron capture in Br (Lugmair and Marti, 1971). This paper reports on the extension of this work to some Apollo 14 samples. The investigated rock fragments (4–10 mm) from sample 14160 were allocated to a consortium, and our results can be correlated with track data (Macdougall *et al.*, 1972). Sample 14257,10E consists of three basaltic fragments (2–4 mm) from the comprehensive fines.

EXPOSURE AGES

The time intervals of exposure to cosmic rays on or near the lunar surface have been determined by the ^{81}Kr–^{83}Kr method (Marti, 1967). This method has been used to date Apollo 11 and 12 materials and has given reliable ages whenever the irradiation history is not too complex. Since ^{81}Kr–^{83}Kr ages obtained from surface material may be affected by recent solar flares, we have only sampled the center portion of the soil fragments. The age obtained from a surface sample of rock 14321 (FM1+2) is about 10% lower than that obtained from a bottom sample (FM5). The ^{81}Kr–^{83}Kr ages are listed in Table 1 together with the relevant ratios. In rock 14321, no evidence is found for neutron capture anomalies from Br and, therefore, P_{81}/P_{83} is calculated from $P_{81}/P_{83} = 0.95(^{80}\text{Kr} + {}^{82}\text{Kr})/2\ {}^{83}\text{Kr}$ (Marti, 1967). However, generally, in Apollo

Table 1. ^{81}Kr–^{83}Kr ages of Apollo 14 samples.

Sample	$^{83}Kr/^{81}Kr$	$^{83}Kr_{sp}/^{81}Kr$	P_{81}/P_{83}	^{81}Kr–^{83}Kr age (m.y.)
14160,4	3765 ± 130	3754	0.615	700 ± 24
14160,6	1879 ± 84	1872	0.618	351 ± 16
14160,8	1377 ± 59	1376	0.634	264 ± 12
14160,10	2311 ± 145	2297	0.605	421 ± 27
14257,10E	858 ± 36	661	0.618	124 ± 5
14310,47	1445 ± 40	1427	0.600	259 ± 7
14321,FM1 + 2	264 ± 6	122	0.645	23.8 ± 0.6
14321,FM5	263 ± 5	142	0.633	27.2 ± 0.5

$\lambda_{81} = 3.3 \times 10^{-6}$ yr^{-1} is used; for the ratio P_{81}/P_{83} see text.
Errors in the ages do not include uncertainties in λ_{81} and in P_{81}/P_{83}.

14 samples, this production ratio cannot be obtained by the interpolation method, because both ^{80}Kr and ^{82}Kr show anomalies from neutron capture in Br. P_{81}/P_{83} ratios were calculated from

$$\frac{P_{81}}{P_{83}} = 0.850\left(\frac{^{78}Kr}{^{83}Kr}\right)_{spall} + 0.442 \qquad (1)$$

a relation which is analogous to equation (5) of Lugmair and Marti (1971), applied to rock 14310. The data of rocks 14321, 10017, 10057, and 10071 are used to obtain relation (1), since the abundance ratios of the major target elements Sr/Zr are similar in these rocks.

Neutron Capture Effects

Enrichments in the $^{158}GdO/^{157}GdO$ due to neutron capture range from <0.02% in rock 14321 up to 0.7% in fragment 14160,4. The analytical techniques and data reduction have been discussed in detail (Lugmair and Marti, 1971). Isotopic ratios of Gd in some additional fragments from sample 14160 are given in Table 2. The $^{158}GdO/^{157}GdO$ ratios and the calculated fluences (Φ_s) and fluxes (ϕ_s) of slow (<0.3 eV) neutrons are compiled in Table 3. Russ *et al.* (1971), from a comparison of Gd and Sm isotopic anomalies, have shown that the lunar neutron energy spectrum is hardened and that, therefore, the effective cross sections may be lower by a factor of about 2.5 (Lingenfelter *et al.*, 1971). The fluxes listed in Table 3 are based on 2200 m/sec cross sections ($\sigma_{157} = 2.54 \times 10^5$ barn) and have not been adjusted.

Rock 14310 was found to be the first lunar sample to show clear evidence for neutron capture anomalies in ^{80}Kr and ^{82}Kr, due to resonance (30–300 eV) neutron capture in Br (Lugmair and Marti, 1971). With the exception of rock 14321, Kr of all our Apollo 14 samples is found to have neutron produced anomalies. This evidence reflects larger concentrations of Br in Apollo 14 material (Morgan *et al.*, 1972; Reed

Table 2. Isotopic ratios of GdO from Apollo 14 samples (corrected for mass fractionation[a])

Sample	$^{152}GdO/^{160}GdO^*$	$^{154}GdO/^{160}GdO^*$	$^{154}GdO/^{160}GdO_{corr}$	$^{155}GdO/^{160}GdO$	$^{156}GdO/^{160}GdO$	$^{157}GdO/^{160}GdO$	$^{158}GdO/^{160}GdO$
Rock fragments:							
14160,4	0.009 28	0.099 63	0.099 63	0.674 63	0.935 14	0.713 37	1.138 51
	± 1	± 3	± 3	± 4	± 7	± 5	± 7
14160,6	0.009 30	0.099 64	0.099 61	0.675 02	0.934 65	0.714 98	1.136 70
	± 3	± 3	± 3	± 2	± 7	± 8	± 4
14160,8	0.009 24	0.099 62	0.099 62	0.675 21	0.934 47	0.715 88	1.135 73
	± 2	± 3	± 3	± 1	± 1	± 7	± 9
14160,10	0.009 29	0.099 61	0.099 61	0.675 06	0.934 69	0.714 98	1.136 64
	± 6	± 3	± 3	± 1	± 6	± 4	± 7
Rocks:							
14310,47	0.009 28	0.099 59	0.099 59	0.674 86	0.934 87	0.714 28	1.137 57
	± 2	± 3	± 3	± 4	± 3	± 6	± 8
14321,FM3	0.009 27	0.099 59	0.099 59	0.675 35	0.934 52	0.716 40	1.135 60
	± 2	± 3	± 3	± 2	± 4	± 8	± 12
Terr. GdO	0.009 27		0.099 60	0.675 33	0.934 41	0.716 37	1.135 30
	± 3		± 1	± 1	± 3	± 2	± 8

* Not corrected for SmO and $^{151}Eu(n,\beta^-)^{152}Gd$ contributions.
[a] For method see (Lugmair and Marti, 1971). The errors given are $2\sigma_{mean}$ (statistical errors only).

Table 3. Neutron capture anomalies in Apollo 14 samples and neutron fluences Φ_s of slow (<0.3 eV) neutrons.

Sample	$^{158}GdO/^{157}GdO$	Φ_s (10^{15} n/cm^2)	$\phi_s = \frac{\Phi_s}{T_r}$ (n/cm^2 sec)	$\frac{^{131}Xe_n}{^{126}Xe_{sp}}$	$\frac{^{80}Kr_n{}^*}{^{83}Kr_{sp}}$	$\frac{^{82}Kr_n{}^*}{^{83}Kr_{sp}}$	$\left(\frac{^{78}Kr}{^{83}Kr}\right)_{sp}$
14160,4	1.595 97	17.00	0.77	2.59	0.1707	0.0635	0.204
	± 15	±0.29			± 19	± 17	± 1
14160,6	1.589 82	7.66	0.70	2.64	0.0649	0.0240	0.207
	± 18	±0.33			± 13	± 16	± 1
14160,8	1.586 48	2.58	0.31	0.92	0.0496	0.0206	0.226
	± 20	±0.35			± 14	± 17	± 1
14160,10	1.589 75	7.55	0.57	—	0.0360	0.0100	0.192
	± 12	±0.25			± 16	± 20	± 1
14310,47	1.592 62	11.92	1.45	3.60	0.1668	0.0563	0.186
	± 18	±0.33			± 18	± 21	± 1
Terr. GdO	1.584 79	≡0					
	± 12						

* Errors include experimental uncertainties only but do not include uncertainties in the spallation correction.

et al., 1972). Relative $^{80}Kr_n$ and $^{82}Kr_n$ neutron capture anomalies are compiled in Table 3. Neutron capture excesses are calculated from

$$\frac{^{m}Kr_n}{^{83}Kr_{sp}} = \left(\frac{^{m}Kr}{^{83}Kr}\right)_{c.r.} - \left(\frac{^{m}Kr}{^{83}Kr}\right)_{sp} \qquad (2)$$

and the spallation ratios $(^{m}Kr/^{83}Kr)_{sp}$ (m = 80, 82) are obtained by interpolation between those found in rock 14321,FM5 and in Apollo 11A rocks 10017, 10057, and 10071. Figure 1 shows the correlation between the relative $^{80}Kr_n$ and $^{82}Kr_n$ excesses. The slope is determined by the ratio $0.92\sigma_{79}/\sigma_{81}$ which is smaller than the thermal

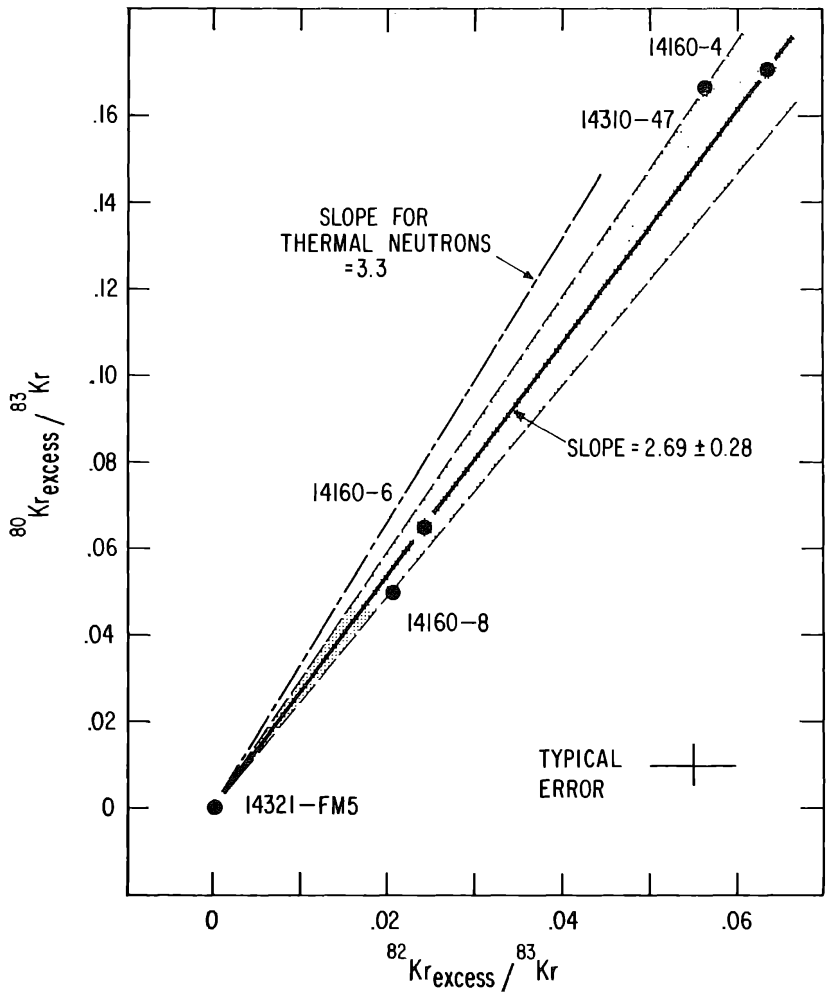

Fig. 1. $^{80}Kr_{excess}/^{83}Kr_{sp}$ versus $^{82}Kr_{excess}/^{83}Kr_{sp}$. The slope of the correlation line is 2.69 ± 0.28 and corresponds to 0.92 σ_r (^{79}Br)/σ_r (^{81}Br). Sub r indicates the resonance energy range 30–300 eV.

cross-section ratio of Br but in agreement with ratios calculated from neutron resonance parameters of Br (Goldberg *et al.*, 1966).

Recent measurements show that the ^{130}Ba cross section for resonance neutrons is 200–300 barn (Kaiser and Berman, 1972; Eberhardt *et al.*, 1971), and that, therefore, the neutron capture contribution to the ^{131}Xe yield is quite large in many lunar samples. We have attempted to calculate the neutron excesses from

$$\frac{^{131}Xe_n}{^{126}Xe_{sp}} = \left(\frac{^{131}Xe}{^{126}Xe}\right)_{c.r.} - \left(\frac{^{131}Xe}{^{126}Xe}\right)_{sp} \qquad (3)$$

analogous to the Kr data. The spallation ratios $(^{131}Xe/^{126}Xe)_{sp}$ cannot be obtained by an interpolation method because no data for spallation *only* are currently known. We have calculated the $^{131}Xe_{sp}$ yield by extrapolation from the best (power) fits to the $^{126,128,129}Xe_{sp}$ yields. The $^{131}Xe_n/^{126}Xe_{sp}$ ratios are also listed in Table 3. A detailed discussion of the rare gas data will be given in a separate paper (Marti *et al.*, 1972).

Discussion

The exposure age of rock 14321 (27 m.y.) is very much shorter than those of the other samples. Rock 14321 was collected on the Cone Crater flank. Similar exposure ages were found in many other rocks from this location (Turner *et al.*, 1971; G. Crozaz *et al.*, 1972) and, therefore, 14321 appears to be one of the Cone Crater ejecta.

Data for three different neutron capture anomalies are given in Table 3. Rock fragment 14160,8 experienced a very small neutron flux of $\phi_s = 0.31$ n/cm^2 sec. This, together with the very high ^{78}Kr/^{83}Kr spallation ratio and the high P_{81}/P_{83} production ratio indicates a close to surface irradiation during most of the time of exposure to cosmic rays. The steep track gradient found in this sample by MacDougall *et al.* (1972) supports this contention.

It is possible to study the correlation between slow and resonance neutron fluxes. Resonance fluxes ϕ_r can be calculated from either $^{80,82}Kr_n$ or $^{131}Xe_n$ data. Flux calculations from the Kr_n data require knowledge of Br abundances. Unfortunately, only Br data for rock 14310 are available. Furthermore, the data obtained by Morgan *et al.* (1972) and Reed *et al.* (1972) differ by a factor of 3.6. If we combine the Kr_n data of 14310 with the Br concentration of Morgan *et al.* (0.235 ppm) a flux $\phi_r(1) = 3.68$ n/cm^2 sec is obtained, and the Reed *et al.* value (0.85 ppm) yields a flux $\phi_r(2) = 1.02$ n/cm^2 sec. This is to be compared to the slow neutron flux $\phi_s = 1.45$ n/cm^2 sec or 3.6 n/cm^2 sec, if the thermal cross section is adjusted according to Lingenfelter *et al.* (1971). The possibility that the resonance flux at or below the lunar surface is smaller than the thermal flux seems very unlikely. Therefore, the Br value by Reed *et al.* (1972) is not applicable to our sample.

If we use $\sigma = 220$ barn for ^{130}Ba (Kaiser and Berman, 1971) and a Ba concentration of 630 ppm, a resonance flux for rock 14310 of ~ 3.5 n/cm^2 sec is calculated. This value is consistent with $\phi_r(1)$ obtained above from neutron produced Kr.

Ba does not only account for the neutron capture excess $^{131}Xe_n$, but it is also the major target element for spallation. We have, therefore, a favorable situation inasmuch as knowledge of the Ba concentration is not required:

$$^{131}Xe_n = [Ba]\frac{^{130}Ba}{Ba}\phi_r T_r \sigma(^{130}Ba), \qquad \text{with } \phi_r \equiv \frac{\Phi_r}{T_r} \tag{4}$$

$$^{126}Xe_{sp} = p_{126}(E)T_r([Ba] + f(E)[La + Ce + Nd])$$

$$^{126}Xe_{sp} = p_{126}(E)T_r[Ba](1 + f(E)R), \qquad \text{with } R = \frac{[La + Ce + Nd]}{[Ba]} \tag{5}$$

$$\frac{^{131}Xe_n}{^{126}Xe_{sp}} = \frac{0.001\sigma(^{130}Ba)}{(1 + f(E)R)p_{126}(E)}\phi_r\,. \tag{6}$$

In a plot of $^{131}Xe_n/^{126}Xe_{sp}$ versus $\phi_s = \Phi_s/T_r$ as calculated from the ^{158}GdO/^{157}GdO data, therefore, essentially ϕ_r and ϕ_s are correlated, and the energy dependence of p_{126} is considered to be small over the depth of $\lesssim 100$ g/cm^2. Figure 2 shows that the two fluxes correlate nearly linearly, which in turn indicates that the ratio of resonance and slow neutron fluxes is not strongly depth dependent. This is in accord with

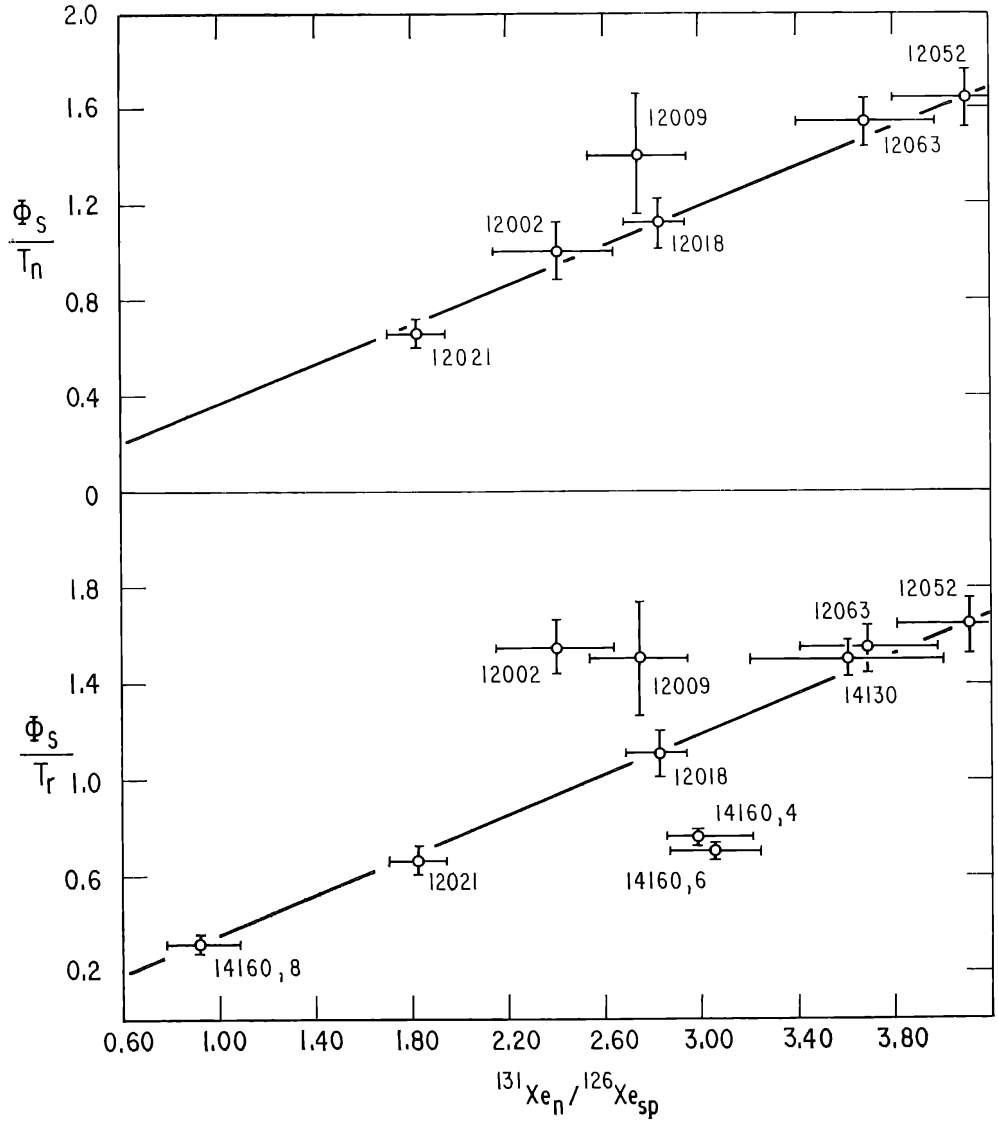

Fig. 2. Correlation of the slow neutron flux $\phi_s = \Phi_s/T$ (in n/cm² sec) and the resonance neutron parameter $^{131}Xe_n/^{126}Xe_{sp}$. The uncertainties of the $^{131}Xe_n/^{126}Xe_{sp}$ ratios shown were compounded including uncertainties in amounts of trapped Xe, fission produced Xe, and of possible neutron produced $^{128}Xe_n$. Assumed excesses $^{128}Xe_n$ are consistent with $^{80}Kr_n$ excesses. Identical isobaric fraction yields were assumed for spallation produced ^{126}Xe, ^{128}Xe, and ^{129}Xe. The use of calculated effective neutron ages T_n (Marti and Lugmair, 1971) instead of ^{81}Kr–^{83}Kr ages T_r for Apollo 12 rocks improves the correlation of the flux parameters (top).

theoretical calculations (Armstrong and Alsmiller, 1971). From spallation systematics (Marti *et al.*, 1966; Burnett *et al.*, 1971), we estimate $^{131}Xe_n/^{126}Xe_{sp}$ ratios for Apollo 14 material to be some 8% larger than for Apollo 12 because of ~20% smaller [La + Ce + Nd]/[Ba] ratio.

Acknowledgments—We gratefully acknowledge the help of K. R. Goldman, B. D. Lightner, T. W. Osborn, and A. Schimmel in the analytical work and in the data reduction. This research was supported by NASA Grant NGR 05-009-150.

References

Armstrong T. W. and Alsmiller R. G. Jr. (1971) Calculation of cosmogenic radionuclides in the moon and comparison with Apollo measurements. *Proc. Second Lunar Sci. Conf., Geochim. Cosmochim. Acta* Suppl. 2, Vol. 2, pp. 1729–1745. MIT Press.

Burnett D. S., Huneke J. C., Podosek F. A., Russ G. P. III, and Wasserburg G. J. (1971) The irradiation history of lunar samples. *Proc. Second Lunar Sci. Conf., Geochim. Cosmochim. Acta* Suppl. 2, Vol. 2, pp. 1671–1679. MIT Press.

Burnett D. S., Huneke J. C., Podosek F. A., Russ G. P. III, Turner G., and Wasserburg G. J. (1972) The irradiation history of lunar samples (abstract). In *Lunar Science—III* (editor C. Watkins), pp. 105–107, Lunar Science Institute Contr. No. 88.

Crozaz G., Drozd R., Graf H., Hohenberg C. M., Monnin M., Rajan D., Ralston C., Seitz M., Shirck J., Walker R. M., and Zimmerman J. (1972) Evidence for extinct ^{244}Pu: Implications for the age of the pre-Imbrium crust (abstract). In *Lunar Science—III* (editor C. Watkins), pp. 164–166, Lunar Science Institute Contr. No. 88.

Eberhardt P., Geiss J., Graf H., and Schwaller H. (1971) On the origin of excess ^{131}Xe in lunar rocks. *Earth Planet. Sci. Lett.* **12,** 260–262.

Eugster O., Tera F., Burnett D. S., and Wasserburg G. J. (1970) The isotopic composition of Gd and neutron capture effects in Apollo 11 samples. *Earth Planet. Sci. Lett.* **8,** 20–30.

Goldberg M. D., Mughabghab S. F., Magurno B. A., and May V. M. (1966) Neutron cross-sections, Vol. 11A, BNL 325, Second Edition, Suppl. No. 2.

Kaiser W. A. and Berman B. L. (1972) The average ^{130}Ba (n, γ) cross-section and the origin of ^{131}Xe on the moon (abstract). In *Lunar Science—III* (editor C. Watkins), p. 444, Lunar Science Institute Contr. No. 88.

Lingenfelter R. E., Canfield E. H., and Hampel V. H. (1971) The lunar neutron flux revisited. *Earth Planet. Sci. Lett.* (to be submitted).

Lugmair G. W. and Marti K. (1971) Neutron capture effects in lunar Gd and the irradiation histories of some lunar rocks. *Earth Planet. Sci. Lett.* **13,** 32–42.

Lugmair G. W. and Marti K. (1972) Neutron and spallation effects in Fra Mauro regolith (abstract). In *Lunar Science—III* (editor C. Watkins), pp. 495–497, Lunar Science Institute Contr. No. 88.

Macdougall D., Martinek B., and Arrhenius G. (1972) Regolith dynamics (abstract). In *Lunar Science—III* (editor C. Watkins), pp. 498–500, Lunar Science Institute Contr. No. 88.

Marti K. (1967) Mass-spectrometric detection of cosmic-ray-produced ^{81}Kr in meteorites and the possibility of Kr–Kr dating. *Phys. Rev. Lett.* **18,** 264–266.

Marti K., Eberhardt P., and Geiss J. (1966) Spallation, fission, and neutron capture anomalies in meteoritic krypton and xenon. *Z. Naturforsch.* **21,** Ser. a, 398–413.

Marti K. and Lugmair G. W. (1971) Kr^{81}–Kr and K–Ar^{40} ages, cosmic-ray spallation products, and neutron effects in lunar samples from Oceanus Procellarum. *Proc. Second Lunar Sci. Conf., Geochim. Cosmochim. Acta* Suppl. 2, Vol. 2, pp. 1591–1605. MIT Press.

Marti K., Lightner B. D., and Osborn T. W. (1972) In preparation.

Morgan J. W., Laul J. C., Krähenbühl U., Ganapathy R., and Anders E. (1972) Major impacts on the moon: Chemical characterization of projectiles (abstract). In *Lunar Science—III* (editor C. Watkins), pp. 552–554, Lunar Science Institute Contr. No. 88.

Reed G. W. Jr., Jovanovic S., and Fuchs L. H. (1972) Concentrations and lability of the halogens, platinum metals and mercury in Apollo 14 and 15 samples (abstract). In *Lunar Science—III* (editor C. Watkins), pp. 637–639, Lunar Science Institute Contr. No. 88.

Russ G. P. III, Burnett D. S., Lingenfelter R. E., and Wasserburg G. J. (1971) Neutron capture on ^{149}Sm in lunar samples. *Earth Planet. Sci. Lett.* **13,** 53–60.

Turner G., Huneke J. C., Podosek F. A., and Wasserburg G. J. (1971) ^{40}Ar–^{39}Ar ages and cosmic-ray exposure ages of Apollo 14 samples. *Earth Planet. Sci. Lett.* **12,** 19–35.